

# Influence of Forest and Rangeland Management on Anadromous Fish Habitat in Western North America

## PROCESSING MILLS AND CAMPS

DONALD C. SCHMIDT



## ABSTRACT

For nearly 50 years, effluents from pulp and paper mills have been known to be toxic to fish and other aquatic animals. Lethal concentrations have been determined for several species of fish and other organisms. Many factors--such as water temperature, size of fish, and additional stresses--affect the ability of fish to withstand pollution. Kraft mill wastes are generally more toxic than sulfite wastes. The high biological oxygen demand of sulfite wastes is often more serious than the chemical toxicity of the effluents. Studies on the effect of kraft effluents on vertebrates show that none of them are more sensitive than juvenile salmonids and some species are more resistant. Fish habitat may also be affected by mill stack emissions. High concentrations of sulfur dioxide may damage or kill trees and other vegetation. The effect of logging camps on fish habitat is largely unknown.

KEYWORDS: Pulp/paper industry, toxic effects (biocide), wood wastes, fish habitat, water quality.



**USDA FOREST SERVICE  
General Technical Report PNW-113**

**INFLUENCE OF FOREST AND  
RANGELAND MANAGEMENT ON  
ANADROMOUS FISH HABITAT IN  
WESTERN NORTH AMERICA**

**William R. Meehan, Technical Editor**

**11. Processing Mills and Camps**

**DONALD C. SCHMIEGE**

**Forestry Sciences Laboratory  
Pacific Northwest Forest and Range Experiment Station  
Juneau, Alaska**

**1980**

## PREFACE

This is one of a series of publications summarizing knowledge about the influences of forest and rangeland management on anadromous fish habitat in the Western United States. This paper addresses the effects of processing mills and camps on anadromous fish habitat. Our intent is to provide managers and users of the forests and rangelands of the Western United States with the most complete information available for estimating the consequences of various management alternatives.

In this series of papers, we summarize published and unpublished reports and data as well as observations of resource scientists and managers. These compilations should be valuable to resource managers in planning uses of forest and rangeland resources, and to scientists in planning future research. The extensive lists of references serve as a bibliography on forest and rangeland resources and their uses.

Previous publications in this series include:

1. "Habitat requirements of anadromous salmonids,"  
by D. W. Reiser and T. C. Bjornn.
2. "Impacts of natural events," by Douglas N. Swanston.
4. "Planning forest roads to protect salmonid habitat,"  
by Carlton S. Yee and Terry D. Roelofs.

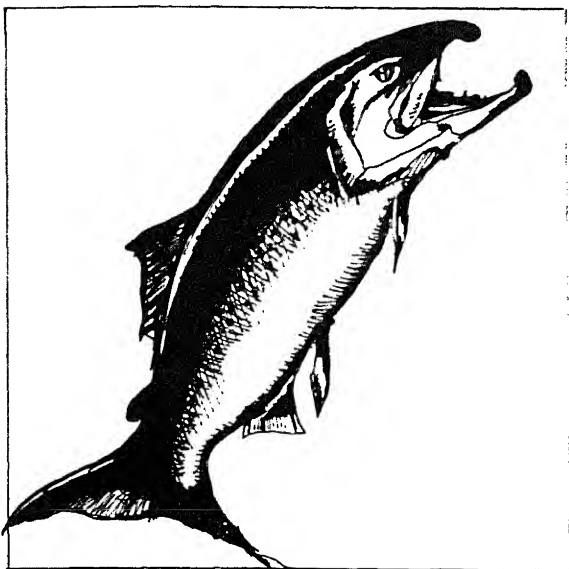
TABLE OF CONTENTS

	Page
INTRODUCTION . . . . .	1
PROCESSING MILLS . . . . .	2
Toxicity of Effluents . . . . .	2
Oxygen Demand . . . . .	5
Suspended Settleable Materials . . . . .	6
Air Pollution . . . . .	8
CAMPS . . . . .	9
Gravel Removal . . . . .	10
Fishing by Residents . . . . .	11
Other Effects of Camps . . . . .	12
SUMMARY AND CONCLUSIONS . . . . .	13
LITERATURE CITED . . . . .	14

## COMMON AND SCIENTIFIC NAMES OF TROUTS, FAMILY SALMONIDAE<sup>1/</sup>

Common name	Scientific name
Pink salmon	<i>Oncorhynchus gorbuscha</i> (Walbaum)
Chum salmon	<i>Oncorhynchus keta</i> (Walbaum)
Coho salmon	<i>Oncorhynchus kisutch</i> (Walbaum)
Sockeye salmon (kokanee)	<i>Oncorhynchus nerka</i> (Walbaum)
Chinook salmon	<i>Oncorhynchus tshawytscha</i> (Walbaum)
Cutthroat trout	<i>Salmo clarki</i> Richardson
Rainbow (steelhead) trout	<i>Salmo gairdneri</i> Richardson
Atlantic salmon	<i>Salmo salar</i> Linnaeus
Brown trout	<i>Salmo trutta</i> Linnaeus
Arctic char	<i>Salvelinus alpinus</i> (Linnaeus)
Brook trout	<i>Salvelinus fontinalis</i> (Mitchill)
Dolly Varden	<i>Salvelinus malma</i> (Walbaum)
Lake trout	<i>Salvelinus namaycush</i> (Walbaum)

<sup>1/</sup> From "A List of Common and Scientific Names of Fishes from the United States and Canada," American Fisheries Society Special Publication No. 6, Third Edition, 1970, 150 p.



## INTRODUCTION

Many pulp and paper mills in North America are either on or near tidal estuaries or on rivers adjacent to estuaries. The anadromous fish that migrate through these estuaries and rivers are valuable for commercial and sport fishing. Inevitably some of these fish contact mill effluents at some concentration.

For nearly 50 years, we have known that effluents from pulp and paper mills may be toxic to fish and other aquatic animals. Effluents from both kraft and sulfite mills are complex mixtures that differ greatly in toxicity, depending on many factors. The toxicity of mill effluents results from the combined activity of a number of chemicals, some of which have not been completely identified. In addition to acute toxicity, pulp and paper mill effluents may be harmful to fish and other aquatic animals because of their biological oxygen demand. High concentrations of wood sugars

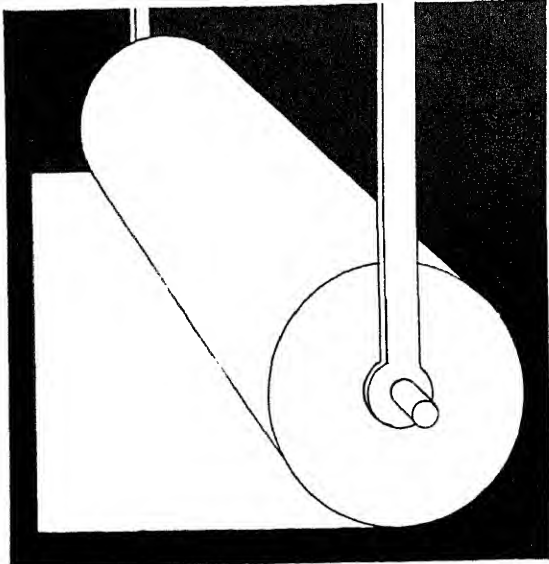
in mill wastes require oxygen during decomposition; hence, as the sugars are stabilized, dissolved oxygen in the receiving water is rapidly depleted. Dissolved oxygen is required by all aquatic animals except anaerobic bacteria.

The difficulty of separating effects of chemical toxicity from effects of biological oxygen demand, and the inability to identify the chemical constituents of effluents, have complicated pollution evaluation studies in the past. The recent development and testing of reproducible bioassay procedures has dramatically changed this situation. Simple, accurate, and sensitive biological assessments are now possible (Walden 1976).

The acute toxicity of various pulp and paper mill effluents is often quite low. Despite their low toxicity, pulp and paper discharges may have a high impact on receiving waters because of the tremendous volumes discharged.

Considerable technological progress in the past decade has reduced harmful effluents. Modern mills that meet Federal and State requirements for pollution abatement differ substantially from the mills that operated 20 or 30 years ago.

Many of the logging camps in Alaska and British Columbia are closely associated with pulp and paper mills because much of the harvested timber goes to the mills. Because of this close association, a discussion of camps and their potential effects on anadromous fish habitat is included in this paper.



## PROCESSING MILLS

### TOXICITY OF EFFLUENTS

The toxicity of effluents from pulp and paper mills has been studied for many years. Some of this work was on the effects of pulp effluents on salmonid fishes (Dimick and Haydu 1952, Lasater 1953, Williams et al. 1953, Alderdice and Brett 1957, Van Horn 1958, Waldichuk 1960, Howard and Walden 1965, Servizi et al. 1968).

A general review of the environmental effects of pulp and paper wastes has been prepared by Marier (1973). Van Horn (1961, 1971) reviewed the pulp and paper industry as it affects aquatic biology. Walden (1976) published an excellent review on the toxicity of effluents from pulp and paper mills.

Effluents from both Kraft and sulfite mills are complex mixtures that differ greatly in toxicity depending on many factors. Because all chemical constituents have not been identified, the effects must be assessed biologically. Several species of fish and many other aquatic organisms have been used for test purposes (Dimick and Haydu 1952, Lasater 1953). Laboratory bioassays have been used to predict toxicity under conditions in natural ecosystems. The definition of reproducible bioassay procedures has been an important step in making bioassays useful (Walden 1976). Simple, accurate, and sensitive bioassays are now possible. Data are converted into toxic units, which may be compared directly, even though bioassay procedures may vary. Maximum accuracy is achieved with 50 percent fish survival. Most toxicity tests require at least 24 hours' exposure time (Walden 1976).

For pulpmill effluents, chemical assays are not feasible. Some toxicants have not yet been identified; consequently, they cannot be assayed chemically. Chemical assays would only be useful if they could be correlated with biological responses.

Because of the low concentration of toxicants in effluents from pulp and paper mills, large amounts of effluent must be used in solutions to be bioassayed. The high biological oxygen demand of these solutions requires oxygenation to maintain fish respiration during the test (Walden 1976).

## EFFLUENTS OF KRAFT MILLS

Reported toxicity of kraft wastes to fish dates back to the work of Ebeling (1931) in Sweden. Many workers since then have confirmed that concentrations of kraft mill effluents needed to kill fish ranged from 10 to 100 percent.

The first studies with salmonids (Dimick and Haydu 1952) demonstrated that sodium hydroxide, methyl mercaptan, sodium sulfide, and hydrogen sulfide were toxic (table 1).

Seven pulpmills were monitored daily for 40 days to determine the amount and duration of effluent toxicity. All sewers in the kraft mills contained toxic chemicals, and substantial daily variation in toxicity was common. Toxicity levels of effluents seldom remained constant more than 12 hours and often varied more frequently (Howard and Walden 1971).

Howard and Walden (1965) studied the toxicity of streams with kraft-process effluents to guppies, Poecilia reticulata (Peters), and sockeye salmon in fresh water at neutral pH. As much as 75 percent of the mortality reported by previous authors was caused by an imbalance in pH. Fish acclimated

to increasing concentrations of effluents in a few days. Test fish exposed to gradually increasing effluent could survive concentrations considerably higher than the values demonstrated as lethal in the bioassays. Thus, concentration values related to various rates of mortality, such as LC<sub>50</sub> (50 percent of the test animals are killed), can be misleading. Length of exposure, other stresses on the fish, pH and temperature of the water, age of the fish, and many other factors can significantly affect pollution concentrations necessary to cause fish mortality.

Effects of kraft effluents on invertebrates indicate that none are more sensitive than juvenile salmonids and some species are much more resistant (Walden 1976).

## SULFITE WASTES

Williams et al. (1953) first demonstrated that sulfite waste liquids were acutely toxic to fish. Previous workers had difficulty demonstrating toxicity, other than the effects of heavy oxygen demand. Kondo et al. (1973), working with neutral sulfite semichemical wastes, showed that they were about one-third as toxic as kraft wastes. Toxicity did not diminish in storage as it did with kraft

Table 1--Threshold concentrations (mg/l) of toxicants in kraft mill wastes lethal to salmonid fishes (after Dimick and Haydu 1952)

Chemical	Chinook salmon	Coho salmon	Cutthroat trout
Hydrogen sulfide	0.3	0.7	0.5
Methyl mercaptan	.5	.7	.9
Sodium sulfide	1.8	1.3	1.0
Sodium hydroxide	27	11	10
Sodium carbonate	58	44	33
Sodium sulfate	--	10,000	2,500

wastes. Holland et al. (1960) found no significant difference in toxicity in ammonia-base and calcium-base pulping liquors.

The toxicity to fish of sulfite pulping wastes is well documented, although the difficulty in segregating toxic effects from those of oxygen demand indicates the limited role toxicity alone plays in natural ecosystems (Walden 1976).

Literature on the effects of sulfite wastes on organisms other than fish is scarce. The available evidence shows that bivalves are especially susceptible. Odlaug (1949) showed that concentrations as low as 100 parts per million of spent sulfite liquor reduced the pumping rate of Olympia oysters (*Ostrea lurida* Carpenter) by 8 percent after immediate exposure. Complete cessation of pumping occurred after 15 days. Stein et al. (1959) showed that concentrations of ammonia-base, spent sulfite liquor greater than 55 parts per million affected spawning of oysters, but lower concentrations stimulated activity. Oysters appear to be more sensitive to spent sulfite wastes than any other species tested (Woelke 1967).

## SUBLETHAL EFFECTS OF PULPMILL EFFLUENTS

Biologists have long recognized that concentrations approaching lethal amounts of pollutants, as determined in bioassays, are not safe for survival and maintenance of fish stocks (Fry 1971). The results of bioassays are valueless and misleading unless they can be related to concentrations producing no harmful effects to the ecosystem. Stresses are cumulative, and any stress on an organism reduces its ability to withstand other stresses.

The known sublethal effects of pulp and paper effluents are attributable to coniferous fibers, hydrogen sulfide, and nonvolatile soluble toxic substances (Walden 1976). The last group is of major environmental concern.

Walden and Howard (1968) described effects displayed by fish after exposure to lethal concentrations of kraft effluent: loss of schooling, respiratory distress, abnormal gill movements, reluctance to eat, loss of equilibrium, convulsive coughing, excessive mucous production, and finally death.

Jones et al. (1956) showed that some species of salmon avoided regions containing pulpmill waste. Chinook salmon were best able to avoid the waste, coho salmon were less able, and steelhead trout showed no noticeable reaction. Inconsistent results were demonstrated in some other studies, such as those of Dimick et al.



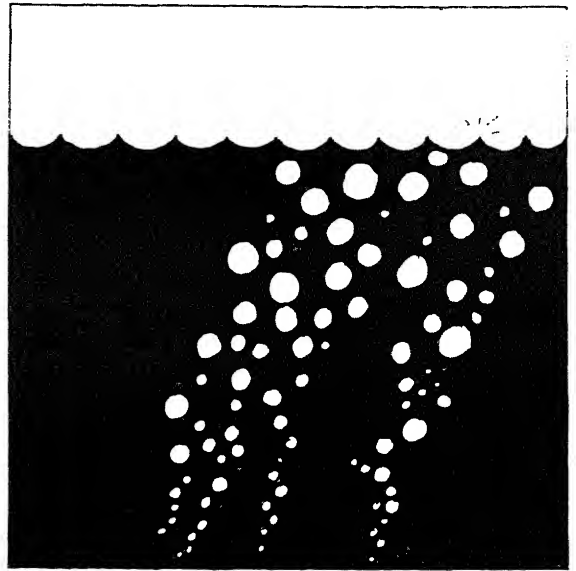
(1957); salmon sometimes avoided concentrations that attracted other test fish.

The ability of fish to swim is affected by pulpmill wastes (Howard 1973, 1975). Howard and Walden (1974) developed techniques to measure swimming; speed and stamina decreased after effluents reached a threshold concentration.

Fish growth may be adversely affected by moderate to high concentrations of kraft mill effluents, but low concentrations stimulated growth (Webb and Brett 1972).

Schaumburg et al. (1967) studied the effects of sublethal concentrations of kraft effluent on fish respiration. They found that stressed fish reversed the flow of water past their gills; this was designated as "coughing." Coughing increased with increasing concentrations of effluents.

Evidence of effects of sublethal concentrations of wastes from pulp and paper mills on organisms other than fish is not extensive. Available data indicate that the threshold at which sublethal concentrations affect invertebrates corresponds roughly to that affecting fish (Walden 1976).



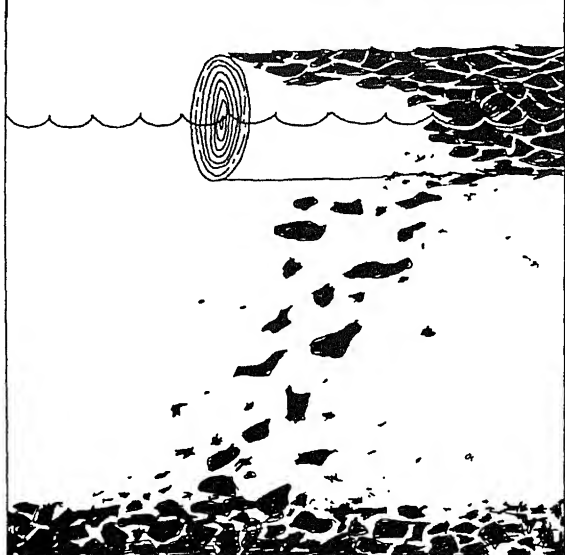
## OXYGEN DEMAND

High concentrations of wood sugars in sulfite wastes require oxygen during decomposition. The oxygen requirements for stabilization of the sugars result in a high biological oxygen demand which can result in rapid depletion of dissolved oxygen in the receiving water (Waldichuk 1960).

Kraft mill wastes also contain high concentrations of organic material, but not nearly as much as in sulfite liquor.

Walden (1976) stated that difficulties in segregating toxic effects from those caused by oxygen demand emphasize the limited role toxicity plays in natural situations, compared to problems arising from potential oxygen depletion. Thus, the primary effect of sulfite wastes is apparently to increase biological oxygen demand.

The dissolved oxygen level required to sustain fish varies considerably, because it depends on other factors such as water temperature, salinity, pH, fish species, and other stresses on the fish. Despite efforts to decrease the biological oxygen demand of wastes from pulp and paper mills, the effect of these wastes on dissolved oxygen remains a problem in some receiving waters.



## **SUSPENDED SETTLEABLE MATERIALS**

Bark, chips, and pulp fibers concern fishery biologists and others because they have long-term effects on the aquatic environment. As these materials begin to cover the bottom, the rich fauna often found there is either destroyed or forced to move. Fish that normally feed on or near the bottom also find the area unattractive and move elsewhere. As the organic materials start to decompose and dissolved oxygen in the water is used up, hydrogen sulfide is released. The bottom layer of water, with low dissolved-oxygen levels, may become very thick and, thus, unsuitable for many species of food fish. This is especially true in inlets and other restricted locations where strong tidal flushing does not occur.

Particles of bark, chips, and fibers come mainly from drum and hydraulic barkers, paper machines, and from transferring chips from scows to the mill. Bark also sloughs off logs during raft transport and during storage in holding ponds. Log-transfer sites often contain heavy accumulations of bark and other wood debris (Schaumburg 1973).

Row and Cook (1971) found that most of the toxicity from mechanical pulping effluents was caused by resin acid soaps. Wilson (1975) studied the toxicity of effluents from newsprint operations. Biotreated effluent had no adverse reaction on any of the zooplankton and invertebrates tested.

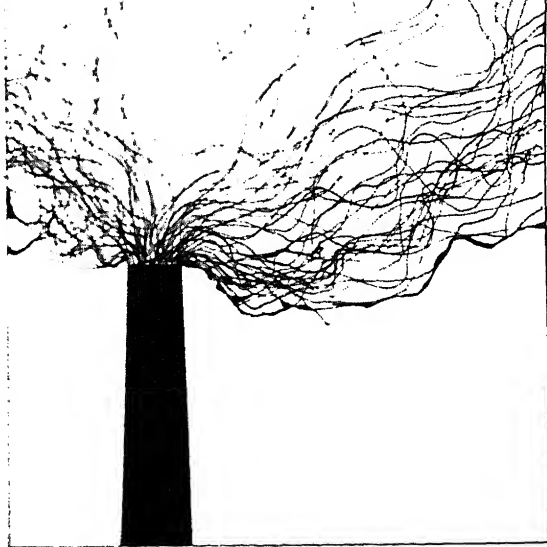
Raw wood is about half cellulose fibers. Modern mills use settling tanks, filters, and other devices to keep fibers out of receiving waters.

Bark accumulations may contaminate salmon spawning grounds (Servizi et al. 1968). Servizi and his coworkers found that the oxygen demand of bark is great enough and of long enough duration that eggs can be killed. Fine bark particles can also clog the gravel, causing egg mortality. These authors estimated that bark concentrations of 4 percent and more were likely to increase egg-to-fry mortality because of oxygen depletion at incubation velocities of 5 cm/h. Even bark concentrations of 1 percent and greater could retard emergence. Egg mortality increased as bark accumulations increased and water flow decreased.

Even though bark leachates are toxic, studies by Schaumburg (1973) showed that leachates from logs in natural waters had little toxic effect. In a study of woodroom effluents, Howard and Leach (1973) found that softwood species tended to be more toxic than hardwood species.

Leachates from logs also contain wood sugar and other biodegradable materials that exert a large biochemical oxygen demand (Schaumburg 1973). Extracts of spruce (Picea sp.) and hemlock (Tsuga sp.) bark are also toxic to fish, shrimp (Pandalus sp.), and dungeness crab (Cancer magister Dana) (Buchanan et al. 1976). Toxic effects on salmon fry were observed as soon as 3 hours after exposure to hemlock bark extracts. After a 96-hour exposure at a concentration of 56 milligrams per liter, 50 percent of the salmon fry were killed. Spruce bark extracts were consistently toxic to all invertebrates tested.

Concentrations of leachates great enough to be toxic are unlikely except in certain locations with little or no tidal flushing, such as log-handling and storage areas.



## AIR POLLUTION

Stack emissions from pulp and paper mills contain many chemicals. Some, such as sulfur dioxide ( $\text{SO}_2$ ), can damage plants if concentrated sufficiently and if exposure continues long enough (Faller 1971, Linzon et al. 1972, Carlson 1974).

Sulfur dioxide is a soluble gas readily absorbed by foliage through the stomata. Absorption can also occur through wet leaf surfaces (Thomas et al. 1950). If  $\text{SO}_2$  is not removed from the air, it oxidizes to  $\text{SO}_3$  and becomes a sulfuric acid mist. This mist is corrosive and can cause lesions on plant tissue.

needles by  $\text{SO}_2$  requires that foliage samples be analyzed for sulfur. Histological examination of needles shows a distinctive syndrome unlike that caused by pathogens, drought, or freezing. Several investigators have established that high sulfur dioxide concentrations can injure or kill plants (Thomas et al. 1950, Faller 1971, Linzon et al. 1972, Ratsch 1974).

When mills are located near rivers used by salmon and other anadromous fish, they can affect fish habitat through air pollution that kills riparian vegetation. Several studies have shown the importance of streamside vegetation in reducing stream temperatures, producing logs in the stream for cover, and forming pools (Meehan et al. 1977). Trees along streambanks also harbor insects that drop into streams and are eaten by fish and other aquatic organisms.

The extent and severity of injury to riparian vegetation resulting from pulpmills depend on wind patterns and surrounding terrain as well as the amount of pollutants emitted from the mill. The presence of a pulpmill does not guarantee that nearby trees will die. If emissions are not great and air currents provide mixing,  $\text{SO}_2$  concentrations may not be high enough to cause damage to trees or other plants (Ratsch 1974).



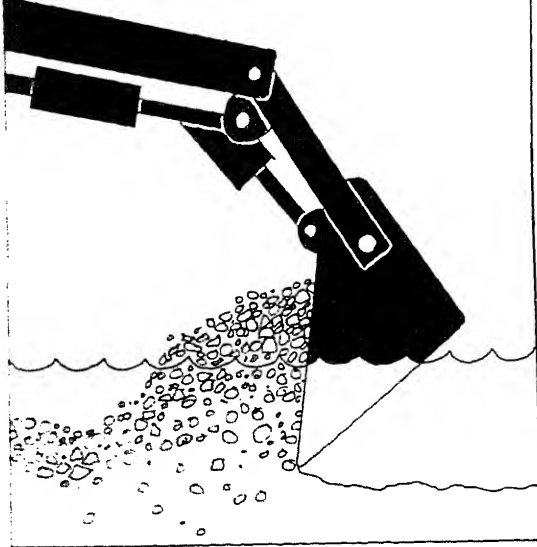
## CAMPS

Except in Alaska and British Columbia, logging camps are nearly nonexistent in North America. A few camps occur in other places, but they are usually not permanent.

About 60 logging companies operate in southeast Alaska (Pease 1974). Some have floating camps that are towed from one anchorage to another but most are land based. They range in size from a one-family operation to a community of 500 people or more. Camps are usually located in protected harbors that serve as log-storage and transfer sites.

In the past, few regulations controlled logging camps. Some activities could have affected anadromous fish, but we have no record of it. Logging camps are now regulated by the Environmental Protection Agency, the USDA Forest Service, and the States. In Alaska, the State Department of Environmental Conservation also has authority. Logging camp sewage or solid wastes are unlikely to affect fish habitat adversely if regulations of these agencies are complied with. The Environmental Protection Agency requires secondary sewage treatment. Chlorinated wastewater could be toxic to fish if concentrations of chlorine were high.

Logging camps used to leave rusting cables, junked machinery, bands from log bundles, spilled fuel, and other debris on or near their sites when a camp was abandoned. No studies document the effects of these materials on fish habitat, however. Present regulations require that the sites be cleaned before the camp is moved.



## GRAVEL REMOVAL

Large amounts of gravel are needed for building logging roads and developing campsites. Some locations have no source of gravel nearby, other than streambeds. Although gravel has been taken from streams in the past, this practice was probably never common and it will no doubt become less common.

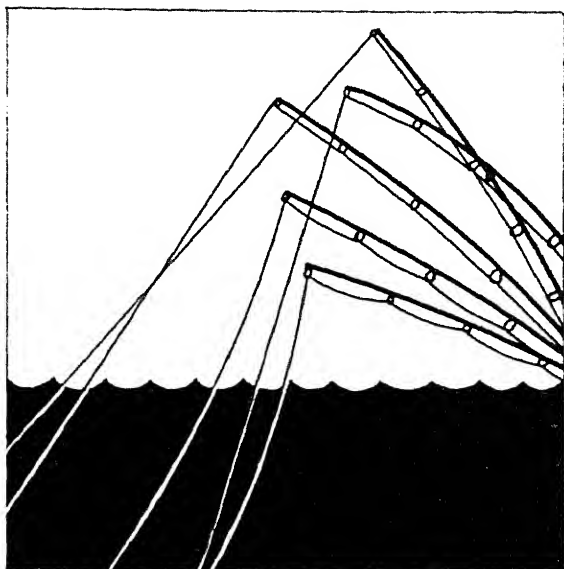
removal from streambeds have been documented in Alaska. Sheridan reported on the removal of gravel from a stream on Baranof Island near Sitka, Alaska.<sup>2/</sup> Road construction and logging were started in the Rodman Creek watershed in 1960 and completed in 1965. Surveys showed that the stream and alluvial flood plain contained the only gravel nearby; 64,000 cubic yards of gravel were taken from 16 borrow pits located on the tideflats, flood plain, and in the stream. Pink and chum salmon spawned in the intertidal area and up to 5 miles upstream. The Alaska Department of Fish and Game had records of escapement before gravel removal and continued these surveys during and after the gravel was removed. The borrow pits filled with gravel in 4 years, no significant changes were observed in streambed gradient, and the pit accelerated bank cutting in their vicinity, causing several trees to fall into the stream and a high intermittent sediment load. The pit-filling probably increased bedload movement and likely increased the instability of spawning beds upstream. Salmon escapement showed no

---

<sup>2/</sup> Unpublished paper, "Effects gravel removal on a salmon spawning stream," by W. L. Sheridan. USDA Forest Serv., 26 p. On file, Forestry Science Laboratory, Juneau, Alaska, 1967.

decrease, even though a short-term decrease in survival of salmon embryos could have occurred because of increased sedimentation. Sheridan cautioned that gravel should be removed from streams only if no other source of gravel is available and the value of timber far exceeds the potential damage to salmon habitat.

During World War II, large amounts of gravel were removed from four salmon streams near the Kodiak Naval Station (McVey 1959). Sections of the streambed were removed to depths of 20 feet. The fish-producing potential was reduced in two streams because the tailings from washing and screening reduced the average size of stream gravel, resulting in instability. In the other two streams, bottom materials broke up and were washed downstream. As a result, streamflow was limited to subterranean seepage during low water flows, and several miles of excellent spawning grounds became inaccessible to spawning fish. By 1958, the gravel of only one of the two streams showed signs of stabilizing.



## FISHING BY RESIDENTS

Logging camps congregate people in remote areas of south-east Alaska and British Columbia. The camps are often near highly productive stream and estuarine fisheries. This combination of people and resources results in heavy use.

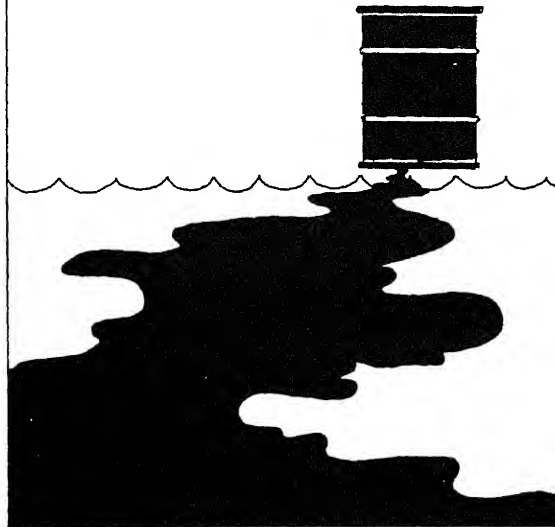
Some biologists believe that logging camps are responsible for unusually heavy fishing pressure in some streams. Depletion of runs has been mentioned, but quantitative data are lacking. Species such as steelhead trout would be especially vulnerable, because the runs are small in some streams. The Alaska Department of Fish and Game has estimated that sport harvest in Rodman Creek, Baranof Island, took over 60 percent of the mature Dolly Varden char in 1963, based on tag returns. This pressure was mainly from nearby logging camps.<sup>3/</sup>

---

<sup>3/</sup> Data on file, Forestry Sciences Laboratory, Juneau, Alaska.

Fish and Game is now conducting a statewide sport fishing survey. Information will be received from high-quality watersheds, including those near logging camps, so sport fishing harvests from logging camps can be estimated.

If anglers all carry proper licenses and observe bag limits, the logging camps only serve to distribute and congregate people, so it may be misleading to view camps as detrimental to the fisheries resource.



## OTHER EFFECTS OF CAMPS

Some logging camps probably have affected the local fisheries by sewage pollution, water diversion, oil and lubricant spills, and gravel removal, although the effects of these activities have not been documented.

In light of the detailed State and Federal water and air quality standards, logging camps are unlikely to have any appreciable effect on fish habitat now or in the future. Logging camps may be viewed as small communities, subject to the same regulations as any other community. If environmental degradation occurs it is because State and Federal regulations are being violated.



# SUMMARY AND CONCLUSIONS

Pulp and paper mills release enormous amounts of effluents daily into receiving waters. The toxicity of these wastes varies widely and is dependent on factors such as chemical processes used, waste recovery, and biological oxygen demand caused by decomposition of sugars in the effluents.

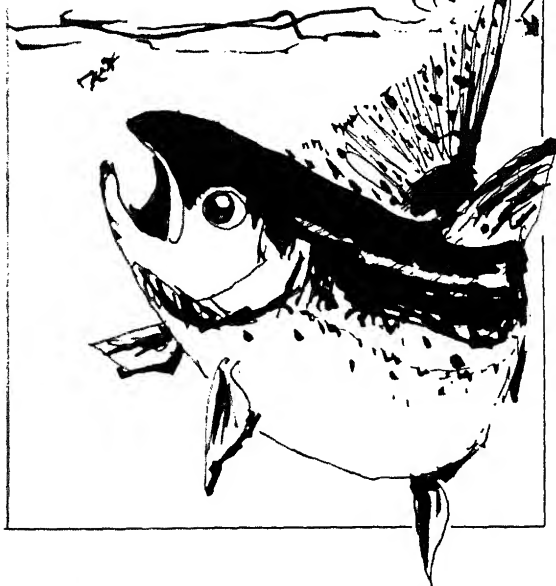
Until recently, assessing the harmful effects of mill wastes was difficult because the chemical constituents are complex, and some remain unidentified. The relation between the concentration of many toxic constituents and biological activity has not been established. In addition, separating chemical toxicity from biological oxygen demand is often difficult. As a result chemical assays cannot be used.

Laboratory and field studies have accumulated the data needed to design accurate and sensitive acute lethal bioassays for effluents from pulp and paper mills. These bioassays have been used to identify thresholds of effluent toxicity for several aquatic animals, including salmonid fishes. This work has demonstrated that the previous history of test animals is very important. Fish and other aquatic animals can be conditioned to withstand increasing levels of pollutants to a point. Stresses tend to be cumulative, however, and such factors as water temperature and pH can compound the effects of other stresses. Despite some shortcomings, recent research on biological assessment has resulted in the development of

tables showing concentrations of effluents associated with effects on various organisms. Threshold concentrations of effluents from paper mills have been based on extensive technical data; this work has been reviewed by Walden (1976).

The acute lethal bioassay is now well established for measuring toxicity of industrial pollution. Using such bioassays to determine safe levels of effluent in the environment is risky, however. Each biological system is unique; plants and animals in the system are subjected to various stresses. The amount and duration of these stresses determine the animal's ability to withstand the added stress of mill pollution. What is needed is a sublethal bioassay, sensitive enough to detect changes in the natural environment as they relate to biological requirements of the animals.

Little information is available on the effects of logging camps on anadromous fish habitat. Because camps are often near productive fish habitat, however, they are potentially hazardous. Present regulations pertaining to camps and associated activities appear adequate to prevent appreciable damage.



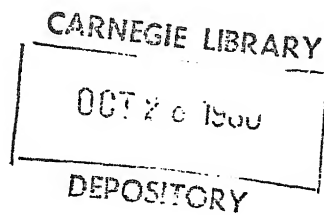
## LITERATURE CITED

- Alderdice, D. F., and J. R. Brett. 1957. Some effects of kraft mill effluent on young Pacific salmon. J. Fish. Res. Board Can. 14(5):783-795.
- Buchanan, D. V., P. S. Tate, and J. R. Moring. 1976. Acute toxicities of spruce and hemlock bark extracts to some estuarine organisms in southeastern Alaska. J. Fish. Res. Board Can. 33(5):1188-1192.
- Carlson, C. E. 1974. Sulfur damage to Douglas-fir near a pulp and paper mill in western Montana. USDA For. Serv. Rep. 74-13, 41 p. Missoula, Mont.
- Dimick, R. E., and E. P. Haydu. 1952. The effects of kraft mill waste liquors and some of their components on certain salmonid fishes of the Pacific Northwest. Natl. Counc. Stream Improv., Inc., New York (Natl. Counc. Stream Improv., Inc., New York (Natl. Counc. Pap. Ind. Air and Stream Improv.) Tech. Bull. 51, 23 p.
- Dimick, R. E., C. E. Warren, B. F. Jones, P. Doudoroff, and H. R. Amberg. 1957. Some preliminary observations on the avoidance reactions of salmonid fishes to pulp mill effluents. Natl. Counc. Stream Improv., Inc., New York (Natl. Counc. Pap. Ind. Air and Stream Improv.) Tech. Bull. 93, 14 p.
- Ebeling, G. 1931. Recent results of the chemical investigation of the effect of waste waters from cellulose plants on fish. Vom Wasser 5:192-200.
- Faller, N. 1971. Effects of atmospheric SO<sub>2</sub> on plants. The Sulfur Inst. J. 6(4):5-7.
- Fry, F. E. J. 1971. The effect of environmental factors on the physiology of fish. In Fish physiology, Vol. 6, p. 1-98. W. S. Hoar and D. J. Randall (eds.). Acad. Press, New York.
- Holland, G. A., J. E. Lasater, E. D. Neumann, and W. E. Eldridge. 1960. Toxic effects of organic and inorganic pollutants on young salmon and trout. Wash. Dep. Fish. Res. Bull. 5, 264 p, Olympia.
- Howard, T. E. 1973. Effects of kraft pulp mill effluents on the stamina, temperature tolerance, and respiration of some salmonid fish. Ph. thesis, Univ. Strathclyde, Glasgow, Scotland. 183 p.

- performance of juvenile coho salmon (Oncorhynchus kisutch) exposed to bleached kraft pulpmill effluent. J. Fish. Res. Board Can. 32(6):789-793.
- Howard, T. E., and J. M. Leach. 1973. Identification and treatment of the toxic materials in woodroom effluents. Can. For. Serv. CPAR Proj. Rep. No. 148-1, 56 p. Ottawa, Ont.
- Howard, T. E., and C. C. Walden. 1965. Pollution and toxicity characteristics of kraft pulp mill effluents. TAPPI 48(3):135-141.
- Howard, T. E., and C. C. Walden. 1971. Effluent characteristics of bleached kraft pulp mills. Pulp and Pap. Mag. Can. 72(1):T3-T9.
- Howard, T. E., and C. C. Walden. 1974. Measuring stress in fish exposed to pulp mill effluents. TAPPI 57(2):133-135.
- Jones, B. F., C. E. Warren, C. E. Bond, and P. Doudoroff. 1956. Avoidance reactions of salmonid fishes to pulp mill effluents. Sewage Ind. Wastes 28(11):1403-1413.
- Kondo, R., K. Sameshima, and T. Kondo. 1973. Spent semi-chemical pulping liquor. (3). Toxicity characteristics of SCP spent liquor and reduction of its toxicity. Japan Tech. Assoc. Pulp and Pap. Ind. 10: 476-485.
- Lasater, J. E. 1953. Effects of sulfite pulp mill waste liquor on salmon food organisms. Pac. Mar. Fish. Comm., Portland, Oregon. 46 p.
- Linzon, S. N., W. D. McIlveen, and P. J. Temple. 1972. Sulphur dioxide injury to vegetation in the vicinity of a sulphite pulp and paper mill. Water, Air, and Soil Pollut. 2(1973):120-134.
- Marier, J. 1973. The effects of pulp and paper wastes with particular attention to fish and bioassay procedure for assessment of harmful effects. Natl. Res. Council. Can., 13501. Environ. Secr. Publ. 73-3, Ottawa, Ont. 33 p.
- McVey, R. 1959. Gravel removal and the fisheries. Alaska Fisheries Briefs. U.S. Fish and Wildl. Serv. Circ. 59, p. 14-18. Bur. Commer. Fish.
- Meehan, W. R., F. J. Swanson, and J. R. Sedell. 1977. Influences of riparian vegetation on aquatic ecosystems with particular reference to salmonid fishes and their food supply. In Importance, preservation and management of riparian habitat: A symposium. USDA For. Serv. Gen. Tech. Rep. RM-43, p. 137-145. Rocky Mt. For. and Range Exp. Stn., Fort Collins, Colo.
- Odlaug, T. O. 1949. Effects of stabilized and unstabilized waste sulfite liquor on the Olympic oyster, Ostrea lurida. Trans. Am. Microsc. Soc. 68(2):163-182.

- Pease, D. C. 1971. Logging and rafting on log dumping and rafting on the marine environment of southeast Alaska. USDA For. Serv. Gen. Tech. Rep. PNW-22, 58 p. Pac. Northwest For. and Range Exp. Stn., Portland, Oreg.
- Ratsch, H. C. 1974. Sulfur content of Douglas-fir foliage near a paper mill. U.S. Environ. Prot. Agency, EPA-660/3-74-018. 13 p. Corvallis, Oreg.
- Row, R., and R. H. Cook. 1971. Resin acid soaps--toxicity and treatability. Sixth Air and Stream Improv. Conf., Tech. Sect., Can. Pulp Pap. Assoc., Quebec City. p. 87-96.
- Schaumburg, F. D. 1973. The influence of log handling on water quality. U.S. Environ. Prot. Agency EPA-R2-73-085, 105 p.
- Schaumburg, F. D., T. E. Howard, and C. C. Walden. 1967. A method to evaluate the effects of water pollutants on fish respiration. Water Res. 1(10):731-737.
- Servizi, J. A., R. W. Gordon, and D. W. Martens. 1968. Toxicity of two chlorinated catechols, possible components of kraft pulp mill bleach waste. Int. Pac. Salmon Fish Comm. Prog. Rep. 17, 43 p. New Westminster, B.C.
- M. Clark, and I. E. Ellis. 1959. The spawning of Olympia oysters (Ostrea lurida) kept in spent sulfite liquor (SSL). Olympia Res. Div. Rep. Rayonnier, Shelton, Wash. 13 p.
- Thomas, M. D., R. H. Hendricks, and G. R. Hill. 1950. The sulfur metabolism of plants. Effects of sulfur dioxide on vegetation. Ind. Eng. Chem. 42(11):2231-2235.
- Van Horn, W. M. 1958. The effect of pulp and paper mill wastes on aquatic life. Paper presented at 5th Ont. Ind. Waste Conf., sponsored by the Water and Pollut. Advis. Comm., p. 60-66. Ont. Water Res. Comm.
- Van Horn, W. M. 1961. Aquatic biology and the pulp and paper industry (Rep. No. 1). Natl. Council of Paper Industry for Air and Stream Improv. Inc., New York, N.Y. Stream Improvement Tech. Bull. 148, 100 p.
- Van Horn, W. M. 1971. Aquatic biology and the pulp and paper industry (Rep. No. 2). Natl. Council of Paper Industry for Air and Stream Improv., New York, N.Y. Stream Improvement Tech. Bull. 251, 45 p.
- Walden, C. C. 1976. The toxicity of pulp and paper mill effluents and corresponding measurements procedures. Water Res. 10(8):639-664.

- Walden, C. C., and T. E. Howard. 1968. A cooperative research program on kraft pulp mill effluent quality. Pulp Pap. Mag. Can. 69: 67-71.
- Waldichuk, M. 1960. Pulp mill pollution in British Columbia. Fish. Res. Board Can. Circ. 57, 14 p. Nanaimo, B.C.
- Webb, P. W., and J. R. Brett. 1972. The effects of sublethal concentrations of whole bleached kraftmill effluent on the growth and food conversion efficiency of underyearling sockeye salmon. J. Fish. Res. Board Can. 29(11):1555-1563.
- Williams, R. W., E. W. Mains, W. E. Eldridge, and J. E. Lasater. 1953. Toxic effects of sulfite waste liquor on young salmon. Wash. Dep. Fish. Res. Bull. 1, 108 p. Olympia.
- Wilson, M. A. 1975. Assessment of the sensitivity of major aquatic food chain organisms to newsprint mill effluents which are not acutely toxic to fish. Can. For. Serv. CPAR Proj. Rep. 328-1, 78 p. Ottawa, Can.
- Woelke, C. E. 1967. Measurement of water quality with the Pacific oyster embryo bioassay. Water quality criteria, ASTM, STP 416, p. 112-120. Am. Soc. Test. Mater., Philadelphia, Pa.



The **Forest Service** of the U.S. Department of Agriculture is dedicated to the principle of multiple use management of the Nation's forest resources for sustained yields of wood, water, forage, wildlife, and recreation. Through forestry research, cooperation with the States and private forest owners, and management of the National Forests and National Grasslands, it strives — as directed by Congress — to provide increasingly greater service to a growing Nation.

The U.S. Department of Agriculture is an Equal Opportunity Employer. Applicants for all Department programs will be given equal consideration without regard to age, race, color, sex, religion, or national origin.

centered curve will now be explained. In order to proceed on the work, it is advisable to first draw the ellipse by the method given above. Let  $AD$  be the given semi-axes. Join  $A$  and  $C$ , and draw a perpendicular to  $AC$ , determining  $E$  and  $O$ , the center. From  $O$ , with  $OC$  as radius, draw an arc  $CK$  at a suitable angle, and join  $K$  with  $O$ . Make  $KG$  equal to  $EO$  and  $G$ . At the center of  $EG$  draw a perpendicular to  $EG$  and note its intersection  $H$  with  $KO$ . From  $H$ , draw an arc to  $HE$  (extended); and from  $O$ , with  $OC$  as radius, complete the curve.

*Parabola.*—The equation of the parabola, Fig. 6,

$$y = \frac{x^2 b}{a^2}$$

Divide the line  $OR$  into any number of convenient parts, and number the points of division 1, 2, 3, etc.,

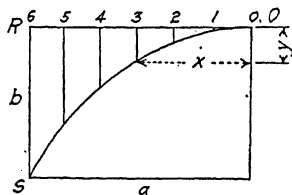


FIG. 6.

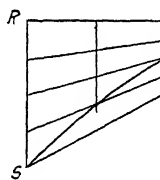


FIG. 7.

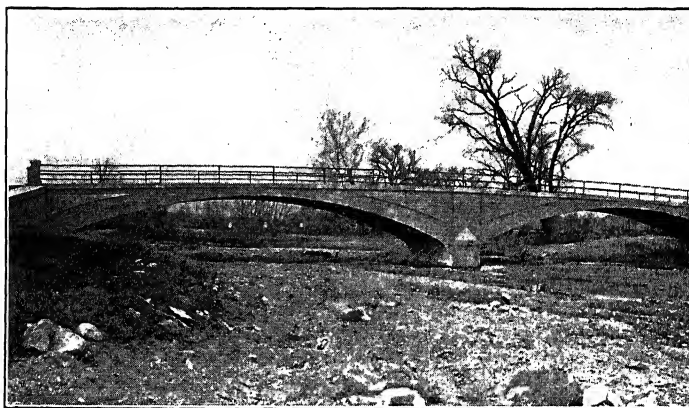
point nearest  $O$ . Then to find the values of the abscissas  $x$ , the numbers 1, 2, 3, etc., should be inserted above the equation for values of  $x$ , and the total number of divisions, in this illustration is 6, should be inserted for the value of  $a$ .

A very simple graphical method of drawing a parabola is shown in Fig. 7. Lay off on the vertical line  $RS$ , Fig. 7, the same number of divisions as are made on the horizontal axis. Draw radiating lines from  $S$  to the divisions on  $RO$ , and draw radiating lines from  $R$  to the divisions on the horizontal axis, such that they intersect the lines from  $S$ . The intersection points are connected to form a parabolic curve.

## GENERAL DATA

of transverse walls (Figs. 9A, 9B, and 9C), or on a continuous superstructure of columns, girders, beams, and slabs (Figs. 10B, and 10C). If, as is rarely the case, a heavy or monumental appearance is desired in open-spandrel construction, the arches and curtain walls may be used and all spandrel openings filled (Fig. 10D). In the open-spandrel type, the arch ring may be either solid or composed of two or more longitudinal ribs. The features of open-spandrel construction are shown in Figs. 10E and 10F.

With filled spandrels, the filling material is held in place laterally by retaining walls which rest upon the arch ring.



*Courtesy of Universal Portland Cement Co.*

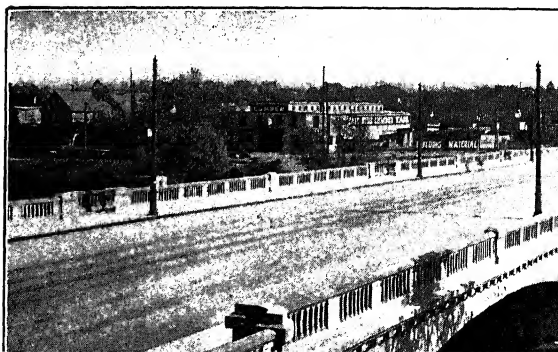
FIG. 8A.—Highway bridge at Ellerton, Ohio.

retaining walls may be of either the gravity or the reinforced type, or they may consist of thin vertical slabs tied together by reinforced-concrete cross walls. Solid fillings increase the weight of the superstructure and make necessary thicker arch rings and larger foundations. Open-spandrel construction, on the



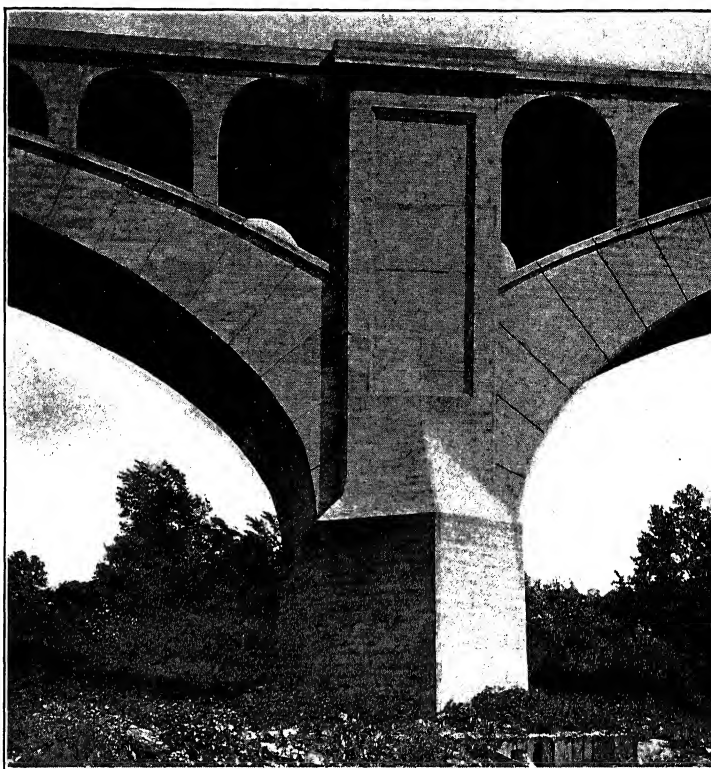


*Courtesy of Mr. Daniel B. Luten, Consulting Engineer, Indianapolis.*  
FIG. 8B.—Georgetown bridge over Wabash River, G.



## GENERAL DATA

**4. Selection of the Most Suitable Intrados.**—The length, span and curve of an arch are often determined by physical conditions. Ample waterway must be provided for over stream and, if possible, piers and abutments should be located where the cost of foundations is a minimum. Sufficient clearances must be allowed over roadways. These and other conditions



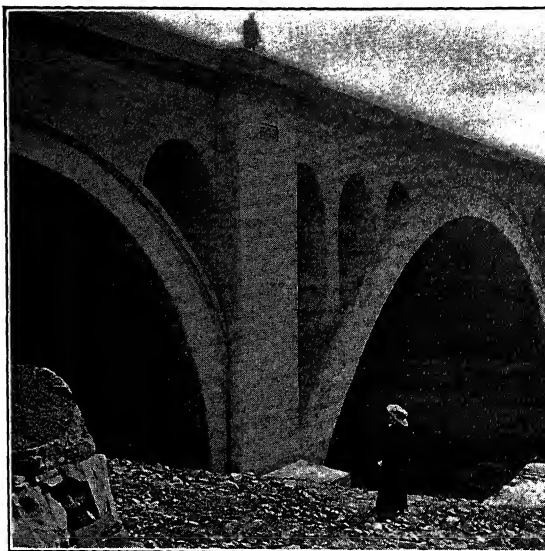
*Courtesy of Assoc. American Portland Cement Mfrs.*

FIG. 9A.—Detailed view of spandrel arches in railroad construction.

span of *less* than one-fourth, the most economical between a circular segment and an ellipse and is obtained by a three-centered intrados.

**5. Piers and Abutments.**—The springing line of an arch, should be located as near the foundation as the soil will permit. This will often make possible a less expensive pier and abutment, where piers are employed, and, where the overturning effect on the piers to a minimum.

In the case of long bridges with a series of



*Courtesy of Sandusky Portland Cement Co.*

FIG. 9B.—Bridge on Lake Shore & Michigan Southern

called abutment piers should be placed at intervals (usually every 5 or 6 spans) so as to act as a check against the failure of one or more of the arches. They should be made of sufficient thickness to resist the pressure of the water standing and the other arch removed, and for the purpose of standing. The ordinary arch pier should be analyzed as a pier with arch without live load and the other adjacent arches with load over the whole span.

GENERAL DATA

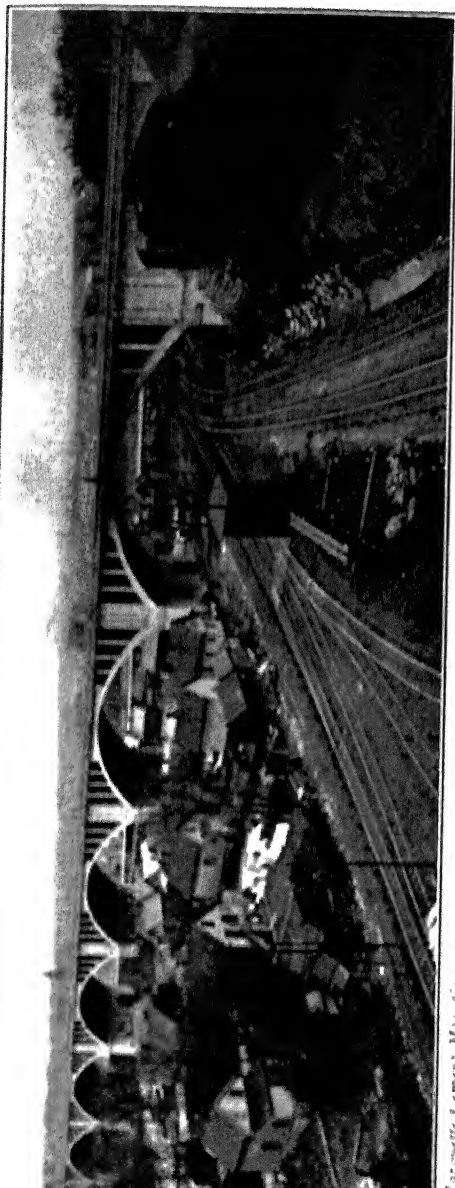
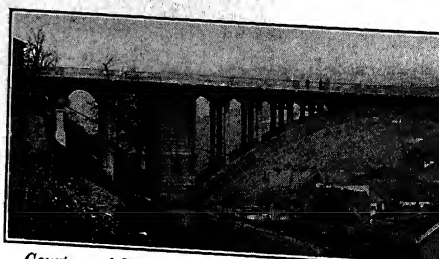


Fig. 90.—Grand Avenue viaduct, Milwaukee, Wis.





*Courtesy of Mr. N. S. Sprague, Superintendent, Boston.*  
FIG. 10B.—Murray Avenue bridge.



*Courtesy of Mr. N. S. Sprague, Superintendent, Boston.*  
FIG. 10C.—Meadow Street bridge.



## GENERAL DATA

be selected and the span lengths should decrease each way from the center of bridge.

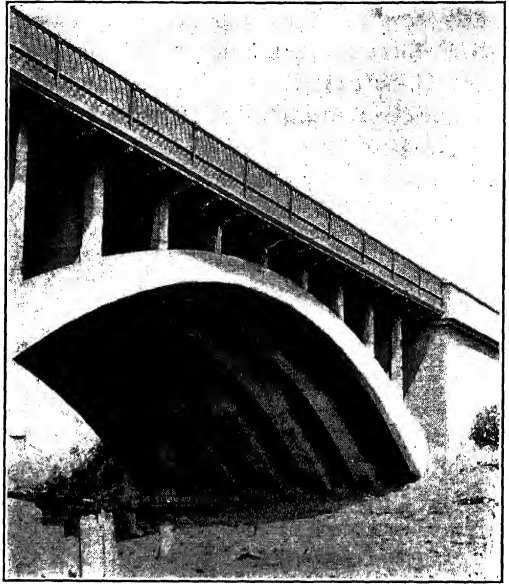
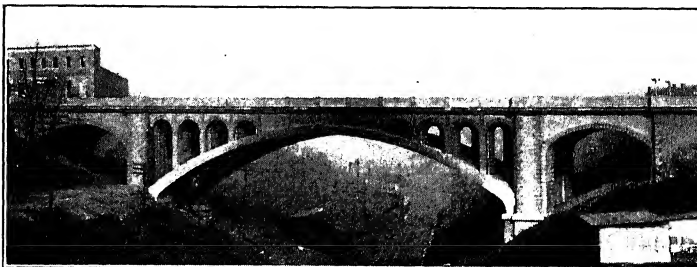


FIG. 10E.—Wealthy Street bridge, Grand Rapids, Mich. Note the space between arch ribs at extrados.

The depth of arch foundations and the shape of abutment piers is dependent upon local conditions, and in some d



*Courtesy of Mr. N. S. Sprague, Superintendent, Board of Public Works, Pittsburgh.*  
FIG. 10F.—Atherton Avenue bridge over P. J. R. R., Pittsburgh. Note fake joints in ribs, posts, and quoins.

and that it is well distributed. Great care should be taken in all cases by the use of hollow, or ribbed, concrete.

**6. Depth of Filling at Crown.**—In the design of an earth-filled arch bridge, it is necessary to determine approximately the required crown thickness of the arch and the amount of earth filling over the crown. In general, in order to determine the remaining distance from the arch springing line—that is, the available height above the highway bridges, a depth of filling in excess of from 1 to 2 ft. will be sufficient; but in some cases a minimum depth of from 2 to 3 ft. be required, in order to form a cushion for the ties, and to absorb the shock from passing traffic.

**7. Loads.**—The dead weight of the earth and any superimposed material, constitute uniformly distributed loads on an arch ring. With open-spandrel concrete arches, the loads act vertically upon the arch ring or upon the abutment or pier walls or columns, and are hence not directly on the filled spandrels, the pressure produced by the earth filling is really inclined and the resultant is not accurately determined.

On flat earth-filled arches, it is better to assume the loads as acting on the arch ring, for the horizontal forces are small and may be neglected. In arches with large rise, the horizontal thrusts are considerable close to the springing lines, and it may be necessary to take these horizontal components into account. In the case of these horizontal thrusts, however, a factor of safety should be used.

A common assumption for weight of earth is that its value is unknown is 100 lb. per cubic foot. In the design its weight should be taken at 120 lb. per cubic foot, assumed as 12 in. thick and as weighing 120 lb. per cubic foot.

The live load to be used in the investigation should be the greatest that comes over the bridge roadway. Each location should be investigated and chosen to fit the requirements. For the design of the roadway and loading is necessary to be determined.

## GENERAL DATA

area of arch ring, uniform live loads are used in the arch design. City highway bridges are generally designed for 5 electric cars and for such bridges, with spans of 200 ft. or more, a uniform load of 1200 lb. per linear foot is usually taken on the railway track together with a uniform load of 80 lb. per square foot over the remaining area of roadway and sidewalks. For spans less than 100 ft., the values corresponding are 1800 lb. per linear foot of each track, and 100 lb. per square foot of remaining area. For spans between 100 and 200 ft., the loads are taken proportionally. The loads specified above for city bridges may be reduced by about 20 per cent to apply to the arch rings of country bridges. The load on each street railway track is generally assumed to cover a width of 9 ft.

In addition to the above loads, city bridges and bridge thoroughfares likely to be used for heavy hauling should be designed to carry 20-ton trucks, with axles about 10 ft. c. to c., 14 tons on rear axle and 6 tons on front axle; wheels about 5 ft. c. to c.

Because of the permanent character of concrete bridges it may be wise to provide a larger margin for increase of loading than the above suggested, or than is usually allowed in steel bridge design. Fortunately, in the case of concrete arch bridges a large increase can be provided for with only a slight increase of expense due, of course, to the controlling influence of the dead load.

Following is an extract from the report of a Committee on Reinforced Concrete Highway Bridges and Culverts, American Concrete Institute, presented at the Annual Convention, Chicago, Feb. 17, 1914:

"Class 'A' Bridges—main thoroughfares leading from large towns. In view of the extensive introduction of the heavy motor trucks and traction engines, and the probable general use of such vehicles in the future, it is recommended that bridges on main thoroughfares and other roads which are likely to be used for heavy hauling, be designed to carry 20-ton trucks, with axles about 10 ft. c. to c., 14 tons on rear axle and 6 tons on fore axle; wheels about 5 ft. c. to c. Outside of large cities it is recommended that only one such vehicle be assumed to be on the bridge at any one time; the likelihood of more than one



impose a load of more than 100 lb. per square foot over a considerable area. The above-mentioned 20-ton truck gives a load of about 140 lb. per square foot, on the area actually occupied, but it is considered extravagant to assume that a large bridge is covered with such heavy loads. One hundred pounds per square foot is thought ample to assume for the loading of spans more than 60 ft. long in designing the trusses or main girders. It is thought to be safe to reduce this assumed load in the case of longer spans, to the following amounts:

Length of span, ft.	Assumed load, lb. per sq. ft.
80.....	90
100.....	80
125.....	75
200 and over.....	70

with all intermediate spans in proportion.

"The greatest load that is liable to be imposed on a bridge sidewalk occurs when there is some excitement in the neighborhood which attracts a large crowd, and for which the bridge affords an especially good point of view. In that case the crowd forms a compact mass against the railing, not more than 4 ft. deep, making a load seldom exceeding 100 lb. per square foot over a very considerable space. The remaining portion of the sidewalk may be covered by a moving crowd which can scarcely weigh more than 40 lb. per square foot. It may be advisable, sometimes, to so design sidewalk slabs, that if a street car or motor truck accidentally gets upon the sidewalk, it will not go through. Such accidents are so rare, that it is thought safe to allow materials to be stressed somewhat beyond the elastic limit in such cases.

"Class 'B' Bridges.—Although it is impossible to determine beforehand, especially in the newer parts of the country, whether any given road is to be used for heavy traffic, it seems extravagant, at least in the cases of larger spans, to design bridges to carry much heavier loads than can be expected to come upon them. It is recommended that bridges of this class be designed to carry 15-ton trucks, with axles 10 ft. apart, 5 tons on the front and 10 tons on the rear axle. This will allow for considerable overloading of existing motor trucks. It is further recommended that only one truck be assumed to be on the bridge at one time, in designing the floor system, that it be assumed to cover a width of 8 ft. and a length of 35 ft. and that the remainder of the bridge be covered with a load of about 90 lb. per square foot, for spans up to 60 ft.

"For longer spans, the trusses and main girders should be designed for the following loads:

Length of span, ft.	Assumed load, lb. per sq. ft.
80.....	80
100.....	70
125.....	65
150.....	60
200 and over.....	55

with intermediate spans in proportion.

"Sidewalks should be designed to carry the same loads as in the case of Class 'A' bridges.

"Special Bridges.—City bridges and bridges carrying traffic connected with mines, quarries, lumber regions, mills, manufactories, etc., require special consideration and should, of course, be designed to carry any load which can reasonably be expected to pass over them, bearing in mind the likelihood of heavy traction engines and motor trucks coming into extensive use in the not distant future.

"Bridges Carrying Electric Cars.—Electric traction is still in its infancy and nobody is able to forecast its future development. It seems probable, however, that it will not be profitable to run cars weighing more than 50 tons each, at a speed that would be permitted on any public road. If very high speeds are desired, the traction company will doubtless be required to operate over its own right-of-way. It is recommended that bridges carrying either urban or interurban electric cars be designed to carry 50-ton cars on two trucks, spaced 30 ft. c. to c., each truck having two axles spaced 7 ft. c. to c. The Committee sees no reason for changing the customary practice of assuming that an axle load is distributed over three ties."

For railroad bridges, Cooper's Standard Loadings are generally specified, the particular loading to be used depending upon the location of the line and the future traffic that may be expected. As regards the arch, in each of the arches, where the thickness of filling is sufficient to resist the concentrated loads over a considerable area, a uniform loading per linear foot perpendicular to the span is specified. A load of 700 lb. per square foot is specified for traffic on spans, say, over 80 ft. in length. A load of 1,000 lb. per square foot is frequently adopted for the impact of live loads. This is not usual for the floors in all arches of the bridge. Braking or tractive stresses are not considered in heavy grades.

A concentrated load is to be distributed downward through the bridge, starting from the ends of

the ties. An axle load is assumed as distributed over three ties in the direction of the track.

**8. Empirical Rules for Thickness of Arch Ring.**—With the trial curvature of the intrados decided upon, the next step in the design of a concrete arch is to choose a trial thickness of the ring at the crown and at the springing. Since the crown thickness depends not only on the thrust, but also upon the location of the line of pressure, it is obvious that it is impossible to devise a formula for its determination. Various empirical formulas, however, have been developed for this trial thickness at the crown and are an aid to the judgment.

Mr. F. F. Weld<sup>1</sup> gives the following formula:

$$h = \sqrt{l} + \frac{l}{10} + \frac{w}{200} + \frac{w'}{400}$$

where

$h$  = crown thickness in inches.

$l$  = clear span in feet.

$w$  = live load in pounds per square foot, uniformly distributed.

$w'$  = weight of dead load above the crown of the arch in pounds per square foot.

Mr. W. J. Douglas gives the following tabulated formulas<sup>2</sup> for different highway spans, the values of  $h$  being given in feet:

Under 20 ft.  $h = 0.03 (6 + l)^*$

20 to 50 ft.  $h = 0.015 (30 + l)^*$

50 to 150 ft.  $h = 0.00010 (11,000 + l^2)^{\dagger}$

Over 150 ft.  $h = 0.016 (75 + l)^{\ddagger}$

\* For railroad arches, add 25 per cent.

† For railroad arches, add 20 per cent.

‡ For railroad arches, add 15 per cent.

Mr. D. B. Luten gives the following formula for solid-spandrel arches:

$$h = 4 + \frac{3l^2(r + 3F)}{4000r - l^2} + \left[ \frac{(w)l^2}{30,000r} \text{ or } \frac{w_c(l + 5r)}{150r} \right]$$

where  $h$  = crown thickness in inches.

$l$  = clear span in feet.

$r$  = the rise from springing line to intrados in feet.

<sup>1</sup> Engineering Record, Nov. 4, 1905, page 529.

<sup>2</sup> Taken by permission from the American Civil Engineers' Pocket Book.

$F$  = the fill over the crown of the extrados in feet.

$w$  = uniform live loads in pounds per square foot.

$w_c$  = concentrated loading consisting of maximum live loading on single track over half-span in tons.

The thickness of an arch should increase from the crown to the springing (except for a hinged arch which is not considered here). The radial thickness of the ring at any section is frequently made equal to the thickness at the crown multiplied by the secant of the angle which the radial section makes with the vertical. For segmental and three-centered curves the radial thickness at the springing ( $a-a$ , Fig. 11) should be taken from two to three times the crown thickness.

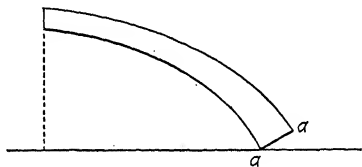


FIG. 11.

The empirical rules given above, it must be remembered, should be used only for trial. The exact shape of the arch ring and the thickness at different sections must be determined by analysis as subsequently explained.

**9. Classification of Arch Rings.**—Arches may be classified as hinged or hingeless. A hingeless arch is one having fixed ends, while a hinged arch may have a hinge at the crown, a hinge at each end, or a hinge at each end and one at the crown. Arches of one and two hinges are not used to any extent in masonry construction since the three-hinged arch offers the advantage of more definitely fixing the line of pressure throughout the ring and thus makes possible a saving of material. Hinges are, however, often an expensive detail and the three-hinged arch is by no means so common as the concrete arch having fixed ends. Friction on hinges is also an important consideration.

Concrete arches without hinges will be treated in the chapters immediately following and later on will be considered the modifications necessary for three-hinged arches.

## CHAPTER II

### DEFLECTION OF CURVED BEAMS

Deflection formulas for curved beams (in which the radius of curvature is large as compared with the depth) are employed in the development of arch theory. Hence, it is important for the student to appreciate the meaning of these deflection formulas before taking up the theory of arches, and this appreciation of the formulas can come only by following through their derivation. A proof for these formulas will now be attempted.

Let  $AB$ , Fig. 12, be any portion of a curved beam in its *unstrained* form and  $A'B$  the same portion in its *strained* form, assuming the beam rigidly fixed at  $B$ . Let  $X - X$  and  $Y - Y$  be rectangular axes with origin at  $A$ , and denote the components of  $A'$  as  $\Delta x$  and  $\Delta y$ .  $AO$ , tangent to the arch axis at  $A$ , moves through the angle  $k$ . It is desired to derive formulas for the following values: (1) angular change of  $AO$ , (2) component  $\Delta x$  of  $A'$ , (3) component  $\Delta y$  of  $A'$ . Only the effects of dead and live loading will be treated in this chapter leaving the effects of temperature change and direct stress for consideration in the chapter on Arch Analysis.

**10. Angular Change.**—Consider  $abcd$  as any small portion of the beam included between two consecutive cross-sections at right angles to the axis. Assume the radius of curvature of the beam as large in proportion to the depth so that the length of all fibers may be assumed equal. Now assume the end  $ad$  as fixed, and let the change in angle between end faces or end tangents of this element (of length  $s$ ) due to bending be denoted by  $k'$ . (See Figs. 12 and 13.) The change in length of a fiber at a distance  $r$  from the neutral axis will be equal to  $rk'$  (the angle  $k'$  being expressed in circular measure) and the deformation per unit length of beam will be equal to  $\frac{rk'}{s}$ . Now,  $E = \frac{\text{unit stress}}{\text{unit deformation}}$  (by definition of modulus of elasticity), or, stress per unit area at distance  $r$  from the neutral axis  $= (E) \times (\text{deformation}) = E \cdot \frac{rk'}{s}$ .

Let  $a$  (Fig. 14) be the area of a small element of the cross-section at a distance  $r$  from the neutral axis. Then the stress on this area equals  $E \cdot \frac{rk'}{s} \cdot a$ , and the moment of this stress about the neutral axis equals  $E \cdot ar^2 \cdot \frac{k'}{s}$ . The total moment of resistance of the cross-section is the sum of all the moments of resistance for

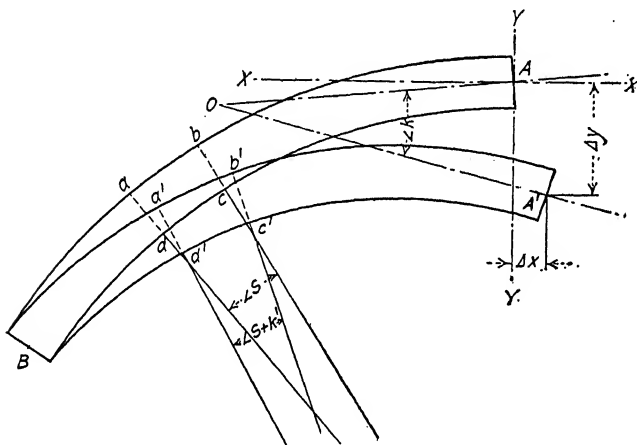


FIG. 12.

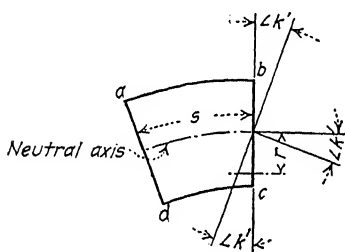


FIG. 13.

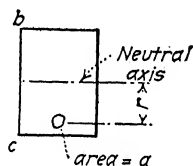


FIG. 14.

the separate elements, which resolves itself into finding the sum of the expressions ( $ar^2$ ).

The term *moment of inertia*,  $I$ , may be defined as follows: The moment of inertia of a plane surface with respect to an axis is the sum of the products obtained by multiplying each elementary area by the square of its distance from that axis. If  $\Sigma$  is taken to mean *the sum of*, then it is evident that  $\Sigma ar^2$  between the limits of the section represents the moment of inertia of the section.

Hence,

$$M = EI \frac{k'}{s}, \text{ or } k' = \frac{Ms}{EI}$$

(This expression might have been obtained more directly by employing the formula derived from the common theory of flexure.) But an expression for the angle  $k$  is desired, and this must be obtained by a summation of all the angles  $k'$  for the elements of the curved beam from  $A$  to  $B$ . Denote this summation by  $\sum_A^B k'$ , then

$$k = \sum_A^B \frac{Ms}{EI}$$

In deriving the foregoing equation, a material with constant  $E$  has been assumed. For beam of reinforced concrete

$$\begin{aligned} M &= E_c I_c \frac{k'}{s} + E_s I_s \frac{k'}{s} \\ &= (E_c I_c + n E_c I_s) \frac{k'}{s} \\ &= E_c (I_c + n I_s) \frac{k'}{s} \\ &= E_c I \frac{k'}{s} \end{aligned}$$

or

$$k' = \frac{Ms}{E_c I} \quad (a)$$

and

$$k = \sum_A^B \frac{Ms}{E_c I} \quad (1)$$

The smaller the elementary lengths of beam considered, the more accurately will Formula (1) apply. The values of  $M$  and  $I$  have been regarded as constant quantities for each particular elementary length considered. Since this is not true in practice on account of each element having appreciable length, a close approximation to the actual  $M$  and  $I$  for a given element may be obtained by taking the values of the bending moment and moment of inertia at the mid-point of  $s$ .

**11. Components of Deflection.**—Consider  $BCDEFA$ , Fig. 15A, to represent the axis of the unstrained form of the beam of Fig. 12 and let the beam pass into its strained form by the bending of each elementary length  $s$  in consecutive order. Bending the

element  $BC$  through the angle  $k'$  causes the portion  $AC$  to turn through this same angle about  $C$  as a center, the point  $A$  moving to  $A_c$  (with radius  $u$ ) through a small distance that we will call  $dv$ , having the components  $dx$  and  $dy$ . Fig. 15B shows clearly the method of bending. Bending the element  $BC$  through the angle  $k'$ , if  $AC$  is kept stationary, would cause  $B$  to move to the point  $B'$ . Now revolving the bent beam about  $C$  as a pivot until  $B'$  is brought back to  $B$ , it should be noticed that  $A$  moves

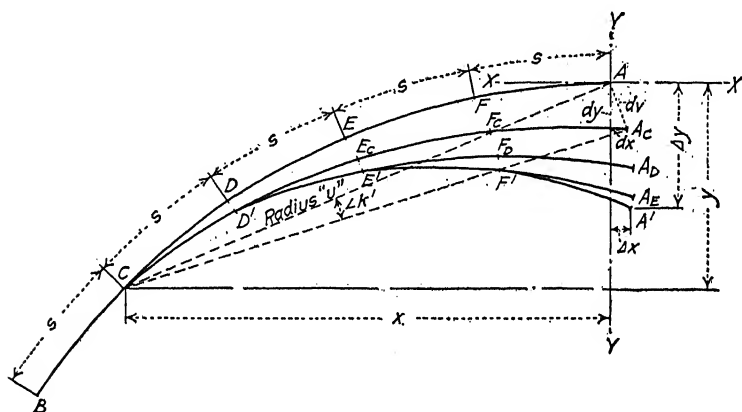


FIG. 15A.

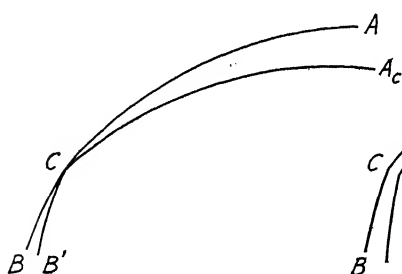


FIG. 15B.

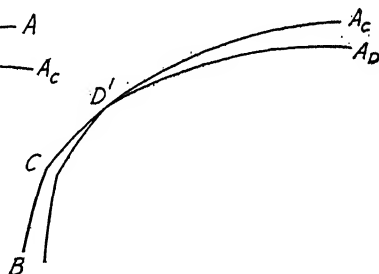


FIG. 15C.

to  $A_c$ . Fig. 15C shows the bending of the element  $CD$ . Thus from the bending of  $CD'$  the point  $A_c$  moves to  $A_D$ , etc.

If  $x$  and  $y$  are the coördinates of any point  $C$ , origin at  $A$ , we have, by similar triangles (triangles are similar since the side  $dv$  is practically at right angles to the radius  $u$ , the movement being very small)

$$\frac{dy}{dv} = \frac{x}{u}, \text{ and } \frac{dx}{dv} = \frac{y}{u}$$



Solving for  $dy$  and  $dx$  and substituting for  $dv$  the value  $uk'$ , we have

$$dy = xk' \quad dx = yk'$$

Substituting the value of  $k'$  from Equation (a), we have

$$dy = x \frac{Ms}{E_c I}, \text{ and } dx = y \frac{Ms}{E_c I}$$

Summing up the value of the components for each change of  $k'$  in angle, the total change of angle made is  $k$ , and  $dy$  and  $dx$  become  $\Delta y$  and  $\Delta x$ , respectively. Then

$$\Delta y = - \sum_A^B \frac{Mxs}{E_c I} \quad (2)$$

and

$$\Delta x = \sum_A^B \frac{Mys}{E_c I} \quad (3)$$

(As in simple beams,  $M$  is considered positive when it tends to increase the compression on the back of the arch. The minus sign is used in Formula (2) because the effect of a positive value of  $M$  in any element causes an upward deflection—that is, a minus value of  $\Delta y$ , considering only the effect of bending in the element in question.)

Formulas (1), (2), and (3) are the fundamental formulas employed in the analysis of masonry arch rings by the elastic theory.

## CHAPTER III

### ANALYSIS OF THE SYMMETRICAL ARCH BY THE ELASTIC THEORY<sup>1</sup>

**12. General Discussion.**—A concrete arch with fixed ends is statically indeterminate. There are, in all, six unknown quantities—three at each support (the vertical and horizontal components of the reaction, and the bending moment; or, what is the same thing, the magnitude, direction, and point of application of the reaction)—and it is possible to determine only three unknowns by the principles of statics. The three additional equations may be found from the following conditions:

The change in span of the arch  $= \Delta x = 0$

The vertical displacement at one end relative  
to the other end  $= \Delta y = 0$

The angle between the tangents to the arch  
axis at the two ends of the arch remain un-  
changed, or  $\angle k = 0$

These three conditions must be true since the arch is fixed at the abutments.

Instead of actually finding the components of the reactions and the moments at the supports as outlined above, it is simpler for symmetrical arches to take the origin of coördinates at the crown and find the thrust, shear, and moment at that point. The method of doing this will be explained later, but it should be clear that, with these three unknowns determined, each half of arch may then be treated as statically determinate.

The analysis of an arch consists in finding the thrust, shear, and bending moment at the crown and at intermediate sections in the arch ring or arch rib, and then finding the stresses resulting therefrom. A longitudinal slice of the arch is considered, having a thickness of 1 ft. The thrust is here taken to be the normal component of the resultant force on the section, and the shear is the component at right angles to the normal. The

<sup>1</sup> Method of analysis is taken by permission from Turneure and Maurer's "Principles of Reinforced-concrete Construction," 2d edition, pages 335 to 344. Copyright 1907, 1909 by F. E. Turneure and E. R. Maurer.

bending moment will be considered positive when it tends to increase the compression on the back of the arch, this being the same convention as for beams.

A horizontal thrust is produced at the crown when the arch is loaded symmetrically. For non-symmetrical loading, an inclined pressure acts at the crown, but its horizontal component is called the horizontal thrust for that loading. Its vertical component is the shear at the crown. Let us assume the arch as cut at the crown and consider each half to act as a cantilever sustaining exactly the same forces as exist in the arch itself. The external forces holding a semi-arch in equilibrium (Fig. 16)

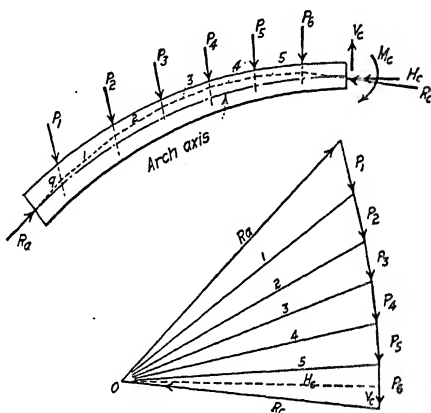


FIG. 16.

are the loads  $P_1, P_2$ , etc.; the horizontal thrust  $H_c$ , the vertical shear  $V_c$ , and the reaction at the skewback  $R_a$ .

After  $H_c$ ,  $V_c$ , and  $M_c$  have been computed, the line of pressure (accurately enough represented by the equilibrium polygon) can be constructed by help of the force polygon, Fig. 16. The value of  $M_c$  definitely determines the point of application of  $H_c$  and makes the construction of the exact line of pressure possible. (For a positive value of  $M_c$ , the thrust  $H_c$  acts above the arch axis.) From this line of pressure and the accompanying force polygon may be obtained the thrusts, shears, and bending moments at intermediate points of the arch. The force polygon gives directly the thrusts and shears, while the line of pressure makes possible the determination of the bending moment at any section, the bending moment being equal to the resultant

pressure at the given point multiplied by the perpendicular distance from the arch axis to the line of pressure. Usually the line of pressure is drawn to serve only as a check on the computations, and the bending moments at the various points are determined algebraically. This algebraic method for finding moment will be employed in the designing work to follow.

The line of pressure of an arch is a continuous curve, but differs very little from an equilibrium polygon for the given loads (Fig. 16). In fact this curve becomes tangent to the equilibrium polygon between the angle points. The greater the number of loads, the nearer the polygon approaches the line of pressure.

With  $H_c$ ,  $V_c$ , and  $M_c$  determined, all external forces are known except the reaction at the skewback, and this is determined by the closing line of the force polygon. An equilibrium polygon may then be constructed as already mentioned, the first side being in the line of  $R_c$  produced, the second parallel to the ray 5, and so on until the last side through  $q$  gives the position of  $R_a$ .

**13. Notation.**—The following notation will be employed in arch analysis:

Let

- $s$  = length of a division of the arch ring measured along the arch axis.
- $n_h$  = number of divisions in one-half the arch.
- $l$  = span of arch axis.
- $c_a$  = average unit compression in concrete of arch ring due to thrust.
- $t_c$  = coefficient of linear temperature expansion.
- $t_D$  = number of degrees rise or fall in temperature.
- $E_c$  = modulus of elasticity of concrete.

At the crown, let

- $H_c$  = horizontal thrust.
- $V_c$  = vertical shear.
- $R_c$  = resultant of  $H_c$  and  $V_c$ .
- $M_c$  = bending moment.

At any point on the arch axis, with coördinates  $x$  and  $y$  referred to the crown as origin, let

- $N$  = thrust (normal) on radial section.
- $S$  = shear on radial section.
- $R$  = resultant force on radial section, resultant of  $N$  and  $S$ .

- $x_o$  = eccentricity of thrust on section, or distance of  $N$  from the arch axis.  
 $t$  = depth of section.  
 $I$  = moment of inertia of section including steel =  $I_c + nI_s$ .  
 $A$  = area of section including steel =  $a_c + na_s$ .  
 $p_o$  = steel ratio for total steel at section.  
 $d'$  = embedment of steel from either upper or lower surface.  
 $M$  = moment =  $Nx_o$ .  
 $m_L$  = moment at any point on left half of arch axis of all external loads ( $P_1, P_2$ , etc.) between the point and the crown.  
 $m_R$  = moment at any point on right half of arch axis of all external loads between the point and the crown.  
 $m$  = moment at any point on either half of arch axis of all external loads ( $P_1, P_2$ , etc.) between the point and the crown.

**14. Formulas for Thrust, Shear, and Moment.**<sup>1</sup>—Let Fig. 17 represent a symmetrical arch loaded in any manner and cut at

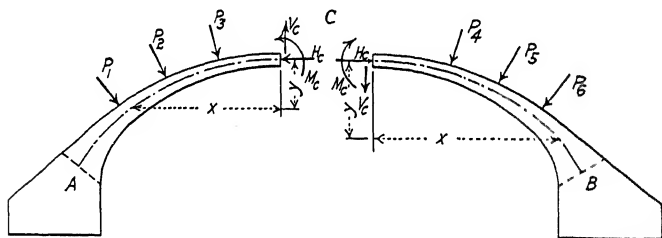


FIG. 17.

the crown, the halves being separated in order to show the forces acting at the section cut.

Formulas for thrust, shear, and moment at the crown will first be developed and then will follow a formula for moment at any section. Thrust and shear at any section may easily be determined graphically.

The horizontal motion of  $C$  as regards the left cantilever, due to bending of the elements between  $A$  and  $C$ , is the same in

<sup>1</sup> Taken by permission from Turneaure and Maurer's "Principles of Reinforced-concrete Construction," 2d edition, pages 338, 339, 343, and 344. Copyright 1907, 1909 by F. E. Turneaure and E. R. Maurer.

amount as the horizontal motion of  $C$  as regards the right cantilever, due to bending of the elements between  $B$  and  $C$ . It should be noticed that a positive bending moment for an element on the left will tend to move  $C$  in the opposite direction from a positive bending moment for an element on the right. Then, from Chapter II on "Deflection of Curved Beams," we have

$$\sum_C^A My \frac{s}{E_c I} = - \sum_C^B My \frac{s}{E_c I}$$

(The coördinates  $x$  and  $y$  refer to the center of each short length of arch ring of length  $s$ , when  $M$  is also taken at the center.) The vertical motions are equal but in the same direction, hence

$$\sum_C^A Mx \frac{s}{E_c I} = \sum_C^B Mx \frac{s}{E_c I}$$

Also the changes in direction of the tangent to the axis at  $C$  are equal but opposite in direction, hence

$$\sum_C^A M \frac{s}{E_c I} = - \sum_C^B M \frac{s}{E_c I}$$

The arch ring will be so divided into sections that  $\frac{s}{I}$  will be made a constant. Then  $E_c$  also being a constant, the quantity  $\frac{s}{E_c I}$  may be placed outside the summation sign. Thus, denoting  $\sum_C^A M$  by  $\sum M_L$  and  $\sum_C^B M$  by  $\sum M_R$ , we have

$$\sum M_L y = - \sum M_R y \quad (b)$$

$$\sum M_L x = \sum M_R x \quad (c)$$

$$\sum M_L = - \sum M_R \quad (d)$$

The bending moment at any point may be expressed as follows:

$$M_L = M_c + H_c y + V_c x - m_L$$

$$M_R = M_c + H_c y - V_c x - m_R$$

where  $M_L$  and  $M_R$  are the moments at the center of any division to the left and right of the crown respectively. Substituting these equations in (b), (c), and (d), combining terms, and noting that  $\sum M_c$  for one-half the arch is equal to  $n_h M_c$ , we have

$$2M_c \sum y + 2H_c \sum y^2 - \sum m_L y - \sum m_R y = 0 \quad (e)$$

$$2V_c \sum x^2 - \sum m_L x + \sum m_R x = 0 \quad (f)$$

$$2n_h M_c + 2H_c \sum y - \sum m_L - \sum m_R = 0 \quad (g)$$

Combining (e) and (g)

$$H_c = \frac{n_h \Sigma(m_L + m_R)y - \Sigma(m_L + m_R) \Sigma y}{2[n_h \Sigma y^2 - (\Sigma y)^2]} \quad (4)$$

From (f)

$$V_c = \frac{\Sigma(m_L - m_R)x}{2 \Sigma x^2} \quad (5)$$

From (g)

$$M_c = \frac{\Sigma(m_L + m_R) - 2H_c \Sigma y}{2n_h} \quad (6)$$

These are the fundamental equations in the analysis of arch rings. All summations refer to one-half the arch axis, and the signs of  $m_L$ ,  $m_R$ ,  $x$ , and  $y$  being taken into account in the derivation of the formulas, their numerical values should be taken as positive when substituting to obtain the corresponding values of  $H_c$ ,  $V_c$ , and  $M_c$ . A positive value of  $V_c$  indicates that the line of pressure at the crown slopes upward toward the left; a negative value, downward toward the left.

The values of the thrust, shear, and moment being found from the above equations, the moment of any section of the left cantilever is

$$M = M_c + H_c y + V_c x - m_L \quad (7)$$

and, at any section of the right cantilever,

$$M = M_c + H_c y - V_c x - m_R \quad (8)$$

To the thrusts, shears, and moments in an arch due to loads must be algebraically added the thrusts, shears, and moments due to a change of temperature. For a rise (or fall) of temperature of the arch ring of  $t_D$  degrees, the span of arch axis  $l$  would *tend* to increase (or decrease) in length an amount expressed by  $t_c t_D l$ ,  $t_c$  being the coefficient of linear expansion. The arch being restrained at the abutments, thrust, shear, and moment would be caused at the different sections of the arch ring.

The method of procedure for determining formulas for  $H_c$  and  $M_c$  due to temperature is similar to that employed in determining the corresponding formulas due to loads. The value  $\Delta x$  of Formula (3) is equal to the amount of the tendency of the half-span to change in length, or  $\frac{t_c t_D l}{2}$ ; and  $k$  of Formula (1) is

zero since the crown section rises and falls in a vertical line as the material of the arch expands and contracts. Thus, we have, considering either half of the arch,

$$\Sigma My \frac{s}{E_c I} - \frac{t_c t_D l}{2} = 0$$

$$\Sigma M \frac{s}{E_c I} = 0$$

Since there are no external loads to be considered in the matter of temperature and since the arch is symmetrical,  $V_c = 0$ , and

$$M = M_c + H_c y$$

Substituting this value of  $M$  in the above equations and remembering that  $\frac{s}{E_c I}$  is to be made a constant, we have

$$M_c \Sigma y + H_c \Sigma y^2 = \frac{t_c t_D l}{2} \cdot \frac{E_c I}{s}$$

$$n_h M_c + H_c \Sigma y = 0$$

From which

$$H_c = \frac{I}{s} \cdot \frac{t_c t_D l n_h E_c}{2[n_h \Sigma y^2 - (\Sigma y)^2]} \quad (9)$$

and

$$M_c = - \frac{H_c \Sigma y}{n_h} \quad (10)$$

The bending moment at any point is

$$M = M_c + H_c y \quad (11)$$

In Formula (9) the value  $t_D$  should be inserted as positive for a rise in temperature and negative for a drop in temperature. The value of  $t_c$  may be taken at 0.000006 per degree Fahrenheit (see Art. 13, Volume I) and the value of  $E_c$  at 2,000,000 lb. per square inch. Moments are usually expressed in foot-pounds and the distance  $y$  in feet, in which case the value of  $E_c$  should be substituted in Formula (9) in pounds per square foot and the value of  $l$  in feet. Since there are no outer loads to consider, the thrust and shear at any point in the arch may be found by resolving  $H_c$  normal and parallel to the arch section at that point.

It should be noted in Formula (9) that, for a given span, the horizontal thrust due to temperature varies inversely as  $[n_h \Sigma y^2 - (\Sigma y)^2]$ , which means that a slight decrease in rise of the arch will produce considerable increase in ring stress.



If the span and rise are kept constant,  $H_c$  and likewise  $M_c$  vary directly with  $I$ , or, in other words, with the cube of the depth of section. On the other hand, fiber stresses for a given moment are known to vary inversely only as the square of the depth of section. Thus in light highway bridges, where temperature moment constitutes a large proportion of the total moment, the resulting fiber stresses may actually be increased by an increase of section.

The thrust acting throughout the arch tends to cause a shortening of the span. Denote  $c_a$  as the average unit compression in concrete of arch ring due to thrust. Then the arch span will tend to shorten the amount  $\frac{c_a l}{E_c}$ . This action tends to produce the same result as a lowering of temperature and the value of the resulting crown thrust may be found by substituting  $\frac{c_a l}{E_c}$  for  $t \alpha_D l$  of Formula (9). Hence,

$$H_c = -\frac{I}{s} \cdot \frac{c_a l n_h}{2 [n_h \Sigma y^2 - (\Sigma y)^2]} \quad (12)$$

and, as for temperature stresses,

$$M_c = -\frac{H_c \Sigma y}{n_h} \quad (13)$$

$$M = M_c + H_c y \quad (14)$$

Thrusts and moments due to rib shortening are usually small except in flat arches, where they may become fairly large.

**15. Division of Arch Ring for Constant  $\frac{s}{I}$ .**—Since the depth of the arch ring generally increases from the crown to the springing, the moment of inertia  $I$  likewise increases, but much more rapidly; in fact, it increases approximately as the cube of the depth. To maintain a constant  $\frac{s}{I}$ , the divisions should be made to increase in length as the arch ring deepens, and some preliminary computations are necessary to do this.

The greater the number of divisions selected, the more accurate the results; but for an arch of ordinary span, the number need not be greater than twenty—sixteen or twenty being the common

rule. Of course, since each half of arch is considered separately, the number of divisions should be even.

To obtain the value of  $\frac{s}{I}$  (the constant), determine first the length of the arch axis. Next, calculate several values of  $\frac{1}{I}$  at equal intervals along the arch and determine its mean value. Then

$$\frac{s}{I} = \frac{l'}{n_h} \cdot \frac{1}{\bar{I}}$$

where  $l'$  is one-half the length of arch axis,  $n_h$  the desired number of divisions in one-half the arch, and  $\frac{1}{\bar{I}}$  the mean value found as previously explained. In determining this value the steel should be considered.

After once the value of  $\frac{s}{I}$  is known, the lengths of the divisions can be readily determined. Assume a length of the first division to one side of the abutment. Determine the value of  $I$  at the center of the assumed division. Then divide the length assumed by the value of  $I$  determined for the center. If the length of the division was assumed correctly, the result should equal the value of  $\frac{s}{I}$  computed above. If not, the necessary adjustment should be made, and so on for each division until the crown is reached. The lengths of the assumed number of divisions should agree with the length of one-half of the arch axis. If an error exists which is not large, it should be divided proportionately among the divisions.

If desired, a graphical means may be employed by which to divide the arch axis into divisions having a constant  $\frac{s}{I}$ . The method to be given will be used in the arch design which follows.

Fig. 18 illustrates the method in detail.  $AB$  is drawn to any convenient scale equal in length to one-half the arch axis. The curve  $EF$  is then drawn through points whose ordinates are the values  $I$  and whose abscissas are the corresponding distances along the arch axis from the skewback. (In order to make the drawing clear, the ordinates and corresponding abscissas which

determine the curve  $EF$  are not shown.) A length  $AH$  is then assumed, a perpendicular  $LC$  erected at its center, and the lines  $AC$  and  $CH$  determined. Starting from point  $H$ , lines are drawn parallel alternately to  $AC$  and  $CH$ , as shown in Fig. 18. Only three or four trials will usually be required to divide the line  $AB$  into the desired number of divisions. The base of each triangle thus formed corresponds to  $s$  and its altitude to  $I$ . Since all the triangles are similar by construction, the term  $\frac{s}{I}$  is constant throughout.

A convenient modification of the above method is to draw a second curve  $E'F'$  below  $AB$ , using the same ordinates as for  $EF$ .  $AH$  is then assumed as before and the perpendicular  $CC'$  erected at its center. Starting with  $C'$ , diagonals and verticals are drawn alternately making the diagonals parallel to  $AC$ . This method

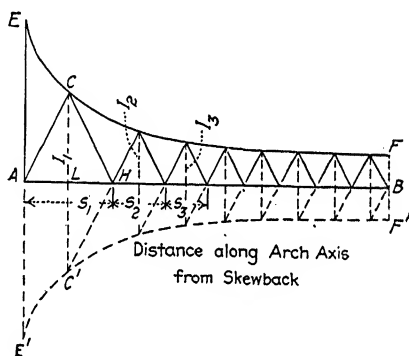


FIG. 18.

offers the advantage of drawing all the diagonals parallel to the same line.

**16. Loadings to Use in Computations.**—Small earth-filled arches should be designed at least for uniform live load over the whole span and the half-span. Large earth-filled arches and arches having the roadway supported on spandrel arches or spandrel columns should be designed for live load over one-third of the span, one-half of the span, two-thirds of the span, the whole span, the middle third of the span, and the end thirds of the span. These uniform loadings are only approximations to the true loadings which produce the maximum stresses. The exact loadings to cause maximum conditions may be found by the use of influence lines, as will be explained in Chapter V.

temperature range in concrete structures. Undoubtedly the most important are those which have recently been completed under the direction of the Engineering Experiment Station at Ames, Iowa, on two highway arch bridges of the earth-filled type. These experiments<sup>1</sup> are described in detail in Bulletin No. 30 of the Iowa State College of Agriculture and Mechanic Arts where a summary is also given of the other tests that have been made on internal temperature variation.

In the Iowa experiments, thermometers were embedded in different parts of the arch ring in such a manner that the thermometers were in direct contact with the concrete at the depth of penetration. Both mercurial soil and electrical resistance thermometers were employed.

The tests of the Squaw Creek arch at Ames extended over the greater part of the school years 1909 to 1912. The west arch of this bridge was the one tested, it being easy of access. The arch is unsymmetrical with a span of 45 ft. and a total rise of 11 ft. 3 in. at the center of span.

The tests on the Walnut Street bridge at Des Moines were made in 1911 and 1912—daily readings being taken covering a period of 1 year. This bridge is composed of six 68-ft. spans with a rise of 11 ft. 6 in. The east arch was selected upon which to make the experiments.

*Internal Range in Temperature.*—The results on the two bridges mentioned were obtained during years in which the extreme atmospheric temperatures, both high and low, were the greatest recorded for many years. With this in mind, the results show that about 75 per cent of the mean atmospheric variation would be effective temperature range in a mass of concrete of less than 5 or 6 ft. in thickness. The atmospheric mean variation at Des Moines was 102°F., 75 per cent of which is 76.5°F. This is only 2.7° less than the average obtained on the Walnut Street bridge during the period January to August, 1912, and but 2.6° less than the average obtained on the Squaw Creek bridge for the same year.

*Heat Generated in Setting.*—The results obtained in the Walnut Street arch tests show a rise to an average maximum temperature of 94.5°F. in an average time of 33 hours after pouring, while other

<sup>1</sup> By Messrs. C. S. Nichols and C. B. McCullough.

results quoted in the bulletin show maximum high temperatures in setting varying from 100° to 130°F. attained in time intervals of from 18 hours to 8 days after placing. All considered, the value of 100° may be taken as a safe average of the final temperature attained by concrete in setting in structures typical of the Walnut Street arch.

The following is quoted from the bulletin above mentioned:

*Temperature Variation.*—"The main point of interest in connection with the temperature rise, due to the setting action, is not so much in the amount of this maximum itself, as in the fact that apparently all the subsequent temperature change is a drop, the stress-producing variation thus becoming more nearly equal to the entire temperature range than to one-half of it. This seems to be the conclusion drawn by Mr. Merriman (from his experiments on the Boonton dam), who says: 'If the maximum temperature attained is 100°F., then the stress-producing range is the difference between 100°F. and the lowest temperature subsequently attained.'

"While at first thought the above conclusion would seem to apply also to concrete arch structures typical of the ones herein described, yet the following facts demand our consideration. The sheer drop in temperature during the first season might induce stresses in the steel of the arch ring exceeding the elastic limit, thus producing a permanent set in the steel. This would operate to raise the elastic limit of the material in the direction of the stress (tension) to about the point of greatest stress, and produce in the arch ring a permanent deformation. The temperature of zero stress would then be, not the initial temperature, but the temperature which originally produced an elongation or distortion in the steel equal to the permanent set. During the subsequent seasonal variations, the variation of temperature would be each way from this new mean. Thus the temperature variation would be reduced to a value more nearly equal to one-half of the temperature range than to the whole range. On the other hand, the elongation of the steel might be so localized at the point of greatest bending as to cause an unsightly crack in the concrete.

"In the Walnut Street arch a temperature drop of the entire range, 87.6°F. plus the entire dead load and rib shortening cause a stress in the steel less than the elastic limit of the material. As a result, there are as yet no cracks in the structure, although it

has passed through a season of maximum external temperature variation.

"In the Squaw Creek bridge at Ames, a temperature drop of  $80^{\circ}$  or even  $60^{\circ}$  will stress the steel at the spring-line above the elastic limit, with the result that at three of the four corners of the structure there are unsightly cracks at the exact point of computed maximum stress. If this cracking is due to a permanent set in the steel, the effective stress-producing variation is now probably each way from a mean corresponding to the amount of the set produced, and the stresses consequently much lower than during the first year.

"In the Locust Street bridge at Des Moines, the steel is also stressed above the elastic limit with a sheer temperature drop equal to the range, and in proof of the theory above advanced, there are cracks at the crown of both the shore spans at the points where a theoretical elongation in the steel corresponds to a temperature drop.

"In spandrel-filled arches it is doubtful if at the coldest period much of the dead load, aside from that of the concrete itself, comes upon the structure by reason of the arching action of the partially frozen fill. However the amount of the arching action is problematical. This might tend to reduce the mathematical stresses produced by the application of all forces.

*Effect of Atmospheric Temperature.*—"It will be noted that the range during the first seasonal variations, which include the high temperatures of setting, exceeded the subsequent seasonal range by about 10 per cent of the former. It is obvious that had the concrete been placed at any other than the extreme high temperature of summer, the heat of setting would have been dissipated to a greater extent, and the range would have been less. This is illustrated by a comparison of the setting temperatures attained in different latitudes. The experiments in the tropical Panama climate showed a rise exceeding those of this country by from  $10^{\circ}$  to  $30^{\circ}$ . Other conditions being equal, a temperature more nearly normal would seem to be better for the concreting of arch structures typical of the ones herein described.

*Lag.*—"The data on the *lag* seem to show that in structures of this type the minimum temperatures are attained in time intervals anywhere from less than 1 day to 4 days after the atmospheric minimum. This interval depends upon the posi-

tion of the portion of the structure considered, and is roughly proportional to the distance from the nearest exposed face."

*Agreement with Theory.*—Levels were taken over the arch rings of both bridges from time to time to determine the rise and fall of the arch ring with variations in temperature. It was found that when uninfluenced by other factors than atmospheric variation, the rise and fall agreed quite closely with theory.

*Conclusions as to Necessary Provision for Temperature Changes.*  
—The writers of the bulletin concluded from the foregoing results and considerations that "to render an arch structurally safe, provision should be made (in the latitude where the bridge tests were conducted) for stresses induced by a temperature variation of *at least* 40°F. each way from an assumed temperature of no stress. Particular circumstances may demand that a greater variation be used for drop in temperature to prevent the appearance of cracks. This will always remain largely a matter of judgment with the designing engineer."

**18. Shrinkage Stresses Due to Setting.**<sup>1</sup>—In arches constructed in longitudinal ribs, shrinkage in the concrete due to setting tends to deform the arch ring in a manner similar to that resulting from a temperature drop. A lowering of the temperature, however, causes contraction of both steel and concrete, while with shrinkage the concrete alone is contracted. As the concrete contracts, the steel is compressed until an equilibrium is established between the compression in the steel and the tension in the concrete which entirely restrains further shrinkage of the mass.

The contraction which results from shrinkage causes a downward deflection of the arch ring, which induces bending stresses. One side of the arch ring is thrown into tension and the other side into compression. On the one side the tension in the steel is offset by the compression due directly to shrinkage. On the other side the compressive effects in the steel are additive, tending to throw quite heavy compressive stresses in the reinforcement.

The primary effect of shrinkage and the bending effect due to the same cause must be considered in the concrete as well. The primary effect is tension, but the bending stresses which result must be taken into account and added algebraically to the direct shrinkage stresses.

<sup>1</sup> The greater portion of this article is taken almost verbatim from Bulletin No. 30 of the Iowa Engineering Experiment Station, by Messrs. C. S. NEALE.

In connection with the temperature range experiments on the Walnut Street bridge described in the preceding article, observations were made on a block of concrete 36 in. long, 10 in. wide, and 6 in. deep, cast at the same time as the arch ring on the east arch. The object of these measurements was to determine the change in dimensions of the concrete during the period of setting. The block was of a 1:2:4 mixture, cast wet, and unreinforced. The measurements, made at a constantly-maintained room temperature of 72° for 100 days, showed a shrinkage of 0.04 per cent. This is somewhat less than the results of Mr. A. T. Goldbeck (see *Concrete Age*, August, 1911), who arrived at a coefficient of shrinkage of about 0.0005.

It is possible theoretically to determine the stresses in steel and concrete due directly to shrinkage. If we let  $c$  denote the coefficient of contraction of the concrete, the contraction per unit length of the reinforced section may be expressed as follows:

$$c_r = c - \frac{f_c}{E_c} = \frac{f'_s}{E_s}$$

Now, for equilibrium,

$$f_c = pf'_s$$

From these equations we get

$$f_c = cE_c \frac{np}{1 + np}$$

$$f'_s = \frac{f_c}{p}$$

The contraction of the reinforced section may be found by the formula

$$c_r = \frac{f'_s}{E_s}, \text{ or } c_r = \frac{c}{1 + np}$$

which is, of course, somewhat less than that of an unreinforced section. It is this contraction which causes the downward deflection of the arch ring and causes bending stresses throughout. Formulas may be determined for thrust, shear, and moment due to this bending, in the same manner as described for temperature in Art. 13.

The following tables have been taken from Bulletin No. 30 of the Iowa Engineering Experiment Station. They give the shrinkage stresses in the Walnut Street arch based upon the



above theory. A value of 0.0004 was taken for  $c$  which gave an average value of  $c_r = 0.0003\frac{1}{2}$ .

### STRESSES AT CROWN

Condition of loading	Stress in steel		Stress in concrete	
	Maximum tension	Maximum compression	Maximum tension	Maximum compression
Dead load and shrinkage.....	7,400	6,400	None	513
Dead load only.....	-2,000	3,130	-136	213
Effect of shrinkage bending....	9,400	3,270	136	318
Primary effect of shrinkage....	-10,000	10,000	130	-130
Net maximum stress induced by shrinkage.....	None	13,270	130	188

— Indicates stress of opposite kind.

### STRESSES AT SPRINGING LINE

Condition of loading	Stress in steel		Stress in concrete	
	Maximum tension	Maximum compression	Maximum tension	Maximum compression
Dead load and shrinkage.....	4,200	2,950	None	218
Dead load only.....	None	1,500	None	110
Effect of shrinkage bending....	4,200	1,450	None	108
Primary effect of shrinkage....	-10,250	10,250	121	-121
Net maximum stresses induced by shrinkage.....	None	11,700	121	None

— Indicates stress of opposite kind.

From the tables the most serious results seem to be the high compressive stresses induced in the steel reinforcement. The ordinary compressive stresses in the steel of arch rings, however, due to dead and live load, temperature, and rib shortening are usually low and, unless these stresses approach the allowable value, the effect of shrinkage need not be considered. The Walnut Street arch has a high percentage of steel and the tables

seem to show that in arches lightly reinforced the compressive stresses in the concrete may need to be investigated.

The above discussion is instructive but should not be taken too seriously. For example, it is doubtful if such large initial stresses occur in concrete (restrained by reinforcing material only) as is represented by a value of  $c_r = 0.0003\frac{1}{2}$ . Considère in his experiments observed a contraction in 1:3 mortar reinforced with  $5\frac{1}{2}$  per cent of steel to be only 0.01 per cent, or one-fifth the amount his tests showed on plain mortar. By the preceding formulas a contraction of about 0.03 per cent could be expected. It is reasonable, then, to conclude that a gradual adjustment takes place in the concrete during the process of hardening which results in less internal stress than theory would indicate. It is also unlikely that the shrinkage in any actual structure would be as great as that found on the laboratory specimen. Investigations of the actual shrinkage in concrete arch bridges will be needed before any very exact computations can be made for shrinkage stresses.

**19. Deflection at Any Point.**—The deflection at any point in an arch may be found by Formula (2), Art. 11, or

$$\Delta y = - \frac{s}{E_c I} \Sigma Mx$$

The arch should be assumed as cut at the point in question, and either portion of the arch may be considered. The cantilever selected should be subjected to exactly the same forces as exist in the arch itself.

If the deflection of the crown of a symmetrical arch is desired, the value of  $M$  due to loading for any section of the left cantilever may be found from Formula (7), Art. 14; or, substituting this value in the above equation, we have

$$\Delta y = - \frac{s}{E_c I} (M_c \Sigma x + H_c \Sigma xy + V_c \Sigma x^2 - \Sigma m_l x)$$

For temperature changes, Formula (11) of Art. 14 may be substituted in place of Formula (7), or

$$\begin{aligned} \Delta y &= - \frac{s}{E_c I} (M_c \Sigma x + H_c \Sigma xy) \\ &= - \frac{t \alpha D l}{E_c I} (n_h \Sigma xy - \Sigma x \Sigma y) \end{aligned}$$

**20. Reliability of the Elastic Theory.**—Formulas based on the elastic theory and actual experiments on arches have been found to give results which agree within practical limits. Whatever error occurs in applying the formulas is due chiefly to the inaccurate assumption that the entire cross-section of the concrete of each section of the arch ring is effective and that the location of the neutral axis, due to bending only, does not change throughout the arch. The neutral axis without any doubt shifts about under the action of different loads (see Art. 39, Volume I) and, as the elastic theory assumes the bending to take place about the neutral axis of each element (see Fig. 13), the values of  $x$  and  $y$  should properly be measured to some kind of an undulating curve. This curve, however, cannot be determined conveniently, so that the assumption is made in arch analysis that the arch axis passes through the neutral axis of each section. This is undoubtedly far from the truth where tension occurs and the steel takes all the tensile stress. Such a condition of stress is limited, however, to small isolated portions of the span and the error in the total result is undoubtedly small.

A comparison of some theoretical and experimental results on arches is given in the *Railroad Age Gazette*, March 26, 1909, in an article by Malverd A. Howe entitled "Experimental Verification of Arch Formulas."

Attention should be called to the uncertainty as to the fixedness of the ends of the arch. This uncertainty can be reduced or entirely eliminated by taking the skewback for purposes of analysis at a plane where the ends of the arch are virtually fixed. Whenever the abutments are of such a form that there is no pronounced change of section at the springing lines, then the analysis should include the whole structure down to the point where the distortion due to the live load on the arch will be inappreciable. In some cases this may be the very bottom of the abutment.

**21. Method of Procedure in Arch-ring Design.**—The main steps that need to be taken in the design of an arch ring may be enumerated as follows:

1. Assume a thickness for the arch ring at the crown and at the springing, using empirical formulas, if desired, as an aid to the judgment.

2. Lay out the curve assumed for the intrados.

3. Lay out a curve for the extrados to give as nearly as possible the assumed ring thickness at the springing.

4. Draw the arch axis between the extrados and intrados.

5. Divide the arch axis into an even number of divisions such that the ratio  $\frac{s}{l}$  is constant for all.

6. Compute the dead and live loads, and indicate these loads properly on the drawing.

7. Compute  $H_c$ ,  $V_c$ , and  $M_c$  at the crown for the different conditions of loading.

8. Draw the force polygons for the different conditions of loading and the corresponding equilibrium polygons, or lines of pressure.

9. Determine the thrusts, shears, bending moments, and eccentric distances at the centers of the  $\frac{s}{l}$  divisions of the arch ring for the different conditions of loading.

10. Compute the thrust and moment at the crown due to variation in temperature; also the moments on the various sections, and the corresponding thrusts and shears by resolving the crown thrust into tangential and radial components.

11. Where necessary, compute the thrust and moment at the crown, and the thrust, shear, and moment at various sections due to rib shortening.

12. Combine the thrusts, shears, and moments due to the different conditions of loading with the thrusts, shears, and moments due to temperature and rib shortening. (The results usually show that the shearing unit stresses are very small and need not be considered.)

13. Compute the maximum stresses—compression in the concrete and tension in the steel—due to the thrusts and moments. If the stresses are either too small or too large, the dimensions or even the shape of the arch ring must be changed and the computations repeated.

*Note.*—A book of multiplication tables such as Dr. A. L. Crelle's "Rechentafeln" is convenient when making computations in arch analysis. The student is advised to procure a book of this nature.

**22. Skew Arches.**—Skew arches may be treated exactly as right arches, the span being taken parallel to the center line of roadway and not at right angles to the springing lines of the arch.

## CHAPTER IV

### DESIGN OF AN EARTH-FILLED ARCH BRIDGE

**23. Data.**—It is proposed to design an electric-railway arch bridge in accordance with the following data:

Rise, 9 ft. 0 in.

Span, 48 ft. 0 in.

Depth of earth filling over crown, 12 in.

Depth of ballast above earth filling (at crown) to base of rail, 16 in.

Dead load:

Earth filling, 120 lb. per cubic foot.

Concrete, including reinforcement, 150 lb. per cubic foot.

Ballast, ties, and rails, 150 lb. per square foot of roadway.

Live load:

A uniform load equivalent to 50-ton electric cars in train.

In view of the considerations presented in Art. 7, it will be sufficiently accurate and on the safe side to consider a uniform load of 200 lb. per square foot extending over a 12-ft. width of arch at the crown. Live load will be applied over only the whole span and half-span. No allowance will be made for impact.

Latitude of Ames, Iowa.

Conditions of calculations:

$f_c$  = 600 lb. per square inch in arch ring for a 1:2:4 concrete—temperature variation of 40° F. each way from an assumed temperature of no stress.

$f_s$  = 16,000 lb. per square inch—temperature variation of 40° F. each way from an assumed temperature of no stress.

$E_s$  = 30,000,000 lb. per square inch.

$E_c$  = 2,000,000 lb. per square inch.

$n$  = 15.

Allowable pressure on foundations shall not exceed 5 tons per square foot.

Steel in the arch ring will be placed in two layers—one layer near the intrados and the other a corresponding distance from the extrados. The writer can give no assurance that the steel arrangement to be used in this design does not infringe one or more of the existing patents on concrete bridges. Assurance of this nature would be unwise since engineers well versed in patent law claim that an efficient, safe, and economical concrete arch bridge cannot be designed at the present time without patent infringement. In this connection the reader is urged to study carefully Chapter XII of this volume.

**24. Selection of the Trial Arch.**—A trial depth of 9 in. will be taken at the crown with a radial depth of 21 in. at the springing. The arch assumed is shown on Designing Sheet No. 1. As explained in Art. 4, the intrados for an earth-filled arch with a ratio of rise to span of less than one-fourth will lie between an ellipse and a segment of a circle, and the trial shape of arch ring must be chosen according to judgment.

**25. Dead Loads and Their Action Lines.**—Now that the trial arch ring has been assumed, the dead loads may be determined.

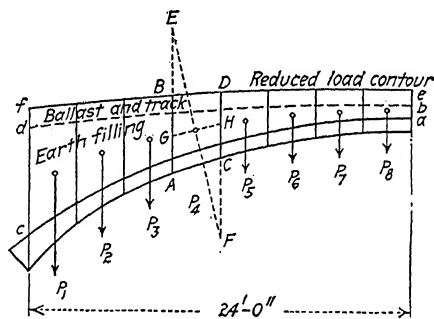


FIG. 19.

The earth filling and ballast, ties, and rails should first be reduced to an equivalent height of masonry, as shown in Fig. 19. For example, since the earth filling reaches 1 ft. above the extrados at the crown, the vertical distance  $ab$  should be laid off equal to  $\frac{120}{150} = 0.8$  ft. In a similar manner the distance  $be$  should be laid off equal to  $\frac{150}{150} = 1$  ft. Points  $d$  and  $f$  should be determined for the loading at  $c$ , and similar points should also be found for other places along the arch ring; a sufficient number

being taken to fully determine the curved line *fe*. This line is called the *reduced-load contour*.

The arch with its load should now be divided by vertical lines into trapezoids, or what are nearly so. For testing the trial arch by the approximate method (to be presented in the following article), the horizontal distance between springing lines may be conveniently divided into divisions of equal horizontal length and, for the trial arch at hand, the number will be made sixteen, that is, eight divisions on each side of the crown.

The next step is to determine the area and center of gravity of each trapezoid. With the area known, the load corresponding to each trapezoid is found by multiplying by the weight of a cubic foot of concrete. (The student must carefully bear in mind that the arch considered is included between two longitudinal vertical planes 1 ft. apart.) The center of gravity for each of the trapezoids may be found as follows: Extend *AB* (Fig. 19) so that *BE* = *CD*, and in the opposite direction extend *CD* so that *CF* = *AB*. The intersection of *EF* and the median *GHI* is the center of gravity sought.

**26. Approximate Method of Testing Trial Arch.**—Since the dead load of earth-filled arches usually controls the shape of the arch ring, the next step will be the testing of the trial arch for this loading, employing an approximate graphical method. In the method referred to, that form of arch in which the line of pressure and the arch axis most closely approach each other is considered to be the best that can be designed. A few words of explanation are needed for the student to understand the limits of this method.

There are two classes of theories of the stability of the masonry arch—the line-of-thrust theories and the elastic theories. The line-of-thrust theories do not consider the elastic properties of the material and are usually employed for arches made up of wedge-shaped stones, called *voussoirs*. For instance, stone arches are generally calculated by these theories and the stability of the arch ring is considered as depending upon the friction and the reaction between the several arch stones. Various assumptions are made in arriving at these different line-of-thrust theories, and the results derived from them are not so accurate as where the elastic properties of the material are employed. They may be made use of, however, in determining the proper shape of the arch ring before applying the elastic theory to monolithic arches.

or even before applying the elastic theory to voussoir arches, since any voussoir arch, whether of stone or brick, will act as an elastic arch as long as the line of resistance remains within the middle third.

A line-of-thrust theory by Winkler may be stated in a general way as follows: "The true line of pressure is the one lying nearest to the center line of the arch ring." The proof of this theorem depends on the assumption that the load is vertical, that the equilibrium polygon coincides with the line of pressure, and that the arch ring has a constant cross-section. This theorem for an earth-filled arch will evidently be more reliable the flatter the arch, since for such a type of arch the less are the conjugate horizontal forces produced on the arch ring by the earth filling. The matter of regarding the equilibrium polygon as coinciding with the line of pressure is assumed in all theories, but a constant cross-section of the arch ring is not usually the case in practice and generally increases, as it should, toward the springing as the thrust increases.

Now if an equilibrium polygon be passed through the centers of the arch ring at the crown and springing, this line will be very near the true line of pressure. In the trial arch mentioned above, if the equilibrium polygon and the arch axis do not closely approach each other there will surely be another shape of arch ring which will fulfill this condition, and hence have probably lower maximum stresses resulting from the live and dead loads. Thus, the method of obtaining the best form of arch is to find for what form the line of pressure for the dead load and the arch axis most nearly coincide. It should be clear that this method will aid us in getting pretty near, at any rate, to the proper form for the arch before applying the elastic theory.

In order to pass an equilibrium polygon through the centers of the arch ring at the crown and springing, the load line should first be laid off as shown on Designing Sheet No. 1 and then any convenient pole  $O'$  selected in the horizontal through the point  $k$  in the load line, this point representing the end of the load nearest the crown. The next step is to draw the rays to the force polygon and then construct the corresponding equilibrium polygon beginning at the center of the arch ring at the skewback (point  $A$ ). If now the first and last strings are prolonged to an intersection at  $B$ , a vertical line is determined which contains the resultant of the loads occurring over the left half of span.



The equilibrium polygon which we have constructed does not pass through the center of the arch ring at the crown and is not the one required. We do know, however, that the first string which passes through *A* must intersect the last string in the vertical through *B* and that the last string must be horizontal due to symmetrical loading. Drawing a horizontal line through the center of the arch ring at the crown determines the point *C* which is the intersection of the first and last strings of the equilibrium polygon required. A line drawn through *m* of the force diagram parallel to *CA* determines the true pole *O* on the horizontal through *k*. If the force diagram is now completed for this pole, the required equilibrium polygon may be easily drawn. The line of pressure is seen to follow the arch axis very closely and the trial arch will be accepted for analysis.

In both preliminary and final analysis the arch ring should be laid out to a scale of 1 in. = 3 ft., and care should be used in the drafting work so as to have the dimensions exact and the lines sharp.

**27. Division of Arch Ring for Constant  $\frac{s}{l}$ .** The method of dividing the arch ring into divisions having constant  $\frac{s}{l}$  is given on Designing Sheet No. 2, and the divisions themselves are shown on Designing Sheet No. 4. The procedure should be clear from a study of Art. 15.

**28. Moments and Thrusts.**—A complete set of formulas, as shown on Designing Sheet No. 3, should be at hand before starting the arch analysis. The notes on this sheet are given for convenience and may aid in preventing errors due to the use of wrong algebraic signs. The formulas show, first of all, that the cantilever bending moments are required at the centers of the  $\frac{s}{l}$  divisions caused by the given external loads (considering the arch as two cantilevers). These moments are found on Designing Sheets Nos. 5 and 5A by both algebraic and graphical methods. The algebraic method should be clear, but the graphical or equilibrium polygon method of finding these moments may need explanation.

*ACB* represents the arch axis and the load line is *acb*. *O* is any convenient pole on a horizontal line through the point *c* — a point on the load line at the junction of the crown loads *P*<sub>8</sub>.

The equilibrium polygon corresponding is  $mnp$  and, since  $Oc = H$  is horizontal, the segment  $no$  is horizontal, and the desired bending moment at any point such as 5 is equal to the intercept on the vertical through this point (included between the equilibrium polygon and the horizontal line  $no$  produced) multiplied by the pole distance  $H$ , or  $m = Hk_5$ .

If desired, the cantilever moments due to live loading may be found somewhat more accurately than indicated in Designing Sheet No. 5. This may be done either by drawing the parabolic curve for moment due to uniform loading or by computing the value of the live moment at the center of each  $\frac{s}{I}$  division in the same manner as for any point in a simple cantilever beam.

Designing Sheet No. 4 shows that the dead load is divided into separate forces in a different manner than in the preliminary analysis of the arch. This second division of the dead-load forces is not common in practice since, theoretically, there is no relation between the divisions of the arch ring and the points of application of the loads, the only requirement being to have such a small subdivision of the arch ring and of the load that the errors of approximation may be neglected. It seems to the writer, however, that taking the separating load-planes through the centers of the  $\frac{s}{I}$  divisions results in more accurate values of the bending moments, which actually bend the separate elements of the arch ring, than are obtained by the common method of load subdivision. Besides, the usual division of the arch requires the perpendicular distance from the arch axis to the line of pressure at a division point to be measured *at* or *near* the load, and this is a most unfortunate selection if the eccentric distances at the sections are to be checked graphically. The load arrangement here proposed eliminates any error in scaling these distances, since between load points the equilibrium polygon and line of pressure coincide.

The live and dead loads near the crown act practically in the same vertical line and hence no sensible error results from assuming them to do so. Near the springing, however, where the horizontal distance between division points is considerable, the live and dead loads may need to be considered separately. In the arch in question a separation of dead and live load is made between division points 1 and 2.

Moments and thrusts for the different conditions of loading and for temperature and rib shortening are given on Designing Sheet No. 6. The writer has tried to arrange the results on this sheet in such a form that the operations involved will be clear and will need but little explanation. The values of  $x$  and  $y$  were scaled, and the values of  $m$  for dead load and for live plus dead load were carried forward from Designing Sheet No. 5. The magnitudes of the thrusts,  $N$ , were scaled from the force polygons on Designing Sheet No. 4, and the computed eccentricities  $x_e$  used simply as a check on the resultant line of pressure determined from the computations. The values of  $M$  and  $N$  for rib shortening were obtained directly from the moments and thrusts due to a fall of temperature by multiplying by the decimal 0.337.

In finding the average unit compression in the concrete due to thrust, only the total thrusts caused by dead load plus live load on right half of span have been considered, and these only at five sections of the arch ring. For light arches, such as the one we are designing, this method is sufficiently accurate for all practical purposes. For heavy arches, however, the effect of temperature (rise and fall) and rib shortening may need to be taken into account. There are two cases to be considered in such arches: (A) That due to dead load, live load, *fall* of temperature, and rib shortening; and (B) that due to dead load, live load, *rise* of temperature, and rib shortening. The method of finding the average unit compression in this more accurate manner will be shown by making the computations for the arch in question, adopting the same position of the live load as previously mentioned.

Case A. Assume  $c_a = 155$  lb. per square inch.

$$H_c = \frac{-(0.016)(155)(144)(49.2)(8)}{490.8} = -287 \text{ lb.}$$

$$c_a \text{ (at crown)} = \frac{22,400 - 890 - 287}{(1)(0.75) + 0.092} = 25,250 \text{ lb. per square foot.}$$

$$c_a \text{ (at point 3)} = \frac{\frac{1}{2}(23,600 + 23,900) - 850 - \frac{850}{890}(287)}{(1)(0.80) + 0.092} = 25,400 \text{ lb. per square foot.}$$

$$c_a \text{ (at springing)} = \frac{\frac{1}{2}(29,200 + 31,600) - 620 - \frac{620}{890}(287)}{(1)(1.75) + 0.092} = 16,050 \text{ lb. per square foot.}$$

$$c_a \text{ (for arch)} = \frac{25,250 + 25,400 + 16,050}{3} = 22,200 \text{ lb. per square foot.}$$

(155) (144) = 22,300 lb., assumed value of  $c_a$  is satisfactory.

$$M_c = - \frac{(-287)(14.65)}{8} = + 526 \text{ ft.-lb.}$$

Case B. Assume  $c_a = 160$  lb. per square inch.

$$H_c = (-287) \left( \frac{160}{155} \right) = 296 \text{ lb.}$$

$$c_a \text{ (at crown)} = \frac{22,400 + 890 - 296}{0.842} = 27,300 \text{ lb. per square foot.}$$

$$c_a \text{ (at point 3)} = \frac{\frac{1}{2}(23,600 + 23,900) + 850 - \frac{850}{890}(296)}{0.892} = 24,300 \text{ lb. per square foot.}$$

$$c_a \text{ (at springing)} = \frac{\frac{1}{2}(29,200 + 31,600) + 620 - \frac{620}{890}(296)}{1.842} = 16,700 \text{ lb. per square foot.}$$

$$c_a \text{ (for arch)} = \frac{27,300 + 24,300 + 16,700}{3} = 22,700 \text{ lb. per square foot.}$$

(160) (144) = 23,000 lb., assumed value of  $c_a$  is satisfactory.

$$M_c = - \frac{(-296)(14.65)}{8} = + 542 \text{ ft.-lb.}$$

TABLE OF SHEARS

Pt.	Live load on right half of span		Live load on whole span	Temperature (fall of 40°, rise of 40°, shears of opposite sign)	Rib shortening	Max. shear	Cross-section (sq. in.)	Max. shear (lb. per sq. in.)
	Left half	Right half						
Cr.	- 820	- 820	0	0	0	- 820	108	8
Spg.	+3200	+1000	+1300	-640	-220	+3620	252	14
1	+1900	- 200	+1100	-535	-180	+2255	161	14
2	- 200	-1600	- 600	-360	-120	-2080	117	18
3	+ 100	- 900	- 300	-280	- 95	-1275	115	11
4	+ 100	- 300	- 100	-230	- 80	- 610	114	5
5	+ 50	+ 100	.....	-175	- 60	+ 215	111	2
6	- 150	+ 400	.....	-120	- 40	+ 480	109	4
7	- 400	+ 600	.....	- 75	- 25	+ 650	108	6
8	- 700	+ 800	.....	- 25	- 10	+ 815	108	8

It is not customary to determine the shears at the centers of the  $\frac{s}{I}$  divisions. The shears for the arch here analyzed are given above in order to show the student that the values obtained are actually very small.

**29. Combining of Moments and Thrusts.**—The method used in combining moments and thrusts for maximum stresses will be explained by giving all the computations needed in finding the maximum stresses at point 1. Reference should be made to Designing Sheets Nos. 6 and 7. Moments and thrusts due to a *fall* of temperature will usually combine with the moments and thrusts on right half of span (live load on right half of span) to give one set of maximum conditions. Moments and thrusts due to a *rise* of temperature will usually combine with the moments and thrusts on left half of span (live load on right half of span) to give a second set of maximum conditions. A third set due to live load on the whole span will need consideration at the crown and at sections near the quarter points. It is convenient to combine rib-shortening moments and thrusts with those for temperature as a preliminary operation. If the values of  $M$ ,  $N$ , and  $x_0$  (or  $\frac{x_0}{t}$ ) of any given set are lower than corresponding values in some other set for the same section, then the first-mentioned set of values need receive no further consideration. Thrusts are likely to control at the crown and moments near the springing.

The necessary computations in combining moments and thrusts at section 1 are as follows:

*Fall of Temperature:*

		$M$	$N$
Temp.		-3900	-710
R. short.		-1300	-240
		-5200	-950
$M$	$N$	$M$	$N$
-5200	-950	-5200	-950
-5200	28,000	+900	31,650
-10,400	27,050	-4300	30,700

*Rise of Temperature:*

	$M$	$N$
Temp.	+3900	+710
R. short.	-1300	-240

$M$	$N$	$M$	$N$
+2600	+ 470	+2600	+ 470
+5500	26,500	+ 900	31,650
<u>+8100</u>	<u>26,970</u>	<u>+3500</u>	<u>32,120</u>

It is quite evident that the other possible combinations could not give maximum conditions. In fact, an experienced designer of arches would recognize immediately that the first set only needs consideration. The set having a value of  $M = +8100$  ft.-lb. should be eliminated at once since the values of  $M$ ,  $N$ , and  $x_0$  of this set are lower than the corresponding values of the first set.

To comply with some types of specifications it is also necessary to find the maximum moments and thrusts with those due to temperature variation excluded, the idea being not to allow the line of pressure to depart from the middle third for such conditions. The method of doing this should be clear from the above example in which the moments and thrusts due to temperature are taken into account.

**30. Maximum Stresses.**—Maximum stresses at each section should be found for the entire arch, using Diagrams 13, 14, and 15 of Volume I, which are based on an embedment of the rods from each surface equal to one-tenth the depth. (Diagrams for other depths of embedment will be given in Chapter V, but these will not be considered here.) In light arches the embedment near the crown will be proportionately much greater than assumed and the stresses as determined by the diagrams of Volume I will be lower than the actual. Those sections where maximum stress is likely to result should then be again considered and the stresses computed accurately by using the formulas on Designing Sheet No. 7 which are reproduced from Volume I for convenience. The determination of  $k$  must be by trial.

The method of finding the *exact* compressive stress at any section when tension exists over part of section (Case II) will be explained by giving the computations for finding the stress at section 1. Since  $k = 0.620$  for one-tenth embedment of the rods, a good value to use for a trial would be 0.600. Substituting in the formula for  $k$ , this value, however, does not satisfy the equation. A value of  $k = 0.596$  is then readily determined. Substituting in the formula for  $L$  gives a value for this term of 0.1066. Then

$$f_c = \frac{(10,400)(12)}{(0.1066)(18)(1.18)(144)} = 540 \text{ lb.}$$

The steel stresses are evidently very small and need be computed in but few cases. The concrete stress at sections 3, 7, and 8 will evidently be lower than that in adjoining sections having approximately the same value of  $t$ . The arch assumed we will consider as satisfactory.

When the stresses in an arch are found to be altogether too small or too large, the dimensions or even the shape of the arch ring should be changed and the computations repeated. Small changes, however, may be made without refiguring the whole arch. For example, the thickness of the arch ring may be decreased throughout by changing the moment of inertia of all sections in the same ratio—that is, by keeping  $\frac{s}{I}$  constant. This may be done since the dead- and live-load stresses will remain sensibly unchanged, and the temperature and rib-shortening stresses will be but slightly modified. The point in the arch where the unit stress is the greatest should be selected, and the depth  $t$  determined by trial which will give the required allowable stress. Of course, this depth should be determined by considering  $M$ ,  $N$ , and  $x_0$  the same as for the unchanged section. The depth at every other section, then, must be changed by such an amount that the percentage change in the moment of inertia will be a constant throughout the arch.

If desired, the modified arch ring may be again tested for maximum stresses. This may be accomplished by finding the new moments due to temperature and rib shortening and combining these with the moments due to loading which can be considered to remain unchanged. The values of the moments and thrusts for temperature change will be increased or decreased in the same ratio as the value of  $I$ . The values of the moments and thrusts for rib shortening will increase or decrease inversely as  $I$ , but obviously not in the same ratio, and will need to be determined in the same manner as in the previous computations.

**31. Design of Abutments.**—The shape of abutment must be such that the load on the foundation will not exceed the allowable and will be well distributed. The shape that will be assumed is shown on Designing Sheet No. 8, the top of the abutment being drawn somewhat above a tangent to the extrados at the skewback.

In general, the so-called lines of pressure through the abutment should be drawn for the following conditions:

1. Dead load and live load on the half span opposite to the abutment.
2. Dead load and live load on the half span adjacent to the abutment, with live load *on* the abutment.
3. Dead load and live load over the whole span, with live load *on* the abutment.
4. In some cases, depending upon the method of procedure adopted in arch construction, an analysis should also be made for dead load only of the arch ring, without earth fill either above or back of the abutment.

The lines of pressure for all cases should be as near to the center of the base as possible in order to obtain a nearly uniform distribution of load over the entire foundation. The analysis and design of the abutment is given on Designing Sheet No. 8, with the exception that for clearness the combination of forces for condition (4) is not shown.

The forces that may act on the foundation consist of (1) the reaction of the arch; (2) the weight of the abutment; (3) the weight of the earth, ballast, and live load directly above the abutment; and (4) the lateral earth pressure. To find the maximum lateral earth pressure, the live-load surcharge should be determined, also the surcharge due to ballast, ties, and rails. The height of the live-load surcharge may be found by dividing the live load per square foot by the weight of a cubic foot of earth. The surcharge due to ballast, ties, and rails may be found in a similar manner. The horizontal pressure on  $AC'$  when the live load is acting is thus equal to the difference between the pressures on  $AG$  and  $C'G$ , and may be determined by the method explained in Art. 3 of Volume II. If we assume an equivalent fluid weight of 25 lb. per cubic foot, then this horizontal pressure

$$P = \frac{1}{2}(25)(19.23^2 - 12.33^2) = 2720 \text{ lb.}$$

and acts at a distance of

$$\frac{6.90^2 + (3)(6.90)(12.33)}{3(6.90 + 2 \times 12.33)} = 3.19 \text{ ft.}$$

above the base. Without the live load,  $P = 2470$  lb. and acts at practically the same distance above the base as when the live load is included. In this design a lateral pressure of 2700 lb. may be considered with sufficient accuracy for all cases.



The weight of the prism of earth whose cross-section is  $BGHC$  and thickness 1 ft. is

$$\frac{(12.33 + 6.90 - 1.00) + 12.33}{2} \times 9.50 \times 120 = 17,500 \text{ lb.}$$

The weight of the prism represented by  $BKLC$   $17,500 - (9.50)(1.67)(120) = 15,600$  lb. The center of gravity of these prisms may be found by the method outlined in Art. 25. The forces representing the weights of the prisms act practically in the same vertical line, and for simplicity we shall use a force of 17,500 lb. for both cases acting 4.45 ft. from the inner edge of abutment.

The weight of the masonry is readily found by dividing the outline of the abutment into a number of triangles and placing the weight represented by a given triangle at its center of gravity. (The center of gravity of a triangle is at the intersection of the medians.) The resultant of all the vertical forces acting (including the weight of the prism of earth) may then be determined by the principle of moments which is explained fully in Art. 2 of Volume II. The resultant is found to have a magnitude of 25,000 lb. and acts 4.94 ft. from the back edge of the abutment.

Designing Sheet No. 8 shows the method of combining forces to find the thrusts on the foundation for the three conditions of loading. The maximum and minimum pressures for any loading may be obtained by using the formulas of Art. 9, Volume II. The true maximum equals

$$p_1 = \frac{51,200}{7.50} \left( 1 + \frac{6 \times 0.65}{7.50} \right) = 10,400 \text{ lb. per square foot}$$

The method of design described above is considerably on the safe side. The student should note that in finding the reactions from the arch ring the assumption is made that the live load of 200 lb. per square foot extends over the entire 16 ft. width of bridge, when, in fact, a load of this intensity covers approximately only 12 ft. at the crown, spreading out at other points so that the unit live load on the back of the arch ring near the abutment is very much less than the maximum. In other words, a much more accurate set of reactions could be obtained with which to analyze the arch abutment by assuming a live load of 200 lb. per square foot at the crown.

abutment is approached. Some allowance for this condition of loading is sometimes made in the abutment design, but since the elastic theory fails if the foundation is not unyielding, the added factor of safety is not usually considered.

Many engineers believe (the writer included) that in many, if not the majority of cases, the dead and live load per linear foot of arch on a strip 1 ft. wide may be determined for purposes of analysis as equal to the total dead load plus total live load divided by the total width of arch. This loading is adopted on the assumption that a 1-ft. strip will not fail separately but will be assisted by the adjoining strips so as to produce average conditions.

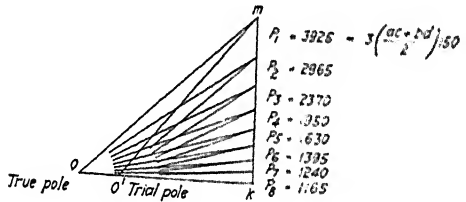
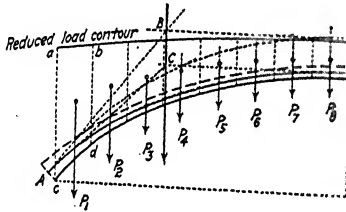
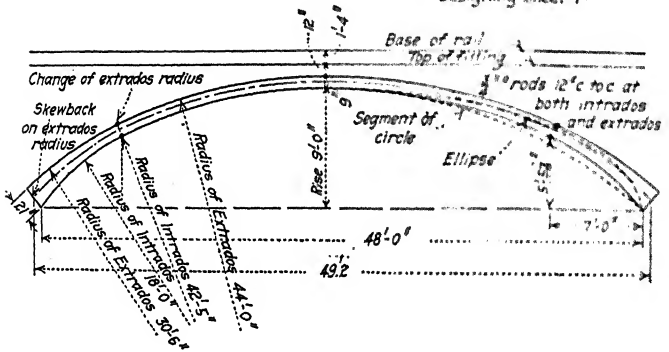
**32. Design of Spandrel Walls.**—The details of the spandrel walls are shown on Plate I which also gives the complete design of bridge. Since cantilever retaining walls would bring indeterminate stresses in the arch near the edges of the ring, which would not be at all desirable in such a thin arch, the curtain-wall type of construction with cross walls was adopted. The method of design is the same as for counterforted retaining walls which is explained in Art. 12 of Volume II.

Expansion joints in the spandrel walls are made at the springing lines (in larger arches additional joints should be made throughout the span) and may be made mere planes of weakness or as actual joints filled with one or more layers of felt or some other partially elastic material. Such expansion joints are desirable to prevent unsightly cracks due to rise and fall of the arch caused by temperature changes. If the arch centers are not struck until after the spandrel walls are constructed, then expansion joints are also necessary to prevent cracking due to settlement of the crown of the arch when the centers are lowered.

Since an arch bridge with a level coping will always appear to sag in the middle, a camber of 4 in. is provided. This slight camber, of course, was not considered in the previous loading calculations.

A batter is given to the back of the cantilever retaining walls resting on the abutments so as to give a low compressive stress per square inch on the abutment concrete, this concrete being only a 1:3:6 mixture. The back of the arch and the lower parts of the spandrel and cross walls should be water-proofed in order to prevent seepage of water through the arch ring and to facilitate drainage.

# Designing Sheet 1.



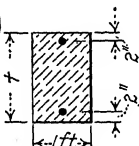
## Designing Sheet 2.

Division of Arch Ring for Constant  $\frac{I}{S}$ Measured length of  $\frac{1}{2}$  arch axis = 26.82Rods -  $\frac{3}{4}$ "  $\phi$ , 12" c to c.Steel area =  $0.44 \times 2 = 0.88$  sq. in

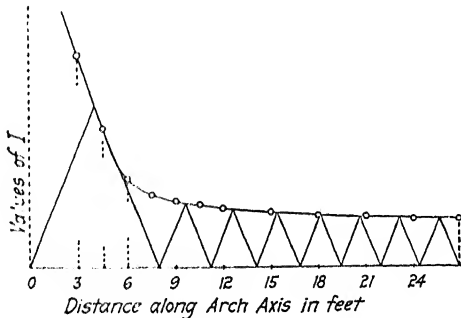
$$p_o = \frac{0.88}{(12 \times 9)} = 0.00815 \left( \frac{\text{sq. in.}}{\text{sq. ft.}} \right)$$

$$a_s = \frac{0.88}{144} = 0.00611 \text{ sq. ft.}$$

$$15a_s = 0.092$$



Distance along the axis from skewbk	$\frac{t}{2}$ (ft.)	$I_c = \frac{t^3}{12}$	$\frac{t}{2}$	$\frac{t}{2} - d'$	$15a_s \left( \frac{t}{2} - d' \right)^2 = 15 I_s$	$I = I_c + 15 I_s$	Division	Lengths of divisions to make $\frac{I}{S}$ constant (by diagram)
3.00	.123	.155	.615	.448	.019	.174	1	8.00
4.50	.107	.102	.535	.368	.012	.114	2	3.23
6.00	.92	.065	.460	.293	.008	.073	3	2.91
7.50	.86	.053	.430	.263	.006	.059	4	2.74
9.00	.83	.048	.415	.248	.006	.054	5	2.60
10.50	.82	.046	.410	.243	.005	.051	6	2.52
12.00	.80	.043	.400	.233	.005	.048	7	2.44
15.00	.78	.040	.390	.223	.005	.045	8	2.38
18.00	.77	.038	.385	.218	.004	.042	$\frac{I}{S} = 0.016$ (from diagram)	
21.00	.76	.037	.380	.213	.004	.041		
24.00	.75	.035	.375	.208	.004	.039		
26.82	.75	.035	.375	.208	.004	.039		



## Formulas Required

Loading:

$$H_c = \frac{n_h \sum (m_L + m_R)y - \sum (m_L + m_R)\sum y}{2[n_h \sum y^2 - (\sum y)^2]} \quad (4)$$

$$V_c = \frac{\sum (m_L - m_R)x}{2\sum x^2} \quad (5)$$

$$M_c = \frac{\sum (m_L + m_R) - 2H_c \sum y}{2n_h} \quad (6)$$

$$M = M_c + H_c y + V_c x - m_L \quad (7)$$

$$M = M_c + H_c y - V_c x - m_R \quad (8)$$

All values of  $m_L$ ,  $m_R$ ,  $x$ , and  $y$  should be substituted as positive. All summations refer to one-half of the arch axis. Positive value of  $V_c$  indicates that the line of pressure slopes upward towards the left; a negative value, downward towards the left. Positive value of  $M_c$  indicates that the thrust  $H_c$  acts above the arch axis. Signs preceding terms  $M_c$  and  $V_c$  in formulas (7) and (8) depend upon the results of (5) and (6).

Temperature:

$$H_c = \frac{I}{s} \cdot \frac{t_0 t_D \ell n_h E_c}{2[n_h \sum y^2 - (\sum y)^2]} \left\{ \begin{array}{l} t_0 \text{ should be} \\ \text{inserted as +} \\ \text{for a rise;} \\ \text{- for a drop.} \end{array} \right\} \quad (9)$$

$$M_c = -\frac{H_c \sum y}{n_h} \quad (10)$$

$$M = M_c + H_c y \quad (11)$$

The value of  $t_0$  should be inserted as plus for a rise of temperature; minus (-) for a drop. Signs preceding  $H_c$  in formulas (10) and (11) depend upon the result of formula (9). Sign preceding  $M_c$  in formula (11) depends upon the result of formula (10). Thus for fall of temperature, thrust and moment are of opposite sign from those for a rise.  $\ell$  = span of arch axis.

Rib Shortening:

$$H_c = -\frac{I}{s} \cdot \frac{c_a \ell n_h}{2[n_h \sum y^2 - (\sum y)^2]} \quad (12)$$

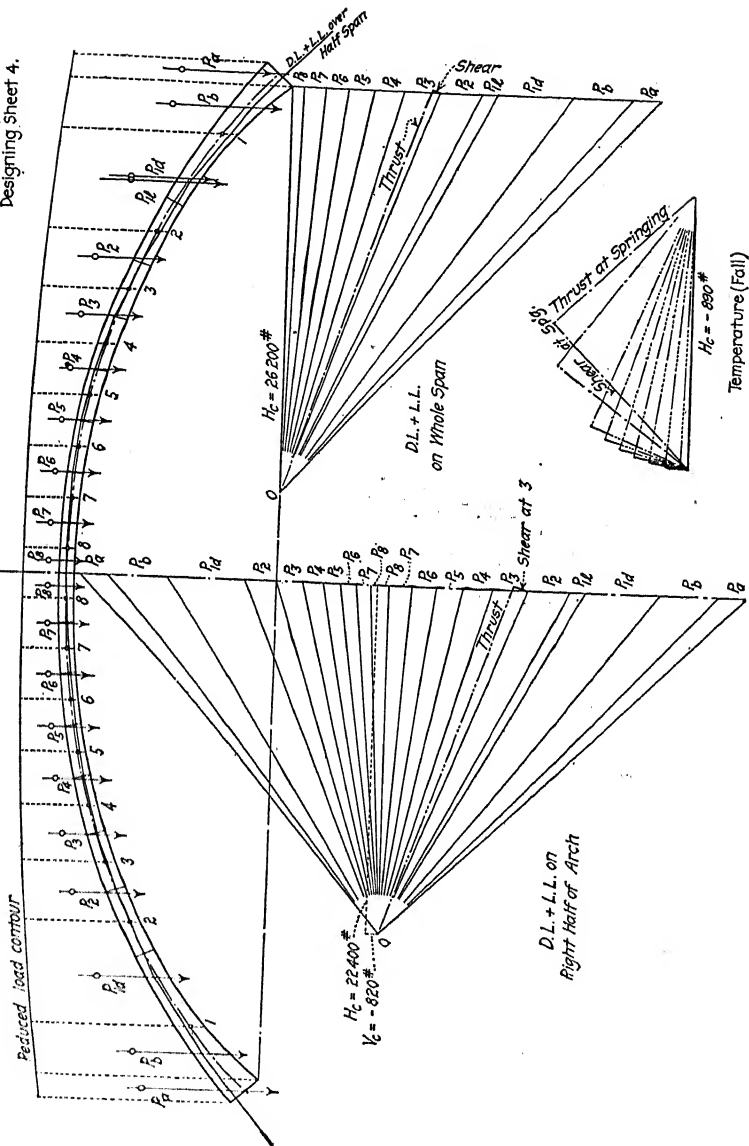
$$M_c = -\frac{H_c \sum y}{n_h} \quad (13)$$

$$M = M_c + H_c y \quad (14)$$

Values of moments and thrusts for rib shortening are of same sign as for temperature fall.  $\ell$  = span of arch axis.

## Stress Sheet

## Designing Sheet 4.



Cantilever Moments  
(Algebraic Method)

Designing Sheet 5.

Point	Hor. dist. from crown	Hor. distance between points	Dead Load				Dead Load plus Live Load				
			Dead Loads	Summation of Dead Loads	Increment of Moment (Dead)	Moments (Dead)	Live Loads	Sum of Live Loads	Increment of moment	Moments	
										Live Load	LL+DL
$P_8$	.61		460	460			240	240			
8	1.19	.58			270	270			140	140	210
$P_7$	2.41	1.22	940	1400	560	830	480	720	290	430	
7	3.60	1.19			1670	2500			860	1290	3790
$P_6$	4.87	1.27	1020	2420	1780	4280	490	1210	910	2200	
6	6.07	1.20			2900	7180			1450	3650	10830
$P_5$	7.37	1.30	1140	3560	3150	10330	500	1710	1570	5220	
5	8.57	1.20			4270	14600			2050	7270	21870
$P_4$	9.89	1.32	1320	4880	4700	19300	510	2220	2260	9530	
4	11.12	1.23			6000	25300			2730	12260	37560
$P_3$	12.51	1.39	1640	6520	6780	32080	540	2760	3090	15350	
3	13.82	1.31			8540	40620			3620	18970	59590
$P_2$	15.28	1.46	2060	8580	9520	50140	570	3330	4030	23000	
2	16.66	1.38			11840	61980			4600	27600	83580
$P_{1d}$	19.26	2.60	4770	13350	22310	84290					
$P_{1e}$	19.09	2.43									
1	21.53	$P_{1d}$ 2.27 $P_{1e}$ 2.44			30300	114590			10490	46180	160170
		1.33	3280	16630	17760	132350	490	4790	5720	51900	
$P_b$	22.86										
$P_{a-f}$	24.55	1.69	1560	18190	28100	160450	220	5010	8100	60000	220450

24.55 18190

160450

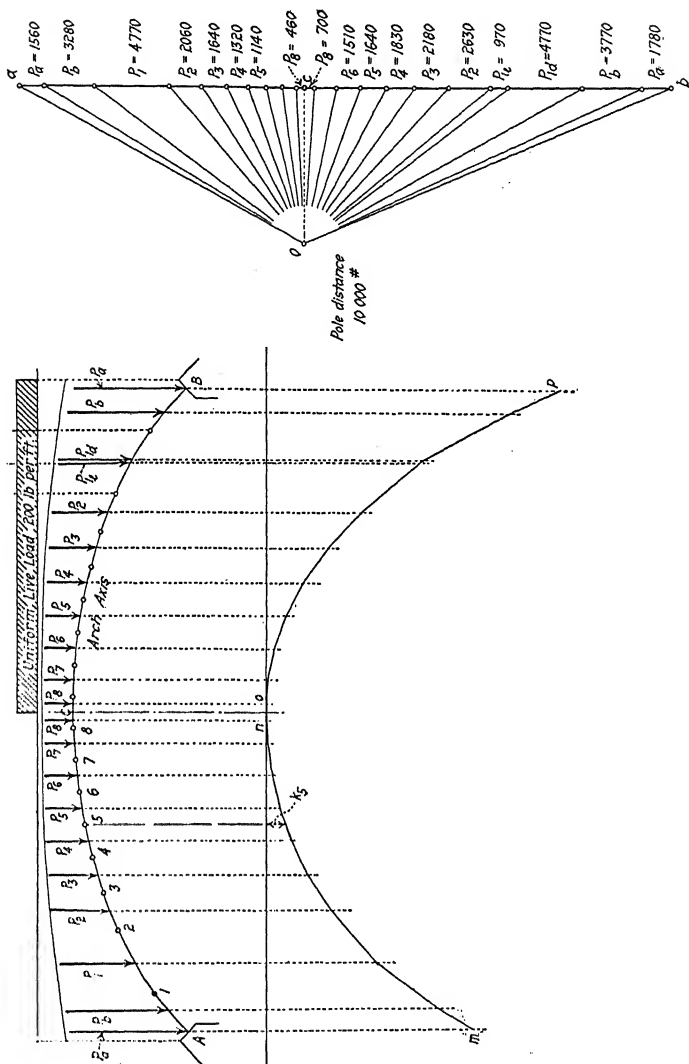
5010

60000

(25.05 X 200) = 5010

Cantilever Moments  
(Graphical Method)

Designing Sheet 5(A)





Designing Sheet 6.

## MOMENTS AND THRUSTS

Pt.	x	y	x <sup>2</sup>	y <sup>2</sup>	Dead Load		Live plus Dead Load		Dead Load plus Live Load on Right Half of Span		D.L. plus L.L. on Whole Span		Temperature		Rib Shortening H <sub>c</sub> =200 H <sub>c</sub> =550 H <sub>c</sub> =550															
					m	mx	m	mx	H <sub>c</sub> y	H <sub>c</sub> x	M	N	H <sub>c</sub> y	M		N	H <sub>c</sub> y	M	N											
																				Left Half		Right Half								
Cr	24.55	8.82	602.7	77.79	160 450	3 319 000	1415 200	220 450	5 412 000	1844 400	187 600	-20 100	-5 500	26 500	-370	22 400	-02	-170	22 400	-02	-50	26 200	-02	-7800	-6200	+1650	-890	+550	300	
1	21.53	6.17	463.5	38.07	114 590	2 467 100	707 000	160 770	3 461 400	982 000	138 200	-17 700	-5 500	26 500	+21	37 650	+03	-19	161 700	+900	37 650	+03	231 100	+10 600	34 900	-5500	-3900	1400	200	
2	16.66	3.35	277.6	11.22	61 980	1 032 600	207 600	89 580	1 492 400	300 100	75 000	-13 700	-1 000	24 300	-04 <th>28 800</th> <th>-05</th> <th>-10</th> <th>87 000</th>	28 800	-05	-10	87 000	-1 800 <th>28 800</th> <th>-06</th> <th>87 000<th>-1 800<th>28 800</th><th>-3000</th><th>-1400</th><th>820</th><th>200</th></th></th>	28 800	-06	87 000 <th>-1 800<th>28 800</th><th>-3000</th><th>-1400</th><th>820</th><th>200</th></th>	-1 800 <th>28 800</th> <th>-3000</th> <th>-1400</th> <th>820</th> <th>200</th>	28 800	-3000	-1400	820	200	
3	13.82	2.28	191.0	5.20	40 620	561 400	92 600	59 590	823 500	135 900	51 100	-11 300	-1 200	23 600	-05 <th>24 500</th> <th>-10</th> <th>-05</th> <th>59 700</th>	24 500	-10	-05	59 700	-1 000 <th>27 800</th> <th>+04</th> <th>59 700<th>-1 000<th>27 800</th><th>-2000</th><th>-400</th><th>500</th><th>200</th></th></th>	27 800	+04	59 700 <th>-1 000<th>27 800</th><th>-2000</th><th>-400</th><th>500</th><th>200</th></th>	-1 000 <th>27 800</th> <th>-2000</th> <th>-400</th> <th>500</th> <th>200</th>	27 800	-2000	-400	500	200	
4	11.12	1.45	123.7	2.10	25 300	281 300	36 700	37 560	417 700	54 500	32 500	-9 100	-2 300	23 100	-10 <th>23 700</th> <th>+16</th> <th>-16</th> <th>38 000</th>	23 700	+16	-16	38 000	+400	27 200	+05	38 000 <td>+400</td> <th>27 200</th> <th>-1300</th> <th>-300</th> <th>300</th> <th>200</th>	+400	27 200	-1300	-300	300	200	
5	8.57	.86	73.4	.74	14 600	125 100	12 600	21 870	187 400	18 800	19 500	-7 000	-2 700	22 650	-12 <th>22 600</th> <th>+18</th> <th>-12</th> <th>22 500</th>	22 600	+18	-12	22 500	+600	26 700	+02	22 500 <td>+600</td> <th>26 700</th> <th>-800</th> <th>-800</th> <th>400</th> <th>200</th>	+600	26 700	-800	-800	400	200	
6	6.07	.40	36.8	.16	7 180	43 600	2 900	3 790	55 800	4 800	9 000	-5 000	-3 600	22 650	-16 <th>22 600</th> <th>+12</th> <th>-16</th> <th>10 500</th>	22 600	+12	-16	10 500	+400	26 500	+05	10 500 <td>+400</td> <th>26 500</th> <th>-400</th> <th>-400</th> <th>200</th> <th>200</th>	+400	26 500	-400	-400	200	200	
7	3.60	.12	13.0	.01	2 500	9 000	300	3 790	13 600	500	2 700	-3 000	-3 200	22 500	-14 <th>22 500</th> <th>+07</th> <th>-14</th> <th>3 100</th>	22 500	+07	-14	3 100	+700	26 300	+03	3 100 <td>+700</td> <th>26 300</th> <th>-100<th>-100</th><th>890</th><th>300</th></th>	+700	26 300	-100 <th>-100</th> <th>890</th> <th>300</th>	-100	890	300	
8	1.19	.02	1.1	.00	270	300	—	410	500	—	400	-1 000	-1 200	22 400	-05 <th>22 400</th> <th>+03</th> <td>500</td> <td>0</td> <th>26 200</th> <td>0</td> <td>500</td> <td>0</td> <th>26 200</th> <td>0</td> <td>+1600</td> <th>-890</th> <th>+550</th> <th>300</th>	22 400	+03	500	0	26 200	0	500	0	26 200	0	+1600	-890	+550	300	
Σ	14.65	1180.4	57.50	267 040	4 520 400	10 39 700	383 400	6 462 300	1506 100	—	—	—	—	—	—	—	—	—	—	—	—	—	—	—	—	—	—	—	—	—

Live Load on Right Half of Span:

$$H_c = \frac{8(1,059,700 + 1,506,100) - (257,040 + 383,400)(14.65)}{2[(57.50) - (14.65)^2]}$$

$$= \frac{10,997,500}{490.8} = 22,400 \text{ lb.}$$

$$V_c = \frac{4,520,400 - 6,462,300}{2(11.804)} = -820 \text{ lb.}$$

$$M_c = \frac{(267,040 - 383,400) - (2,224,000 - 1,465,000)}{2(1.19)} = -570 \text{ ft. lb.}$$

Live Load on Whole Span:

$$H_c = \frac{(8)(2,119,500 + 1,506,100) - 2(383,400)(14.65)}{490.8}$$

$$= \frac{12,984,000}{490.8} = 26,200 \text{ lb.}$$

$$V_c = 0$$

$$M_c = \frac{2(383,400) - 2(26,200)(14.65)}{15} = -570 \text{ ft. lb.}$$

Temperature (fall):

$$H_c = \frac{(0.06)(100000)(10)(14.65)(14.65)}{490.8}$$

$$V_c = 0$$

$$M_c = \frac{(800)(14.65)}{8} = +1630 \text{ ft. lb.}$$

Rib Shortening (live load on one-half span):

$$\text{Assume } C_u = 160 \text{ lb. per sq. in.}$$

$$H_c = \frac{(0.06)(160)(144)(14.65)(14.65)}{490.8} = -300$$

$$C_u \text{ (at crown)} = \frac{22,400}{(1)(14.65)} = 26600$$

$$C_u \text{ (at point 3)} = \frac{1}{2} \left( \frac{23,600 + 23,900}{(1)(14.65)} \right) = 26600$$

$$M_c = \frac{(300)(14.65)}{8} = +550 \text{ ft. lb.}$$

$$M_c = \frac{(29300 + 16500)}{2(11.15)} = 16500$$

$$\text{Ratio of } H_c \text{ for rib shortening} = \frac{300}{800} = .375$$

$$(160)(144) = 23000 \text{ lb. per ft. of } 23,250$$

Designing Sheet 7.

## Maximum Stresses

Point	+	$p_o$	Combination of Moments and Thrusts and Resulting Stresses				
			M	N	$\frac{x_o}{r}$	$f_c$	$f_s$
Crown	0.75	.00815	* 2130	25 010	.113 (f)	* 335	
Springing	1.75	.0035	+20800 *+14 700	29 610 35 310	.401 (r) .238 (r)	472 *324	6100 (Exact 540)
1	1.12	.0054	-10 400	27 050	.343 (f)	516	2800
2	0.81	.0075	* -3 700	27 700	.165 (f)	* 408	
3	0.80	.0076	+ 2 700	24 460	.138 (r)		
4	0.79	.0077	+ 4 100	22 150	.235 (f)	406	(Exact 572)
5	0.77	.0079	+ 5 200 - 3 200	21 640 23 430	.312 (f) .177 (r)	508 371	
6	0.76	.0080	- 4 400	23 230	.249 (r)	458	
7	0.75	.0081	- 4 200	23 090	.243 (r)		
8	0.75	.00815	- 3 300 *+ 2 100	22 990 25 010	.192 (r) .112 (f)		

\* means due to live load on whole span

Formulas for Bending and Direct Stress

$$\left\{ \begin{array}{l} \text{Compression over entire section} \\ \text{Tension over part of section} \end{array} \right\} \left\{ \begin{array}{l} f_c = \frac{N}{bt} \left( \frac{1}{1 + np_o} + \frac{6x_o t}{t^2 + 12 np_o r^2} \right) = \frac{N}{bt} (K) \\ K^3 - 3 \left( \frac{1}{2} - \frac{x_o}{t} \right) K^2 + 6 np_o K \frac{x_o}{t} = 3 np_o \left( \frac{x_o}{t} + 2 \frac{r^2}{t^2} \right) \\ L = \left[ \frac{np_o r^2}{K^2} + \frac{K}{12} (3 - 2K) \right] \\ f_c = \frac{M}{L bt^2} \\ f_s = n f_c \left( \frac{d}{Kt} - 1 \right) \end{array} \right.$$

## Analysis of Abutment

Designing Sheet 8.

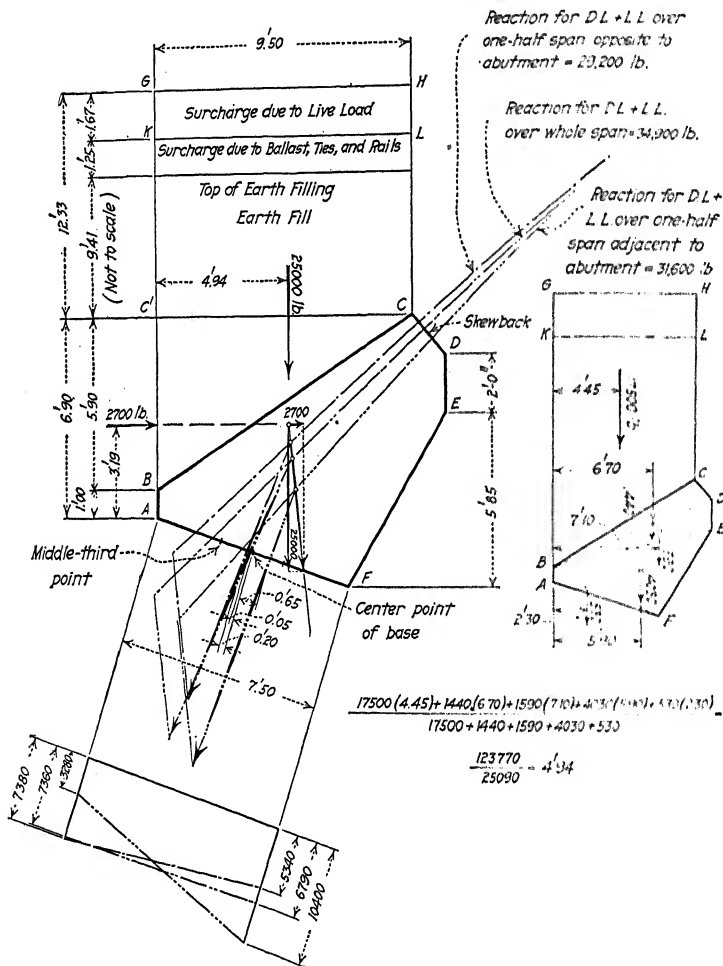
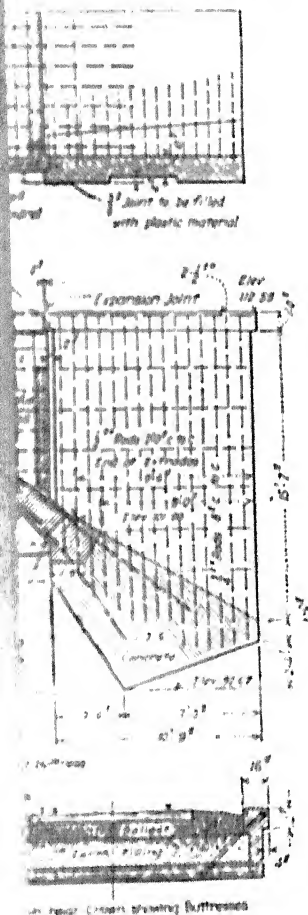


# PLATE 1



(Facing Page 66.)

S

ion prac-  
ling over  
at these  
, in the  
ned that  
greatest  
a general  
and con-  
of pro-  
uctures,  
resses is  
method.  
unity at  
awn for

aximum  
ance in  
ll show  
imilarly  
ccurate  
lines as  
definite  
fluence-  
sen for  
degree

tion.—  
; prac-  
ring in  
averse  
divid-

The

K-7380

## CHAPTER V

### USE OF INFLUENCE LINES IN ARCH ANALYSIS

**33. Advantage of Using Influence Lines.**—It is common practice in arch design to consider the live load as extending over certain definite portions of the span and to assume that these loadings produce the maximum effects. For example, in the design of the arch in the preceding chapter it was assumed that by loading either the whole span or the half span the greatest possible stresses at any given section were obtained. In general this assumption is only a very rough approximation, and considerable inaccuracy may result from such a method of procedure. In fact, in the case of large and important structures, the only satisfactory way to analyze for maximum stresses is by what might be called a *unit-load* or *influence-line* method. By this method the arch is first analyzed for a load of unity at the several load points and then influence lines<sup>1</sup> are drawn for either moment and thrust or for fiber stress.

The position of the live load on an arch to cause maximum stress at any given section cannot be determined in advance in the common method of analysis. An investigation will show that different loadings are required for sections similarly located in arches of different proportions. The only accurate method, then, is to draw a proper number of influence lines as above described. In arches continuously loaded no definite load points exist at which to place the load of unity in influence-line analysis, but in arches of this class points may be chosen for this purpose sufficiently close together to give any desired degree of accuracy.

**34. Analysis of an Arch Ring in Open-spandrel Construction.**—The use of influence lines will be illustrated by giving practically complete computations for the design of an arch ring in open-spandrel construction supporting a series of transverse walls. The only computations omitted will be those for dividing the half arch into ten divisions having constant  $\frac{s}{l}$ . The

<sup>1</sup> Influence lines are treated in "The Elements of Structures" by the same author.

arch to be analyzed is shown in Fig. 20. Loads apply to a longitudinal strip of arch ring 12 in. in width. The notation that will be used is given in Art. 13.

Designing Sheet No. 9 gives the computations needed in determining the moments and thrusts at the crown for a load of unity placed successively at the load points  $L_1, L_2, L_3$ , and  $L_4$ . In a symmetrical arch such as the one under analysis, load points need be taken only to one side of the center of span. The quantity  $m$  (cantilever moment) at a given section for a load of unity at a given load point is equal to the value of  $x$  for the section in question minus the value of  $x$  for the given load point. For example, the value of  $m$  for section 1 with a unit load at  $L_1$

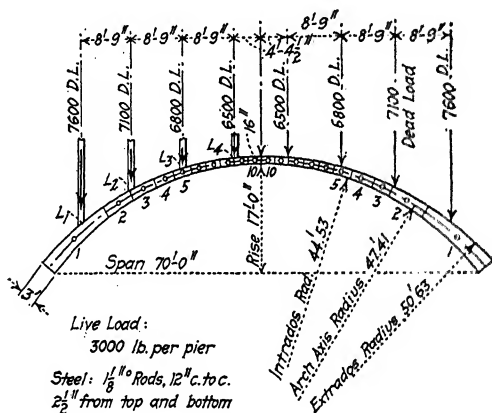


FIG. 20.

equals  $31.70 - 30.62 = 1.08$  ft.-lb. Also the value of  $m$  for section 1 with a unit load at  $L_4$  equals  $31.70 - 4.37 = 27.33$  ft.-lb. The values of the moments and thrusts at the crown were determined by the formulas given on Designing Sheet No. 3.

Designing Sheets Nos. 10 and 10A give the computations and graphical work required in determining the moments and thrusts at the various sections due to the above loadings. The moments and thrusts could all be determined algebraically, but the graphical method is much the simpler. The method of procedure in constructing Designing Sheet No. 10A will be explained by considering a unit load at  $L_4$ .

The values of  $H_c$ ,  $V_c$ , and  $x_c$  (at crown) for this loading are known, having been computed on Designing Sheet No. 9. These

values determine the magnitude, direction, and point of application of the reaction at the crown. The point of application, designated as  $a$  on Designing Sheet No. 10A, is 1.06 ft. from the arch axis and should be laid off above the same, since the sign is plus. The value of  $V_c$  is positive and indicates that the line of pressure slopes upward toward the left. The force polygon for the unit load at  $L_4$  is designated as  $AOC$ . The side  $OA$  is determined by laying off  $AB$  on the vertical side  $AC$  equal to  $V_c$ , and making the horizontal distance  $BO$  equal to  $H_c$ . With  $AC$  as one side of the force polygon made equal to the load of unity, and with  $OA$  equal to the reaction on the right of the arch, the reaction to the left of the point  $L_4$  must equal  $OC$ , or the closing side of the polygon. In order for the forces acting on the arch to be in equilibrium, the forces must act in order around the triangle. This fact shows that  $OC$  acts upward toward the right, as was to be expected.

The equilibrium polygon may thus be determined by drawing a line through the point  $a$  parallel to  $OA$ , and then drawing a line on the left portion of the arch parallel to  $OC$ , both lines intersecting in the load vertical at  $b$ . The bending moment at any section, due to the unit load at  $L_4$ , is therefore equal to the vertical ordinate measured from the arch axis to the equilibrium polygon, multiplied by the force  $H_c$ . If the vertical ordinates be designated in general as  $v_a$ , then, at any section,  $M = H_c v_a$ . The thrusts and shears at any section may be found by resolving the proper reaction into components perpendicular and parallel respectively to the section in question. The values of the moments and thrusts are given in the proper columns on Designing Sheet No. 10. Moments and thrusts for other loadings may be determined in a similar manner.

Influence lines could now be drawn for moment and thrust, but maximum fiber stress does not occur in general for either maximum moment or maximum thrust. Obviously, the true maximum stress occurs for the loading that makes the algebraic sum of the stresses due to moment and thrust a maximum. Influence lines, therefore, should often be drawn directly for outer fiber stress, as such procedure eliminates any necessity for trial loadings.

Before influence lines are plotted, there is no way of telling, for a given maximum condition of loading, whether the stress analysis of a given section will fall under Case I or under Case II



(see Arts. 75 and 76, Volume I)—that is, whether compression will be produced over the entire section or whether a tension will exist over part of the section greater than the allowable tensile strength of the concrete. If the latter condition (Case II) should result, an influence line for fiber stress cannot be employed to determine the corresponding maximum stress, due to the fact that it is impossible, when computing values of the fiber stress for a load of unity at separate load points, to take properly into consideration the exact amount of tensile stress in the concrete that would be neglected if the analysis should be made for the maximum loading using total moment and total thrust. This is not serious, however, since no matter whether maximum stress is desired at an upper or lower fiber, the loading that will produce a maximum value, assuming a Case I distribu-

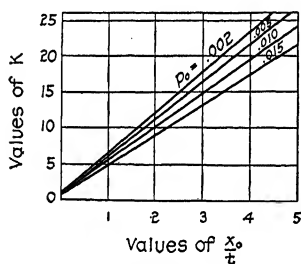


DIAGRAM 1.

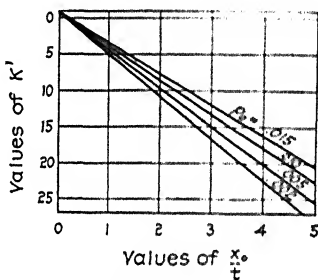


DIAGRAM 2.

tion of stress, will always be the same loading that will cause maximum stress for Case II distribution. Consequently, the influence lines should all be drawn assuming Case I distribution, and, if tension is found greater than the allowable tensile strength of the concrete, the Case II conditions should be separately considered by drawing influence lines for moment and thrust and finding the values of the moments and thrusts that correspond to the Case I loadings for maximum stress.

(If no tension greater than the tensile strength of the concrete is likely to result at any section of the arch, then Designing Sheet No. 10 may be omitted. The values of  $x_0$  and  $N$  may be scaled and used directly in Designing Sheets Nos. 11 and 11A. In fact, even with considerable tension at some sections, not all of Designing Sheet No. 10 will be needed and only those values should be determined as are later found necessary. The de-

signing sheet is given in full here, however, for convenience and for instructive purposes.)

The following formulas refer to Case I:

$$f_c = \frac{NK}{bt}$$

$$f'_c = \frac{NK'}{bt}$$

in which, for reinforcement symmetrical about the center of section,

$$\frac{(K)}{(K')} = \left[ \frac{1}{1 + np_o} \begin{matrix} (+) \\ (-) \end{matrix} \frac{6x_o t}{t^2 + 12np_o r^2} \right]$$

For an embedment of rods equal to one-tenth the depth, and  $n = 15$ ,

$$\frac{(K)}{(K')} = \left[ \frac{1}{1 + 15p_o} \begin{matrix} (+) \\ (-) \end{matrix} \frac{x_o}{t} \cdot \frac{6}{1 + 28.8p_o} \right]$$

Diagrams 1 and 2 give values of  $K$  and  $K'$  for various values of  $p_o$  and  $\frac{x_o}{t}$ , and for one-tenth embedment. These diagrams as

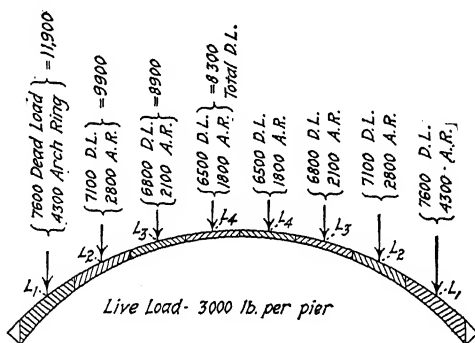


FIG. 21.

presented here are too small for actual use, but illustrate the construction of diagrams which should be drawn to a large scale in practice for at least three depths of embedment—that is, for  $d'$  equal to  $0.05t$ ,  $0.10t$ , and  $0.15t$ . The size of the diagrams should be approximately 30 in. square to obtain a reasonable degree of accuracy. The few values above  $\frac{x_o}{t} = 5.0$  may easily be computed directly from the formulas.

minimum fiber stress (Case I) remain constant for any given section, influence lines drawn for the quantities  $NK$  and  $NK'$  will serve as influence lines for fiber stress. (See Art. 44 for another method of determining fiber stresses.) The values of  $K$  and  $K'$  on Designing Sheets Nos. 11 and 11A have been determined directly from the diagrams, making the assumption, for simplicity, that  $d' = 0.10t$  at all sections. The influence lines resulting from multiplying these values by the thrusts are shown on Designing Sheet No. 12, making no attempt to obtain smooth curves. The full lines are for upper fiber stress and the dot-dash lines for lower fiber stress. Ordinates above the base line indicate compression for both upper and lower fibers.

The maximum fiber stresses (assuming Case I to apply at all sections) are given on Designing Sheet No. 13, considering the weight of the arch ring as applied at the centers of the supports (Fig. 21). The computations are given on this sheet for the maximum stresses at the crown and springing. Notice that tension exists at the springing for loading No. 1—that is, loading for maximum compression in upper fiber—and influence lines for moment and thrust should be drawn if the stresses to loading only are to be determined.

The student should note that where all the loads on an arch are at load points, the actual influence lines need not be drawn. In such a case a table as on Designing Sheet No. 14 may be convenient, the values being taken directly from Designing Sheets Nos. 11 and 11A.

The stresses given on Designing Sheet No. 13 are for loading only, assuming Case I. When stresses are required including temperature and rib shortening, these stresses due to loading should be combined with those for temperature and rib shortening and the resulting stresses computed. When tension exists at any section, due to Case I loading combined with temperature and rib shortening, then influence lines for moment and thrust should be drawn, whether or not such lines are required for loading alone.

Designing Sheet No. 15 gives the total maximum stresses for the four conditions of loading shown, assuming Case I to apply at all sections. The last column gives the sections and loadings that need to be considered for a Case II distribution of stresses. Although the depth of section gradually decreases toward the crown, it is obvious that, for Case II conditions, the stresses

Determination of Moments and Thrusts at Crown  
(Unit Load at Definite Points)

Designing Sheet 9.

Pt.	x	y	x <sup>2</sup>	y <sup>2</sup>	Unit Load at L <sub>1</sub>		Unit Load at L <sub>2</sub>		Unit Load at L <sub>3</sub>		Unit Load at L <sub>4</sub>		
					m	mx	my	m	mx	my	m	mx	my
L <sub>1</sub>	30.62												
L <sub>2</sub>	21.87												
L <sub>3</sub>	13.12												
L <sub>4</sub>	4.37												
1	31.70	12.16	1004.9	147.87	1.08	34.2	13.13	9.83	311.6	119.53	18.58	589.0	225.93
2	24.18	6.63	584.7	43.96				2.31	55.9	15.32	11.06	267.4	73.33
3	19.61	4.25	384.6	18.06							6.49	127.3	27.58
4	16.08	2.80	258.6	7.84							2.96	47.6	8.29
5	13.06	1.85	170.6	3.42									
6	10.33	1.13	106.7	1.28									
7	7.80	.64	60.8	.41									
8	5.43	.30	29.5	.09									
9	3.18	.12	10.1	.01									
10	1.05	.02	1.1	.00									
Σ	29.90	2611.6	222.94	1.08	34.2	13.13	12.14	367.5	134.85	39.09	1031.3	335.13	93.23

Unit Load at L<sub>1</sub>

$$H_c = \frac{10(13.13) - (1.08)(29.90)}{2[10(222.94) - (29.90)^2]} =$$

$$\frac{99.0}{2670.8} = 0.037$$

$$V_c = \frac{34.2}{2(2611.6)} = \frac{34.2}{5223.2} = 0.007$$

$$M_c = \frac{(1.08) - 2(0.037)(29.90)}{(2)(10)} = \frac{-0.057}{20} = -0.003$$

$$x_0 \text{ (at crown)} = \frac{-0.057}{0.037} = -1.54$$

Unit Load at L<sub>2</sub>

$$H_c = \frac{10(134.85) - (12.14)(29.90)}{2670.8} =$$

$$\frac{985.5}{2670.8} = 0.369$$

$$V_c = \frac{367.5}{5223.2} = 0.070$$

$$M_c = \frac{12.14 - (2)(0.369)(29.90)}{20} = \frac{-0.496}{20} = -0.025$$

$$x_0 \text{ (at crown)} = \frac{-0.496}{0.369} = -1.35$$

Unit Load at L<sub>3</sub>

$$H_c = \frac{10(335.13) - (39.09)(29.90)}{2670.8} =$$

$$\frac{2182.5}{2670.8} = 0.818$$

$$V_c = \frac{1031.3}{5223.2} = 0.197$$

$$M_c = \frac{(39.09) - 2(0.197)(29.90)}{20} = \frac{-0.491}{20} = -0.025$$

$$x_0 \text{ (at crown)} = \frac{-0.491}{0.818} = -0.60$$

Unit Load at L<sub>4</sub>

$$H_c = \frac{10(586.56) - (93.23)(29.90)}{2670.8} =$$

$$\frac{3078.0}{2670.8} = 1.151$$

$$V_c = \frac{2040.2}{5223.2} = 0.391$$

$$M_c = \frac{93.23 - (2)(1.151)(29.90)}{20} = \frac{+1.22}{20} = +0.061$$

$$x_0 \text{ (at crown)} = \frac{+1.22}{1.151} = +1.06$$

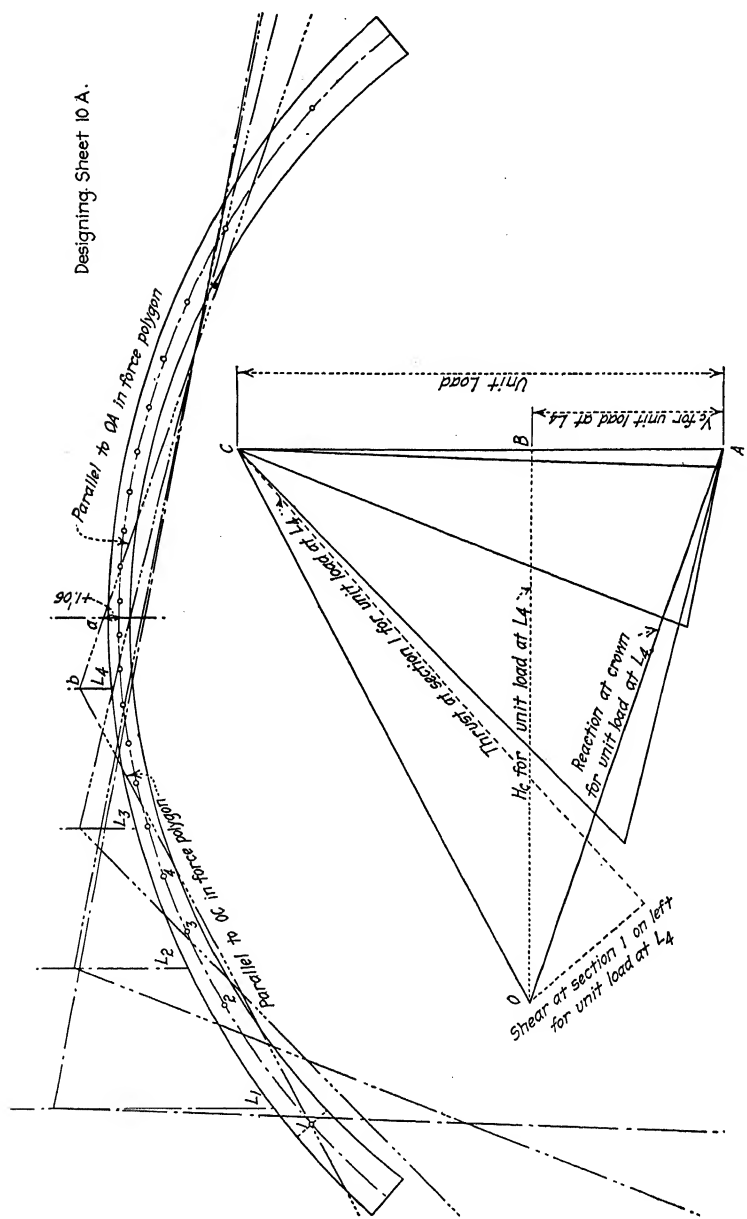
Moments and Thrusts at the Various Sections  
(Unit Load at Definite Points)

Designing Sheet 10

Pt.	Unit Load at $L_1$						Unit Load at $L_2$						Unit Load at $L_3$						Unit Load at $L_4$																	
	$H_c = 0.037$			$M_c = -0.057$			$H_c = 0.369$			$V_c = 0.070$			$M_c = -0.496$			$H_c = 0.818$			$V_c = 0.197$			$M_c = -0.491$			$H_c = 1.151$			$V_c = 0.391$			$M_c = +1.22$					
	Left Half			Right Half			Left Half			Right Half			Left Half			Right Half			Left Half			Right Half			Left Half			Right Half			Left Half			Right Half		
	$V_d$	$M_d$	$H_c V_d$	$N$	$V_d$	$H_c V_d$	$N$	$V_d$	$M_d$	$H_c V_d$	$N$	$V_d$	$M_d$	$H_c V_d$	$N$	$V_d$	$M_d$	$H_c V_d$	$N$	$V_d$	$M_d$	$H_c V_d$	$N$	$V_d$	$M_d$	$H_c V_d$	$N$	$V_d$	$M_d$	$H_c V_d$	$N$	$V_d$	$M_d$	$H_c V_d$	$N$	
Cr	-1.54	-0.57	0.37				-1.35	-0.496	3.69				-0.60	-0.491	8.18																					
Sp	-125.60	-4.647	7.83	+8.62	+319.030		-16.27	-6.004	950	+8.46	+3.122	2.83	-3.21	-2.626	1.142	+7.32	+5.988	6.80	+2.45	+2.850	1.211	+5.50	+6.331	1.044												
1	-11.95	-4.42	6.92	+4.87	+180.035		-9.74	-3.594	8.97	+4.75	+1.753	3.21	-3.42	-2.798	1.145	+3.85	+3.149	7.41	+0.26	+2.293	1.263	+2.40	+2.762	1.119												
2	+9.39	+3.47	0.28	+0.70	+0.26	0.36	+3.58	+1.321	7.95	+0.67	+2.347	3.53	-1.62	-1.325	1.114	+0.15	+1.123	8.04	-1.30	-1.496	1.301	-0.55	-0.633	1.188												
3	+6.23	+2.31	0.90	-0.84	-0.31	0.38	+6.62	+2.443	3.08	-0.82	-3.023	3.65	+0.45	+3.668	1.077	-1.11	-1.908	8.26	-1.23	-1.416	1.298	-1.37	-1.577	1.207												
4	+4.14	+1.53	0.32	-1.63	-0.60	0.38	+4.52	+1.668	3.24	-1.60	-0.590	3.71	+2.49	+2.037	1.043	-1.70	-1.391	8.36	-0.80	-0.921	1.288	-1.60	-1.842	1.215												
5	+2.63	+0.97	0.34	-2.07	-0.77	0.38	+2.95	+1.089	3.37	-2.01	-1.742	3.74	+4.41	+3.607	0.731	-1.95	-1.595	8.41	-0.20	-0.230	1.274	-1.55	-1.764	1.214												
6	+1.45	+0.54	0.35	-2.25	-0.83	0.38	+1.77	+0.653	3.45	-2.18	-0.804	3.75	+3.05	+2.495	0.755	-1.97	-1.611	8.40	+0.56	+0.645	1.255	-1.30	-1.496	1.207												
7	+0.49	+0.18	0.36	-2.30	-0.85	0.38	+0.78	+0.288	3.53	-2.19	-0.808	3.76	+1.83	+1.497	0.776	-1.83	-1.497	8.39	+1.42	+1.634	1.237	-0.92	-1.059	1.200												
8	-0.25	-0.09	0.37	-2.20	-0.81	0.37	0.00	0.000	3.58	-2.06	-0.760	3.75	+1.05	+0.859	0.791	-1.69	-1.309	8.36	+2.35	+2.705	1.213	-0.45	-0.518	1.187												
9	-0.83	-0.31	0.37	-2.01	-0.74	0.37	-0.60	-0.221	3.63	-1.82	-0.672	3.73	+0.34	+0.278	0.804	-1.24	-1.014	8.30	+2.30	+2.647	1.122	+0.12	+0.138	1.174												
10	-1.37	-0.51	0.37	-1.72	-0.64	0.37	-1.15	-0.424	3.68	-1.54	-0.568	3.70	-0.35	-0.286	0.815	-0.83	-0.679	8.24	+1.40	+1.611	1.142	+0.72	+0.829	1.159												

Graphical work on Designing Sheet 10A.

Designing Sheet 10 A.



Designing Sheet 11-

Data for Influence Lines  
 Values of NK and NK' in formulas  $f_c = \frac{NK}{bt}$  and  $f_c' = \frac{NK'}{bt}$  respectively  
 (Unit Load at Definite Points)

Point	P <sub>o</sub>	Unit Load at L <sub>1</sub>										Unit Load at L <sub>2</sub>									
		Left Half					Right Half					Left Half					Right Half				
		$\frac{x_o M}{t}$	K	NK	K'	NK'	$\frac{x_o M}{t}$	K	NK	K'	NK'	$\frac{x_o M}{t}$	K	NK	K'	NK'	$\frac{x_o M}{t}$	K	NK	K'	NK'
Cr.	1.33	0.004	-1.16	6.23	-0.231	4.49	+0.166					-1.01	5.52	-2.037	3.79	+1.399					
Spg.	3.00	0.046	-1.98	11.42	-8.942	9.54	+7.470	+3.55	19.74	+592	17.86	-536	-2.11	12.10	-11.471	10.22	+9.689	+3.56	19.77	+5.793	17.89
1	2.50	0.055	-0.26	2.27	-1.571	0.43	+2.98	+2.06	11.61	+406	9.77	-342	-1.60	9.22	-8.270	7.38	+6.620	+2.18	12.20	+3.916	10.38
2	1.97	0.070	-0.29	32.27	+9.04	30.45	-8.53	+0.37	2.76	+0.99	0.94	-0.34	+0.84	5.10	+4.055	3.28	-2.608	+0.36	2.70	+0.953	0.88
3	1.74	0.079	-0.42	22.45	+6.74	20.77	-6.23	-0.47	3.14	-1.19	1.46	+0.55	+4.56	23.14	+7.127	21.46	-6.610	-0.48	3.19	-1.164	1.51
4	1.56	0.089	-0.06	15.51	+4.96	13.75	-4.40	-1.01	5.71	-2.17	3.95	+1.50	+3.30	16.80	+5.443	15.04	-4.873	-1.02	5.76	-2.137	4.04
5	1.47	0.094	-1.94	10.04	+3.41	8.28	-2.82	-1.36	7.39	-2.81	5.63	+2.14	+2.20	11.26	+3.795	9.50	-3.202	-1.35	7.25	-2.712	5.49
6	1.42	0.097	-1.09	5.98	+2.09	4.24	-1.48	-1.54	8.09	-3.07	6.35	+2.41	+1.33	7.11	+2.453	5.37	-1.853	-1.51	7.95	-2.981	6.21
7	1.37	0.101	-0.37	2.59	+0.93	0.85	-0.31	-1.63	6.45	-3.21	6.71	+2.55	+0.60	3.66	+1.341	1.92	-0.730	-1.57	8.17	-3.105	6.43
8	1.35	0.102	-0.19	1.70	-0.63	0.04	+0.01	-1.62	8.37	-3.10	6.63	+2.45	0.00	0.87	+3.11	0.87	-0.311	-1.50	7.81	-2.929	6.07
9	1.33	0.104	-0.63	3.78	-1.40	2.34	-0.75	-1.50	-2.0	-2.89	6.06	+2.24	-0.46	3.00	-1.089	1.26	+4.57	-1.35	7.11	-2.652	5.37
10	1.33	0.104	-1.04	5.66	-2.09	3.92	+1.46	-1.70	6.2	-2.54	5.15	-1.91	-0.87	4.88	-1.736	3.16	+1.163	-1.15	6.17	-2.283	4.45

\* indicates tension except as noted.

- indicates over fiber

+ indicates under fiber

### Data for Influence Lines

Values of  $NK$  and  $NK'$  in formulas  $f_c = \frac{NK}{b\tau}$  and  $f_c' = \frac{NK'}{b\tau}$  respectively

### Unit Load at Definite Points:

[illegible]

# Indicates upper fiber

— Indicates lower fiber

\* Indicates tension except as noted.



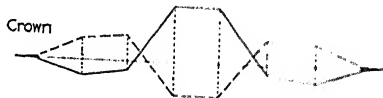
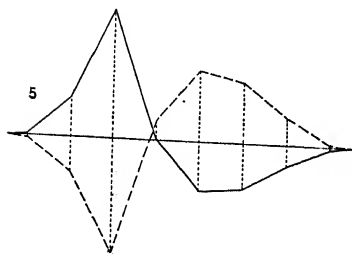
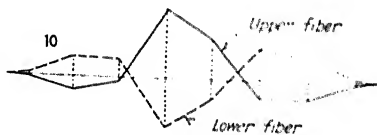
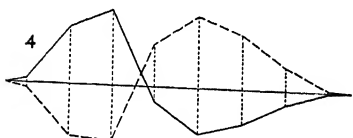
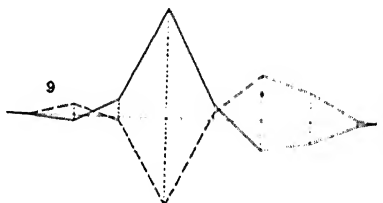
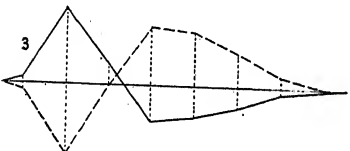
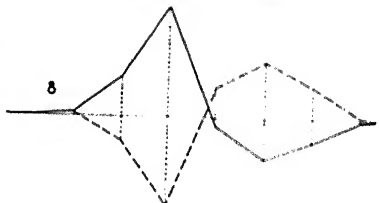
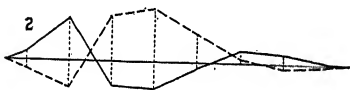
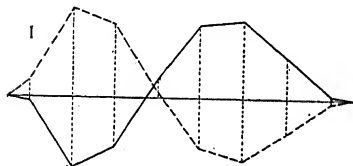
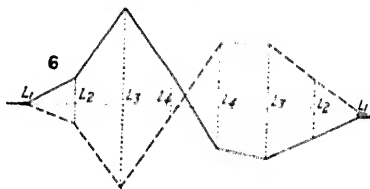
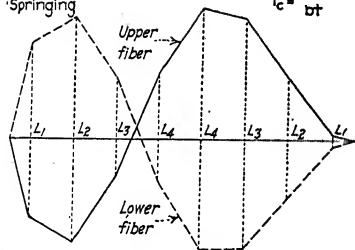
# Influence Lines for NK and NK

Designing Sheet 12.

Springing

$$f_c = \frac{NK}{bt}$$

$$f_c' = \frac{NK'}{bt'}$$



Maximum Stresses Due to Loading Assuming Case I to Apply at All Sections.

Designing Sheet 13.

Maximum Stresses (Loading)

Stress	No. 1 Loading		No. 2 Loading	
	Upper	Lower	Upper	Lower
Max Comp in Upper Fiber	362	81	118	329
Max Comp in Lower Fiber	477	-189	84	199
	354	-5	104	233
	161	198	40	364
	200	131	-22	400
	281	106	-47	488
	489	-76	97	351
	360	44	2	424
	376	59	20	417
	510	-65	187	270
	521	-52	248	214
	362	77	118	324

Crown:

$$\text{Upper} \quad -2(.166)(11,900) - 2(1.399)(9,900) - 2(.990)(8,900) + 2(5.249)(11,300) = 2(34,700)$$

$$f_c = \frac{2(34,700)}{(1.33)(144)} = 362$$

$$\text{Lower} \quad 2(.231)(11,900) + 2(2.037)(9,900) + 2(2.413)(8,900) - 2(3.246)(11,300) = 2(7,700)$$

$$f_c' = \frac{2(7,700)}{(1.33)(144)} = 81$$

$$\text{Upper} \quad -2(.166)(14,900) - 2(1.399)(12,900) - 2(.990)(11,900) + 2(5.249)(8,300) = 2(11,300) - 2(166 + 1,399 + 990) + 5,249(3000)$$

$$f_c' = \frac{2(11,300)}{(1.33)(144)} = 118$$

$$\text{Lower} \quad 2(.231)(14,900) + 2(2.037)(12,900) + 2(2.413)(11,900) - 2(3.246)(8,300) = 2(31,500) - 2(7700) + 2(231 + 2,037 + 2,413 + 3,246)(3000)$$

$$f_c = \frac{2(31,500)}{(1.33)(144)} = 329$$

Springing:

$$\text{Upper} \quad - (7.470)(11,900) + (.592)(14,900) - (9.699)(9,900) + (5.793)(12,900) - (3.586)(8,900) + (11.227)(11,900) + (18.198)(11,300) = 206,100$$

$$f_c = \frac{206,100}{(3.00)(144)} = 477$$

$$\text{Lower} \quad (8.942)(11,900) - (.536)(14,900) + (11.471)(9,900) - (5.242)(12,900) + (5.721)(8,900) - (9.948)(11,900) - (14.032)(11,300) = -81,700$$

$$f_c' = \frac{-81,700}{(3.00)(144)} = 189 \text{ lb. tension}$$

etc.

(For method of computing No. 2 Loading see Designing Sheet 13)

Point	Fiber	L <sub>1</sub>				L <sub>2</sub>				L <sub>3</sub>				L <sub>4</sub>			
		DL=11,900		DL+LL=14,900		DL=9900		DL+LL=12,900		DL=8,900		DL+LL=11,900		DL=6,900		DL+LL=11,300	
		Comp.		Ten.		Comp.		Ten.		Comp.		Ten.		Comp.		Ten.	
		Comp.	Ten.	Comp.	Ten.	Comp.	Ten.	Comp.	Ten.	Comp.	Ten.	Comp.	Ten.	Comp.	Ten.	Comp.	Ten.
Crown	Upper		2(.166)				2(.139)				2(.990)					2(.5249)	
	Lower	2(.231)				2(.203)				2(.2413)							2(.3246)
Spgs	Upper		7.470	.592			9.669	5.793			3.586	11.227				16.067 12.131	
	Lower	8.942			.536	11.471			5.242	5.721			9.948				3.863 10.189
1	Upper		.298	.406			6.620	3.916			4.763	7.217				11.758 16.770	
	Lower	1.571			.342	8.270			3.332	6.870			5.854			.581	4.711
2	Upper			.904 .099				4.055 .953			2.317	1.053				12.576 .523	
	Lower				.853 .034				12.608 .311	4.345		.410			14.944 12.685		
3	Upper		.055	.674			.551	7.127			1.850	1.960				12.908 3.416	
	Lower	.119			.623	1.164			6.610	3.238			.151		13.088 15.444		
4	Upper		.150	.496			1.499	5.443			3.545	7.155				11.700 4.508	
	Lower	.217			.440	2.137			4.873	5.016			5.319		13.967 16.646		
5	Upper		.214	.341			2.053	3.795			4.382	12.237				4.662	.395
	Lower	.281			.282	2.712			3.202	5.862			10.950	6.798		1.847	
6	Upper		.241	.209			2.329	2.453			4.586	8.871				3.874	3.213
	Lower	.307			.148	2.981			1.853	6.048			7.558	5.975			1.029
7	Upper		.255	.093			2.443	1.341			4.398	5.766				2.580	6.655
	Lower	.321			.031	3.105			.730	5.797			4.415	4.668			4.503
8	Upper		.245	.001			2.276	.311			3.762	3.654				7.24	10.323
	Lower	.310		.063		2.929			.311	5.217			2.278	2.789			8.212
9	Upper		.075 .224				.457 12.003				2.805	1.664				10.154 1.514	
	Lower	.140 .289				11.089 12.652				4.250			2.65			.528	8.202
10	Upper		.146 .191				.1163 11.647				1.277 11.648					6.878 3.883	
	Lower	.209 .264				11.796 12.283				11.679 13.065							4.614 1.689

the sections shown on Designing Sheet No. 16 will control. In fact, section 5 might well be omitted, but is given here with the others to show the influence of the depth of section upon the resulting fiber stresses. Notice that although the maximum stress at the springing, given for loading (b) on Designing Sheet No. 15, is very much less than at section 9 for loading (a), the effect of neglecting the tension is much greater for the deeper section, and the actual springing stress is not far from the maximum for the entire arch.

The formulas for fiber stress for Case II are as follows:

$$f_c = \frac{M}{Lbt^2}$$

$$f_s = nf_c \left( \frac{d}{kt} - 1 \right)$$

The value of  $L$  may be determined by means of Diagrams 3 to 6 inclusive. These diagrams are similar to Diagrams 14 and 15



Point	+	P <sub>o</sub>	Type of Loading	Moments and Thrusts										Total Maximum Stresses (Case II)				
				Loading				Fall of Temperature and Rib Shortening		Rise of Temperature and Rib Shortening		Totals						
				No.1 Loading		No.2 Loading		M	N	M	N							
				M	N	M	N											
Spg.	3.00	.0046	(b)	+81,600	76,670			+2,300	-1,990	+3,200	+150	+84,800	76,820	368	.57	.108	606	5,300
5	1.47	.0094	(a)	+18,600	49,700							+20,900	47,710	298	.74	.124	540	1,800
8	1.35	.0102	(a)	+16,200	49,700			+5,600	-2,050			+21,800	47,650	339	.68	.129	644	3,100
9	1.33	.0104	(a)	+15,700	51,070			+5,900	-2,050			+21,600	49,020	331	.695	.129	658	2,900

of Volume I, but are plotted in such a manner as to give greater accuracy.

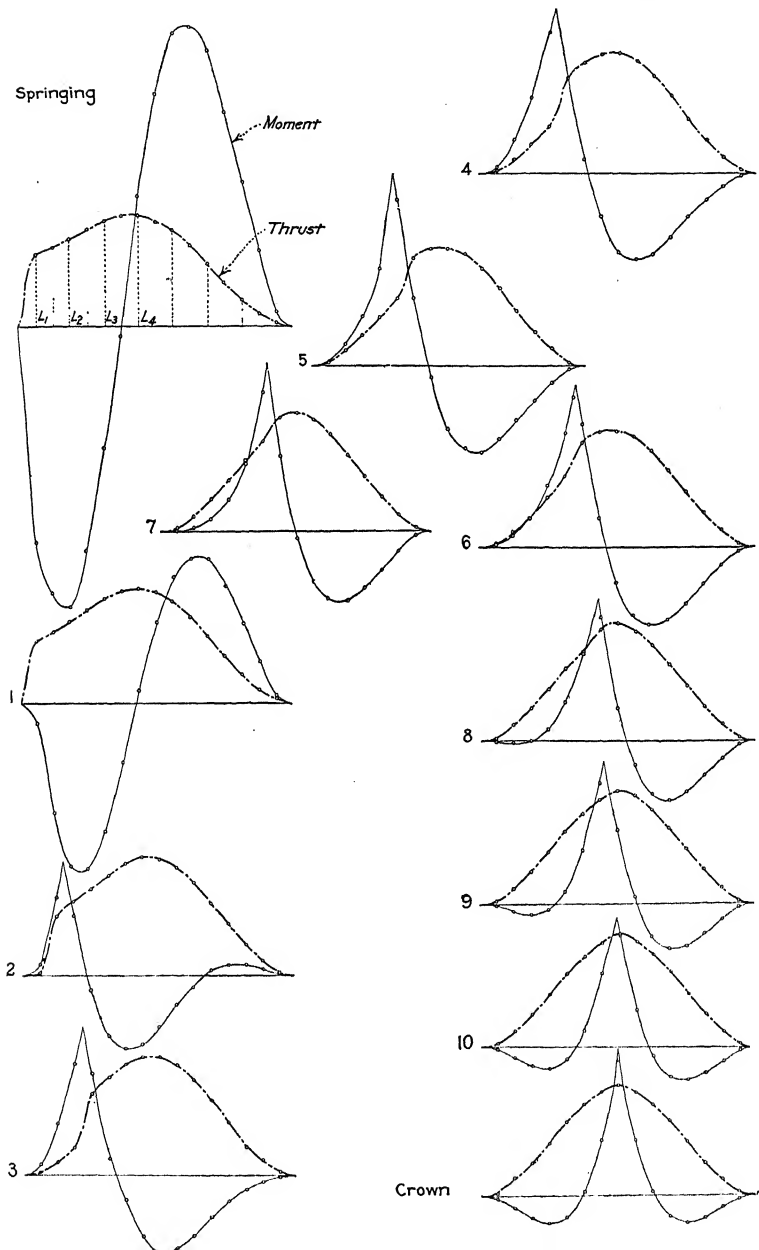
Designing Sheet No. 17 gives the influence lines for moment and thrust for all sections. Although these lines are not actually needed in the problem under consideration, they are presented for instructive purposes. In order to show smooth curves, additional load points have been taken intermediate between the first set, and values of moment and thrust have been computed and plotted at these points.

If the dead weight of the arch ring had been considered as concentrated at seventeen load points (Fig. 21A) instead of eight as in the preceding analysis, a maximum fiber stress at section 9 of 640 lb. per square inch would have been the result. This gives some idea of the increased accuracy that may be obtained by doubling the number of load points. A greater number of such points, however, than just sufficient to determine accurately smooth curves for the influence lines are entirely unnecessary. This is due to the fact that, with influence lines properly drawn, loads may be placed at any point and the values scaled with a reasonable degree of accuracy. Thus for continuous loadings, such as occur in earth-filled arches, four to eight load points on each half of the arch may be sufficient to determine properly the curves of the influence lines, but the continuous loading should be broken up into a greater number of loads than represented by the number of load points in order to obtain accurate values of the maximum fiber stresses at the various sections.

A general discussion in regard to the use of influence lines for moment and thrust may serve to make this part of the subject more clear. Consider influence lines as shown in Fig. 22 and assume uniform live loading. A load placed anywhere on the structure is seen to cause a positive thrust at the given section. For this reason it might seem on first thought that

Influence Lines for Moment and Thrust

Designing Sheet 17



maximum compression on the *upper* fiber will be obtained if the live load extends from *C* to *F*. Loads to the left of *C* and to the right of *F*, however, will also be found to give compression in the upper fiber, although the resultant moment for such loads is

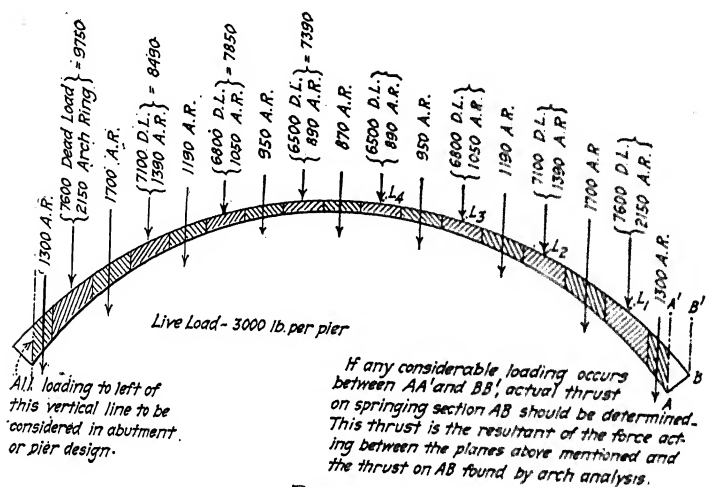


FIG. 21A.

negative. The live load, for example, should extend to points such as *B* and *G* where a load placed at such points will be found to give a zero stress at the upper fiber. Likewise, for maximum compression in the *lower* fiber, the live loading should extend from *A* to *D* and from *E* to *H*. Thus, the termination of the proper

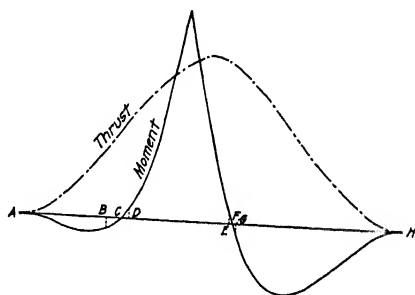
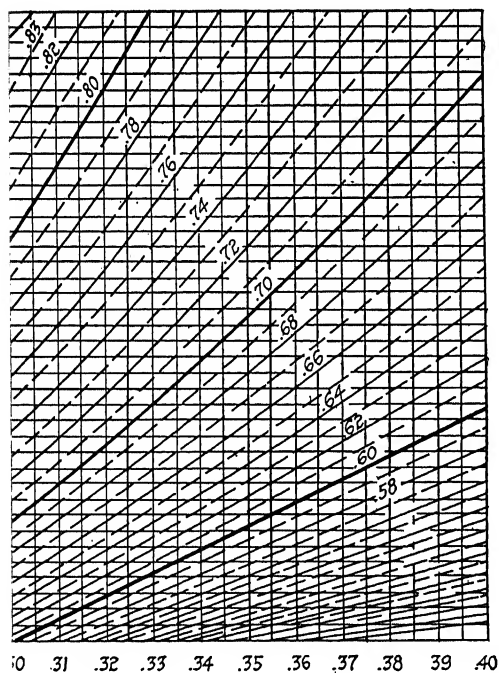
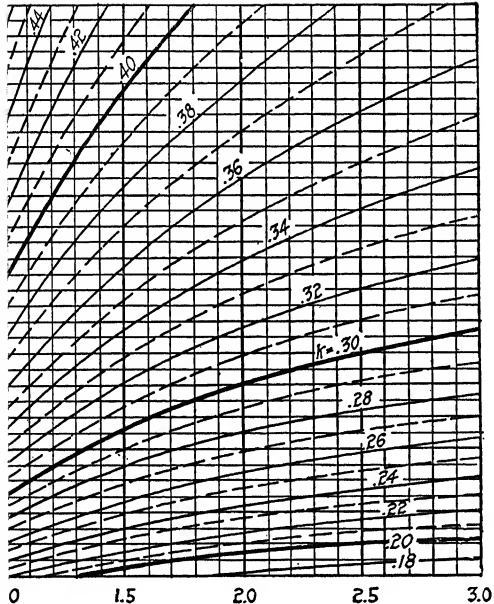


FIG. 22.

steel percentage curve in Diagram 13 of Volume I will give the value of  $\frac{M}{Nt} = \frac{x_o}{t}$  for which there is no tension or compression at the outer fiber, and points *B*, *D*, *E*, and *G* may be determined by trial when influence lines are plotted.



ling  
re-  
sec-  
1A.  
s in  
1 D  
is is  
1 A  
wer  
om-

lear  
axi-  
lb.  
oad  
the  
nch  
hus  
the  
s in  
has  
7 to  
ess.  
ions  
the  
ions  
oad



maxi  
live  
right  
the

1200 A B  
  
All  
this  
'corrs'  
or ph

nega  
such  
to gi  
comp  
A to

steel  
value  
the c  
by ti

stress. With load points widely separated, as in the preceding analysis, it is not often that load points enter the spaces corresponding to  $BD$  and  $EG$ , but this sometimes occurs, as at sections 1, 2, 5, 8, and 9 on Designing Sheets Nos. 11 and 11A. For the section represented in Fig. 22, maximum tensile stress in the lower steel would occur for the live load extending from  $D$  to  $E$ , and for the upper steel from  $A$  to  $B$  and  $G$  to  $H$ . This is obvious when it is considered that a load anywhere between  $A$  and  $D$  and between  $E$  and  $H$  will cause compression in the *lower* steel, while a load anywhere between  $D$  and  $E$  will cause compression in the *upper* steel.

Referring to Designing Sheet No. 16, it should now be clear that the steel stresses there given are not necessarily the maximum stresses. For example, a greater steel stress than 2900 lb. per square inch may be obtained at section 9 if only the dead load is placed at point  $L_4$  on the right half of the arch. Removing the live load at this point causes a stress of 640 lb. per square inch in the concrete and a tensile stress of 3300 lb. in the steel. Thus adding the live load is seen to cause a greater stress in the concrete at the upper fiber, but decreases the tensile stress in the lower steel. In some analyses, where the steel stress has its greatest value under such conditions, it may be necessary to consider the exact loading which will give the maximum stress.

Maximum and minimum pressures on abutment foundations are not necessarily obtained for any of the positions of the live load which give maximum stresses at the various sections in the arch. For abutment design, consideration of live load over the half span and the whole span will usually suffice.

## CHAPTER VI

### UNSYMMETRICAL ARCHES

Unsymmetrical arches are sometimes desirable in the end spans of a series of two or more arches in order to reduce material in abutments and, at the same time, to provide ample waterway area over streams. Also, arches of this type are often necessary under other conditions, as, for example, when a river in a deep ravine is bordered by a railway requiring maximum clearance near the abutments.

**35. Method of Analysis.**—In the analysis of unsymmetrical arches, the entire arch ring should be divided into a sufficient number of  $\frac{s}{l}$  divisions to obtain the desired degree of accuracy. The origin of coördinates may then be taken at the center of any

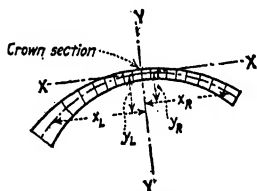


FIG. 23.

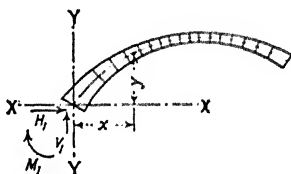


FIG. 24.

one of the sections occurring between the divisional lengths, but, for convenience in scaling the values of  $x$  and  $y$ , this origin should be placed at one of the sections near the crown—which we shall call the crown section. The  $X$  and  $Y$  axes should be drawn perpendicular and parallel respectively to this section so as to permit the crown thrust to be determined directly without composition and resolution of forces. Fig. 23 shows how these axes should be drawn.

The flexure formulas for  $H_c$ ,  $V_c$ , and  $M_c$  for unsymmetrical arches, considering the origin of coördinates near the crown, are exceedingly complex and inconvenient for use in practice. The best plan is to use formulas similar to those designated as (c), (f), and (g), Art. 14, and to solve simultaneously for the above

values after the numerical values of the coefficients are substituted. Following are the formulas to be solved in this way (see also Designing Sheet No. 18):

$$\begin{aligned} H_c \Sigma y^2 + V_c(\Sigma x_{LYL} - \Sigma x_{RYR}) + M_c \Sigma y - \Sigma m y &= 0 \\ H_c(\Sigma x_{LYL} - \Sigma x_{RYR}) + V_c \Sigma x^2 + M_c(\Sigma x_L - \Sigma x_R) \\ &\quad - \Sigma m_L x_L + \Sigma m_R x_R = 0 \\ H_c \Sigma y + V_c(\Sigma x_L - \Sigma x_R) + n M_c - \Sigma m &= 0 \end{aligned}$$

The subscripts *L* and *R* in these formulas refer to summations to the left and right of the crown section respectively. No subscript indicates that the summation is to be taken for the entire arch.

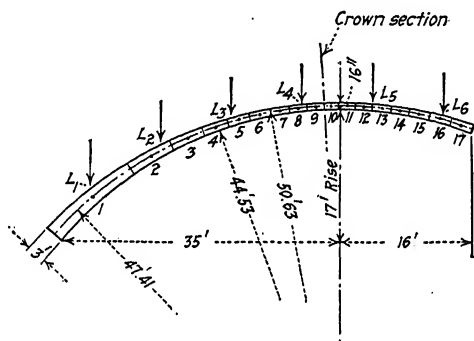


FIG. 25.

The three corresponding equations for temperature are as follows:

$$\begin{aligned} H_c \Sigma y^2 + V_c(\Sigma x_{LYL} - \Sigma x_{RYR}) + M_c \Sigma y - \frac{I}{s} \cdot t_c t_D l E_c &= 0 \\ H_c(\Sigma x_{LYL} - \Sigma x_{RYR}) + V_c \Sigma x^2 + M_c(\Sigma x_L - \Sigma x_R) &= 0 \\ H_c \Sigma y + V_c(\Sigma x_L - \Sigma x_R) + n M_c &= 0 \end{aligned}$$

The value of  $t_D$  should be inserted as plus (+) for a rise of temperature; minus (−) for a drop.

Rib shortening causes the same effect as a lowering of the temperature. By referring to Art. 14, it should be clear that the following formula may be employed to solve for the equivalent temperature drop:

$$\frac{c_a l}{E_c} = t_c t_D l, \text{ or } t_D = \frac{c_a}{E_c t_c}$$

The writer believes that for unsymmetrical arches it is convenient to assume the origin of coördinates at the center of the section through the springing. Fig. 24 shows how the coördi-

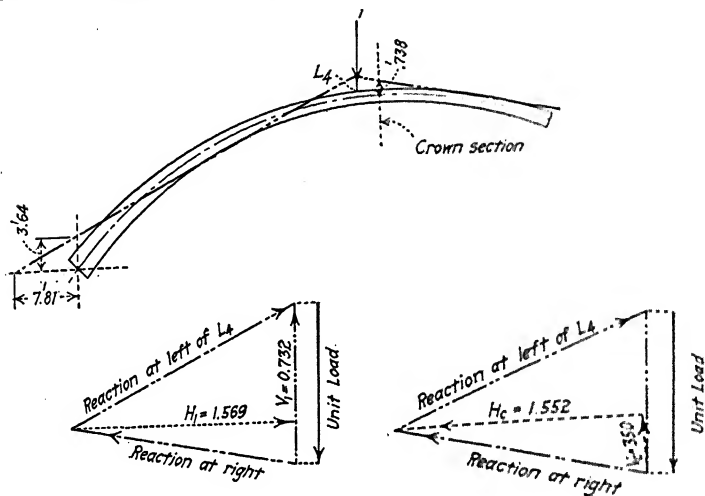


FIG. 26.

ates  $x$  and  $y$  should be measured. The directions of  $H_1$ ,  $V_1$ , and  $M_1$  are shown for values considered as positive in the formulas given on Designing Sheet No. 19. Special note should be made of

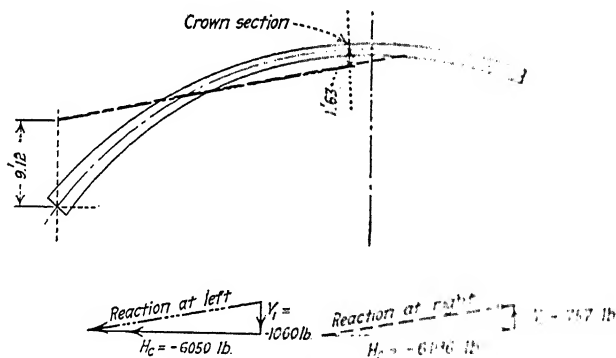


FIG. 27

the fact that values of  $y$  measured below the axis  $X-X$  should always be considered as negative.

**36. Examples of Computations in Unsymmetrical Arch Analysis.**—In order to show the method of analyzing unsym-

metrical arches, the computations are given on Designing Sheet No. 20 for finding the thrust, shear, and moment at the crown section of the arch shown in Fig. 25 due to a unit load at  $L_4$ . (This unsymmetrical arch was obtained by simply shortening the arch of Fig. 20.) Similar computations are given on Designing Sheet No. 21 for finding  $H_1$ ,  $V_1$ , and  $M_1$  at the springing due to the same loading. Fig. 26 shows the agreement between the two methods, the equilibrium polygon being drawn for the unit load at  $L_4$ .

Designing Sheets Nos. 20A and 21A show the temperature computations by the two methods for the arch in question, assuming a drop of temperature of  $40^\circ\text{F}$ . The equilibrium polygon for temperature is a straight line, and Fig. 27 shows the method of determining this line by the two methods.

## Designing Sheet 18.

Formulas Required for Unsymmetrical Arches  
Origin of Coördinates near Crown

Loading:

$$H_c \Sigma y^2 + V_c (\Sigma x_L y_L - \Sigma x_R y_R) + M_c \Sigma y - \Sigma m y = 0$$

$$H_c (\Sigma x_L y_L - \Sigma x_R y_R) + V_c \Sigma x^2 + M_c (\Sigma x_L - \Sigma x_R) - \Sigma m_L x_L + \Sigma m_R x_R = 0$$

$$H_c \Sigma y + V_c (\Sigma x_L - \Sigma x_R) + n M_c - \Sigma m = 0$$

$$M_L = M_c + H_c y_L + V_c x_L - m_L$$

$$M_R = M_c + H_c y_R - V_c x_R - m_R$$

All values of  $m_L$ ,  $m_R$ ,  $x_L$ ,  $x_R$ ,  $y_L$ , and  $y_R$  should be substituted as positive. The subscripts  $L$  and  $R$  refer to summations to left and right of the crown section respectively. No subscript indicates that summation is for entire arch. Positive value of  $M_c$  indicates that the thrust  $H_c$  acts above the arch axis. Considering the crown section as vertical, a positive value of  $V_c$  indicates that the line of pressure slopes upward towards the left; a negative value, downward towards the left. Signs preceding terms  $M_c$ ,  $V_c x_L$ , and  $V_c x_R$  in the last two formulas depend upon the signs of  $M_c$  and  $V_c$  resulting from the three simultaneous equations.

Temperature.

$$H_c \Sigma y^2 + V_c (\Sigma x_L y_L - \Sigma x_R y_R) + M_c \Sigma y - \Sigma t_D \ell E_c = 0$$

$$H_c (\Sigma x_L y_L - \Sigma x_R y_R) + V_c \Sigma x^2 + M_c (\Sigma x_L - \Sigma x_R) = 0$$

$$H_c \Sigma y + V_c (\Sigma x_L - \Sigma x_R) + n M_c = 0$$

$$M_L = M_c + H_c y_L + V_c x_L$$

$$M_R = M_c + H_c y_R - V_c x_R$$

The value of  $t_D$  should be inserted as plus (+) for a rise of temperature; minus (-) for a drop. Signs preceding terms  $M_c$ ,  $H_c y_L$ ,  $H_c y_R$ ,  $V_c x_L$ , and  $V_c x_R$  in the last two formulas depend upon the signs of  $M_c$ ,  $H_c$ , and  $V_c$  resulting from the three simultaneous equations.  $l$  = span of arch axis measured parallel to  $X$  axis.

Rib Shortening:

$$t_D = \frac{c_a}{E_c t_c}$$

Rib shortening causes the same effect as a lowering of the temperature. Solving for  $t_D$  gives equivalent temperature drop.

## Formulas Required for Unsymmetrical Arches

## Origin of Coördinates at Left Springing

Loading:

$$H_1 \Sigma y^2 - V_1 \Sigma xy - M_1 \Sigma y + \Sigma my = 0$$

$$H_1 \Sigma xy - V_1 \Sigma x^2 - M_1 \Sigma x + \Sigma mx = 0$$

$$H_1 \Sigma y - V_1 \Sigma x - nM_1 + \Sigma m = 0$$

$$H_1 = \frac{ab - cd}{ae - cf} \quad \text{or} \quad V_1 = \frac{d - H_1 f}{a} \quad M_1 = \frac{H_1 \Sigma y - V_1 \Sigma x + \Sigma m}{n}$$

in which

$$a = \Sigma x \Sigma y - n \Sigma xy$$

$$b = \Sigma mx \Sigma y - \Sigma x \Sigma my$$

$$c = \Sigma x^2 \Sigma y - \Sigma x \Sigma xy$$

$$d = \Sigma m \Sigma y - n \Sigma my$$

$$e = \Sigma x \Sigma y^2 - \Sigma xy \Sigma y$$

$$f = n \Sigma y^2 - (\Sigma y)^2$$

$$\text{Then } M = M_1 + V_1 x - H_1 y - m$$

All values of  $m$  and  $x$  should be substituted as positive. Values of  $y$  below the  $x - x$  axis should be taken as negative. The summations refer to entire arch. Positive value of  $M_1$  indicates that the reaction acts to the left of the arch axis at the springing. Positive values of  $H_1$  and  $V_1$  indicate that the reaction acts upward to the right. Signs preceding terms  $M_1$ ,  $V_1 x$ , and  $H_1 y$  in the last formula depend upon the signs of  $M_1$ ,  $V_1$ , and  $H_1$  resulting from the preceding equations.

Temperature:

$$H_1 \Sigma y^2 - V_1 \Sigma xy - M_1 \Sigma y = \frac{l}{5} t_c t_D \ell E c$$

$$H_1 \Sigma xy - V_1 \Sigma x^2 - M_1 \Sigma x = 0$$

$$H_1 \Sigma y - V_1 \Sigma x - nM_1 = 0$$

$$H_1 = \frac{a \Sigma x - nc}{ae - cf} (k) \quad \text{or} \quad V_1 = \frac{k \Sigma x - H_1 c}{c} \quad M_1 = \frac{H_1 \Sigma y - V_1 \Sigma x}{n}$$

in which

$$k = \frac{l}{5} t_c t_D \ell E c$$

Then

$$M = M_1 + V_1 x - H_1 y$$

The value of  $t_D$  should be inserted as plus (+) for a rise of temperature; minus (-) for a drop. Signs preceding terms  $M_1$ ,  $V_1$ , and  $H_1$  in the last formula depend upon the signs of  $M_1$ ,  $V_1$ , and  $H_1$  resulting from the preceding equations.  $l$  = span of arch axis measured horizontally; that is, parallel to  $X$  axis.

Rib Shortening.

$$t_D = \frac{c \alpha}{E_c t_c}$$

Rib shortening causes the same effect as a lowering of the temperature. Solving for  $t_D$  gives equivalent temperature drop.



**Determination of Moments and Thrusts at Crown Section - Unsymmetrical Arch  
(Unit Load at Definite Points)**

Designing Sheet 20

$$H_c \ddot{\Sigma} \dot{V}^2 + V_c (\Sigma \ddot{x}_i \dot{V}_i - \Sigma x_{oi} \dot{V}_{oi}) + M_c \Sigma \dot{V} - \Sigma m \dot{V} = 0$$

$$H(\sum x_i v_i - \sum x_p v_p) + V(\sum x^2 + M(\sum x_i - \sum x_p) - \sum m_i x_i + \sum m_p x_p = 0$$

$$H_L \Sigma V + V_L (\Sigma X_i - \Sigma X_P) + \pi M_C - \Sigma \pi = 0$$

$$180.36 H_C + 431.73 V_C + 33.01 M_C - 468.81 = 0 \quad (a)$$

$$431.73 H_C + 2950.6 V_C + 43.60 M_C - 1752.3 = 0 \quad (b)$$

$$33.01 H_C + 43.60 V_C + 17 M_C - 85.96 = 0 \quad (c)$$

MuLtIplIvIng (a) bY 17 and (c) bY 33.01

$$3066.12 H_c + 7339.41 V_c + (33.01 \times 171) M_c - 7969.77 = 0$$

$$1089.66 H_c + 1439.24 V_c + (33.01X/7) M_c - 2837.54 = 0$$

$$1976.46 H_c + 5900.17 V_c - 5132.23 = 0 \quad (d)$$

MuLtIplying (b) by 17 and (c) by 43 60

$$T339.41 \text{ H}_2 + 50.1602 \text{ V}_2 + (43.60 \text{ K } 17) \text{ M}_2 - 29.7891 = 0$$

$$1439.24 \text{ H} + 1900.95 \text{ K} + (43.60 \times 171 \text{ M}) - 37479 = 0$$

5000 17 H + 4825024 V - 36 041250 101

LI 0065 A9 (a) PUB #2 652787 A9 (P) BULK:3417M

$$0 = 0.5 \text{ L} \cdot \text{P} - 1 \text{ L} \cdot 0.05 \text{ M} \cdot \text{P} + 1 \text{ L} \cdot 0.5 \text{ M} \cdot \text{P}$$

[illegible]

**WALSH & COMPANY**

$H_c = 38, 43, 47, 50, 53, 56, 59, 62, 65, 68, 71, 74, 77, 80, 83, 86, 89, 92, 95, 98, 101, 104, 107, 110, 113, 116, 119, 122, 125, 128, 131, 134, 137, 140, 143, 146, 149, 152, 155, 158, 161, 164, 167, 170, 173, 176, 179, 182, 185, 188, 191, 194, 197, 200, 203, 206, 209, 212, 215, 218, 221, 224, 227, 230, 233, 236, 239, 242, 245, 248, 251, 254, 257, 260, 263, 266, 269, 272, 275, 278, 281, 284, 287, 290, 293, 296, 299, 302, 305, 308, 311, 314, 317, 320, 323, 326, 329, 332, 335, 338, 341, 344, 347, 350, 353, 356, 359, 362, 365, 368, 371, 374, 377, 380, 383, 386, 389, 392, 395, 398, 401, 404, 407, 410, 413, 416, 419, 422, 425, 428, 431, 434, 437, 440, 443, 446, 449, 452, 455, 458, 461, 464, 467, 470, 473, 476, 479, 482, 485, 488, 491, 494, 497, 500, 503, 506, 509, 512, 515, 518, 521, 524, 527, 530, 533, 536, 539, 542, 545, 548, 551, 554, 557, 560, 563, 566, 569, 572, 575, 578, 581, 584, 587, 590, 593, 596, 599, 602, 605, 608, 611, 614, 617, 620, 623, 626, 629, 632, 635, 638, 641, 644, 647, 650, 653, 656, 659, 662, 665, 668, 671, 674, 677, 680, 683, 686, 689, 692, 695, 698, 701, 704, 707, 710, 713, 716, 719, 722, 725, 728, 731, 734, 737, 740, 743, 746, 749, 752, 755, 758, 761, 764, 767, 770, 773, 776, 779, 782, 785, 788, 791, 794, 797, 800, 803, 806, 809, 812, 815, 818, 821, 824, 827, 830, 833, 836, 839, 842, 845, 848, 851, 854, 857, 860, 863, 866, 869, 872, 875, 878, 881, 884, 887, 890, 893, 896, 899, 902, 905, 908, 911, 914, 917, 920, 923, 926, 929, 932, 935, 938, 941, 944, 947, 950, 953, 956, 959, 962, 965, 968, 971, 974, 977, 980, 983, 986, 989, 992, 995, 998, 1001, 1004, 1007, 1010, 1013, 1016, 1019, 1022, 1025, 1028, 1031, 1034, 1037, 1040, 1043, 1046, 1049, 1052, 1055, 1058, 1061, 1064, 1067, 1070, 1073, 1076, 1079, 1082, 1085, 1088, 1091, 1094, 1097, 1100, 1103, 1106, 1109, 1112, 1115, 1118, 1121, 1124, 1127, 1130, 1133, 1136, 1139, 1142, 1145, 1148, 1151, 1154, 1157, 1160, 1163, 1166, 1169, 1172, 1175, 1178, 1181, 1184, 1187, 1190, 1193, 1196, 1199, 1202, 1205, 1208, 1211, 1214, 1217, 1220, 1223, 1226, 1229, 1232, 1235, 1238, 1241, 1244, 1247, 1250, 1253, 1256, 1259, 1262, 1265, 1268, 1271, 1274, 1277, 1280, 1283, 1286, 1289, 1292, 1295, 1298, 1301, 1304, 1307, 1310, 1313, 1316, 1319, 1322, 1325, 1328, 1331, 1334, 1337, 1340, 1343, 1346, 1349, 1352, 1355, 1358, 1361, 1364, 1367, 1370, 1373, 1376, 1379, 1382, 1385, 1388, 1391, 1394, 1397, 1400, 1403, 1406, 1409, 1412, 1415, 1418, 1421, 1424, 1427, 1430, 1433, 1436, 1439, 1442, 1445, 1448, 1451, 1454, 1457, 1460, 1463, 1466, 1469, 1472, 1475, 1478, 1481, 1484, 1487, 1490, 1493, 1496, 1499, 1502, 1505, 1508, 1511, 1514, 1517, 1520, 1523, 1526, 1529, 1532, 1535, 1538, 1541, 1544, 1547, 1550, 1553, 1556, 1559, 1562, 1565, 1568, 1571, 1574, 1577, 1580, 1583, 1586, 1589, 1592, 1595, 1598, 1601, 1604, 1607, 1610, 1613, 1616, 1619, 1622, 1625, 1628, 1631, 1634, 1637, 1640, 1643, 1646, 1649, 1652, 1655, 1658, 1661, 1664, 1667, 1670, 1673, 1676, 1679, 1682, 1685, 1688, 1691, 1694, 1697, 1700, 1703, 1706, 1709, 1712, 1715, 1718, 1721, 1724, 1727, 1730, 1733, 1736, 1739, 1742, 1745, 1748, 1751, 1754, 1757, 1760, 1763, 1766, 1769, 1772, 1775, 1778, 1781, 1784, 1787, 1790, 1793, 1796, 1799, 1802, 1805, 1808, 1811, 1814, 1817, 1820, 1823, 1826, 1829, 1832, 1835, 1838, 1841, 1844, 1847, 1850, 1853, 1856, 1859, 1862, 1865, 1868, 1871, 1874, 1877, 1880, 1883, 1886, 1889, 1892, 1895, 1898, 1901, 1904, 1907, 1910, 1913, 1916, 1919, 1922, 1925, 1928, 1931, 1934, 1937, 1940, 1943, 1946, 1949, 1952, 1955, 1958, 1961, 1964, 1967, 1970, 1973, 1976, 1979, 1982, 1985, 1988, 1991, 1994, 1997, 2000, 2003, 2006, 2009, 2012, 2015, 2018, 2021, 2024, 2027, 2030, 2033, 2036, 2039, 2042, 2045, 2048, 2051, 2054, 2057, 2060, 2063, 2066, 2069, 2072, 2075, 2078, 2081, 2084, 2087, 2090, 2093, 2096, 2099, 2102, 2105, 2108, 2111, 2114, 2117, 2120, 2123, 2126, 2129, 2132, 2135, 2138, 2141, 2144, 2147, 2150, 2153, 2156, 2159, 2162, 2165, 2168, 2171, 2174, 2177, 2180, 2183, 2186, 2189, 2192, 2195, 2198, 2201, 2204, 2207, 2210, 2213, 2216, 2219, 2222, 2225, 2228, 2231, 2234, 2237, 2240, 2243, 2246, 2249, 2252, 22$

Subject: *History of the U.S.*

306747 + 5000 17 1/2 - 51323 = 0

2007/08

Substituting values of  $H_2$  and  $K_2$  in (2)

6-23-82-1711-0506-3

1961

$$x_0 = \frac{1.145}{.001} = 738 \text{ ft.}$$

$$x_0 = \frac{57}{1}$$

# UNSYMMETRICAL ARCHES

Determination of Moment and Thrust at Crown Section- Unsymmetrical Arch  
(Temperature Fall of 40°F.)

Designing Sheet 20 A.

$$H_c \Sigma y^2 + V_c (\Sigma x_L y_L - \Sigma x_R y_R) + M_c \Sigma y - \frac{I}{3} \cdot \frac{t_c}{D} \cdot \ell E_c = 0$$

$$H_c (\Sigma x_L y_L - \Sigma x_R y_R) + V_c \Sigma x^2 + M_c (\Sigma x_L - \Sigma x_R) = 0$$

$$H_c \Sigma y + V_c (\Sigma x_L - \Sigma x_R) + n M_c = 0$$

$$180.36 H_c + 431.73 V_c + 33.01 M_c + (.125)(.000006)(40)(52.95)(2,000,000)(144) = 0$$

$$431.73 H_c + 2950.6 V_c + 43.60 M_c = 0 \quad (b)$$

$$33.01 H_c + 43.60 V_c + 17 M_c = 0 \quad (c)$$

Multiplying (a) by 17 and (c) by 33.01

$$3066.12 H_c + 7339.41 V_c + (33.01)(17) M_c + 7,777,296 = 0$$

$$1089.66 H_c + 1439.24 V_c + (33.01)(17) M_c = 0$$

$$1976.46 H_c + 5900.17 V_c + 7,777,296 = 0 \quad (d)$$

Multiplying (b) by 17 and (c) by 43.60

$$7339.41 H_c + 50,160.2 V_c + (43.60)(17) M_c = 0$$

$$1439.24 H_c + 1900.96 V_c + (43.60)(17) M_c = 0$$

$$5900.17 H_c + 48,259.24 V_c = 0 \quad (e)$$

Multiplying (d) by 48,259.24 and (e) by 5900.17

$$95,382,457.49 H_c + (48,259.24)(5900.17) V_c + 375,326,394,215 = 0$$

$$34,812,006.03 H_c + (48,259.24)(5900.17) V_c = 0$$

$$60,570,451 H_c = -375,326,394,215$$

$$H_c = -6,196 \text{ lb}$$

Substituting value of  $H_c$  in (d)

$$-12,246,146 + 5900.17 V_c + 7,777,296 = 0$$

$$V_c = \frac{4,468,850}{5900.17} = 757 \text{ lb.}$$

Substituting values of  $H_c$  and  $V_c$  in (c)

$$-204,530 + 33,005 + 17 M_c = 0$$

$$M_c = \frac{171,525}{17} = 10,090 \text{ ft lb}$$

$$x_o = \frac{10,090}{6196} = -1.63 \text{ ft.}$$

Determination of Moments and Thrusts at Springing - Unsymmetrical Arch  
(Unit Load at Definite Points)

Pt.	x	y	xy	x <sup>2</sup>	y <sup>2</sup>	Unit Load at L <sub>4</sub>		
						m	mx	my
L <sub>1</sub>	4.38				20.25			
L <sub>2</sub>	13.13			138.8	100.00			
L <sub>3</sub>	21.08			266.7	153.76			
L <sub>4</sub>	30.63			393.6	190.99			
L <sub>5</sub>	39.37			522.6	239.93			
L <sub>6</sub>	48.12			652.3	241.18			
1	4.33	4.50	19.49	18.7	20.25	96	61.3	32.32
2	11.78	10.00	117.60	138.8	100.00	4.5	14.7	62.39
3	16.33	12.40	202.49	266.7	153.76	6.7	23.4	24.89
4	19.84	13.82	274.19	393.6	190.99	8.7	32.6	32.86
5	22.86	14.23	325.21	522.6	239.93	8.4	42.8	32.26
6	23.84	5.53	132.64	652.3	241.18	2.5	12.5	2.50
7	23.27	5.02	117.24	535.5	252.64	2.2	11.2	2.20
8	21.77	5.29	115.16	465.7	279.83	2.7	13.7	2.70
9	21.12	5.42	115.67	447.0	293.77	2.7	13.7	2.70
10	24.74	5.77	142.52	612.9	332.89	2.4	12.4	2.40
11	31.30	6.77	211.71	979.1	458.29	2.0	10.0	2.00
12	34.36	6.87	236.02	1180.6	470.93	2.0	10.0	2.00
13	40.00	6.87	273.00	1600.0	470.93	2.0	10.0	2.00
14	43.22	6.87	296.83	1868.6	470.93	2.0	10.0	2.00
15	43.13	5.79	249.81	1860.6	335.24	2.0	10.0	2.00
16	43.13	1.3	56.07	1860.6	1.69	2.0	10.0	2.00
17	43.13	1.3	56.07	1860.6	1.69	2.0	10.0	2.00
Σ	571.8	242.55	1242.15	1242.15	2720.85	96.2	432.9	5.64

Designing Sheet 21.

$$H_1 = \frac{ab - cd}{ae - cf}$$

$$a = \Sigma x \Sigma y - n \Sigma xy$$

$$b = \Sigma mx \Sigma y - \Sigma x \Sigma my$$

$$c = \Sigma x^2 \Sigma y - \Sigma x \Sigma xy$$

$$d = \Sigma m \Sigma y - n \Sigma my$$

$$e = \Sigma x \Sigma y^2 - \Sigma xy \Sigma y$$

$$f = n \Sigma y^2 - (\Sigma y)^2$$

$$V_1 = \frac{d - H_1 f}{a}$$

$$H_1 = \frac{H_1 \Sigma y - V_1 \Sigma x + \Sigma m}{n}$$

$$a = (531.38)(248.25) - (17)(8248.06) = -8,301.93$$

$$b = (4307.9)(248.25) - (531.38)(1517.64) = 261,751.39$$

$$c = (19,407.0)(248.25) - (531.38)(8248.06) = 434,933.63$$

$$d = (96.63)(248.25) - (17)(1517.64) = -1,811.48$$

$$e = (531.38)(3785.23) - (8248.06)(248.25) = -36,185.38$$

$$f = (17)(3785.23) - (248.25)^2 = 2720.85$$

$$H_1 = \frac{(-8,301.93)(261,751.39) - (434,933.63)(-1,811.48)}{(-8,301.93)(-36,185.38) - (434,933.63)(2,720.85)} = \frac{-2,138,568.45}{-882,980.675} = 2.423$$

$$V_1 = \frac{d - H_1 f}{a} = \frac{(-1,811.48) - (2.423)(2,720.85)}{-8,301.93} = \frac{-6,260.49}{-8,301.93} = 0.753$$

$$H_1 = \frac{(1,569)(248.25) - (10)(32,453.38) + 96.63}{17} = \frac{97.16}{17} = 5.715$$

$$x_2 = \frac{5.715}{0.712} = 7.81 \text{ ft.}$$

$$x_2 = \frac{5.715}{0.712} = 7.81 \text{ ft.}$$

$$x_2 = \frac{5.715}{0.712} = 7.81 \text{ ft.}$$

Determination of Moment and Thrust at Springing - Unsymmetrical Arch  
(Temperature fall of 40°F.)

Designing Sheet 21A.

$$H_1 = \frac{a \Sigma x - \pi c}{ae - cf} \cdot (k)$$

$$k = \frac{I}{S} \cdot t_c \cdot t_b \cdot \ell E_c$$

$$V_1 = \frac{k \Sigma x - H_1 a}{c}$$

$$= (.125)(.000006)(-40)(52.4)(2,000,000)(.144) \\ = -452,736$$

$$M_1 = \frac{H_1 I y - V_1 \Sigma x}{n}$$

$$H_1 = \frac{(-8301.93)(531.38) - (17)(434,933.63)}{-882,980,675} \cdot (-452,736) = -6050 \text{ lb.}$$

$$V_1 = \frac{(-452,736)(531.38) - (6050)(-36,185.38)}{434,933.63} = -1060 \text{ lb.}$$

$$M_1 = \frac{(-6050)(248.25) - (-1060)(531.38)}{17} = -55,215 \text{ ft. lb.}$$

$$x_o \text{ (vertically)} = \frac{-55,215}{-6050} = 9.12 \text{ ft.}$$

## CHAPTER VII

### ARCHES WITH ELASTIC PIERS

The necessity for considering relatively thin piers elastic was probably brought to public attention by Mr. Daniel B. Luten of Indianapolis, as early as the year 1904. Undoubtedly the idea came from his experience with the design of the arch bridge across the Wabash River at Peru, Ind., in which the conditions for a satisfactory design required the balancing of thrusts of unequal spans by introducing a moment in the piers.<sup>1</sup> Whether or not the idea was brought forward in this way, it is a fact that Mr. Luten since the Peru bridge experience has built many arch bridges with unusually thin piers, two of the more pronounced



*Courtesy of Mr. Daniel B. Luten, Consulting Engineer, Indianapolis.*

FIG. 28.—Venore bridge over Tellico River, Venore, Tenn.  
(Twin spans of 65 ft. each.)

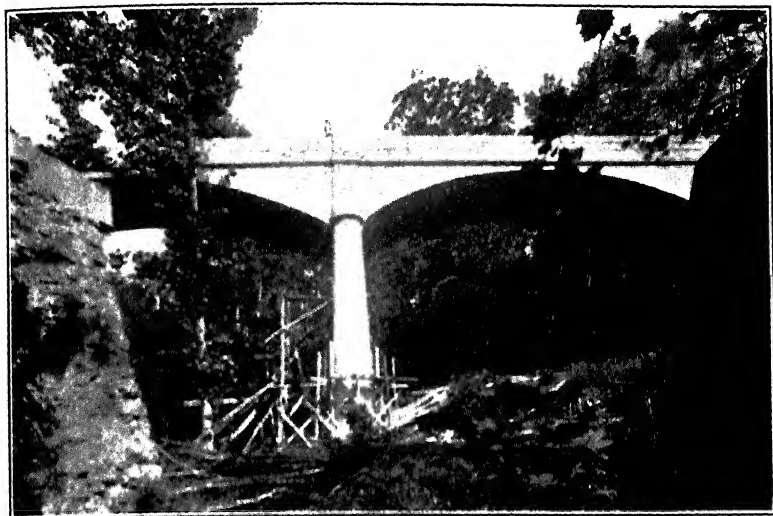
structures of this class being shown in Figs. 28 and 29. Mr. A. C. Janni has also made use of the elastic-pier principle in the Kings-highway viaduct, recently constructed at St. Louis, in which the arches and piers were analyzed as a continuous elastic body.

Arches with elastic piers are undoubtedly somewhat more difficult to analyze than single arches extending only from springing to springing, but this does not change the fact that a great number of arch bridges of multiple spans have piers which should be considered as elastic if a thorough analysis is to be made. In any given structure, good judgment should be exercised in determining whether or not the piers are of such slender pro-

<sup>1</sup>*Engineering News*, Mar. 29, 1906.

portions that the bending due to unequal arch thrusts should be considered.

Thin piers not only save concrete in most cases but increase the area of waterway and, on this account, it is quite likely that elastic piers will be much used in the future where architectural appearance is satisfied with this type of construction. In some cases, however, increased thickness of arch rings in elastic-pier construction will offset any advantage gained from diminishing the cross-sectional area of the piers.



*Courtesy of Mr. Daniel B. Luten, Consulting Engineer, Indianapolis.*

FIG. 29. Paint Branch bridge near Washington, D. C.  
(Three spans of 60 ft. each.)

**37. Method of Analysis.** Very few American engineers have made any attempt to analyze arches having elastic piers, due undoubtedly to a lack of textbook material on the subject. Up to the present time,<sup>1</sup> the method outlined by Mr. A. C. Janni in the *Journal of the Western Society of Engineers*, May, 1913, and described in the next chapter, is, as far as the writer knows, the only published treatment of arch analysis in this country giving some attention to elastic-pier construction. In the paper referred to, Mr. Janni presents a graphical treatment for the analysis of arches for any and all conditions based on the theory of the ellipse of elasticity. The method to be proposed

in this article, however, will not differ in principle from the analysis previously presented in this text for single symmetrical and unsymmetrical arches.

Consider first the two-span arch structure represented in Fig. 30. The points indicated as fixed may be the bottoms of the pier and abutments, or they may be at intermediate sections, depending upon where the designer considers the structure fixed. The method proposed is to take a horizontal section  $A - A$  where arches and pier join and study the movement at that section.

In Art. 14 the method employed in deriving formulas for the thrust, shear, and moment at the crown of a symmetrical arch was to cut the arch at the crown and study the horizontal,

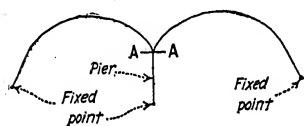


FIG. 30.

vertical, and angular moments of the cantilever on the left with respect to similar movements of the cantilever on the right. From the formulas for deflection of curved beams, three independent equa-

tions were possible and expressions for the three unknowns ( $H_c$ ,  $V_c$ , and  $M_c$ ) were then derived.

A similar method may be followed in finding expressions for the forces acting at the horizontal section  $A - A$  in Fig. 30. The thrust from the left arch and the thrust from the right arch combine to produce a resultant thrust on the pier. There are three unknowns with respect to each arch—that is, six unknowns in all, since there is a known relation between the thrust on the pier and the thrusts from the arches. Three independent equations may be written by placing the vertical, horizontal, and angular movements of the pier end of the left arch algebraically equal to similar movements respectively of the pier end of the right arch. The other three independent equations required may be written by placing the vertical, horizontal, and angular movements of the pier end of either arch algebraically equal to similar movements respectively of the top of the pier. These independent equations may be simplified and changed somewhat by placing the vertical movement of the section  $A - A$  (due to loading) equal to zero, since this may be done without any appreciable error.

In Fig. 31 the top of the pier is shown in detail. The horizontal section  $A - A$  may be assumed to be at the top of the pier, which

arches. What may be called the skewbacks of the arches are shown. The weight of the material between the skewbacks and the section  $A - A$  need be considered only in finding the resultant thrusts on the pier sections. The origin of coördinates  $x$  and  $y$  for each arch may be taken at the middle point  $C$  of the section  $A - A$  instead of at the center of the skewbacks. This should be obvious from a study of the derivation of the deflection formulas of Chapter II.

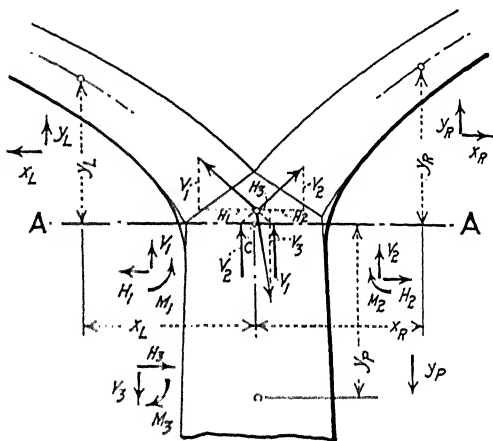


FIG. 31.

The following notation will be employed:

Let

$x_L, y_L$  coördinates of any point on the axis of the left arch referred to the center of the section  $A - A$  as origin. Values of  $y_L$  should be considered plus when measured above the axis  $A - A$ , and as negative when measured below that axis.

$x_R, y_R$  coördinates of any point on the axis of the right arch referred to the center of the section  $A - A$  as origin. Values of  $y_R$  should be considered plus when measured above the axis  $A - A$ , and as negative when measured below that axis.

$y_P$  depth of any point on the vertical axis of the pier below the section  $A - A$ .



$m_L, m_R$  = moment at any point on axis of left arch and right arch respectively of all external loads between the point in question and the top of the pier.

$M_L, M_R, M_P$  = moment at any point on axis of left arch, right arch, and pier respectively.

$n_L, n_R, n_P$  = number of  $\frac{S}{I}$  divisions in the left arch, right arch, and pier respectively.

$c_L, c_R, c_P$  = values of  $\frac{S}{I}$  for left arch, right arch, and pier respectively.

$H_1, V_1$  = horizontal and vertical components of the thrust from the left arch at the top of pier.

$M_1$  = moment at section  $A-A$  due to thrust from left arch vertical component of thrust from left arch multiplied by the distance from the point  $C$  (the center of the section) to where this thrust produced cuts the section  $A-A$ .

$H_2, V_2$  = horizontal and vertical components of the thrust from the right arch at the top of pier.

$M_2$  = moment at section  $A-A$  due to thrust from right arch.

$H_3$  = resultant shear on section  $A-A = H_1 - H_2$ .

$V_3$  = resultant thrust normal on section  $A-A = V_1 + V_2$ .

$M_3$  = resultant moment on section  $A-A = M_1 - M_2$ .

Other notation that will be used is given in Art. 13. The arrows in Fig. 31 indicate what will be considered positive values of the quantities.

Referring to Chapter II on "Deflection of Curved Beams," we have

$$\begin{array}{ll} c_L \Sigma M_L y_L & c_R \Sigma M_R y_R \\ c_L \Sigma M_L x_L & 0 \\ c_R \Sigma M_R x_R & 0 \\ c_L \Sigma M_L & c_R \Sigma M_R \\ c_P \Sigma M_P y_P & c_P \Sigma M_P y_P \\ c_P \Sigma M_P & c_P \Sigma M_P \end{array}$$

## Designing Sheet 22.

## Formulas Required-Arches with Elastic Piers

Loading:

$$\begin{aligned} C_L (M_1 \Sigma y_L - H_1 \Sigma y_L^2 + V_1 \Sigma x_L y_L - \Sigma m_L y_L) = \\ - C_R (M_2 \Sigma y_R - H_2 \Sigma y_R^2 + V_2 \Sigma x_R y_R - \Sigma m_R y_R) \end{aligned}$$

$$M_1 \Sigma x_L - H_1 \Sigma x_L y_L + V_1 \Sigma x_L^2 - \Sigma m_L x_L = 0$$

$$M_2 \Sigma x_R - H_2 \Sigma x_R y_R + V_2 \Sigma x_R^2 - \Sigma m_R x_R = 0$$

$$\begin{aligned} C_L (\pi_L M_1 - H_1 \Sigma y_L + V_1 \Sigma x_L - \Sigma m_L) = \\ - C_R (\pi_R M_2 - H_2 \Sigma y_R + V_2 \Sigma x_R - \Sigma m_R) \end{aligned}$$

$$\begin{aligned} C_P [(M_1 - M_2) \Sigma y_P + (H_1 - H_2) \Sigma y_P^2] = C_L [M_1 \Sigma y_L - H_1 \Sigma y_L^2 + V_1 \Sigma x_L y_L - \Sigma m_L y_L] \\ C_P [\pi_P (M_1 - M_2) + (H_1 - H_2) \Sigma y_P] = -C_L [\pi_L M_1 - H_1 \Sigma y_L + V_1 \Sigma x_L - \Sigma m_L] \end{aligned}$$

Bending Moment at any point:

$$M_L = M_1 - H_1 y_L + V_1 x_L - m_L$$

$$M_R = M_2 - H_2 y_R + V_2 x_R - m_R$$

$$M_P = (M_1 - M_2) + (H_1 - H_2) y_P$$

Values of  $y_L$  and  $y_R$  should be considered plus when measured above the axis  $A-A$ , and as negative when measured below that axis. The values of  $H_3$ ,  $V_3$ , and  $M_3$  may be obtained from the following relations:

$$H_3 = H_1 - H_2$$

$$V_3 = V_1 + V_2$$

$$M_3 = M_1 - M_2$$

All values of  $m_L$  and  $m_R$  should be substituted as positive.

The bending moment at any point may be expressed as follows:

$$M_L = M_1 - H_1 y_L + V_1 x_L - m_L$$

$$M_R = M_2 - H_2 y_R + V_2 x_R - m_R$$

$$M_P = M_3 + H_3 y_P = (M_1 - M_2) + (H_1 - H_2) y_P$$

Substituting these expressions in the preceding equations and combining terms, we have the six simultaneous equations given on Designing Sheet No. 22. These six equations may now be solved simultaneously for the values of  $H_1$ ,  $V_1$ ,  $M_1$ ,  $H_2$ ,  $V_2$ , and  $M_2$ . The values of  $H_3$ ,  $V_3$ , and  $M_3$  may then be obtained from the following relations:

$$H_3 = H_1 - H_2$$

$$V_3 = V_1 + V_2$$

$$M_3 = M_1 - M_2$$

For arch bridges symmetrical about the center line of pier, the labor involved in solving the simultaneous equations mentioned above will be greatly reduced.

All the simultaneous equations given above pertain to the unknown forces acting at the section  $A - A$ . With these completely determined, however, the moment and thrust at any section may be found in the manner described for the single symmetrical arch. Each of the three members, of course, must be considered separately and each subjected to exactly the same force that is found to act upon it at the top of pier in the monolithic structure.

Consider now the case of a three-span arch bridge, as represented in Fig. 32. The portion of the structure shown by a solid line should be treated first, solving for the unknowns at section  $A$ . The dotted portion should next be considered, solving for the unknowns at section  $B$  but placing at  $A$  the thrust coming from (or acting upon) the left arch for the given loading. The process may now be repeated by considering the solid portion again and solving for the unknowns at  $A$ , but placing at  $B$  the thrust coming from (or acting upon) the right arch for the given loading. Likewise in treating the dotted portion the second time, more accurate values of the unknowns at  $B$  may be determined by placing at  $A$  the second value obtained for the thrust.

from (or acting upon) the left arch. It will be only in exceptional cases that the unknowns at sections *A* and *B* will need to be solved more than once in order to obtain sufficient accuracy. In fact, solving for the unknowns at *A* twice and at *B* once is usually all that is desired.

Fig. 33 shows how the method may be applied to four spans and Fig. 34 represents its use in five, or any greater number of spans. It is very seldom that arch bridges of more than six or seven spans are constructed without an intermediate abutment

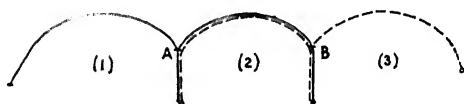


FIG. 32.

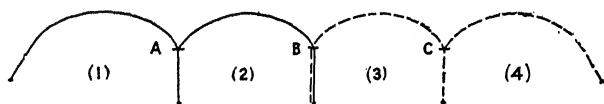


FIG. 33.

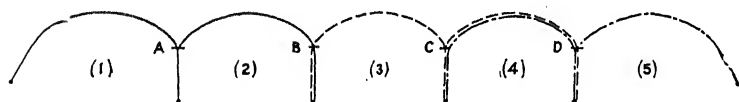


FIG. 34.

pier. The method for a large number of arches may be simplified by the fact that the effect of a load on any one span extends principally over the span itself and the two spans immediately adjacent.

In a series of arches with elastic piers, there is seldom, if ever, any radical change in span lengths between successive arches. On this account the unbalanced thrust acting on any pier due to a maximum change in temperature will be relatively small, and each arch of a series when analyzed for temperature stresses may be considered in nearly all cases as having immovable or

this method of analysis will give exact results since the piers are not acted upon by any unbalanced thrusts.

Rib shortening causes the same effect as a lowering of the temperature. By referring to Arts. 14 and 34, it should be clear that the following formula may be employed to solve for the equivalent temperature drop:

$$t_D = \frac{c_a}{E_{ctc}}$$

### 38. Analysis of a Two-span Arch Bridge with Pier Elastic.—

The earth-filled bridge shown in Designing Sheet No. 23 will be partially analyzed for loading only, assuming a live load of 150 lb. per linear foot over the entire right arch—that is, considering a strip of bridge 1 ft. in width—and dead load only on the left arch. This loading causes the greatest stresses in the pier and also causes the resultant thrust on the base of pier to act at the maximum distance from the center line.

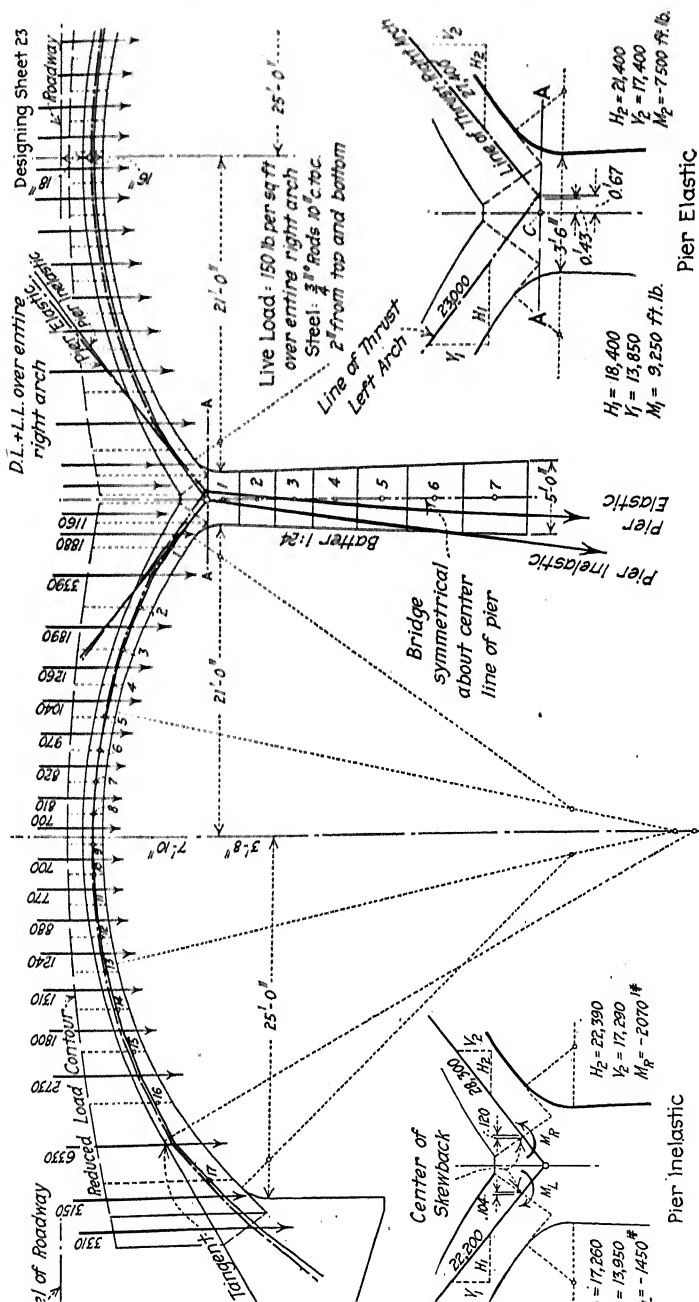
The structure represented is symmetrical about the center line of pier and  $x_L = x_R$ ,  $y_L = y_R$ . The following values may then be determined in the manner described in previous chapters:

$\Sigma x$	=	403.85	$\Sigma m_L$	=	3,908,000	$c_L = c_R$	=	9.40
$\Sigma y$	=	100.00	$\Sigma m_L x$	=	128,241,600	$c_P$	=	0.41
$\Sigma xy$	=	2258.74	$\Sigma m_L y$	=	19,918,500	$n_L = n_R$	=	17
$\Sigma x^2$	=	11,986.6	$\Sigma m_R$	=	4,752,100	$n_P$	=	7
$\Sigma y^2$	=	671.65	$\Sigma m_R x$	=	156,842,600			
$\Sigma y_P$	=	64.99	$\Sigma m_R y$	=	24,056,500			
$\Sigma y_P^2$	=	867.13						

Substituting these values in the six simultaneous equations of Designing Sheet No. 22 and solving, we have

$H_1$	=	18,400 lb.	$H_2$	=	21,400 lb.
$V_1$	=	13,850 lb.	$V_2$	=	17,400 lb.
$M_1$	=	9250 ft.-lb.	$M_2$	=	-7500 ft.-lb.

Thus both arch thrusts act to the right of the center of the section A - A (Fig. 35). The thrust from the left arch acts through a point  $\frac{9250}{13,850} = 0.67$  ft. from C and the thrust from the right arch acts through a point  $\frac{7500}{17,400} = 0.43$  ft. from the same point, both distances measured to the right.



Designing Sheet No. 23 shows the lines of pressure in the arches and the pier. The resultant thrust on the base of pier is seen to act outside the middle-third point. This should not be allowed in good construction and either the shape of the arches should be changed or a reinforced-concrete footing should be added to the pier to make a more nearly uniform distribution of pressure over the pier base. If the structure should be analyzed assuming the arches to have fixed ends, the resultant thrust would fall even farther from the middle third point, as shown, indicating that the elastic properties of the pier tend to prevent failure in so far as that is possible. It should be noted that if the pier should tip due to unequal intensity of pressure on its foundation, the thrust from the right arch would be somewhat reduced and the thrust from the left arch increased. This would cause a certain righting moment at the top of pier and would tend to prevent failure. Relying on such a possible factor of safety, however, would not be acting according to good practice as unknown stresses might be set up in the arch rings which would otherwise endanger the structure. Of course, it is possible to determine these stresses for any predetermined amount of unequal settling.

If desired, each arch in the above design may be considered as fixed for dead load only. The live-load stresses should then be combined with those due to dead load in order to give the correct maximum stresses. If the arches had been taken unequal, the resultant for dead load should be made to pass through the middle third of the pier base if the arches are to be considered as fixed for this loading. This may be done by overloading the arch having the shorter span.

## CHAPTER VIII

### ARCH ANALYSIS BY THE METHOD OF THE ELLIPSE OF ELASTICITY<sup>1</sup>

The ellipse-of-elasticity method of arch analysis is almost entirely graphical and is unique in the fact that by its use influence lines may be readily constructed for finding the stresses at any section. Even arches with elastic piers may be rigorously analyzed by this method without any great difficulty. The method is rapid and easily applied, and is likely to be in great favor with American engineers as soon as it becomes well known. A number of underlying principles must be explained before this method can be completely understood.

**39. Preliminary Considerations Pertaining to the Method of Treating the Symmetrical Arch.**—Let Figs. 13 and 14 in Chapter II represent any given element of an arch, and let  $k'$  represent the angle of rotation of the face  $bc$  with respect to the face  $ad$  which would be caused by a bending moment  $M$ . From Art. 10 we know that

$$k' = \frac{Ms}{E_c I} \quad (1)$$

Now if we consider the symmetrical arch shown in Fig. 35A as fixed at the right end and free at the left end, each element will cause a rotation of the left skewback equal to  $\frac{Ms}{E_c I}$ , where  $M$  is the moment acting upon a given element,  $s$  its length, and  $I$  the moment of inertia of its average cross-section. If the element considered is  $abcd$ , then  $s$  is the distance between the intersections of the neutral axis of the arch with the faces  $ad$  and  $bc$ , and  $I$  is the moment of inertia of the cross-section at the center of gravity of the element. Since the quantity  $\frac{s}{E_c I}$  is a characteristic of the given element and shows the amount of its

<sup>1</sup> Method taken by permission from a paper presented before the Western Society of Engineers, January 13, 1913, by Mr. A. C. Janni, C. E. Printed in the Journal of the Western Society of Engineers, May, 1913. Most of the data in this chapter other than that



ability to cause rotation if acted upon by a moment, we may treat this quantity as a force acting at the center of gravity of the area  $abcd$ . We shall call this quantity the *elastic weight* of the element.

Suppose the bending moment acting on the element  $abcd$  is due to a force  $P$  having a leverage of  $x'$  about the center of gravity of the element. Then the rotation of the left skewback due only

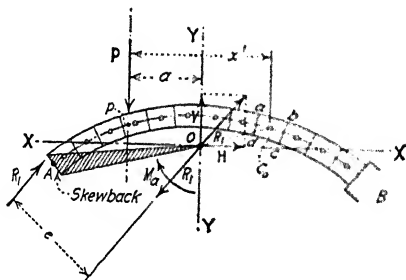
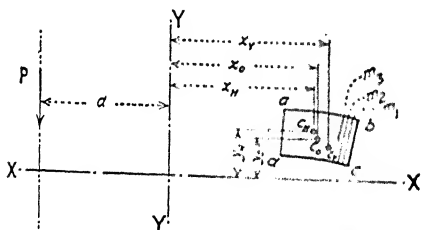


FIG. 35A.



$C_g$  = center of gravity of the element  $abcd$ ,  
which is also the center of gravity of the  $\frac{S}{E_c I}$   
forces corresponding to the small elements  
 $m_1, m_2, m_3$ , etc.

$C_h$  = center of gravity of the moments of  
the small  $\frac{S}{E_c I}$  forces about the axis  $\begin{cases} Y-Y \\ X-X \end{cases}$

FIG. 35B.

to the bending of this element will be  $Px' \cdot \frac{S}{E_c I}$ . Considering  $\frac{S}{E_c I}$  (the elastic weight of  $abcd$ ) as a force, this angle of rotation may also be determined by multiplying the force  $P$  by the moment of the elastic weight of  $abcd$  about an axis through the line of action of  $P$ , or

$$k' = P \cdot \frac{S}{E_c I} x'$$

Designating the elastic weight by the letter  $G$ , we have

$$k' = P(Gx') \quad (2)$$

The total angle of rotation of the left skewback due to the force  $P$  will equal the sum of all the moments of the elastic weights to the right of the line of action of the force  $P$  with respect to this line of action, or

$$k = P \sum_p^B Gx' \quad (3)$$

In Art. 10 the moment of inertia has been defined as follows: "The moment of inertia of a plane surface with respect to an axis is the sum of the products obtained by multiplying each elementary area by the square of its distance from that axis." If each elementary area is considered a force, then the moment of inertia becomes the sum of the products obtained by multiplying each force by the square of its distance from the given axis. From this interpretation of the definition we may consider the same term to apply in the case of the elastic weights of the arch elements. In other words, whenever we obtain the sum of the products mentioned above for a system of elastic weights with respect to a given axis, we shall designate such sum as the moment of inertia of these weights about the axis in question. Thus if each product  $Gx'$  in the expression  $\sum_p^B Gx'$  in the above formula should be multiplied again by  $x'$  the result of the expression would be the moment of inertia of all the elastic weights to the right of the line of action of  $P$  with respect to this line of action. If any given horizontal axis is also considered, the expression  $\sum Gx'y$ , or in general  $\sum Gxy$ , will be called the *product of inertia*. If two vertical axes are considered, the expression for the product of inertia takes the form  $\sum Gxx'$ . It should be clear that "moment of inertia" is found with respect to one axis only, while "product of inertia" is found with respect to two axes at any inclination whatever and making any angle with each other.

In Art. 11 it is shown that the vertical and horizontal displacements (Fig. 15) of the free end of the arch due to the moment  $M$  acting upon a given element may be expressed respectively by the formulas

$$dy = x \frac{Ms}{EI} \quad \text{and} \quad dx = y \frac{Ms}{EI} \quad (4)$$

CONCRETE CONSTRUCTION

where  $x$  and  $y$  refer to coördinate axes with the origin at the free end. These formulas if applied to the element  $abcd$  of Fig. 35A may be put in the form

$$dy = x \cdot Px' \cdot G \quad \text{and} \quad dx = y \cdot Px' \cdot G$$

Suppose now that a certain point  $O$  is assumed to be rigidly connected with the cross-section of the left skewback and let it be desired to find the displacements of this point  $O$  due only to the rotation of the element  $abcd$ , this rotation being caused by the bending moment  $Px'$ .

First of all it should be noted that the angle of rotation of the free end ( $A$ ) of the arch which is determined above by the formula  $k' = P(Gx')$  refers to the angle of rotation at any point to the left of the element  $abcd$ , and also to the point  $O$  since this point is in rigid connection with  $A$ . If we consider  $C_o$ , the center of gravity of the element  $abcd$ , as the center of rotation (considered so simply for illustration as the student will find later that the center of rotation is not at  $C_o$ ), then the preceding statement means that the line  $C_oO$  turns through the same angle as a line connecting  $C_o$  and  $A$ . Thus the above formulas for vertical and horizontal displacements can be applied with respect to axes through the point  $O$  as well as through  $A$  or any other point which is rigidly connected with the arch and is to the left of the given element. We have then the formulas

$$dy = P \cdot Gx' \cdot x \quad \text{and} \quad dx = P \cdot Gx' \cdot y \tag{5}$$

which give the displacements at point  $O$  provided  $x$  and  $y$  are measured with respect to the axes  $X - X$  and  $Y - Y$ .

The total vertical and horizontal displacements of  $O$  due to the force  $P$  causing bending in all elements to the right of its line of action are

$$\Delta y = -P \sum_p^B Gx' \cdot x' \quad \text{and} \quad \Delta x = P \sum_p^B Gy' \cdot x' \tag{6}$$

considering positive values of  $y$  above the axis  $X - X$  and positive values of  $x$  to the right of  $Y - Y$ . The expression  $\sum_p^B Gy' \cdot x'$  represents the product of inertia of the elastic weights at the right of  $P$  with respect to the axis  $X - X$  and to the axis through the line of action of  $P$ . The expression  $\sum_p^B Gx' \cdot x'$  represents the

product of inertia of the same elastic weights above mentioned with respect to the axis  $Y - Y$  and to the axis through the line of action of  $P$ .

Suppose now that a force or reaction  $R_1$  acts upon the structure so as to cause equilibrium, and suppose this same reaction  $R_1$  is applied twice at the point  $O$  (rigidly connected with left skewback), but acting in opposite directions as shown. It will be possible to resolve one of these two forces at  $O$  into two components  $V$  and  $H$ , and then the opposite force  $R_1$  can be combined with the actual skewback reaction so as to form a couple  $R_1e$ . Thus at the point  $O$  we have the three unknowns  $V$ ,  $H$ , and  $M_a = R_1e$ .

The angle of rotation at the point  $O$  due to the moment  $M_a = R_1e$  is given by the formula

$$k = M_a \sum_A^B G \quad (7)$$

where  $\sum_A^B G$  represents the sum of all the elastic weights from  $A$  to  $B$ . This expression comes directly from Formula (1), taking into consideration the fact that the moment  $R_1e$  acts upon the entire arch. Therefore

$$M_a \sum_A^B G = P \sum_p^B Gx' \quad (8)$$

since the angles of rotation at  $O$  due to the force  $P$  and to the reaction moment  $M_a = R_1e$  must be the same.

It will be convenient to take the point  $O$  at the center of gravity of all the elastic weights. By center of gravity is meant the point through which the resultant elastic weight will always pass no matter in what parallel direction the weights are supposed to act. This point may be readily determined by finding the lines of action of the vertical and horizontal resultants. The intersection of these two resultants is the center of gravity of the system.

With the point  $O$  located as above mentioned, the vertical displacement of this point due to the vertical reaction  $V$  is, by Formula (6),

$$\Delta y = V \sum_A^B Gx^2 \quad (9)$$

This means that the vertical displacement of  $O$  from this cause is equal to the product obtained by multiplying the force  $V$  by the

moment of inertia of the whole elastic system with respect to the vertical axis through  $O$ . This displacement must be equal to that previously found due to the load  $P$ , or

$$V \sum_A^B Gx^2 = P \sum_p^B Gx \cdot x' \quad (10)$$

The horizontal reaction  $H$  does not cause any vertical displacement at the point  $O$  since it acts at right angles to  $V$  and through the center of gravity of the system of elastic weights. The expression for the vertical displacement of point  $O$  due to force  $H$  is as follows:  $H \sum_A^B Gxy$ . The arch, however, is symmetrical, so that  $\sum_A^B Gxy$  reduces to zero and no vertical displacement results.

The horizontal displacement of  $O$  due to the horizontal reaction  $H$  is, by Formula (6),

$$\Delta x = H \sum_A^B Gy^2 \quad (11)$$

that is, the horizontal displacement of  $O$  is equal to the product obtained by multiplying the force  $H$  by the moment of inertia of the elastic weights of the whole elastic system with respect to the horizontal axis through  $O$ . Placing this equal to the horizontal displacement previously found, we have

$$H \sum_A^B Gy^2 = -P \sum_p^B Gy \cdot x' \quad (12)$$

With a known force  $P$  (which should be considered as unity in order to plot influence lines), Formulas (8), (10), and (12) may be employed to determine the values of  $M_a = R_1e$ ,  $V$ , and  $H$ . The moments and products of inertia of the elastic weights may be found readily by graphical methods. The magnitude of the reaction  $R_1$  is equal to the resultant of  $V$  and  $H$ , and its actual position may be determined by drawing a tangent parallel to this resultant at a distance

$$e = \frac{M_a}{R_1}$$

from the point  $O$ . The reaction at the right of the structure may be obtained in the manner shown on Designing Sheet No. 104.

Following is another method of deriving Formulas (8), (10), and (12): Consider the element  $abcd$  (Fig. 35A) with the forces  $P$  and  $R$  simultaneously applied. The bending moment acting on this element will be

$$M = -Px' + M_a + Vx - Hy$$

If this value of  $M$  is inserted in our three fundamental equations for the deflection of curved beams, we have

$$\begin{aligned} k &= \sum_A^B (-Px' + M_a + Vx - Hy)G = 0 \\ \Delta y &= \sum_A^B (-Px' + M_a + Vx - Hy)Gx = 0 \\ \Delta x &= \sum_A^B (-Px' + M_a + Vx - Hy)Gy = 0 \end{aligned}$$

The arch being symmetrical, and with the coördinate axes at the point  $O$ , we know that  $\sum_A^B Gx = 0$ ,  $\sum_A^B Gy = 0$ , and  $\sum_A^B Gxy = 0$ . Substituting these values, we obtain

$$\begin{aligned} \sum_A^B M_a G - P \sum_A^B Gx' &= 0 \\ V \sum_A^B Gx^2 - P \sum_A^B Gx \cdot x' &= 0 \\ -H \sum_A^B Gy^2 - P \sum_A^B Gy \cdot x' &= 0 \end{aligned}$$

Since  $Px'$  becomes zero for all elements to the left of the force  $P$ ,

$$\begin{aligned} M_a \sum_A^B G &= P \sum_p^B Gx' \\ V \sum_A^B Gx^2 &= P \sum_p^B Gx \cdot x' \\ H \sum_A^B Gy^2 &= -P \sum_p^B Gy \cdot x' \end{aligned}$$

These equations for  $k$ ,  $\Delta y$ , and  $\Delta x$  are the same as Formulas (8), (10), and (12) respectively.

It should be remembered that each part of a given element has an elastic weight of its own. In the element  $abcd$  (Fig. 35B), for example, the elastic weights of the smaller elements should be considered at their respective centers of gravity. Let  $g_1$ ,  $g_2$ , and  $g_3$ , etc., represent respectively the elastic weights of the small elements  $m_1$ ,  $m_2$ , and  $m_3$ , etc., and let  $C_o$  be the center of gravity of all these weights. Consider now the moments of these elastic weights about the axis  $Y - Y = g_1x_1 + g_2x_2 + g_3x_3 +$

etc. =  $Gx_o$ , and the moments about the axis  $X - X = g_1y_1 + g_2y_2 + g_3y_3 + \text{etc.} = Gy_o$ . If each small element is now assumed to have an elastic weight acting in a vertical direction equal to the moment of its real elastic weight about the axis  $Y - Y$ , the center of gravity of these elastic moments will not fall necessarily at the center of gravity ( $C_o$ ) of the element  $abcd$ , but at some point as  $C_V$ . Likewise the center of gravity of the elastic moments with respect to the axis  $X - X$  will fall at some point as  $C_H$ . This means that, in finding the moment of inertia of all the elastic weights of these smaller elements, the elastic moments should not be considered to act at the center of gravity ( $C_o$ ) of the total elastic weight of the element, but at  $C_V$  or  $C_H$  as the case may be. If the distance from the point  $C_V$  to the axis  $Y - Y$  is designated as  $x_V$ , then the moment of inertia of the elastic weight of the element  $abcd$  about this axis is

$$I_Y = Gx_o x_V$$

Similarly, the moment of inertia of the elastic weight of  $abcd$  about the axis  $X - X$  is

$$I_X = Gy_o y_H$$

The product of inertia of the elastic weight of the same element with respect to the axes  $X - X$  and the line of action of  $P$  is

$$I_{XP} = Gy_o \cdot (x_H + a)$$

and with respect to  $Y - Y$  and the line of action of  $P$  is

$$I_{YP} = Gx_o \cdot (x_V + a)$$

The points  $C_V$  and  $C_H$  may readily be determined graphically, as shown later on. These points will be termed *centers* in the articles which follow.

The finding of these centers is a refinement over the method given in the preceding chapters of this book. It should be noted that the elements, as  $abcd$  (Fig. 35A), may be of any given length and the work of dividing the arch into constant  $\frac{s}{l}$  divisions is avoided.

**40. Properties of an Ellipse.**—In the preceding article the reason has been given for finding the points  $C_V$  and  $C_H$  (Fig. 35B) for each element of the arch. A simple graphical construction will suffice to find these points for any given element. Before

presenting this method, however, it may be desirable to explain certain properties of an ellipse.

If through a fixed point ( $C'$ , Figs. 36A and 36B) any number of secants be drawn to an ellipse, and tangents to the latter be drawn at the points of intersection of each secant with the ellipse, then each pair of tangents will intersect upon a straight line ( $RS$  and  $MN$ , Figs. 36A and 36B), called the *polar* of the fixed

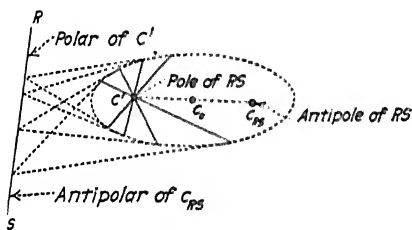


FIG. 36A.

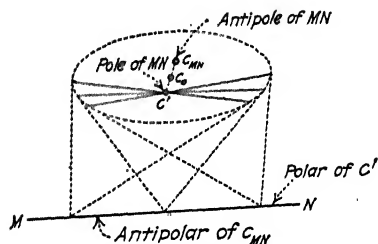


FIG. 36B.

point ( $C'$ ). Reciprocally the fixed point is called the *pole* of the straight line. The fixed point symmetrical with the pole with respect to the center of the ellipse is called the *antipole* of the straight line.

In Figs. 36A and 36B the pole  $C'$  is shown inside the ellipse, but the same property holds true for any point outside. The meaning of the term *antipolar* is clearly shown in these figures and no definition is necessary.

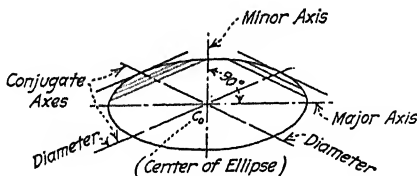


FIG. 36C.

If the pole lies on the ellipse, it follows from the above definition that the polar is simply the tangent to the ellipse at the pole. For such a case the antipole is also on the ellipse since it is diametrically opposite the pole and at the same distance from the center.

A diameter is any straight line passing through the center of the ellipse, and is the locus of the middle points of a system



of an ellipse are the only diameters perpendicular to the chords they bisect.

Two diameters are said to be *conjugate* when each diameter bisects all chords parallel to the other. The tangent at the extremity of any diameter is parallel to the conjugate diameter.

If the antipole relative to a polar falls upon another polar, the antipole relative to the latter will fall upon the first. Thus in Fig. 37A, the antipole of  $RS$  falls upon  $MN$ . Reciprocally the

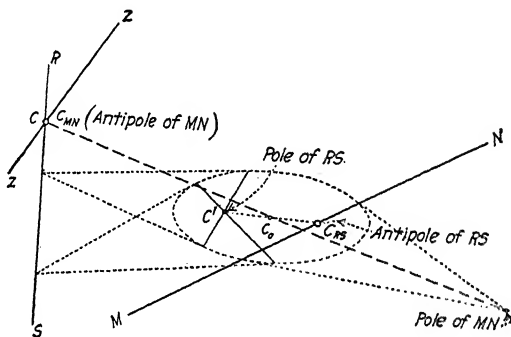


FIG. 37A.

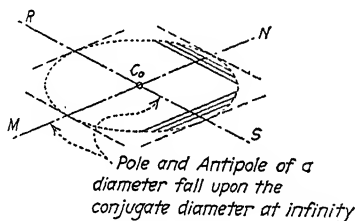


FIG. 37B.

antipole of  $MN$  falls upon  $RS$ . Any line as  $ZZ$  (or even  $C_{MN}C_0$  which passes through the center of the ellipse) passing through  $C_{MN}$ , the antipole of the line  $MN$ , will have its antipole somewhere on the line  $MN$ . (The above statements hold with respect to poles and polars, as well as antipoles and polars or poles and antipolars.)

The pole and antipole of a diameter fall upon the conjugate diameter at infinity (Fig. 37B). In Fig. 37A a line through the center  $C_0$  parallel to  $MN$  and the line  $C_{MN}C_0$  are conjugate axes.

If the lengths of the semi-major and semi-minor axes of an ellipse are known, the antipole of any line or axis can be determined by a simple graphical construction. For example, in Fig. 38 the antipole ( $C_{MN}$ ) of  $MN$  may be found in the following manner:

Lay off  $C_oB' = C_oB$ , and  $C_oD' = C_oD$ .

Connect  $B'$  with  $F$ , and  $D'$  with  $G$ .

Draw  $B'B''$  perpendicular to  $B'F$ , and  $D'D''$  perpendicular to  $D'G$ .

From  $B''$  draw a line parallel to  $C_oD$ , and from  $D''$  draw a line parallel to  $AB$ .

The intersection of these lines is the antipole  $C_{MN}$ .

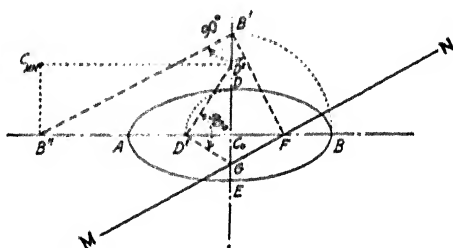


FIG. 38.

#### 41. Properties of the Center of Gravity of Static Moments.—

Let  $C_o$  of Fig. 39 be the center of gravity of the given element, which is the center of gravity of all the small elastic weights. Also let  $C_{RS}$  be the *center* (see Art. 39) relative to the axis  $RS$ , and  $C_{MN}$  the *center* relative to the axis  $MN$ . Then the product of inertia of all the small elastic weights of the given element about  $RS$  and  $MN$  is

$$Gx_o y_{RS} = G y_o x_{MN}$$

This equation shows that if  $y_{RS}$  should be zero, then also  $x_{MN}$  would be equal to zero. Thus it follows that if the center relative to an axis falls upon another axis, the center relative to the latter will fall upon the first. (It should be noted that this is the same relation which exists between the poles and polars, or antipoles and polars, of an ellipse, Fig. 37.) Also any axis passing through the center relative to another axis will have its center somewhere on that other axis. For such axes, which are *conjugate axes*, the product of inertia of the small elastic weights is zero.

The moment of inertia of the weights about the axis  $RS$  may be expressed as follows:

$$I_{RS} = Gx_0x_{RS}$$

or

$$x_{RS} = \frac{I_{RS}}{Gx_0}$$

If the axis  $RS$  should pass through the center of gravity  $C_0$ , then  $x_0$  would equal zero and  $x_{RS}$  would equal infinity, which is the same relation which exists between the poles and diameters, or antipoles and diameters, of an ellipse (Fig. 37B).

It should now be clear that the centers  $C_V$  and  $C_H$  (Fig. 35B) for the given element with respect to given axes must be either the poles or antipoles of some ellipse which has its center at the center of gravity of the element and one axis lying in the geometrical axis of the arch.

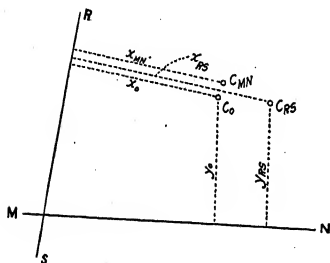


FIG. 39.

The lengths of the major and minor axes of this ellipse, however, we have not yet determined.

**42. Determination of the Ellipse of Elasticity.**—Points  $C_V$  and  $C_H$  in Fig. 35B are termed *centers* in Art. 39. They are in reality centers of rotation of the element  $abcd$  if forces are considered to act on the element along the axes  $Y - Y$  and  $X - X$  respectively. For example, a force along  $Y - Y$  causes a bending moment in each of the small elements  $m_1, m_2, m_3$ , etc., and the center of gravity of all these bending moments considered as forces will be the instantaneous center of rotation of the element  $abcd$ —that is, the point  $C_V$ .

In order to show conclusively that this is true, consider the very small elements  $m_1$  and  $m_2$  of  $abcd$  (Fig. 40), with centers of gravity  $C_1$  and  $C_2$  respectively, and assume that bending is caused in these elements by a force acting along an axis  $Y - Y$ . The vertical displacement of some point  $A$  to the left of  $abcd$  due to the force acting on the small element  $m_1 = M_1x_1g$  (see Formula 4, Art. 39), where  $M_1$  is the moment acting on this given element. Likewise, the vertical displacement of  $A$  due to the force acting on the small element  $m_2 = M_2x_2g$ . Thus the total vertical displacement of  $A$  due to the force acting on both  $m_1$  and  $m_2 = M_1x_1g + M_2x_2g = g(M_1x_1 + M_2x_2)$ . In like manner it may be shown that the total horizontal displacement of  $A$  due to the bending in the elements  $m_1$  and  $m_2$  is  $g(M_1y_1 + M_2y_2)$ .

Suppose we select a point  $C_{1-2}$  on the straight line joining  $C_1$  and  $C_2$ , such that  $\frac{C_1 C_{1-2}}{C_{1-2} C_2} = \frac{M_2}{M_1}$ . In other words, we will choose a point  $C_{1-2}$  which is the center of gravity of forces equal to  $M_1$  and  $M_2$  applied at  $C_1$  and  $C_2$  respectively. If the point  $A$  should rotate about this point due to the force acting on the elements  $m_1$  and  $m_2$ , the vertical displacement of  $A$  would be

$$M_1 x_{1-2} g + M_2 x_{1-2} g = (M_1 + M_2) x_{1-2} g$$

Since  $x_{1-2} = x_2 + \frac{M_1}{M_1 + M_2} (x_1 - x_2)$ , we have

$$(M_1 + M_2) x_{1-2} g = g(M_1 x_1 + M_2 x_2)$$

In a similar manner, the horizontal displacement of  $A$  under the same conditions would be

$$(M_1 + M_2) y_{1-2} g = g(M_1 y_1 + M_2 y_2)$$

But these values are identical with those found above for the sums of the components of the two displacements. Thus the rotation caused by the force along  $Y-Y$  acting on the elements  $m_1$  and  $m_2$  is about a point  $C_{1-2}$  which is the center of gravity of the moments  $M_1$  and  $M_2$ , when these

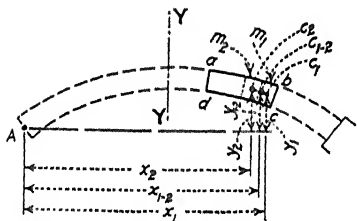


FIG. 40.

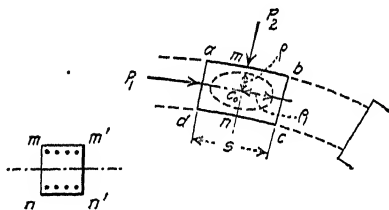


FIG. 41.

moments are considered as forces and applied at the centers of gravity of their respective elements. It should be evident that this same proof will hold with respect to any number of small elements and we have then the rule that the center of gravity of the bending moments of the small elements, when these moments are considered as forces, is the center of rotation of the large element  $abcd$ .

Now in Art. 41 it is shown that instantaneous centers  $C_Y$  or  $C_H$ , Fig. 35B, are either poles or antipoles of some ellipse with respect, of course, to the lines  $X-X$  and  $Y-Y$ . If the centers were the poles of  $X-X$  and  $Y-Y$ , there would be positions of each axis (polar) for which its corresponding center (pole) would lie on itself. (A polar is tangent to an ellipse at its pole, Art. 40.) This, however, cannot happen since a center of rotation can never lie on the line of action of a force. The centers, therefore, are the antipoles of the ellipse for the given

In order to determine the lengths of the major and minor axes of the ellipse, consider a force  $P_1$  lying in the arch axis and acting on the section  $ad$  of the element  $abcd$ , Fig. 41. Since  $P_1$  acts through the center of gravity  $C_o$  of the element, the shortening due to this force will be

$$\Delta s = \frac{P_1 s}{E_c A} = P_1 \cdot \frac{s}{E_c I} \cdot \frac{I}{A} = P_1 \cdot G \cdot \frac{I}{A}$$

where  $A$  (representing the cross-sectional area)  $= a_c + na_s$ , and  $I = I_c + nI_s$ . From Art. 39, we also know that the displacement of the face  $ad$  is equal to the product of the force by the moment of inertia of the elastic weight  $G$  with respect to the line of action of the force  $P_1$ . If  $\rho$  is the semi-minor axis (radius of gyration) of the ellipse of elasticity in question, then  $G\rho^2$  will be the moment of inertia we desire, and  $P_1 G\rho^2$  will be the displacement of the section  $ad$  with respect to the section  $bc$ , so that

$$\Delta s = P_1 \cdot G \cdot \rho^2$$

It should be clear that this displacement, computed by two different methods, must be the same. Hence

$$P_1 \cdot G \cdot \frac{I}{A} = P_1 \cdot G \cdot \rho^2$$

or

$$\rho = \sqrt{\frac{I(\text{of } mm'n'n)}{A(\text{of } mm'n'n)}}$$

which is the semi-axis of the ellipse of elasticity normal to the geometrical axis of the arch, and which also turns out to be the radius of gyration of the central cross-section of the element  $abcd$ . In a somewhat similar manner, using force  $P_2$  rigidly connected with face  $ad$ , the semi-axis of the ellipse lying on the arch axis may be shown to be

$$\rho_1 = \sqrt{\frac{I(\text{of } abcd)}{A(\text{of } abcd)}} = s \sqrt{\frac{1}{12}} = 0.289s$$

The graphical construction in Fig. 38 (Art. 39) may now be employed to determine centers or antipoles relative to any given axis.

It should be clear from the above that we may treat the elastic weights of the elements (as  $abcd$ ) for the whole arch in the same manner as we have the small elastic weights.

Then it follows that an ellipse with its center at  $O$ , Fig. 35A (major and minor axes horizontal and vertical respectively for a symmetrical arch) may be employed to find the "centers" of the *entire* system of elastic weights with respect to given axes—that is, the antipole of such an ellipse, with respect to an axis through the line of action of a given force, will be the center of rotation of the free end of the arch ( $A$ , Fig. 35A) due to this given force. The length of the semi-minor axis would be equal to

$$\sqrt{\frac{I}{\sum_A^B G}}$$

where  $I$  represents the moment of inertia of all the elastic weights about the axis  $X - X$ , and  $\sum_A^B G$  represents the *sum* of all these weights. The length of the semi-major axis may be found by the same general expression, but  $I$  would be taken about the axis  $Y - Y$ . Of course, the ellipse for an unsymmetrical arch would not have vertical and horizontal axes as above described. The method of determining the position of the ellipse for such arches will be given in Arts. 45 and 46.

For a symmetrical arch (Fig. 35A), it is shown in Art. 39 that any vertical force  $V$  acting through the point  $O$  would cause only vertical displacement of this point. This same conclusion is reached from the theory of the ellipse of elasticity. For example, the force  $V$  acts along the minor axis of the ellipse and the antipole, or instantaneous center of rotation, falls upon the major axis at infinity (Art. 40); which means that this force causes a rotation about a point at infinity—that is, a displacement in a straight line perpendicular to the major axis.

**43. Graphical Constructions for Finding Moments and Products of Inertia of the Elastic Weights.**—In Art. 39 the following formulas are derived:

$$\begin{aligned} M_a \sum_A^B G &= P \sum_p^B Gx' \\ V \sum_A^B Gx^2 &= P \sum_p^B Gx \cdot x' \\ H \sum_A^B Gy^2 &= -P \sum_p^B Gy \cdot x' \end{aligned}$$

by which it is possible to determine the moment and the horizontal and vertical components of the reaction acting at the point

O, Fig. 35A. In order to find  $M_a$ ,  $V$ , and  $H$ , it is first necessary to determine the values of the following expressions:

$$\begin{array}{ll} \sum_A^B G & \sum_p^B Gx' \\ \sum_A^B Gx^2 & \sum_p^B Gx \cdot x' \\ \sum_A^B Gy^2 & \sum_p^B Gy \cdot x' \end{array}$$

This may be done graphically. In fact it will be shown later that the graphical constructions for finding moments and products of inertia of the elastic weights will give directly the values of  $M_a$ ,  $V$ , and  $H$ , if the constructions are made with this result in view.

For the present it will suffice to show the general method to be followed in finding the above expressions graphically. In order to gain clearness in the explanation of this method, the weights assumed—namely:  $G_1$ ,  $G_2$ ,  $G_3$ ,  $G_4$ , and  $G_5$  (Fig. 42)—will be considered as the weights of heavy particles concentrated at the points 1, 2, 3, 4, and 5 respectively. In other words, five concentrated weights will be assumed and these will be applied at any five selected points, thus eliminating any consideration of “centers” or antipoles in this preliminary discussion. The method will be shown as perfectly general by choosing coördinate axes oblique to each other.

The first consideration is to find the center of gravity  $O$  of the system and this may be accomplished by means of equilibrium polygons  $f_a$  and  $f_b$ .<sup>1</sup> For example, to determine the axis  $X - X$  (the inclination of which is previously decided upon), the weights are assumed to act parallel to this axis, next the force polygon  $F_a$  is constructed, and then the corresponding equilibrium polygon  $f_a$ . The line  $X - X$  through the intersection  $p'$  of the first and last sides of the equilibrium polygon  $f_a$  will contain the center of gravity of the system. Also, the sides of the polygon  $f_a$  will determine, on this line, segments proportional to the moments of the corresponding weights with respect to this same axis through the center of the system. The axis  $Y - Y$  may be determined in a like manner employing the force polygon  $F_b$  and the equilibrium polygon  $f_b$ . The intersection of the axes  $X - X$  and  $Y - Y$  determines the center of gravity  $O$  of the system.

<sup>1</sup> See “Elements of Structures,” by the same author.

If verticals are drawn through the points of application of the weights, the segments cut off on any given vertical by the

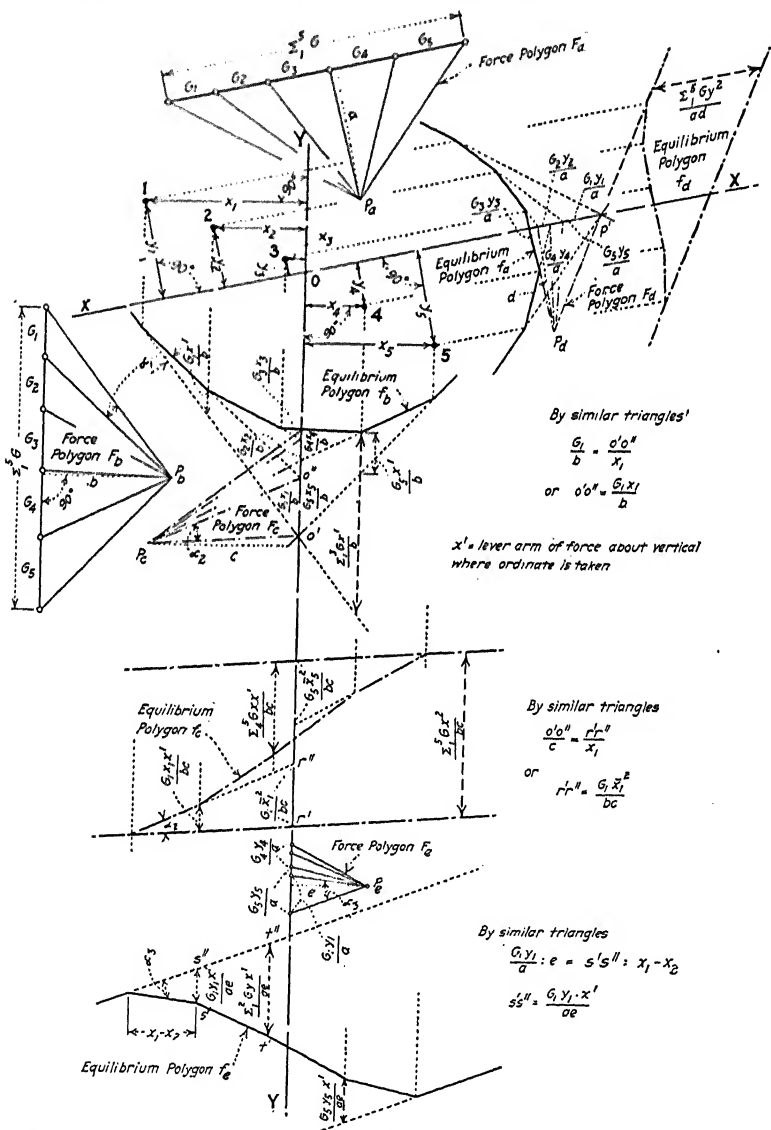


FIG. 42.

equilibrium polygon  $f_b$  will be proportional to the moment of all



Fig. 42 shows what intercepts should be considered to give desired moments.

As stated above for polygon  $f_a$ , the sides of the equilibrium polygon  $f_b$  intercept, on the axis  $Y - Y$ , segments proportional to the moments of the weights with respect to this axis. If these segments are treated as vertical forces applied at the points of application of the original weights, the equilibrium polygon  $f_c$  (constructed by means of the force polygon  $F_c$ ) will intercept, on the axis  $Y - Y$ , a segment which will be proportional to the moment of inertia of the weights with respect to this axis. This segment is determined by the first and last sides of the polygon  $f_c$ . As shown in Fig. 42 the intercepts on verticals through the points of application of the weights correspond to the general expression  $\sum Gx \cdot x'$ . If equilibrium polygon  $f_d$  is constructed in a similar manner to polygon  $f_c$  (only with respect to the axis  $X - X$  instead of  $Y - Y$ ), then the segment cut off on the axis  $X - X$ , between the first and last sides of the polygon  $f_d$ , is the moment of inertia of the weights about this coördinate axis.

The equilibrium polygon  $f_a$  determines the moments of the weights with respect to the axis  $X - X$ . If these moments are considered as forces and applied at the points of application of the original weights, but this time acting vertically, the equilibrium polygon  $f_e$  (corresponding to force polygon  $F_e$ ) will intercept on a vertical through any weight, a segment proportional to the product of inertia of the weights to one side of the given vertical with respect to this vertical and the  $X - X$  axis. Fig. 42 shows what intercepts to consider for moments of the weights to the right and those for moments of the weights to the left of any given vertical.

**44. Method of Analyzing Symmetrical Arches for Loading Only.**—The graphical constructions in Fig. 43 are similar to those given in Fig. 42 except that  $G_1, G_2$ , etc., apply to the elastic weights of arch elements (made of equal lengths for convenience) instead of to the weights of concentrated loads. Each part of a given element has an elastic weight of its own (Art. 39), consequently the *centers* of each element with respect to axes  $X - X$  and  $Y - Y$  must be determined. These may be found by means of the ellipse of elasticity, as explained in Art. 40. Since the arch is symmetrical about a center line, only one-half of the structure need be considered. The arch is divided into a small number of



(1V, 2V, etc.). Similarly, the moment of inertia of the elastic weights about the axis  $X - X$  (see equilibrium polygon  $f_a$ ) should be determined by assuming the moments of the elastic weights, given by equilibrium polygon  $f_a$ , to act as horizontal forces applied at the *centers* of the arch elements relative to the axis  $X - X$ . The equilibrium polygon  $f_c$  should be drawn by assuming the forces corresponding to the moments with respect to the axis  $X - X$  to be placed at the *centers* relative to the same axis, but acting vertically. (The results from equilibrium polygons  $f_a$  and  $f_d$  should be checked analytically in many cases as the intersections are not advantageous and may lead to cumulative errors. The force polygon with  $P_c$  as pole may be drawn to a larger scale for convenience in drawing the corresponding equilibrium polygon  $f_c$ .)

It should be noted in Fig. 43 that the pole distance  $b$  is taken equal to  $\Sigma G$ ; that  $d$  is made equal to  $\frac{\Sigma Gx^2}{bc}$  and considered as unity in scaling; that  $e$  is given a value equal to  $\frac{\Sigma G'y^2}{ad}$ ; and that the pole  $P_c$  is taken on the end string of the equilibrium polygon  $f_b$  which occurs at the right of the entire arch, this string being produced backward to the left side of the axis  $Y - Y$ . By so doing the values of the reactions and the moment  $M_a$  for a load unity at any given point may be scaled directly.

The truth of the preceding statement may be proved as follows: From the preceding article we know that

$$M_a = \frac{P \sum_P^B Gx'}{\sum_A^B G}$$

With  $P = 1$  and  $b = \Sigma G$ , we have

$$M_a = \frac{\sum_P^B Gx'}{b}$$

which may be scaled from Fig. 43 in the manner shown for a load unity at  $p$ . (See also Fig. 42.) Likewise

$$V_1 = \frac{P \sum_P^B Gx \cdot x'}{\sum_A^B Gx^2} = \frac{\sum_P^B Gx \cdot x'}{bc} \times \frac{bc}{\sum_A^B Gx^2} = \frac{\sum_P^B Gx \cdot x'}{bc}$$

$$\begin{aligned}
 H &= \frac{P \sum_P^B Gy \cdot x'}{\sum_A^B Gy^2} = \frac{\sum_P^B Gy \cdot x'}{ae} \times \frac{ae}{\sum_A^B Gy^2} \\
 &= \frac{\sum_P^B Gy \cdot x'}{ae} \quad \left( \text{since } \frac{\sum_A^B Gy^2}{ad} = e, \text{ or } \sum_A^B Gy^2 = ae \right)
 \end{aligned}$$

The student should note that the first and last sides of the equilibrium polygon  $f_e$  in Fig. 43 would coincide if the right-hand half of the polygon were completed. This occurrence is due to the fact that the directions of the coördinate axes are conjugated and the product of inertia of all the elastic weights with respect to these axes must be zero (Art. 41). Thus the values of  $M_a$ ,  $V_1$ ,  $V_2$ , and  $H$  due to a load unity at any given point  $p$  may be determined by drawing a vertical line through the point in question and, in the manner shown in Fig. 43, scaling the intercepts which are cut off on this line by the sides of the equilibrium polygons  $f_b$ ,  $f_c$ , and  $f_e$ . By laying off  $H$  horizontally as in the drawing and joining the point  $p'$  to the ends of  $V_1$  and  $V_2$ , the magnitude and directions of the reactions may be determined. The actual position of  $R_1$  may be found by drawing a tangent parallel to  $p'q$  at a distance  $\frac{M_a}{R_1}$  from the point  $O$ . The right reaction  $R_2$  may then be drawn from the intersection of  $R_1$  with the vertical through  $p$  parallel to  $p'm$ .

Considering  $d$  equal to 1 lb. in scaling, we have, for a 1-lb. load at  $p$  in Fig. 43,  $R_1 = 1.05$  lb. and  $M = 17.7$  ft.-lb. The lever arm of  $R_1$  about  $O = \frac{17.7}{1.05} = 16.9$  ft. In a similar manner the reactions may be found for a 1-lb. load at other points on the arch. The intersection line shown passing through  $n$  (Fig. 43) is intended to represent the line of intersection of all reactions with their corresponding loads. It is shown as horizontal in this case in order to save the labor of determining its exact location.

Influence lines may now be drawn in the manner described in Art. 34 and the maximum stresses computed. Another and more graphical method, however, of determining values of ordinates to influence lines to represent maximum stress is shown in Fig. 44 with reference to a given section designated as  $S$ . It is convenient in this method to determine the envelopes of the reactions and the

influence line for horizontal thrust ( $H$ ) which, of course, may be plotted directly from the data given in Fig. 43. Seven positions of the unit load are shown.

Assuming no tension at a given section greater than the tensile strength of the concrete, we have, from Art. 74, Volume I, that the stress on the extreme fiber

$$f_c = \frac{N}{A} \pm \frac{N x_0 x_1}{I}$$

where  $N$  is the thrust normal to the section, and  $x_0$  and  $x_1$  are the distances from the gravity axis to the point of application of the

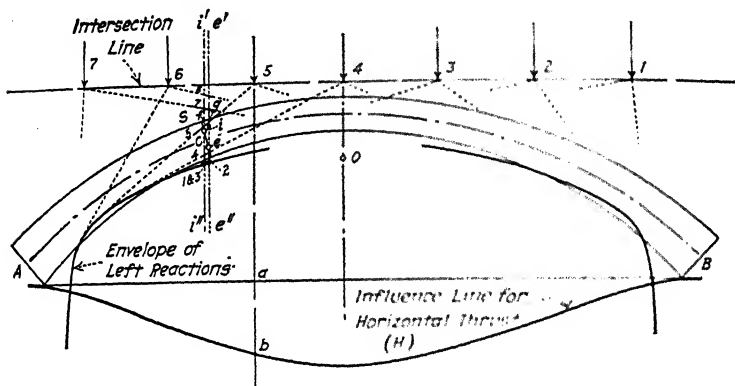


FIG. 44.

thrust and to the extreme fiber respectively. Let  $\rho$  be the letter used for the radius of gyration of the section, then

$$f_c = \frac{N(\rho^2 \pm x_0)x_1}{A\rho^2} \quad \frac{N(\rho^2 \pm x_0)}{A \cdot \frac{\rho^2}{x_1}}$$

If the stress in the *upper* fiber is desired, the numerator in the above expression represents the moment about a point a distance  $\frac{\rho^2}{x_1}$  below the gravity axis of the section, where  $x_1$  is the distance from the gravity axis to the *upper* fiber. Similarly the moment for the *lower* fiber would be taken about a point a distance  $\frac{\rho^2}{x_1}$  above the gravity axis where  $x_1$  is the distance from the gravity axis to the *lower* fiber. If we denote these moments by  $M_a$

and  $M_i$ , and the maximum fiber stresses by  $f_e$  and  $f_i$  respectively, then

$$f_e = \frac{M_e}{A \cdot \rho^2} = \frac{M_e}{A(ce)} \quad (\text{See Fig. 45})$$

$$f_i = \frac{M_i}{A \cdot \rho^2} = \frac{M_i}{A(ci)} \quad (\text{See Fig. 45})$$

$M_e$  and  $M_i$  are given graphically in Fig. 45 as the products  $R(ae)$  and  $R(bi)$  respectively. It will be more convenient, however, to draw vertical lines through the points  $e$  and  $i$ , and to determine the products  $H(ge)$  and  $H(fi)$ .

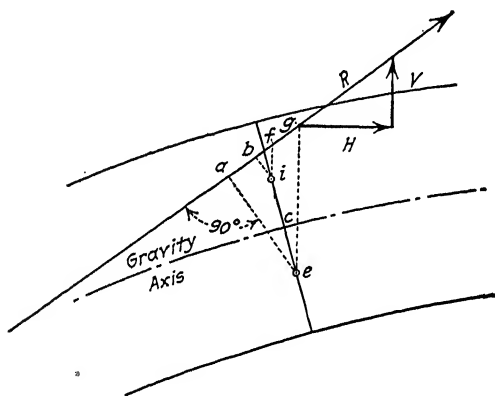


FIG. 45.

With the above discussion in mind, let us consider the influence on section  $S$ , Fig. 44, of a 1-lb. load at point 5. A vertical through this point shows the horizontal thrust to have a value  $ab = 0.98$  lb., and a line drawn from the same point on the intersection line, tangent to the envelope of the left reaction, cuts off the distances  $ge$  and  $fi$  on the verticals through points  $e$  and  $i$  of the given section  $S$ .  $ge = 2.00$  ft.  $fi = 0.35$  ft. Therefore  $M_e = 1.96$  ft.-lb. and  $M_i = 0.34$  ft.-lb., and these moments may be plotted as the influence lines for fiber stress since the denominators in the preceding equations are constants.

**45. Method of Analyzing Unsymmetrical Arches for Loading Only.**—In deriving equations (8), (10), and (12) of Art. 39, the

= 0. The first two assumptions express the condition that the origin of coördinates is taken at the center of gravity of the elastic weights, while the third assumption is satisfied when the product of inertia of these weights referred to the two coördinate axes is zero. In Arts. 41 and 42 it is shown that the latter is the case when the two axes are conjugate diameters with reference to an ellipse for the entire arch with its center at the center of gravity

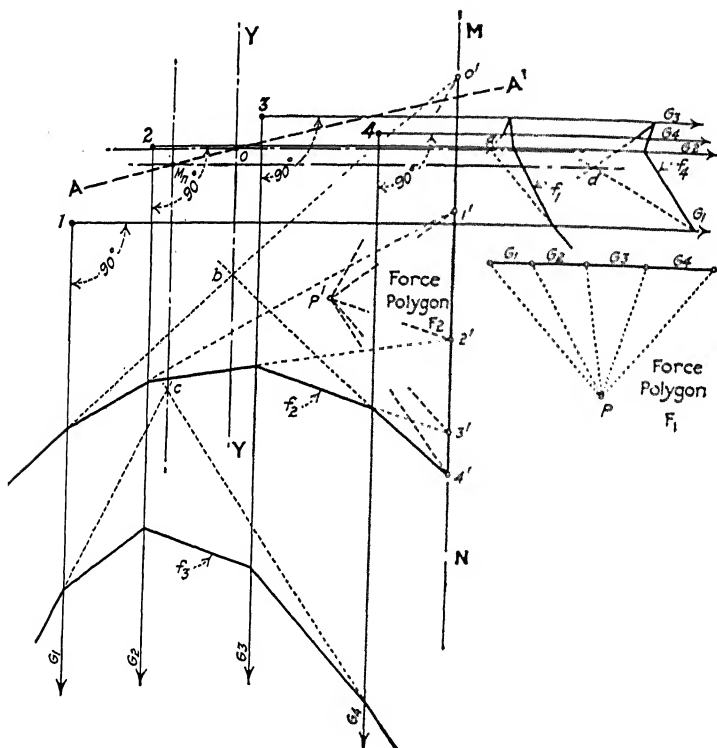


FIG. 46.

of the elastic weights. It will be convenient to assume a vertical direction for one of the coördinate axes. In a symmetrical arch it is then recognized at once that the horizontal axis is conjugate to the vertical, but this is not so for an arch that is unsymmetrical. For such an arch the additional problem is presented of finding a coördinate axis which will be conjugate to the assumed vertical axis. This may readily be accomplished graphically.

In Fig. 46 let points 1, 2, 3, and 4 be the centers of gravity

of elements with elastic weights  $G_1, G_2, G_3$ , and  $G_4$ , respectively.  $O$  is the center of gravity of all the elastic weights and may be found as usual by assuming the elastic weights to act, first horizontally, and then vertically, and finding the line of action of the resultant in each case. The intersection of these two lines locates the center of gravity of all the weights. The construction to find  $O$  is all shown by means of force polygon  $F_1$  and equilibrium polygons  $f_1$  and  $f_2$ .

Now in order to find a conjugate diameter  $AA'$  to a vertical through  $O$ , take any vertical axis  $MN$  and extend all sides of the equilibrium polygon  $f_2$  to intersect this axis at  $0', 1', 2', 3'$ , and  $4'$ . The segments, as we know, will be proportional to the moments of the elastic weights with respect to  $MN$ . Consider these segments  $0'1', 1'2', 2'3'$ , and  $3'4'$  as forces and find their center of gravity  $M_n$  assuming that they are applied at the same points 1, 2, 3, and 4. The construction is the same as for finding  $O$  except that the acting forces are  $0'1', 1'2'$ , etc., instead of  $G_1, G_2$ , etc. The force polygon  $F_2$  and the equilibrium polygons  $f_3$  and  $f_4$  furnish the solution. The vertical passing through the intersection  $c$  of the first and last sides of  $f_3$  will contain the point  $M_n$ . Rotating by  $90^\circ$  the forces  $0'1', 1'2'$ , etc., about points 1, 2, 3, and 4, the horizontal through the intersection  $d$  of the first and last side of  $f_4$  will also contain  $M_n$ . Thus the meeting point of the vertical through  $c$  and the horizontal through  $d$  will definitely determine the point  $M_n$  which is the antipole of the ellipse of the entire arch with respect to the vertical axis  $MN$ . As shown in Fig. 37A, a line through this point  $M_n$  and the center  $O$  of the ellipse is a conjugate diameter to the line  $MN$  or to a parallel or vertical line through  $O$ . Thus  $AA'$  is conjugate to a vertical through the center of gravity of the elastic weights—that is,  $AA'$  is the proper coördinate axis  $X - X$  corresponding to a vertical axis  $Y - Y$ .

Once the conjugate axes for an unsymmetrical arch have been determined, the remainder of the arch analysis is similar in every way to the analysis of a symmetrical arch described in the preceding article with the exception, of course, that the entire arch must be considered. The method of analysis should be clear from a study of Figs. 42, 43, and 44.

**46. Temperature and Rib Shortening.**—If the left end of the unsymmetrical arch  $AB$ , Fig. 47, is assumed as free, a variation of  $t$  degrees in temperature will change any unit linear dimension



to a length  $1 + t_e t_D$ ,  $t_e$  being the coefficient of linear temperature expansion. The length of arch chord,  $l'$ , will become  $l'(1 + t_e t_D)$  and this will be accomplished without any rotation. The reaction at the free end of the arch to return the arch axis to its original position must be such that no rotation is produced, which means that the line of action of such reaction due to temperature must pass through the elastic center  $O$ , and lie in the diameter conjugate to the normal to the chord of the arch (see Arts. 40 and 41). The method of finding a conjugate axis to the normal is the same in principle as the method explained in the preceding article for finding a conjugate axis to the vertical. By

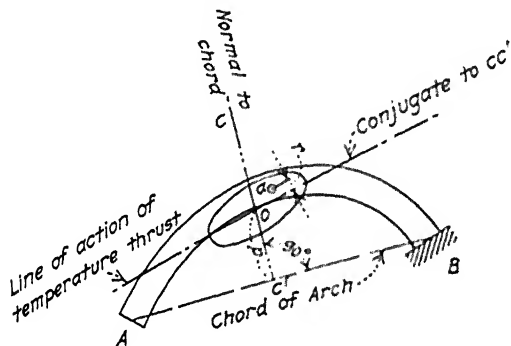


FIG. 47.

formula (6) Art. 39, the displacement of  $O$  (rigidly fastened to  $A$ ) is as follows:

$$H \sum_A^B G y \cdot x' = l' t_e t_D$$

in which  $H$  is the reaction and  $\sum_A^B G y \cdot x'$  is the product of inertia of the entire elastic system with respect to the line of action of the force  $H$  and to the arch chord. If  $a$ , Fig. 47, is the antipole of the ellipse with respect to the chord  $AB$ , then the displacement along  $AB$  is equal to  $H(OO'')(r) \sum_A^B G$ , or

$$H \cdot d \cdot r \cdot \sum G = l' t_e t_D$$

$$H = \frac{l' t_e t_D}{d \cdot r \cdot \sum G}$$

In order to determine the antipole  $a$  of the ellipse with respect to the chord  $AB$  using the graphical construction of Fig. 38, the location and lengths of the principal axes of the ellipse need to be found. The quantities already determined by the graphical constructions for loading, admit drawing tan-

gents to the ellipse of elasticity of the system parallel to the conjugate axes  $X$  and  $Y$ . For example, in Fig. 48 the normal distance to axis  $X - X$  is

$$ab = \sqrt{\frac{I_x}{\sum_A^B G}}$$

where  $I_x$  represents the moment of inertia of all the elastic weights about the axis  $X - X$  and  $\sum_A^B G$  represents the *sum* of all these weights (see Art. 42). Likewise

$$cd = \sqrt{\frac{I_y}{\sum_A^B G}}$$

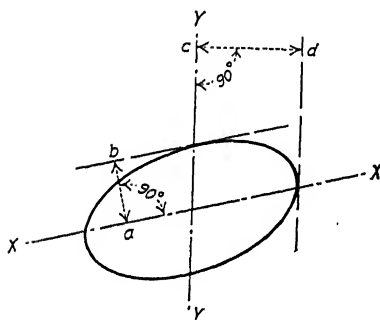


FIG. 48.

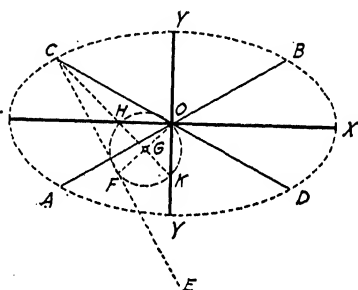


FIG. 49.

The lengths of the conjugate diameters being determined in the above manner, the graphical construction shown in Fig. 49 may be employed to determine the directions and lengths of the principal axes.

Let  $AB$  and  $CD$  be two conjugate diameters of an ellipse. From  $C$  draw  $CE$  normal to  $AB$  and upon it, starting from  $C$ , lay off  $CF = OA$ . Join  $F$  with  $O$  and on  $FO$ , as diameter, describe the circle  $G$ . Join  $C$  with the center  $G$  obtaining the two intersections  $H$  and  $K$ . Then  $OK$  and  $OH$  will determine the direction of the principal axes.  $CH$  will be the length of  $OY$ , and  $CK$  that of  $OX$ . (In order to obtain sufficient accuracy it will be necessary in many cases to assume an ellipse with the lengths of its conjugate diameters some suitable multiple of the lengths of the conjugate diameters of the true ellipse.)

If the arch is symmetrical, then the force  $H$  acts along the horizontal or major axis of the ellipse of elasticity and

$$H \sum_A^B G y^2 = l l_c t_D$$

or

$$H = \frac{l l_c t_D}{\sum_A^B G y^2}$$

The value of  $\sum_A^B Gy^2$  is easily found from the graphical construction of Fig. 43—that is, from the equilibrium polygon  $f_d$ . (If  $E_c$  has been considered as unity in calculating the elastic weights for Fig. 43, then the above value of  $H$  should be multiplied by the actual value of  $E_c$ . It is permissible to assume  $E_c$  as unity in analyzing for loading since equations 8, 10, and 12, Art. 39, contain the value of  $E_c$  on each side of the equality sign.)

Rib shortening causes the same effect as a lowering of the temperature. By referring to Arts. 14 and 34, it should be clear that the following formula may be employed to solve for the equivalent temperature drop:

$$t_D = \frac{c_a}{E_c t_c}$$

where  $c_a$  is the average unit compression in concrete of arch ring due to thrust.

**47. Analysis of a Symmetrical Arch**—By A. C. JANNI, Consulting Engineer, New York City, Designer of the Carondelet Park Bridge, St. Louis, Mo.—The arch of the Carondelet Park bridge (see Plates XII, XIII, and XIV of Chapter XIII) is a reinforced-concrete hingeless arch of the solid barrel type, with segmental intrados and extrados. Its principal dimensions are as follows:

Span.....	95.00 ft.
Rise.....	7.50 ft.
Thickness at key.....	1.50 ft.
Thickness at springing.....	2.50 ft.
Intrados radius.....	154.00 ft.
Extrados radius.....	179.00 ft.

A longitudinal section of the barrel of the arch 1 ft. in width was considered, and the graphical constructions were confined to one-half the arch on account of its symmetry.

Since the length of the geometrical axis of one-half the arch was found to be 48.80 ft., the dividing of the arch into eight equal parts (made equal for convenience) gave each element a length of 6.10 ft., and the semi-axes of all the ellipses of elasticity of the various elements lying in the arch axis had the same value, namely:

$$\rho_1 = 6.10 \times \sqrt{\frac{1}{12}} = 6.10 \times 0.289 = 1.76 \text{ ft.}$$

Taking into account the steel reinforcement in the various cross-sections of the elements, the area,  $A$ , and moments of inertia,  $I$ , were found to be as follows:

	$A$	$I$
1.....	2.48 sq. ft.	0.46
2.....	2.48 sq. ft.	0.46
3.....	1.93 sq. ft.	0.46
4.....	2.03 sq. ft.	0.55
5.....	2.13 sq. ft.	0.64
6.....	2.33 sq. ft.	0.87
7.....	3.18 sq. ft.	1.48
8.....	3.38 sq. ft.	1.92

The elastic weights of the elements  $\left(\frac{\Delta S}{E_c I} = G\right)$ , assuming  $E_c = 1$  for the sake of simplicity, were found to have the following values:

	$G$		$G$
1.....	13.26	5.....	9.53
2.....	13.26	6.....	7.01
3.....	13.26	7.....	4.12
4.....	11.09	8.....	3.18

The semi-axes of the ellipses of elasticity  $\left(\sqrt{\frac{I}{A}}\right)$ , normal to the axis of the arch, were as follows:

1.....	0.43 ft.	5.....	0.55 ft.
2.....	0.43 ft.	6.....	0.61 ft.
3.....	0.49 ft.	7.....	0.68 ft.
4.....	0.52 ft.	8.....	0.75 ft.

The graphical constructions on Designing Sheet No. 24 were made in the following manner:

*Polygon  $p_1$ .*—The elastic weights given above were considered as vertical forces applied at the corresponding centers of gravity of the elements. The static moments of these forces with respect to center line  $Y$  were then found by means of the force polygon with the pole distance  $\Sigma G$ , and the corresponding equilibrium polygon  $p_1$ . The sides of  $P_1$ , produced, cut on the vertical through  $O$  the static moments required.

*Polygon  $p_2$ .*—The same elastic weights given above were next assumed as applied *horizontally* at the centers of the elements, and the polygon  $p_2$  was constructed to find the position of the center of gravity  $O$  of the elastic weights, as well as the static moments of these weights with respect to the horizontal passing through  $O$ .

*Polygon  $p_3$ .*—Knowing the semi-axes of the ellipses of elasticity of the various elements of the arch, the next step was to locate the antipoles  $O'_1$ . . . .  $O'_8$  of the vertical through  $O$  with respect to each one of these ellipses. The static moments obtained by polygon  $p_1$  were then regarded as vertical forces applied at the corresponding antipoles of the elements, and the equilibrium polygon  $p_3$  constructed. It should be clear that this polygon gave the moment of inertia of the whole arch with respect to the vertical  $Y$ . (The pole  $P_3$  was chosen arbitrarily.)

*Polygon  $p_4$ .*—The antipoles of the horizontal  $OX$  were next located with respect to the various ellipses, and these points designated as  $O''_1$ . . . .  $O''_8$ . The static moments, obtained by polygon  $p_2$ , were regarded as horizontal forces applied respectively at the points  $O''_1$ . . . .  $O''_8$ . (The pole or center  $P_4$  was selected at a distance below  $OX$  equal to the vertical distance between the first and the last sides of the polygon  $p_3$ .) The corresponding equilibrium polygon  $p_4$  gave the moment of inertia of the elastic system with respect to  $OX$ .

*Polygon  $p_5$ .*—The polygon  $p_5$  was constructed by considering the same static moments as were used in determining the polygon  $p_4$ , assuming also these moments to act as forces at the same points  $O''_1$ . . . .  $O''_8$ , but this time in a vertical direction. (The pole distance of the force polygon  $P_5$  was made equal to  $e$ . In Designing Sheet No. 24 this distance is shown as  $2e$ , but this is because the entire force polygon was made twice the usual size for convenience in drawing the corresponding equilibrium polygon  $p_6$ .)

Polygons  $p_1$ ,  $p_3$ , and  $p_5$  are the only polygons necessary for the study of the arch. They are, so to speak, characteristics peculiar to the arch, by means of which moments, vertical reactions, and horizontal thrusts can be determined immediately for any hypothesis of loading.

*Dead Load.*—For 1-ft. width the following loads were computed:

	Weight of elements	Weight of fill over elements
1.....	0.686 ton	0.457 ton
2.....	0.686 ton	0.457 ton
3.....	0.732 ton	0.518 ton
4.....	0.778 ton	0.670 ton
5.....	0.823 ton	0.854 ton
6.....	0.915 ton	1.110 tons
7.....	1.006 tons	1.386 tons
8.....	1.098 tons	1.590 tons

The verticals of these loads, applied at the respective centers of gravity, cut the polygons  $p_1$ ,  $p_3$ , and  $p_5$ . The intercepts on these verticals with polygon  $p_1$ , measured to the scale of the drawing and multiplied each by its corresponding load, gave in each instance the amount of the moment at the point  $O$  for the load in question. Adding together all these partial moments, the total moment at  $O$  was obtained due to the dead load of the entire arch.

Similarly, the intercepts on these verticals with polygon  $p_5$  (measured on a scale having as a unit the vertical distance between the first and last side of polygon  $p_3$ ) multiplied each by its corresponding load, gave in each instance the amount of horizontal thrust due to the load under consideration. Adding together all these partial horizontal thrusts, the total horizontal thrust was obtained.

The results were as follows:

$$\Sigma M = 442.816 \text{ ft.-tons}$$

$$\Sigma H = 33.458 \text{ tons}$$

Knowing the total dead load of the arch = 13.766 tons, the points where the resultant reaction crossed the axes  $X$  and  $Y$  were found in the following manner, the values of  $x$  and  $y$  being given with respect to the center  $O$ :

$$x = \frac{442.816}{13.766} = 32.16 \text{ ft.} \quad y = \frac{442.816}{33.458} = 13.20 \text{ ft.}$$

The exact position of the polygon of pressure, therefore, was located, and the maximum stresses (tons per square foot) in the four sections  $S_1$ ,  $S_2$ ,  $S_3$ , and  $S_4$  due to dead load were found to be as follows:

Section	Intrados	Extrados
$S_1$ .....	11.354	17.034
$S_2$ .....	8.663	26.447
$S_3$ .....	11.686	19.481
$S_4$ .....	33.400	-105.000 (steel)

A short graphical method of analyzing an arch for dead load (including temperature and rib shortening) is shown in Designing Sheet No. 25. Since dead load usually controls in the shape of an arch ring, this method should be used for making preliminary investigations with a view to determine the probable adequacy of the arch dimensions assumed. Proof of the correctness of the graphical construction may be found in the Journal of the Western Society of Engineers, issue of May, 1913. The method in detail is as follows: Construct equilibrium polygons  $p_2$  and  $p_4$  as in Designing Sheet No. 24. On an arbitrary vertical  $ab$  lay off the dead loads and assume the pole  $P_0$  on the horizontal through  $a$ . Draw the corresponding equilibrium polygon  $p_0$  intersecting with the verticals through the points of application of the loads. Now load the polygon  $p_0$  horizontally with the same elastic weights as determined for the arch, at the points where the verticals through the centers of gravity of the elements meet the polygon  $p_0$ . Then intersecting these horizontals with an equilibrium polygon  $p'_2$ , corresponding to the force polygon  $P_2$ , the center of gravity  $O'$  of this new elastic system is determined. Again load the polygon  $p_0$  with the static moments found for the construction of polygon  $p_4$ , but this time assume them applied at the meeting point of the verticals through the antipoles with the sides of the polygon  $p_0$ . The equilibrium polygon  $p'_4$ , corresponding to the force polygon  $P_4$ , determines a distance  $\frac{1}{2}e'$  between its first and last sides. This distance is proportional to the moment of inertia of the elastic weights acting on this new elastic system, in the same manner that  $\frac{1}{2}e$  is proportional to the moment of inertia of the system of elastic weights with respect to the horizontal passing through  $O$ .

Between the polygon  $p_0$  and the true pressure polygon  $p$  there is a geometrical relation. For example, the distance of any point on the true pressure polygon  $p$  from the horizontal through  $O$  can be obtained by multiplying by the ratio  $\frac{e}{e'}$  the distance from the horizontal through  $O'$  to the point of the polygon  $p_0$  on the same vertical with the point in question. Thus any distance as  $kk$  equals  $k'k'$  multiplied by  $\frac{e}{e'}$ . The horizontal thrust  $aP$ , likewise, may be found by multiplying the assumed thrust  $aP_0$  by the inverse of the ratio, or  $\frac{e'}{e}$ .

In the arch in question  $\frac{e'}{e} = \frac{0.59}{0.44} = 1.34$  and the assumed horizontal thrust = 25 tons. The true thrust, therefore, was  $1.34 \times 25 = 33.5$  tons. The ratio  $\frac{e}{e'} = \frac{0.44}{0.59} = 0.745$ , and the vertical distance between  $O'$  and the polygon  $p_0 = 0.70$ . Then  $0.745 \times 0.70 = 0.52$  determined the exact point where the true horizontal thrust intersected the key of the arch.

Note that the coördinates of the resultant obtained by the method of Designing Sheet No. 24 checked exactly with those obtained by this method. The horizontal thrust also checked by the two methods.

*Temperature.*—The horizontal thrust, due to temperature changes, passed through  $O$  and its intensity was given by the formula:

$$H = \frac{lt_c E_c}{\Sigma Gy^2}$$

where

$t_c$  = coefficient of expansion = 0.0000066.

$l$  = span of the geometrical axis = 95.7 ft.

$E_c$  = modulus of elasticity of concrete = 144,000 tons per sq. ft.

$\Sigma Gy^2$  = moment of inertia of the arch with respect to the horizontal passing through  $O = e \times 14.16 \times 11.76 = 2.64 \times 14.16 \times 11.76 = 439.61$ .

( $e$  was measured to the same scale as the elastic weights—that is, 1 in. = 6 units. The polar distances were measured to the same scale as the drawing, namely: 1 in. = 3 ft.)

Substituting these values

$$H = \frac{0.0000066 \times 95.7 \times 144,000}{439.61} = 0.20$$

for  $1^\circ$  change of temperature. For a change of  $30^\circ\text{F}$ .

$$H = 6.00 \text{ tons.}$$

For a drop of temperature of  $30^\circ$ , which was the only case needing consideration, the following stresses were obtained in tons per square foot:

Intrados

Extrados



*Shortening of Arch Due to Dead Load and Shrinkage.*—The shortening of the geometrical axis of the arch due to dead load, at the time when the arch is allowed to bear upon its supports, may be considered as a shortening due to a drop in temperature.

Knowing, by means of the pressure polygon, the amount of compression on each cross-section, and knowing also the modulus  $E_c$ , the shortening of the arch was calculated and found to correspond to a drop in temperature of  $23.4^\circ\text{F}$ .

The arch was concreted by the alternate block method (see Art. 53) and the shrinkage of the arch was confined to the shrinkage of its keys only. The total key space was 6 ft., and  $\frac{1}{2000}$  was considered the ratio of shrinkage in a 1:2:4 concrete. The shortening of the arch axis, using these values, was found to correspond to a drop of  $4.6^\circ\text{F}$ . in the arch.

The total drop of temperature due to the above two causes was assumed at  $28^\circ\text{F}$ . The corresponding horizontal thrust which, of course, passed through  $O$ , induced the following stresses (tons per square foot) in sections  $S_1$  and  $S_4$  of the arch.

	Intrados	Extrados
At spring (section $S_1$ ). 8.30 (concrete)		—315.00 (steel)
At key (section $S_4$ ). —42.00 (steel)		5.80 (concrete)

It might be interesting to note that had the arch been concreted by longitudinal sections from springing to springing in one operation, the shrinkage in the concrete would have induced in the arch, stresses equivalent to a drop of temperature of  $75^\circ\text{F}$ .

*Stresses Due to Live Load.*—From Designing Sheet No. 24 it should be clear how the envelope lines and the intersection line can be constructed, the construction being fully indicated for position 4 of the load.

In Designing Sheet No. 26, which represents the whole arch, the envelope lines, the intersection line, and the polygon  $p_6$  have been redrawn.

By means of the above lines, the various reactions corresponding to the several positions of the unit live load, together with the corresponding horizontal thrust in each case, have been determined. Moments have been determined, likewise, for the kern points  $i$  and  $e$  of each section and the results obtained are given in the following table:

Influence lines for kern moments have been plotted in Design-

Positions	H	S <sub>1</sub>				S <sub>2</sub>				S <sub>3</sub>				S <sub>4</sub>			
		ci	ce	M <sub>i</sub>	M <sub>e</sub>	ci	ce	M <sub>i</sub>	M <sub>e</sub>	ci	ce	M <sub>i</sub>	M <sub>e</sub>	ci	ce	M <sub>i</sub>	M <sub>e</sub>
1	0.09	2.08	3.05	0.18	0.27	-0.52	0.25	-0.05	0.02	-1.96	-1.30	-0.17	-0.12	-1.60	-1.10	-0.14	-0.10
2	0.50	2.02	3.00	1.01	1.50	-0.53	0.25	-0.26	0.12	-1.90	-1.25	-0.95	-0.62	-1.43	-0.93	-0.71	-0.47
3	1.10	1.90	2.86	2.09	3.15	-0.55	0.22	-0.60	0.24	-1.80	-1.20	-1.98	-1.32	-1.27	-0.77	-1.39	-0.85
4	1.88	1.65	2.62	3.10	4.92	-0.60	0.18	-1.13	0.34	-1.60	-1.00	-3.00	-1.88	-0.90	-0.40	-1.69	-0.75
5	2.65	1.40	2.38	3.71	6.31	-0.66	0.12	-1.70	0.32	-1.40	-0.78	-3.71	-2.07	-0.48	0.02	-1.27	0.05
6	3.16	1.02	2.00	3.22	6.32	-0.73	0.08	-2.31	0.25	-1.10	-0.45	-3.47	-1.42	0.13	0.63	0.41	1.99
7	3.30	0.50	1.50	1.65	4.95	-0.82	-0.05	-2.70	-0.16	-0.70	0.0	-2.31	0.0	1.04	1.54	4.51	5.08
8	3.16	-0.35	0.68	-1.11	2.15	-0.98	-0.19	-3.09	-0.60	0.02	0.68	0.06	2.15	.....	.....	.....	.....
9	2.65	-1.70	-0.62	-4.50	-1.64	-1.15	-0.30	-3.05	-0.79	1.32	2.00	3.49	5.30	.....	.....	.....	.....
.....	2.53	.....	.....	.....	.....	.....	.....	.....	.....	1.65	.....	4.17	.....	.....	.....	.....	.....
.....	2.54	.....	.....	.....	.....	.....	.....	.....	.....	.....	2.30	.....	5.84	.....	.....	.....	.....
10	1.88	-4.10	-3.00	-7.71	-5.64	-1.17	-0.29	-2.20	-0.54	1.12	1.78	2.10	3.34	.....	.....	.....	.....
11	1.10	-8.50	-7.30	-9.35	-8.03	0.0	0.91	0.0	1.00	0.57	1.20	0.63	1.32	.....	.....	.....	.....
.....	0.63	.....	.....	.....	.....	4.30	.....	2.71	.....	.....	.....	.....	.....	.....	.....	.....	.....
.....	0.65	.....	.....	.....	.....	.....	5.05	.....	3.28	.....	.....	.....	.....	.....	.....	.....	.....
12	0.50	-17.45	-15.90	-8.72	-7.95	4.20	4.93	2.10	2.47	0.30	0.92	0.15	0.46	.....	.....	.....	.....
13	0.09	-46.85	-42.90	-4.22	-3.86	4.02	4.75	0.36	0.43	0.15	0.80	0.01	0.07	.....	.....	.....	.....

ing Sheet No. 26. These influence lines have no direct importance in a design of a reinforced-concrete arch section where the tension in concrete is omitted, and the intention in showing them in this case is to demonstrate how careful a designer should be in applying certain empirical rules of loading in order, as he thinks, to find the maximum stresses in the arch. These lines show clearly that the maximum stresses at intrados and extrados for the same section do not happen with the same hypothesis of loading.

The stresses at section  $S_1$  due to the live load of 100 lb. per square foot were found to be as follows in tons per square foot:

Intrados	Extrados
10.60 (concrete)	-243.0 (steel)

Total stresses in section  $S_1$  of the arch were finally determined and found to be:

$$\begin{aligned} f_s &= 12,750 \text{ lb. per square inch (steel)} \\ f_c &= 850 \text{ lb. per square inch (concrete)} \end{aligned}$$

The computations of the stresses in the sections  $S_2$ ,  $S_3$ , and  $S_4$  have been omitted, as they would have shown smaller stresses than those found above for section  $S_1$ .

*Design of Abutment.*—The resultant due to the dead load of the arch was found to be 36.2 tons (per 1-ft. length of abutment) and the vertical dead load on the abutment itself, 45.00 tons. The resultant of these two forces was 67.500 tons, and its vertical component 58.7 tons. (See Designing Sheet No. 27.) The resultant dead load intersected the base at point  $E$  which is not the center of the base. Using formulas for bending and direct stress for compression over the whole section, there resulted a pressure of 2.5 tons per square foot at  $C$  and a pressure of 0.38 ton per square foot at  $D$ .

$K_2$  and  $K_1$  are shown as the middle third points of the rectangular base  $CD \times 1$  ft. If from  $K_1$  we draw the tangent  $K_1B$  to the left envelope line, all positions of the live load to the right of  $B$  will cause compression at  $C$ . Also if we draw from  $K_1$  the vertical  $K_1F$ , and from  $C$  the vertical  $CG$ , all positions of the live load between  $G$  and  $F$  will affect the point  $C$  in the same manner, so that the most prejudicial hypothesis of loading, as far as pressure at  $C$  is concerned, is when it is assumed that all arch and abutment is loaded except the space  $FB$ .

Assuming, as for the arch, a live load of 100 lb. per square foot,

the maximum compression at *C* was found to be 0.50 ton per square foot.

On account of a rise in temperature, an additional pressure at *C* was taken into account. Assuming that there would be a rise of 30°F., which corresponds to a horizontal thrust of 6.0 tons, the corresponding pressure at *C* was found to be 0.48 ton per square foot.

The total maximum pressure at *C* was found to be as follows:

$$2.50 + 0.50 + 0.48 = 3.48 \text{ tons per square foot}$$

The part *PD* of the footing slab was designed as a slab supported on two sides (counterforts) and loaded as shown by the pressure diagram.

The part *CP* was reinforced to stand a deflection indicated by the arrow.

For shear, it was necessary only to ascertain the intensity at *P*, where it was 22.5 tons per 1-ft. depth of slab, safely absorbed by the sections of concrete, longitudinal upper reinforcement, and stirrups.

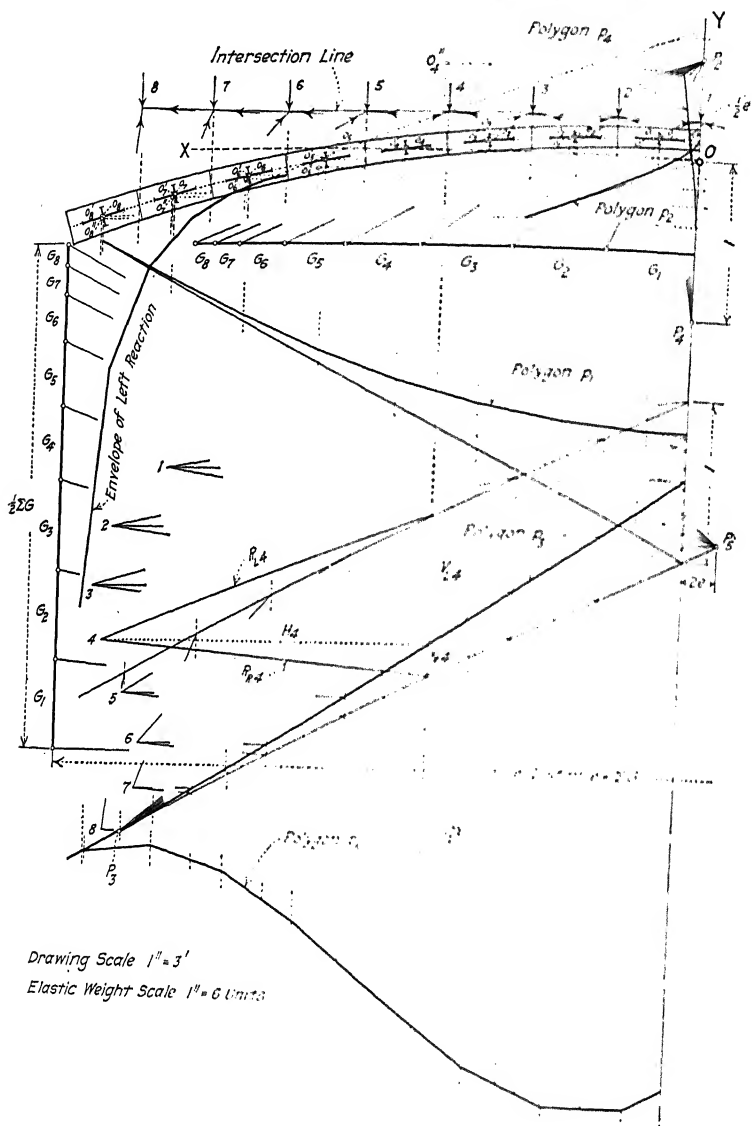
Of course the shear (likewise the moment) increased going from *P* to *E*, where it reached the maximum; but it is not necessary to go into details for the sections on the right of the section *PQ*, since the shape and area of these sections preclude any possibility of maximum conditions. The maximum compression at *Q* was found to be 601 lb. per square inch.

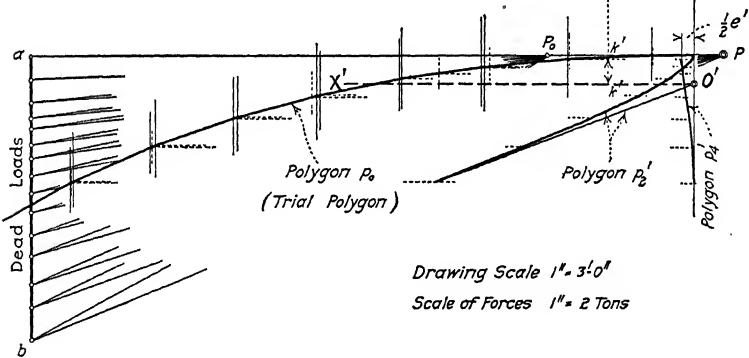
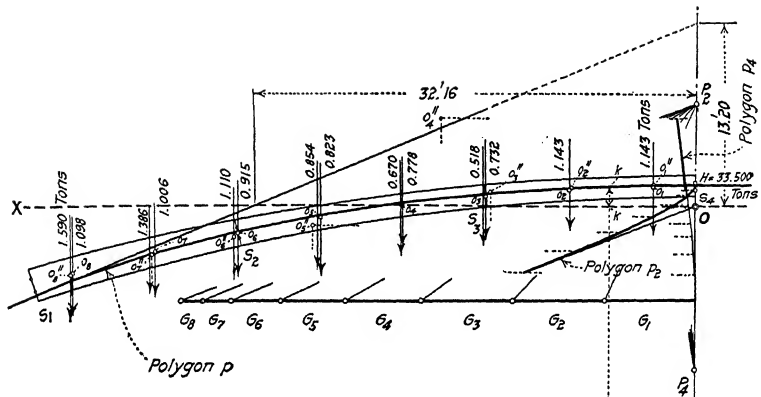
The front wall of the pier (2 ft. thick) was found to safely support the vertical component of the total reaction, or 13.76 tons + 4.70 tons.

Concerning now the horizontal component of the above reaction, two sections were considered for shear—namely: sections *HL* and *MN*. The maximum shear in concrete at section *HL* was found to be 52 lb. per square inch (considering the steel reinforcement to be 12.5 sq. in. per linear foot depth), and at section *MN*, 64 lb. per square inch. Considering that a good vertical compression acted on these two sections, it will be seen that the above stresses were quite legitimate.

Finally, the counterforts were designed as solids under combined action of direct compression and bending with regard to the thrust of the arch. Fig. 50 on Designing Sheet No. 27 gives an idea of how the problem was solved by means of the formula for bending and direct stress. *E* is the resultant acting upon the counterfort.

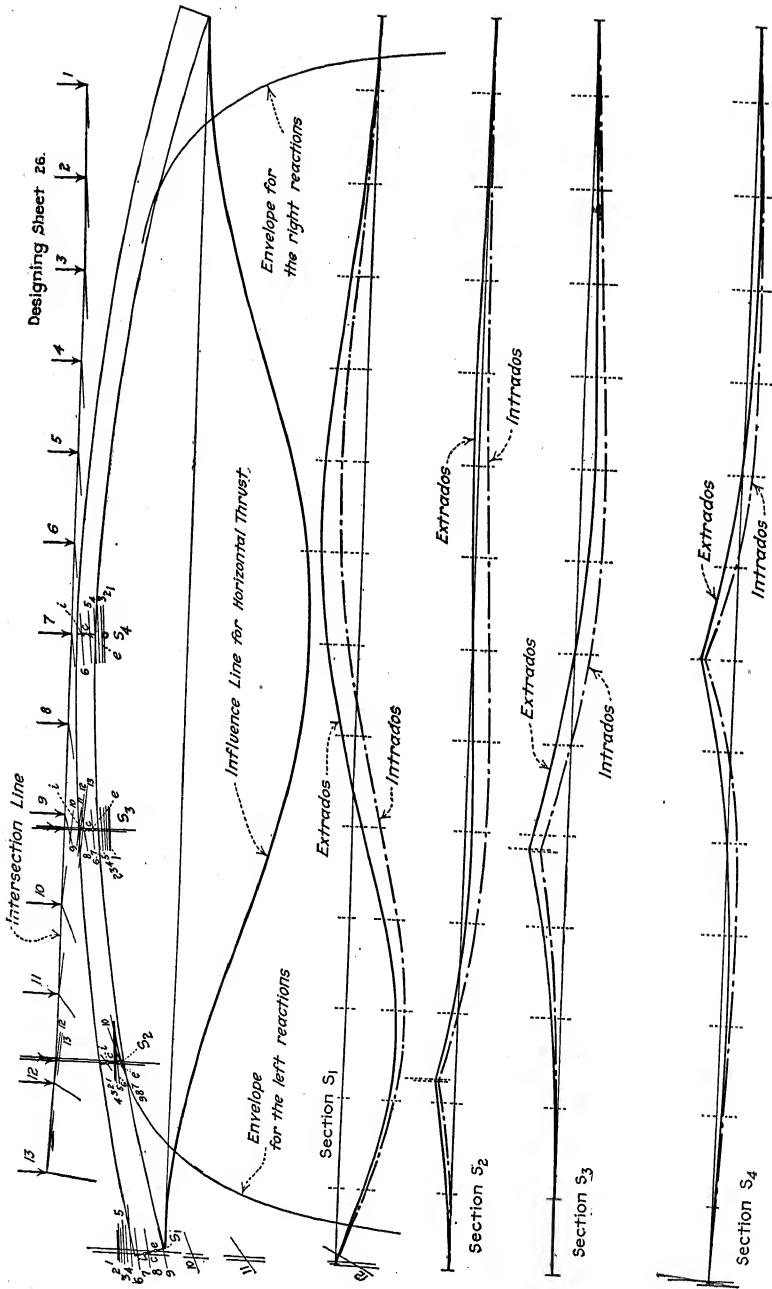
Designing Sheet 24



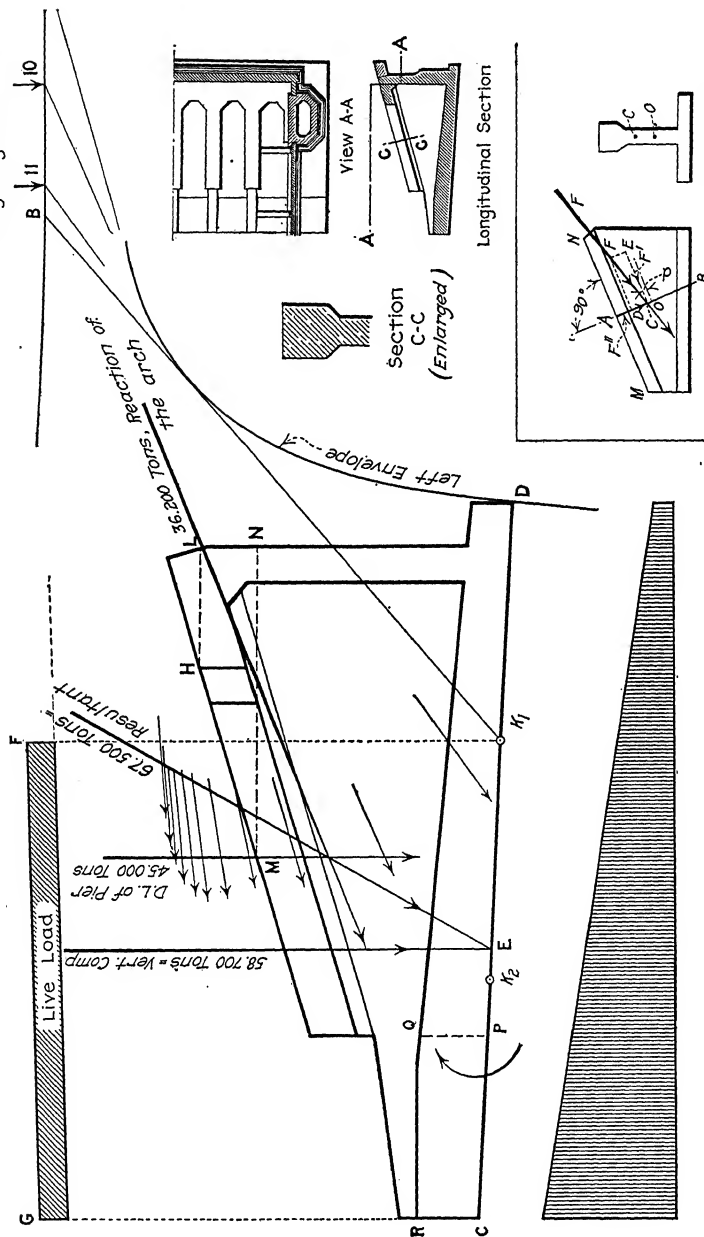


Drawing Scale 1" = 3'-0"

Scale of Forces 1" = 2 Tons



Designing Sheet 27.





fort, and  $AB$  is a section taken normally to  $MN$ .  $F'$  is the compressive force on the section and  $F''$  the shear.  $O$  is the center of gravity of the cross-section  $AB$ .

**48. Method of Analyzing a Series of Arches with Deformable Supports.**—Consider first a three-span symmetrical arch structure as shown in Fig. 51, whose piers  $P_1$  and  $P_2$  are of such dimensions that they can be regarded as deformable. If the arches  $A_1$ ,  $A_2$ , and  $A_3$  were equal, then, as far as the dead load is concerned, each of them could be regarded as a fixed arch. If they are unequal as shown, then, with the overloading of the short spans, it is usually possible to drive the resultant to the center or near the center of the base of the pier. This result being accomplished, it is then permissible to consider each arch as fixed.

The live load, in every case, requires a totally different treat-

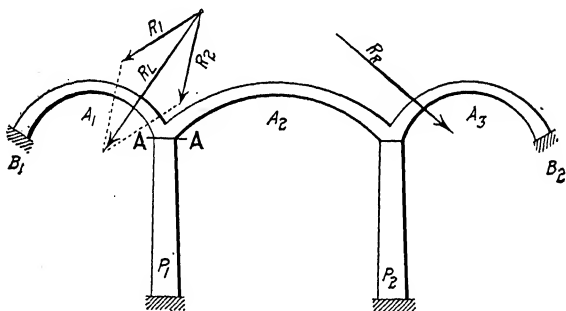


FIG. 51.

ment from that mentioned above. It is evident that the middle arch  $A_2$  is supported by two elastic systems— $A_1P_1$  on the left and  $A_3P_2$  on the right. The method is to construct the ellipse of elasticity for the arch  $A_1$  and for the pier  $P_1$  (Fig. 52)—that is to say, to construct the ellipse  $O_a$  (ellipse of elasticity of the arch with respect to its terminal section  $A - A$ ) and the ellipse  $O_p$  (ellipse of elasticity of the pier with respect to its terminal section  $A - A$ )—and then to construct the ellipse of elasticity with respect to the same section  $A - A$  when this section is regarded as a section of the entire system  $A_1P_1$ .

A horizontal displacement without rotation of section  $A - A$ , regarded as the terminal section of  $P_1$ , cannot happen but for the action of a horizontal force  $F_p$  passing through  $O_p$ , and

if  $\Sigma G_p$  is the elastic weight of the pier  $P_1$ , this displacement of  $A - A$  will be given by (see Art. 42)

$$F_p \cdot \Sigma G_p \cdot \rho_p^2$$

This same displacement of  $A - A$ , when  $A - A$  is regarded as a terminal section of  $A_1$ , is given by (see Fig. 52)

$$F_a \cdot \Sigma G_a \cdot \rho_a^2$$

where  $\Sigma G_a$  is the elastic weight of the arch  $A_1$ .

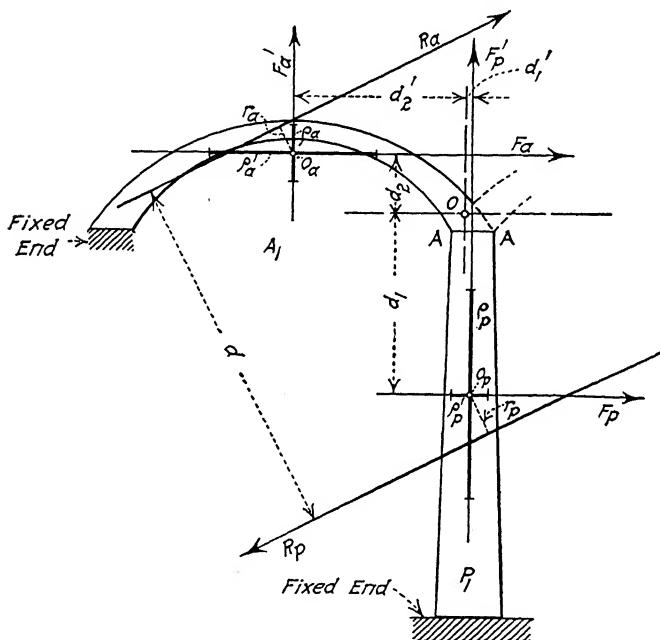


FIG. 52.

We have, therefore:

$$F_p \cdot \Sigma G_p \cdot \rho_p^2 = F_a \cdot \Sigma G_a \cdot \rho_a^2$$

or

$$\frac{F_a}{F_p} = \frac{\Sigma G_p \cdot \rho_p^2}{\Sigma G_a \cdot \rho_a^2} \quad (1)$$

which gives the position of the horizontal passing through the center  $O$ . In fact, if we regard  $A - A$  as a section of the elastic system  $A_1P_1$ , its horizontal displacement must be caused by a horizontal force  $F_a + F_p$  passing through  $O$ . If we designate

$d_1$  and  $d_2$  as the perpendicular distances from  $O$  to  $F_p$  and  $F_a$  respectively, then

$$\frac{d_1}{d_2} = \frac{\Sigma G_p \cdot \rho_p^2}{\Sigma G_a \cdot \rho_a^2}$$

or

$$d_1 = \frac{d_1 + d_2}{1 + \frac{\Sigma G_a \cdot \rho_a^2}{\Sigma G_p \cdot \rho_p^2}} \quad (2)$$

In exactly the same way, we obtain

$$\frac{F'_a}{F'_p} = \frac{\Sigma G_p \cdot (\rho'_p)^2}{\Sigma G_a \cdot (\rho'_a)^2} = \frac{d'_1}{d'_2}$$

or

$$d'_1 = \frac{d'_1 + d'_2}{1 + \frac{\Sigma G_a \cdot (\rho'_a)^2}{\Sigma G_p \cdot (\rho'_p)^2}} \quad (3)$$

This expression gives the position of the vertical through  $O$ .

The point  $O$  being located, the elastic weight of the combined arch and pier must now be determined. Since  $O$  is the center of the ellipse, any rotation of section  $A - A$  (as belonging to  $A_1P_1$ ) about  $O$  cannot be caused but by a couple. (A force of which  $O$  is the antipole must lie at infinity—that is, will act along the antipolar of  $O$ —which is the same thing as saying that the rotation is caused by that of a couple.) On the other hand, the same rotation of  $A - A$ , regarded as terminal section of  $A_1$ , is caused by a force  $R_a$  acting along the antipolar of  $O$  with respect to the ellipse  $O_a$ ; also the same rotation of  $A - A$ , regarded as terminal of  $P_1$ , is caused by a force  $R_p$  acting along the antipolar of  $O$  with respect to the ellipse  $O_p$ . Hence the forces  $R_a$  and  $R_p$  will constitute a couple, or  $R_a = R_p = R$ . The angle of rotation is given by the formula (Art. 39)

$$k = M \Sigma G = R d \Sigma G$$

and considering the section  $A - A$  as belonging first to  $A_1$  and then to  $P_1$ , we have

$$k = R r_a \Sigma G_a = R r_p \Sigma G_p$$

or

$$\Sigma G = \frac{r_a \Sigma G_a}{d} = \frac{r_p \Sigma G_p}{d} \quad (4)$$

which determines the total elastic weight of arch and pier.

The horizontal displacement of  $A - A$  as belonging to  $A_1P_1$  is

$$(F_a + F_p) \Sigma G \cdot \rho^2$$

This displacement must be the same as that due to the force  $F_p$ , or

$$(F_a + F_p) \Sigma G \cdot \rho^2 = F_p \cdot \Sigma G_p \cdot \rho_p^2$$

$$\rho^2 = \frac{\Sigma G_p \cdot \rho_p^2}{\Sigma G \left(1 + \frac{F_a}{F_p}\right)}$$

Substituting the value of  $\frac{F_a}{F_p}$  from Equation (1)

$$\rho^2 = \frac{\Sigma G_p \cdot \rho_p^2}{\Sigma G \left(1 + \frac{\Sigma G_p \cdot \rho_p^2}{\Sigma G_a \cdot \rho_a^2}\right)}$$

or

$$\rho^2 = \frac{\Sigma G_p \cdot \rho_p^2}{\Sigma G \left(1 + \frac{d_1}{d_2}\right)} \quad (5)$$

Similarly

$$(\rho')^2 = \frac{\Sigma G_p (\rho'_p)^2}{\Sigma G \left(1 + \frac{d'_1}{d'_2}\right)} \quad (6)$$

Equations (5) and (6) determine the lengths of the semi-minor and semi-major axes of the ellipse at  $O$ .

The ellipse of elasticity for the system  $A_1P_1$  (Fig. 51) is now fully determined. In a like manner the ellipse may be drawn for the system  $A_1P_1A_2$  by combining the ellipse for  $A_1P_1$  with the ellipse for  $A_2$ , and so on. The same operation can be carried out starting from the right abutment.

Suppose the effect of loads on the arch  $A_2$  is to be determined. The method of doing this is to find the ellipse of elasticity for the system  $A_1P_1$  and for the system  $A_3P_2$ . (If the entire arch system is symmetrical about the center line between piers  $P_1$  and  $P_2$ , there is a great deal of work saved.) The arch  $A_2$  is then studied in the usual way, with the only variation that it is assumed that the arch is constituted by its elements plus two *ideal* elements, one on each side of the arch  $A_2$  (Fig. 53), each having the ellipse of elasticity as above determined. These ellipses of the ideal elements are considered as any other of the ellipses of the arch elements.

Having found by the above method the reactions  $R_L$  and  $R_R$  due to the actions of the elastic systems  $A_1P_1$  and  $P_2A_3$  respectively against the arch  $A_2$ , it becomes necessary to determine which com-

ponent of  $R_L$  belongs to the arch  $A_1$  and which belongs to the pier  $P_1$ . (In Fig. 51 consider  $R_1$  the component acting upon  $A_1$ , and  $R_2$  the component acting upon the pier.) This is most easily accomplished by means of the three ellipses  $O_a$ ,  $O_p$ , and  $O$ , already found (Fig. 52). Consider the section  $A - A$  as a section of the system  $A_1P_1$  under the action of the force  $R_L$ . A rotation of this section will be performed about a certain point  $D$  (not shown), which is the antipole of  $R_L$  with respect to the ellipse  $O$ . The same rotation of  $A - A$ , if we regard  $A - A$  as the terminal section of  $P_1$ , will be caused by a force  $R_2$  acting

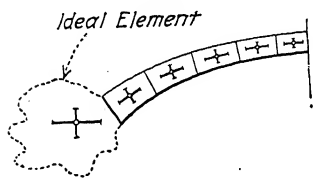


FIG. 53.

along the antipolar line of the same point  $D$  with respect to the ellipse  $O_p$ . Similarly, if  $A - A$  is regarded as the terminal section of  $A_1$ , then the same rotation of this section will be caused by a force  $R_1$  acting along the antipolar of  $D$  with respect to  $O_a$ . With the usual construction for finding polar and antipole, or, what is the same thing, for finding antipolar and pole, the lines of action of  $R_1$  and  $R_2$  can be located. Of course, as a check, the two components as found above must meet on  $R_L$ . A similar method of finding components can be applied to the system  $P_2A_3$  for finding the forces acting on  $P_2$  and  $A_3$ .

In the case of a bridge of two spans, each arch could be regarded as fixed at one end and supported at the other end by the elastic system, including arch and pier. The end arch of a three-span structure could be regarded in a similar manner except that the elastic system would consist of two arches and two piers.

It can be readily appreciated that the analysis of a large series of arches in the manner above suggested would be exceedingly laborious on account of the large number of ellipses of elasticity which would need to be determined and the consequent resolving of reactions into components. The method may be greatly simplified by the fact that the effect of a load on any one span extends principally over the span itself and the two spans immediately adjacent. For example, if  $A_2$  in Fig. 51 is assumed as an arch of a large series of arches, it is permissible for all practical purposes to consider the arches  $A_1$  and  $A_3$  as fixed at  $B_1$  and  $B_2$  and to analyze arch  $A_2$  with its supports  $A_1P_1$  and  $A_3P_2$  without regard to any of the remaining arches of the system. If the arches are

all equal, then the same calculations will serve for any three arches of the series.

It is possible to take into account the stresses in an arch resulting from the yielding of the soil beneath the piers due to an eccentricity of the resultant thrust on the base. Knowing  $E$  of the ground, which is the same thing as knowing the load necessary to have the soil yield 1 in., and neglecting the even or horizontal displacements of the soil, an ellipse of elasticity may be deter-

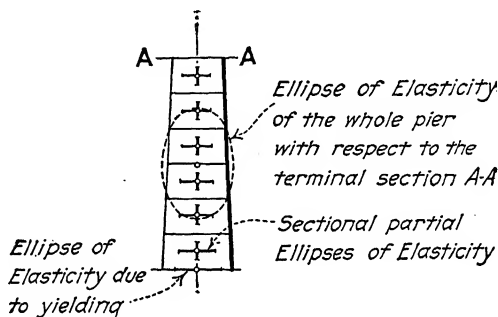


FIG. 54.

mined due to yielding. If we call  $I$  the moment of inertia of the supporting surface in contact with the footing of the pier, and  $g_p$  the amount of yielding found as above, then the expression

$$G_g = \frac{1}{g_p I}$$

will be the elastic weight to be applied at the center of gravity of that section. The ellipse of elasticity of this point (Fig. 54) will have only the horizontal axis, since the vertical one will be zero on account of the assumption that the horizontal displacements may be neglected.

The method of analyzing a series of unsymmetrical arches with elastic piers is the same in principle as the method already explained for symmetrical arches. A graphical construction is convenient, however, to find the lengths and directions of the principal axes of an ellipse when two pairs of conjugate axes are known.

These principal axes are required in order to use the construction of Fig. 38 to find antipoles from polars or antipolars from poles. A brief description of the method of combining ellipses for unsymmetrical arches will be given.

Referring to Fig. 55, consider first the arch  $AB$ , and let us determine a force  $F_a$  which will cause the point  $A$  to undergo a horizontal displacement, without rotation. The line of action of this force  $F_a$  will be along the conjugate diameter of the vertical

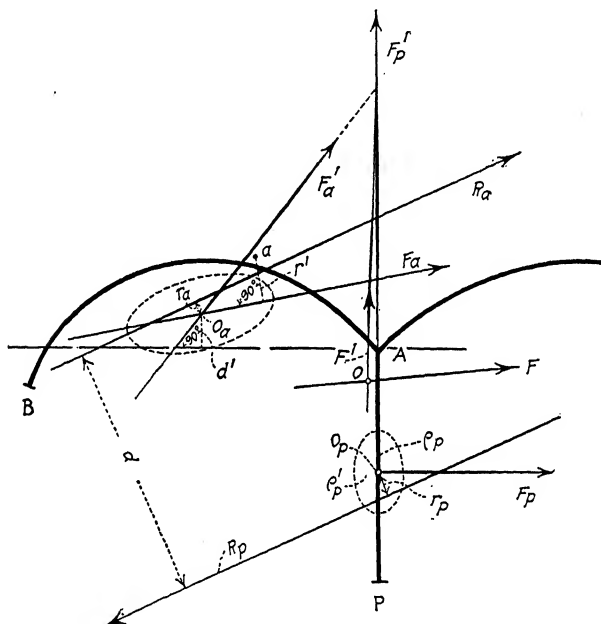


FIG. 55.

through the center of the ellipse  $O_a$ . The horizontal displacement is equal to

$$F_a \cdot \Sigma G_a \cdot r' \cdot d'$$

considering  $a$  the antipole of the horizontal through the point  $A$ . (See Art. 46.) The horizontal displacement of the point  $A$  due to force  $F_p$  is, as before,

$$F_p \cdot \Sigma G_p \cdot \rho_p^2$$

Then

$$F_p \cdot \Sigma G_p \cdot \rho_p^2 = F_a \cdot \Sigma G_a \cdot r' \cdot d'$$

or

$$\frac{F_a}{F_p} = \frac{\Sigma G_p \cdot \rho_p^2}{\Sigma G_a \cdot r' \cdot d'}$$

If  $F_a$  and  $F_p$  are prolonged until they intersect, then the resultant  $F$  of these two forces, the direction of which may be determined by means of the above equation, will cause  $A$  of the system  $BAP$  to move, without rotation, through the same horizontal distance as the force  $F_a$  acting on the system  $AB$  or the force  $F_p$  acting on the system  $AP$ .

Considering the vertical displacement of  $A$ , we obtain a similar equation to the above. The resultant  $F'$  of the forces  $F'_a$  and  $F'_p$  will cause point  $A$  of the system  $BAP$  to move through the same vertical displacement without rotation.

The two forces  $F$  and  $F'$  will cause point  $A$  to be displaced along a line passing through the center of the ellipse of elasticity of the system. Consequently the center of the ellipse is at the inter-

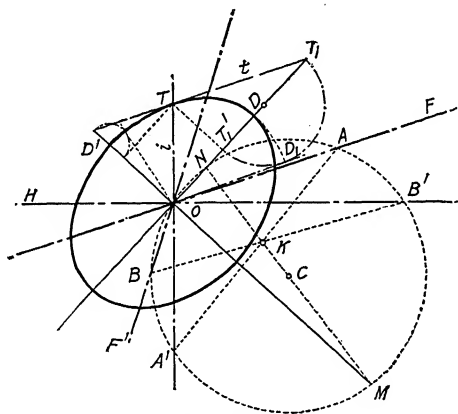


FIG. 55A.

section of the forces. The elastic weight  $\Sigma G$  of the system  $BAP$  may be found in the identical manner previously explained for the symmetrical arch and pier.

The graphical construction of Fig. 55A<sup>1</sup> serves to determine the principal axes of the ellipse  $O$ . Considering ellipse  $O$ , the line of action of the force  $F$  and a vertical ( $V$ ) through  $O$  on the one hand, and the line of action of the force  $F'$  and a horizontal ( $H$ ) through  $O$  on the other hand, constitute two pairs of conjugate elements of the ellipse by means of which the principal axes may be determined.

To find the major and minor axes, describe an arbitrary circle

<sup>1</sup> Taken from an article by Prof. H. Lossier of the University of Lausanne in the "Genie Civil," volume of 1903. Translation by Mr. Samuel Morell, Jr., Bridge Designing Engineer for City of Chicago.



(with center  $C$ ) passing through  $O$ . This circle will intersect the straight lines  $F$ ,  $V$ ,  $F'$ , and  $H$  in the points  $A$ ,  $A'$ ,  $B$ , and  $B'$  respectively. The point of intersection  $K$  of the straight lines  $AA'$  and  $BB'$  will be the center of the figure  $AA'BB'$ . Connect points  $C$  and  $K$  and prolong to intersections  $M$  and  $N$  on the circumference of the circle. The two conjugate diameters  $OM$  and  $ON$  will be perpendicular and determine the direction of the principal axes of the ellipse. The length of the axes required may be found by drawing the tangent  $t$  to the ellipse  $O$ , parallel to  $F$ . The point of contact  $T$  of  $t$  lies on the vertical  $V$  at a distance  $OT$  from  $O$  equal to  $i = \sqrt{\frac{1}{\Sigma G \cdot H_o}}$ , where  $H_o$  is the horizontal projection of the force  $F$  which causes a horizontal displacement of the point  $O$  equal to unity without rotation. Let  $T_1$  be the point of intersection of the tangent  $t$  with the axis  $ON$  and let  $T'_1$  be the projection of  $T$  on this axis. Then the length of the semi-axis is

$$OD = \sqrt{(OT'_1)(OT_1)}$$

that is,  $OD$  may be measured by the length  $OD_1$  of the tangent passing through  $O$  to the circle described on  $T_1T'_1$  as a diameter. The length of the other principal axis may be found in a like manner.

The statements made in the preceding chapter in regard to temperature and rib shortening in a series of arches with elastic piers should be noted.

## CHAPTER IX

### DETAILS OF ARCH BRIDGES

**49. Spandrel Details in Earth-filled Bridges.**—As stated in Art. 3, the filling material in solid-spandrel bridges is held in place laterally by retaining walls which rest upon the arch ring. These retaining walls may be of either the gravity or the reinforced type, or they may consist of thin vertical slabs tied together by reinforced-concrete cross walls as employed in the design of the arch bridge of Chapter IV. In the usual type of solid-spandrel construction the sidewalk rests upon the earth filling, which is the type shown in Fig. 56. Where the counterforted type of spandrel wall is employed, sidewalks are sometimes cantilevered beyond the faces of the arch ring, as illustrated in Figs. 57, 58,

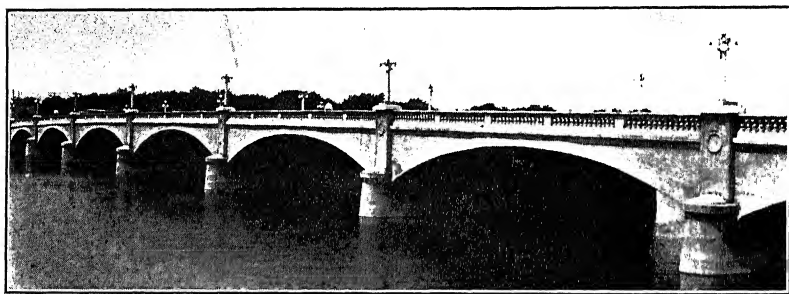


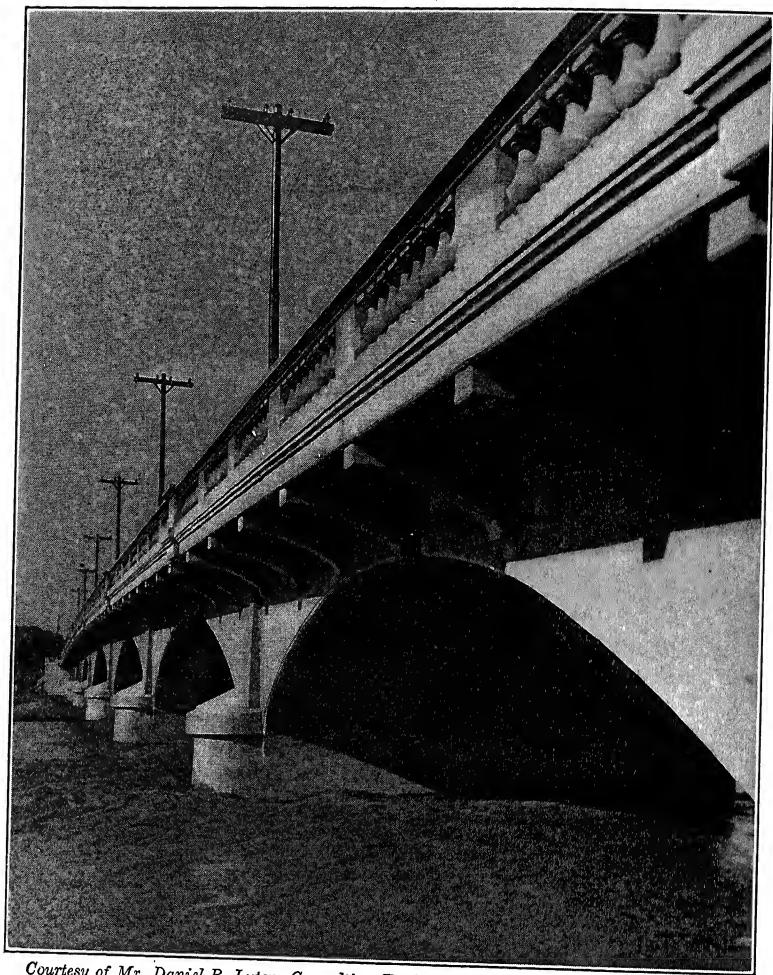
FIG. 56.—Leonard Street bridge over Grand River, Grand Rapids, Michigan.

and 59. The faces of spandrel walls may be entirely plain (Fig. 57), or panels of approximately a triangular shape may be formed either by indenting the portion above the arch ring or by nailing beveled strips to the form work with the result shown in Fig. 60. Brick and stone are used in some cases as a facing for arch rings and spandrel walls.

Figs. 61A and 61B show a portion of a flat arch bridge designed for the city of Lima, Ohio. The spandrel walls are of the reinforced cantilever type. Other examples of this form of spandrel wall and sidewalk construction may be found in Chapter XIII.

A bridge with gravity spandrel walls is shown in Fig. 62. The

brick facing for the arch ring and the cast concrete and brick belt courses should be noted. The spandrel walls rest partly on the brick facing and partly on the concrete portion of the arch,



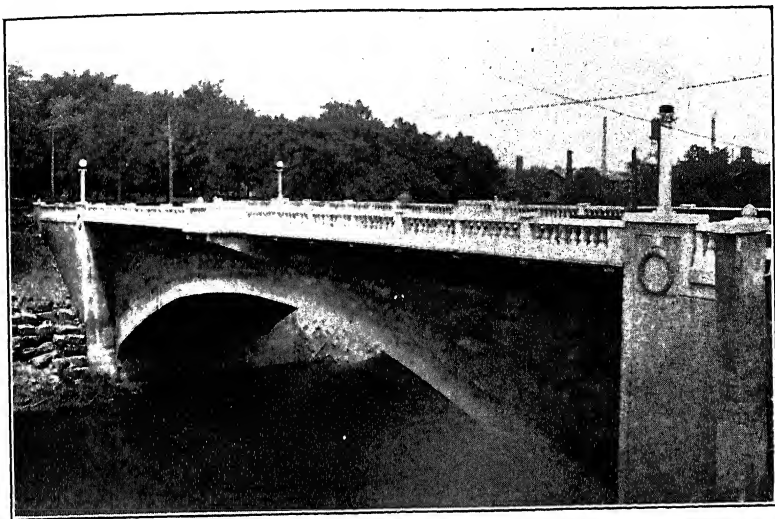
*Courtesy of Mr. Daniel B. Luten, Consulting Engineer, Indianapolis.*

FIG. 57.—Bridge at La Junta, Colorado.

and are keyed into the concrete portion by means of a projection which fits into a 6 in. by 12-in. groove in the arch.

Engineering and Contracting, issue of Oct. 7, 1914, describes the character of the cast concrete and brick masonry as follows:

"The cast concrete blocks for the belt courses and copings are composed of 1 part cement and 3 parts crushed stone chips, the chips being of



*Courtesy of Mr. Daniel B. Luten, Consulting Engineer, Indianapolis.*

FIG. 58.—Washington Avenue bridge, Elyria, Ohio.

such sizes as to pass through a  $\frac{3}{8}$ -in. mesh screen. Waterproofing material is incorporated in the concrete of the cast stone. After being

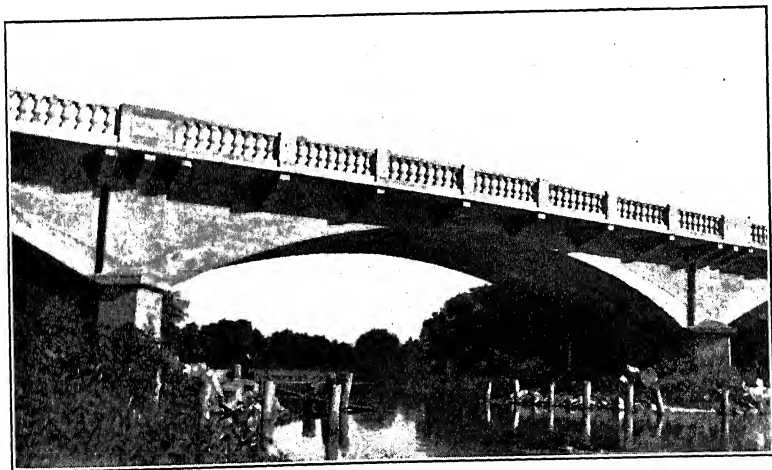
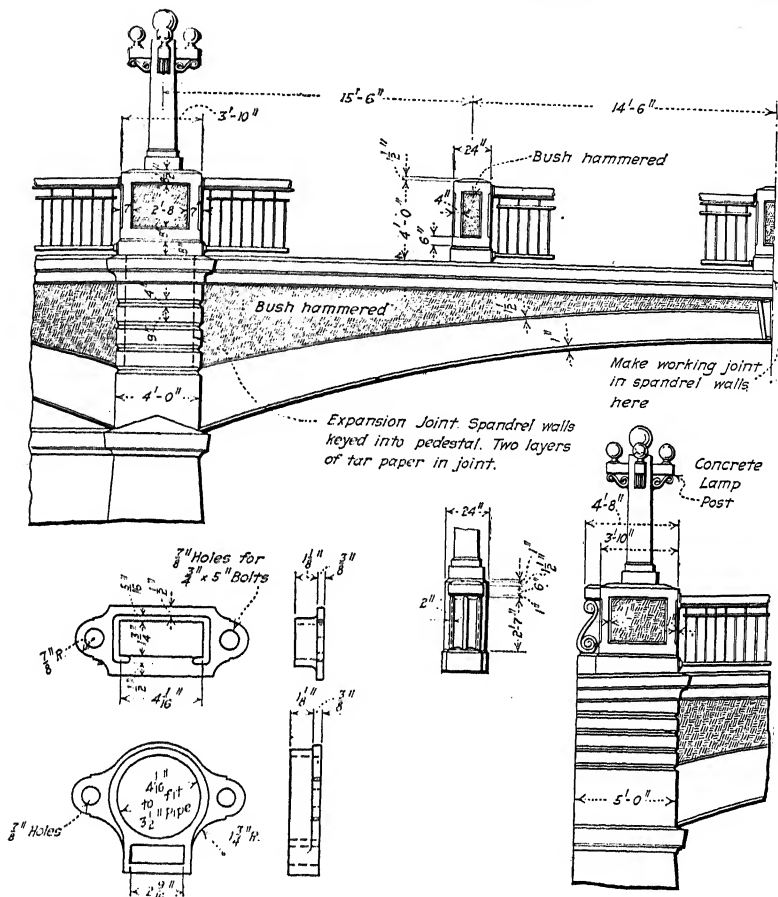


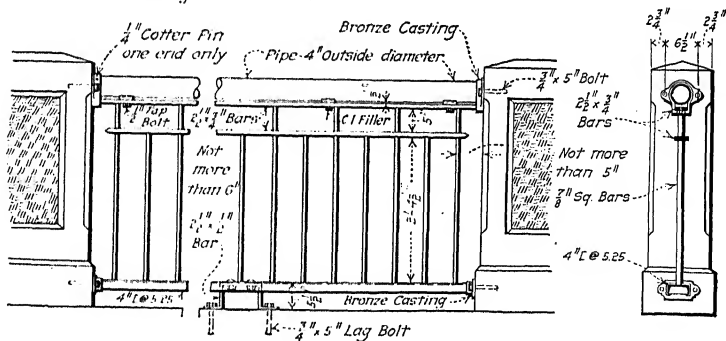
FIG. 59.—Adams Street bridge, Troy, Ohio.

cast from 40 to 60 days, all exposed surfaces of the stones were dressed with six-cut bush hammers. The cast concrete blocks are laid in 1:2





Bronze Castings for Hand Rail



Details of Railing

Section

Portland cement mortar, with joints of not more than  $\frac{1}{4}$  in. Before the mortar had set the joints were raked out for a depth of 3 in. and pointed with 1:1 Portland cement mortar.

"The bricks used for facing the arch rings and for the ornamental courses are up-and-down, hard-burned, dark, water-struck bricks. They are laid in 1:3 Portland cement mortar, except the outer 4-in. faces where "Puzzolan" cement is used. One pail of lime putty was allowed to be added for each barrel of cement."

A counterforted type of spandrel wall is shown in Fig. 63. These walls are 12 in. thick and are reinforced on both faces with a double system of rods. The counterforts occur at about 9-ft.

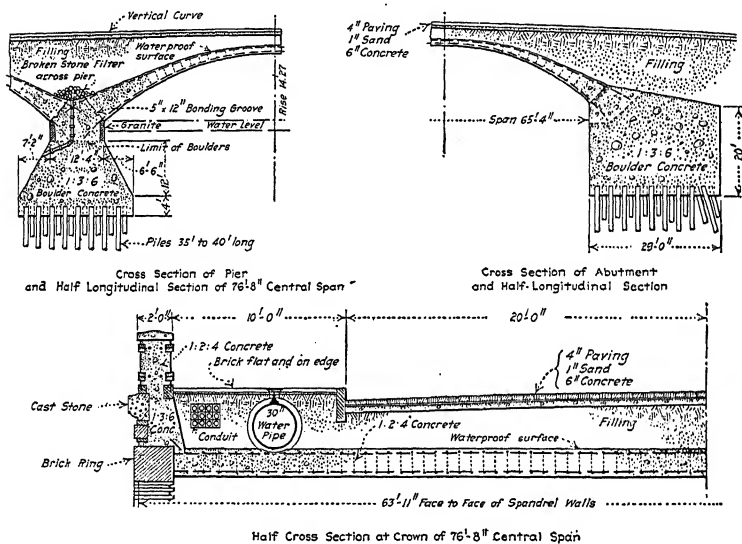


FIG. 62.—Details of Larz Anderson bridge over the Charles River, Cambridge and Boston, Mass.

intervals, and cantilever brackets are placed at these counterforts to support the sidewalks. The following description is taken from Engineering Record, issue of February 22, 1913.

"The entire width of the arch ring between outside faces of spandrel walls is 35 ft., and the roadway above is 39 ft. wide, thus giving an overhang of 2 ft. on each side of the bridge between the curb lines. This 2-ft. overhang constitutes the concrete gutter of the roadway and, as such, will be subject to heavy concentrated wheel loads coming upon the cantilever section. It was, therefore, built as a heavily-reinforced concrete beam. This beam is 2 ft. 9 in. wide, having a depth of 15 in.

at the spandrel wall and 10 in. at the curb, and is reinforced with fourteen  $\frac{3}{4}$ -in. rods, with additional reinforcement at the brackets.

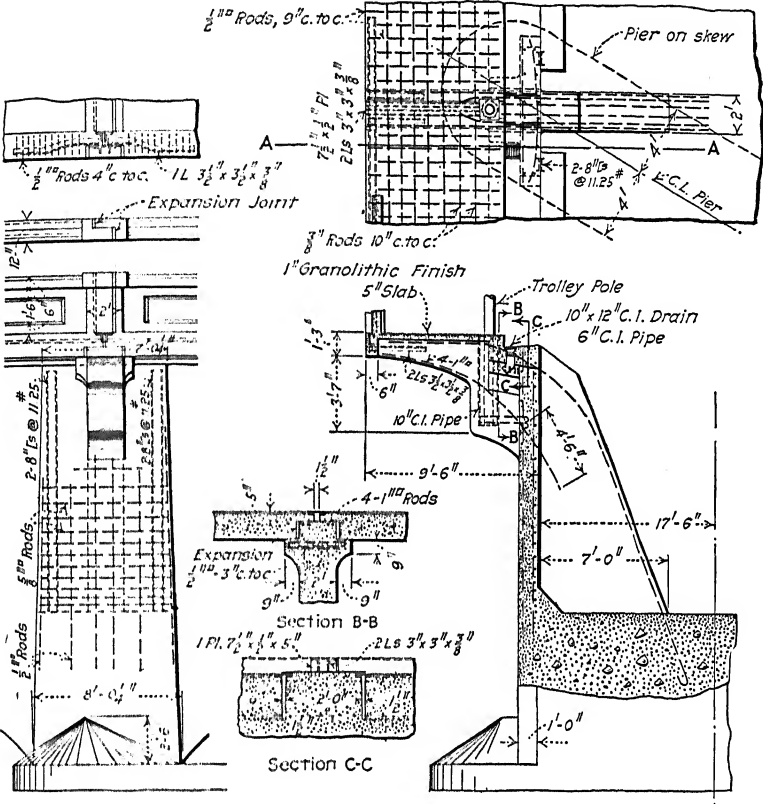


FIG. 63.—Counterforted spandrel wall, highway bridge at Ansonia, Conn.

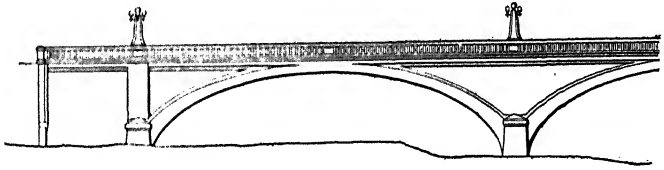
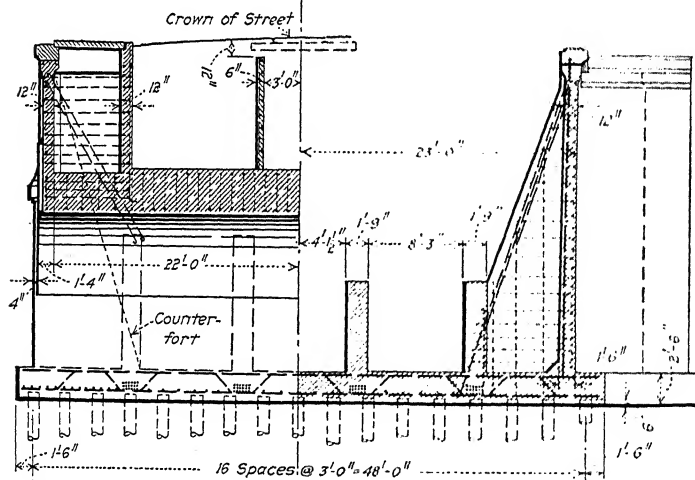


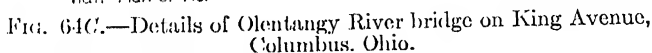
FIG. 64A.—Elevation of west end of Olentangy River bridge on King Avenue, Columbus, Ohio.

"The bridge is designed for trolley traffic, and provision is made for the trolley poles by anchoring sections of 10-in. cast-iron waterpipe in the





Section A-A



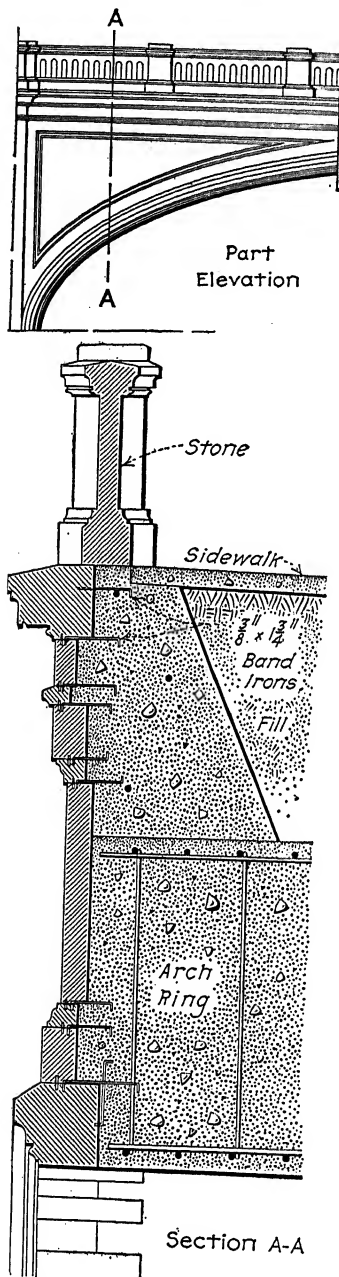


FIG. 65.—Details of stone facing of Michigan Street bridge over St. Joseph River, South Bend, Ind.

brackets of the piers and abutments. Drainage is provided by means of 6-in. cast-iron drains in the gutters over the piers."

Details of the arch bridge over the Olentangy River on King Avenue, Columbus, Ohio, is shown in Figs. 64A, 64B, and 64C. The type of spandrel walls without pilasters over piers should be noted. Since the space beneath each sidewalk is hollow, the inner wall was designed as a slab with the principal steel placed horizontally between cross walls. The longitudinal walls under

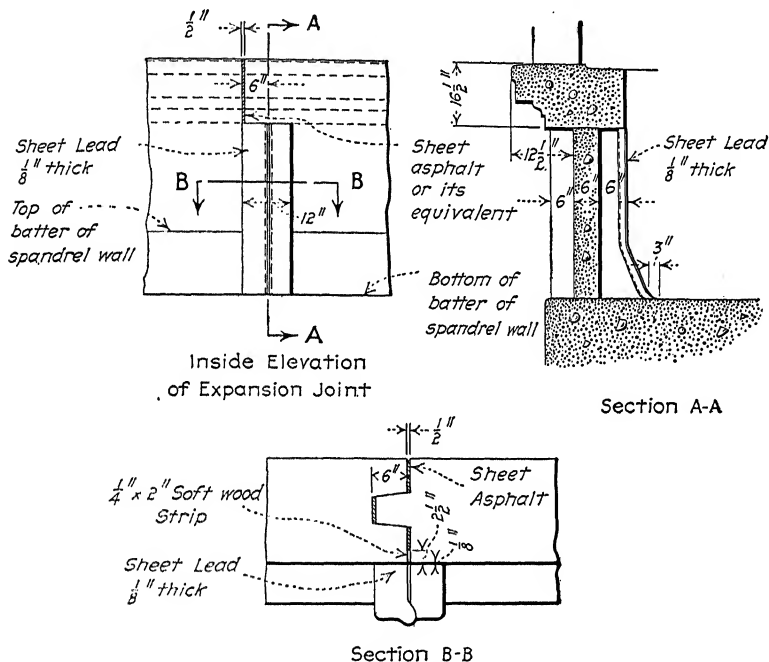


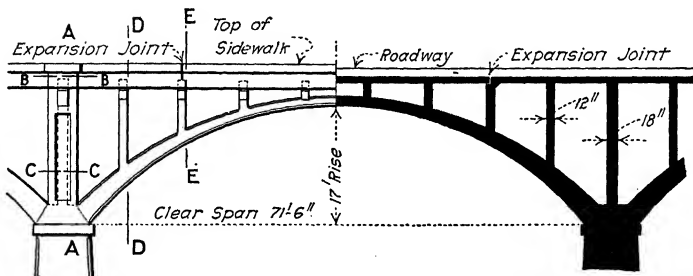
FIG. 66.—Details of expansion joint in highway arch bridge over Chattahoochee River at Columbus, Georgia.

the car track were employed to prevent the usual settlement of the track when laid on a new fill. The ties were laid directly on top of these walls and earth filling was dumped both sides of, and also between, the longitudinal walls.

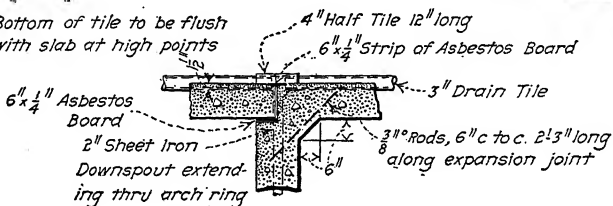
An earth-filled arch faced entirely with stone is shown in Fig. 65. The bonding irons should be noted.

Drains should be placed on each side of the roadway of a concrete bridge at intervals of 30 to 40 ft. when the roadway is level and about every 100 ft. when on a grade. These drains should

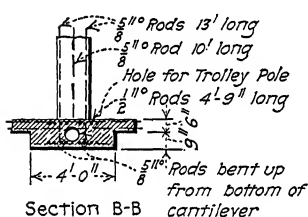




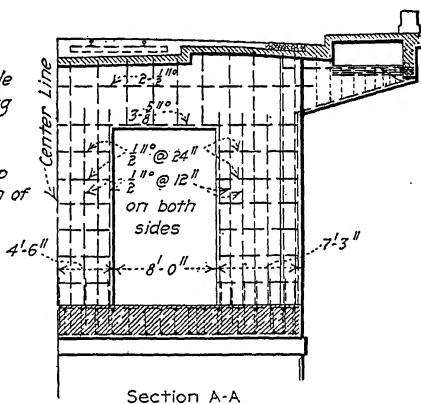
Bottom of tile to be flush with slab at high points



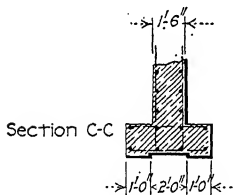
Section through Expansion Joint at Center Drain



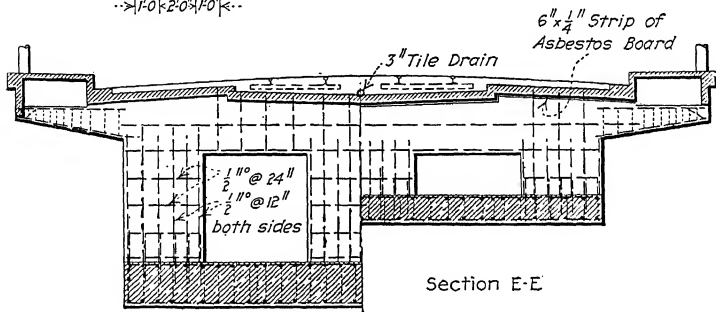
Section B-B



Section A-A



Section C-C



Section E-E

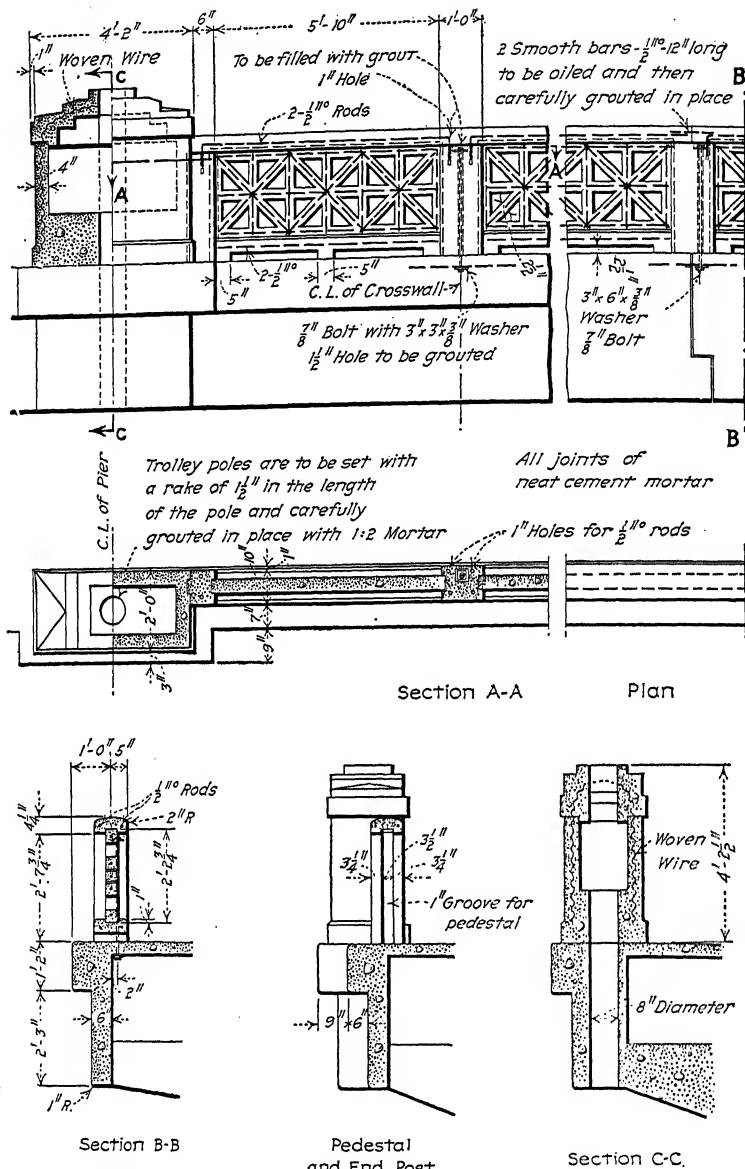


FIG. 68B.—Details of the Dallas-Oak Cliff viaduct, Dallas, Texas.

have a diameter of not less than 3 in. The minimum area of a drain in square inches may be computed by the formula

$$a = \frac{A}{200}$$

where  $A$  = area of the surface drained in square feet.

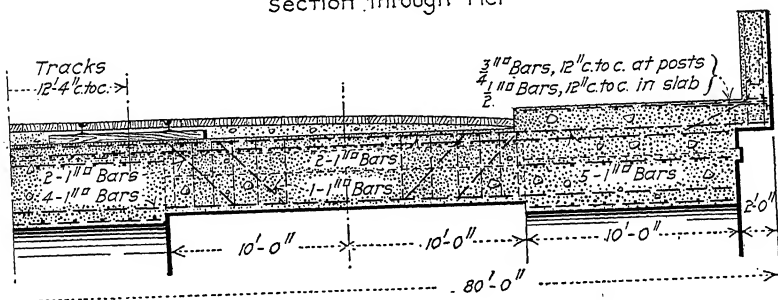
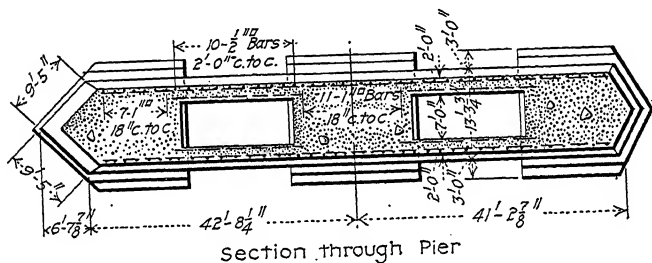
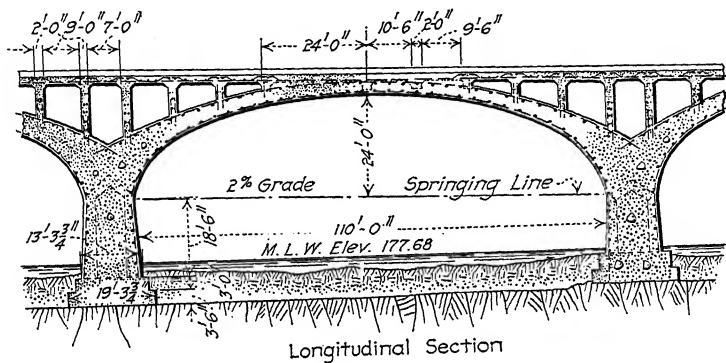


FIG. 69.—Details of Penn Street viaduct, Reading, Pa.

For remarks concerning expansion joints, see Art. 32. One type of expansion joint in a simple cantilever wall is shown



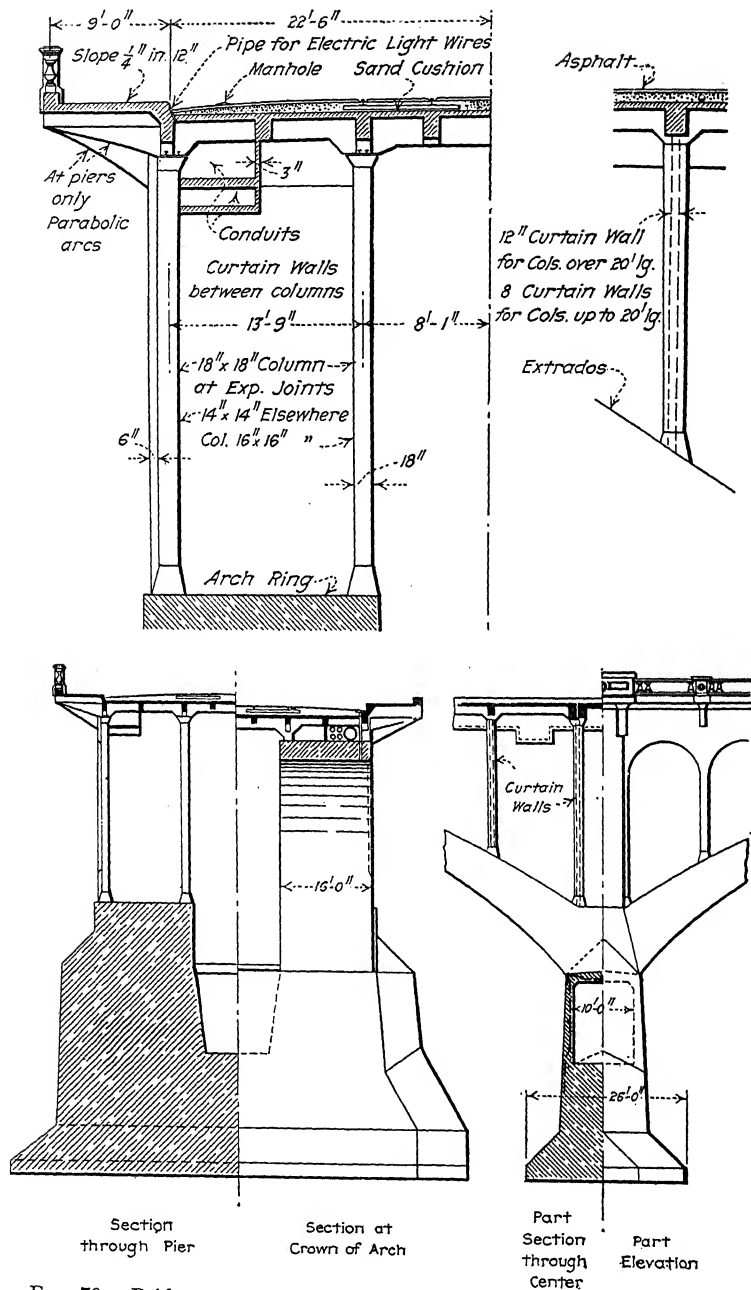


FIG. 70.—Bridge over Saskatchewan River at Saskatoon, Canada.

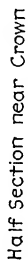
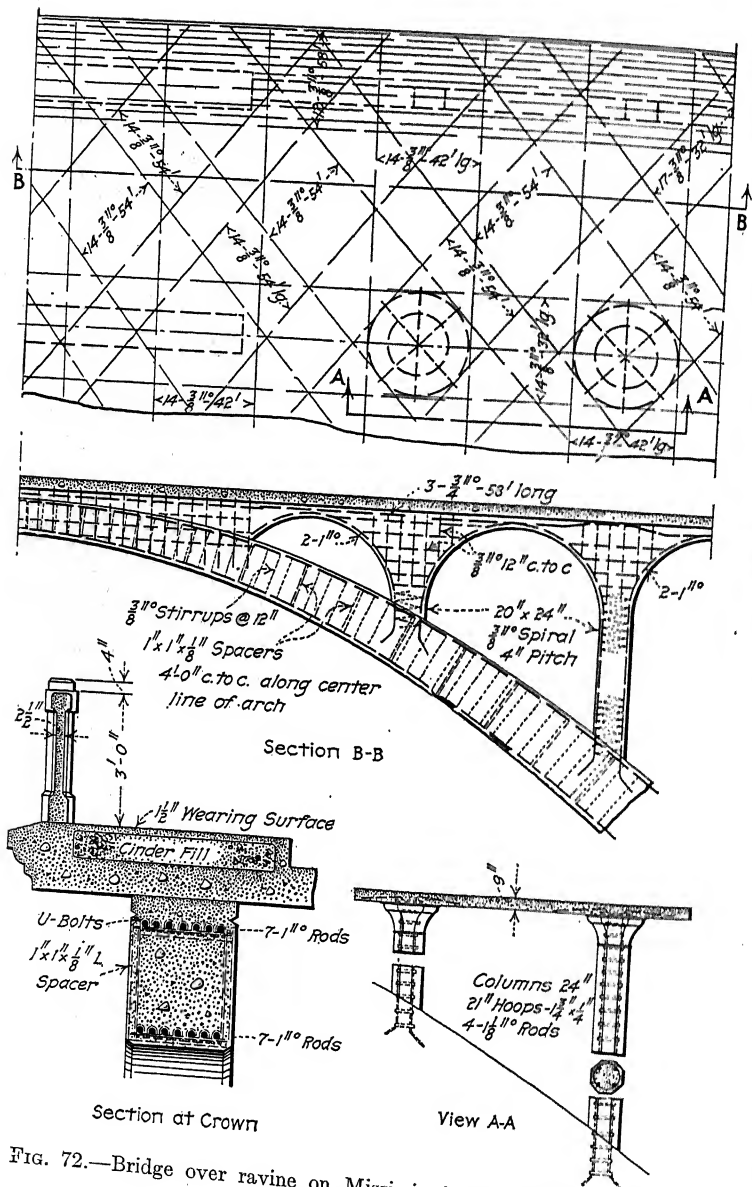


FIG. 71.—Wisconsin approach to high wagon bridge at Winona, Minn.



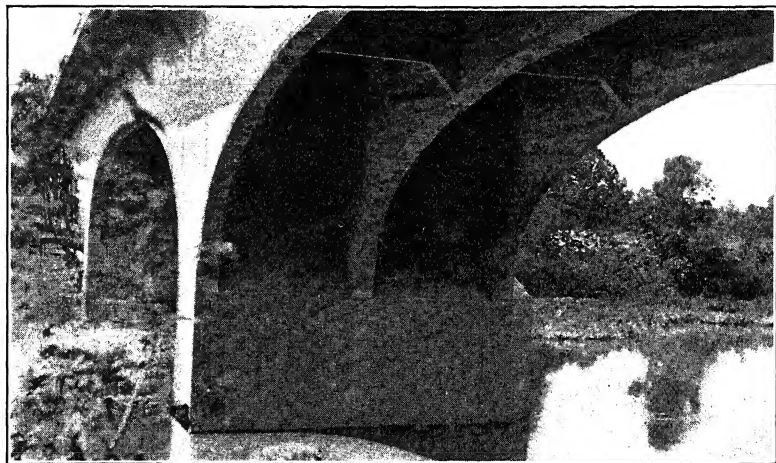


FIG. 73.—Highway bridge at Covington, Ohio.

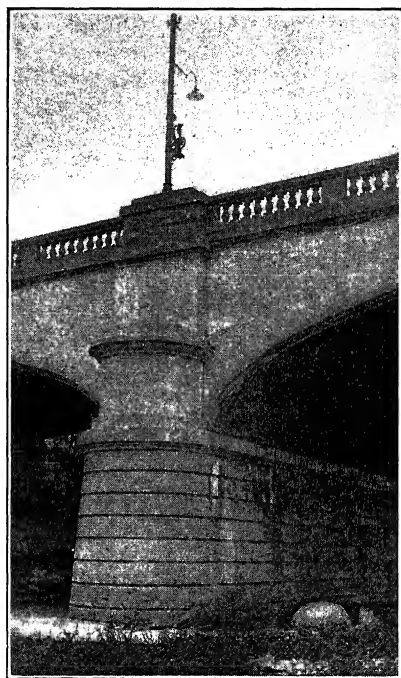


FIG. 74.—Third Street bridge, Dayton, Ohio.

in Fig. 66. Other types of expansion joints may be found in Chapter XIII.

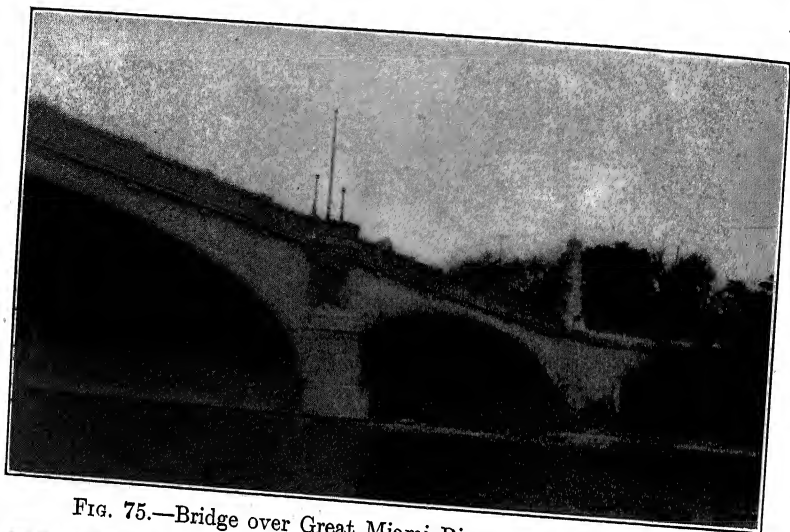
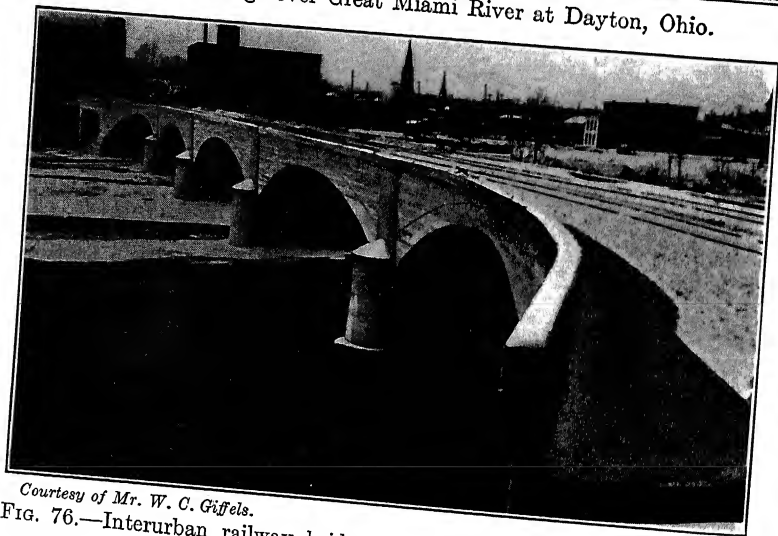


FIG. 75.—Bridge over Great Miami River at Dayton, Ohio.



*Courtesy of Mr. W. C. Giffels.*  
FIG. 76.—Interurban railway bridge over Grand River, Grand Rapids, Michigan.

**50. Spandrel Details in Open-spandrel Bridges.**—The general types of open-spandrel bridges have been described in Art. 3. Figs. 67 to 72 inclusive will serve to illustrate details of some of these types. Other details may be found in Chapter XIII.

Fig. 67 shows a full-barrelled arch reinforced with typical Melan trusses made up of 3 in. by 3 in. by  $\frac{5}{16}$ -in. angles and  $2\frac{1}{4}$  in. by  $\frac{1}{4}$ -in. lattice bars. The floor system is carried on a series of transverse spandrel walls and the floor slab is provided with expansion joints as shown. The sidewalks leave an overhang of about 3 ft. and are supported on cantilever brackets. The cantilever section of the sidewalk is cast in units 5 ft. long and laid in place. Tile conduits are provided under each sidewalk for the necessary wires, and a 4-in. gas pipe and 12-in. water main are laid in specially-designed reinforced-concrete troughs beneath the roadway.

Transverse spandrel walls with openings to save material are shown in Figs. 68A and 68B. The method of carrying the sidewalk should be noted.

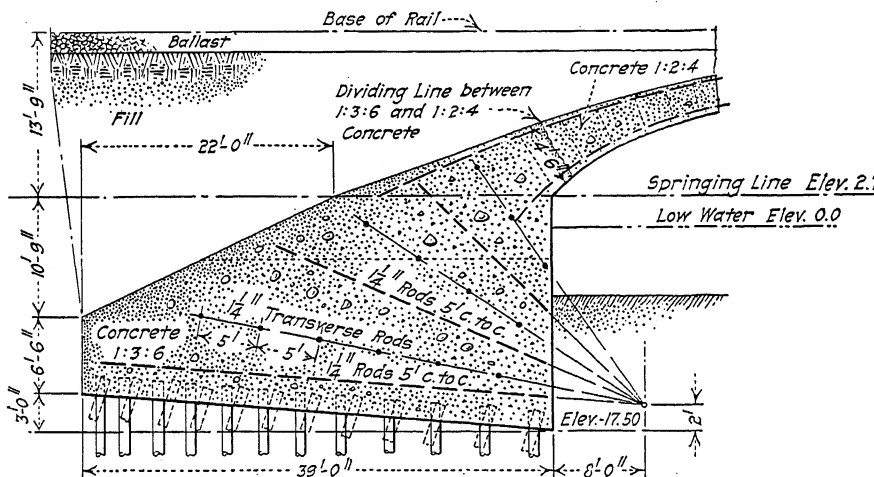


FIG. 77.—Abutment of causeway arch construction, Galveston, Texas.

The details of the ribbed arches in Figs. 69, 70, 71, and 72 should need no explanation. Fig. 73 shows a ribbed arch structure in which the ribs extend up to the floor level throughout each entire span.

The curtain walls between columns in Fig. 70 were considered simply as a bracing system. The columns were designed to carry all loads, but doubtless the curtain walls help to distribute the total loading. In taking the loading for the arch rings, it was assumed that the loading from columns was equally distributed over 12 ft. of arch ring instead of having two loads concentrated on an arch ring 16 ft. wide.

to the passage of water varies with the type of starling. Experiments show that the value in this respect of the different shapes of piers is in the following order: first, elliptical horizontal sections; second, rectangular body with starlings formed by two circular arcs, tangent to the sides and described on the sides of an equilateral triangle; third, rectangular body with semicircular starlings; fourth, rectangular body with triangular starlings, the angle at the nose being  $90^\circ$ ; and fifth, rectangular body without starlings. Piers of the third type mentioned are shown in Figs. 74, 75, and 76. Other types may be found in the many illustrations scattered throughout the book.

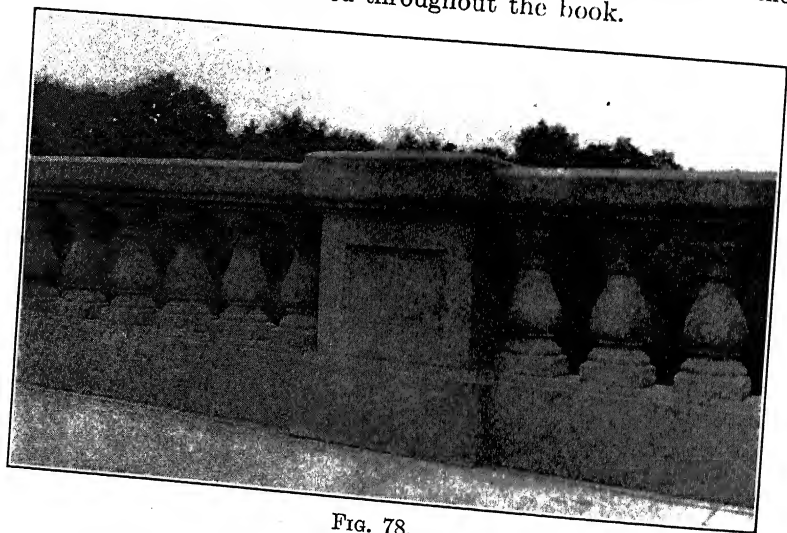


FIG. 78.

The ordinary type of abutment in earth-filled arches is shown in Plate I, Chapter IV. What might be called a buttressed abutment is shown in detail in Fig. 64B. Fig. 77 represents a very wide abutment in which a network of rods has been employed to make the entire abutment act as a unit. Hollow piers for ribbed-arch structures are shown in Figs. 69 and 70. See Chapter XIII for other examples of cellular construction.

**52. Railing and Ornamental Details.**—A common type of spindle balustrade is shown in Fig. 78. In such railings the spindles or balusters are usually the only members which are not cast in place. Expansion joints should be provided each side of the posts and also over the spandrel joints. Railing and ornamental details





of various kinds are shown in Figs. 61B, 64C, 67, 68B, and in Chapter XIII.

A typical unit-built handrail is shown in Figs. 79 and 80. This particular design was used on the viaducts of the Kansas City Terminal Railway Company. The following description of the design and construction of this railing is taken from the Engineering Record, issue of Dec. 19, 1914:

"The railing consists of a top and bottom rail set parallel to the pavement and grooved to receive the  $3\frac{3}{4}$  in. by 5-in. spindles, which are set



*Courtesy of Horton Concrete Construction Co., Kansas City.*

FIG. 80.—Unit-built handrail on Kansas City viaduct.

truly vertical, regardless of the grade of the rails. For this purpose the tops and bottoms of the spindles are shaped to the required angle.

"The panels between the hollow posts are usually 20 ft. long, but vary from 10 to 22 ft. The bottom rail rests on blocks 3 in. above the floor to give a detached appearance. Both rails extend into the post beyond the post shell. Projecting reinforcing rods in the rails entering from the high side, bond with the green concrete subsequently filled into the posts, but an expansion joint has been secured on the opposite and lower side of the post by wrapping the rail ends in tar paper.

"A basket reinforcement of four  $\frac{1}{4}$ -in. rods wrapped with No. 2 wire cloth has been provided for the post shells, which are set in concrete.

held down by a wire embedded in the cap during its construction. This wire was forced down into the soft concrete after the shell was filled.

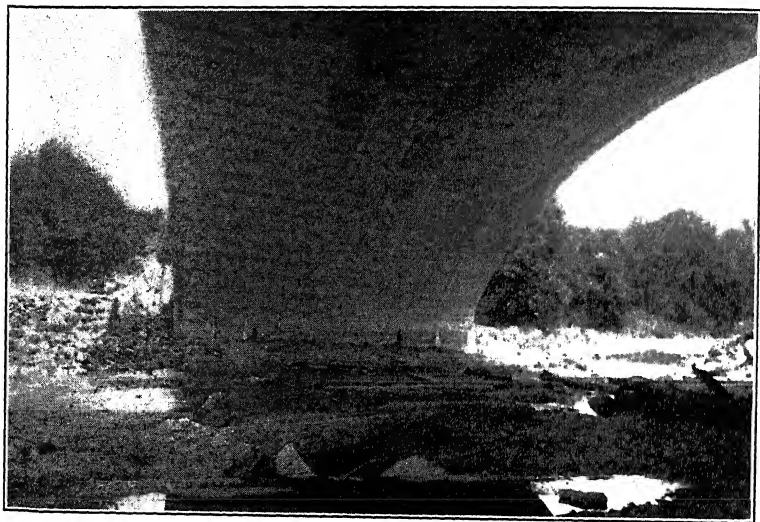
"Separate members were cast near the slab plant used to construct the large units for the subways, as described in the Engineering Record of Aug. 30, 1913, page 288. A pug mill, steam house, and gantry crane comprised the equipment. The pug mill was used to obtain uniformity of mixture, as mortar in it could be observed and the foreman was relied upon to obtain the proper consistency. Wood forms were employed to prevent craze and sand marks. In cold weather the steam house facilitated setting, while in summer 45 minutes in the steam retarded setting a sufficient amount to avoid crazing. The aggregate consisted of 1 part cement,  $2\frac{1}{2}$  parts Kaw River sand, considered exceptionally good, and 1 part of crusher-run soft native limestone passing a  $\frac{3}{4}$ -in. mesh. All measurements were made by hand in a 1-cu. ft. box.

"The rails were turned upon a sand cushion 24 hours after being poured. The posts were cast at three separate pourings so that shrinkage would not crack them at the points of top and bottom enlargement."

## CHAPTER X

### CONSTRUCTION OF ARCH BRIDGES

No attempt will be made in this chapter to describe at length the character of the materials required for concrete; the kind of lumber to use for forms; the types of forms for ordinary column, beam, and slab construction; the methods of bending and placing reinforcement; the proportioning, mixing, and placing of concrete; the finishing of concrete surfaces; or the various methods of

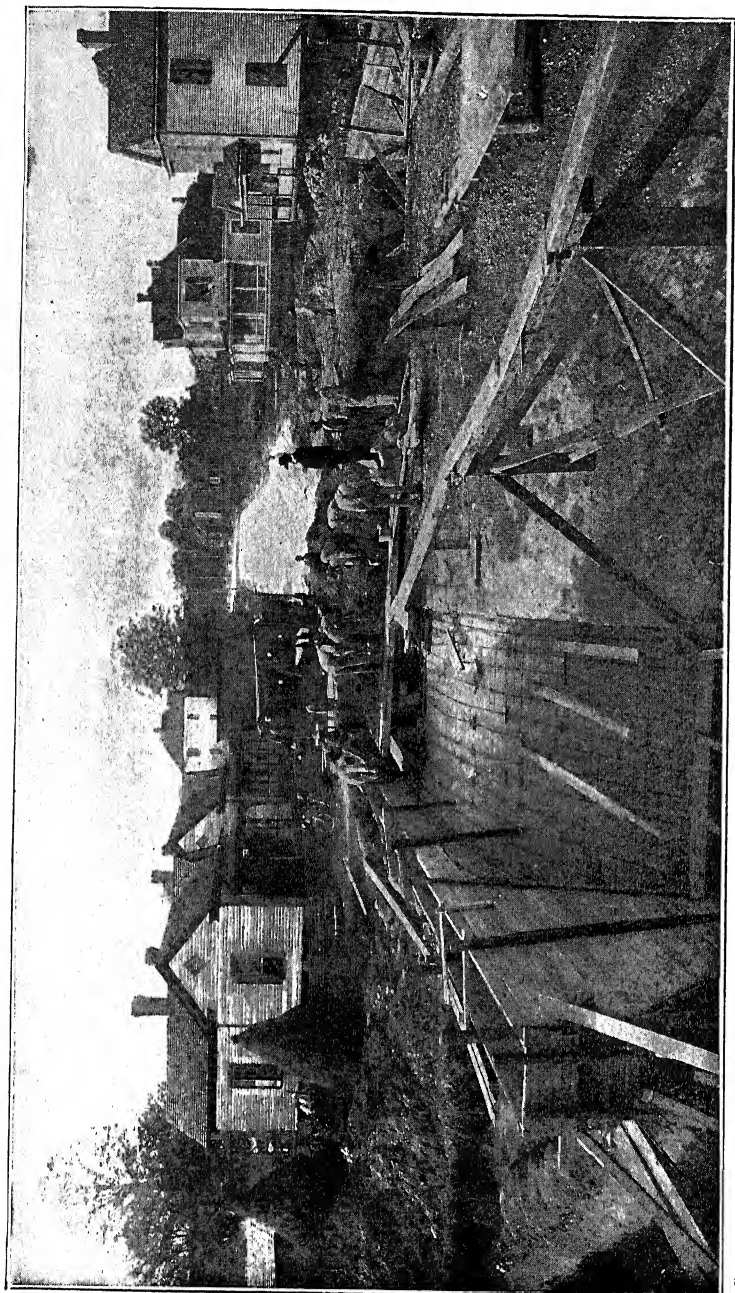


*Courtesy of Mr. Daniel B. Luten, Consulting Engineer, Indianapolis.*

FIG. 81.—Harford Avenue bridge over Hering Run, Baltimore, Md. Showing method of construction of arch ring in longitudinal sections.

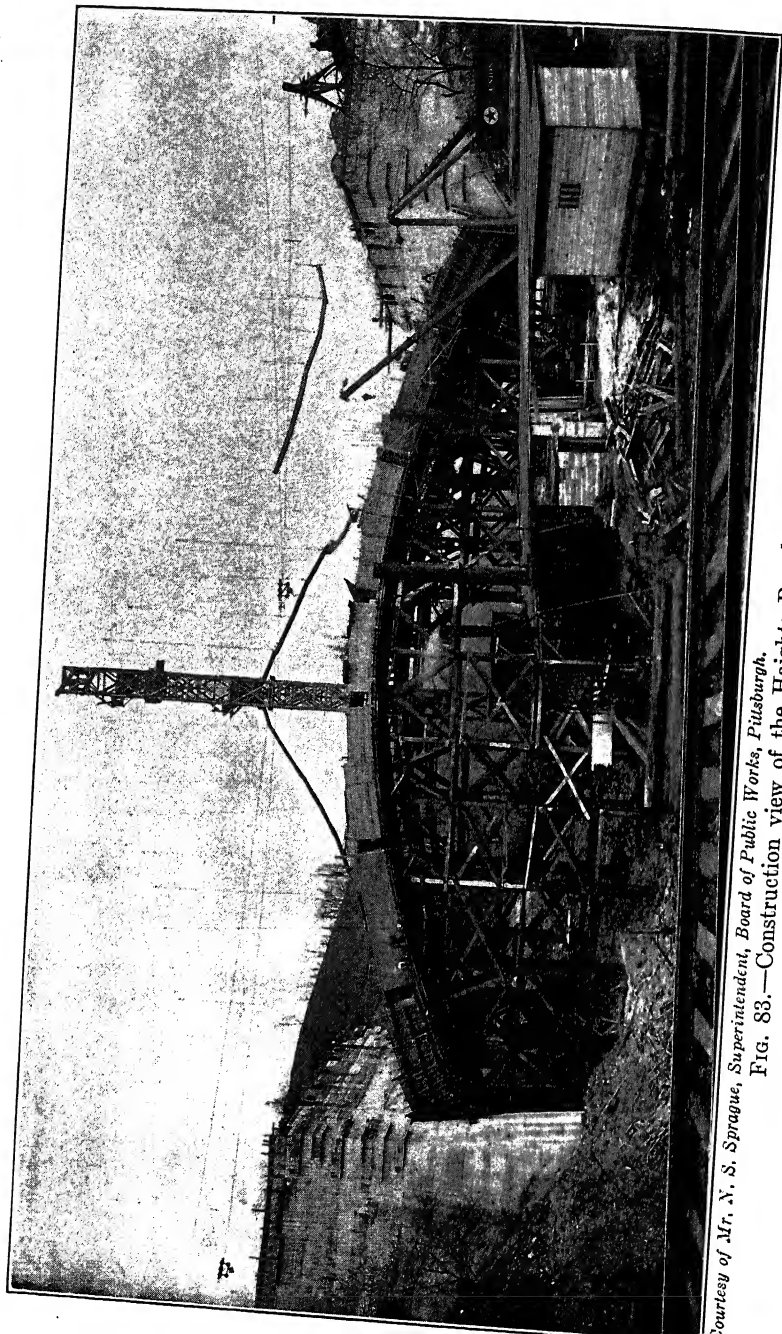
waterproofing. These subjects are all treated in detail in Volume II. Special consideration, however, must be given in this volume to the methods of arch construction; the centering for arches; and the forms for spandrel walls, piers, and abutments.

**53. Arch-ring Construction.**—Arch rings with span lengths less than about 90 ft. are usually constructed in longitudinal ribs 3 or 4 ft. wide (Figs. 81 and 82), or in fact of such width that one entire rib can be poured in approximately 1 day's time. In



*Courtesy of Mr. Daniel B. Luten, Consulting Engineer, Indianapolis.*

fig. 82.—Elizabeth Avenue bridge, Charlotte, North Carolina. View showing arch concreted in longitudinal rings; reinforcement in place for one 12-ft. concentric ring. Forms constructed for spandrel wall.



Courtesy of Mr. N. S. Sprague, Superintendent, Board of Public Works, Pittsburgh.  
FIG. 83.—Construction view of the Hights Run bridge, Pittsburgh, Pa.

narrow arches the entire arch ring is sometimes poured at one operation. This method of construction has been successfully used for much greater spans than 90 ft. but, unless special care

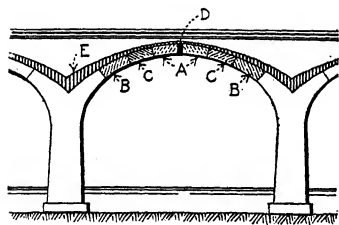


FIG. 84.

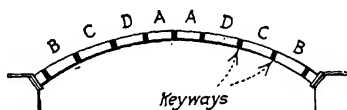


FIG. 85.

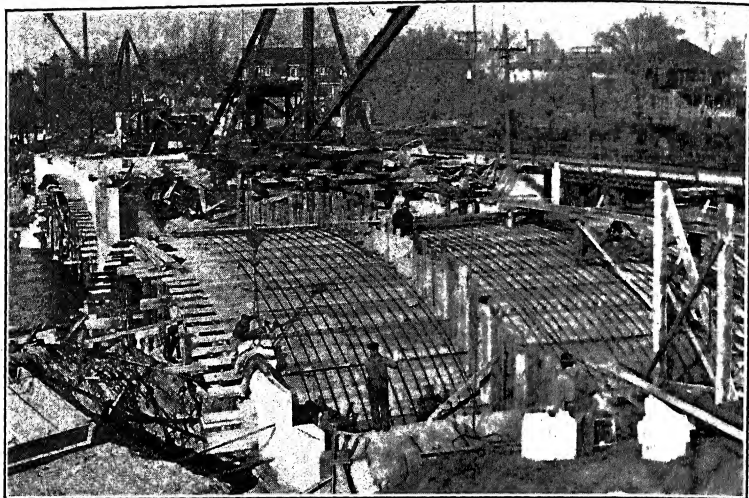
is taken to make the centering very stiff, the construction of any one rib may deform the arch center to such an extent as practically to strike the center under the completed ribs. Of course,



*Courtesy of Mr. Daniel B. Luten, Consulting Engineer, Indianapolis.*

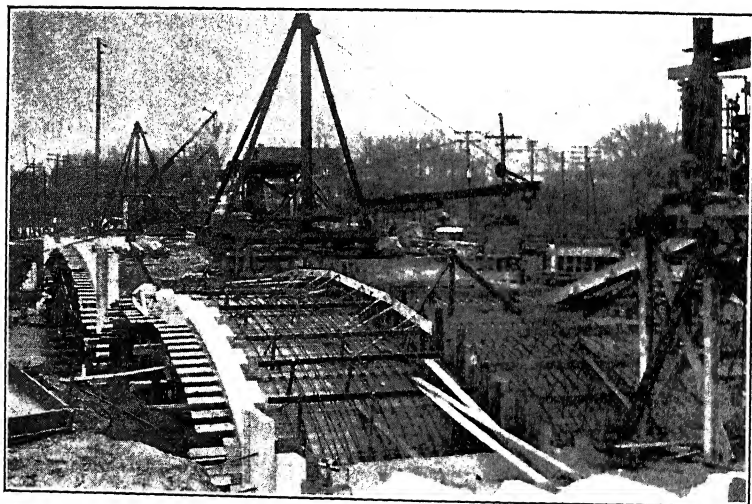
FIG. 86.—Concreting longitudinal rings, 50-ft. span, Plymouth, Mass.

the ribs should be poured continuously from each abutment toward the crown so as to obtain a symmetrical loading on the false-work and thus eliminate distortion of the centering as far as possible.



*Courtesy of Mr. Charles W. Cole, City Engineer, Mishawaka, Ind.*

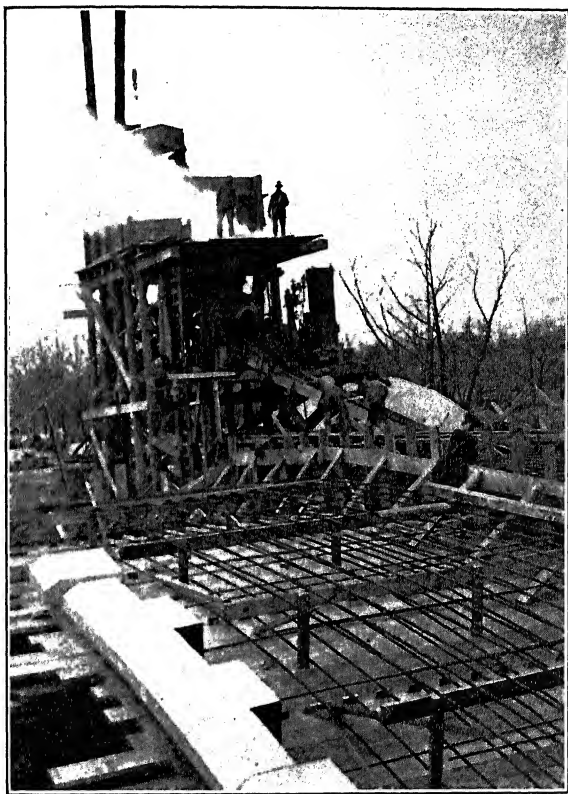
FIG. 87.—Construction view of North Michigan Street bridge, South Bend, Indiana.



*Courtesy of Mr. Charles W. Cole, City Engineer, Mishawaka, Ind.*

FIG. 88.—Construction view of North Michigan Street bridge, South Bend, Indiana.

For spans of 90 ft. or over it is usually preferable to construct an arch ring or arch rib by what is known as the alternate block or voussoir method. The arch is constructed in transverse blocks (Fig. 83) of such size that each block can be completed at one pouring, or with about a day's work. Obviously this method reduces shrinkage stresses in the arch ring to a minimum.



*Courtesy of Mr. Charles W. Cole, City Engineer, Mishawaka, Ind.*

FIG. 89.—Construction view of North Michigan Street bridge, South Bend, Indiana.

For the best results the blocks should be poured in such order as to give a uniform settlement of the centering, and also prevent the crown of the arch from rising as the lower arch loads are placed. If blocks close to the crown section are not placed before the blocks at the haunch and springing sections, the centering will rise at the crown and the placing of the crown loads will be likely to cause



cracks at the middle of the haunch. Even in the construction of an arch by the longitudinal rib method, a temporary loading of the crown is often necessary.

The order followed in the construction of the Philadelphia and Reading R. R. bridge across the Delaware River at Yardley, Pa.—an earth-filled bridge with clear span of 90 ft. 9-in.—is shown in Fig. 84, the sections being concreted in the alphabetical order shown. The section *D* is the keying section, and the section *E* a haunching section (quite unusual construction) which was added after the lower portion of the arch ring was completed. The part of the arch ring close to the springing lines was placed monolithic



*Courtesy of Mr. Charles W. Cole, City Engineer, Mishawaka, Ind.*

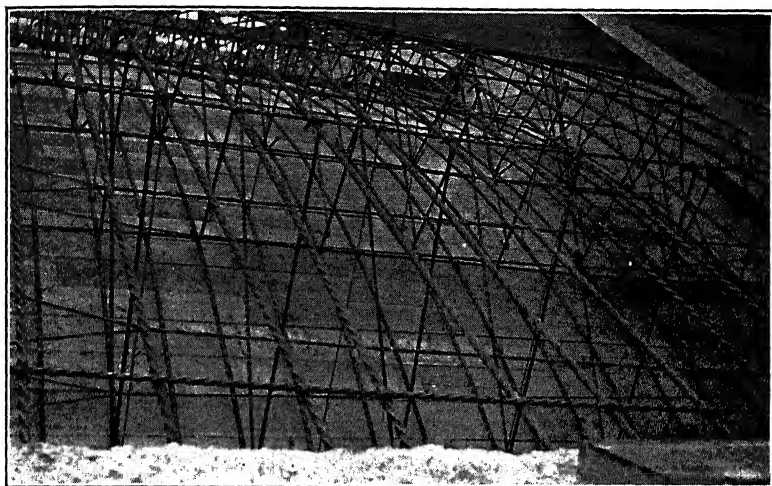
FIG. 90.—North Michigan Street bridge, South Bend, Indiana. Reinforcement supported in place.

with the piers and abutments, making what is called an umbrella form for the piers. In large arches this umbrella type of construction is frequently adopted. The pier forms in such cases are more expensive, but this increase in expense for the piers is usually more than offset by the saving in the falsework for the arch ring.

Fig. 85 shows the method of constructing the Larimer Ave. bridge at Pittsburgh—a bridge of the open-spandrel type, with two ribs, having a clear span of approximately 300 ft. The blocks were placed in alphabetical order and later the keys between them were concreted to make the closure.

In constructing an arch rib or arch ring by the alternate block method the individual sections or block spaces are closed off at the ends by timber bulkheads. On the steepest slopes of the lagging these bulkheads adjoining keying sections are held in place by temporary struts between voussoirs. A top form is usually needed for the block sections near the piers and abutments. This top form should be laid up as the concreting progresses. Fig. 86 shows a top form being used in the construction of an arch ring by the longitudinal rib method.

If arch reinforcement for large arches is put in place in long



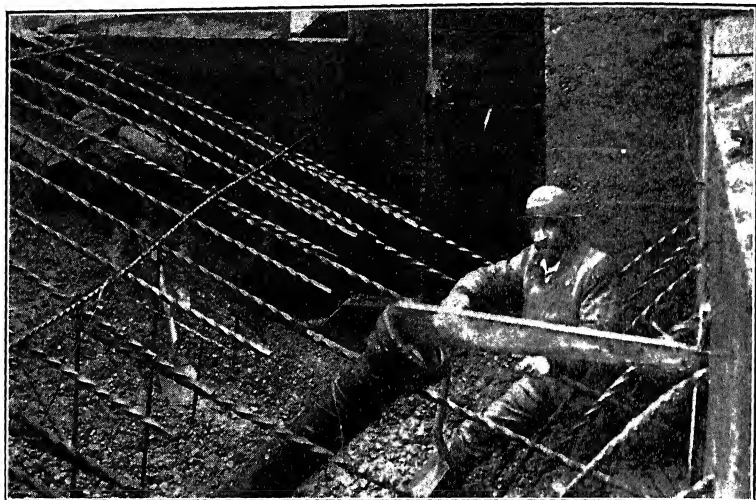
*Courtesy of Mr. Charles W. Cole, City Engineer, Mishawaka, Ind.*

FIG. 91.—North Michigan Street bridge, South Bend, Indiana. Reinforcement in place held by overhead timbers.

lengths, the settlement and deformation of the centering during the pouring of the concrete will cause buckling of the steel which will prevent the reinforcement from lying in its theoretical position. For this reason steel lengths should not exceed about 30 ft. and the splicing should occur in the keyways. An effort should be made to stagger the splices of adjacent rods and to locate the splices where the tension in the steel is a minimum.

Figs. 87 to 92 inclusive show the reinforcement in place in the North Michigan Street bridge at South Bend, Ind. The lower steel was wired together and blocked up as shown in Fig. 87; props were then erected for the upper steel (Figs. 88, 89, and 90); after which the diagonal rods were placed. Instead of blocking

out these blocks and spacing boards as the concrete was brought up (a method sometimes followed), all the wood used in erection



*Courtesy of Mr. Charles W. Cole, City Engineer, Michawaka, Ind.*

FIG. 92.—North Michigan Street bridge, South Bend, Indiana. Concrete being put in place.

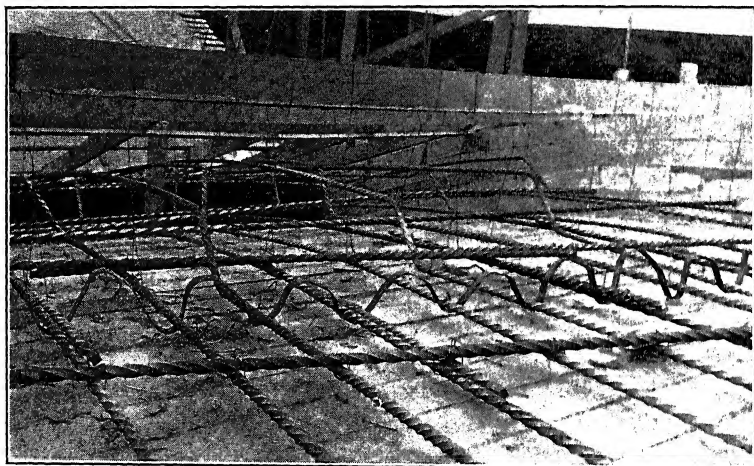
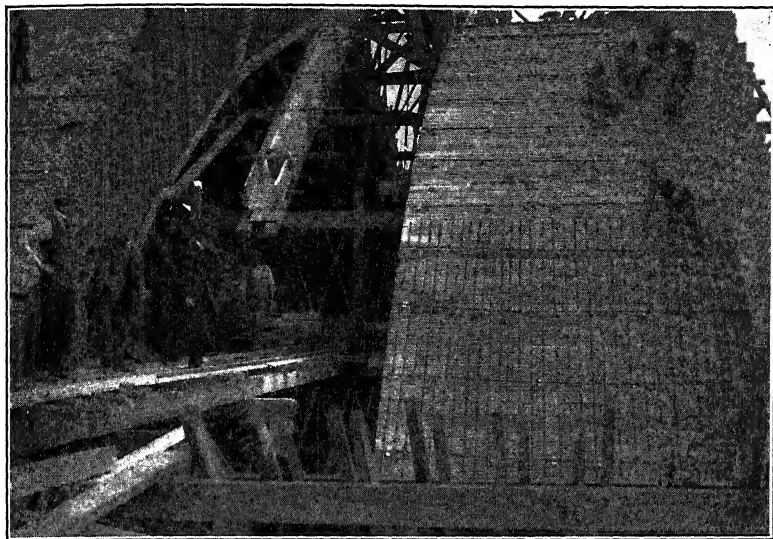


FIG. 93.—Arch reinforcement held in place by being wired to transverse timbers supported above the surface of the finished concrete. Bridge of Luten Design.

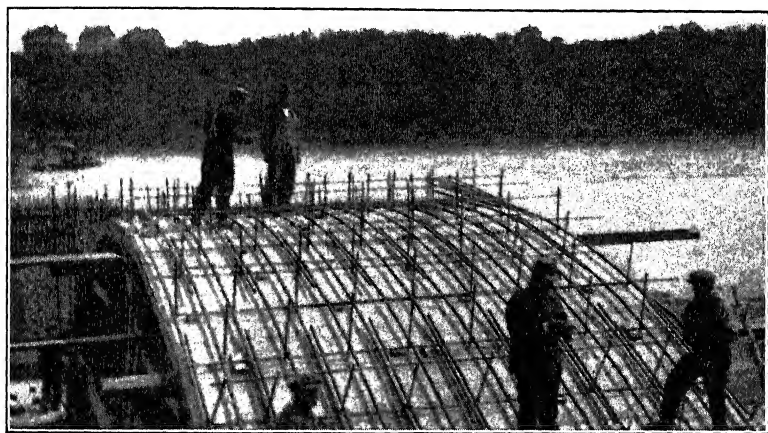
was removed before concreting was started and the system of rods was held in place by being wired to transverse timbers supported

above the surface of the finished concrete (Fig. 91). By this method the likelihood of disturbing the steel during the pouring



*Courtesy of Mr. Daniel B. Luten, Consulting Engineer, Indianapolis.*

FIG. 94.—Bridge over Saskatchewan River at Saskatoon, Canada. Placing reinforcement in arch ribs.

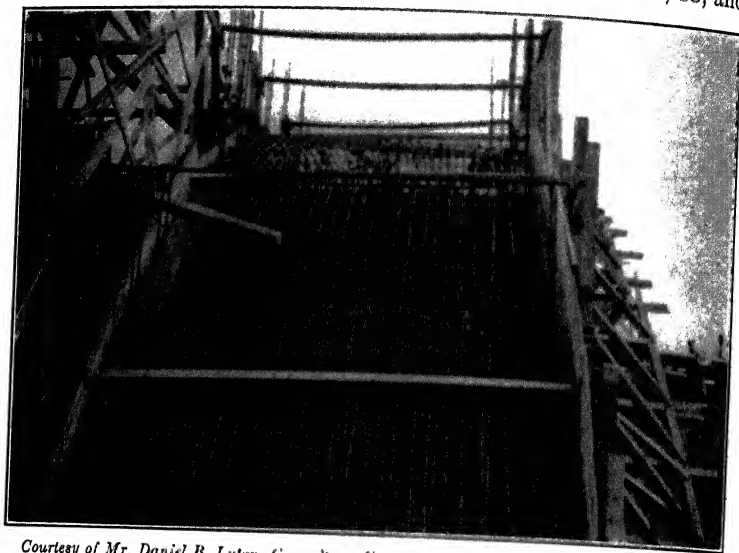


*Courtesy of Mr. Daniel B. Luten, Consulting Engineer, Indianapolis.*

FIG. 95.—Bridge over Saskatchewan River at Saskatoon, Canada. Reinforcement in place on one of the arch ribs.

of the concrete was reduced to a minimum and, of course, there was no chance of trouble arising from failure to remove all the

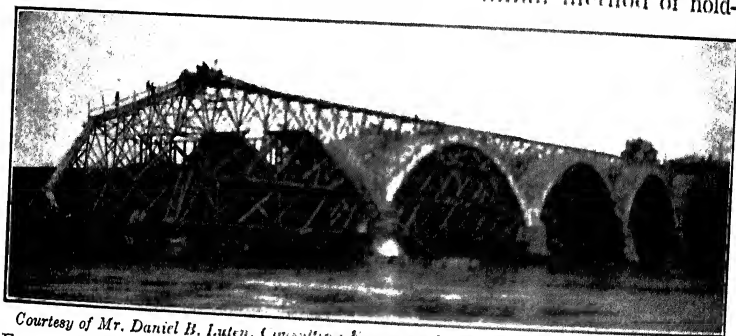
spacing blocks. The bridge in question has a stone facing. Some of the stone work may be seen in place in Figs. 87, 88, and



*Courtesy of Mr. Daniel B. Luten, Consulting Engineer, Indianapolis*

Fig. 96.—Bridge over Saskatchewan River at Saskatoon, Canada. Arch rib ready for concreting.

89. Narrow gauge distributing track should be noted, also longitudinal bulkheads used in the longitudinal rib method of arch-ring construction. Fig. 93 shows a similar method of hold-



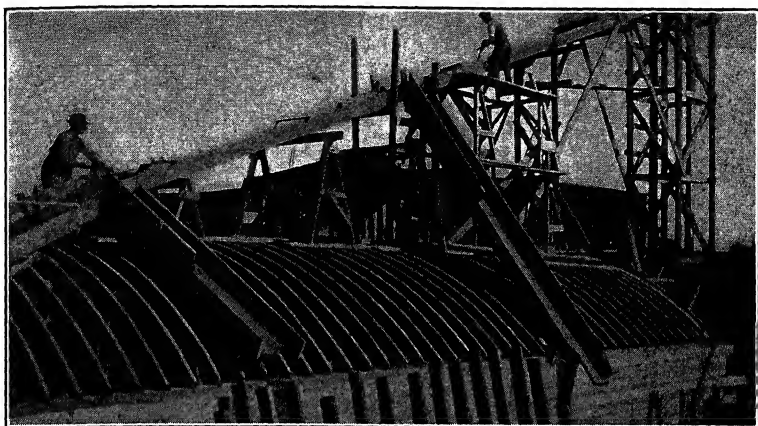
*Courtesy of Mr. Daniel B. Luten, Consulting Engineer, Indianapolis*

Fig. 97.—Construction view of bridge over Saskatchewan River at Saskatoon, Canada.

ing steel in position employed in a Luten Design bridge (see Chapter XII) at Collinsville, Ohio.

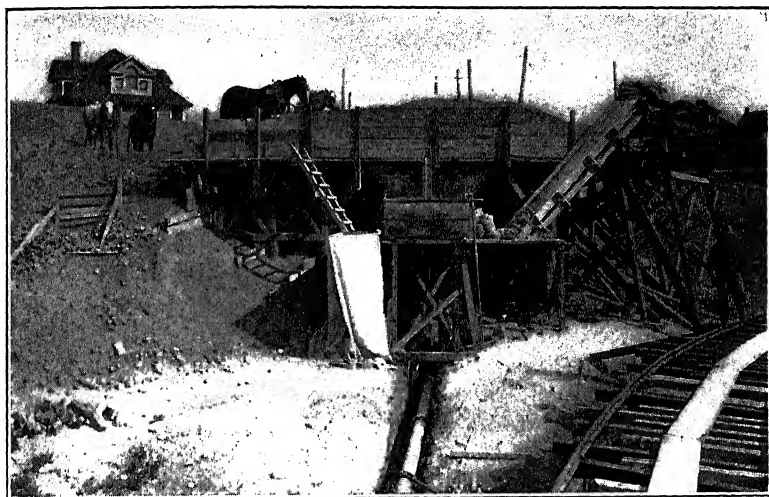
Figs. 94, 95, and 96 show the placing of reinforcement in a two-

ribbed open-spandrel arch bridge at Saskatoon, Saskatchewan, Canada. Two tracks were used for distributing materials, one



*Courtesy of Mr. Daniel B. Luten, Consulting Engineer, Indianapolis.*

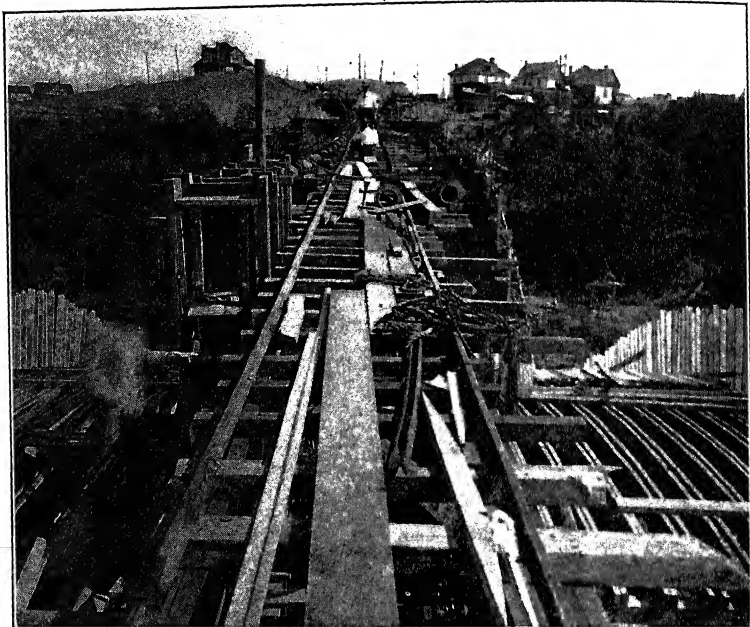
FIG. 98.—Bridge over Saskatchewan River at Saskatoon, Canada. Placing concrete by hoist and chutes.



*Courtesy of Mr. A. P. Linton, Asst. Chief Engineer, Board of Highway Commissioners, Sask.*

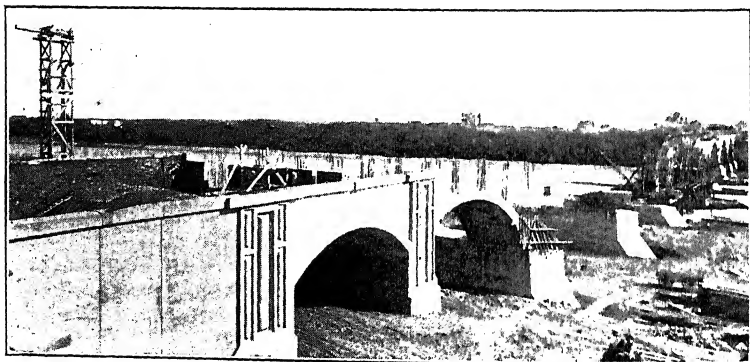
FIG. 99A.—Pneumatic mixing plant at bridge over Saskatchewan River, Saskatoon, Canada. View showing hopper for measuring gravel; tank for measuring water; method used in handling cement; pneumatic mixing machine; and pipes leading to discharge box.

just above the spring line shown in Fig. 94, and another on top of the arches (Fig. 97).



*Courtesy of Mr. A. P. Linton, Ass't. Chief Engineer, Board of Highway Commissioners, Sask.*

FIG. 99B.—Pipe line from pneumatic mixer at bridge over Saskatchewan River, Saskatoon, Canada. Notice discharge box. (Troughs are not shown in this view.)



*Courtesy of Mr. Daniel B. Luten, Consulting Engineer, Indianapolis.*

FIG. 100.—Bridge over Saskatchewan River at Saskatoon, Canada. General construction view.

bridge was placed by compressed air; the remainder by hoist and chutes (Fig. 98). In Fig. 99A is shown the pneumatic mixing plant used in the construction of this bridge with pipes leading to discharge box on the upper material track (Figs. 97 and 99B). Troughs leading from the discharge box to the work are shown in Fig. 97 but not in Fig. 99B. In Fig. 99A should be noted

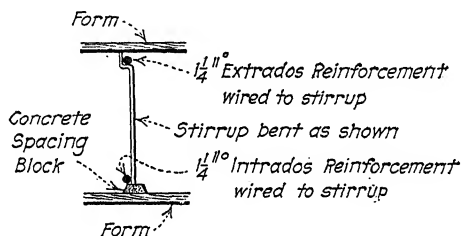
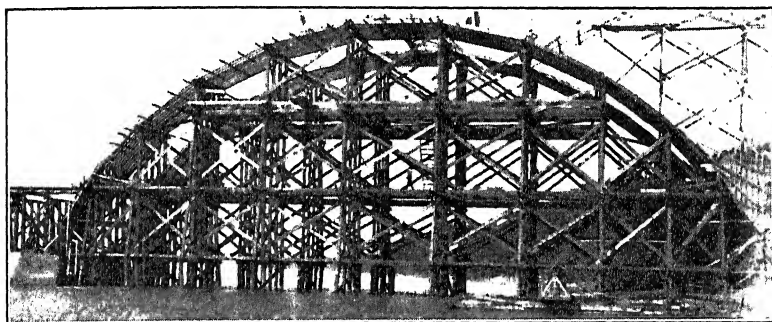


FIG. 101.

the hopper for measuring gravel, tank for measuring water, and method of handling cement. A general view of the Saskatoon bridge during construction is shown in Fig. 100.

The short radial rods in the arch ring, shown in Figs. 95, 96, and 101 were not looped around either upper or lower steel,



*Courtesy of Mr. Daniel B. Luten, Consulting Engineer, Indianapolis.*

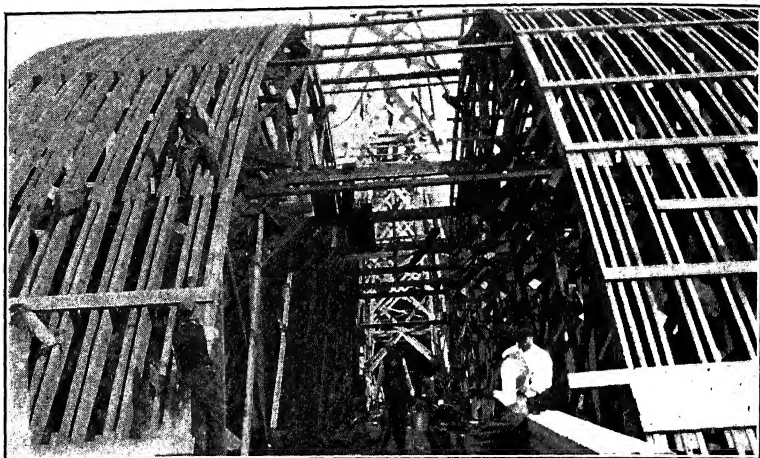
FIG. 102.—Timber falsework and centering for arches. Bridge over Saskatchewan River at Saskatoon, Canada.

but simply wired thereto. They were intended simply for framing.

When steel ribs (either rolled sections or built-up lattice girders) are used as arch reinforcement, great care should be taken to fix the ribs in the proper position, and in this position they should be braced until the concrete is placed. The use of such ribs is known as the Melan system.



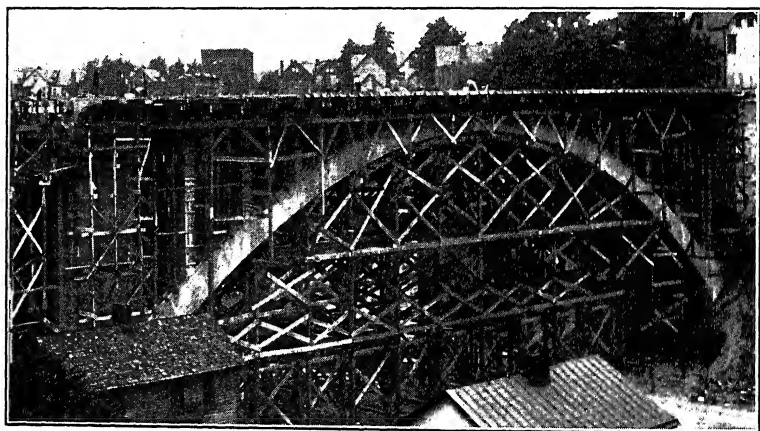
**54. Centering.**—The bent type of timber falsework (Figs. 102, 103, 104, and 105) is the type of centering generally employed in



*Courtesy of Mr. Daniel B. Luten, Consulting Engineer, Indianapolis.*

FIG. 103.—View of upper part of centering. Bridge over Saskatchewan River at Saskatoon, Canada.

arch construction except where a deep gorge is to be spanned or where a large clearance under the arch is necessary while the

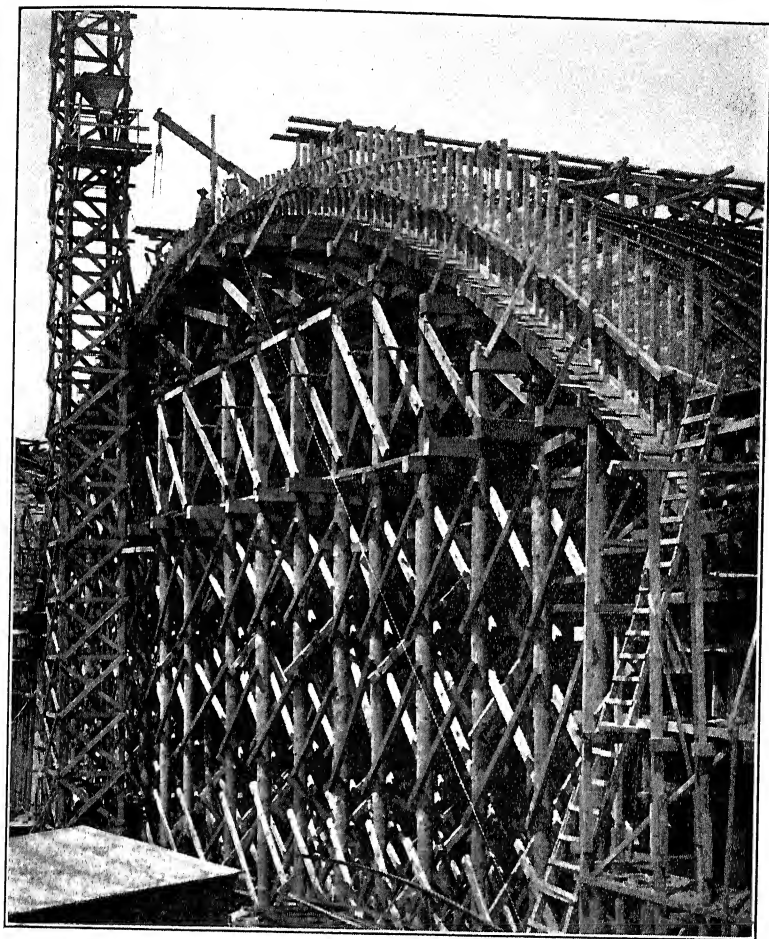


*Courtesy of Mr. N. S. Sprague, Superintendent, Dep't. of Public Works, Pittsburgh.*

FIG. 104.—Centering for Meadow Street bridge, Pittsburgh, Pa.

bridge is under erection. Timber arches, Howe trusses, and bow-string trusses are sometimes employed when it is impossible to use the bent type of centering, but these forms are expensive to build.

deform badly under loading, and have but small salvage value. (Fig. 106 shows a combination of the bent and Howe-truss types of centering.) Before using any of these types, consideration should be given to the use of steel centers (Fig. 107); or, in some

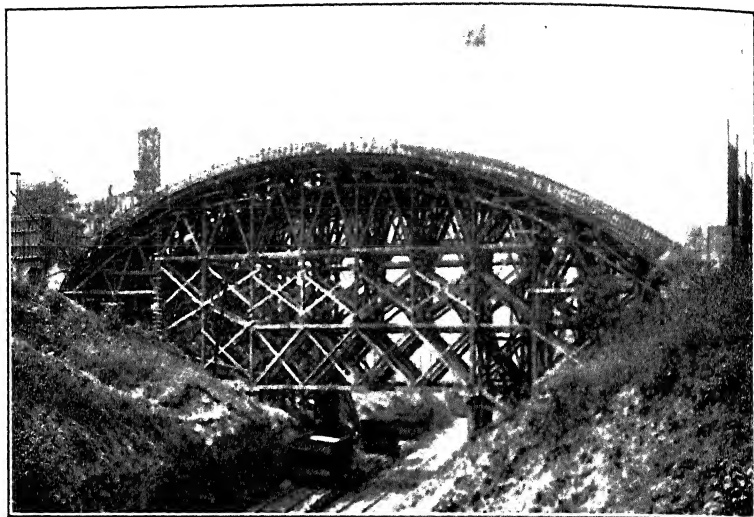


*Courtesy of Marquette Cement Mfg. Co.*

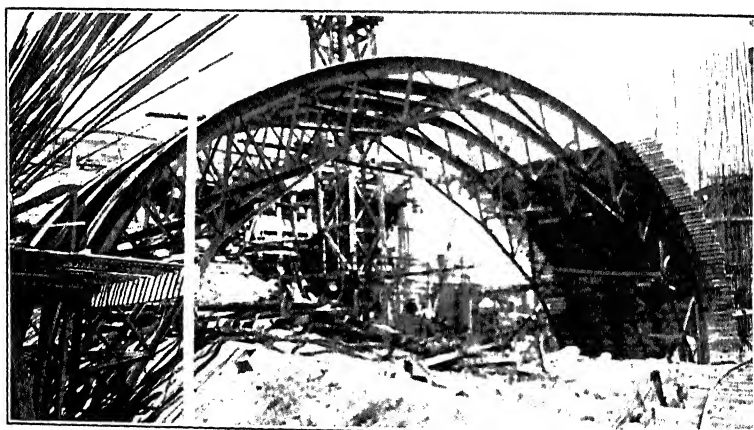
FIG. 105.—Centering for Grand Avenue viaduct, Milwaukee, Wis.

cases, to the use of suspended centering (Figs. 108, 109, and 110), if the writer may be permitted to refer in this manner to patented methods of arch construction. In some special cases

to carry a suspended arch form together with the dead load of the wet concrete (Fig. 111).



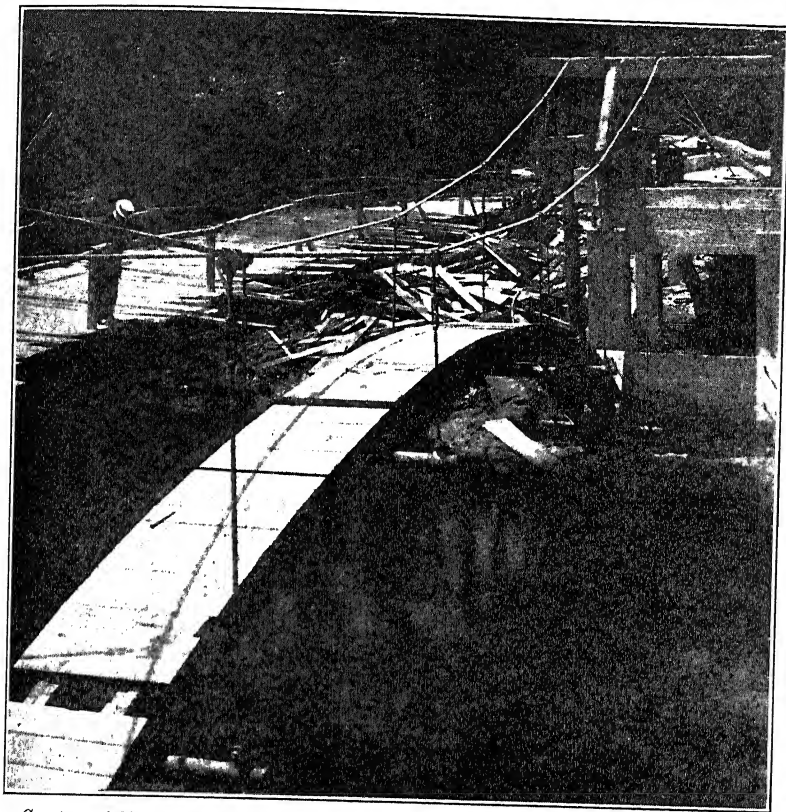
*Courtesy of Mr. N. S. Sprague, Superintendent, Dep't. of Public Works, Pittsburgh.*  
FIG. 106.—Centering for Atherton Avenue bridge over Pittsburgh Junction R. R., Pittsburgh, Pa.



*Courtesy of Mr. N. S. Sprague, Superintendent, Dep't. of Public Works, Pittsburgh.*  
FIG. 107.—Steel centering for North Side Point bridge, Pittsburgh, Pa.

*Timber Centers.*—A simple and common form of timber centering for arches of low rise is shown in Fig. 112. The lagging had not been placed at the time this photograph was taken, but some

of the joists for supporting the lagging were already in place. The joists, of course, extended from abutment to abutment and were supported by transverse bents of round timber resting on sills the full length of each bent. The falsework rested on the concrete floor of a spillway channel so that mud sills, piles, or specially-constructed concrete footings were not necessary. Wedges



*Courtesy of Mr. Philip Aylett, Civil Engineer, St. Louis.*

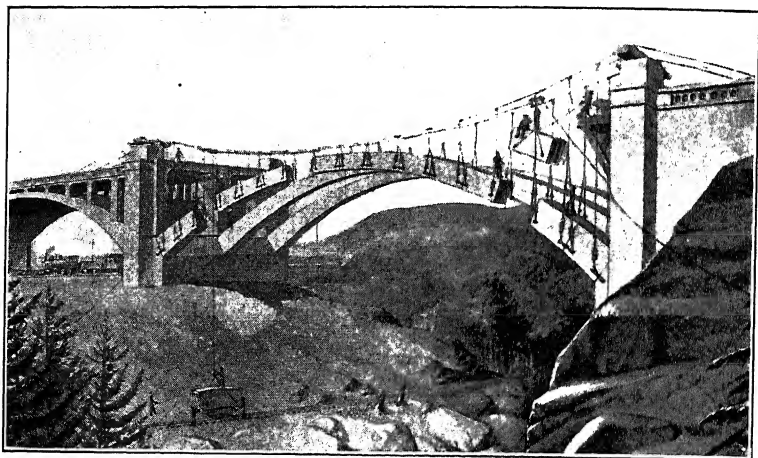
FIG. 108.—Construction view of Chickahominy River bridge near Richmond, Va. Suspended centering in place.

were placed at the bottom of the posts so that the center might be lowered conveniently after the arch ring was completed and ready to bear its load. Fig. 113 shows a similar type of centering partly removed. In the constructing of this bridge, however, the wedges were placed at the top of the posts, as can be plainly seen in the

Timber centering varies so greatly in design to meet different conditions, that plans and photographs of a number of centers which have actually been built, with a few statements (quoted or otherwise) concerning each, will do more to give the reader a clear idea of this type of construction than any general descriptions which might be given.

The centering used in the Third Avenue bridge at Cedar Rapids, Iowa is shown in Fig. 114. In a paper presented before the Western Society of Engineers, April 13, 1914, Mr. Barton J. Sweatt described the construction of this centering as follows:

"The falsework for supporting the arches consisted of pile bents, the first bent being 6 ft. 6 in. from the face of piers and abutments, the

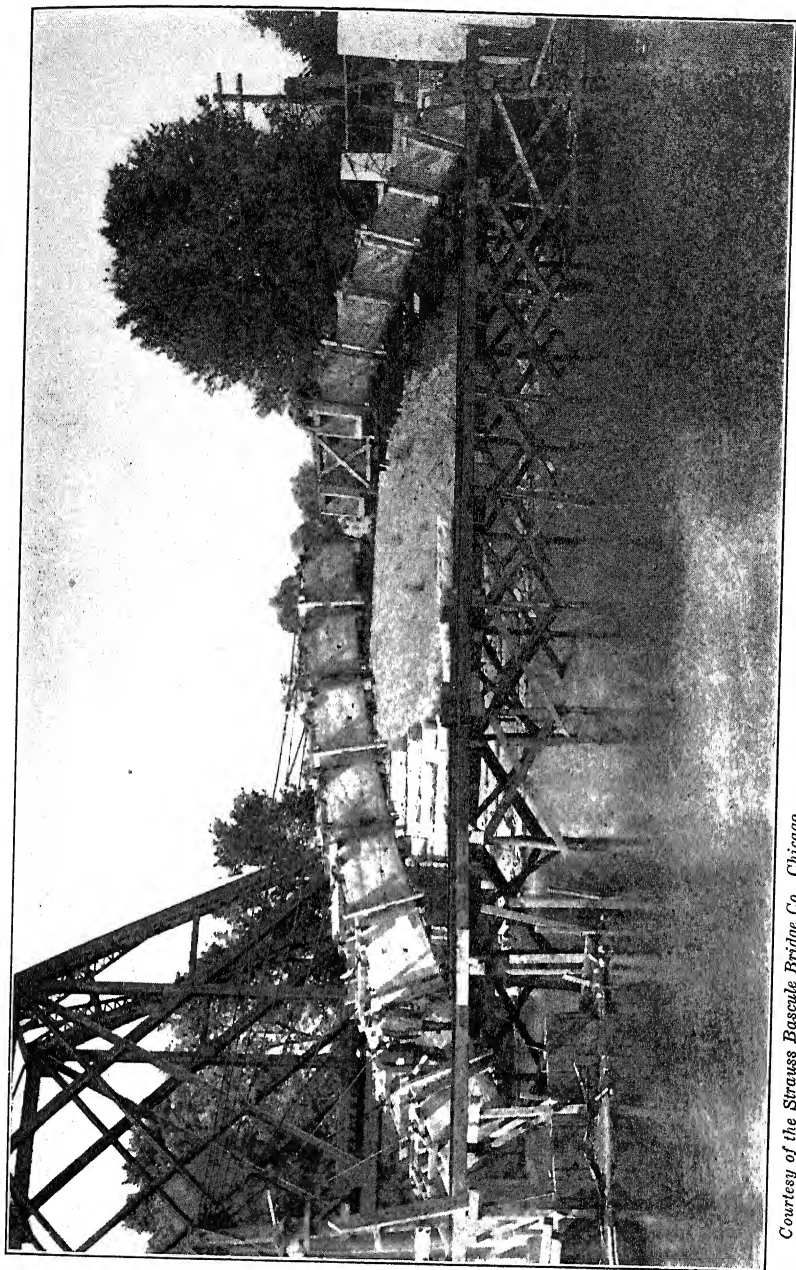


*Courtesy of Mr. Philip Aylett, Civil Engineer, St. Louis.*

FIG. 109.—Pre-casted voussoir method of arch construction.

second bent 12 ft. 6 in. from the first, and the intermediate bents were 14 ft. 6 in. centers. Oak piles were used and as a rule were driven to bed rock, the spacing was 6 ft. 0 in. for the three outside piles and 8 ft. 0 in. for the intermediate. The caps used were 12 in. by 12-in. yellow pine, false caps 6 in. by 10 in., joints 4 in. by 14 in., spaced 24 in. on centers and the lagging was 2 in. by 8 in. The proper curve for the intrados was obtained by the use of 2-in. strips cut to the proper curve and tacked to the regular joists. Oak wedges were used between the main and false caps. These wedges were placed in pairs and spaced about 4 ft. apart. Small wedges were used under the ends of the joists to bring them to the proper height.

"In constructing the centering, an all-around falsework was built up of

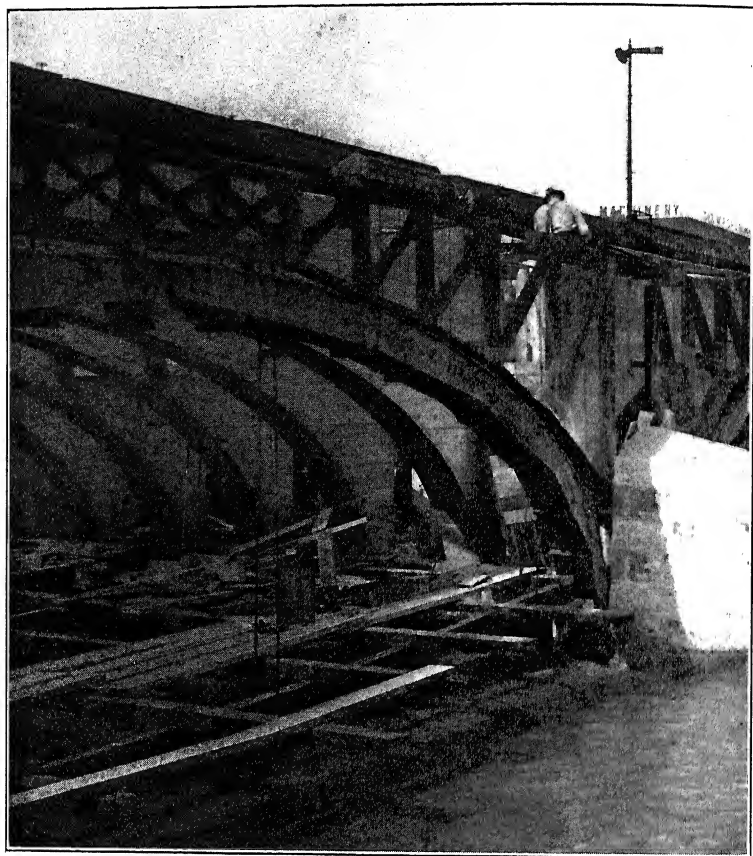


*Courtesy of the Strauss Bascule Bridge Co., Chicago.*

Fig. 110.—Strauss system of bridge construction.

camber and  $\frac{1}{2}$  in. for settlement after the centering was removed. The actual settlement of the crown after removing the centering was  $\frac{3}{8}$  in."

An article in *Cement Age*, March, 1912, describes the construction of the centering shown in Fig. 115 in the following manner:



*Courtesy of Mr. John F. Skinner, Prin. Ass't. Engineer, Dep't. of Engineering, City of Rochester.*

FIG. 111.—Bridge at Central Avenue, Rochester, N. Y. Structural reinforcement and arch-rib forms in place.

"The centering for the arch consisted of four pile bents of four piles each, and two center pile bents of five piles each. These bents were capped, top of caps being elevation of spring line of arch, and four lines of 6 in. by 8-in. stringers were placed continuous from abutment to abutment, the ends, at elevation of the spring line bearing 4 in. on the concrete abutments. At completion the ends of stringers were bolted to the



holes in the abutments filled with concrete. On these four lines of stringers were placed a set of pine wedges over each pile, there being four and five sets of wedges to each bent; 3 in. by 12-in. timber was laid on the wedges over each bent through the width of the arch. On these 3 in. by 12-in. timbers, the arch bents were erected, each having four and five 6 in. by 8-in. vertical posts V-braced, with 6 in. by 8-in. caps set edge-ways, top of caps 12 in. below intrados of arch. On these caps were placed 2 in. by 12-in. ribs, dapped to take square bearing on caps. These ribs were placed 18 in. centers across the arch and were cut from timber of

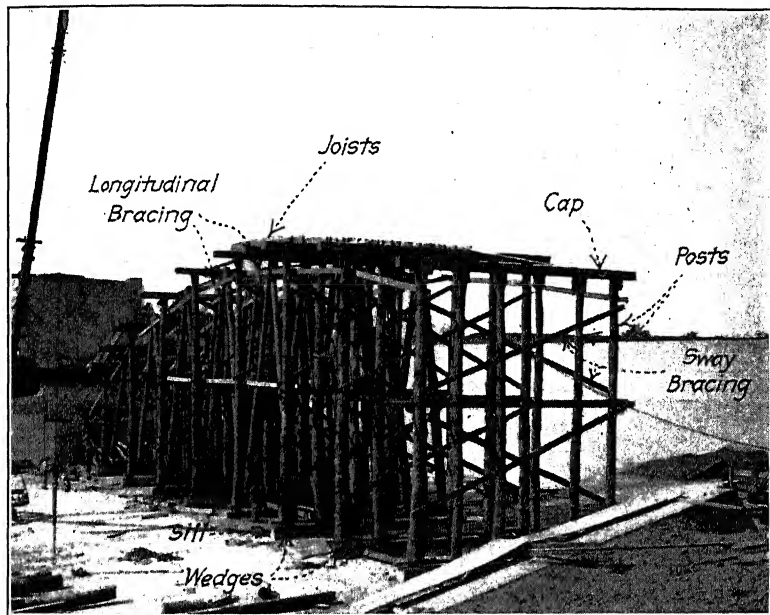


FIG. 112.—Common form of timber centering for arches of low rise.

sufficient dimensions to make them lap over alternate caps. The ribs were covered with 2-in. planking to form the intrados of the arch.

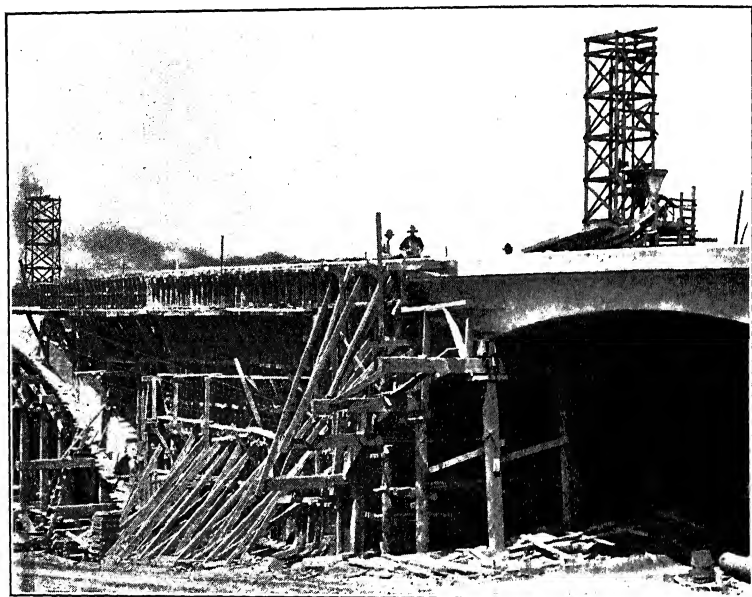
"A very simple and accurate method of laying out the ribs was used which consisted of laying out the full-size arch intrados radii on a level place near the bridge site. The timber for the ribs was, therefore, marked by a full-size drawing. Probably the most interesting feature of this arch centering was the simple straight work giving maximum strength and maximum safety in every respect at the lowest cost. The five steel floor beams of the old bridge were utilized to make an 18-ft. clear opening of maximum height in the centering. This was economical and safe, but it was not a true bent, but its main



purpose was to allow drift to pass through in case of high water during construction."

Figs. 116, 117, 118, and 119 show timber centers similar to the one just described.

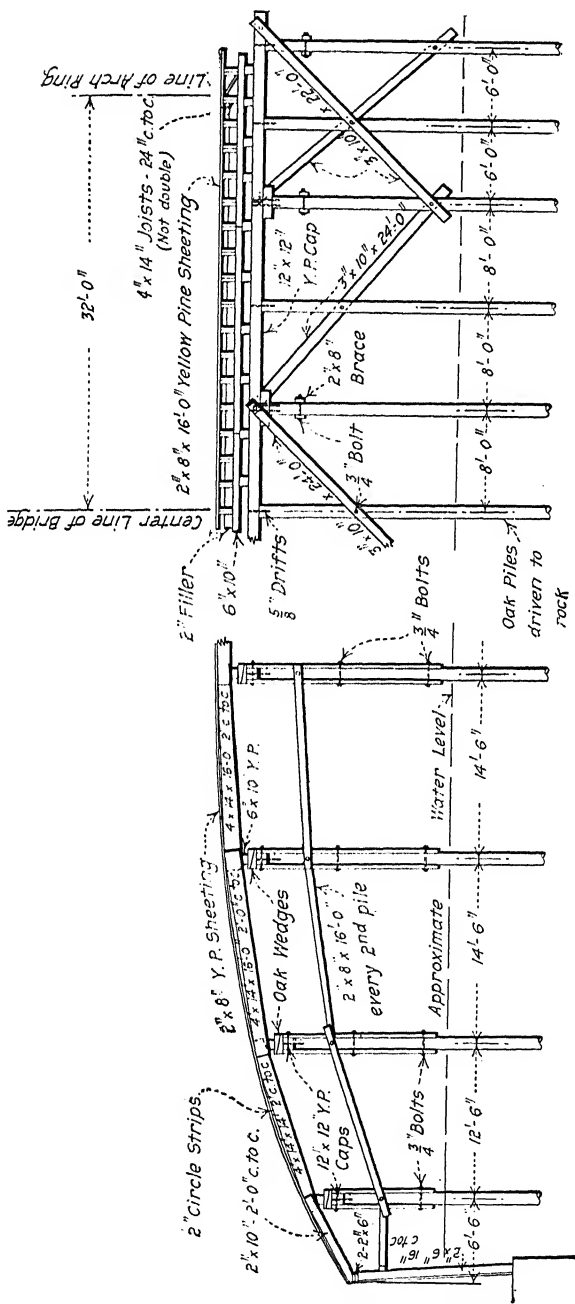
A patented type of centering is shown in Figs. 120A, 120B, 120C, and 120D, known as the Luten arch centering (see Chapter XII). The idea in this center is to dispense with the usual wedges employed in lowering the falsework. The top part of the uprights consist of two thin members with major dimensions transverse



*Courtesy of Marquette Cement Mfg. Co.*

FIG. 113.—Centering for arches of low rise, Grand Avenue viaduct, Milwaukee, Wis.

to each other. These are arranged in the form of a T-column, and wired together at frequent intervals. Each member separately is made too light to carry its loading so that clipping the wires permits each member to buckle, which lowers the center. Fig. 120B shows the first stage in construction. The joists are nailed to the uprights which consist originally of only one member each. The transverse members of the uprights are then added to form the T-columns. The V-bracing is put in position after all the joists and uprights are in place



Half Side View

Half Side View

Section showing Half of Center Bent

FIG. 114.—Centering for Third Avenue bridge, Cedar Rapids, Iowa.

FIG. 114.—Centering for Third Avenue bridge, Cedar Rapids, Iowa.

All Plumb Posts, Caps, and Stringers - 6" x 8" Yellow Pine Timber  
 All Batter Posts - 4" x 6" Y. P. Timber  
 Arch Ribs - 2" x 12" Y. P. Timber  
 Arch Flooring - 2" x 10" Y. P. Timber  
 Other Braces - 2" x 6" Y. P. Timber

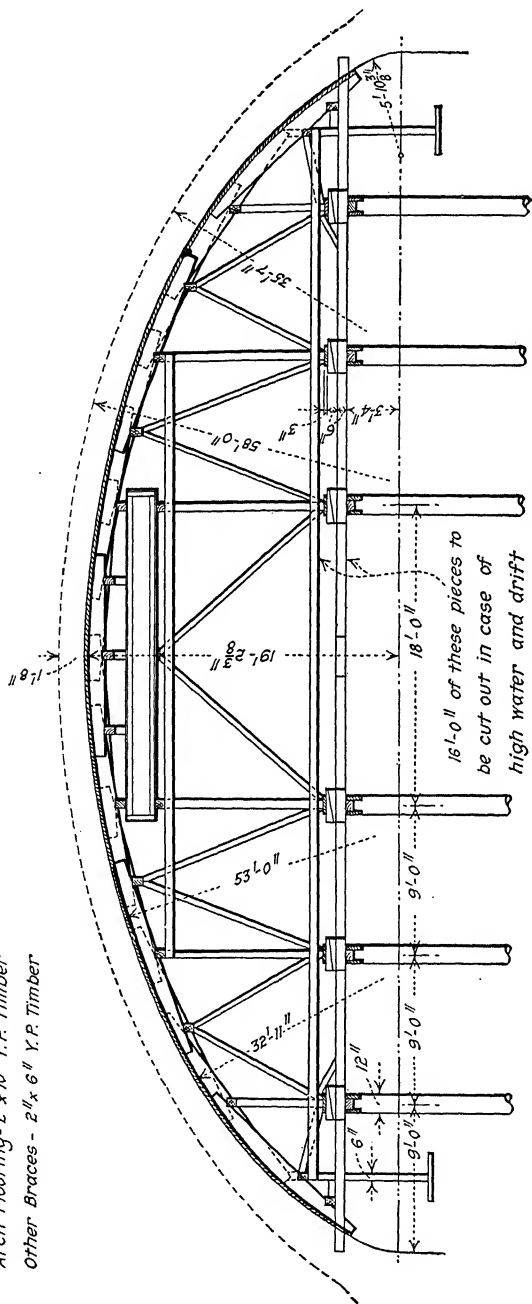
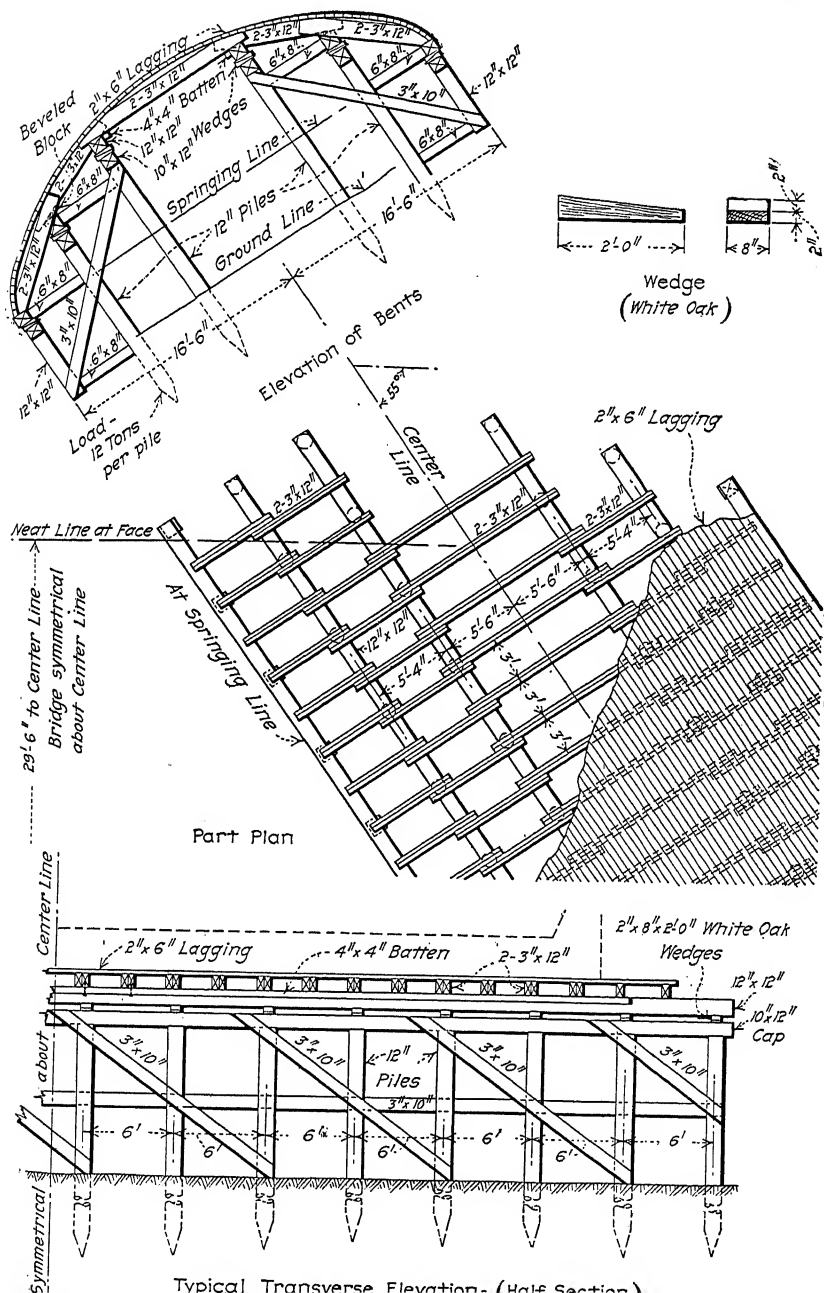


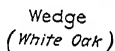
FIG. 115.—Falsework and centering for Cleveland Avenue bridge, Kansas City, Mo. Note structural steel girder carrying the center of the span to allow for flood.



in Fig. 121:

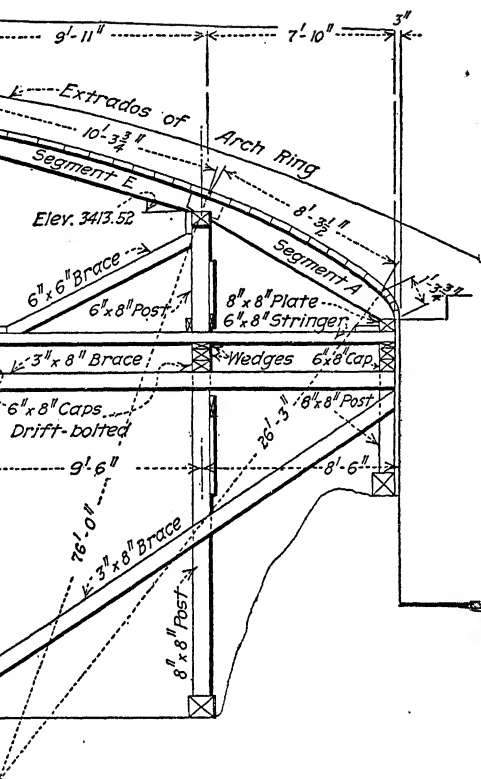


All lumber to be Yellow Pine unless otherwise stated. All bolts,  $\frac{3}{4}$ " with two standard C.I. washers. Lagging to be matched and dressed to a uniform thickness so as to form a smooth and true surface. All lagging to be 2"x4" tongue and groove



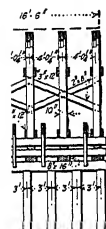
Section A-A  
FIG. 117.—Details of arch centers for Center Street bridge,  
Phillipsburg, N. J.

"Since Buffalo Bayou is a navigable stream it was necessary



average  
passage-  
ing in the  
ing nine  
ed in the

much as  
wn as the  
l, special  
care of all  
at right



Half  
Section A-A

Wedges are to be  
th, surfaced on  
a thoroughly soaked

. R. R.

Material.

	No.	Size	Ordered Length	Location
	18	3" x 8"	24'-0"	Bracing
	9	3 1/2 x 8"	22'-0"	"
	9	3 1/2 x 8"	18'-0"	"
	55	3 1/2 x 8"	16'-0"	"
	9	3 1/2 x 8"	14'-0"	"
	116	3 1/2 x 8"	18'-0"	Lagging D&M.
	116	3 1/2 x 8"	16'-0"	"
	116	3 1/2 x 8"	12'-0"	"
	16	3 1/2 x 6"	16'-0"	Bracing
	40	3 1/2 x 6"	14'-0"	Bracing
	11	3 1/2 x 4"	18'-0"	Lagging S-2-S & 2-E
	11	3 1/2 x 4"	16'-0"	"
	11	3 1/2 x 4"	12'-0"	"
	140	6" x 8"	2'-0"	Wedges
	140	3/4" x 1 1/4"	Drift Bolt's without heads or	

ed a load

ll River,  
Record,

ovide for  
ne shown

3 ft. at a  
between  
he top of  
ted with-  
centering  
e lagging

M  
 Aug  
 in l



A  
 O  
 n  
 n  
 S  
 L

during construction. This opening was 24 ft. vertically above average water level and 38 ft. wide. Protection piles on each side of the passage-way were necessary, consequently the total span of the opening in the arch centering was 49 ft. To carry the load over this opening nine 30-in., 200-lb. I-beams were used. These I-beams will be used in the construction of other bridges.

"Longitudinal bracing was arranged so as to counter, as much as possible, the 'bucking up' tendency of the centering at the crown as the arch was concreted. On account of the arch being skewed, special study was given during the placing of braces, etc., so as to take care of all side thrusts. Struts were placed diagonally between bents at right

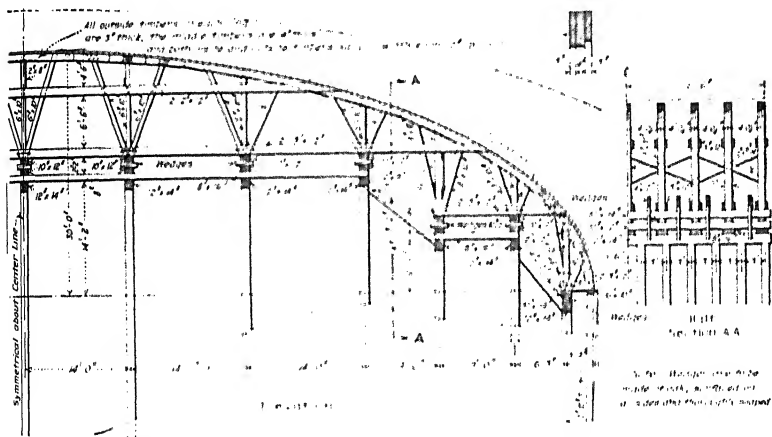


FIG. 119. Falsework for bridge over Big Muddy River, I. C. R. R.

angles. Spacing of centering piles was such that no pile received a load of over 12 tons."

Timber centering for a bridge over railroad tracks at Fall River, Mass., is shown in Fig. 122 and described in Engineering Record, issue of April 26, 1913, as follows:

"In building the arch centering it was necessary to provide for certain requirements that necessitated a design similar to the one shown in the accompanying drawing.

"These requirements called for an overhead clearance of 18 ft. at a point 11 ft. 3 in. from the property line, a clear span of 40 ft. between inside vertical posts, and a minimum clearance of 15 ft. from the top of rail to the under side of the truss. The work had to be conducted without interruption of train service. The uprights supporting the centering



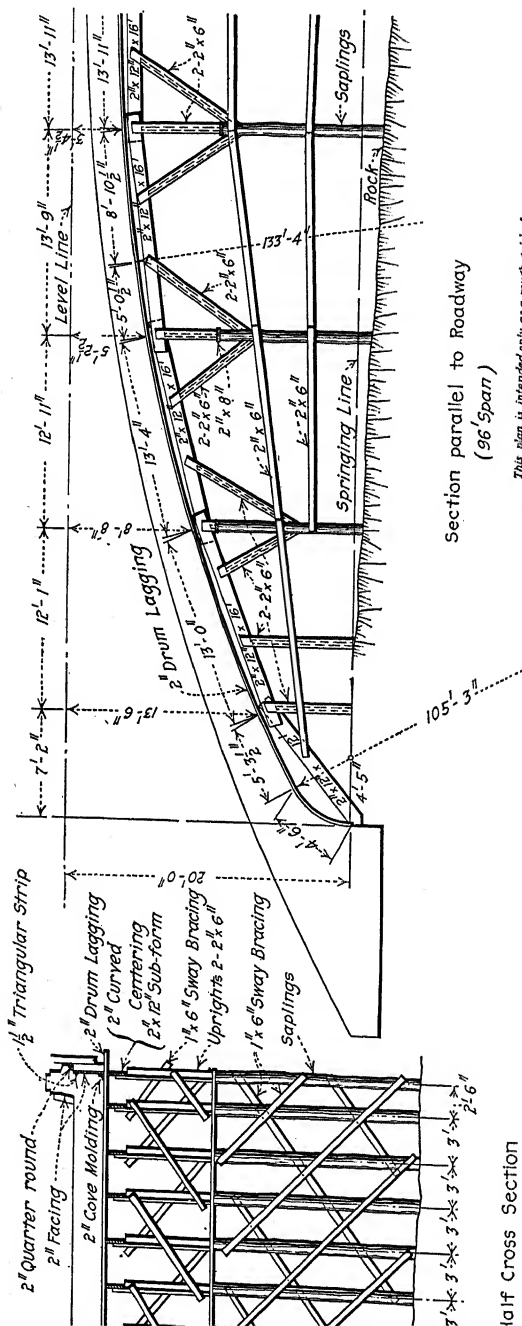


Fig. 120.A.—Centers of Luten Design for Cicott Street bridge over Wabash River, Logansport, Ind.

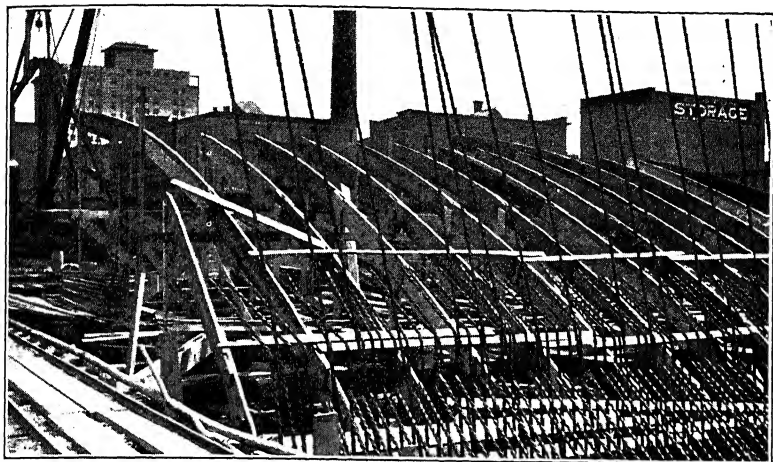


FIG. 120B.—Luten arch centering.

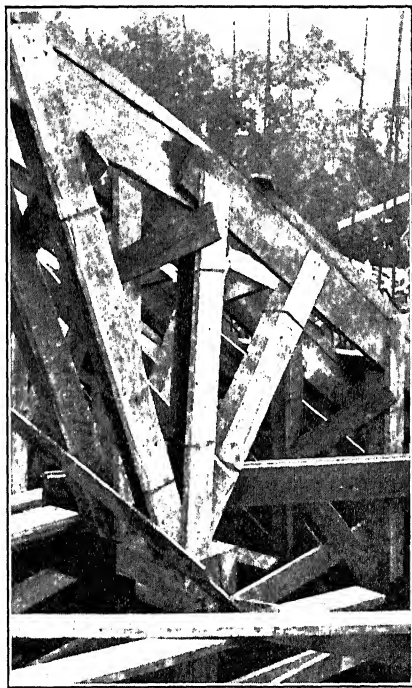


FIG. 120C.—Luten arch centering.

was used over the entire arch ring. The centering was designed for a deflection equal to one eight-hundredth of the span."

In the construction of the Hights Run bridge shown in Fig. 83 the two arch ribs were constructed in sections and each section cast at one operation. The false work consisted of braced timber posts supporting I-beams which carried the lagging for the arch ribs. All adjustments for the arch rib were made by wedges immediately under the I-beams. Two bents of posts of the false

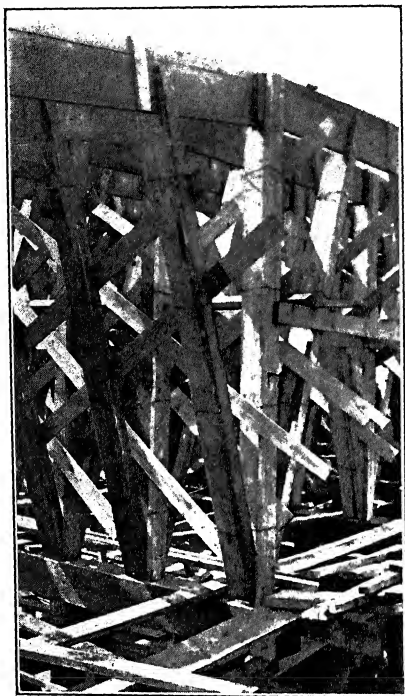
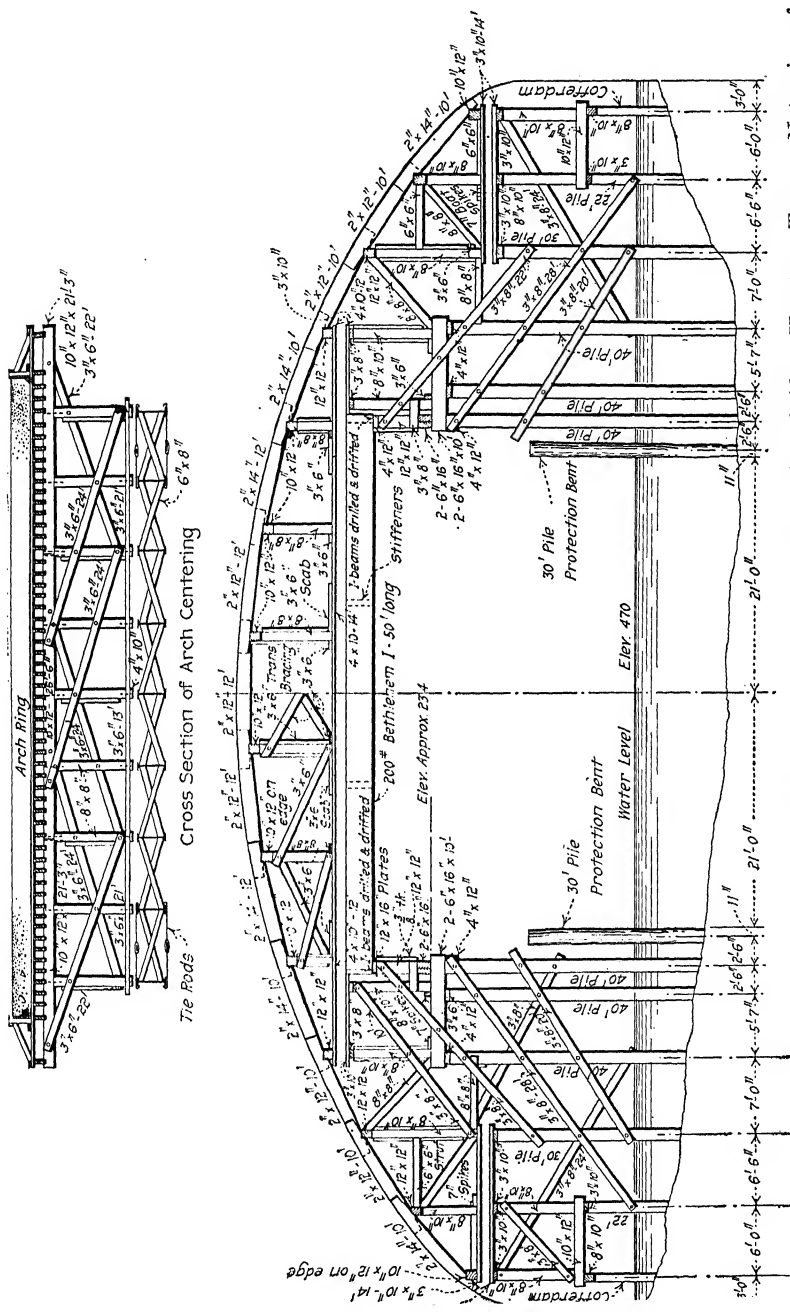


FIG. 120D.—Luten arch centering.

work were located under each section of the arch rib, and located so that the center of gravity of the section fell between the posts which were braced together like a single tower; thus each section of the rib was independently supported and adjusted. In designing the falsework no soft lumber was subjected to cross-grain compression, hard wood being used for sills and caps. Posts and bracing were of yellow pine.

Figs. 123A and 123B show the type of arch centering used in



G. 121.—Details of arch centering and supports for 110-ft. span of San Jacinto bridge, Houston, Texas. Note size of opening for navigation.



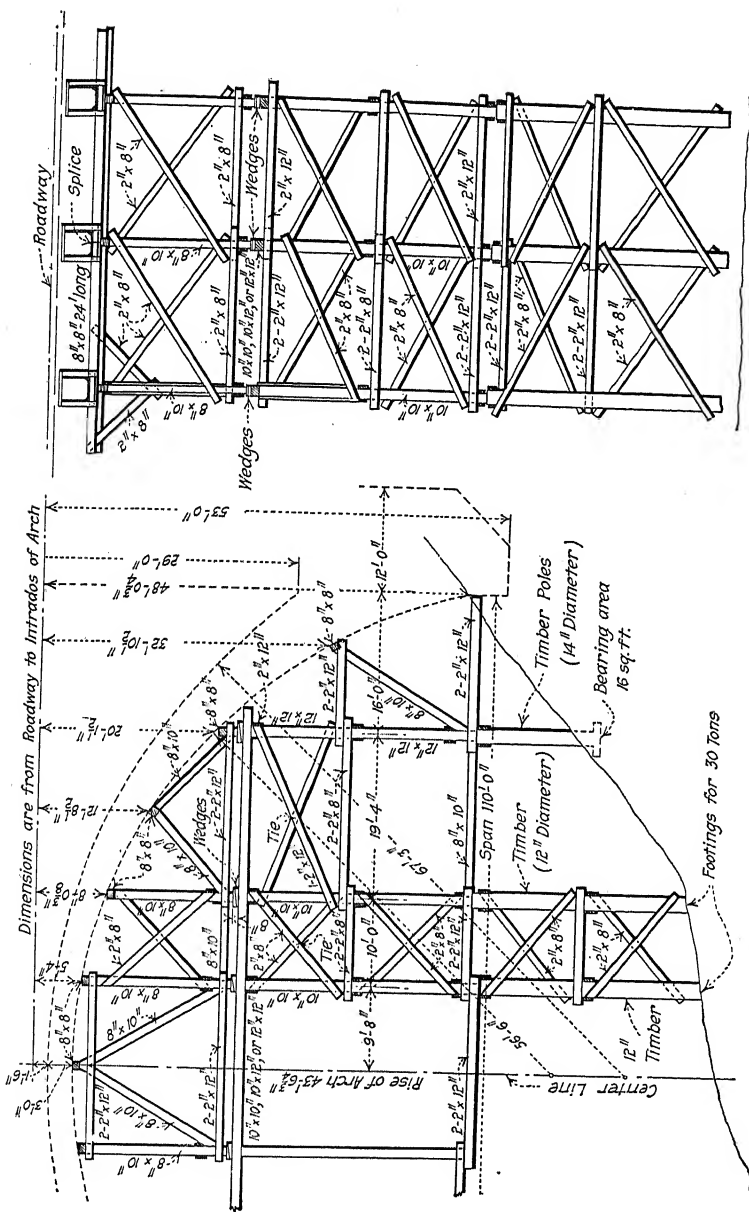


Fig. 123A.—Centering for bridge over ravine on Mississippi River Boulevard, St. Paul, Minn.

A sand box used in the main arch of the Edmondson Avenue bridge, Baltimore, is shown in Fig. 125. The center was lowered by allowing the sand to run out through a 1-in. circular hole in the oak bottom of the steel-plate cylinder. This hole was closed by a wooden plug while the centering supported its load. A disadvantage in the use of sand boxes lies in the fact that the centering cannot be raised before the arch ring is poured in order to adjust the top members to the curve of the arch intrados.

In the design of large arch centers an uncertainty exists regarding the pressures from voussoirs placed on the steepest portions of the lagging. Either of two assumptions are usually made as to the forces acting on the centering due to the weight of such voussoirs. In the common method of design, the assumption is made

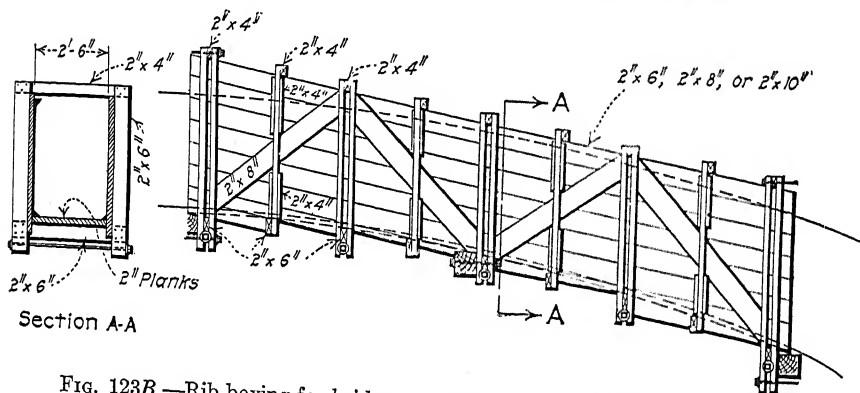


FIG. 123B.—Rib boxing for bridge over ravine on Mississippi River Boulevard, St. Paul, Minn.

that the centering sustains only the radial components of the voussoir weights, the tangential components being resisted by temporary struts between voussoirs so as to be transferred to the abutments. The more accurate method is to assume that tangential pressures (in addition to the radial pressures) act on the centering which, from any voussoir, may be as great as the product of the radial component and the coefficient of friction between the voussoirs and lagging. The original tangential component is then reduced by this amount.

Since a timber center is only a temporary structure and has a high salvage value, great accuracy in the design of the separate members is not necessary. The method of design need only be such that the size of each member is well on the safe side. Then

too, rigidity is quite as important as strength, so that all things considered, close figuring is out of the question. Obviously the weight of centering may be omitted except for high arches. For

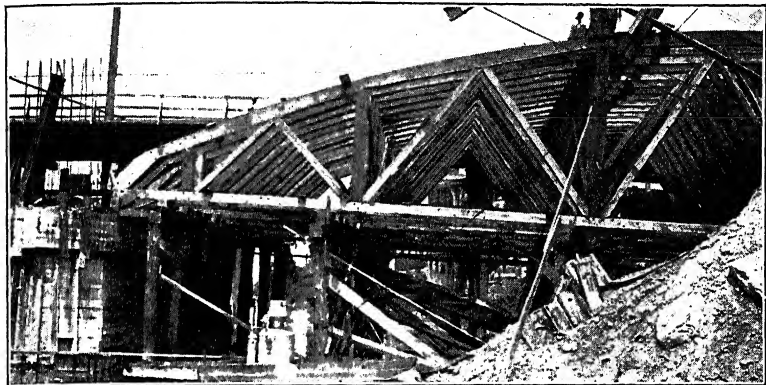


FIG. 124A.—Centering for High Street bridge, Hamilton, Ohio.

the method of designing lagging, joists, and posts see Art. 88, Volume II.

As a rule, only hard wood should be used for caps and sills,

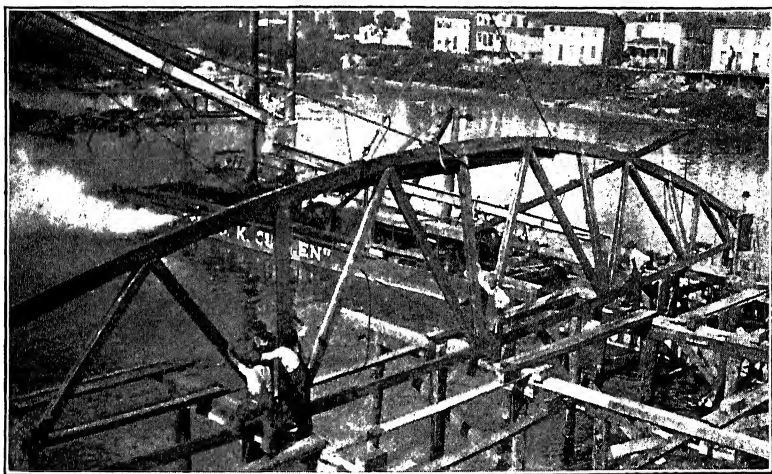


FIG. 124B.—Centering for High Street bridge, Hamilton, Ohio.

although long-leaf pine may be sufficiently hard in many cases. Wedges, however, should be made of hard wood without exception. It is also well to consider the number of joists in side walls



compression to a minimum on account of the low bearing value of timber across the grain. Steel distributing plates are of advantage in this connection.

Care should be taken to prevent lateral displacement of vertical posts due to radial pressure from the arch ring. This may be avoided either by proper longitudinal bracing or by notching out the joists and shimming them tight against the caps.

Many practical notes on the design and erection of falsework may be found in Section 7 of the American Civil Engineers' Pocket Book.

In striking arch centers, wedges should be lowered gradually beginning at the crown and working toward the springing lines. The lowering should be done symmetrically with respect to the center of the arch ring. In a series of arches, centers between

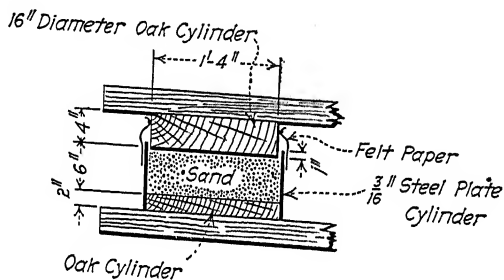


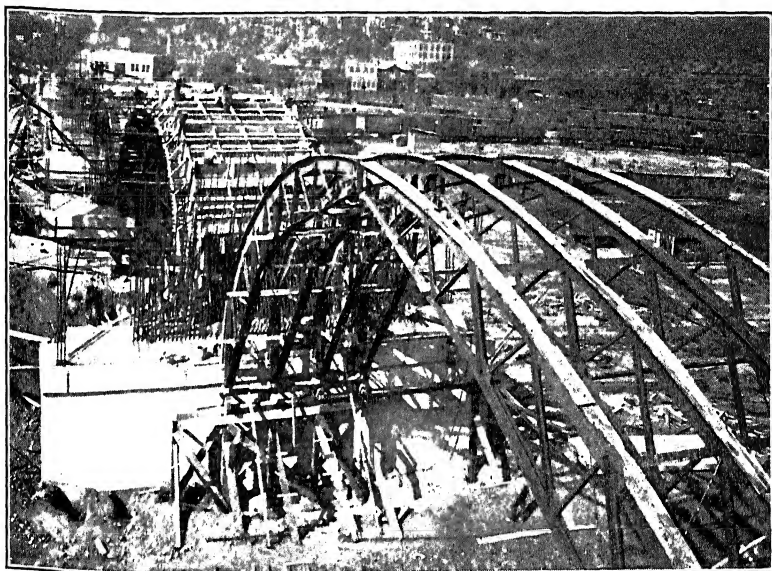
FIG. 125.—Sand box.

abutments or abutment piers should be struck simultaneously. As a rule, centers should not be struck from arches in less than 28 days under favorable weather conditions, and it is desirable that a longer period should elapse if possible.

*Steel Centers.*—Steel centers of the arch-trussed type (Fig. 126) should receive consideration when arches are to be built in series or where the character of the stream or crossing renders timber and pile falsework impossible or expensive. Undoubtedly the cost of a steel center is usually high, but if it can be used a number of times, as in a large series of arches, it may not prove any more costly than timber. Mention should be made of the fact that in the Cummings-Watson system, to be described later on, the steel arch centering consists of triangular units which can be adapted to any shape and can be used for any span or curve by connecting and adjusting the units to fit. It is quite likely that with these

units as part of a regular contractor's equipment, the steel center may be used with economy even in ordinary construction.

It is generally recognized that there are some well-defined advantages in using three-hinged arch centers. In the first place, the crown deflection using steel centers is usually much less than that obtained by employing timber falsework. Furthermore, it is possible to compute the deflection of each point of a steel center with some degree of accuracy while, in the case of a wooden center, the probable settlement at each bent is pretty much a matter of guesswork. Steel centers also have the additional ad-



*Courtesy of Mr. N. S. Sprague, Superintendent, Dep't. of Public Works, Pittsburgh.*

FIG. 126. —Steel centers for North Side Point bridge, Pittsburgh, Pa.

vantages of allowing an obstructed opening for railroad or other traffic and of eliminating danger from flood and ice in the construction of arches over streams. The advantage of allowing the deflection to be quite accurately computed makes it possible to give the centers a preliminary camber so that when the concrete is in place and the centering withdrawn, the arch ring will assume its true position.

One disadvantage of using steel in arch centering lies in the fact that it is materially affected by temperature changes. For this reason, in constructing large arches, only the alternate block method should be used.

The steel centering used in constructing the three-span earth-filled arch structure which carries Atherton Avenue in the city of Pittsburgh across the four tracks of the Pennsylvania Railroad is shown in Fig. 127. This centering, fabricated by the Blaw Steel Construction Company, consisted of steel arch trusses spaced 5 ft. 5¼ in. on centers. The trusses carried timbers and lagging, and were supported on framed trestle bents placed close to the pier faces. Sufficient trusses were at first erected to concrete one-half the width of each arch ring, then the centers were shifted transversely to themselves and the concrete placed for the second half of the structure. The method used in construction and the details of the arch centering are described in *Engineering and Contracting*, issue of February 19, 1913, as follows:

"A six-post bent was erected on the footing shelf of the pier, the idea being to have a bent-post under each arch rib. On the bent caps over each post was placed a block and double wedge and on these supports a 12 in. by 12-in. plate on which rested the ribs. Between each pair of ribs a dolly was fastened to the bent-caps.

"The shifting of the center to construct the second half of the arch was accomplished as follows: Jacks were set up on the bent-caps alongside the dollies, and a strain taken on them until the wedges were loosened sufficiently to be easily removed. The jacks were then lowered until the weight of the centers rested on the dollies. To prevent the lagging and cross timbers from being lifted off the ribs by sticking to the soffit of the arch ring, one end of the center was lowered ahead of the other so as to give a stripping action in freeing the lagging. When lowered into the dollies the whole center was shifted sidewise rubbing on the dollies, until it rested on the six-post bents under the second half of the arch. The jacks were then placed on the caps of the second bents and the center raised and the blocks and wedges inserted. A steamboat ratchet was used to pull the center on the dollies. Four men working 8 hours shifted a center. Incidentally the tie rods connecting the opposite ends of the ribs were found, when planked across, to provide a most convenient bridge for the workmen engaged in shifting and adjusting the centers.

"The lateral thrust on the centers due to their skewed position was taken care of by suitable lateral bracing of the ribs. In anticipation of the center rising at the crown in concreting from the haunches upward, the ribs were anchored back to the pier masonry as shown in Fig. 41. The joining carried by the ribs consisted of cross-timbers over which were notched stringers with curved top edges. The stringers were spaced 11½ in. apart and were lagged with ¾-in. boards. The bearings of the stringer ends against the piers were formed by wedges."

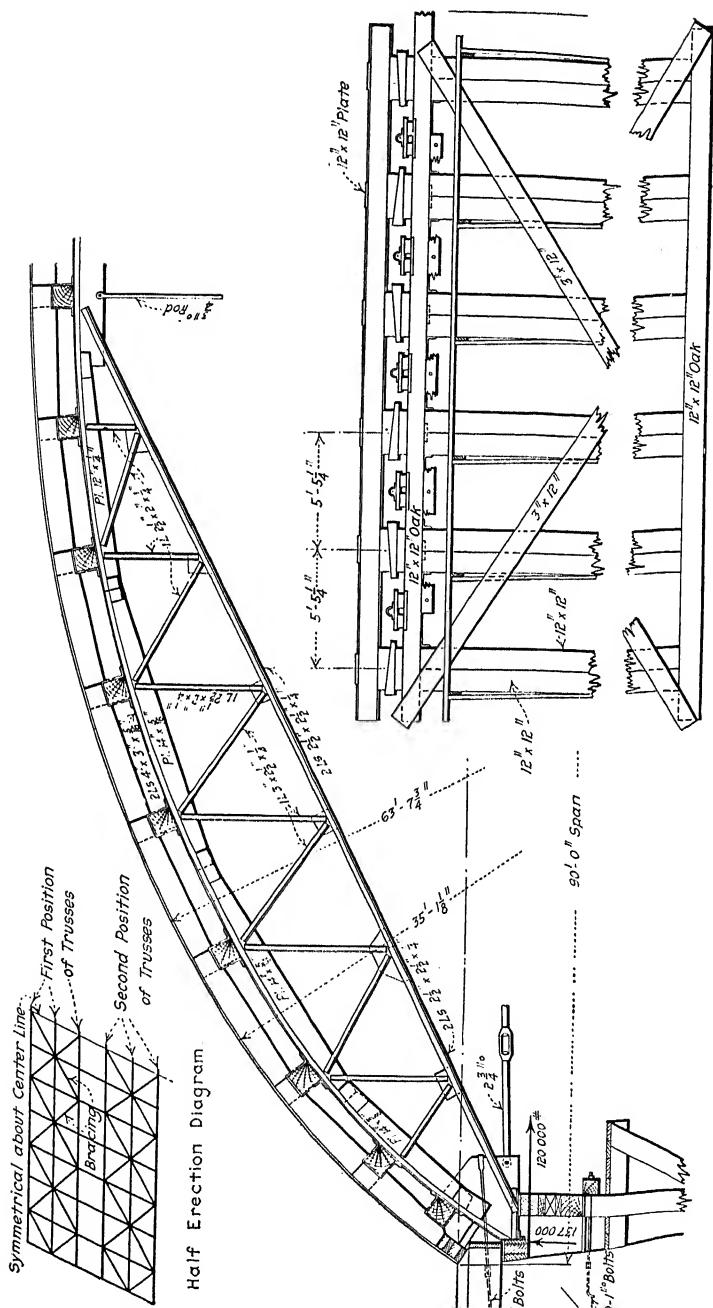


Fig. 127.—Steel centering for Atherton Avenue bridge, Pittsburgh, Pa.

Steel centering employed in the construction of the South Eighth St. Viaduct, Allentown, Pa. (a two-ribbed arch structure of nine 120-ft. spans) is shown in Fig. 128. The Engineering News, issue of April 17, 1913, describes this centering as follows:

"For the nine 120-ft. arches three full sets of steel arch centers were used, using each set for three of the arches. Each set of centers consisted of two independent-trussed arches of the outlines shown in Fig. 128, each arch supporting one of the twin concrete arch ribs and being itself made up of two steel arch ribs interbraced with steel struts. Across

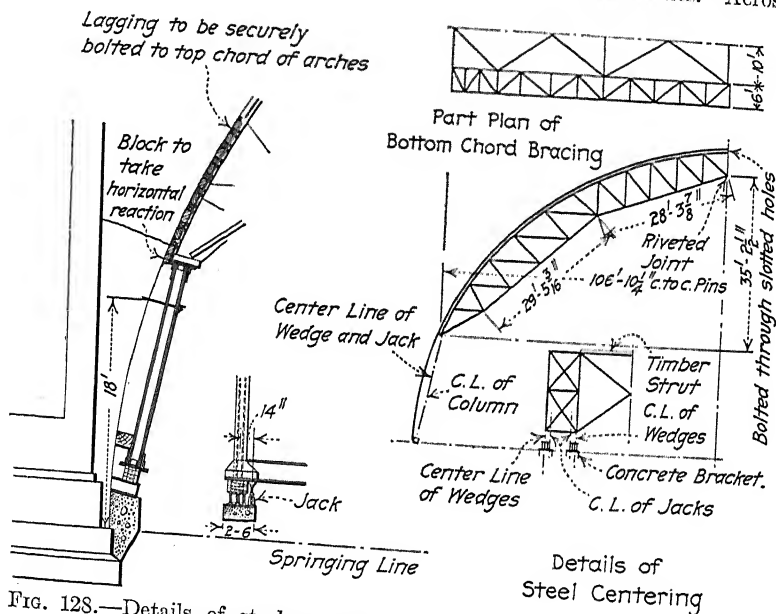
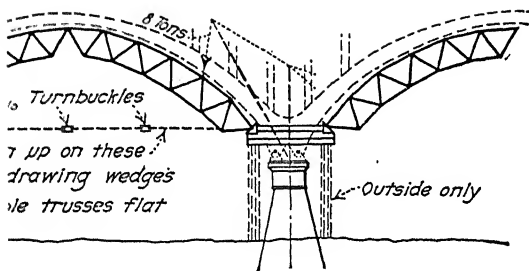


FIG. 128.—Details of steel centering for South Eighth Street viaduct, Allentown, Pa.

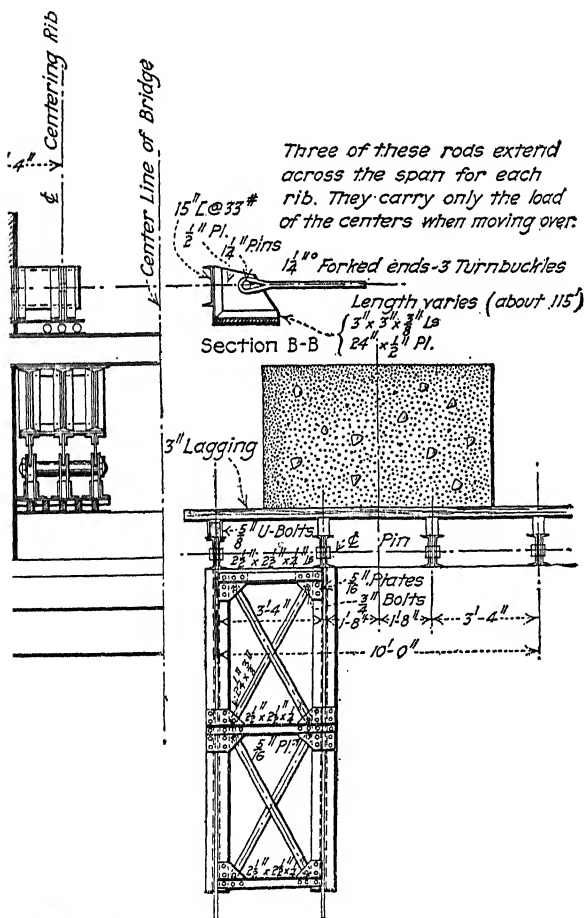
the upper chords of these steel ribs, which were curved to the curve of the concrete arch, was bolted the wooden lagging on which the concrete was deposited. The twin centering arches were held together by a timber cross-beam and diagonal steel rods.

"The arch trusses were fabricated in six sections and riveted on the ground into semi-arches, which were lifted by derricks into place, to be bolted at the base to the supporting columns. At the crown it was riveted solidly in the bottom chord, but bolted through slotted holes at the upper chord, to insure the stress passing through the lower chord.

"The centers were supported on inclined steel columns which footed on concrete steps purposely projected from the main section of the pier.



of the  
illages,  
en the  
used to  
wed to  
which  
a. bolt  
lges to  
or the



ation.  
n off

ting  
rela-  
able  
rip-  
pter

own  
pin-  
bers  
to



Ej  
of  
N.

us  
sis  
ea  
m:

—

=

—

=

—

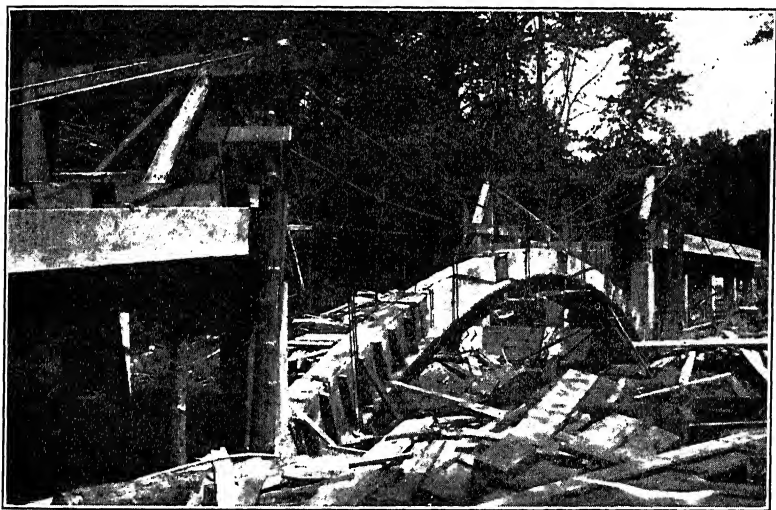
F<sub>1</sub>

th  
co  
de  
cr

gr  
bc  
ri  
at

or

and cut off after the centers were struck. The base plates of the columns rest on cast-iron wedges which in turn rest on I-beam grillages, footing on the afore-mentioned concrete projection. Between the column base and the projection, 10-ton screw jacks are interposed to aid in the alignment and leveling of the centers; they are allowed to remain in place, though the load passes directly to the wedges which are used for striking centers. A U-shaped clamp, made of a 1-in. bolt (not shown in the drawing), is passed around each pair of wedges to prevent any possible lateral motion. A similar bolt is used for the same purpose higher up on the main column."



*Courtesy of Mr. Philip Aylett, Civil Engineer, St. Louis.*

FIG. 130.—View of Chickahominy River bridge during construction. Key spaces have just been filled with concrete. Forms are being taken off rib in order to hasten setting of concrete.

The unique feature in the steel centering used in constructing the Tunkhannock Creek viaduct on the relocation of the Delaware, Lackawanna, and Western Railroad was an adjustable panel at the crown of the steel arch trusses. A detailed description of these trusses and their erection may be found in Chapter XXXII.

The Cummings-Watson system of steel arch centering is shown in Fig. 129. The centering consists of triangular units, pin-connected at their apices, and with extra adjustable members which serve to connect the units and at the same time serve to form the lower chords of the arch trusses.



*Suspended Systems.*—Suspended systems of arch construction refer only to arches of the ribbed type.

The Aylett System (patented)<sup>1</sup> of suspended centering, pre-



*Courtesy of Mr. Philip Aylett, Civil Engineer, St. Louis.*

Fig. 131.—View of Chickahominy River bridge during construction. One rib completed and suspended centering ready to be removed.

viously illustrated in Fig. 108, is shown in detail in Figs. 130 and 131, which are construction views of the Chickahominy River bridge, Richmond, Va. (Fig. 132 is a view of the completed

<sup>1</sup> See *Engineering and Contracting*, June 21, 1911, or *Cement Age* for June, July, and September, 1911, for detailed account of this method of construction.

arch structure.) Another Aylett method of arch construction is shown in Fig. 133, known as the pre-casted voussoir method.

A patented system of arch erection without falsework, originated by Mr. J. B. Strauss and tried out in the construction of a bridge over the Kiswaukee River near Belvidere, Ill., in 1906, is illustrated in Fig. 110. Voussoir forms are made of reinforced concrete in sheet-metal molds (Fig. 134). After these forms are raised to position they are held in place by suspension rods which pass over A-frames supported on top of the piers and anchored by means of steel rods. The concrete forms when self-supporting form an arch trough in which the reinforcing steel and concrete



*Courtesy of Mr. Philip Aylett, Civil Engineer, St. Louis.*

FIG. 132.—View of completed Chickahominy River bridge near Richmond, Va.

are placed. The concrete forms are designed to safely carry their own weight and the weight of the concrete deposited therein. (Fig. 135 shows the completed Belvidere bridge.) Fig. 110, previously referred to, shows a traveller on falsework used in connection with the construction of the Belvidere bridge. This is not the way, however, that the Strauss System is intended to be used, since the particular object of the construction is to avoid any falsework whatever in the stream. In the erection of the Belvidere structure it was impossible to procure a cableway in time to start the work, and the traveller method was used on that account.

Reinforcement in the form of steel arch trusses to carry the

arch rib forms are shown in Figs. 111 and 136. These trusses were designed to carry the weight of the arch forms together with the dead load of the wet concrete, both as to tension and compression, the result being that the steel reinforcement of the arches was stressed by the weight of the forms and wet concrete

*Note: Voussoirs are suspended and coupled together at floor level on both abutments, L and R, simultaneously. As the resulting "voussoir-chains" grow in length, link by link, they descend to junction at crown of arch. Final adjustment and keying of entire arch-rib then proceeds.*

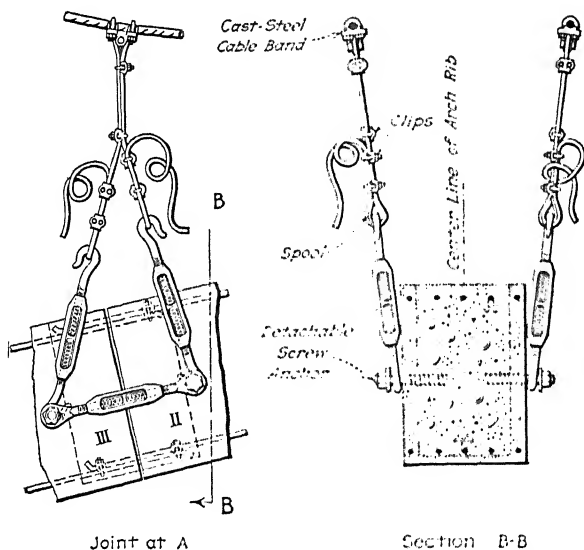
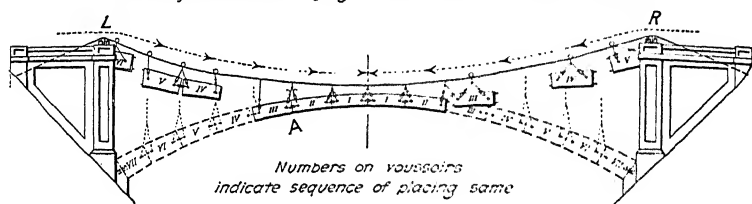
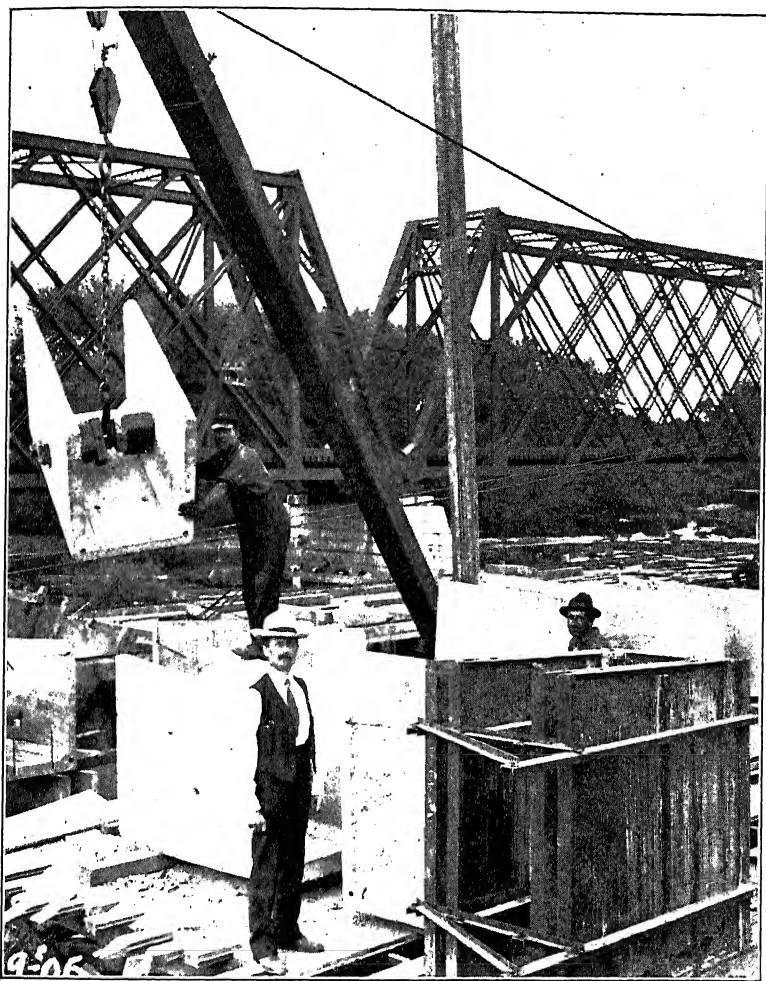


FIG. 133.—Pre-casted voussoir method of arch erection.

before the concrete obtained its set. In the finished structure the reinforcement was also considered to do its share in carrying the live load.

In Fig. 111 a wire mesh is shown on the outside of the outer line of arch ribs. This was stiffened by means of small vertical rods

and supported from the steel arch trusses at a distance of 2 in. from the face form. The white Portland cement and crushed granite aggregate were carried up next the form and



*Courtesy of the Strauss Bascule Bridge Co., Chicago.*

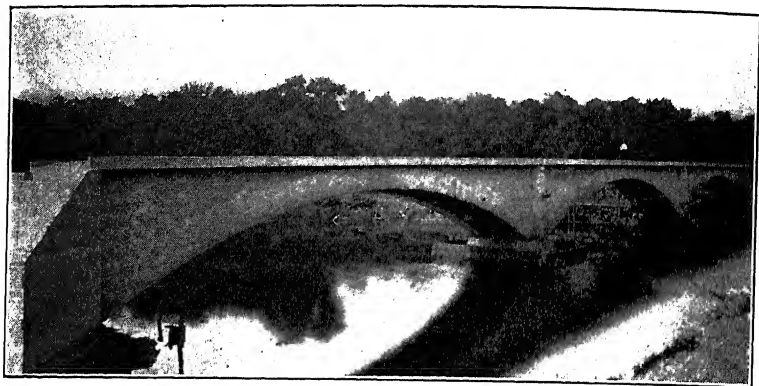
FIG. 134.—Voussoir forms used in the Strauss system of bridge construction.

outside of this mesh, a little ahead of the gray Portland cement concrete in the body of the arch. The mesh of the wire screen was large enough to admit stones from the granite aggregate passing through, but too small to allow the gray limestone of

the main aggregate from passing outward toward the face. The advantage of this construction was, of course, the carrying up of the two masses simultaneously, and did not require the pulling of an intermediate form with the consequent dislodgment of material and breaking of the bond between them.

Figs. 136 and 137 show that the upper chords at the ends of the arches were each connected by two tension rods. Boxes of clay were arranged back of the nuts of these rods, so that in case of any lengthening of the arches the rods would slide through their bearings, but would come into action in tension under heavy loads.

Figs. 111 and 136 show also working platforms suspended from

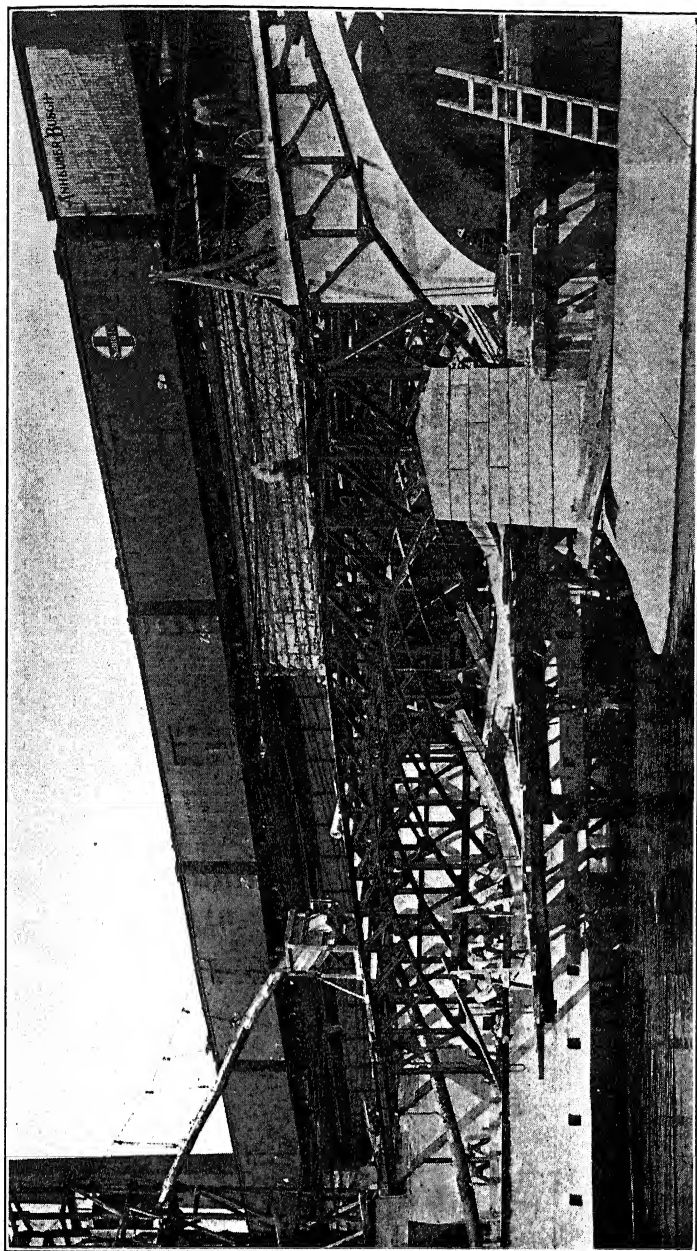


*Courtesy of the Strauss Bascule Bridge Co., Chicago.*

FIG. 135.—Bridge over the Kishwaukee River near Belvidere, Ill. Built by the Strauss system.

the steel arch ribs. The reason for suspending these platforms rather than building up falsework may be seen in Fig. 111, where high water is passing under the bridge and a low power dam crosses the river 10 ft. upstream. A 98-ft. fall also occurs a few hundred feet downstream. Fig. 138 is a view of the completed structure. Incidentally it might be stated that the floor has a 2-ft. camber in its entire length, the ends of the structure being at the same elevation.

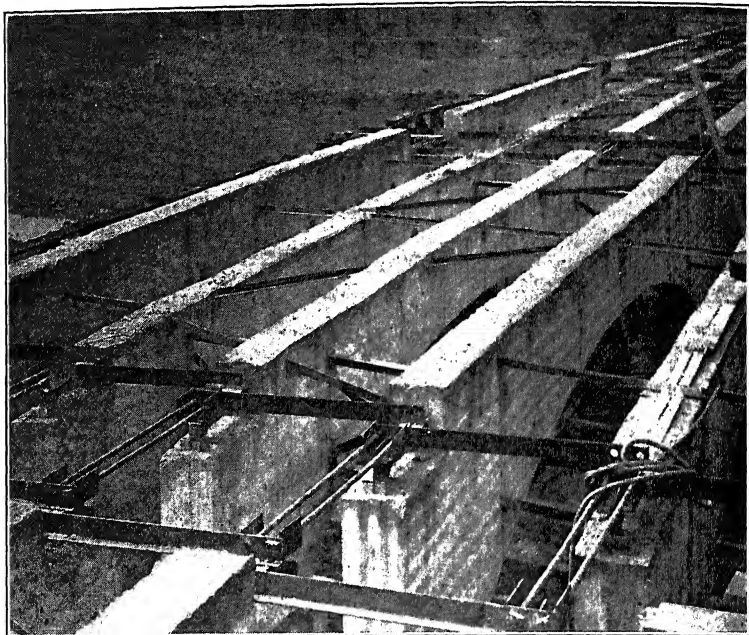
**55. Forms.**—Forms for piers and walls are usually constructed of either 1-in. or 2-in. plank nailed to studs and held by horizontal waling pieces, with tie bolts extending across the pier or wall between opposite wales. The wales, which consist generally of two planks fastened together but separated by



*Courtesy of Mr. John F. Skinner, Prin. Ass't. Engineer, Dep't. of Engineering, City of Rochester.*

FIG. 136.—Bridge at Central Avenue, Rochester, N. Y. under construction.

spacing blocks, are set edgewise against the form studs and the tie bolts are carried through the openings which occur in the waling pieces. Wire is sometimes used for bracing and is tightened either by wedges or by twisting. The wire pulls against spreaders which are inserted between forms and which are removed as the concrete level rises. As in most form work, bridge forms are either erected in sections of a size for easy

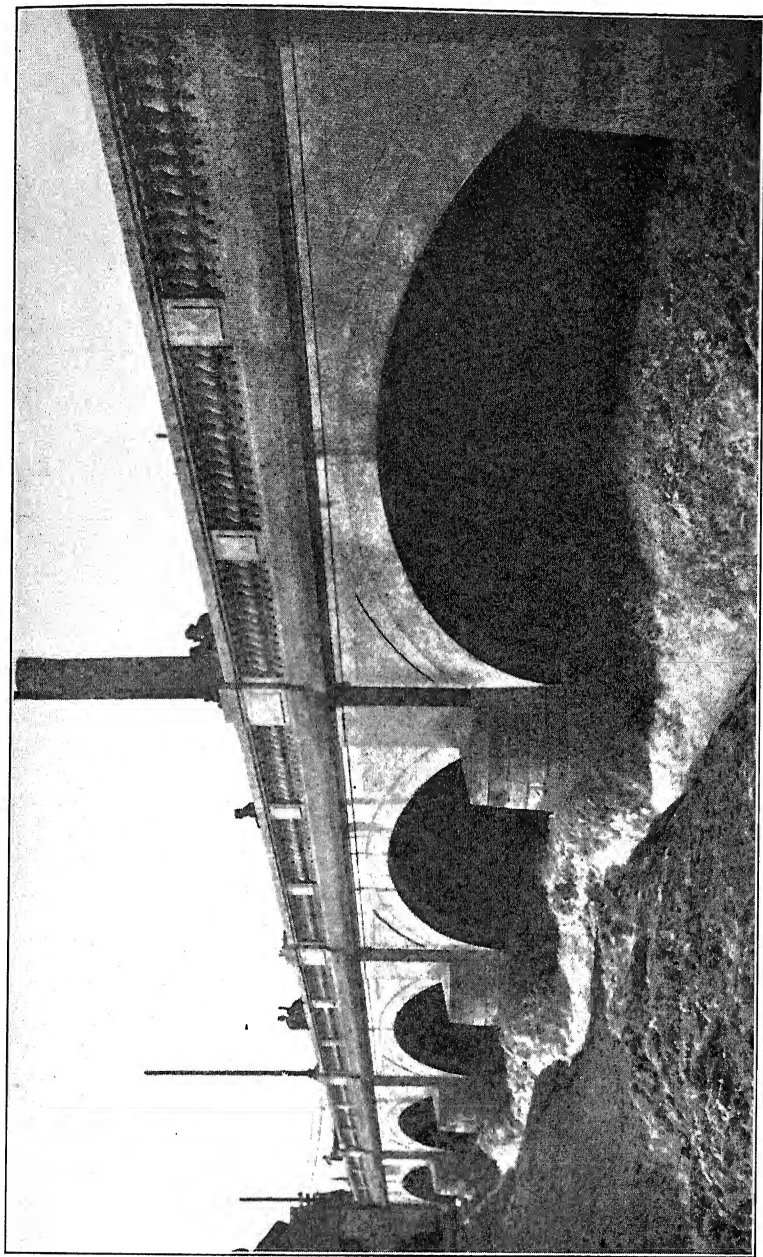


*Courtesy of Mr. John F. Skinner, Priv. Ass't. Engineer, Dep't. of Engineering, City of Rochester.*

FIG. 137.—Bridge at Central Avenue, Rochester, N. Y. under construction.

handling or built in place (Fig. 139). Forms of small height may be braced by only battered posts outside.

Where bolts are employed in pier and wall construction, a number of different methods are used for withdrawing the bolts. One method is to cover each bolt with old pipe cut somewhat shorter than the inside dimensions of the forms, and to place a wood washer at each end of the pipe. When the forms are taken down, the bolts are easily drawn out of the pipes, the wood washers are then cut out of the face of the concrete, and the holes pointed up. Another method is to make the bolts



*Courtesy of Mr. John F. Skinner, Prin. Ass't. Engineer, Dep't. of Engineering, City of Rochester.*

FIG. 138.—View of completed bridge at Central Avenue, Rochester, N. Y.



in three pieces, with the middle piece occupying the same position between the forms as the pipe above described. This middle section is connected with the end pieces by means of ordinary unions. When the concrete has set sufficiently, one turn releases the end sections and the holes left in the work are plugged with mortar.

The following specification for the construction of forms is

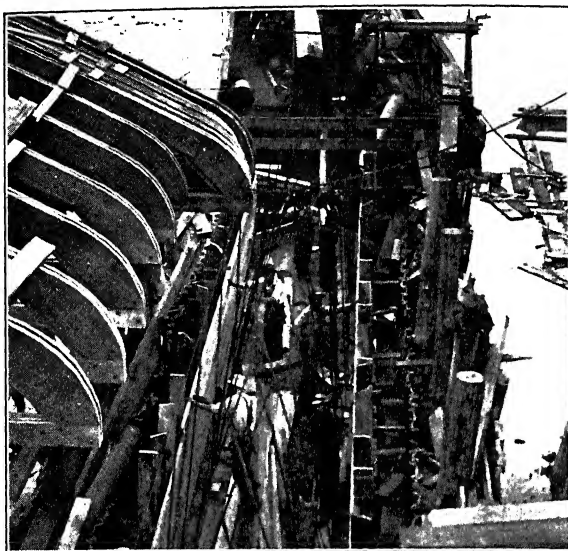


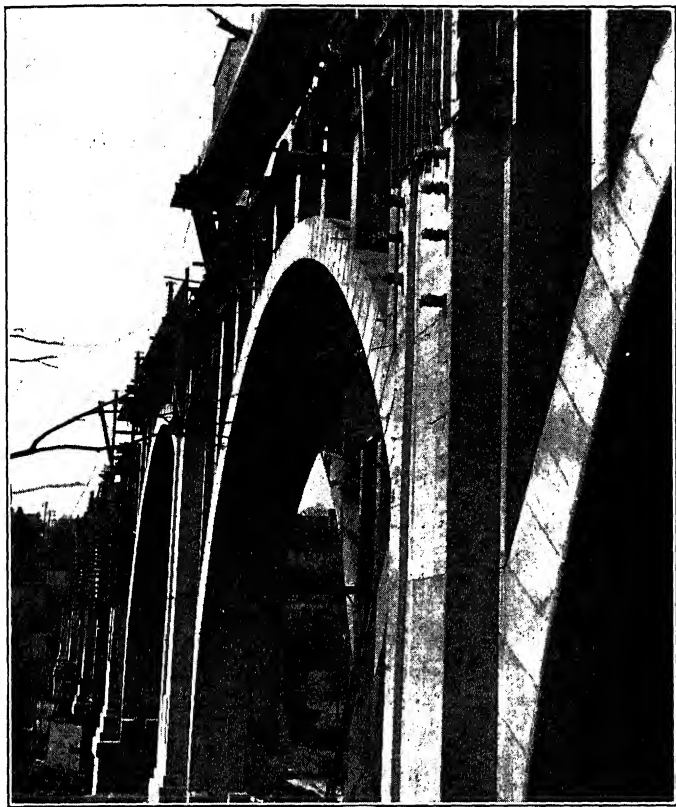
FIG. 139.—Constructing pier of Main and High Street bridge, Hamilton, Ohio.

taken from the "Specifications of the Piney Creek concrete bridge, Washington, D. C."

"All forms for all classes of concrete shall be closely laid and strongly braced. The contractor shall, before proceeding with the work, submit drawings of the forms to the engineer for his approval. All lagging shall be tongue-and-grooved, and the studding for all the work shall be dressed or sawed to an even thickness. All forms, except by the consent of the engineer, shall be held in place by means of bolts, so made that the outer 3 in. of the bolts can be removed after the forms are taken down and the remaining holes shall be filled with mortar. If  $\frac{3}{4}$ -in. lagging is used, the studs shall not exceed 18 in. on centers; and, if 2 in. by 8-in. studs are used, the wales shall not be less than 8 in. by 8 in. These wales on a basis of 2 in. by 8-in. studs shall not be farther apart than

8 ft., nor shall the bolts which hold them and which have diameters of  $\frac{3}{4}$  in. be farther apart than 8 ft.

"If lagging, studs, wales, or bolts are proposed by the contractor other than those described herein before, they shall be such as to make a form of equal strength and stiffness to that described.



*Courtesy of Lehigh Portland Cement Co.*

FIG. 140.—Construction view of Eighth Street viaduct, Allentown, Pa.

"Washers shall be used under all bolt heads and nuts, and, before proceeding with the concrete work, forms shall be brought true to line and grade, and all bolts shall be taut."

Where especially good work is desired, forms are lined with galvanized iron. For high piers or walls, the forms are constructed in large panels. After the concrete has been constructed to a proper height and the last course has set several days, the panels are disconnected and hoisted to a higher posi-

tion and then reassembled for concreting, and so on. The same practice is followed in pilaster construction (Fig. 140).

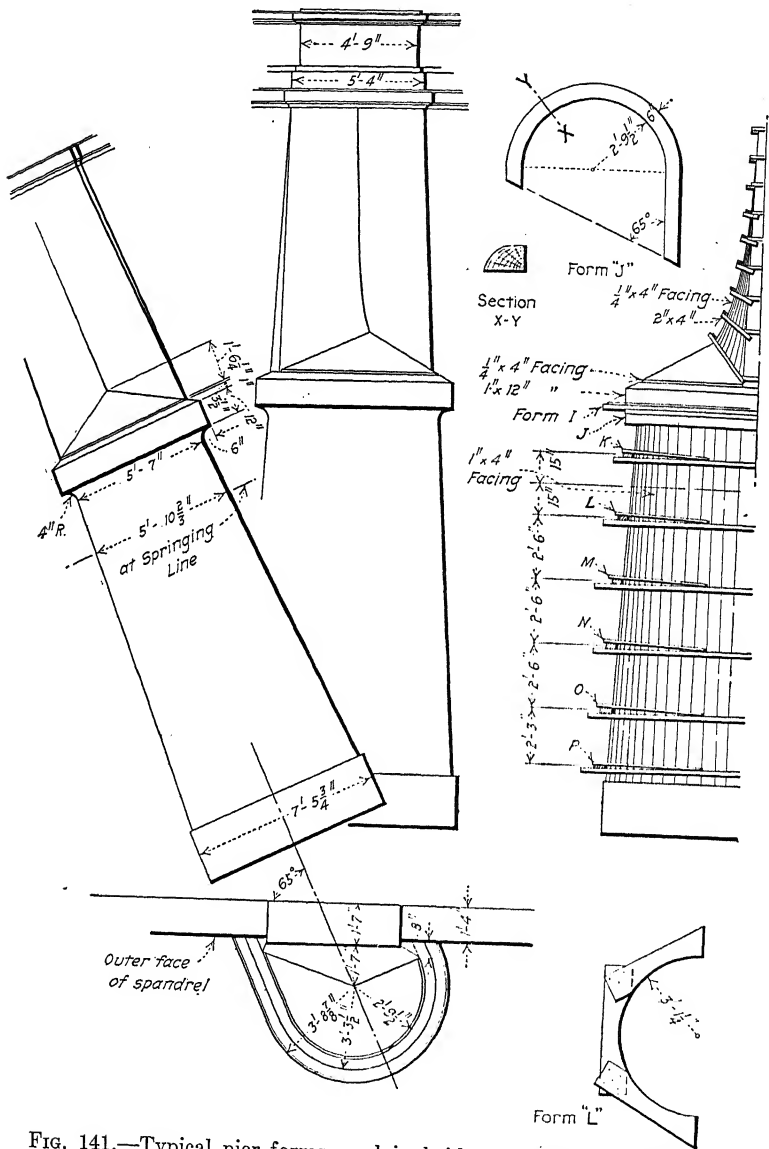
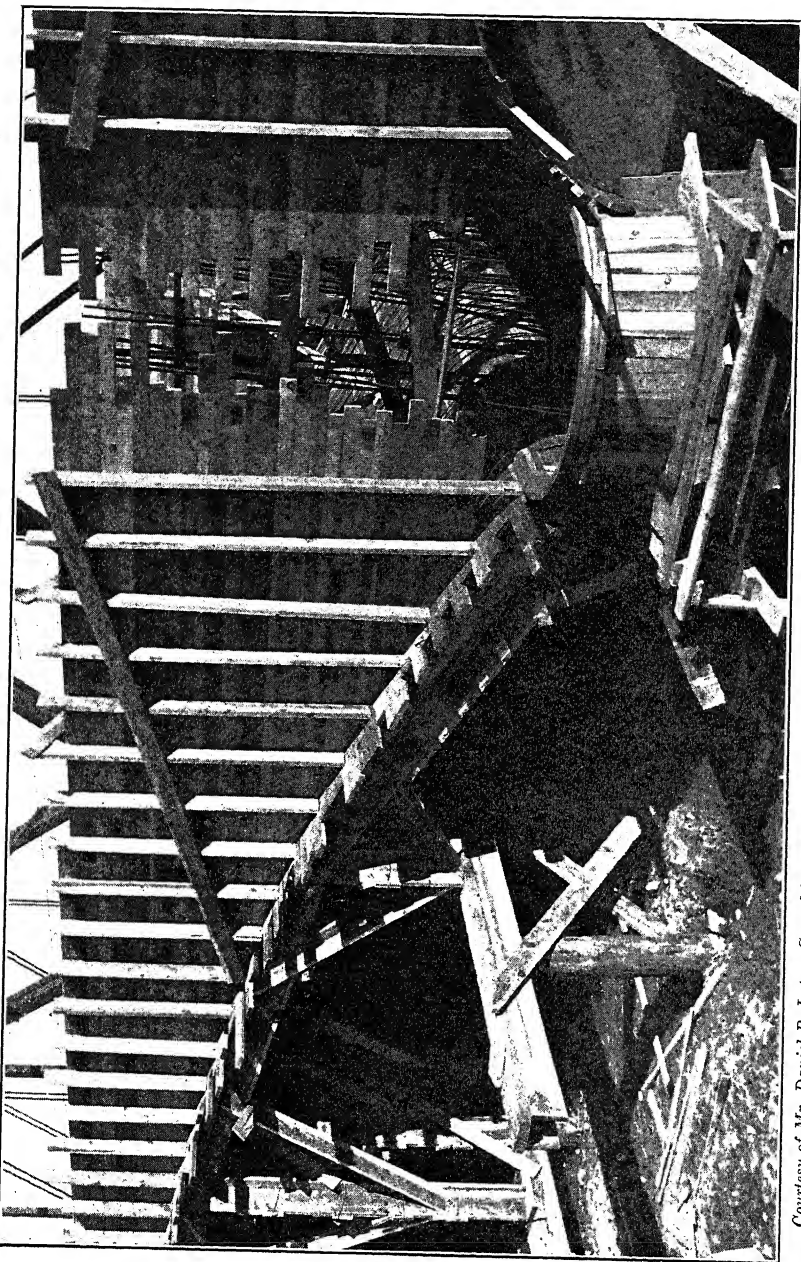


FIG. 141.—Typical pier forms used in bridges of Luten Design.

When the ends of piers are rounding, special forms are necessary. In the construction of the Athol Pier, Athol, Mass.,



*Courtesy of Mr. Daniel B. Luten, Consulting Engineer, Indianapolis.*

FIG. 142.—Centering and curved pier forms used in bridges of Luten Design.

the Pennsylvania R. R. tracks in Pittsburgh, the forms for the curved ends of the piers were built of 1 in. by 2-in. strips nailed to horizontal segmental wales. These wales were nailed to the wales of the side forms. The rounding forms were kept in place by wiring to dowels set in the foundation concrete. Before starting the erection of the form work, a flexible panel was made by nailing galvanized-iron sheets to the 1 in. by 2-in. strips. This panel was bent against the wales, which acted like hoops.

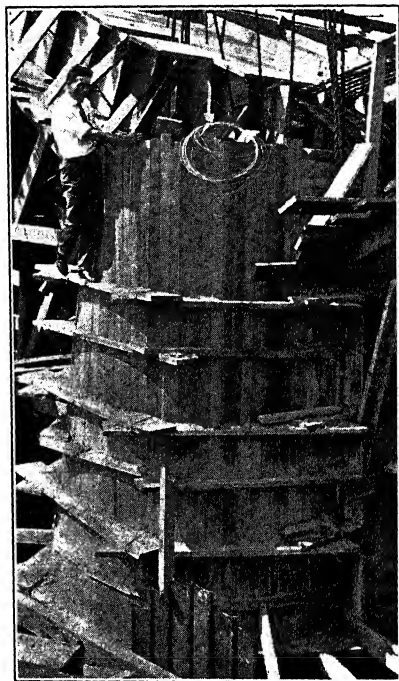
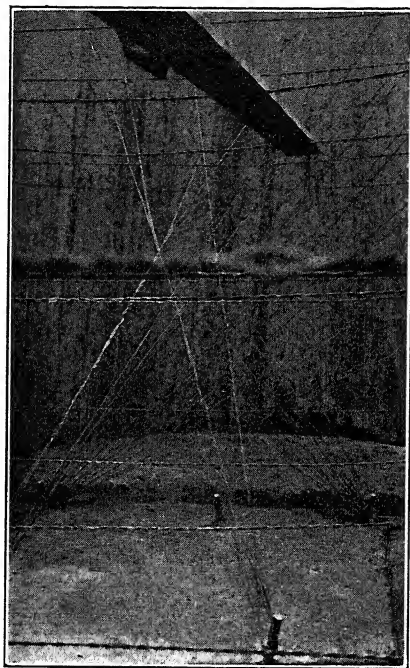


FIG. 143.—Detail view of curved pier forms.

Curved pier forms used in bridges of Luten Design are shown in Figs. 141, 142, and 143. Fig. 144 shows the wiring of the forms to prevent spreading. Fig. 145 shows the pier form removed, and Fig. 146 shows it set in place for use in constructing another pier end.

In the bridge shown in Fig. 147 the pier starlings were constructed of granite from an old bridge. Pilaster forms are seen resting on the upper course of stone.

The common form of longitudinal bulkhead used in arch ring



*Courtesy of Mr. W. C. Giffels.*

FIG. 144.—Wiring of curved pier forms to foundation concrete.

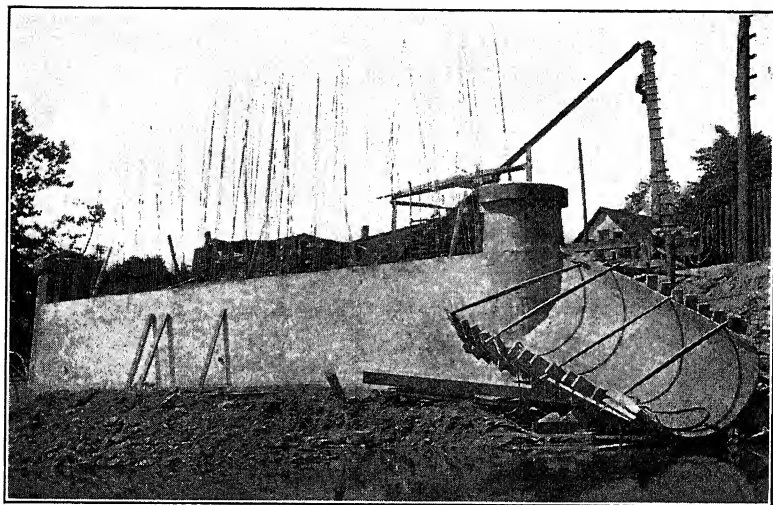
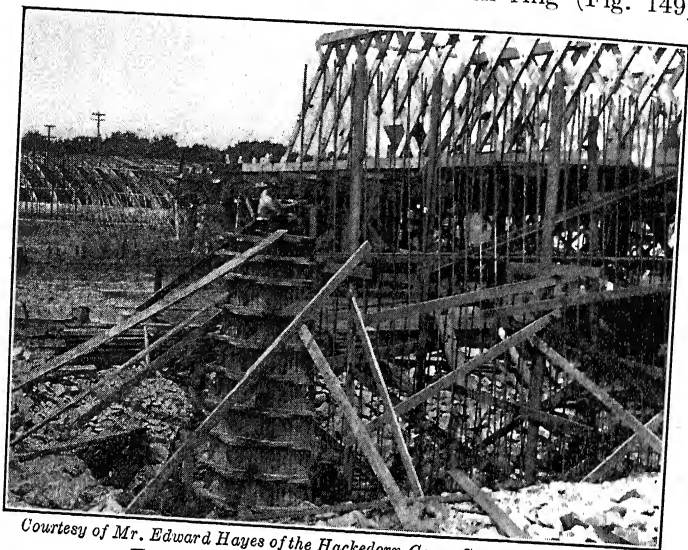


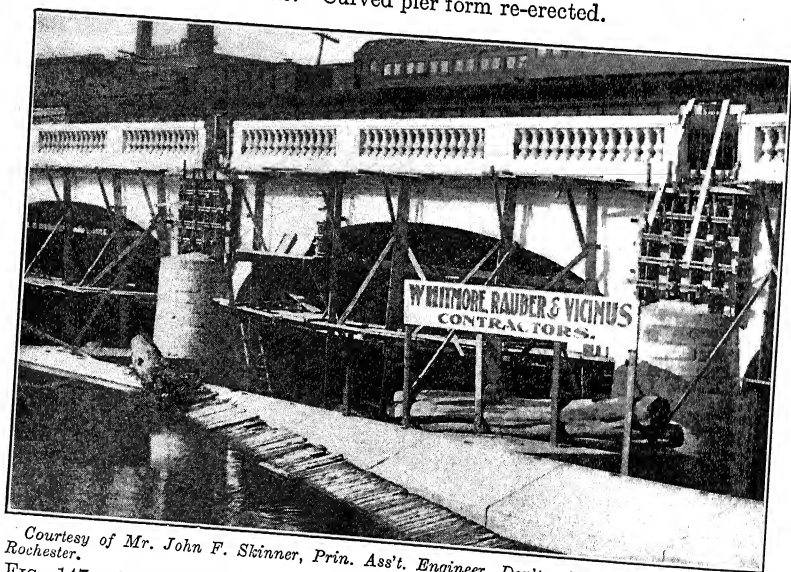
FIG. 145.—Curved pier form removed.

construction is shown in Fig. 148. Spandrel walls for earth-filled arches are either built on top of the arch ring (Fig. 149), or



*Courtesy of Mr. Edward Hayes of the Hackedorn Cons. Co.*

FIG. 146.—Curved pier form re-erected.



*Courtesy of Mr. John F. Skinner, Prin. Asst. Engineer, Dept. of Engineering, City of Rochester.*

FIG. 147.—Pilaster forms. Bridge at Central Avenue, Rochester, N. Y. include a portion of the arch, the bottom inner edge of the spandrel retaining wall lapping a short distance over the

pleted arch ring (Fig. 150). Forms for spandrel walls of the latter class are shown in Figs. 151 and 152.

Prepared sheet metal forms are often employed for special

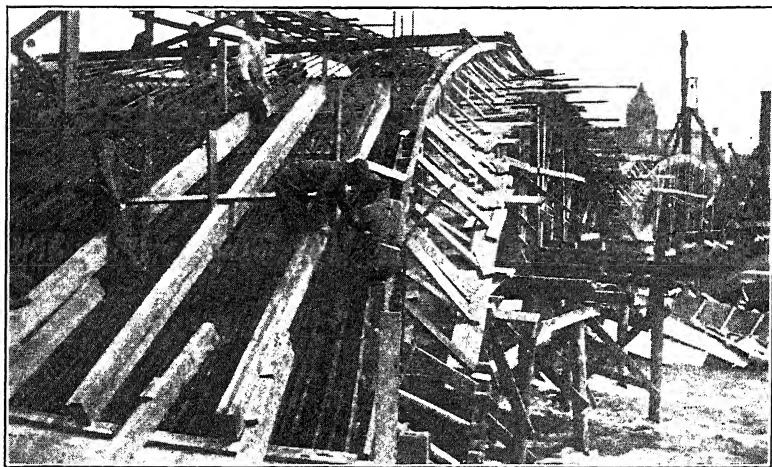


FIG. 148.—Longitudinal bulkhead used in arch-ring construction.

work such as cantilever beams, capitals on spandrel columns, and other small projections. These sheet metal forms are fastened to the wood forms at successive positions.

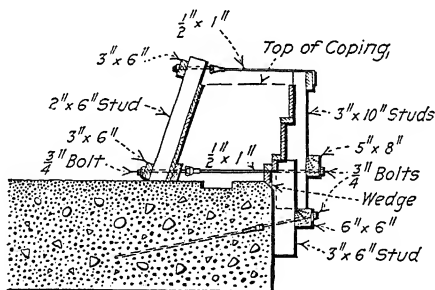


FIG. 149.—Spandrel wall forms used in constructing the Yardley bridge, Philadelphia & Reading Ry. Co.

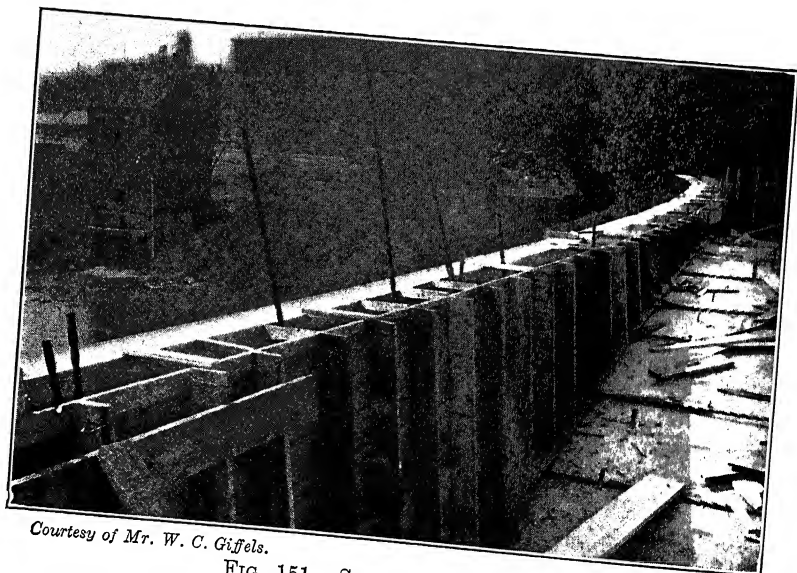
The railing or balustrade of Greek cross panels shown in Fig. 153 was cast in units on a horizontal plane. Cement Age, issue of March, 1912 describes the construction of the panels of this balustrade as follows:





*Courtesy of Mr. W. C. Giffels.*

FIG. 150.—Arch ready for the building of spandrel walls.



*Courtesy of Mr. W. C. Giffels.*

FIG. 151.—Spandrel-wall forms.



*Courtesy of Mr. W. C. Giffels.*

FIG. 152.—Spandrel-wall forms.



*Courtesy of Waddell & Harrington, Consulting Engineers, Kansas City.*

FIG. 153.—Cleveland Avenue bridge, Kansas City, Mo.

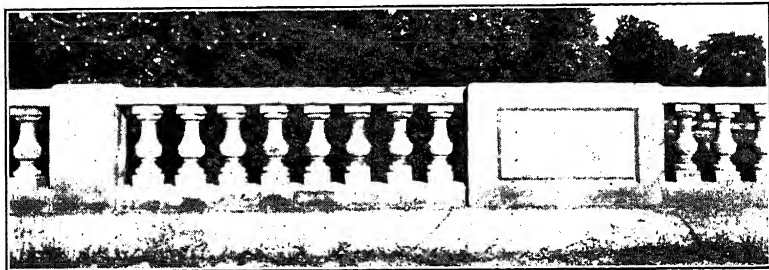


FIG. 154.

"The forms consisted of a wooden base 6 in. wider and longer than the concrete panel. A wooden rail the thickness of the panel was bolted around the outer edges of this base, the measurements between the rails being the size of the panel. On this base were also bolted triangular

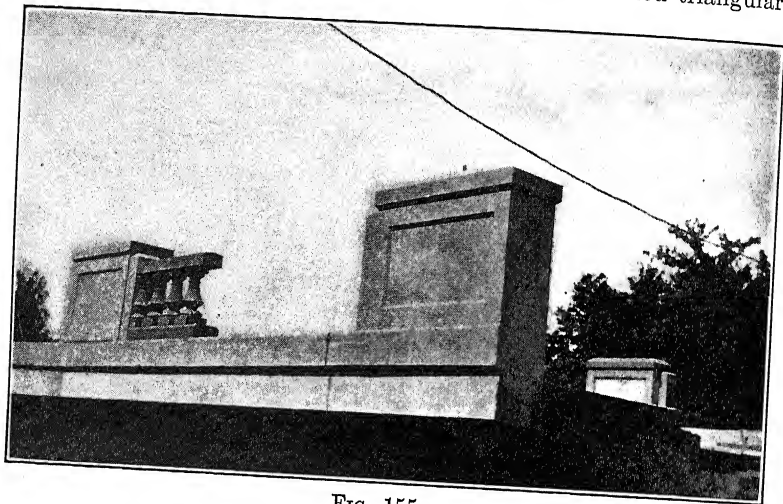


FIG. 155.

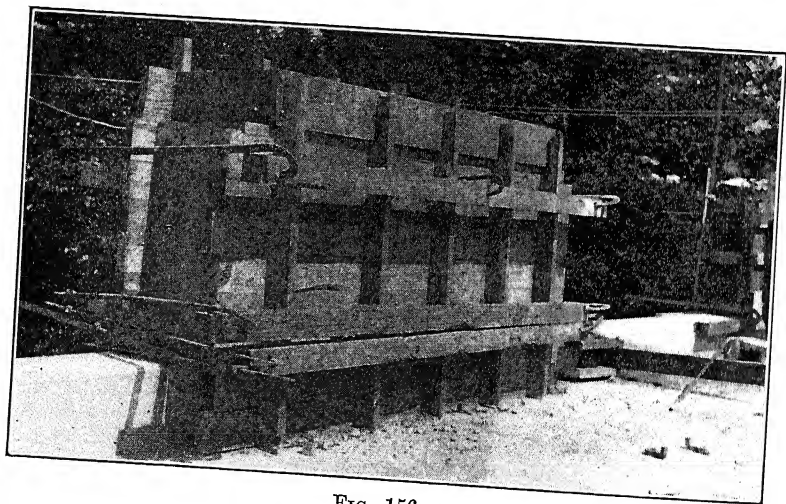


FIG. 156.

blocks, split in half horizontally, with a slight bevel or draw to each half. These blocks were bolted together, and, bolted to the base in place, form the triangular openings of the Greek cross design of the panel. After the forms were bolted together the base was laid level horizontally

on two horses or bents, about 3 ft. above the work floor level. The form was then filled with water and allowed to soak over 1 night. The following morning the water was let out; the form cleaned and re-levelled;  $\frac{1}{2}$  in. of concrete was put in bottom and well tamped with small hand tampers; one set of reinforcing wires were placed; 3 in. more concrete was put in, well tamped; a second set of reinforcing wires was then placed; concrete finally finished to the top and struck off with a

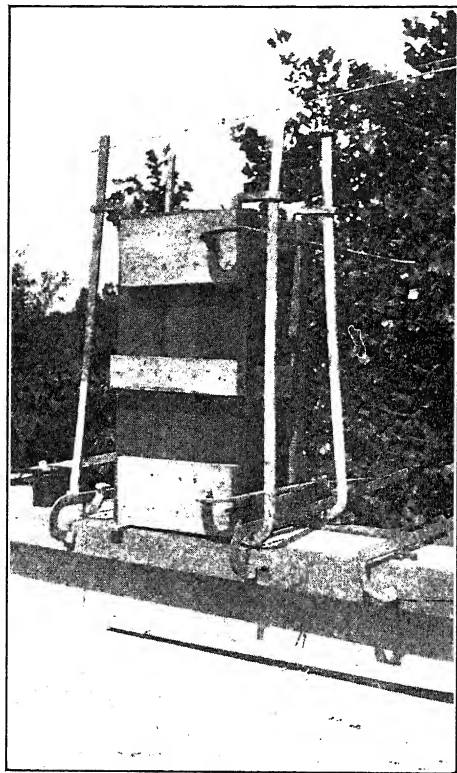


FIG. 157.

straight edge run over top of outer railing and triangular blocks, all of which were made the exact thickness of the panel. After the concrete was sufficiently set the top was finished with smoothing trowel. Concrete in the panel was allowed to stay in the form undisturbed 3 days; the outer railing of the form was then removed and the base to which the triangular blocks were bolted and on which the concrete was resting, was set up on edge, the panel resting on a piece of timber on the ground. The blocks were then unbolted from the base and the base

removed. Forty-eight hours from the time the base was removed, the triangular blocks were withdrawn from the concrete panel by taking one-half of the block out from one side and the other half from the opposite side, the slight bevel and shrinkage of the blocks allowed them to be removed without injury to the edges of the concrete."

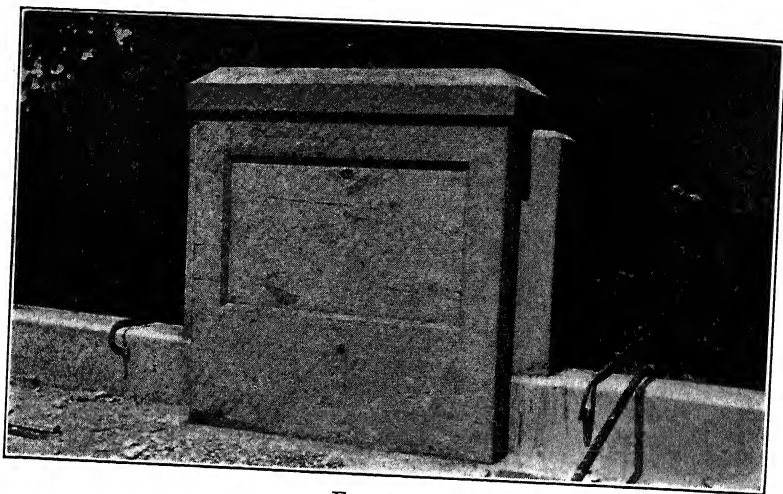


FIG. 158.

Railing of the type shown in Fig. 154 may be either constructed entirely in separate units and afterward erected, or the spindles or balusters may be poured separately in wooden or cast-iron molds and the top and bottom rails and posts cast in place. Figs. 155 to 158 inclusive show the construction of a railing of this balustrade type.

## CHAPTER XI

### THREE-HINGED ARCHES

**56. General Discussion.**—An arch with three hinges is statically determinate and consequently can be analyzed much more readily for a given loading than is possible in the case of a fixed-ended or solid arch. Furthermore, three-hinged arches do not need to be analyzed for temperature changes, the hinges allowing contraction and expansion of the ribs without causing any stress throughout the arch. Obviously this statement does not take into account the effect which results from friction on the hinges, but such effect is usually considered to be negligible. Whether or not hinge friction is likely to cause appreciable error in the analysis of three-hinged arches is still a matter, however, in regard to which there seems to be a decided difference of opinion.

Three-hinged arches are especially adapted to sites where abutments and piers must be founded on compressible soil or on piles. The hinges permit of considerable settlement without failure of the arch or without causing the huge cracks which are sure to develop in a fixed-ended structure under like conditions. Of course, a solid arch may be designed on the assumption that the abutments are yielding, but this is rarely done and such computations in any event could not take into account such settlement as might come from an unexpected source.

Hinges in arch-bridge construction are likely to be an expensive detail, especially in short-span structures. The claim is made, however, that in arches of large span, the saving in concrete as compared with the fixed-ended type much more than pays for the hinges.

It is generally admitted that the three-hinged arch is usually awkward in appearance and has not the graceful form that is characteristic of the majority of the solid arch structures. This lack of artistic proportions is caused by the increased thickness at the haunches, and cannot be avoided in economical design.

**57. Methods of Analysis.**—Three-hinged arches should be analyzed for at least the same conditions of loading that are

recommended in Art. 16 for arches with fixed ends. It should be stated, however, that, for large arches, an analysis by influence lines for the exact maximum loadings is much to be preferred to the common method referred to in the above article, by reason of the fact that the common method assumes the live loads as fixed at only a few definite locations on the span.

*Common Method.*—Consider first the general case of an unsymmetrical three-hinged arch subjected to a number of vertical concentrated loads. By referring to Fig. 159, it is seen that there are four unknown quantities—namely: the horizontal and vertical components of each reaction—and four independent equations

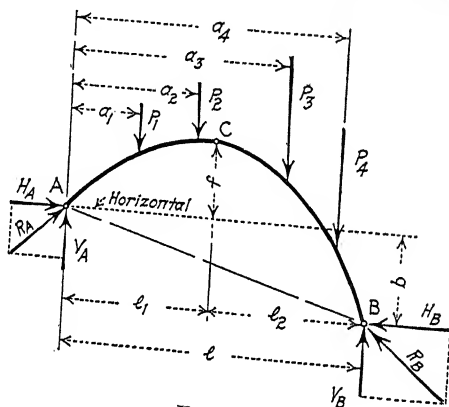


FIG. 159.

tions are necessary to solve for these unknowns. We have the following three equations from statics:

$\Sigma V$  = algebraic sum of the vertical components = 0.

$\Sigma H$  = algebraic sum of the horizontal components = 0.

$\Sigma M$  = algebraic sum of moments of all the forces about any point = 0.

The additional equation may be obtained from the fact that the bending moment is zero at the crown hinge. Thus we have the following four equations with respect to the arch of Fig. 159:

$$V_A + V_B - \Sigma P = 0$$

$$H_A - H_B = 0$$

Taking moments about the left hinge

$$H_B b - V_B l + \Sigma P a = 0$$

Since the moment at the crown hinge is zero

$$V_A l_1 - H_A f - \sum_0^{l_1} P(l_1 - a) = 0$$

These four equations may be solved simultaneously to obtain the horizontal and vertical components of the two reactions.

The calculations may be simplified by resolving each reaction into a vertical force and a force in the direction of the closing chord (Fig. 160). The four equations in this case are as follows (since  $H_A = H_B$  from Fig. 159):

$$V_1 + V_2 - \sum P = 0$$

$$H_1 - H_2 = 0$$

$$-V_2 l + \sum P a = 0$$

$$V_1 l_1 - \sum_0^{l_1} P(l_1 - a) - H_1 r = 0$$

or

$$V_1 l_1 - \sum_0^{l_1} P(l_1 - a) - H_A c = 0$$

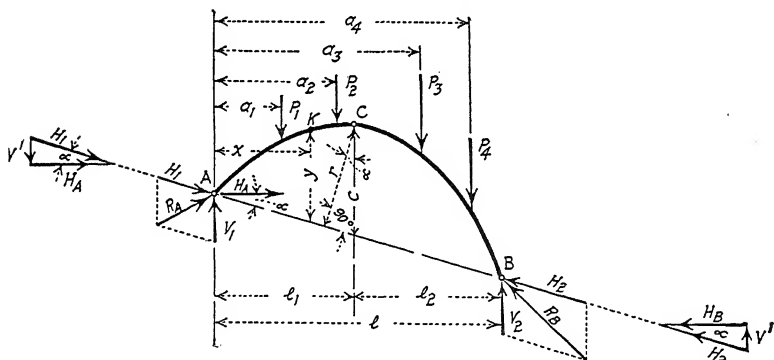


FIG. 160.

(The values of  $V'$  have not been considered in the first equation as they are equal and opposite in direction.) With the components of either reaction determined by these equations, the line of thrust may be drawn throughout the arch as described in Art. 12 for the arch with fixed ends.

It should be noted that the values of  $V_1$  and  $V_2$  may be obtained from the above equations (or by using  $\sum M = 0$  at both points A and B) in the following form:

$$V_1 = \frac{1}{l} \sum P(l - a) \quad (1)$$

$$V_2 = \frac{1}{l} \sum P a \quad (2)$$



These forces are thus identical with the reactions of a simple beam of the same span and similarly loaded.

The bending moment at any point  $K$  (Fig. 160) may be expressed as follows:

$$\begin{aligned} M &= V_1x - \sum_0^x P(x-a) - H_Ay \\ &= M_K - H_Ay \end{aligned} \quad (3)$$

where  $M_K$  is the bending moment at the point  $K$  of a similarly loaded beam. At the crown hinge, letting  $M_C$  denote the moment of the vertical forces about the point  $C$ , we have

$$M = M_C - H_Ac = 0$$

or

$$H_A = \frac{M_C}{c} \quad (4)$$

Equations (1) to (4) inclusive are the formulas commonly employed in the analysis of three-hinged arches—supplemented, of course, with the force and equilibrium polygons as in the case of arches with fixed ends.

For symmetrical arches,  $H_1$  and  $H_2$  are horizontal and the line of thrust need be drawn for only one-half the arch when the loading is symmetrical about the crown hinge. In such a case of loading, the thrust at the crown hinge is horizontal and the line of thrust may be determined by trial in the manner described in Art. 26. This trial method gives exact results when applied to a three-hinged symmetrical arch on account of there being two known points (hinge points) on the line of thrust for each half of arch.

The computations for uniform live loading are extremely simple and should be made separately from those for dead load or concentrated live loads. For full loading, with the crown-hinge at mid-span, Formula (4) gives:

$$H_A = \frac{1}{8} \cdot \frac{wl^2}{c} \quad (5)$$

where  $w$  is the uniform load per foot. The following equation, determined by substituting in Formula (3) gives the bending moment at any point (coördinates  $x$  and  $y$ ):

$$M = \frac{1}{2} wx(l-x) - \frac{1}{8} \cdot \frac{wl^2}{c} \cdot y \quad (6)$$

(For an arch of parabolic form,  $M = 0$ , and only axial stress occurs throughout the arch for full uniform loading.) With only one-half of the span loaded

$$H_A = \frac{1}{16} \cdot \frac{wl^2}{c} \quad (7)$$

or one-half that due to full loading. The bending moment at any point in the loaded half equals

$$M = \frac{1}{8} wx(3l - 4x) - \frac{1}{16} \cdot \frac{wl^2}{c} \cdot y \quad (8)$$

and in the unloaded half

$$M = \frac{1}{8} wlx - \frac{1}{16} \cdot \frac{wl^2}{c} \cdot y \quad (9)$$

(In Equations (8) and (9), the value of  $x$  is measured from that end of the arch which is nearer to the point in question.)

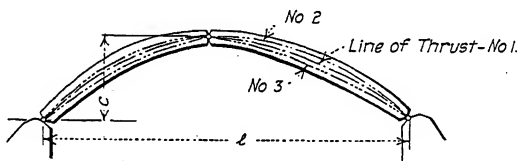


FIG. 161.

A three-hinged arch is commonly analyzed for (1) dead and uniform live load over the entire span, (2) for dead and uniform live load over the right half of span, and (3) for dead and uniform live load over the left half of span. Full loading gives maximum stresses for the sections near the hinges, while the half-span loadings give the greatest stresses near the quarter points of the span. The usual method of design is to locate the hinges at the proper points and to draw the force lines representing the load concentrations. These loads can be determined quite accurately by making a complete design of the spandrels prior to the arch design and by approximating the weight of the arch ring—the arch ring, however, need not be drawn. The lines of thrust for the three conditions of loading stated above are then drawn as shown in Fig. 161. With the lines of thrust known, it then becomes possible to determine the correct thickness of the arch at any point and decide upon a suitable arch ring which, of course, should not differ appreciably in weight or position from

the arch ring previously assumed or else a second analysis should be made.

*Influence-line Method.*—The method of analyzing arches by the use of influence lines is explained at length in Chapter V for fixed arches. (See also Chapter VIII.) The method is the same for three-hinged arches but is simplified by the fact that for a single concentration—as, for example, a load of unity at the point  $L_2$  in Fig. 162—the direction of one of the reaction lines is given by the line connecting the two hinges to one side of the load. The direction of the other reaction is then known. Thus, designing sheets similar to Designing Sheets Nos. 11 and 11A

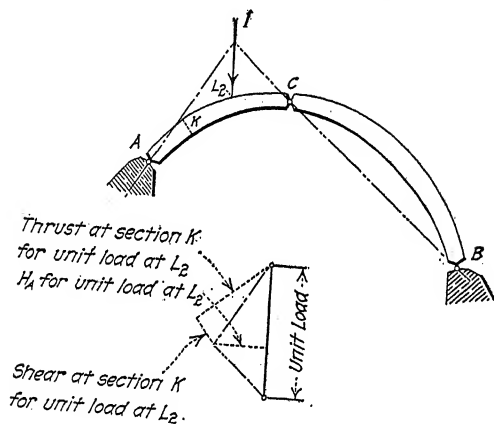


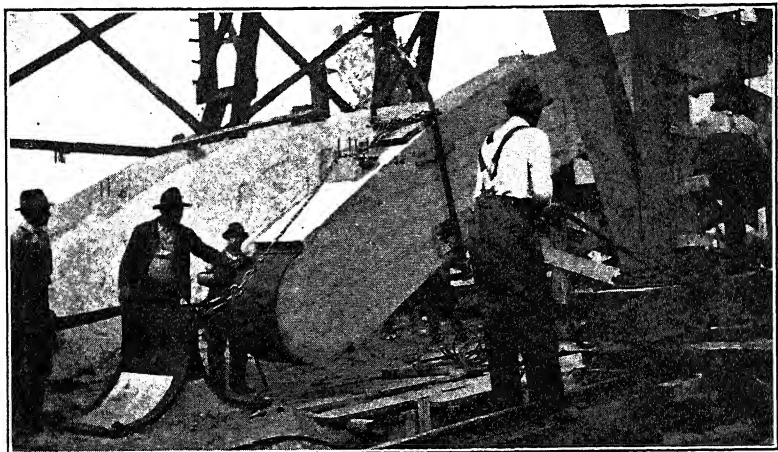
FIG. 162.

may be readily prepared and the remainder of the analysis followed in exactly the same manner as for the fixed arch.

**58. Types of Hinges.**—The most common form of arch hinge consists of a structural or cast-steel pin bearing on two steel castings. Hinges of this type are shown in Figs. 174 to 177 inclusive. A form similar to the one above mentioned consists of two steel castings with ball-and-socket joints. Details of this type of hinge are given on Plate XL, Chapter XIII.

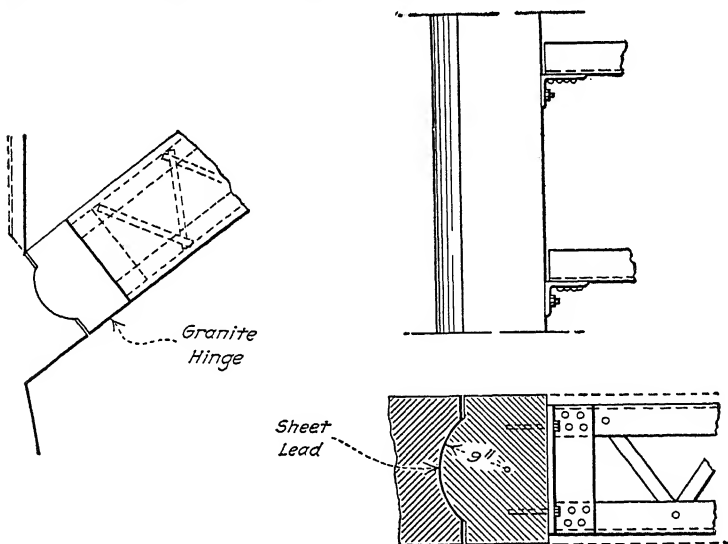
A patented method of hinge construction is shown in Fig. 198, Chapter XII. The reinforcement of each section of arch rib is connected at the crown end to cylindrical plates of steel having a ball joint mated into a cup in the opposite rib. The lower hinge (see also Fig. 163) consists of a semicircular plate attached to the rib and a cast-iron shoe bolted to the pier or abutment.

A flat lead plate has been used to a limited extent in three-hinged arch construction. A plate of this kind cannot be truly



*Courtesy of Mr. Wm. M. Thomas, Consulting Engineer, Los Angeles, Cal.*

FIG. 163.—Thomas Method of arch construction.



Longitudinal Section

FIG. 164.—Details of stone hinge.

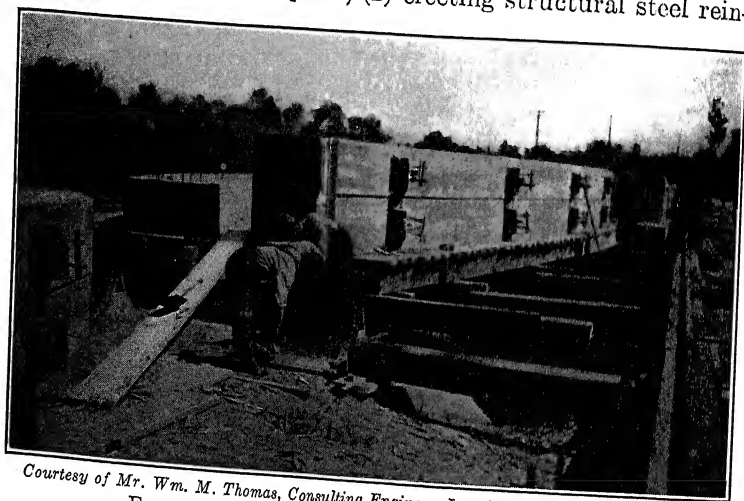
called a hinge, but does limit the line of thrust to a definite area. It should be used only for arches which are to be erected as three-

hinged (due to a possible excessive settlement of the centering), but which are afterward to be converted into solid arches by encasing the hinges in mortar or concrete.

A type of stone hinge which has been used in a few bridges is shown in Fig. 164. The details of an unusual hinge are given in Fig. 178.

It should be evident that all types of hinges are not equally effective in definitely locating the line of thrust.

**59. Methods of Construction.**—Three distinct methods of construction have been employed in the erection of three-hinged arches: (1) casting the concrete ribs in forms on the ground and then hoisting them into place; (2) erecting structural steel rein-



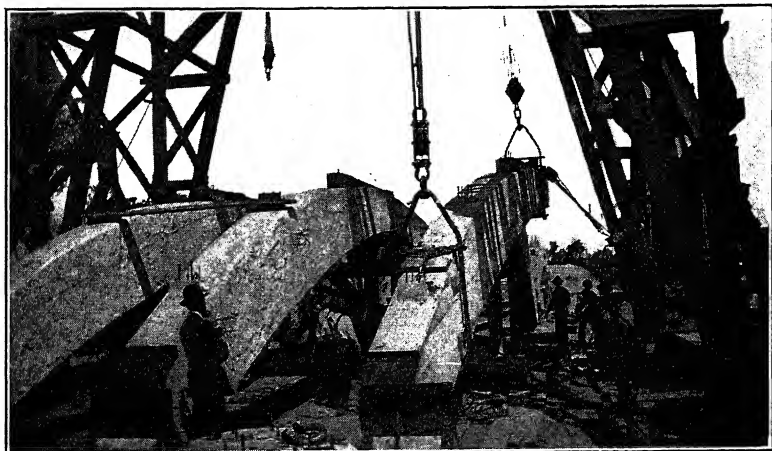
*Courtesy of Mr. Wm. M. Thomas, Consulting Engineer, Los Angeles, Cal.*

FIG. 165.—Thomas Method of arch construction.

forcement to be employed in the arch ribs and using this reinforcement to support the weight of the forms and plastic concrete during construction; and (3) employing the usual type of centering and casting the ribs in place. The first method is the one usually followed. Method No. 2 is of advantage when a stream to be spanned is subject to sudden freshets and a minimum of falsework is required. (See Fig. 175 and Plate XL of Chapter XIII.) Method No. 3 is necessary only under unusual conditions.

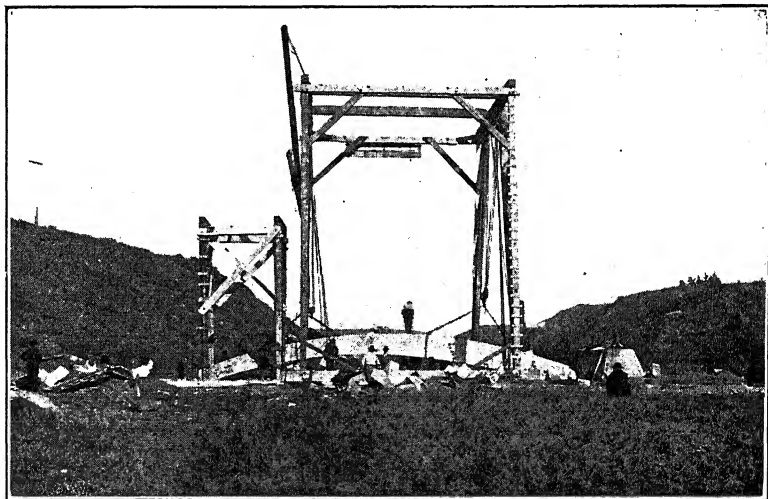
The cheapest type of the three-hinged arch and also the type that is lightest and best adapted to the use of hinges is one of detached ribs supporting spandrel columns. Such a type of arch lends itself readily to the unit method of construction should

this form of erection be desired, and also eliminates the necessity for waterproofing which is a serious problem in the case of a solid filled arch.



*Courtesy of Mr. Wm. M. Thomas, Consulting Engineer, Los Angeles, Cal.*

FIG. 166.—Thomas Method of arch construction.

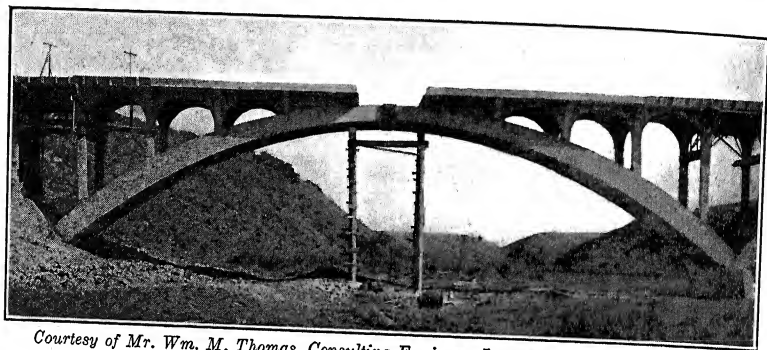


*Courtesy of Mr. Wm. M. Thomas, Consulting Engineer, Los Angeles, Cal.*

FIG. 167.—Thomas Method of arch construction.

The Thomas Method of unit construction is shown in Figs. 165 to 172 inclusive and the designing details in Fig. 178. The illustrations are self-explanatory.

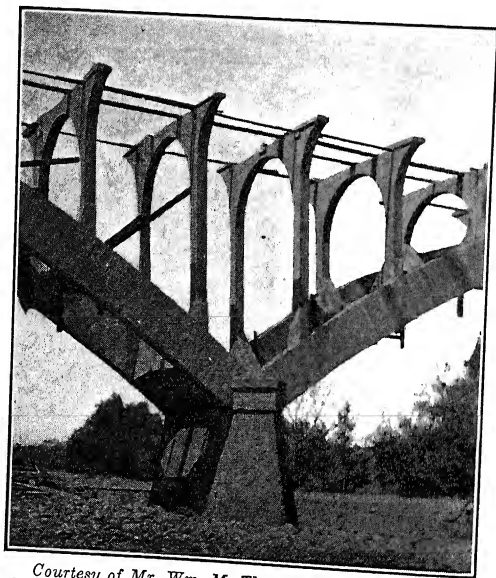
60. Details of Design.—Figs 174 to 178 inclusive give typical details of three-hinged arches.



*Courtesy of Mr. Wm. M. Thomas, Consulting Engineer, Los Angeles, Cal.*

FIG. 168.—Thomas Method of arch construction.

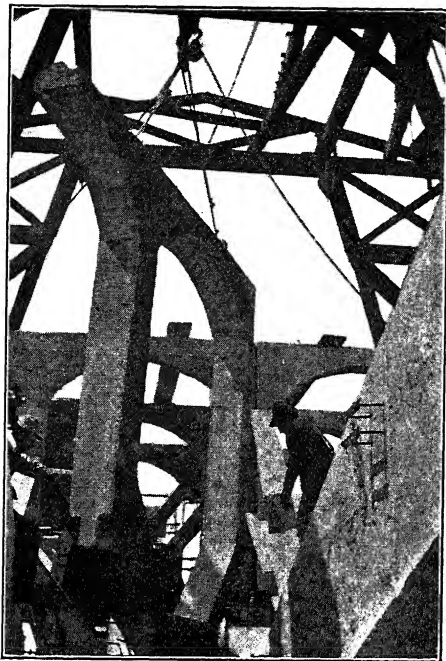
The arch shown in Figs. 173 and 174 is founded on Ohio River mud, Raymond concrete piles being used for the foundations.



*Courtesy of Mr. Wm. M. Thomas, Consulting Engineer,  
Los Angeles, Cal.*

FIG. 169.—Thomas Method of arch construction.

The reason for the use of the cast hinges in this case is thus apparent, as settlement of foundations was anticipated. No appreciable settlement, however, has ever taken place.



*Courtesy of Mr. Wm. M. Thomas, Consulting Engineer, Los Angeles, Cal.*

FIG. 170.—Thomas Method of arch construction.

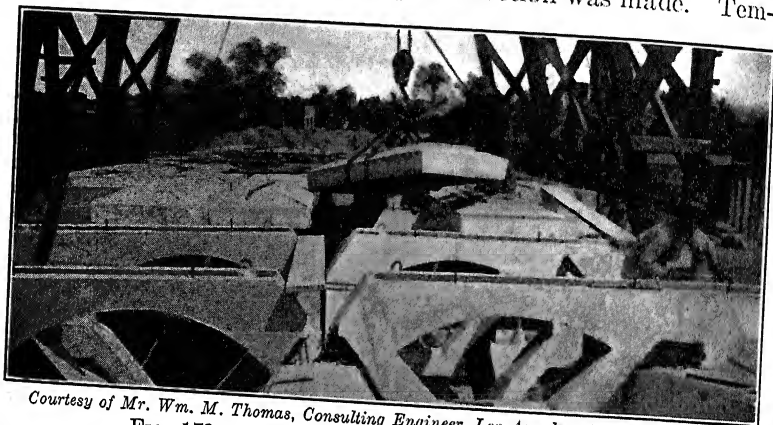


*Courtesy of Mr. Wm. M. Thomas, Consulting Engineer, Los Angeles, Cal.*

FIG. 171.—Thomas Method of arch construction.



The two halves of each rib of the bridge shown in Fig. 175 were designed to be erected simultaneously, without falsework, by derricks on opposite sides of the stream, and to be self-supporting as soon as the crown hinge connection was made. Tem-

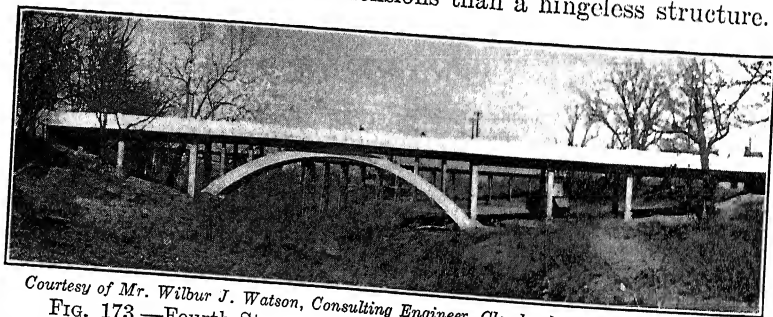


*Courtesy of Mr. Wm. M. Thomas, Consulting Engineer, Los Angeles, Cal.*

FIG. 172.—Thomas Method of arch construction.

porary sway bracing was provided to insure lateral stability while the forms were being built and filled with concrete.

The three-hinged arch construction with cantilever ends, shown in Fig. 176, is unusual, but was found to be more economical for an arch of this type and dimensions than a hingeless structure.



*Courtesy of Mr. Wilbur J. Watson, Consulting Engineer, Cleveland, Ohio.*

FIG. 173.—Fourth Street bridge over Island Creek, Paducah, Ky.

The cantilever ends were rendered necessary on account of the fact that there were no stable foundations for abutments at the top of the fill at the ends of the bridge. The cantilever ends decreased the dead load thrust on the center hinges about one-quarter and decreased considerably the angle which the resultant thrust on the lower hinges made with the vertical, thus decreasing

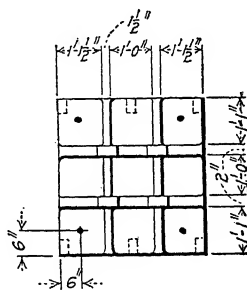
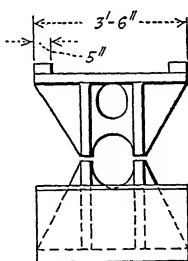
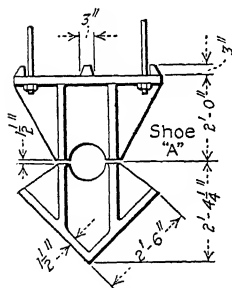
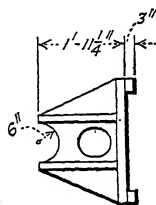
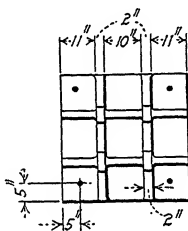
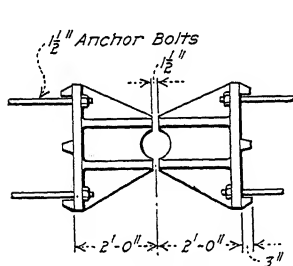
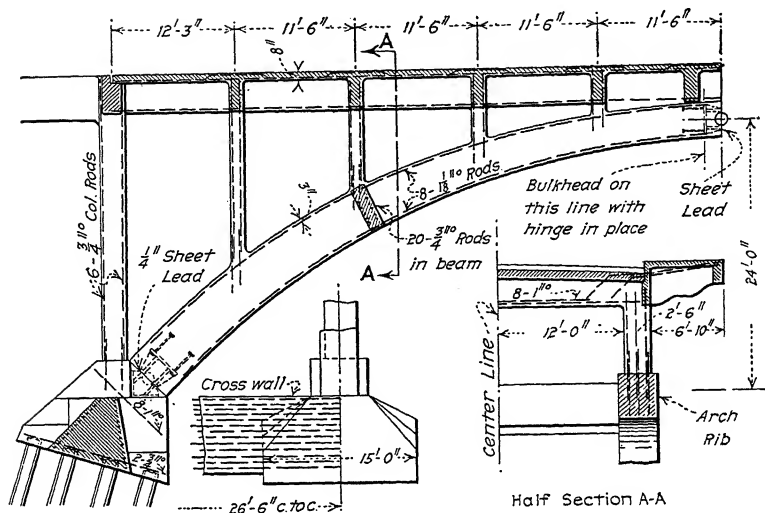


FIG. 174.—Details of Fourth Street bridge, Paducah, Ky.

Section C-C

Section

← Elev. 12.75      ← Top of Pavement

4-2.5% Grade

C

$\frac{1}{2}'' \times 16'' \times 2'-7''$  Plate

*Rip Hinge*

Crown:

Section

Diagram illustrating the assembly of a lattice bar. The diagram shows a cross-section of a structure with a lattice bar. The dimensions are labeled as  $\frac{1}{2} \times 3$ " Lattice Bars and  $6 \times 6 \times \frac{5}{8}$ " Ls.

Section A-A

Abutment

←----- 2!

-----  $2' - 0''$  .

1.5" 1.5"

11

\_\_\_\_\_

12/12

11

\_\_\_\_\_

**I**

linge

Baltimore, Md.

n the hing

en the en

the extro

THE CASE

### Cast Steel Rib Hinge

to take care of the additional bending moments in the hingeless arch. No connection whatever was needed between the ends of the cantilevers and the abutments on account of the extremely

small amount of vertical motion at these points. A common type of centering was used in constructing the arch ribs in place. The cast-steel hinges were entirely encased in concrete after the centers were struck, a  $\frac{1}{4}$ -in. plate of sheet lead having been placed at the center of each hinge to allow the necessary motion of the

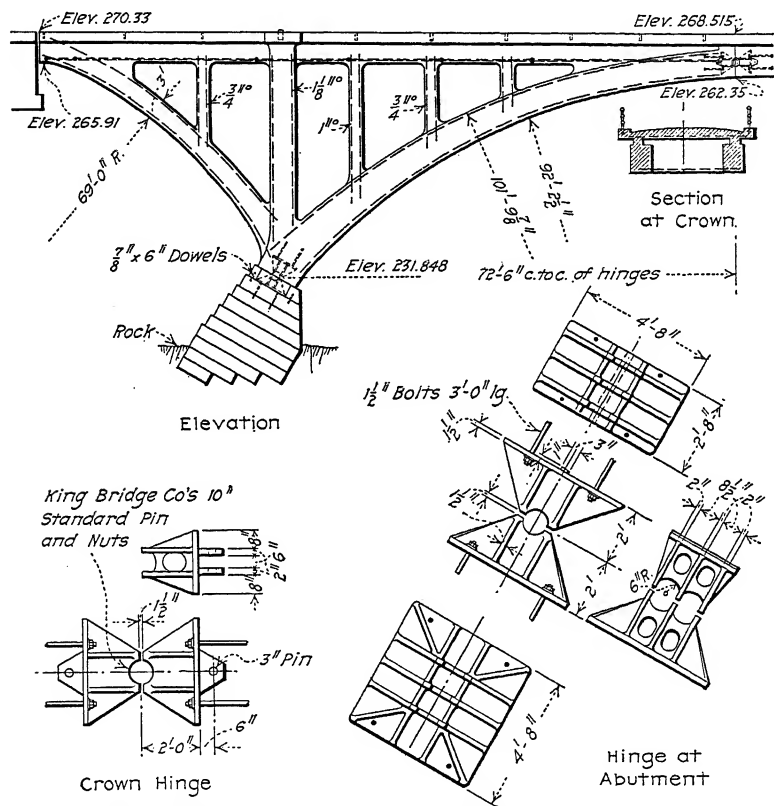


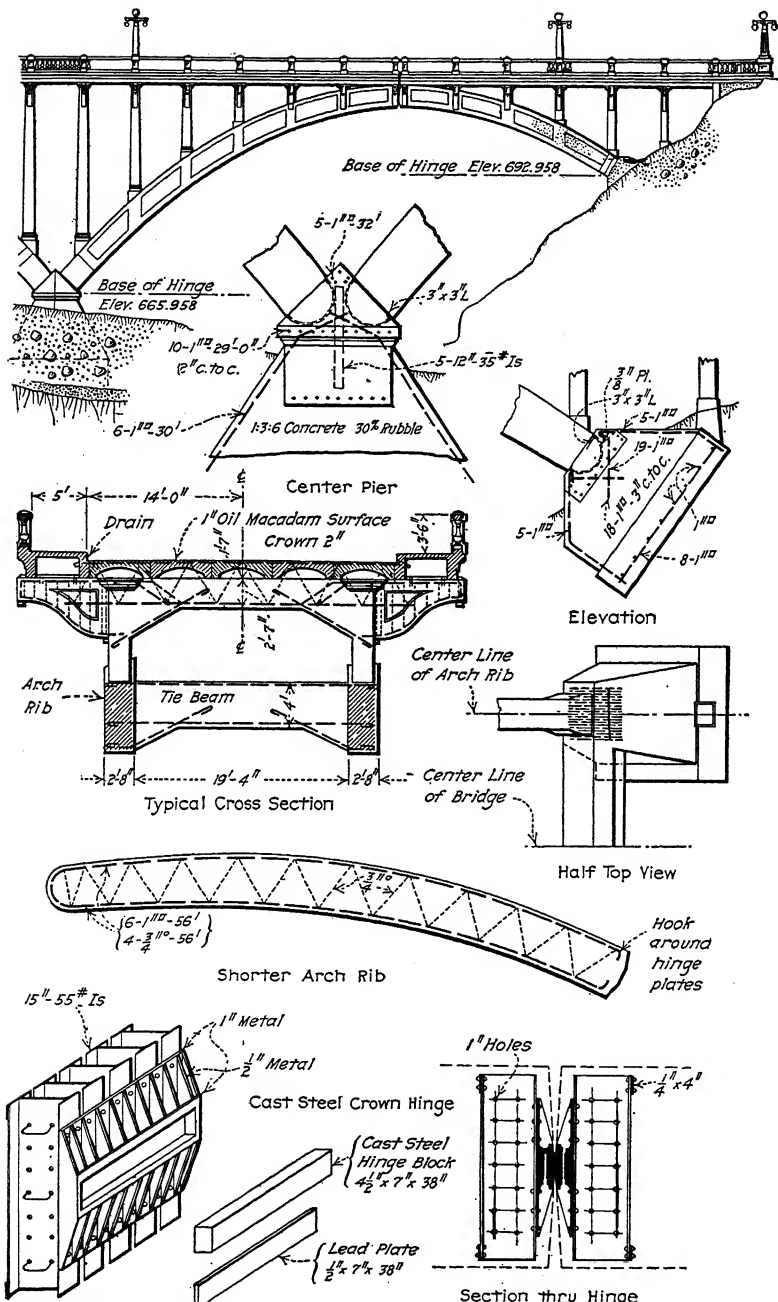
FIG. 176.—Bridge over the Vermillion River at Wakeman, Ohio

arch rib under live load and temperature stresses. In this way all possibility of corrosion of the steel hinges was avoided.

What is believed will be the longest three-hinged concrete arch ever built is shown in Fig. 177. When completed it will be one of the show bridges of the United States.

Fig. 178 gives details of the Thomas Method of arch construction already referred to in Arts. 58 and 59.

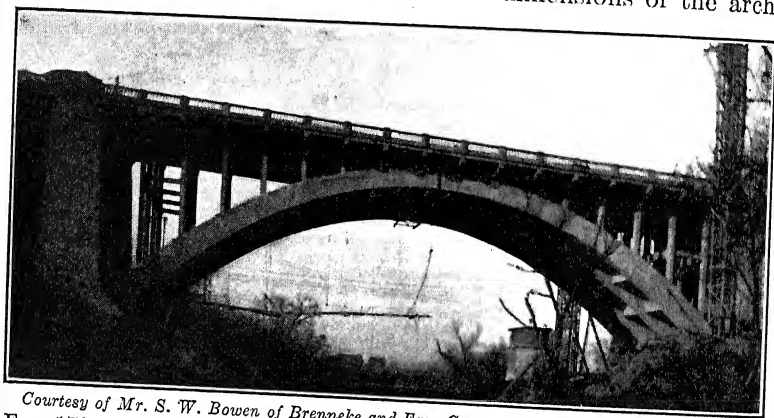




Assumptions as to the dimensions of the arch ribs and braces were then made to determine the dead load from these portions of the structure.

The next step was to draw the lines of thrust in the arch ribs, for full live and dead load and for dead load combined with live load on each half of the span. This gave the position of the neutral axis, or center line of the arch rib, which was taken midway between the extreme lines of thrust, and coincided closely with the line of thrust for full live and dead load. It might be mentioned that the center line of the arch rib, thus determined, agreed closely with a parabola, with its vertex at the crown of the arch.

The general outline and approximate dimensions of the arch



*Courtesy of Mr. S. W. Bowen of Brenneke and Fay, Consulting Engineers, St. Louis.*  
FIG. 179.—225-ft. arch span of the Main Street viaduct, Fort Worth, Texas.

ribs being determined, the next step was to design the structural steel reinforcement of the ribs. This reinforcement consisted of curved lattice girders, three in each inner, and two in each outer rib. These girders were laced together in the plane of the top and bottom flanges. They were also connected under each post by vertical cross frames. The weight of the concrete in the arch ribs and braces was computed, and also the weight of the forms. An allowance was also made for the weight of the structural reinforcement. Concrete was assumed to be placed simultaneously in each half of the span, from the haunches to the crown. The stresses in the structural reinforcement were then found for each successive stage of the concreting—that is, for the forms of the ribs and braces filled with concrete up to the first, second,

etc., panel points, counting from the haunches. All of these stresses were found graphically, and the members proportioned for the maximum conditions. The unit stresses used were 12,500 lb. per square inch in compression, and 16,000 lb. per square inch in tension. No stress whatever was assumed to be taken by the concrete, as it was unlikely that the concrete near the haunches would be sufficiently set to take stress, by the time the ribs were finished.

In the design of the arch ribs, which was next undertaken, the stresses caused by the construction of the columns and deck were considered as well as those due to live and dead loads on the finished structure. The columns were assumed to be built out from each pier, panel by panel, until the crown was reached; then the deck was assumed to be concreted; panel by panel, working from the crown toward the haunches. The stresses in the rib were found for each stage of the construction. For live-load stresses, five conditions were considered, as follows: First, live load on entire span; then each half of span loaded; next the two end quarters loaded; and finally the live load on the two middle quarters of the span. A maximum unit stress of 500 lb. per square inch was used in the extreme fiber of the rib, and sufficient reinforcement was provided to keep the stress in the concrete down to this figure. In case the structural reinforcement at any point was not sufficient for this purpose, additional metal in the shape of bars was provided. The stresses and reinforcement required were computed at each panel point, and these bars were stopped off when not required. In case the computed amount of steel at any point exceeded 5 per cent of the gross area of the rib at that point, a redesign was made. It will be seen from the above that the structural steel reinforcement takes stress in two ways: (1) that due to the weight of the plastic concrete in the ribs and braces, together with their forms; and (2) that due to the construction of the columns and deck, and to the loads on the finished structure. The first of these may be called an initial stress, which remains in the steel as the concrete sets. The second must be added to the first to get the total compressive stress in the steel. In this case the maximum possible compressive unit stress in the structural steel would be 12,500 lb., plus  $15 \times 500$  lb., or a total of 20,000 lb. per square inch. As a matter of fact, the total unit stress was about 16,000 lb. per square inch.





expansion joints in the deck at each pier and near the center of the span. There is no doubt, however, that a very considerable portion of these forces pass directly through the deck to the piers, which correspondingly relieves the bracing system.

While the arch ribs were assumed to be hinged at the haunches and crown, rods were provided at these points which tended to fix them transversely. In other words, the arch ribs are three-hinged in vertical planes but are hingeless, or practically so, transversely.

Fig. 181 shows half of the bracing system developed. The similarity to the columns and girders of an office building is apparent.

Fig. 182 shows a portion of Fig. 181 enlarged with the various forces acting on it, and the points of inflection indicated.

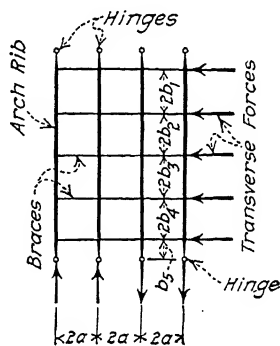


FIG. 181.

From the three conditions of equilibrium—namely: (1) the sum of the horizontal forces must equal zero, (2) the sum of the vertical forces must equal zero, and (3) the sum of the moments about any point must equal zero—and knowing the external

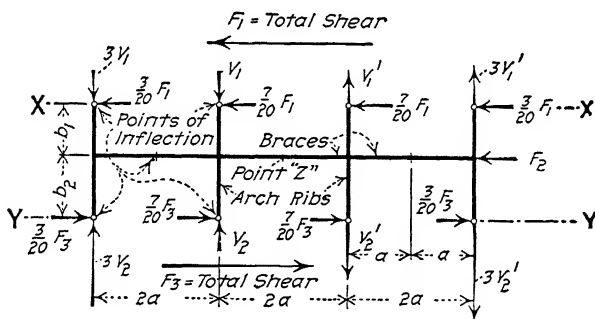


FIG. 182.

forces  $F_1$  and  $F_2$  and all dimensions, the thrusts, shears, and bending moments in the various members are readily calculated.

For example, the horizontal force  $F_1$  is the total of the transverse forces acting on the structure above the plane  $X - X$  where the forces  $F_1$  are shown.  $F_2$  is the total transverse force acting on one panel of the structure, and  $F_3$  is the total shear at

the plane  $Y - Y$ . Then from the first condition of equilibrium,

$$F_3 = F_1 + F_2 \quad (1)$$

The vertical forces  $3V_1$ ,  $V_1$ ,  $V'_1$ , and  $3V'_1$  are those produced by the action of the horizontal forces acting above the plane  $X - X$ . Similarly, the forces  $3V_2$ ,  $V_2$ ,  $V'_2$ , and  $3V'_2$  are those produced by the action of all horizontal forces above the plane  $Y - Y$ . The term "vertical" has been applied to the forces indicated in the figure as acting at right angles to the forces  $F_1$ , etc. These forces are, of course, not vertical in the structure, but act in the direction of the axis of the arch rib.

For the sake of simplicity, let  $V_2 - V_1 = V_3$ . Then from the second condition of equilibrium,

$$3V_3 + V_3 = V'_3 + 3V'_3$$

$$\text{or} \quad V_3 = V'_3 \quad (2)$$

From the third condition of equilibrium, taking moments about point  $Z$ ,

$$F_1 b_1 + F_3 b_2 = 2 \times 3V_3 \times 3a + 2 \times V_3 \times a$$

$$\text{or} \quad V_3 = \frac{F_1 b_1 + F_3 b_2}{20a} \quad (3)$$

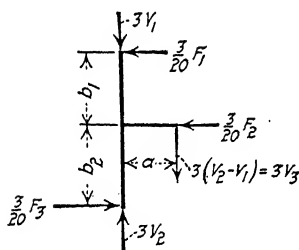


FIG. 183.

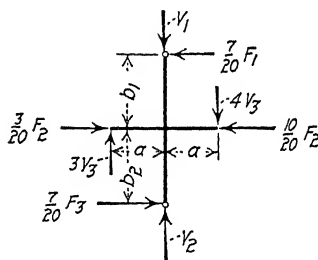


FIG. 184.

Fig. 183 shows a portion of Fig. 182. As before

$$\frac{3}{20} F_3 = \frac{3}{20} F_1 + \frac{3}{20} F_2$$

$$\text{or} \quad F_3 = F_1 + F_2 \quad (1')$$

$$3V_2 - 3V_1 = 3V_3$$

$$\text{or} \quad V_2 - V_1 = V_3 \quad (2')$$

$$\frac{3}{20} F_1 b_1 + \frac{3}{20} F_3 b_2 = 3V_3 a$$

$$\text{or} \quad V_3 = \frac{F_1 b_1 + F_3 b_2}{20a} \quad (3')$$

Fig. 184 shows the remaining portion of half of Fig. 182. The same equations apply here.

$$\frac{7}{20} F_1 + \frac{7}{20} F_2 = \frac{7}{20} F_3$$

or

$$F_3 = F_1 + F_2 \quad (1'')$$

$$3V_3 + (V_2 - V_1) = 4V_3$$

or

$$V_2 - V_1 = V_3 \quad (2'')$$

$$\frac{7}{20} F_1 b_1 + \frac{7}{20} F_3 b_2 = 3V_3 a + 4V_3 a$$

or

$$V_3 = \frac{F_1 b_1 + F_3 b_2}{20a} \quad (3'')$$

The maximum bending moment in the upper portion of the outer rib is  $\frac{3}{20} F_1 b_1$ , in the lower portion  $\frac{3}{20} F_3 b_2$ , in the upper portion of the inner rib  $\frac{7}{20} F_1 b_1$ , and on the lower portion  $\frac{7}{20} F_3 b_2$ . The maximum bending moment in the outer brace is  $3V_3 a$ , and in the inner brace  $4V_3 a$ .

The hinge castings were designed in much the same manner as a cast column base. The area in contact with the concrete was determined by dividing the total load by 800 lb. per square inch. The diameter of the ball-and-socket joint was determined by dividing the total load by 20,000 lb. per square inch, which gave the projected area of the ball.

The shears and moments on the ribs were then computed, and their thickness and that of the base determined.

In the design of the piers, several stages in the construction of the spans were considered, as well as the conditions existing in the finished structure.

For example, with the pier finished up to the roadway, the arch ribs and braces of one span (the longer) were considered as finished, but nothing was done on the adjoining span. Next the full dead load, exclusive of paving but including forms, was considered on the long span, and only the ribs and braces of the adjoining span finished. Then the finished structure was considered, first with live load on the long span only, and second with live load on both spans. In each case the resultant force

was kept within the middle third of the base. The uplift of the water was considered in each case, the stage being taken as the top of the levee.

No impact was considered in the design of the piers.

Pier No. 2 was supported on timber piles driven into a mixture of sand and gravel overlying bed rock. This method was used instead of founding the pier on bed rock in order to reduce the cost, the amount of the appropriation being limited. The piles were not driven to rock in order to take advantage of the bearing of the pier base on the stratum of gravel, and also to take advantage of the friction to help resist sliding. The pier was protected against scour by sheet piling and rip-rap.

Piles were assumed to take 20,000 lb. each and the remainder of the load was assumed to be carried by bearing on the soil at about 5000 lb. per square foot.

## CHAPTER XII

### PATENTS

The number of patents that have been granted by the United States Government for improvements in reinforced-concrete construction has increased from a yearly average of three or four between the years 1890 and 1900 to about 150 per year at the present time—that is, not considering patents on concrete mixers, fence posts, and other minor structures. Undoubtedly some of these patents are worthless, impractical, and possibly invalid, but others unquestionably are of considerable importance. The mere granting of a patent does not establish its validity under the United States patent law, and many of these patents may be invalidated by litigation. In spite of this fact, however, the engineer has no right to consider any patent invalid unless he has positive proof to that effect.

**62. Patents in General.**—The Constitution of the United States contains the following clause:

“The Congress shall have power to promote the progress of science and useful arts, by securing for a limited time for authors and inventors the exclusive right to their respective writings and discoveries.”

Under this provision of the Constitution, Federal statutes have been passed authorizing the issue of a patent to the original inventor of any new and useful improvement and granting to him the exclusive right to make, to sell, or to use the patented improvement for a period of 17 years after date of issue of the patent. The patent is, in effect, an agreement between the United States Government and the inventor of a new and useful improvement, whereby the Government grants to the inventor the right to exclude others from making, using, or selling his

invention for 17 years from the date of issue of the patent, in return for complete publicity of the invention. Under this agreement the inventor's reward is valuable or worthless as the invention proves valuable or worthless to others. If the invention is one desired by the general public, the exclusion of others may enable the patentee to reap a rich reward; or if the invention is worthless, the reward will be equally valueless.

By means of patents, publicity for new ideas is encouraged; for the owner of a valid patent is secure for 17 years, after that the subject of the patent becomes public property. It is for this reason that the patent consists of drawings and specifications to make a complete disclosure of the invention, so that anyone skilled in that particular industry may reproduce it. In addition to the drawings and specifications there are what are called claims. These claims define the actual limits to the patentee's rights to exclude others. Without adequate protection, there would be a tendency to suppress public information regarding new inventions, the inventor relying upon secrecy instead to gain his reward. The patent actually withdraws nothing from the public, but merely withholds for a limited time what otherwise might have been kept secret and perhaps lost forever. It must add to the sum of human knowledge, for in so far as it does not do that, it is to that extent invalid. All that is necessary to establish invalidity is to prove that nothing has been added to the sum of human knowledge by the patent. If it is plainly apparent to an engineer that a patent is invalid, the engineer should be able to so convince the court.

Patents pertaining to reinforced concrete may be divided into two classes: (1) those that apply to improvements in manufactured details, such as reinforcements, and which have been described in Art. 18 of Volume I and in Chapter V of Volume II; and (2) those which may more properly be called engineering patents and which relate to improvements in the structure itself as, for example, the *location* of reinforcement, or the processes of erection. Patents on manufactured details develop a field for the sale of special types of reinforcement, the royalty being included in an enhanced selling price. In other words, this class of patents is used to promote the business of the manufacturer rather than that of the engineer. The second class above mentioned is used more often by the engineer as a support for specialization in engineering, and the royalty is ordinarily

in  
erces  
by e  
vic  
nt  
ut  
f

## CHAPTER XII

### PATENTS

**I**f patents that have been granted by the United States Government for improvements in reinforced-concrete have increased from a yearly average of three or four years 1890 and 1900 to about 150 per year at the present time, that is, not considering patents on concrete mixers, and other minor structures. Undoubtedly some of these are worthless, impractical, and possibly invalid, but unquestionably are of considerable importance. The granting of a patent does not establish its validity under United States patent law, and many of these patents have been annulled by litigation. In spite of this fact, however, we have no right to consider any patent invalid unless there is proof to that effect.

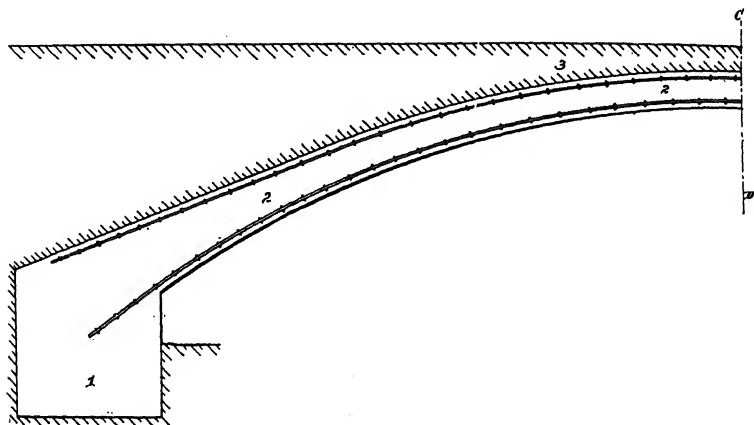
**in General.**—The Constitution of the United States contains the following clause:

"Congress shall have power to promote the progress of science and useful arts by securing for a limited time for authors and inventors the exclusive right to their respective writings and discoveries."

Under the provision of the Constitution, Federal statutes have been enacted authorizing the issue of a patent to the original inventor of any new and useful improvement and granting to the inventor the exclusive right to make, to sell, or to use the patented invention for a period of 17 years after date of issue of the patent is, in effect, an agreement between the Government and the inventor of a new and useful invention whereby the Government grants to the inventor the exclusive right to exclude others from making, using, or selling his



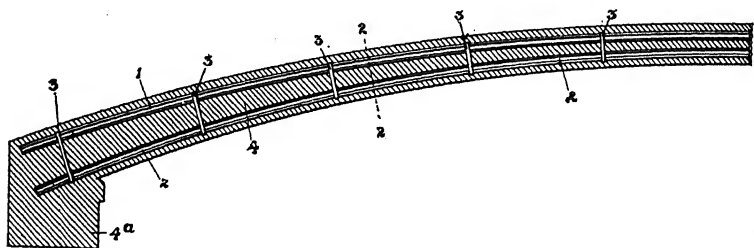
the patent drawings and include more than is covered by the claims cited. The reason for this is due to the fact that a claim is for an improvement while the patent drawings must show how to construct a complete working structure.)



CLAIM 3.—The combination with abutments, and a concrete arch spanning the space between the abutments, of a series of metal bars in pairs, one bar of each pair above the other bar, near the extrados and intrados of the arch, each bar of a pair being independent of the other, and one bar of each pair extending well into the abutment, substantially as described.

FIG. 185.—Thacher patent.

A somewhat similar reinforcement is shown in the patent to Arnold, No. 749,771, issued, Jan. 19, 1904, on an application filed Sept. 13, 1902. The bars are arranged in pairs, but bonded



CLAIM 2.—In a bridge, an arch of concrete or other masonry, having embedded therein ribs, arranged one above but separated from each other and by the masonry and composed of railroad rails or other iron, said ribs being bonded together by metallic straps wound around them and at intervals of the length thereof, substantially as described.

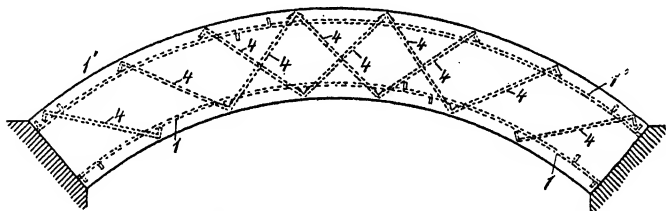
FIG. 186.—Arnold patent.

together by metallic straps as indicated in Fig. 186, thus differing from the Thacher patent in which the bars are claimed as independent of one another.

Another modification of the Thacher patent is shown in Melber,

No. 660,518, issued Oct. 23, 1900, on an application filed August 24, 1899, in which shear members cross diagonally from one reinforcing member to another (Fig. 187).

The Parmley patent, No. 696,838, issued April 1, 1902, on an

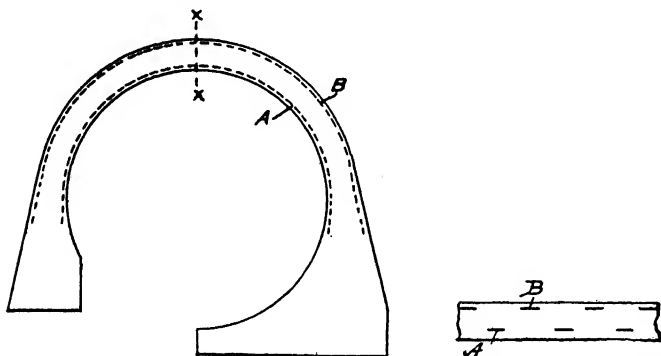


CLAIM 1.—In cement or other concrete construction metal reinforcing bars, unattached at their ends to other metal reinforcing bars, embedded therein transverse to the calculated shearing strains.

FIG. 187.—Melber patent.

application filed June 4, 1901, differs from the Thacher patent in having the bars near intrados and extrados alternating with one another instead of being arranged in pairs (Fig. 188).

A materially different form of arch reinforcement is shown in the patent to Luten, No. 1,009,676, Nov. 21, 1911; application

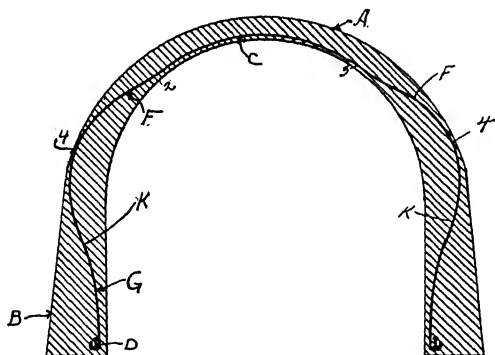


CLAIM 3.—A concrete arch having bars embedded therein, both in intrados and extrados at the regions of tension and extending continuously through the regions of tension and sufficiently into the abutments to obtain a secure anchorage, the bars in the extrados being opposite the spaces between those in the intrados.

FIG. 188.—Parmley patent.

filed April 29, 1901. This patent shows the arch reinforced with but a single series of reinforcing members (Fig. 189) instead of the double row of the Thacher, Arnold, Melber, and Parmley patents. A modification of this device is shown in another patent to Luten, No. 818,386, April 17, 1906; application filed May 17,

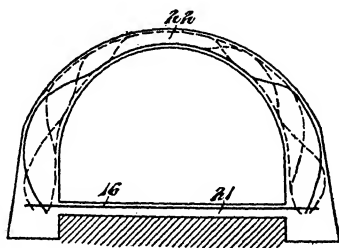
1902. In this patent the points of crossing the arch ring for various rods of the single series have been displaced laterally along the arch ring, so that the arch is reinforced on both sides through a short region where there is doubt as to whether the



CLAIM 2.—In an arched structure of concrete the combination with a curved or arched member and abutments to support the same, of a series of tension members embedded in said curved or arched member, and passing close to the interior face of the abutments.

FIG. 189.—Luten patent.

bending moments will be positive or negative (Fig. 190). The reason for placing the reinforcement in this way is based on the theory that tension will occur at alternately opposite regions of an arch in limited regions only, and that steel is located in those regions and extends continuously from one to the other for

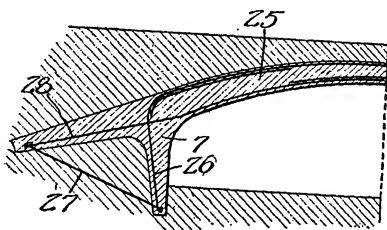


CLAIM 7.—An arch having embedded therein rods, bars, or other tension members in two or more series following one face of the arch rib, thence across and following the other face of the rib, the points of crossing for the different series being angularly or laterally displaced with respect to each other, substantially as described.

FIG. 190.—Luten patent.

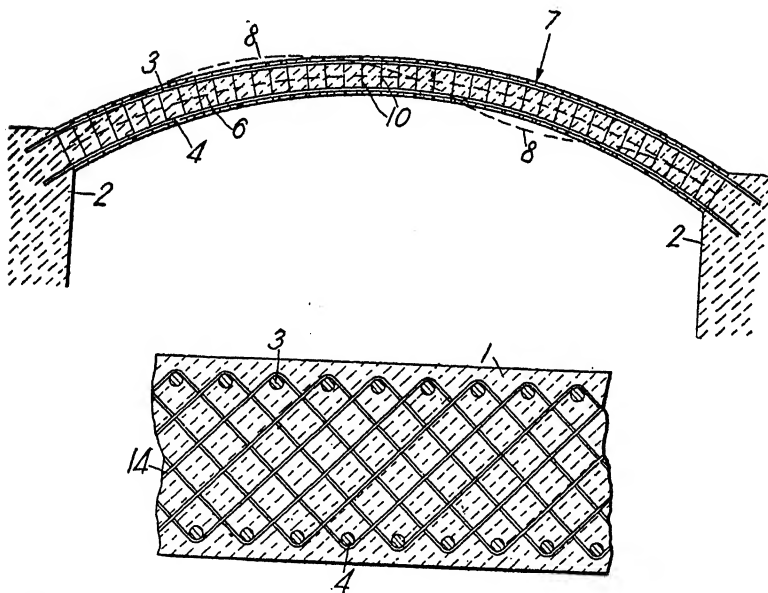
convenience in placing. A similar object may be accomplished with non-continuous rods as shown in patent to Luten No. 852,971, May 7, 1907; application filed June 30, 1906. (See Fig. 191.) The difficulty of placing this form of reinforcement probably offsets the saving in metal.

The Cummings patent, No. 978,361, issued Dec. 13, 1910, on an application filed June 11, 1909, relates entirely to



CLAIM 9.—A concrete arch having reinforcement near both surfaces alternately heavy and light on opposite sides of points of calculated change of moment.

FIG. 191.—Luten patent.



CLAIM 4.—A reinforced concrete arch or girder comprising longitudinal reinforcement bars arranged near the upper and lower surfaces thereof, a series of open metal sheet or mesh members arranged close together and all parts of each lying in substantially a single plane substantially normal to the neutral equilibrium curve of the arch or girder and extending from top to bottom and side to side thereof and comprising a substantial portion of the cross-sectional area thereof, whereby said reinforcement members resist vertical tension stresses throughout the width of the arch or girder, and cementitious material enveloping and embedding said longitudinal and transverse reinforcement members.

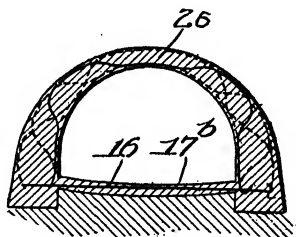
FIG. 192.—Cummings patent.

transverse reinforcement in the arch ring or arch rib. A typical claim is given in Fig. 192.

In any of the above patents the reinforcement may be of



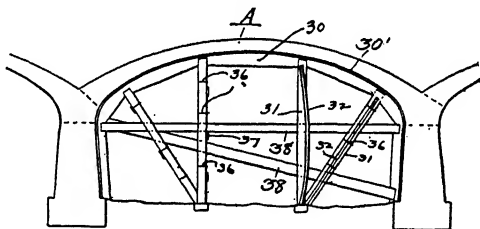
with elimination of possible settlement cracks. The old method was to remove the centers from beneath an arch before the spandrels, fill, and railings were added, the arch thus assuming its settlement stresses before their addition; but the erection of spandrels or fill after centers are removed is dangerous unless the arch ring is made excessively heavy. The process of the Luten



CLAIM 9.—An arch or bridge having the bed of stream paved with concrete with tension members embedded transverse to the course of the stream.

FIG. 194.—Luten patent.

patent referred to covers the building of the arch and *part* of the spandrel *before* striking centers, and the addition of the coping and railings *after* striking centers. The addition of the lower part of the spandrel walls before striking centers permits the addition of the earth fill supported by these walls and this applies



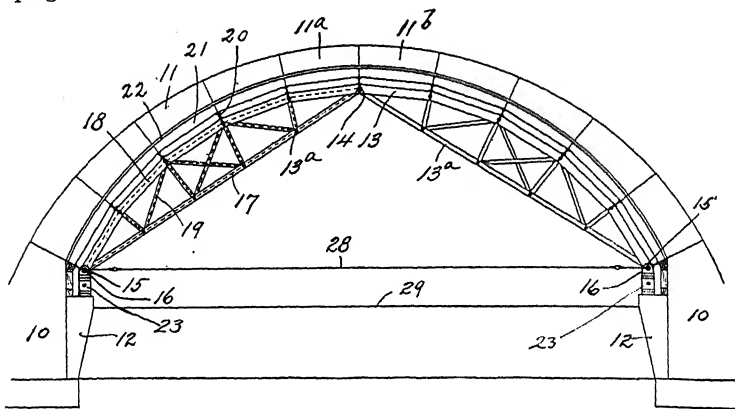
CLAIM 4.—A falsework centering containing compound compression members for supporting a load and each composed of a plurality of pieces having major and minor dimensions transverse to their lengths, the major dimension of one piece being arranged transversely to the major dimension of another piece, and a withdrawable connection to unite the pieces of each compression member.

FIG. 195.—Luten patent.

to the arch its normal loading at the time the centers are struck. The part spandrel serves to stiffen the arch and render it secure, making possible the use of a light arch ring, yet with elimination of settlement cracks. One of the broader claims (claim 14) is as follows:

“That improvement in the art of building an arch or girder comprising erecting the arch or girder together with part of the spandrel or super-

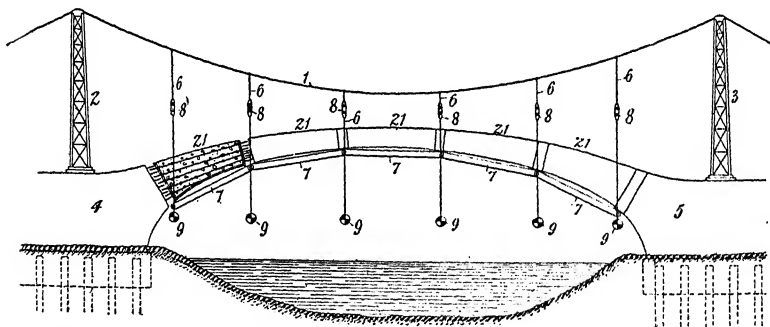
structure on centers, then lowering the centers and subsequently adding coping or railing."



CLAIM.—A centering or temporary falsework for masonry, or concrete arches comprising a three-point pinned arch composed of two sections supported solely at their lower ends and connected together at their upper ends at the center plane of the arch by a single pin through which stresses are transmitted from one section to the other, supports at the lower ends of the two sections each connected to the corresponding section by a single pin.

FIG. 196.—Watson patent.

An improved form of centering is disclosed in Luten patent No. 1,106,880, Aug. 11, 1914; application filed Nov. 1, 1906. The uprights consist of compound T-columns fastened together with wires (Fig. 195) and consisting usually of 2 in. by 6-in. or

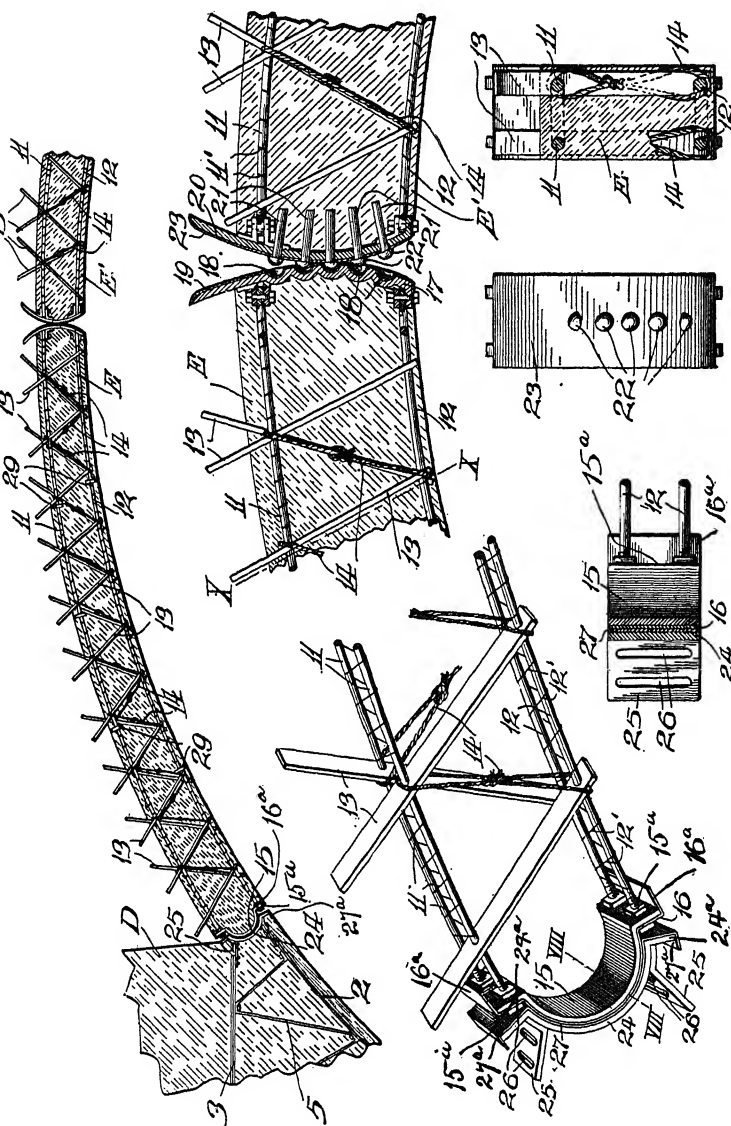


CLAIM 2.—In a system of concrete construction, the combination of supporting cables, arranged over a space to be spanned, a centering comprising a plurality of flexibly jointed sections, and hangers suspending the said sections from the cables.

FIG. 197.—Aylett Patent.

2 in. by 8-in. timbers. No wedges or sand boxes are used for striking centers, but by clipping the wires, the compound columns are resolved into their simple elements, which buckle, lowering the center, and the arch thus gradually assumes its load.

A three-pin type of centering is shown in the patent to Watson, No. 1,071,118, issued Aug. 26, 1913, on an application filed



CLAIM 7.—In a bridge construction, a pair of mating concrete arch sections having hinge plates at their crown ends the hinge plate of one of the sections being provided with pockets and the hinge plate of the other section being provided with pins having heads adapted to enter the pockets in the mating hinge plate, substantially as set forth.

CLAIM 11.—A bridge construction comprising a concrete abutment formed with a cantilever arm having reinforcing framework, segmental shaped socket plates having wings connected to the framework of the cantilever arm, and an arch section having semi-circular hinge members fitted to the socket plates.

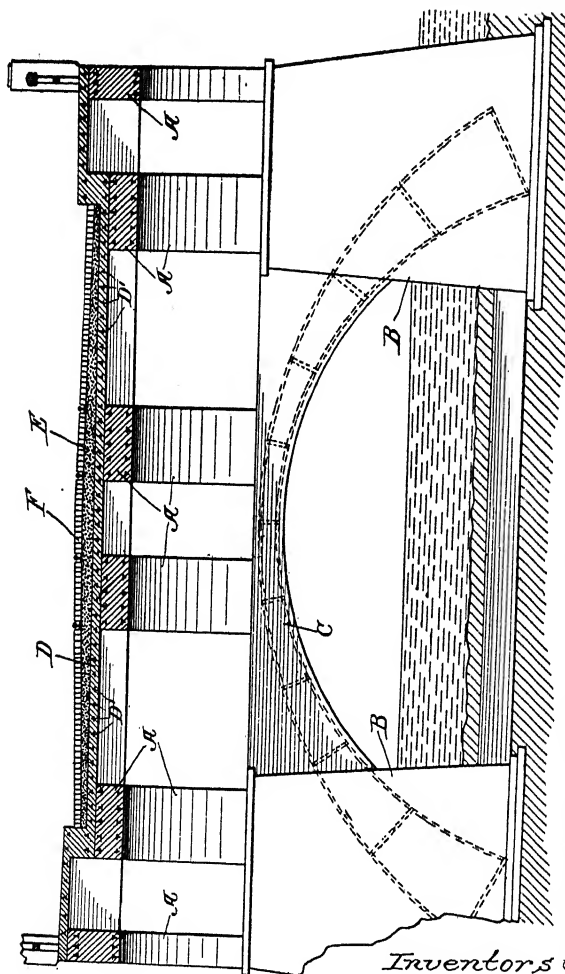
Fig. 198.—Thomas patent.

Jan. 27, 1911. One of the objects of the invention is to provide a centering which can be used repeatedly, which has a minimum deflection when the load is applied, and which is well adapted



for construction of arch bridges where obstruction to traffic under the bridge must be avoided. (See Fig. 196.)

A suspended system of arch construction is described in the Aylett patent No. 965,358, July 26, 1910; application filed Oct. 26,



CLAIM 6.—A concrete bridge comprising a series of piers separated longitudinally and transversely, a super-structure supported upon said piers and comprising a series of longitudinal ribs connected by a floor integral therewith and having a less thickness than the ribs.

FIG. 199.—Strauss and Collins patent.

1907. (See Fig. 197.) The Aylett patents also cover the method of attaching the main cables directly to the voussoirs without any centering whatever—or what might be called a suspended pre-casted voussoir method.

A three-hinged arch patent is disclosed in the patent to Thomas,

No. 915,316, Mar. 16, 1909; application filed Jan. 30, 1908. (See Fig. 198.)

The Strauss and Collins patent No. 762,361, issued June 14, 1904, on an application filed Jan. 25, 1904, describes a special type of arch bridge, as indicated in Fig. 199.

**64. Patent Litigation.**—There has been much activity in litigation of arch patents. Of the suits won, many have been concluded by consent decrees, but none have thoroughly contested the validity of the patents. Many of the pending suits are being hotly contested at the present time and will undoubtedly result in decrees that will definitely determine the validity of some of the patents. A single favorable opinion in a thoroughly contested case will go a long way to fix the standing of the patents before the public. An unfavorable opinion on the other hand will not be conclusive, because it will determine the validity of only a few claims, and the Luten patents alone contain hundreds of claims. Any one suit might invalidate a possible half-dozen of these claims but would not be conclusive as to the patents themselves or the other claims that were not involved. Hence no early conclusion of litigation under these various patents can be expected.

Since a patent is a Federal grant, litigation for violation of the patent itself must always be in the Federal court. Property rights in patents and contracts under patents may come within the jurisdiction of the State courts, but infringement of a patent is a matter for correction exclusively in the Federal court. A patent is infringed by anyone who makes, sells, or uses any device that includes all of the elements named in any one claim of the patent. If any element of the claim be absent from the device the patent is not infringed. But the presence of more elements than called for by the claim does not avoid infringement. The drawings and specifications have very little to do with the question of infringement, being principally useful to the court in determining any ambiguity that may arise as to the claim. In the Thatcher patent illustrated in Fig. 185 the reinforcement is shown consisting of deformed bars, but the claims are not thus limited. Hence smooth rods or bars or their equivalent would infringe the patent if arranged as claimed.

The remedy for infringement may be a suit at law before a jury to collect damages, or it may be a suit in equity before a judge for an injunction which, if granted, carries with it an ac-

counting for damages and profits. Nearly all infringement suits are consequently suits in equity, having the injunction against future infringement as their primary object. An injunction to prevent infringement may be granted either before or after there has been infringement, a past infringement being construed by the court as a threat to infringe again. If one claim of a valid patent is shown to be infringed, the court will grant an injunction forever restraining the future infringement of that patent. The suit may be against any party violating the patent. Thus the builder and the purchaser are both liable and neither can relieve the other. The designer may also be held liable under certain conditions, even though he has not actually made, used, or sold the infringing structure itself. The courts have held that there may be contributory infringement by one who assists others to make, sell, or use patented devices, as in the case of an engineer designing and supervising an infringing structure.

There are many possible defenses to a suit for infringement, but none of them are ordinarily of much practical value, except the proof that the patent was not granted to the original inventor in this country. The most convincing test of the validity of a patent is: Did it add anything to the sum of human knowledge? If it did, it is to just that extent valid. One or more claims of a patent may be found invalid and the remaining claims of the patent still remain valid. And the patent itself is not void until all of its claims have been proved invalid.

Suits for infringements are begun in district courts of the United States. From this court there may be an appeal to the Circuit Court of Appeals of the Circuit, and its decision is final. There are nine Federal Circuits in the United States and nine courts of appeal, and the decision of one of these courts is not binding upon any other, although it is persuasive. In case of conflicting decisions a remedy may be had in the Supreme Court of the United States, but this is possible only in case such court consents to a hearing. Consequently a patent may be valid in one district and invalid in another, and adverse decisions are necessary in nine district courts to completely invalidate it throughout the United States. Usually one or two thoroughly contested decisions are considered conclusive.

The damages that may be secured in a suit for infringement are usually measured by the customary royalty charged for the use of the patent. In case the infringement was done knowingly

and wilfully, treble damages may be awarded at the pleasure of the court. But even so the cost of litigation usually far exceeds the damages secured and the primary object of a suit for infringement must be the injunction to stop further infringement. Under the old rules of Federal court procedure the cost of a patent suit not infrequently ran into tens of thousands of dollars. The total cost of the suit that established the validity of the Cameron Septic Tank patent is said to have exceeded \$50,000, and the Warren Bitulithic Paving patent, \$60,000. But on Feb. 1, 1913, the new rules of Federal court procedure went into effect and infringement suits may now be tried in open court with but little delay, so that lower court decisions may now be had in 1 or 2 years, where formerly 5 years was not unusual, and Mr. Edison is said to have contested one suit through 30 years of litigation.

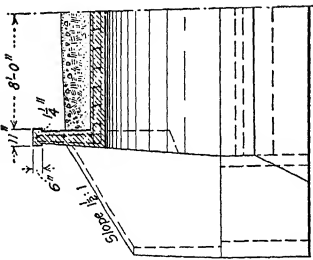


## CHAPTER XIII

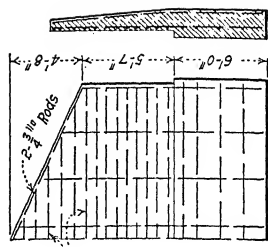
### TYPICAL DESIGNS OF THE VARIOUS TYPES OF ARCH BRIDGES

The bridges illustrated in this chapter have been selected as representative of the various types of arch bridges built in this country, and much can be gained, the writer believes, by a careful study of the details shown. In fact, it is thought that the practical designing of concrete arch bridges can be taught in no other way than by requiring a well-directed study of a representative collection of typical detailed designs, such as those shown, in addition to the usual problems of analysis. The construction views included should prove instructive.

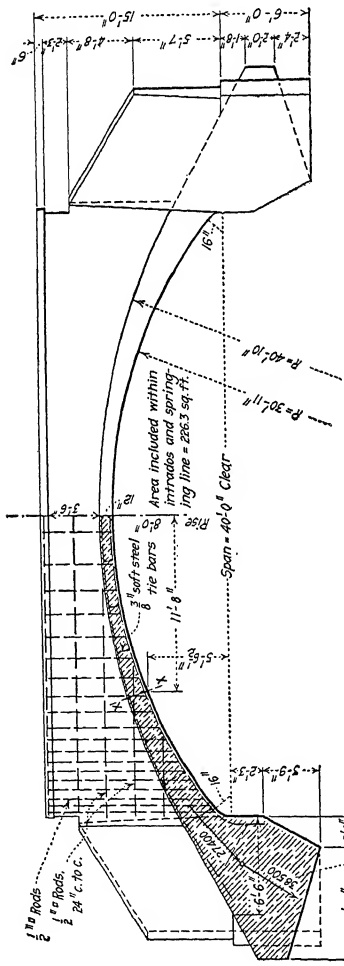
The construction in detail of the Yardley bridge (Plates IV, V, and VI) may be found in Chapter XXXI. The Third Street bridge at Logansport, Ind. (Plate VII) is a bridge of Luten Design—a patented type of bridge referred to in Chapters X and XII. The lattice girders set across the arch ring in the Atherton Avenue bridge (Fig. 207 and Plate IX) should be especially noted as they are somewhat unusual, being employed to provide positive spacing and locking together of the arch reinforcement. The analysis of the Carondelet Park bridge (Plates XII, XIII, and XIV) and also of the Main Street viaduct (Plates XL and XLI) may be found in Arts. 47 and 61 respectively. The Latah Creek bridge (Figs. 232 and 233) was included to show one method of providing rigidity and at the same time reducing the number of ribs showing on the arch soffit—this being done by connecting each outer rib with the adjacent inner one by a thin slab at the intrados. The highway bridge at Danville, Va. (Plate XXXVIII) shows a type of bridge with the arch ribs extending up to the roadway and the reinforcement so placed that the greater part of rib may be considered as effective arch depth. The Benson Street bridge at Lockland, Ohio (Plate XXXIX), is a through arch bridge with the horizontal component of the arch thrust taken by steel rods extending between the skewbacks and fastened to the steel in the ribs.



Half Section through Crown



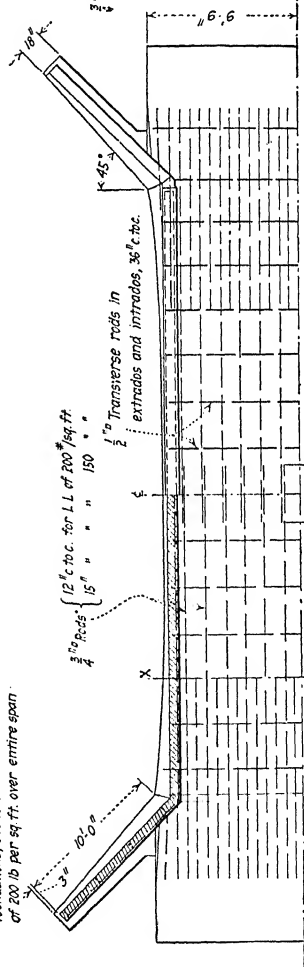
Wing Wall



Half Elevation

Half Section

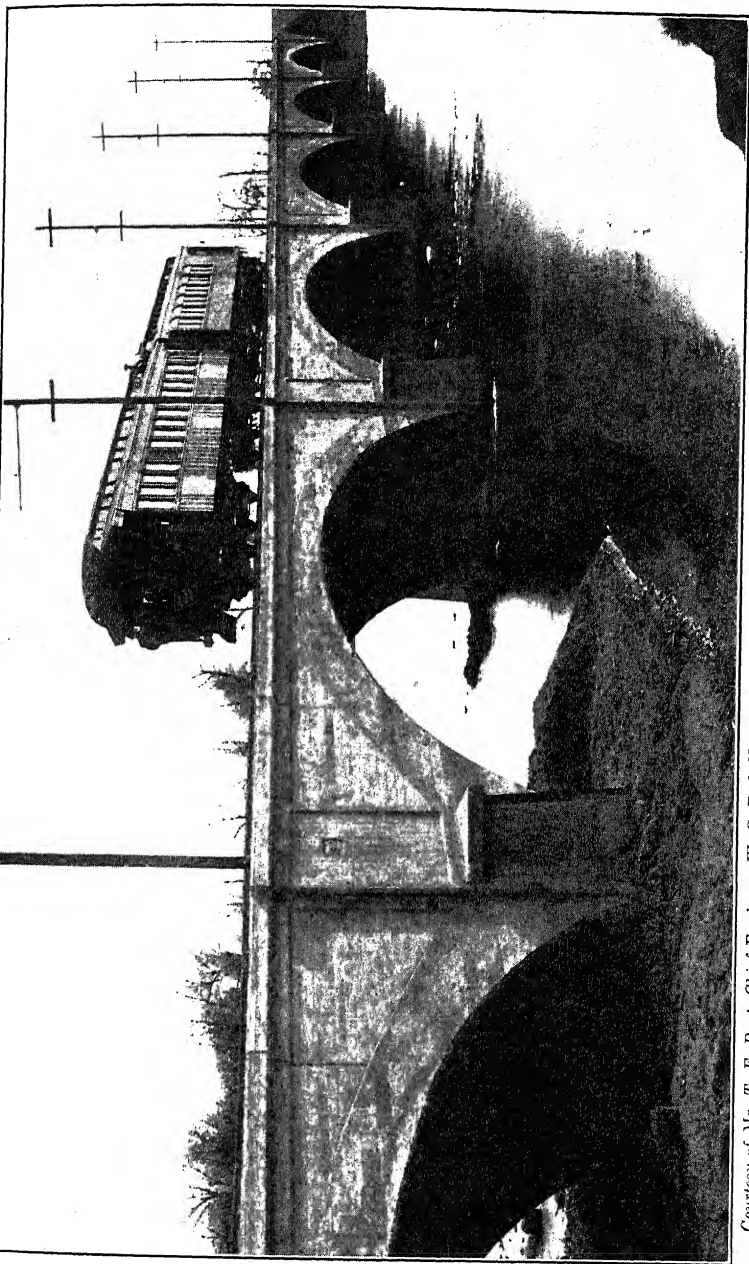
Direction and intensity of maximum pressure on foundations, due to D.L. + L.L. of 200 lb per sq ft. over entire span.



Section of Headwall

Plan

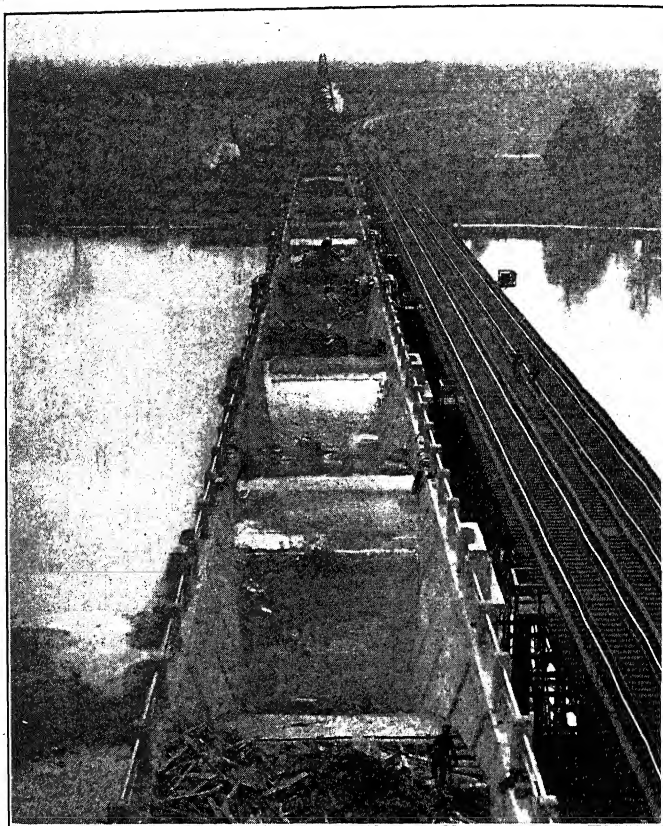
Standard 40-ft. arch, State of Missouri Highway Department.



*Courtesy of Mr. T. E. Rust, Chief Engineer, W. C. F. & N. Ry.*

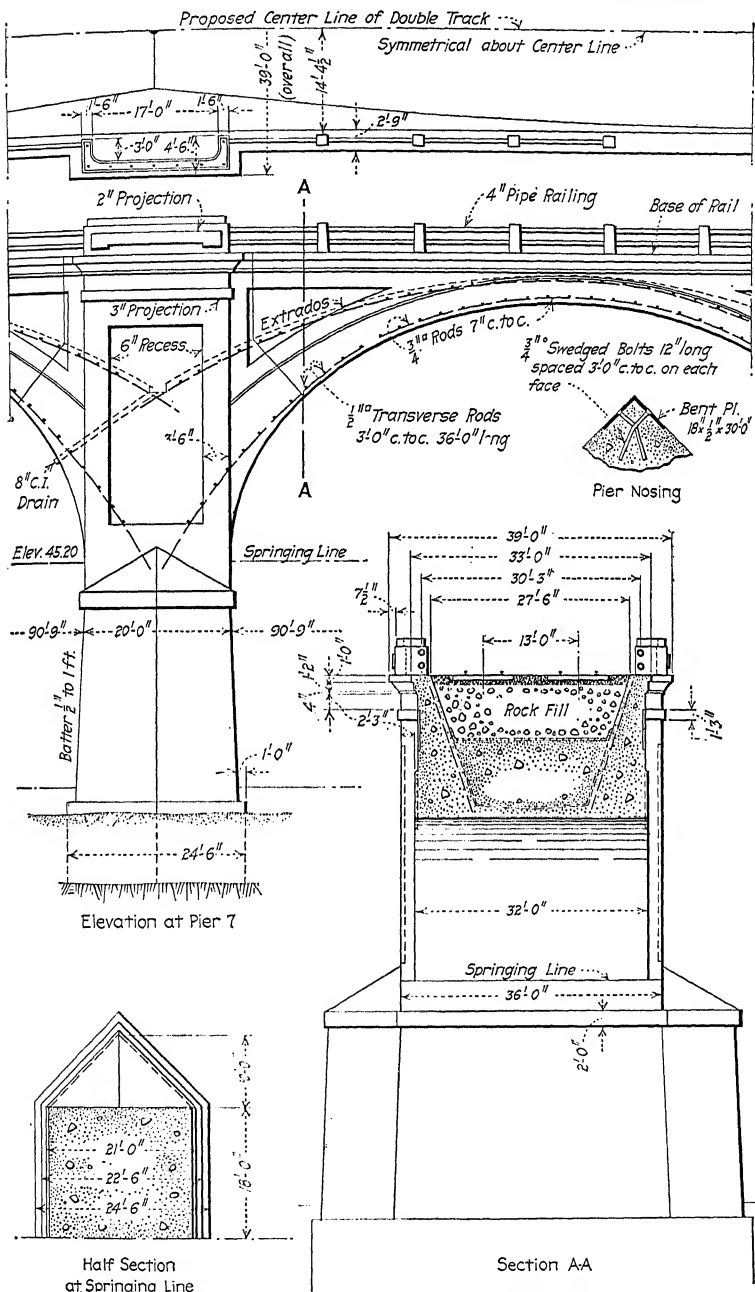
FIG. 200.—Elk Run bridge across Cedar River, Waterloo, Cedar Falls & Northern Ry. Co.

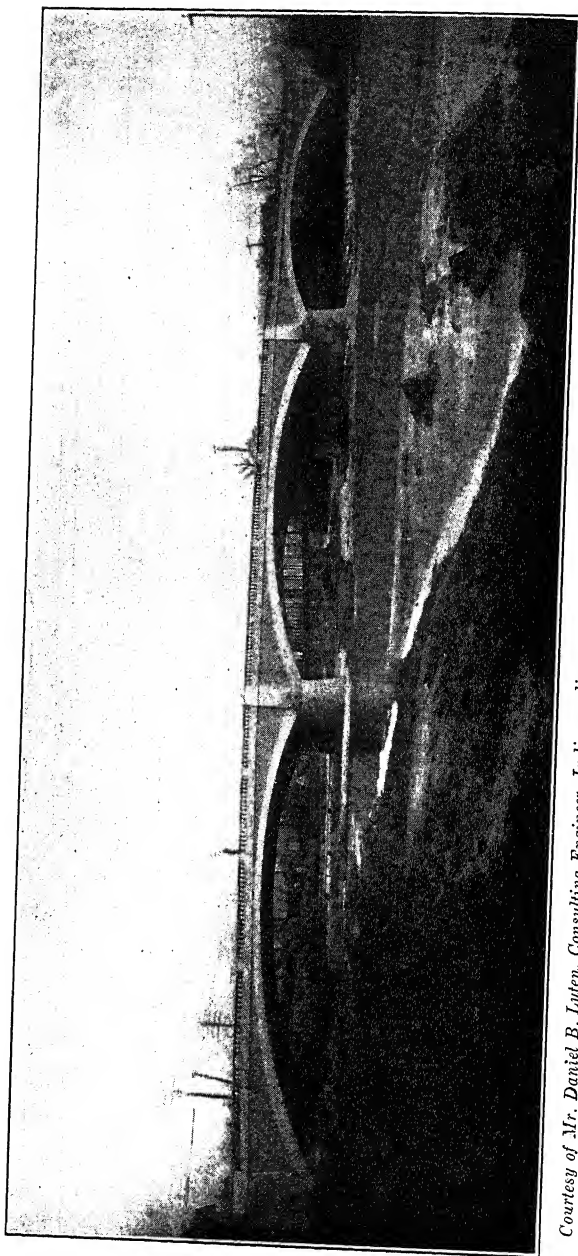




*Courtesy of Mr. William Hunter, late Chief Engineer, P. & R. Ry. Co.*  
FIG. 202.—Yardley bridge, Philadelphia & Reading Ry. Co.

## PLATE IV

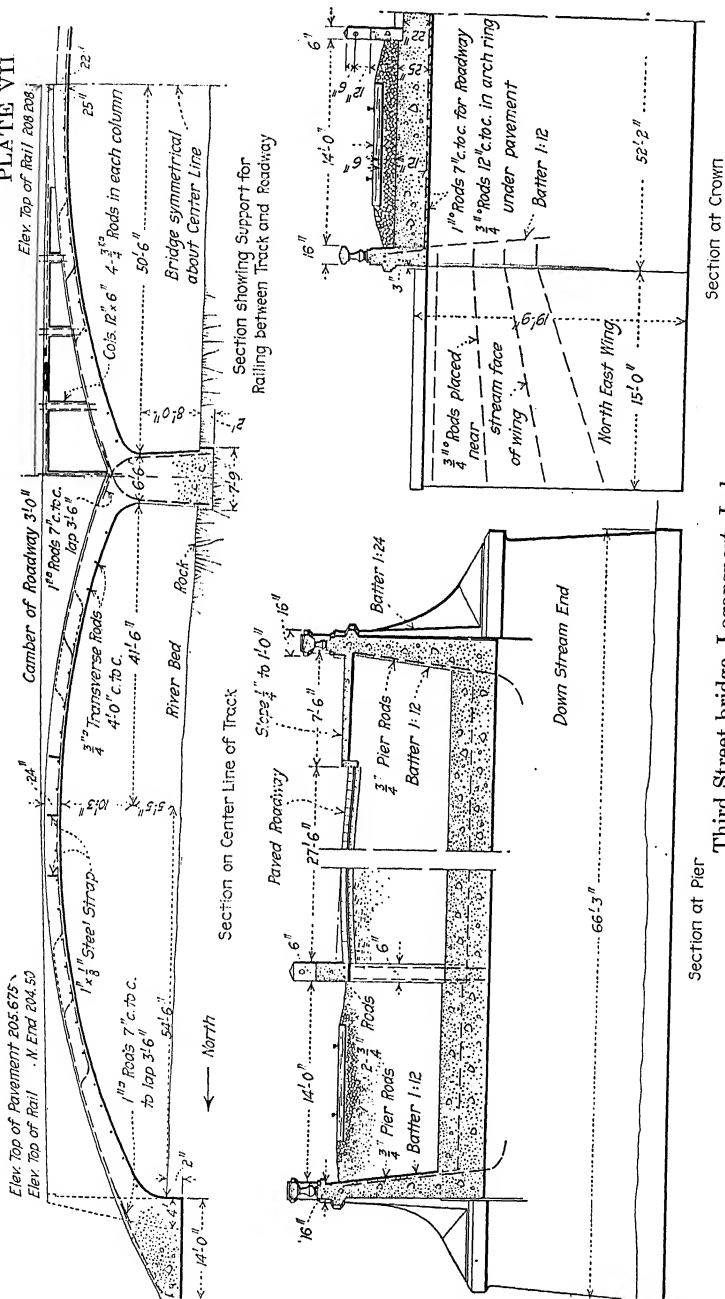




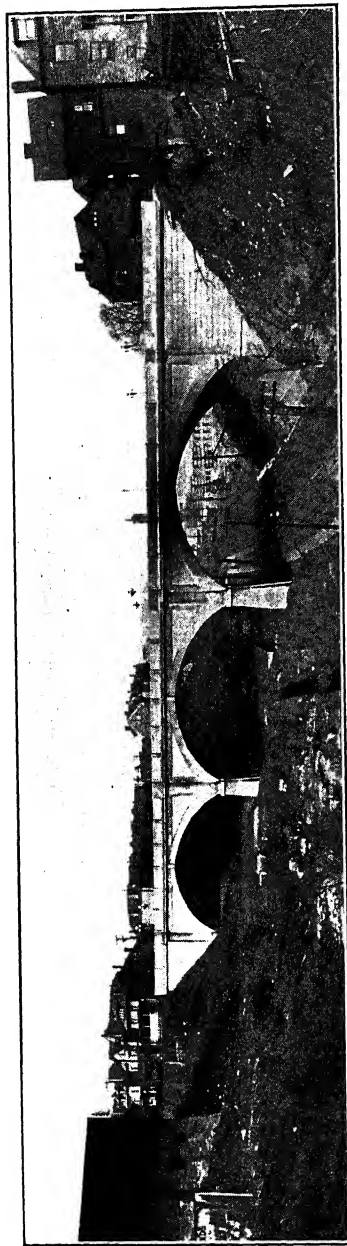
*Courtesy of Mr. Daniel B. Luten, Consulting Engineer, Indianapolis.*

FIG. 203.—Third Street bridge, Logansport, Ind.

Elev. Top of Pavement 205.675、  
Elev. Top of Rail . N. End 204.50

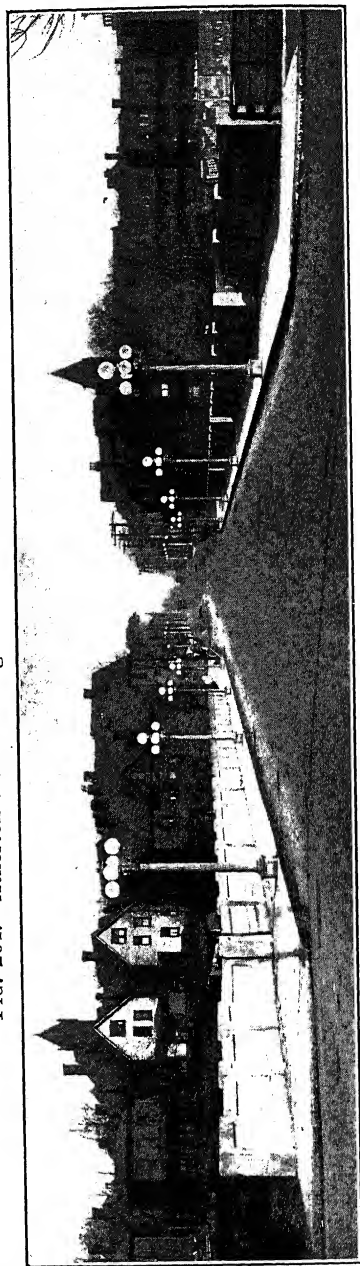


Third Street bridge, Logansport, Ind.



*Courtesy of Mr. N. S. Sprague, Superintendent, Dep't. of Public Works, Pittsburgh.*

FIG. 204.—Atherton Avenue bridge over P. R. R., City of Pittsburgh.

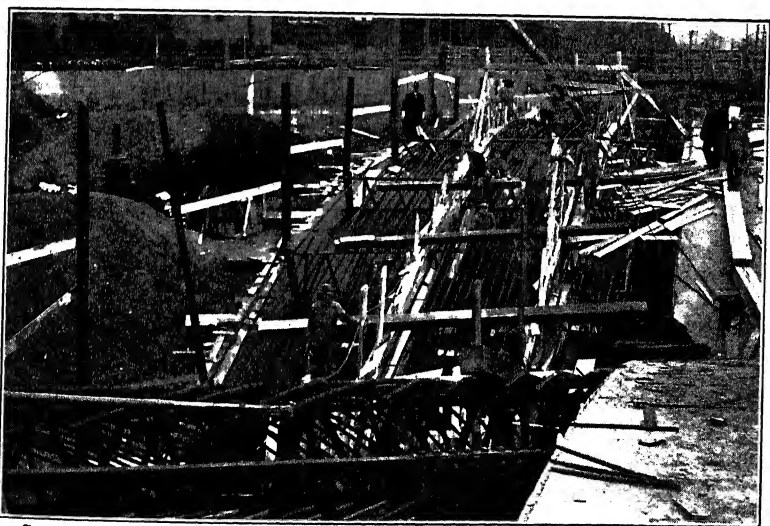


*Courtesy of Mr. N. S. Sprague, Superintendent, Dep't. of Public Works, Pittsburgh.*

FIG. 205.—Roadway of Atherton Avenue bridge over P. R. R., City of Pittsburgh.



*Courtesy of Mr. N. S. Sprague, Superintendent, Dep't. of Public Works, Pittsburgh.*  
FIG. 206.—Steel centers—Atherton Avenue bridge, Pittsburgh.



*Courtesy of Mr. N. S. Sprague, Superintendent, Dep't. of Public Works, Pittsburgh.*  
FIG. 207.—Construction view—Atherton Avenue bridge, Pittsburgh.

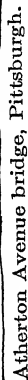
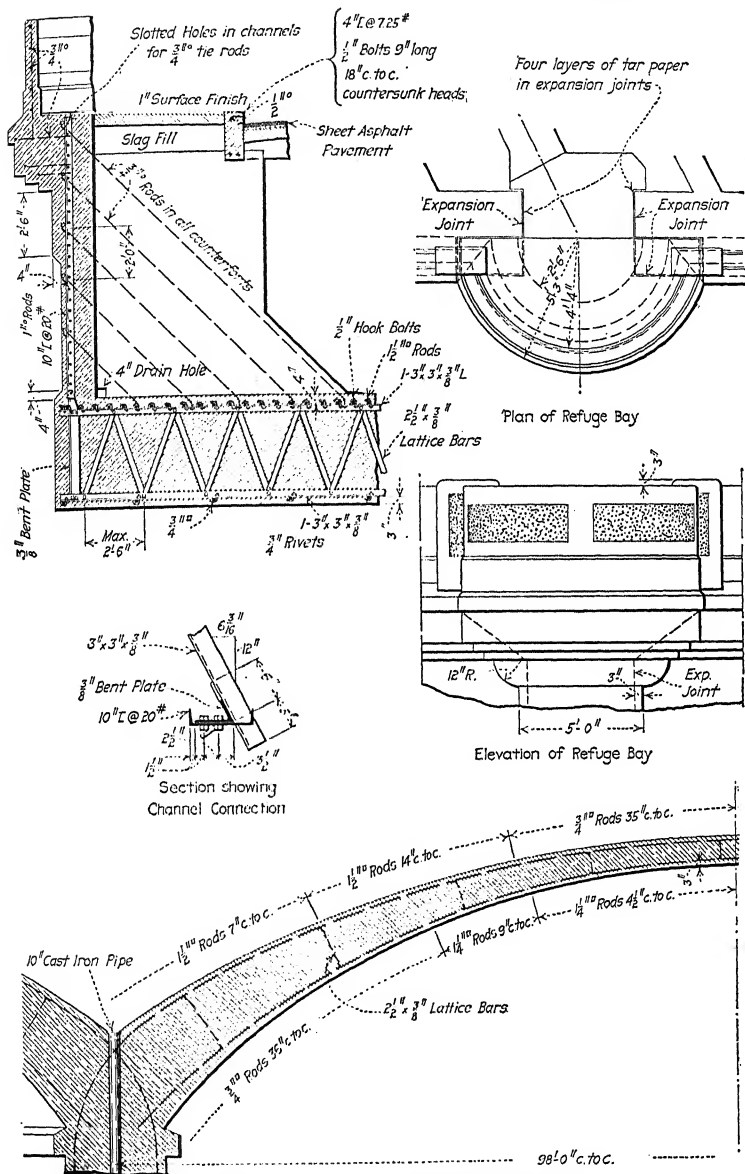
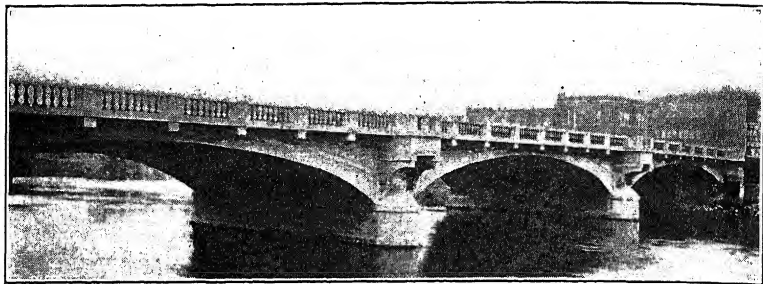


PLATE IX



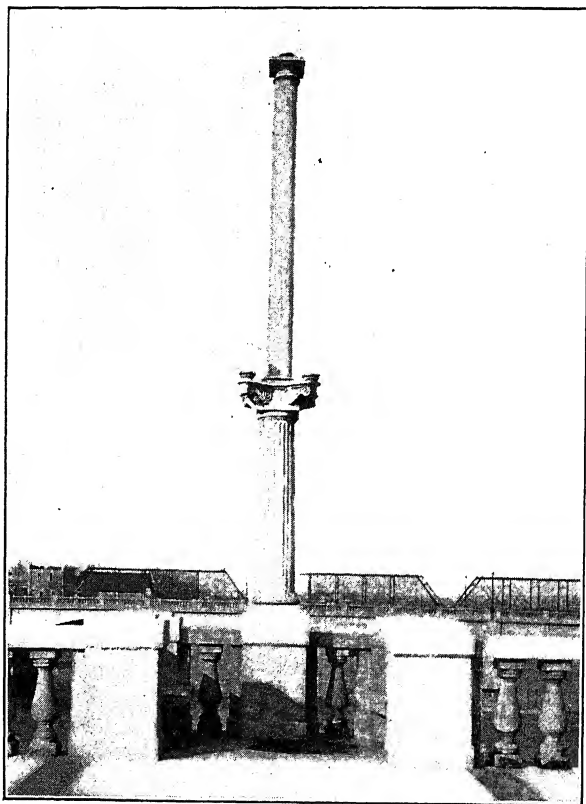
Atherton Avenue bridge, Pittsburgh.





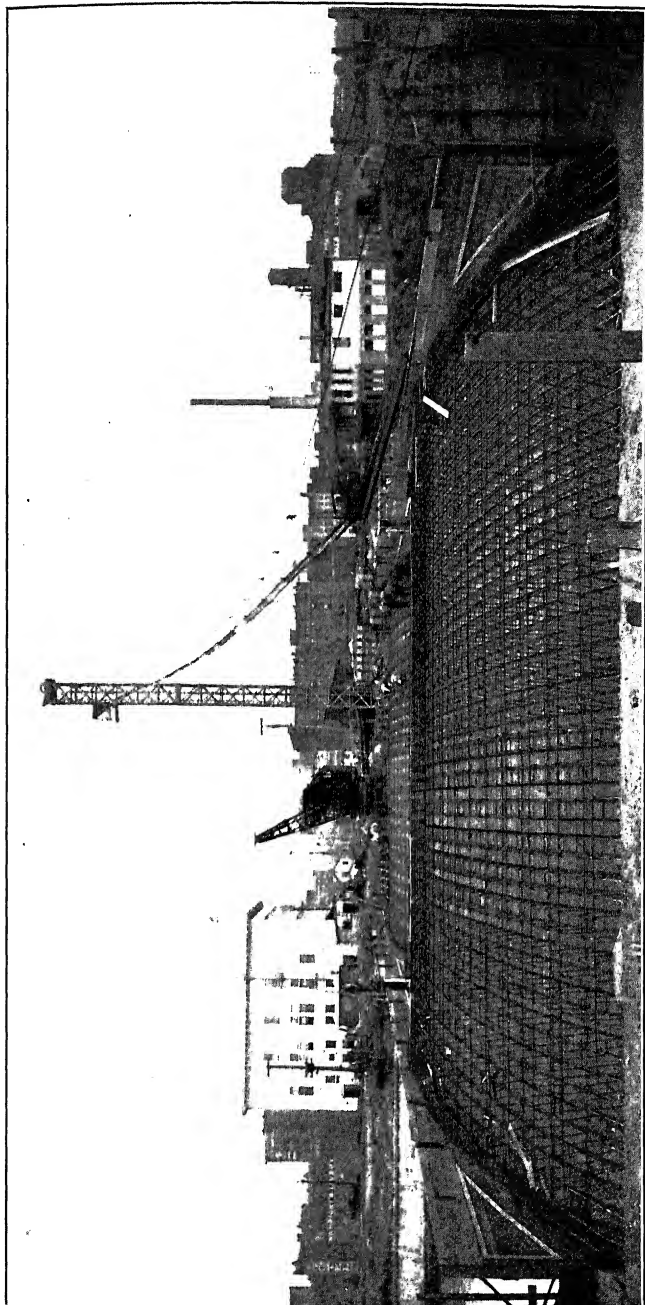
*Courtesy of Engineering and Contracting.*

FIG. 208.—Third Avenue bridge over Cedar River, Cedar Rapids, Iowa.



*Courtesy of Engineering and Contracting.*

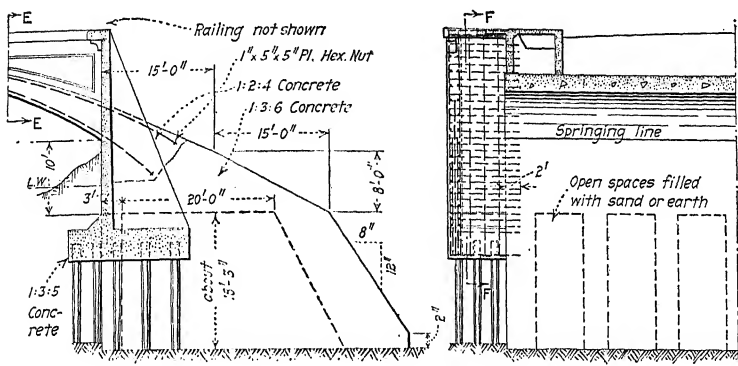
FIG. 209.—Refuge bay of Third Avenue bridge, Cedar Rapids, Iowa.



*Courtesy of Engineering and Contracting.*

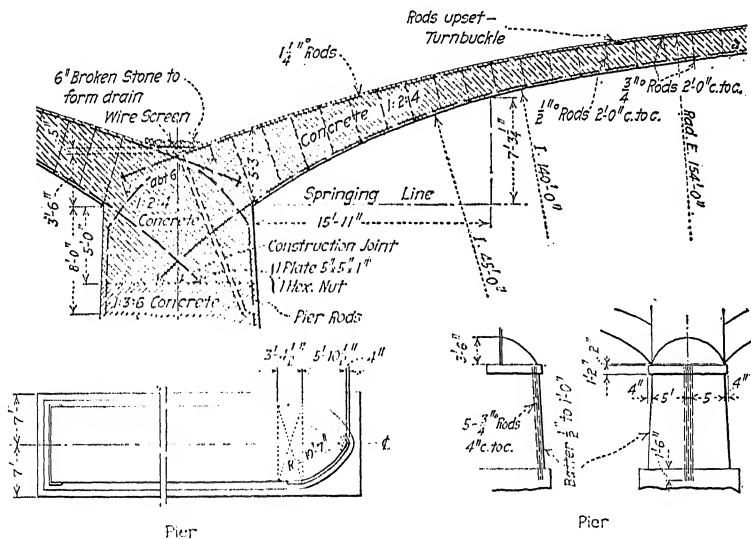
Fig. 210.—Construction view of Third Avenue bridge, Cedar Rapids, Iowa.





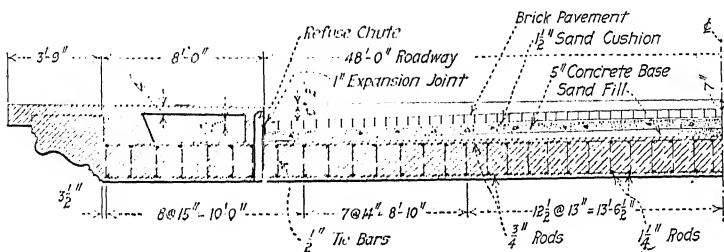
Section F-F through Retaining Wall

Section E-E



Pier

Pier



Half Section through Crown

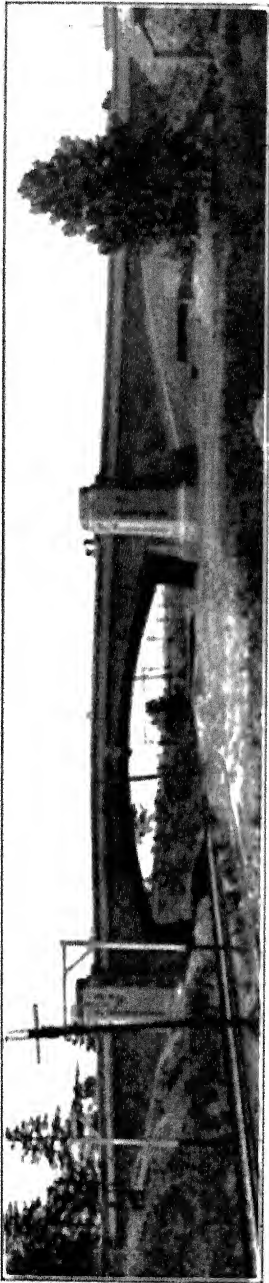


Fig. 211.—Carondelet Park bridge, St. Louis.

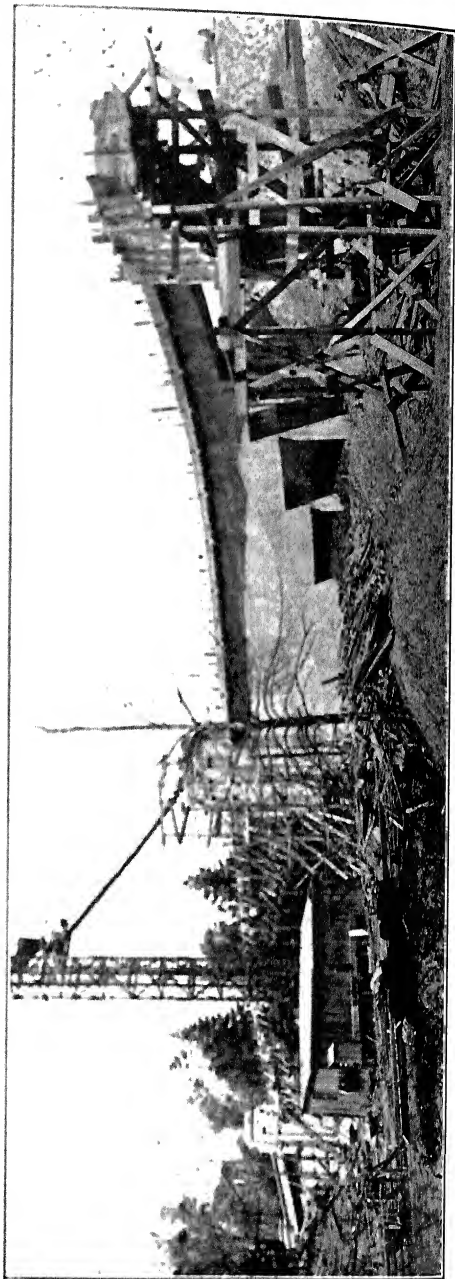
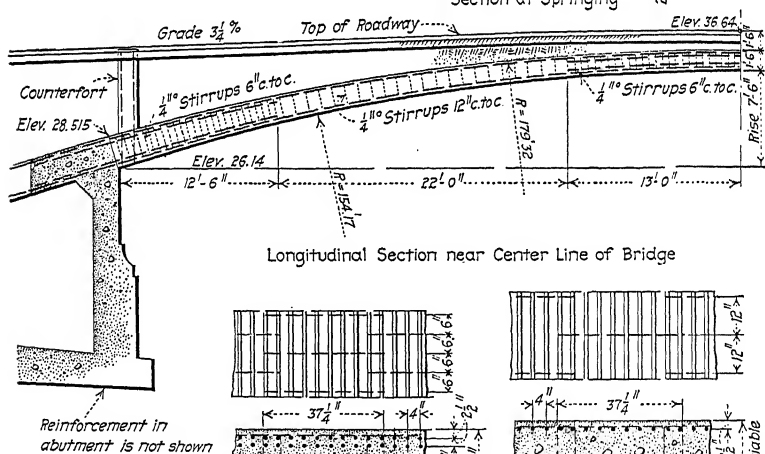
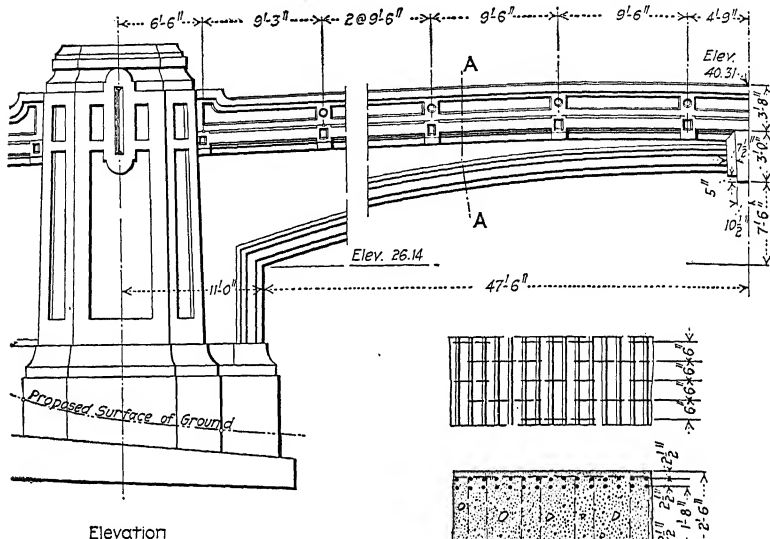


Fig. 212.—Construction view of Carondelet Park bridge, St. Louis.



FIG. 213.—Abutments of Carondelet Park bridge, St. Louis.

## PLATE XII



Section at Crown  
Section near Quarter Point  
Carondelet Park bridge, St. Louis.







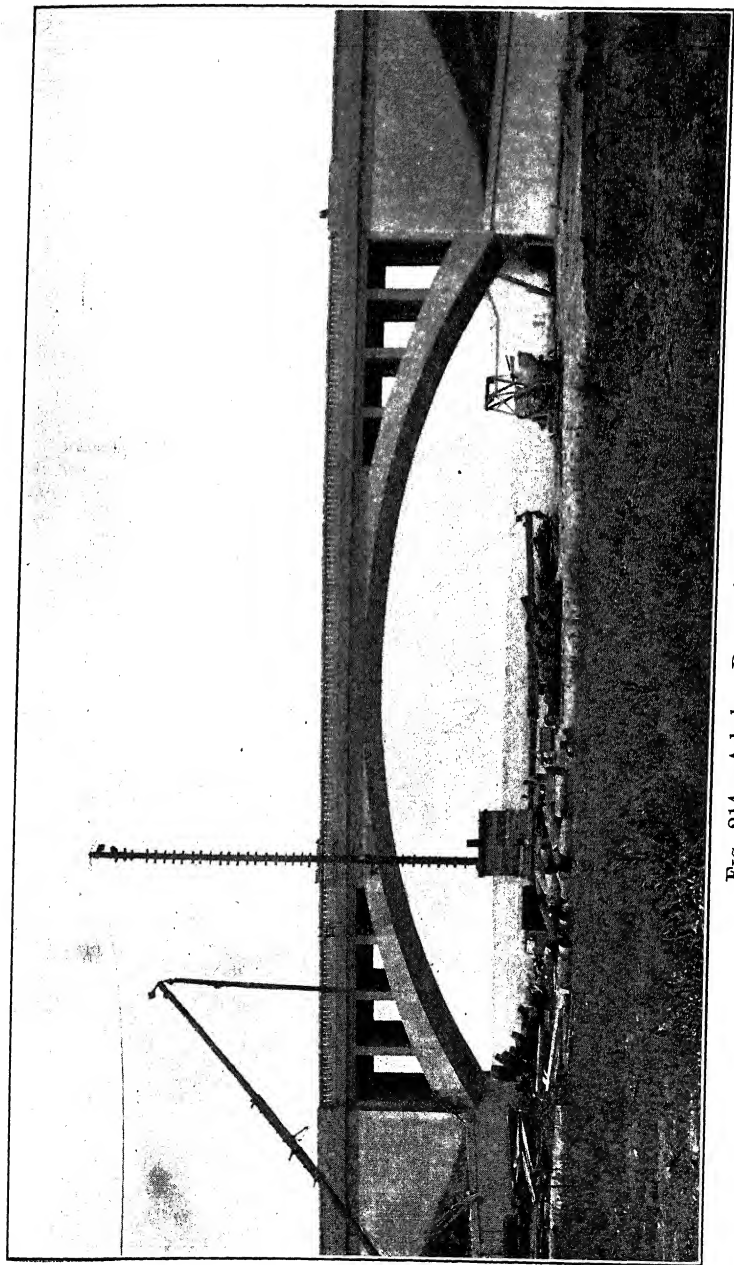


Fig. 214.—Ashokan Reservoir Spillway bridge.

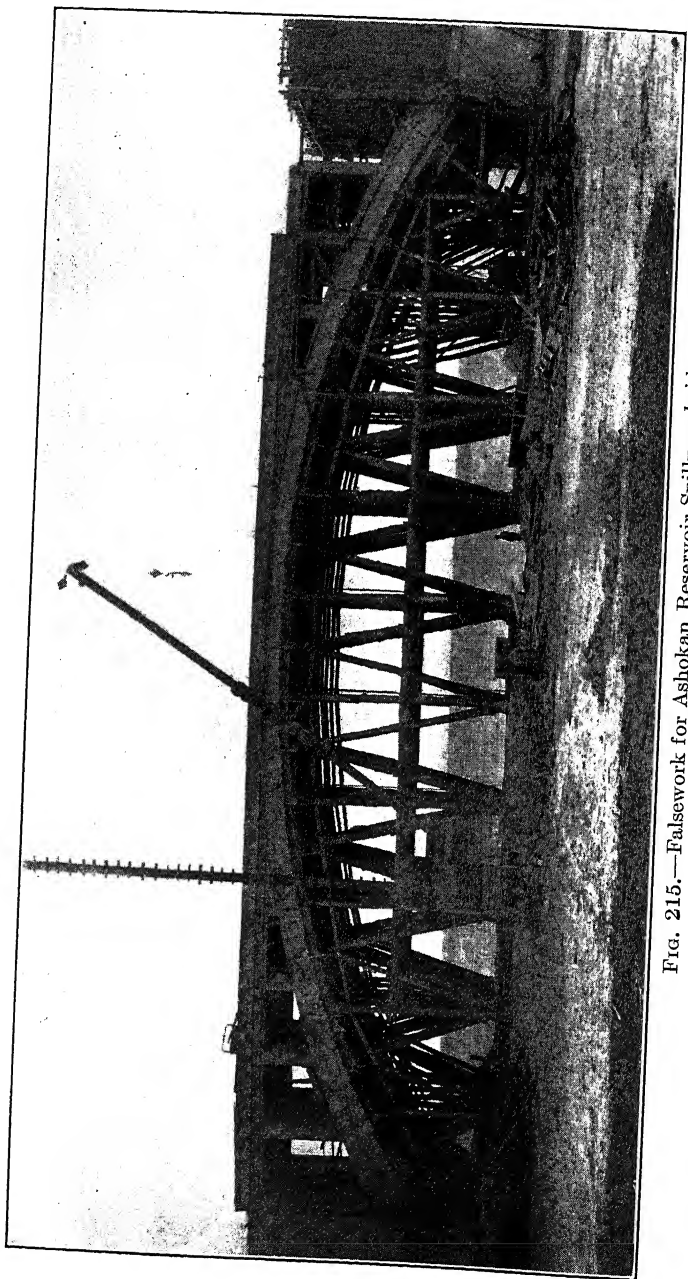
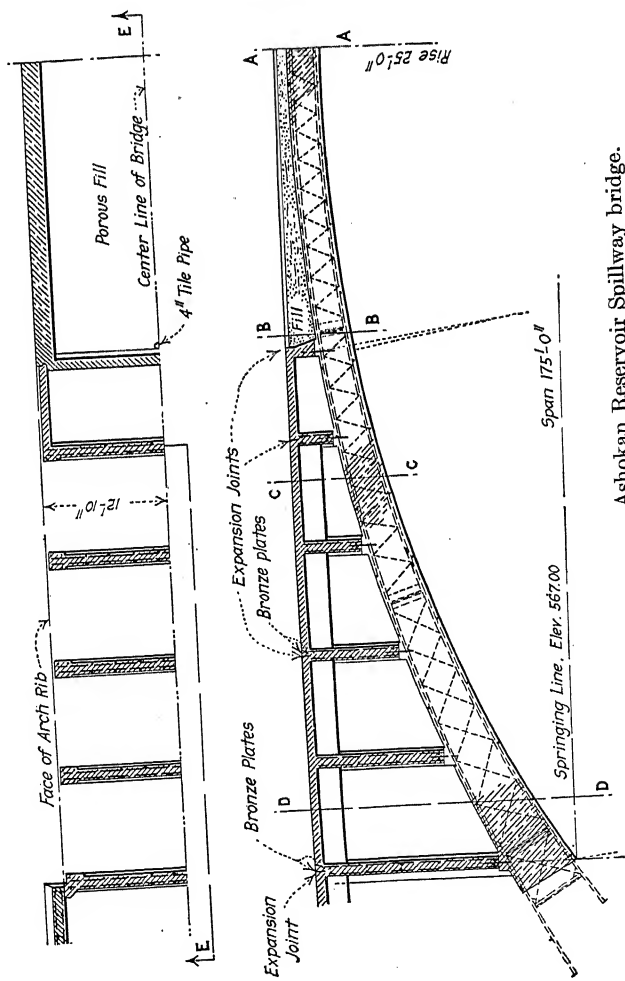
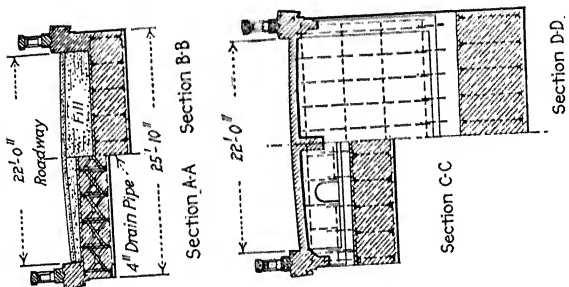
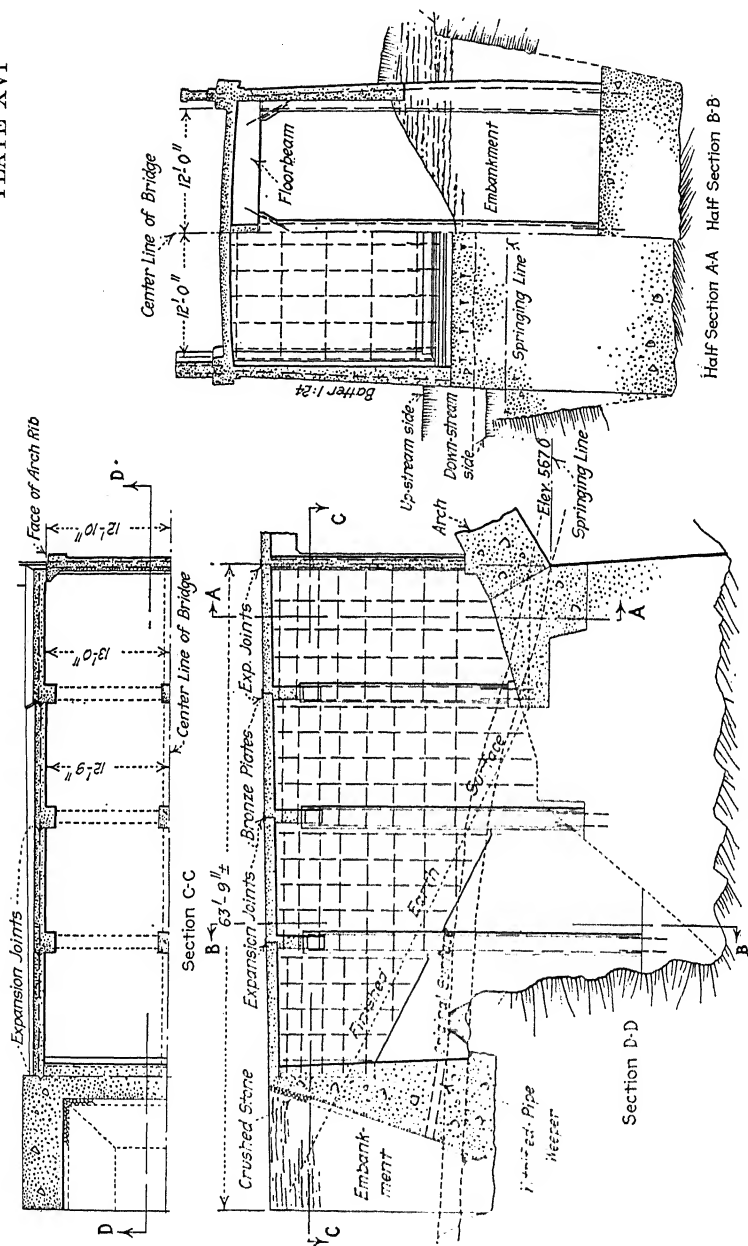


FIG. 215.—Falsework for Ashokan Reservoir Spillway bridge.

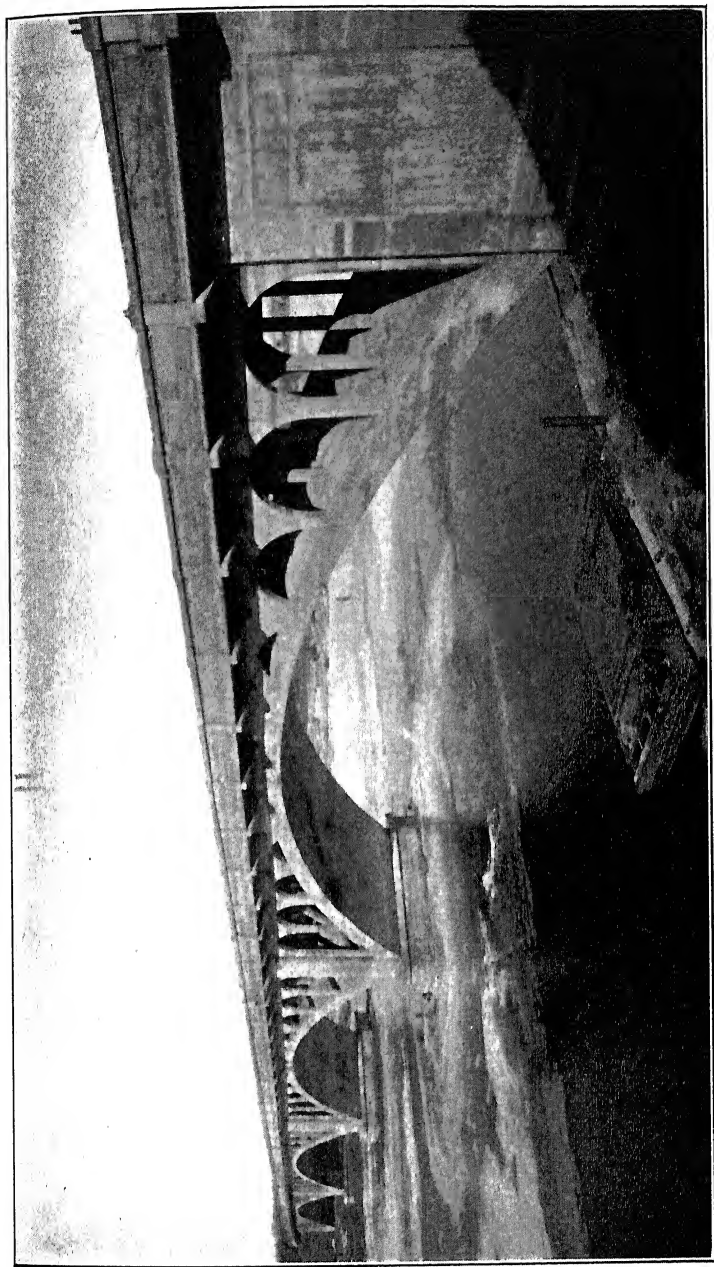
PLATE XV



Ashokan Reservoir Spillway bridge.

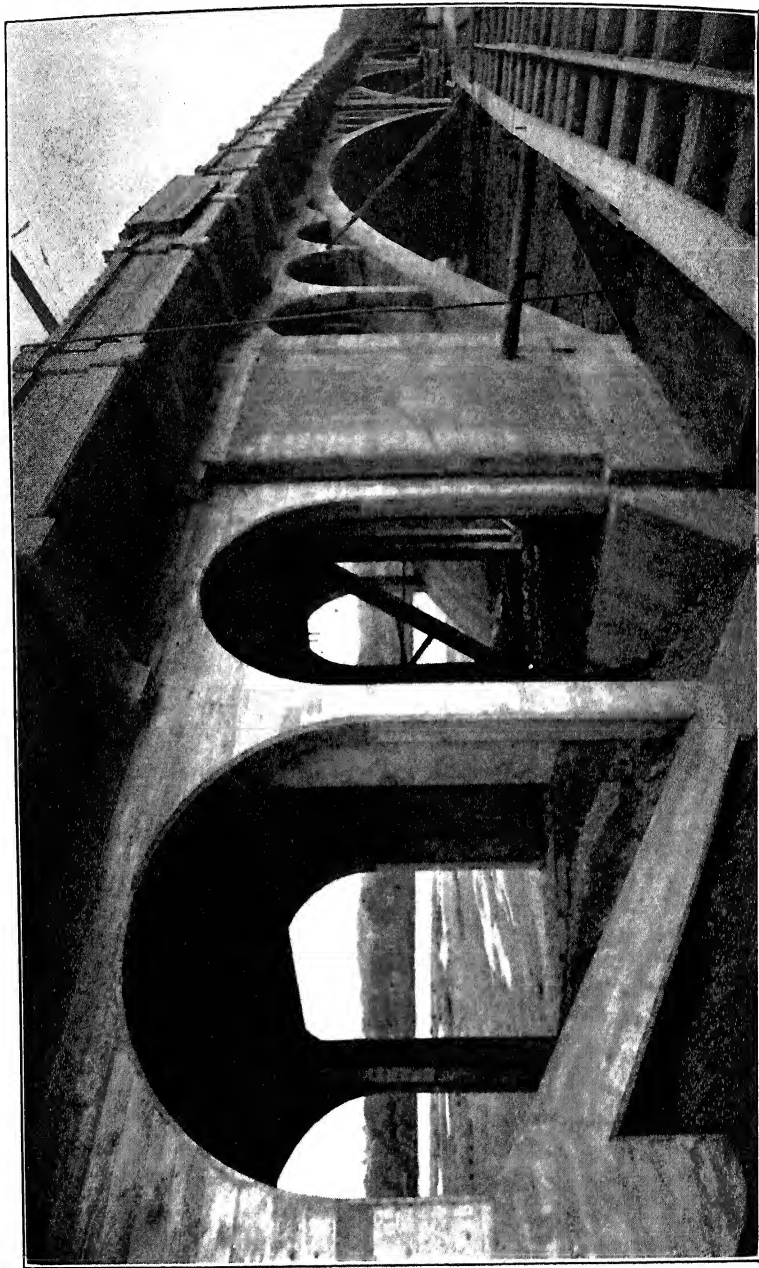


Ashokan Reservoir Spillway bridge.



*Courtesy of Mr. Louis P. Wolf, Consulting Engineer, St. Paul, Minn.*

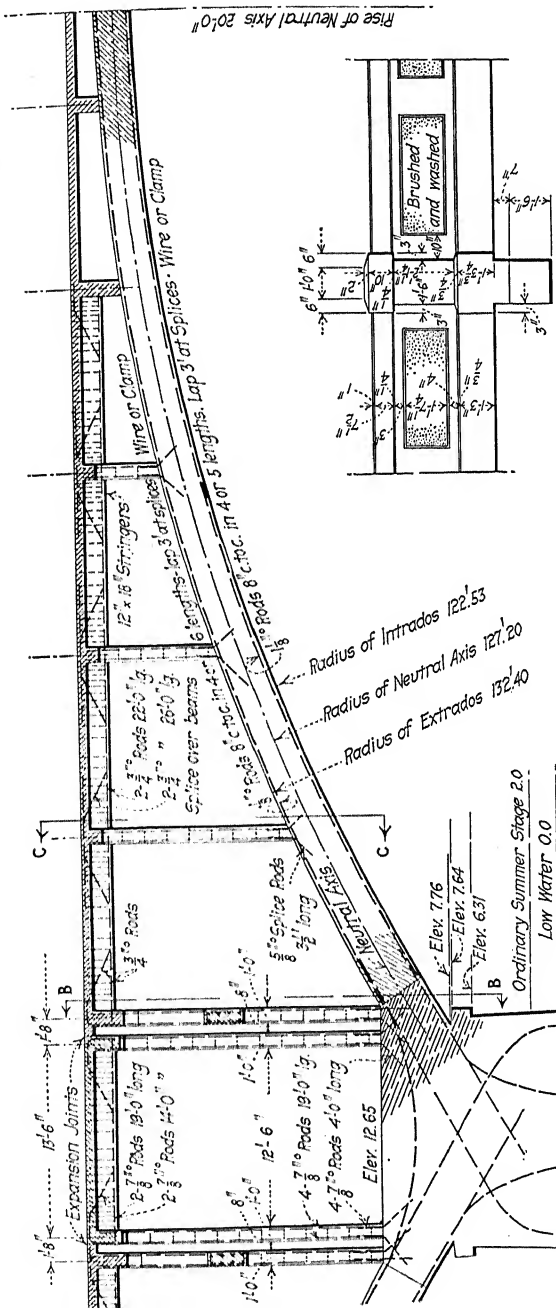
Fig. 216.—Chippewa River bridge, Eau Claire, Wis.



*Courtesy of Sandusky Portland Cement Co.*

FIG. 217.—Chippewa River bridge, Eau Claire, Wis.

PLATE XVII



### Railing between Piers

Chippewa River bridge, Eau Claire, Wis.

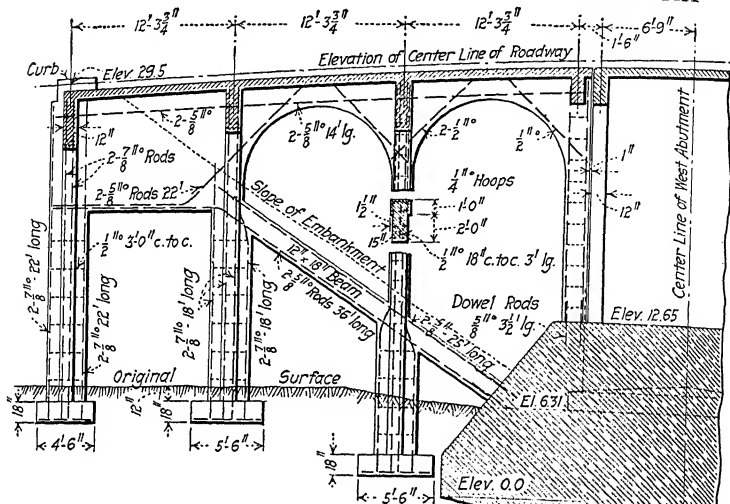
Wet Summer Stage 2.0  
Low Water 0.0



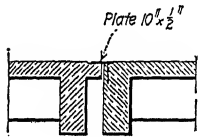




PLATE XX

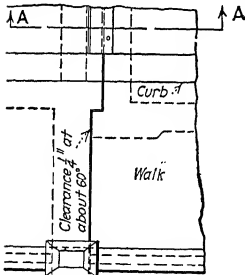
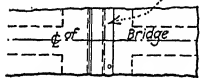


Longitudinal Section  
of West Approach

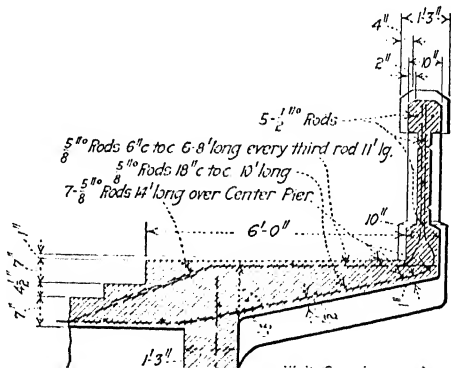
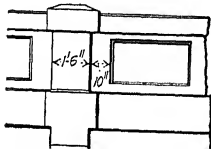


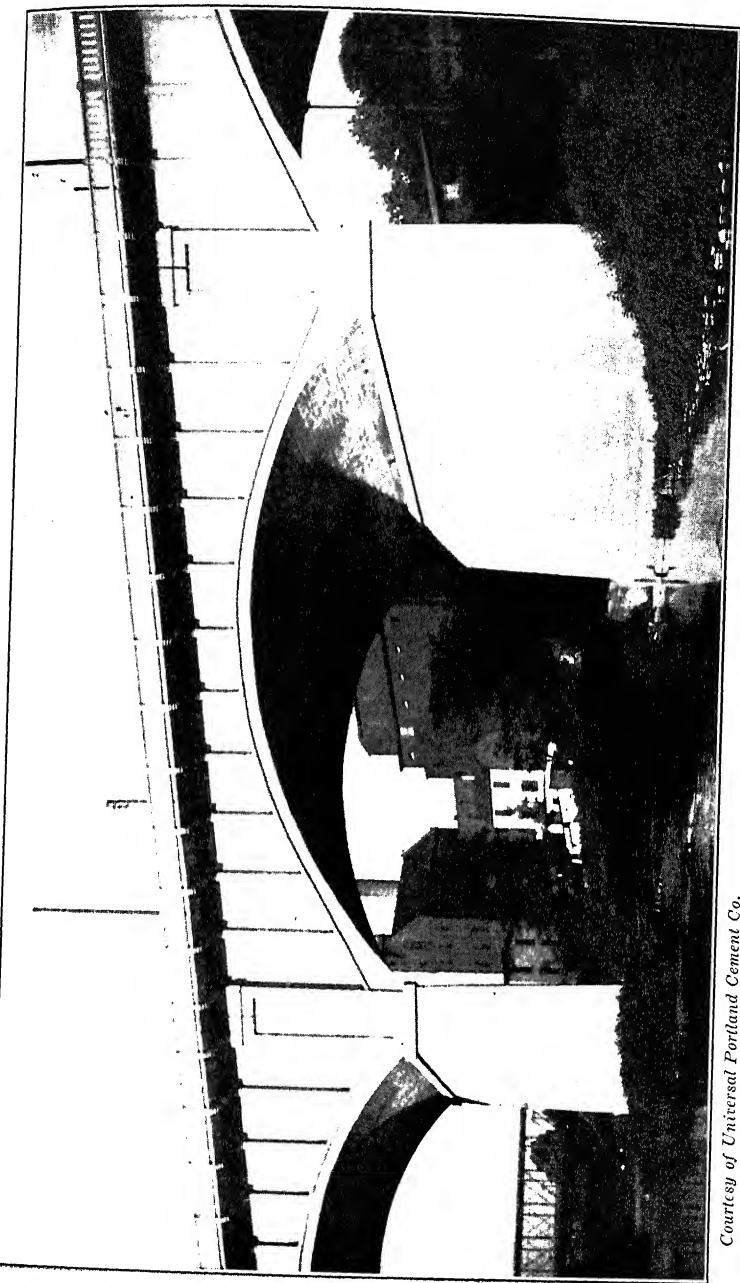
Section A-A

10" x  $\frac{1}{2}$ " x 21'-10" Plate over Expansion Joint  
anchored with  $\frac{5}{8}$ " Bolts with countersunk  
heads spaced about 2'-0" c. to c.



## Plan





*Courtesy of Universal Portland Cement Co.*

Fig. 218.—Ludlow Avenue viaduct, Cincinnati, Ohio.

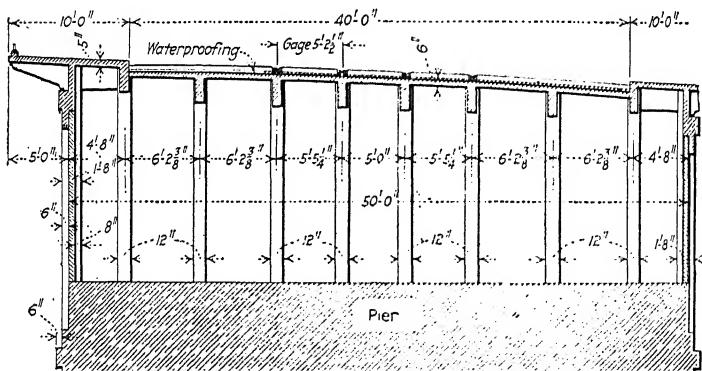
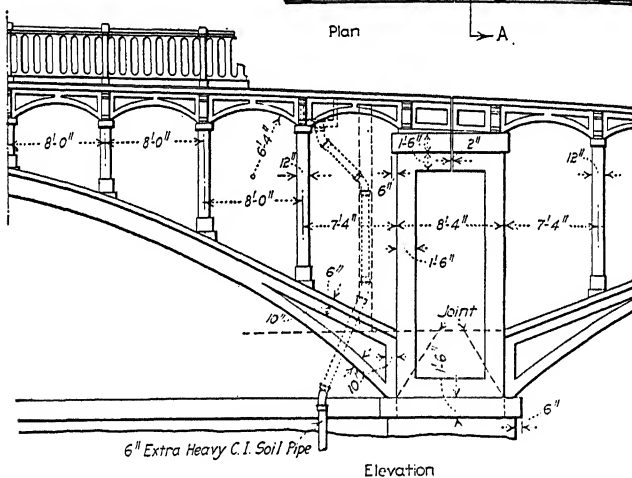
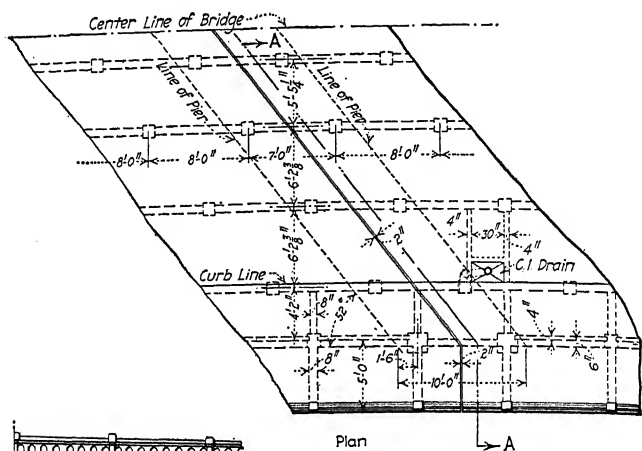
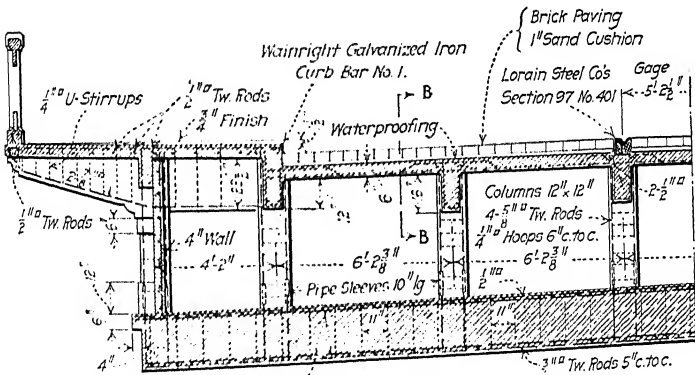
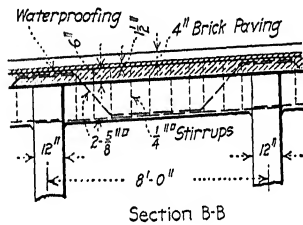
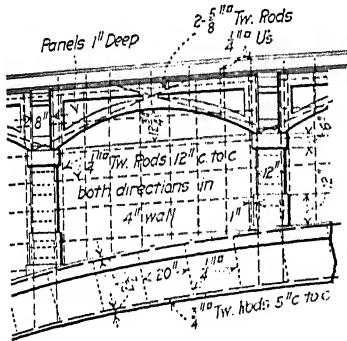
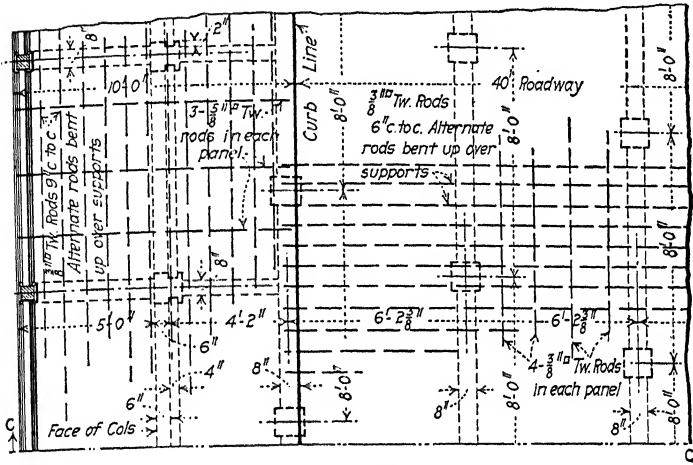
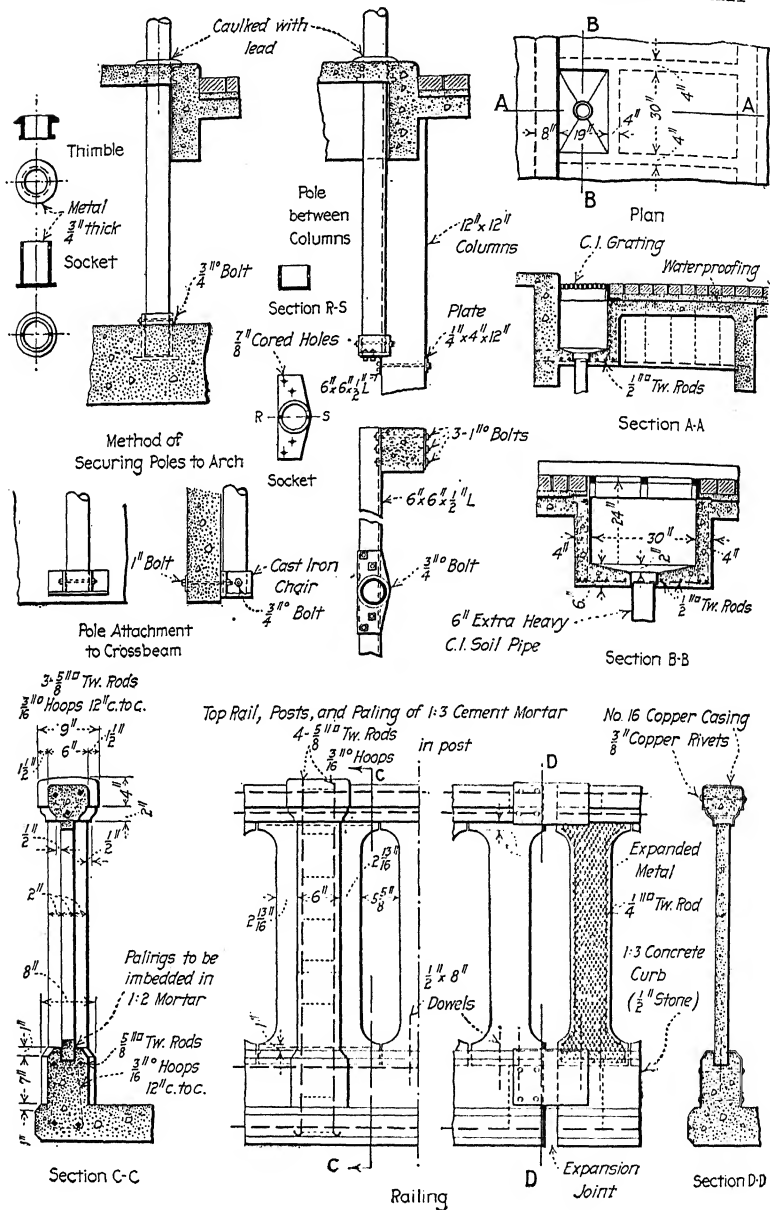
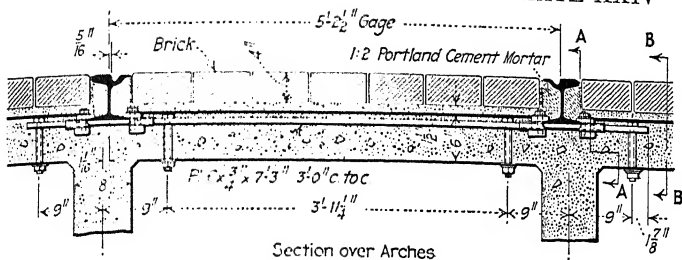


PLATE XXII

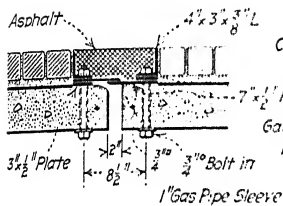




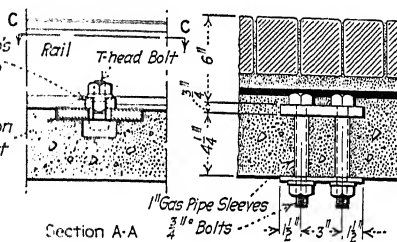
Ludlow Avenue viaduct, Cincinnati, Ohio.



Section over Arches

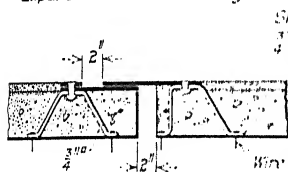


Detail of Expansion Joint in Roadway

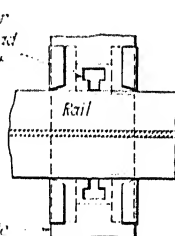


Section A-A

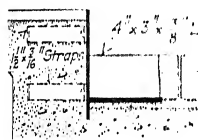
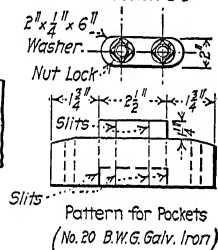
Section B-B



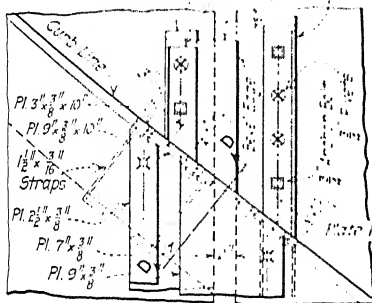
Detail of Expansion Joint in Sidewalk



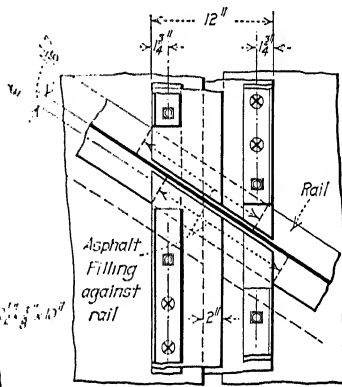
Section C-C



Section D-D showing Straps

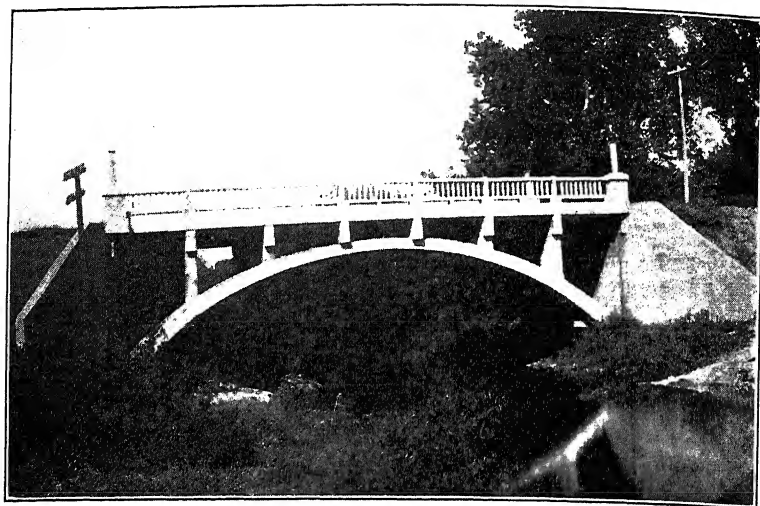


Expansion Joint Detail at Curb Line



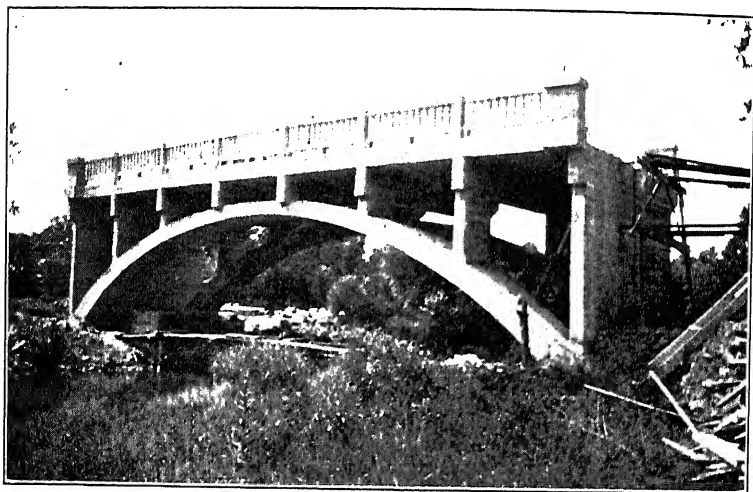
Plan of Expansion Joint in Roadway





*Courtesy of Mr. E. C. L. Wagner, Civil Engineer, Kansas City.*

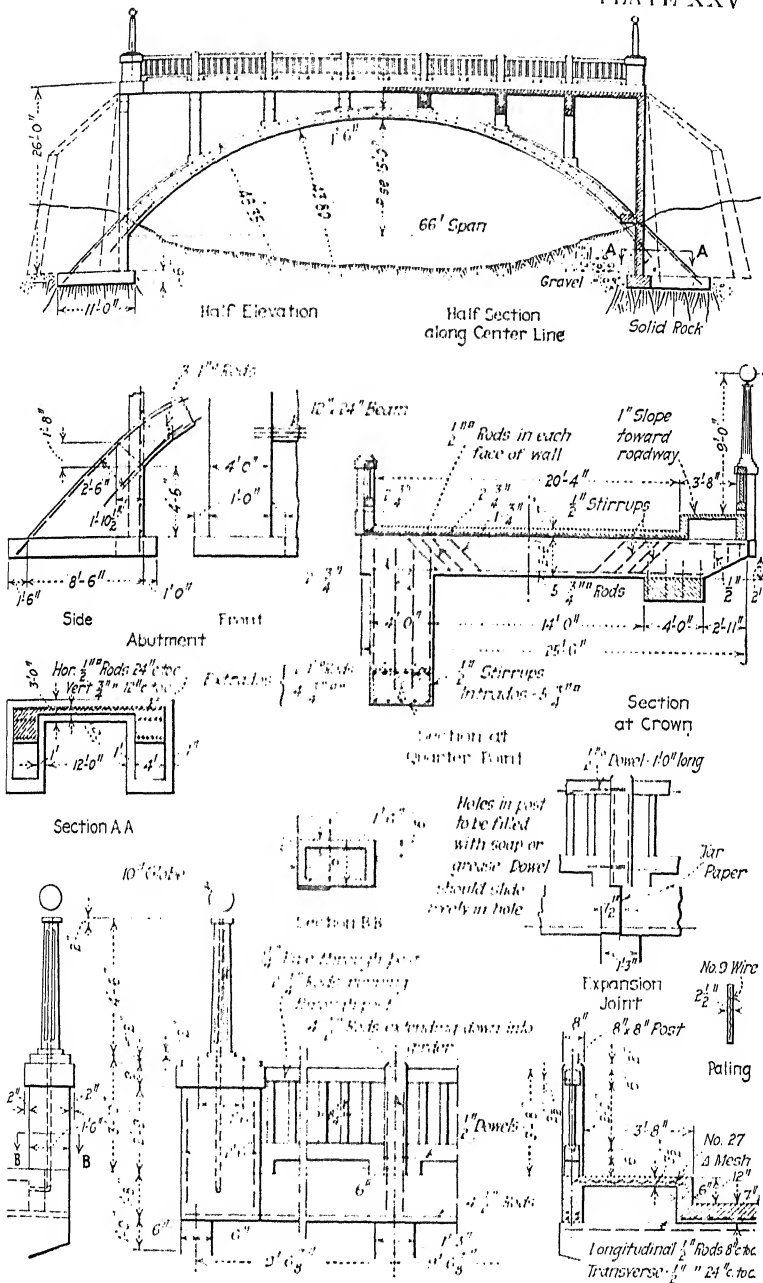
FIG. 219.—Stimson Creek bridge, Fulton, Mo.

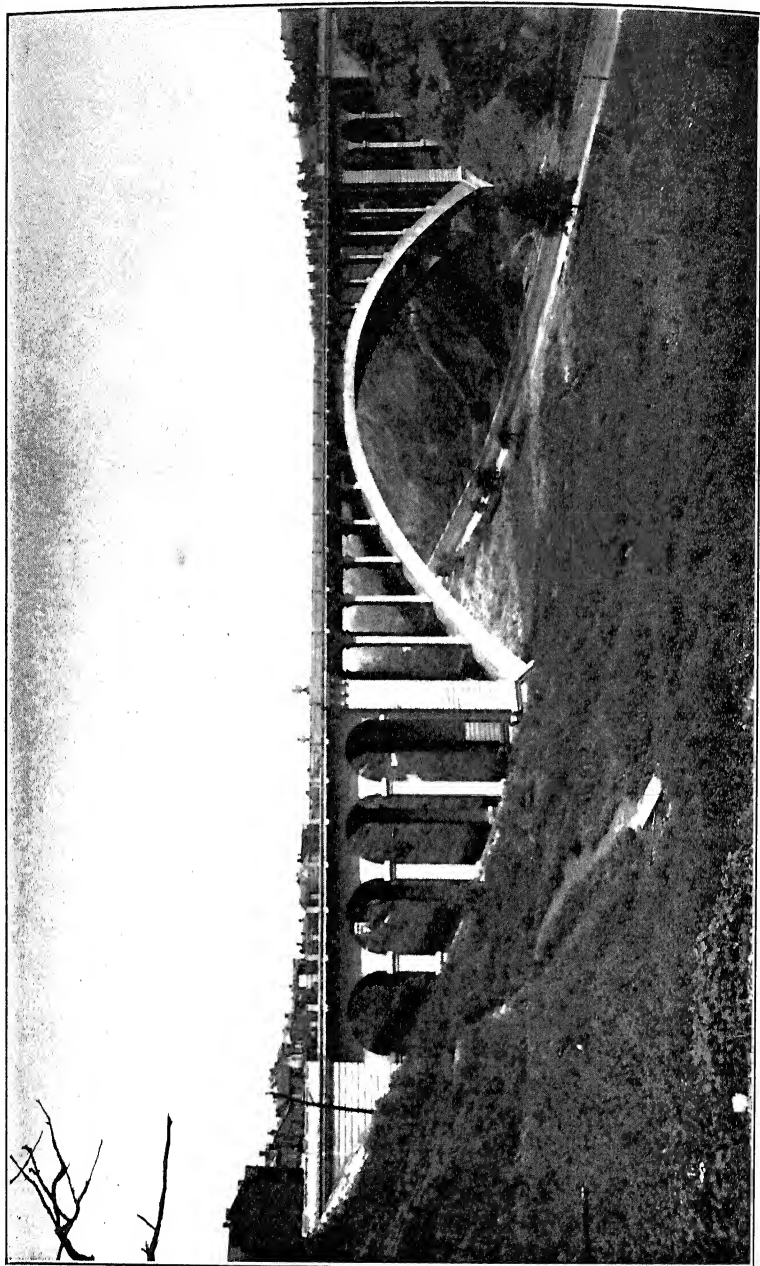


*Courtesy of Mr. E. C. L. Wagner, Civil Engineer, Kansas City.*

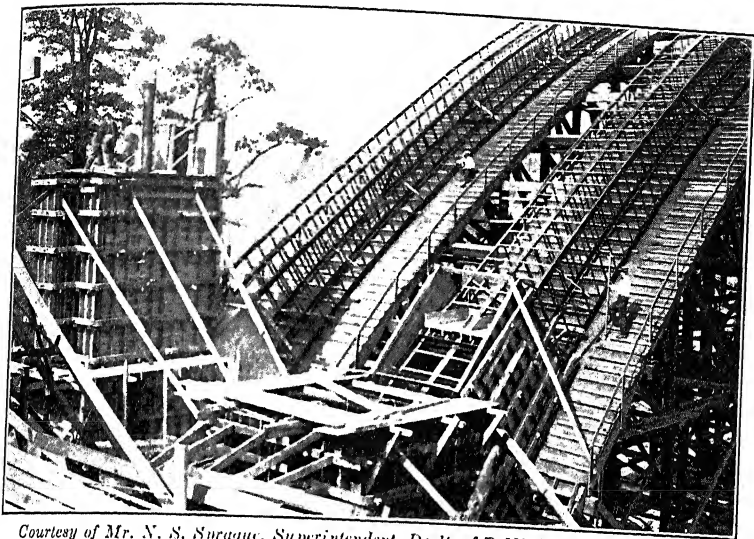
FIG. 220.—Construction view of Stimson Creek bridge, Fulton, Mo.

PLATE XXV



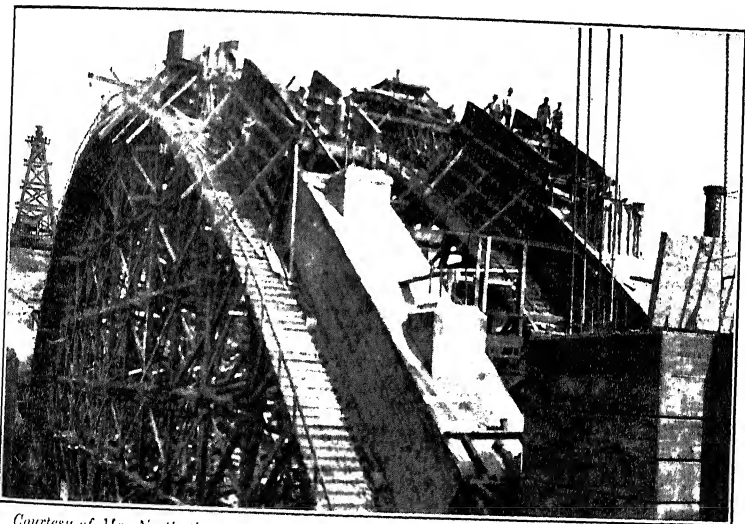


*Courtesy of Mr. N. S. Sprague, Superintendent, Dep't. of Public Works, Pittsburgh.*  
FIG. 221.—Larimer Avenue bridge, Pittsburgh, Pa.



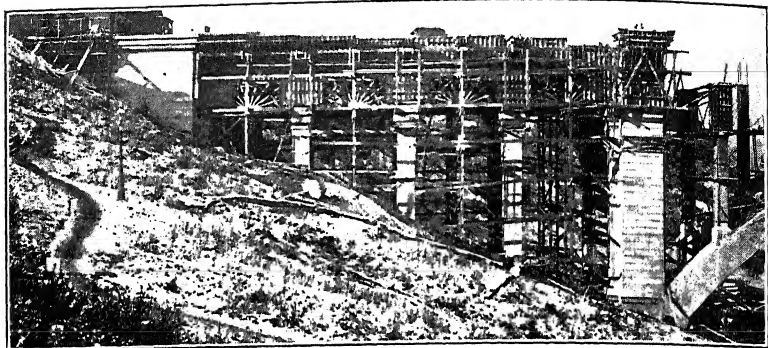
*Courtesy of Mr. N. S. Sprague, Superintendent, Dep't. of Public Works, Pittsburgh.*

FIG. 222.—Arch-rib reinforcement in place, Larimer Avenue bridge, Pittsburgh.



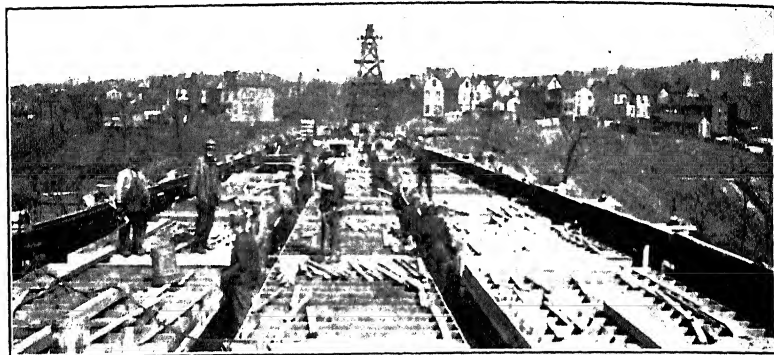
*Courtesy of Mr. N. S. Sprague, Superintendent, Dep't. of Public Works, Pittsburgh.*

FIG. 223.—Concreting of arch ribs, Larimer Avenue bridge, Pittsburgh.



*Courtesy of Engineering and Contracting.*

FIG. 224.—Construction view of west approach, Larimer Avenue bridge, Pittsburgh.



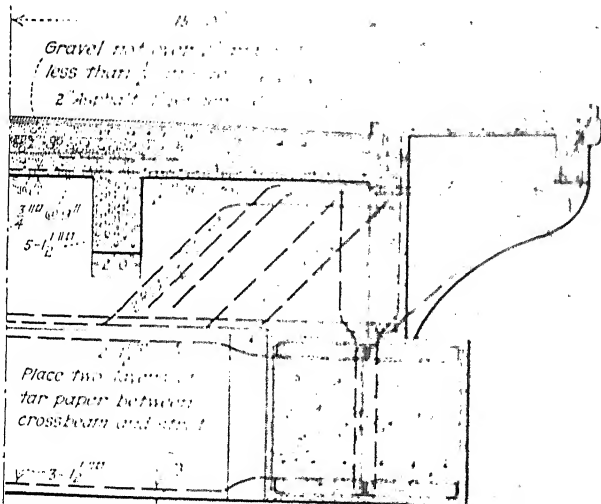
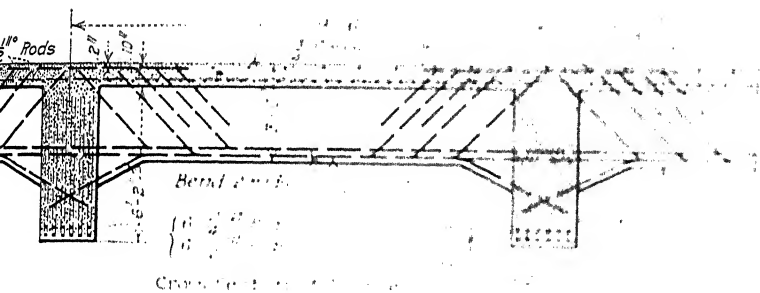
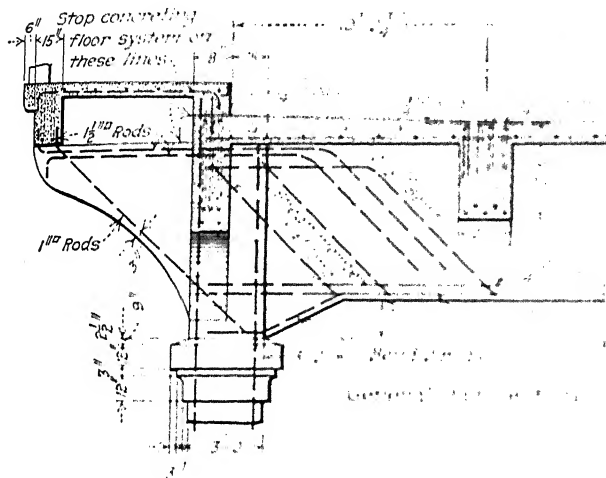
*Courtesy of Engineering and Contracting.*

FIG. 225.—Forms for floor system over main arch, Larimer Avenue bridge, Pittsburgh.



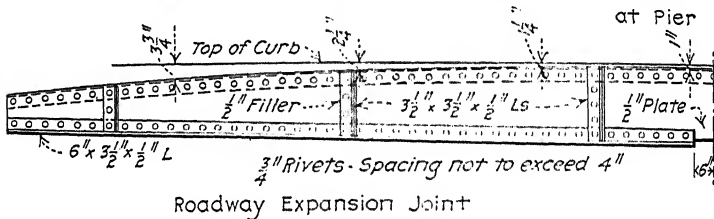
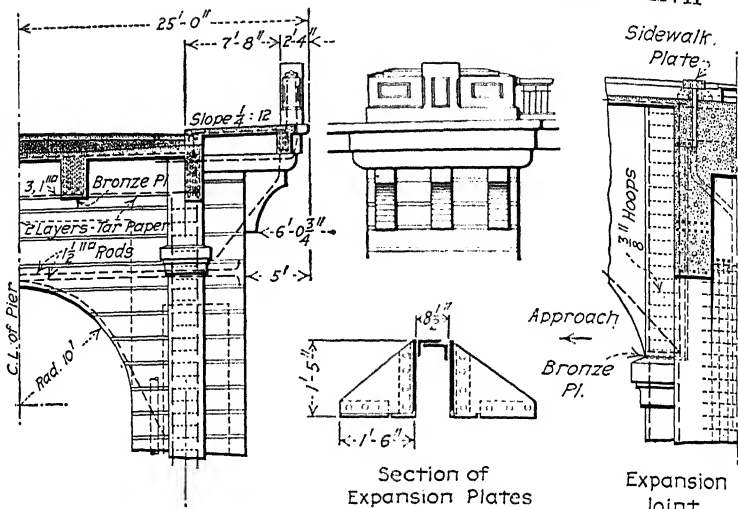
*Courtesy of Engineering and Contracting.*

FIG. 226.—View of traveler for suspending working scaffolds for bushhammer work, Larimer Avenue bridge, Pittsburgh.

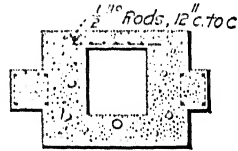
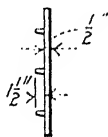


Place two layers of  
tar paper between  
crossbeams and rafters.

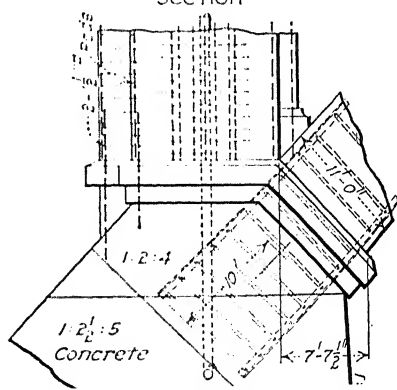
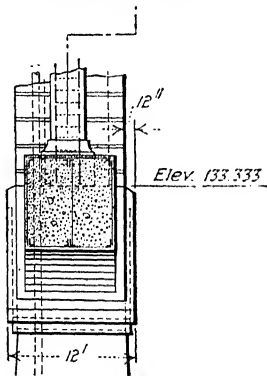
4-3-12



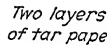
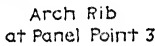
Bronze Plate



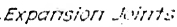
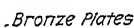
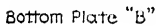
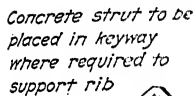
Section



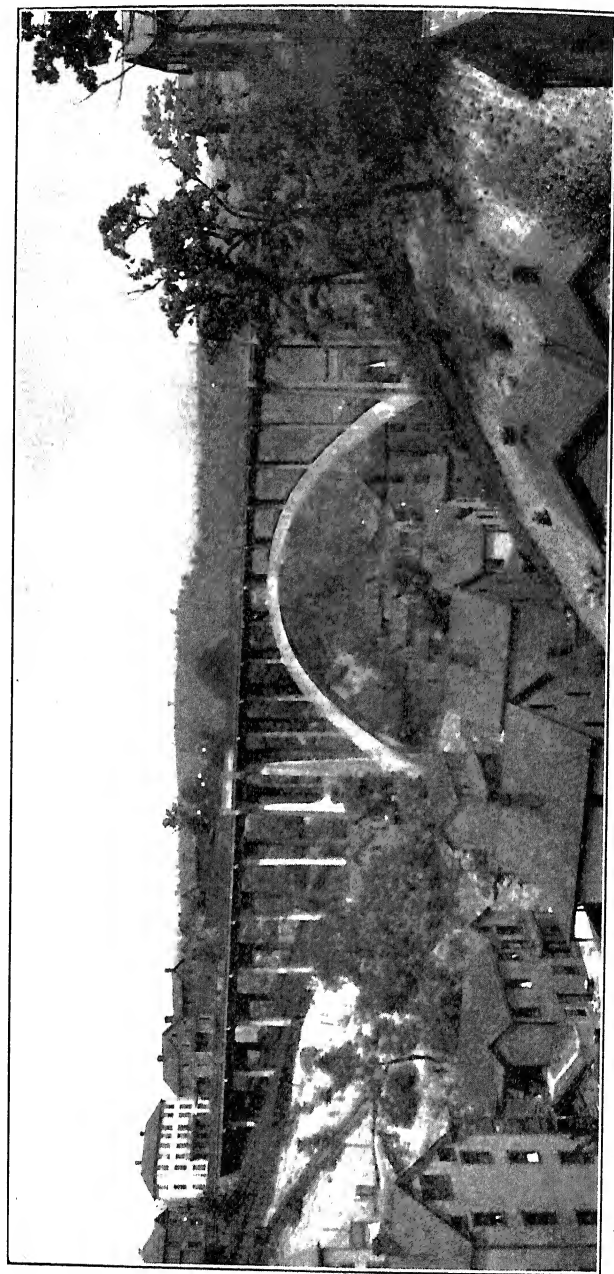
## PLATE XXVIII



Section  
showing  
Double Floorbeam

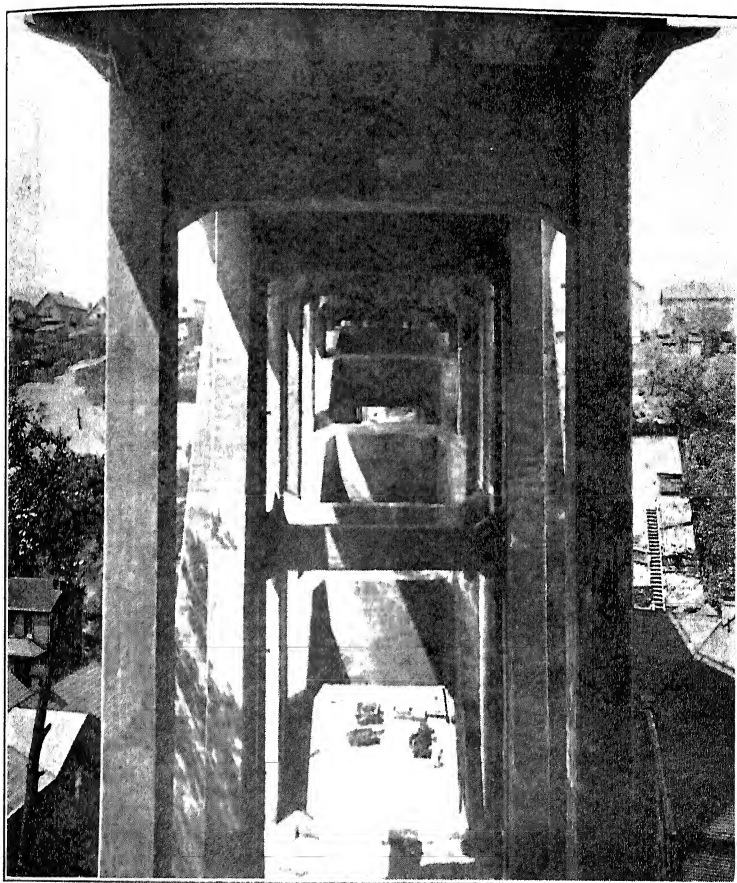






*Courtesy of Chester & Fleming, Engineers, Pittsburgh.*

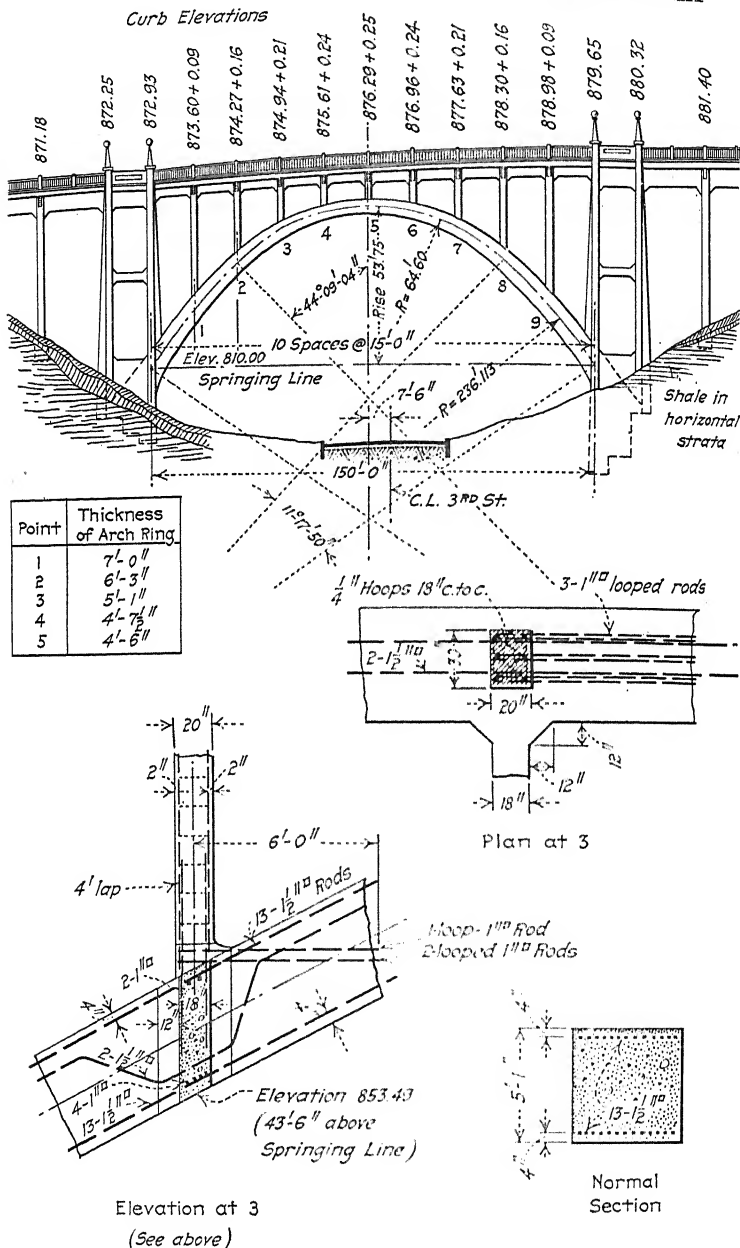
FIG. 227.—Monessen viaduct, Monessen, Pa.



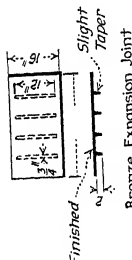
*Courtesy of Chester & Fleming, Engineers, Pittsburgh.*

FIG. 228.—Monessen viaduct, Monessen, Pa.

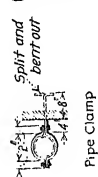
## PLATE XXIX





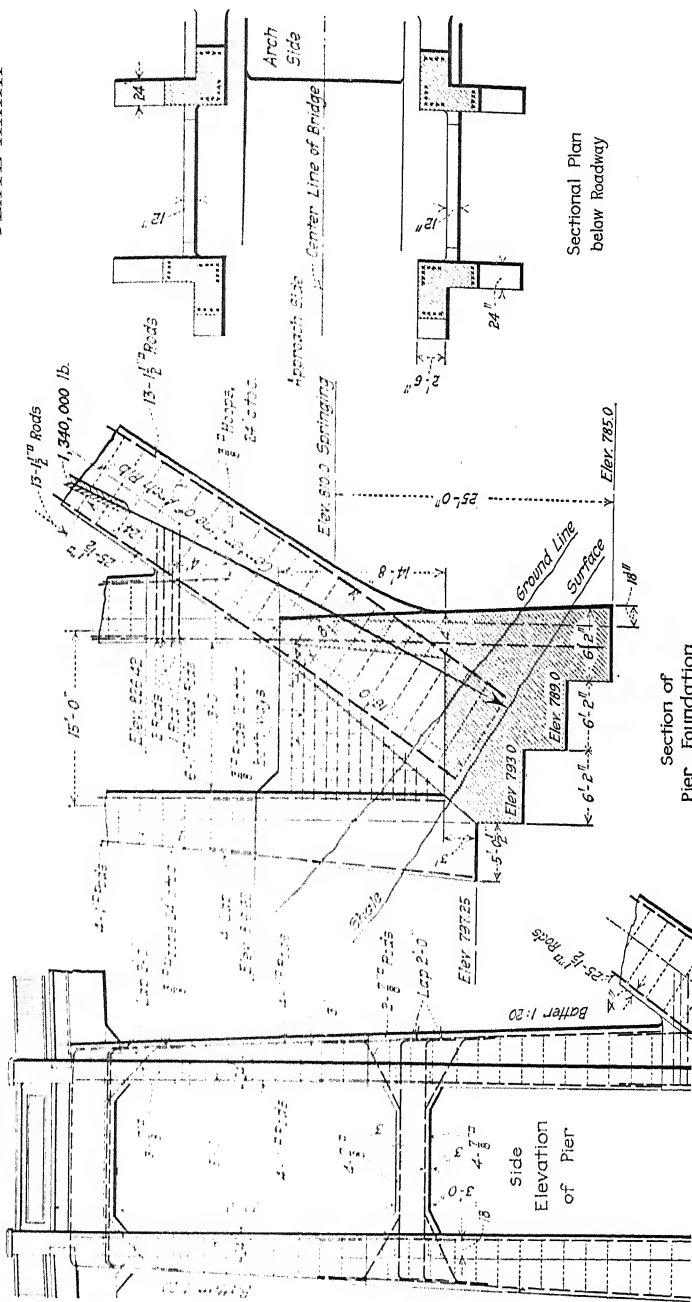


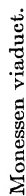
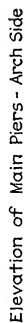
End View of Pier - Arch Side

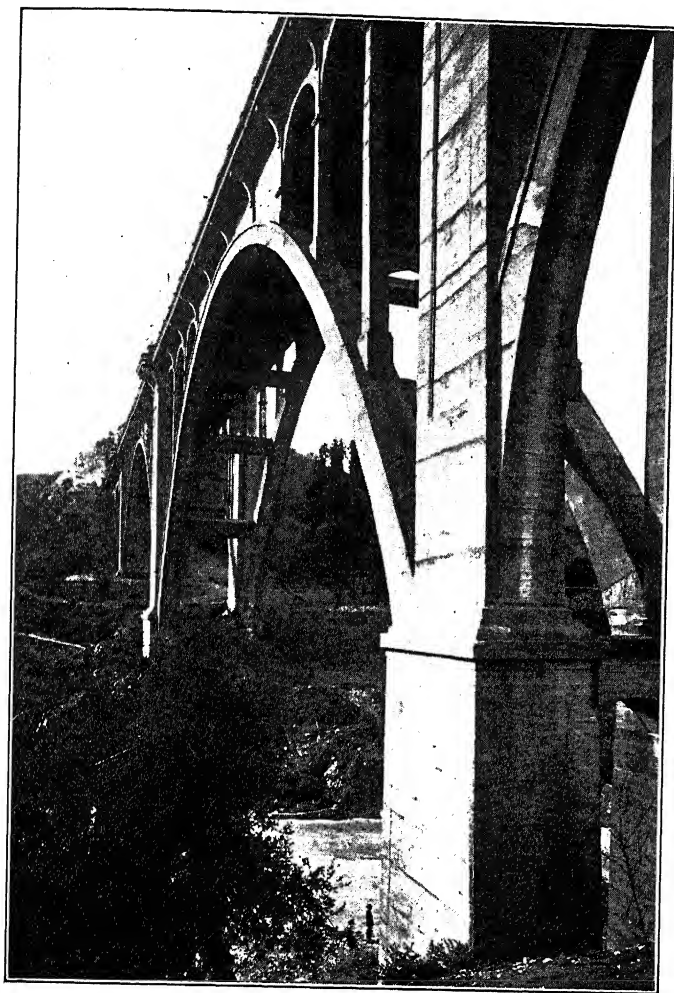


Section on Center Line of Bridge

Monessen viaduct.



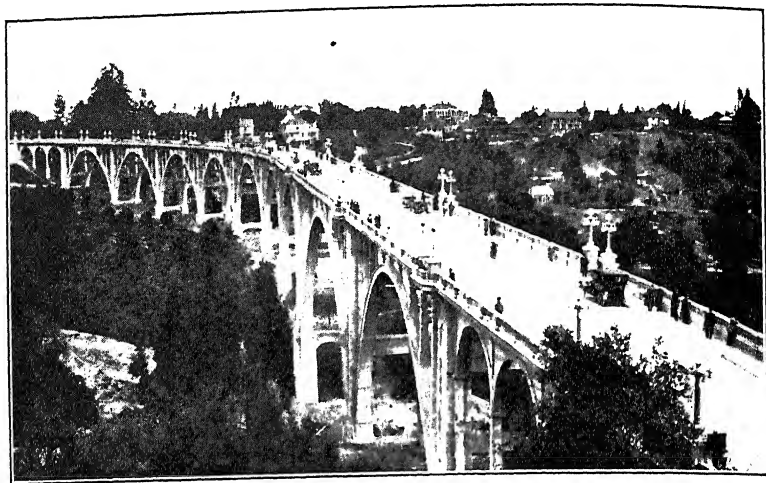
Rear  
Elevation



*Courtesy of Concrete-Cement Age.*

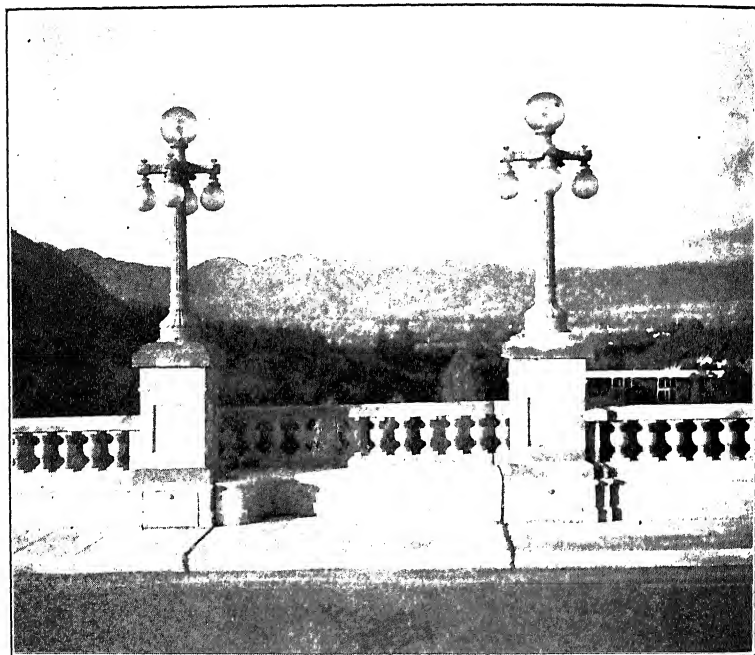
FIG. 229.—Bridge over the Arroyo Seco, Pasadena, Cal.





*Courtesy of Mr. Charles A. Byers, Los Angeles, Cal.*

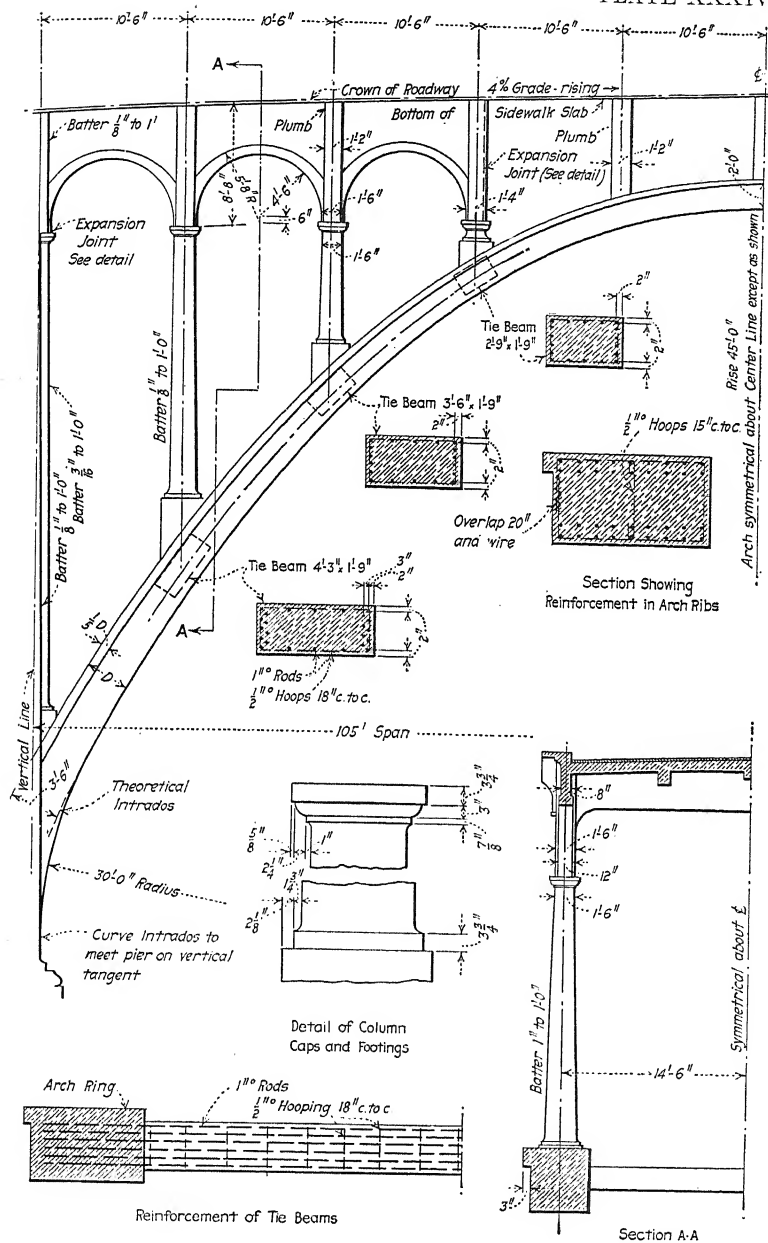
FIG. 230.—General view of bridge over the Arroyo Seco, Pasadena, Cal.



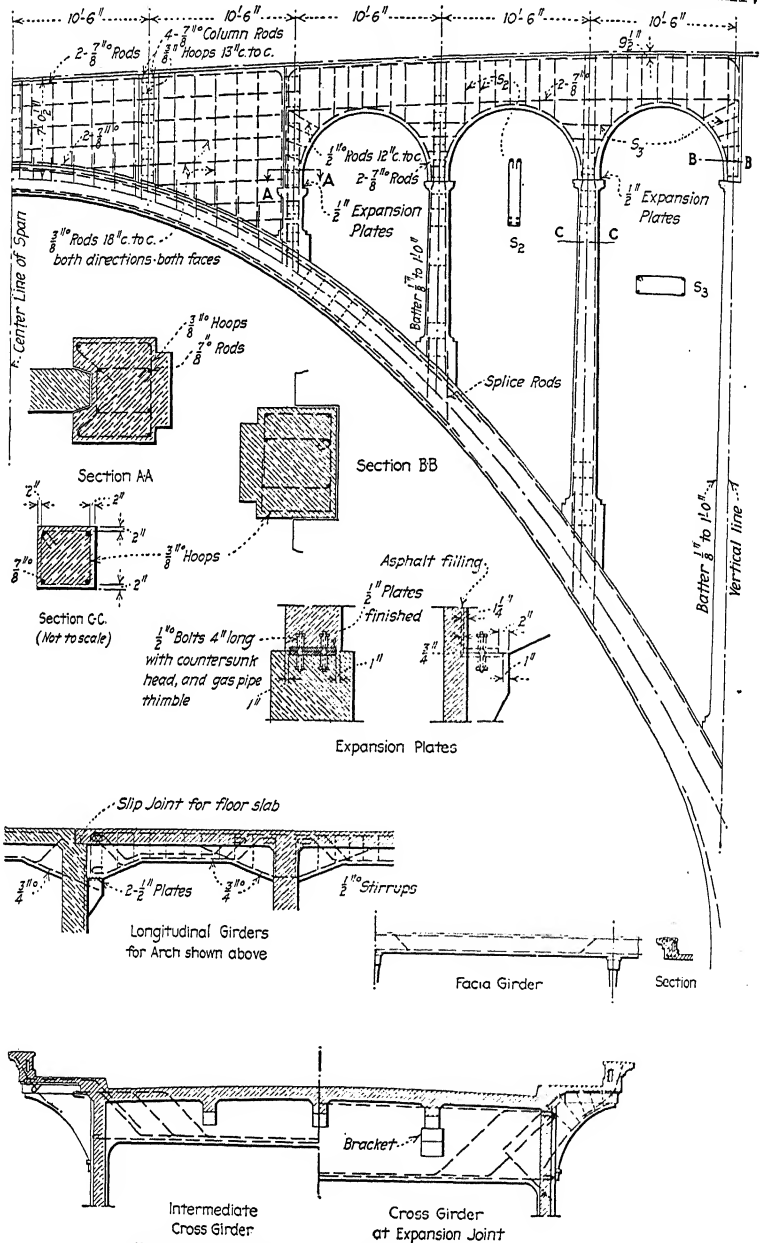
*Courtesy of Mr. Charles A. Byers, Los Angeles, Cal.*

FIG. 231.—Refuge bay on bridge over the Arroyo Seco, Pasadena, Cal.

## PLATE XXXIV

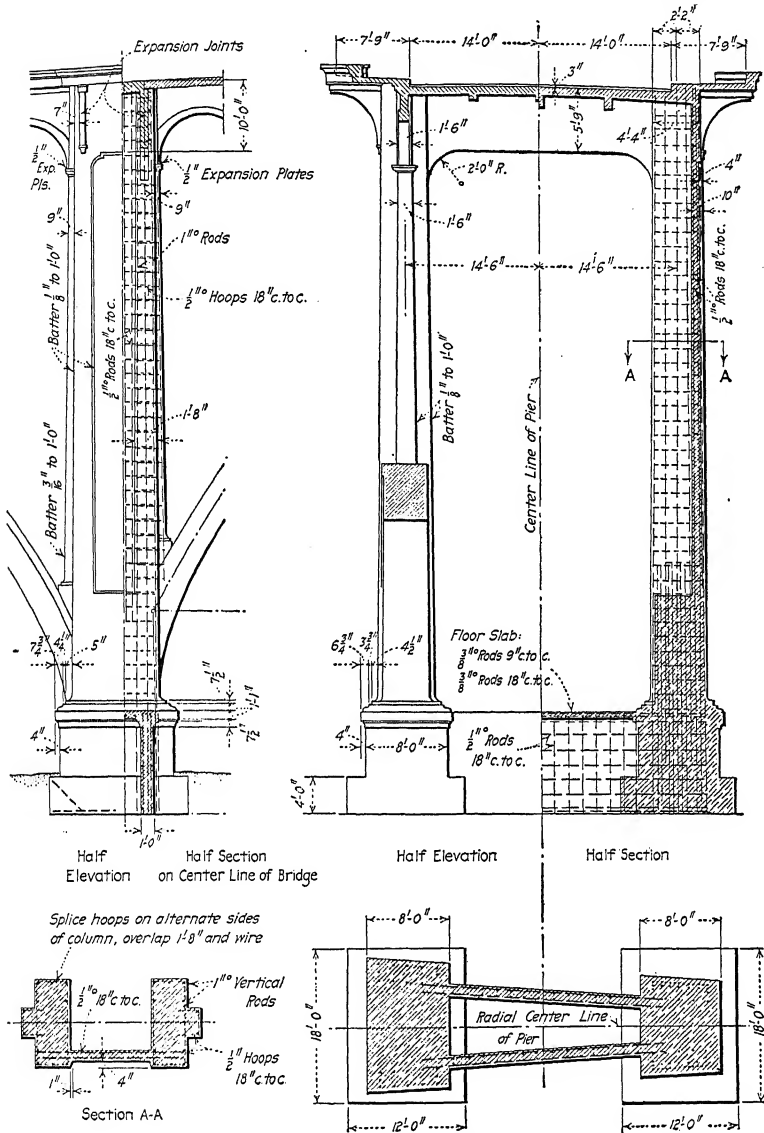


Bridge over the Arroyo Seco, Pasadena, Cal.

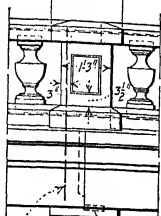
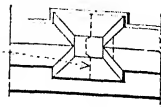


Bridge over the Arroyo Seco, Pasadena, Cal.

## PLATE XXXVI

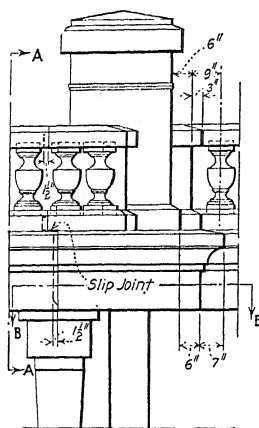


Bridge over the Arroyo Seco, Pasadena, Cal.

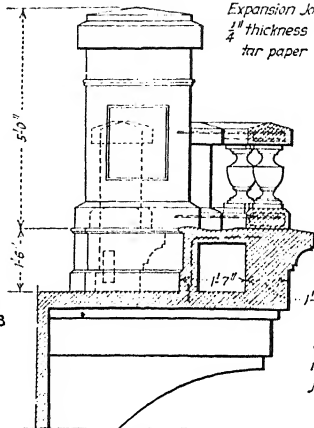


4 -  $\frac{3}{8}$ " Rods  
in posts at  
joints only

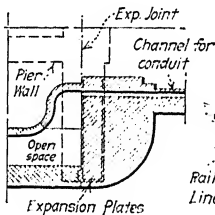
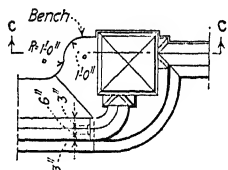
Exp  
P/s.



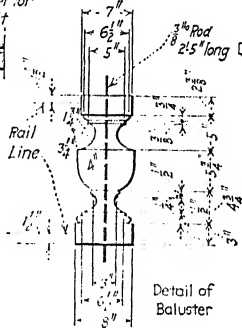
Main Post and Refuge Bay



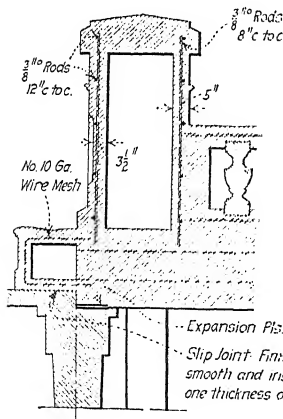
Section A-A through Bench



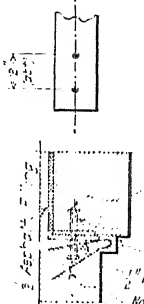
Section BB



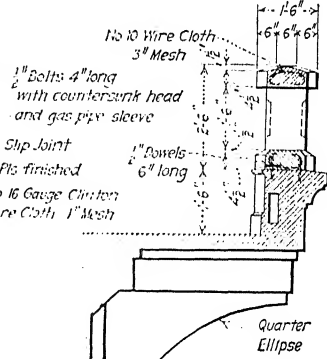
### Detail of Baluster



Section C-C

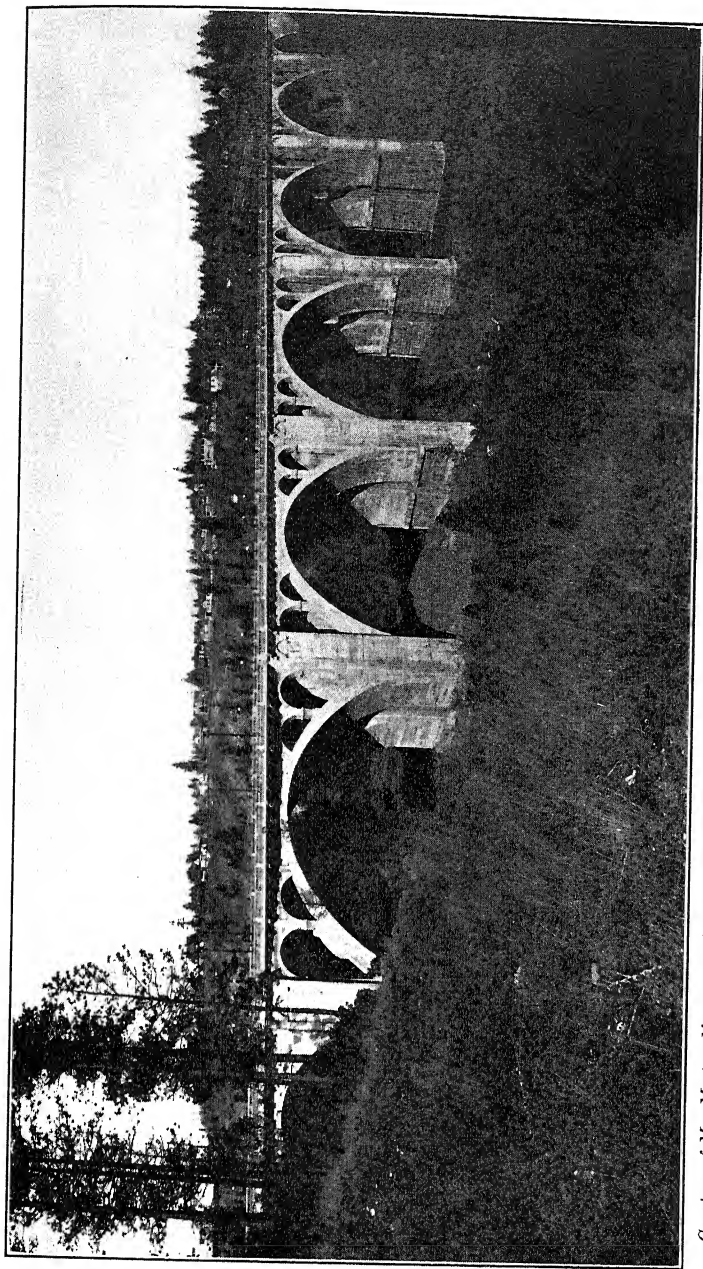


### Details of Expansion Plates for Facia



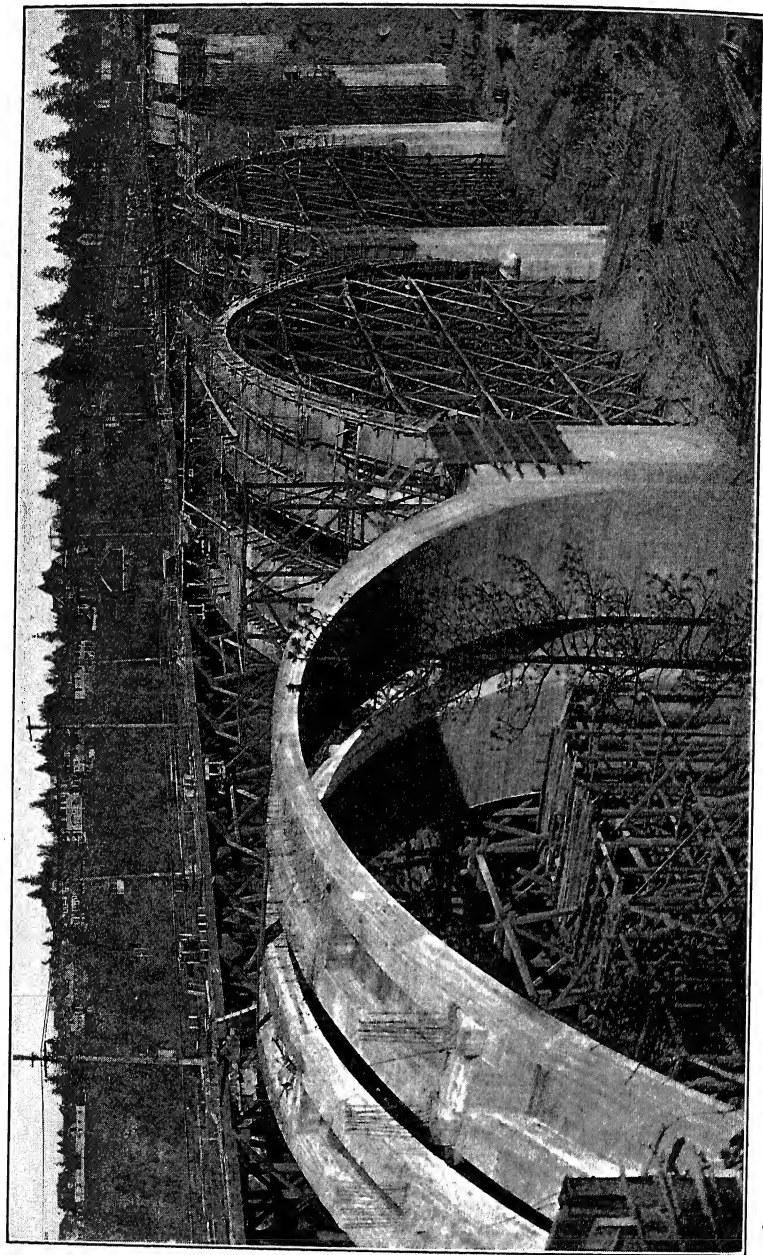
Quarter  
Ellipse

Bridge over the Arroyo Seco, Pasadena, Cal.



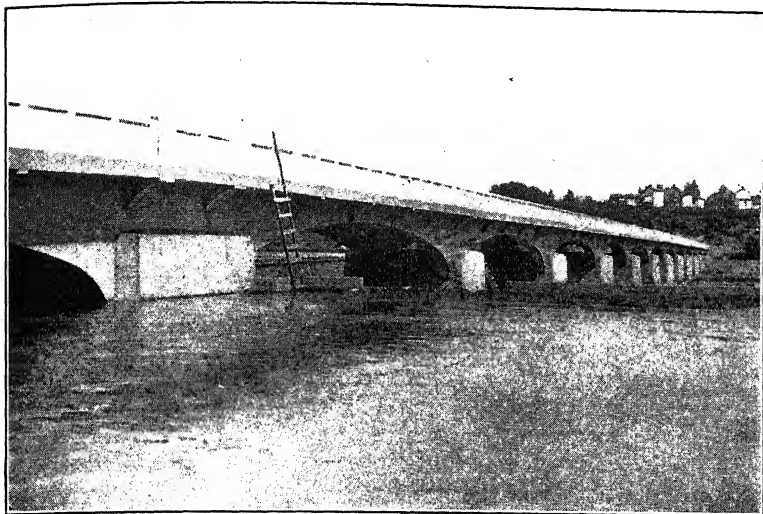
*Courtesy of Mr. Morton Macartney, City Engineer, Spokane.*

FIG. 232.—Latah Creek bridge, Spokane, Wash.



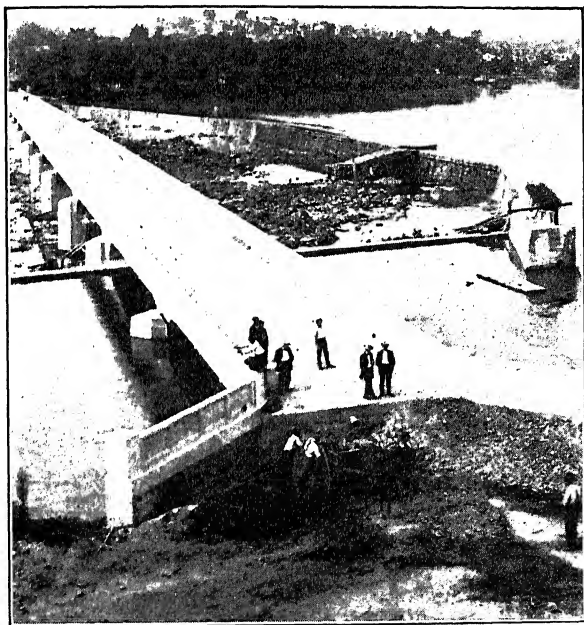
*Courtesy of Mr. Morton Macartney, City Engineer, Spokane.*

FIG. 233.—Construction view of Latah Creek bridge, Spokane, Wash.



*Courtesy of Mr. Wilbur J. Watson, Consulting Engineer, Cleveland.*

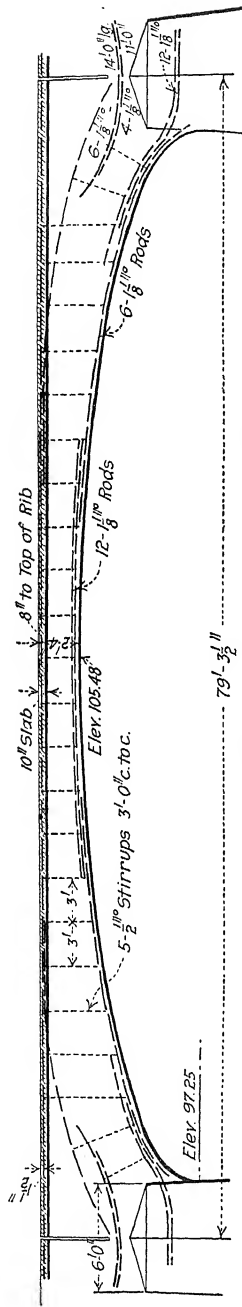
FIG. 234.—Highway bridge at Danville, Va.



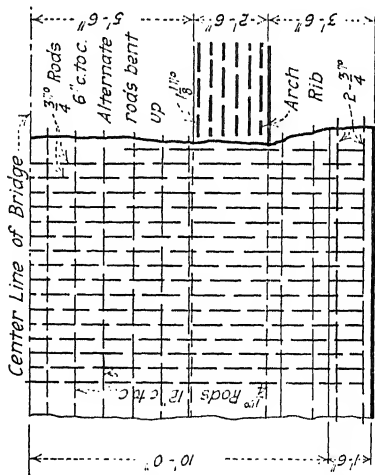
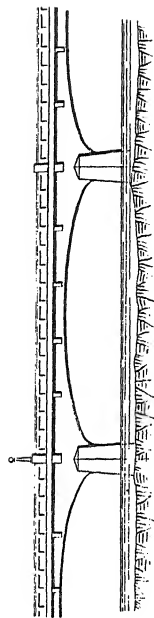
*Courtesy of Mr. Wilbur J. Watson, Consulting Engineer, Cleveland.*

FIG. 235.—General view of highway bridge at Danville, Va.

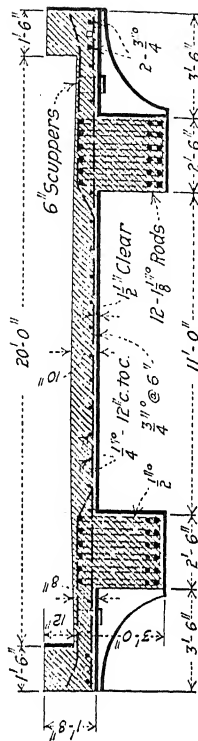




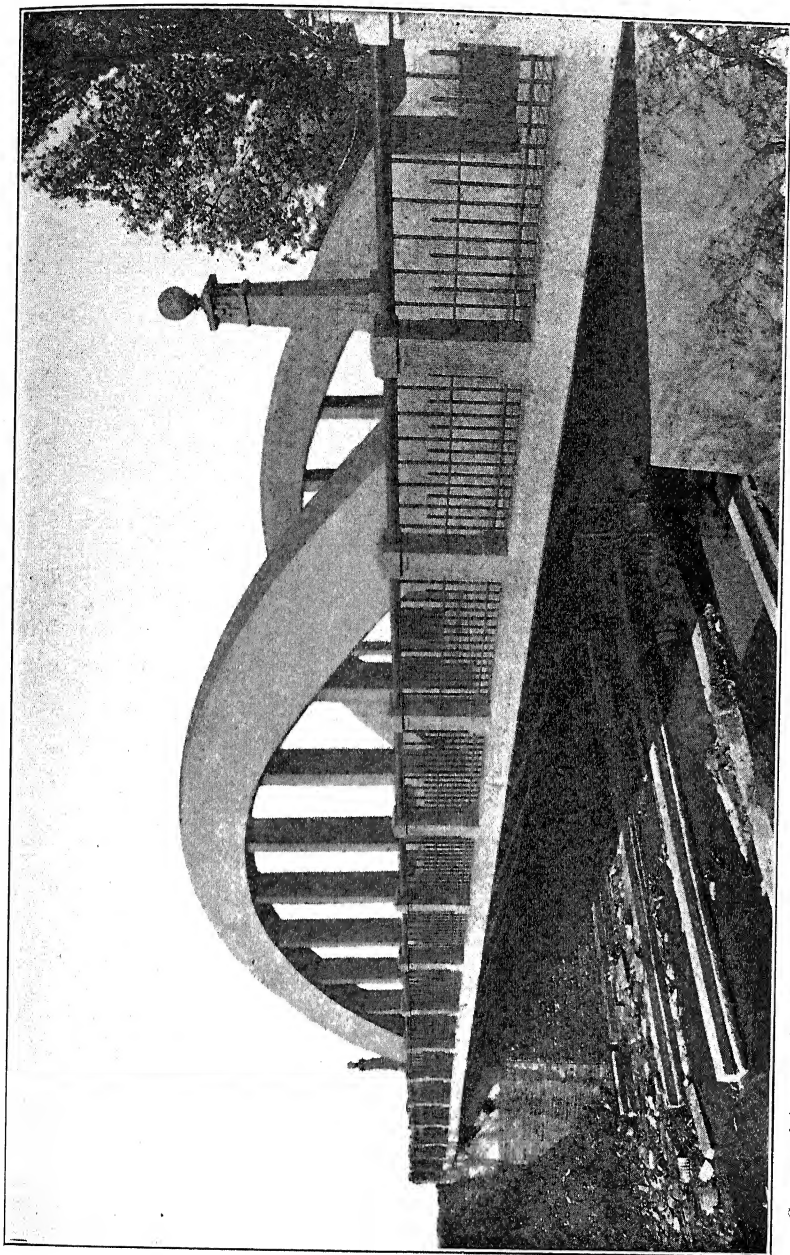
Longitudinal Section on Center Line of Bridge.



Part Plan of Floor Slab

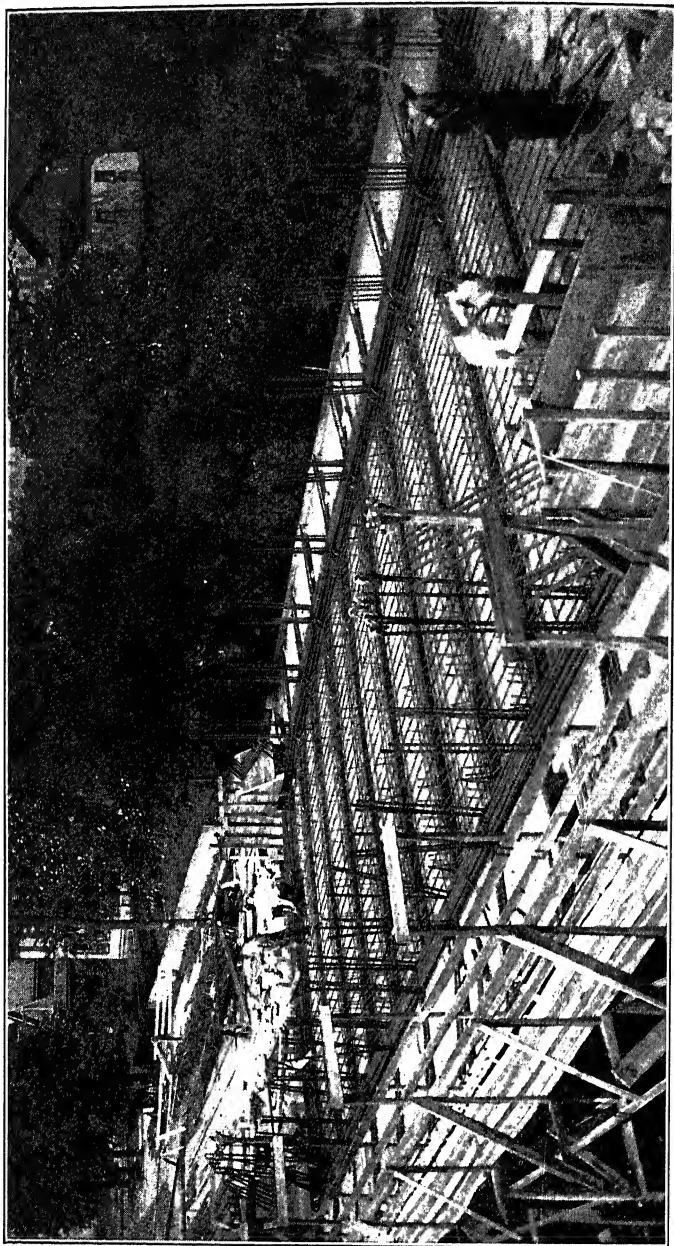


Highway bridge at Danville, Va.



*Courtesy of Assoc. of American Portland Cement Mfrs.*

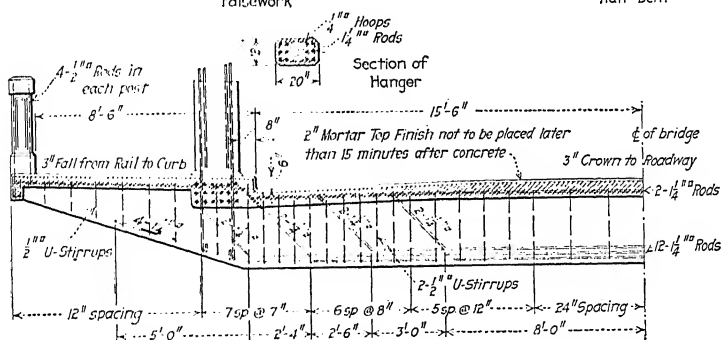
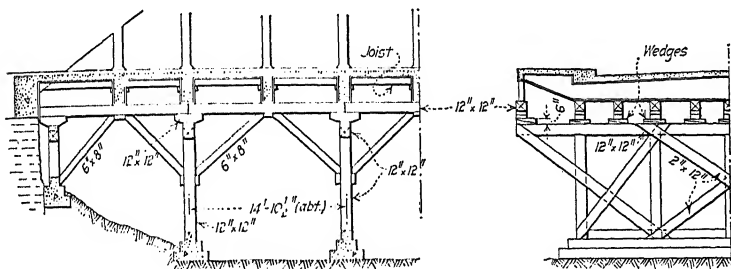
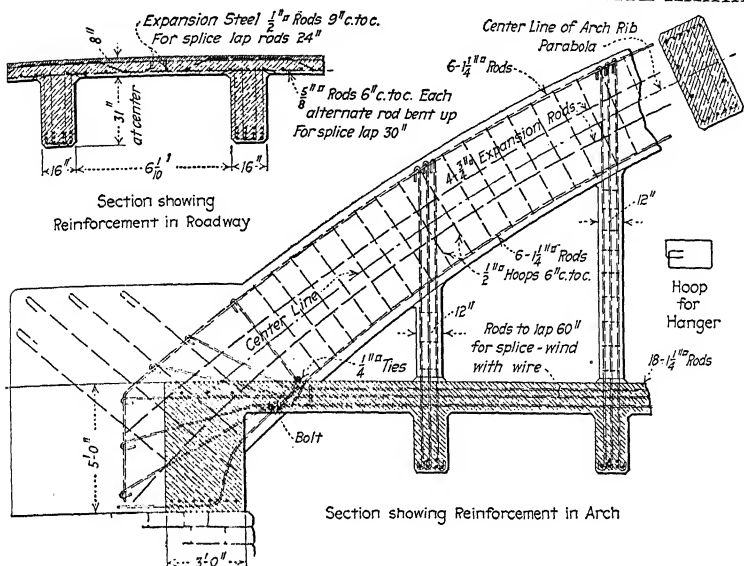
Fig. 236.—Benson Street bridge over Mill Creek at Lockland, Ohio.



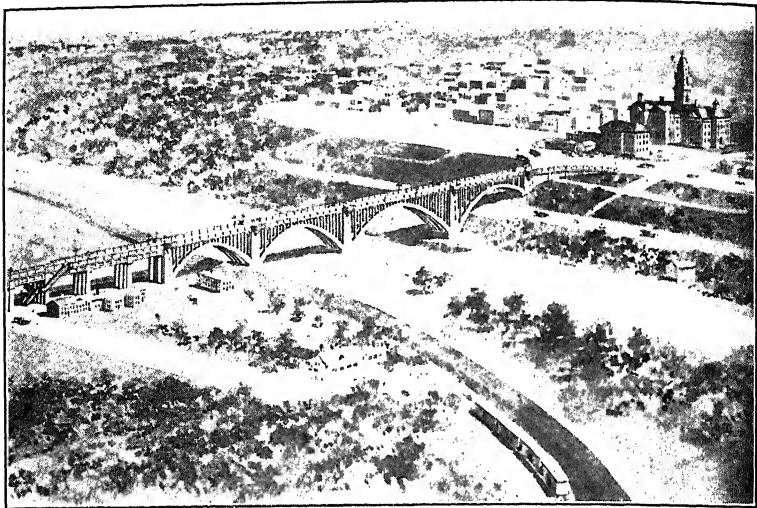
*Courtesy of Mr. E. A. Gast, Deputy County Surveyor, Hamilton County, Ohio.*

FIG. 237.—Construction view, Benson Street bridge over Mill Creek at Lockland, Ohio.

## PLATE XXXIX

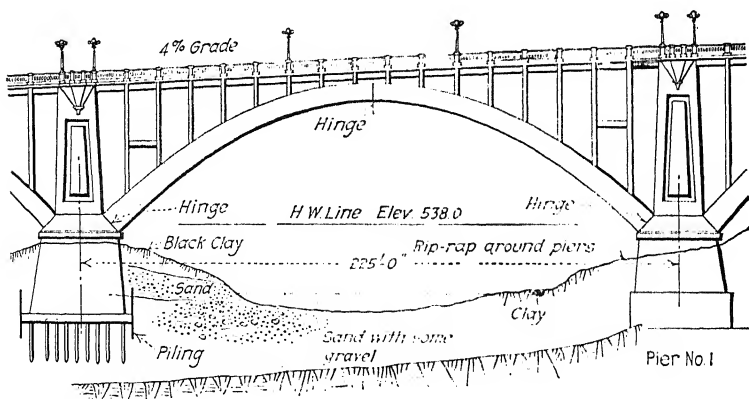


Benson Street bridge over Mill Creek at Lockland, Ohio.



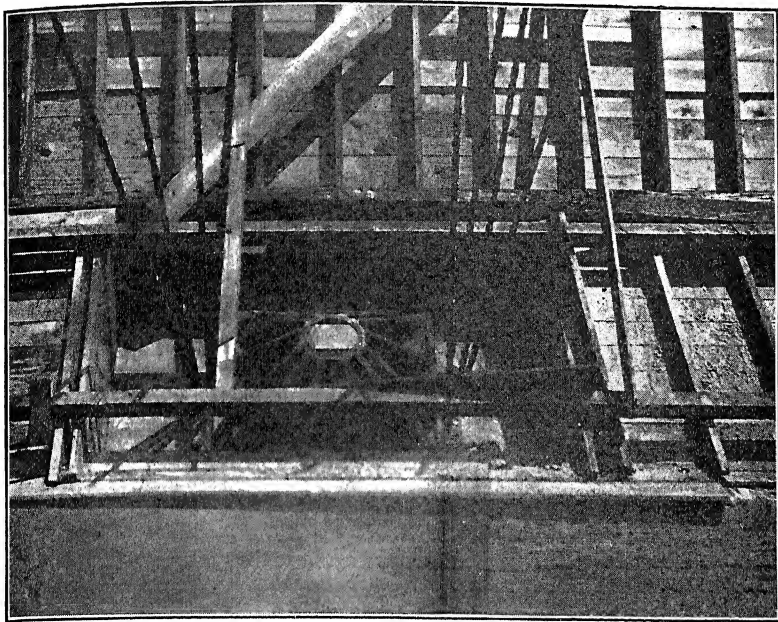
*Courtesy of Mr. S. W. Bowen of Brenneke and Fay, Consulting Engineers, St. Louis.*

FIG. 238.—Main Street viaduct, Fort Worth, Texas, from an artist's perspective.



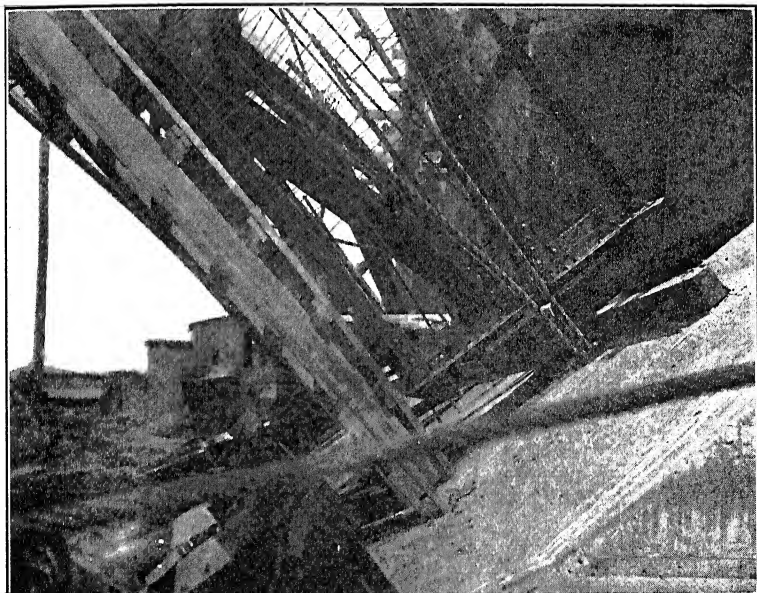
Pier No. 2

FIG. 239.—River span, Main Street viaduct, Fort Worth, Texas.

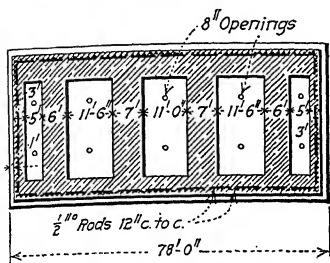


*Courtesy of Mr. S. W. Bowen, St. Louis.*

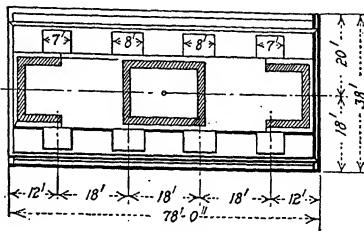
FIG. 240.—Pier casting of center rib, Main Street viaduct, Fort Worth, Texas. Casting ready to be concreted in.



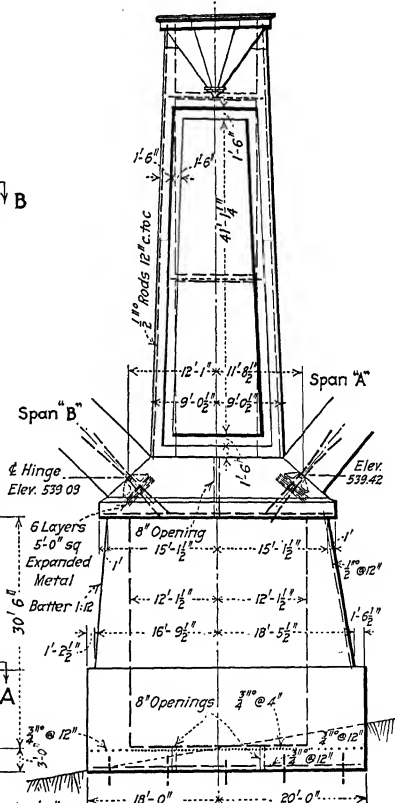
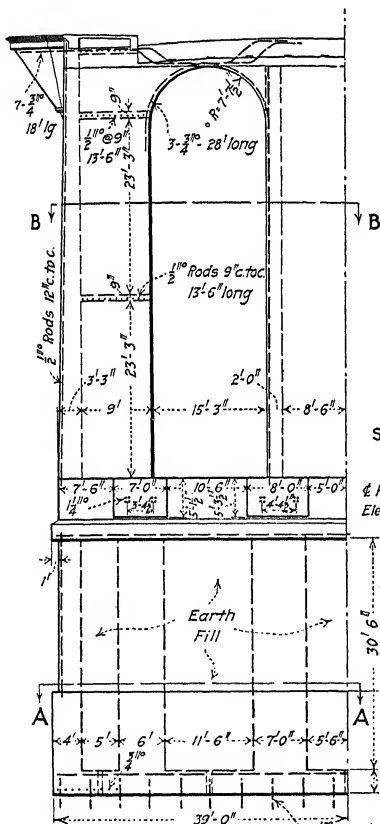




Section A-A



Section B-B



Half Elevation - Span "B" Side

End Elevation

Main Street viaduct, Fort Worth, Texas.





## PART II

### SLAB AND GIRDER BRIDGES

Since the methods of designing slabs, beams, and girders have been explained at length in Volumes I and II, no attempt will be made in the following chapters to treat of these methods in detail. Many things must be considered, however, in designing bridges of this class, aside from the proportioning of simple and continuous beams, and such matters will be given due consideration.

The erection of forms and other operations in slab-and-girder bridge construction are essentially the same for ordinary conditions as the corresponding operations in the construction of buildings. On this account, constructional methods will be referred to only incidentally under this heading.

The loadings to use in design are, of course, the same as for the floors in arch bridges of open-spandrel construction (see Art. 7). In fact, it should be noted that the framed structure which is supported by a ribbed arch is virtually a trestle form of girder bridge and the loadings and general design are identical.

Impact may properly be neglected in arch-ring analysis but becomes important in bridge-floor design. An increase of 25 per cent is usually made in the live load or live-load stresses for highway bridges and 50 per cent in those for railroad bridges.

From the standpoint of economy, slab bridges should in general be limited in span length to about 25 ft., and ordinary girder bridges to about 50 ft.

## CHAPTER XIV

### SLAB BRIDGES

**65. Slabs Under Concentrated Loading.**—Recent tests made on simply-supported slabs at the University of Illinois and at the United States Office of Public Roads gave results in sufficient agreement to permit of simple rules being formulated for estimating the effective width of slabs supporting concentrated loads. In one series of tests,  $\frac{1}{2}$ -in. plain round rods were used and the loads were applied centrally over a bearing area 6 in. in diameter. In another series somewhat similar loads were applied at the one-third points of the span. In a discussion of the tests above mentioned before the American Society for Testing Materials,

June, 1913, Mr. W. A. Slater, first assistant of the Engineering Experiment Station, University of Illinois, recommended that where the total width of slab is greater than twice the span, the effective width  $e$  (Fig. 242) be assumed as

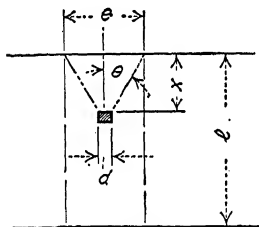


FIG. 242.

$$e = \frac{4}{3}x + d$$

where  $x$  is the distance from the concentrated load to the nearest support and  $d$  is the width at right angles to the span over which the load is applied. Mr. Slater pointed out that the tests so far made showed the effective width to be but little influenced by the depth of the slab or by the percentage of longitudinal reinforcement. He stated, however, that he would limit the latter to 1 per cent. "because of the possibility that in a beam with a large amount of longitudinal reinforcement and a relatively small depth, failure may be caused by transverse tension in the concrete and not by longitudinal steel stress."

Tests were made on beams having various percentages of transverse reinforcement, but results did not show conclusively that such reinforcement is economical when used for the purpose of resisting transverse bending stress. Additional tests are needed to

determine what increase may be made in the effective width for different percentages of transverse steel. At least a small amount should be used in every case for the purpose of distributing deformation due to variations in temperature.

The formula given above for finding effective width shows that this width is very nearly a constant proportion of the span; and consequently it follows that the depth of slab required to support a given concentrated load is approximately the same for all spans. Of course, the depth referred to here is only that necessary to support the live load. Considering both dead and live load, an increase in span length would obviously cause considerable increase in depth or in percentage of reinforcement.

The above discussion refers to a total width of slab greater than twice the span. For a slab whose total width is less than

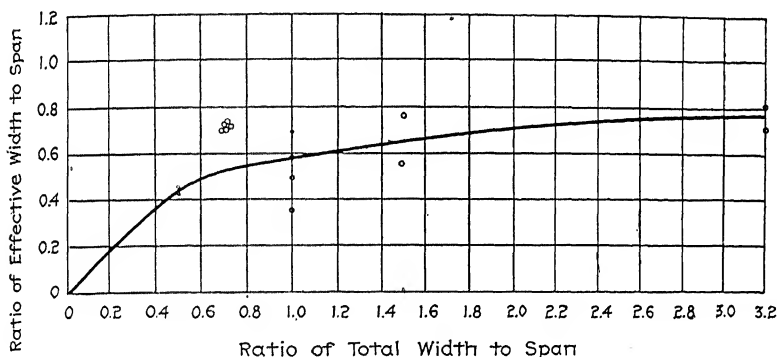


FIG. 243.

this, the effective width may be found from Fig. 243 which shows the ratio of the effective width of the span as determined from the measured steel stresses in the University of Illinois tests.

Mr. C. R. Young, Assistant Professor of Structural Engineering in the University of Toronto, in an article in *Engineering News*, issue of July 30, 1914, calls attention to the fact that the loads caused by wheels or rollers on highway bridges are applied over considerably elongated areas. In view of the tests referred to above, he presents a practical method of estimating the effective width of slabs supporting the type of concentrated loads found in practice. The following is taken from the article mentioned:

"Let a concentrated load, bearing on an area of length  $c$  and width  $d$ , be applied in any general position to a slab having a total width  $b$  not

less than twice the span length  $l$ , as shown in Fig. 244. If any small element of this load, as  $mn$ , distant  $x$  from the nearer support, be considered, it is directly evident from the experimental investigations cited above, that such part of it as is delivered to the nearer support may be regarded as wholly transferred to that support within lines drawn through the end points of the element making angles  $\theta$  with the direction of the span of the slab, the tangent of which angle is between 0.67 and 0.80. For brevity, the angle between these two bounding lines, that is  $2\theta$ , may be called the *effective angle*. The reaction at the near support may thus be regarded as uniformly distributed over a width of  $r = 2x \tan \theta + d$ , or if  $\tan \theta$  be assumed as 0.67, a conservative value in the light of experimental results, this width becomes  $1.33x + d$ .

"Although there is no direct experimental evidence that the effective angle to the farther support is the same as to the nearer, careful con-

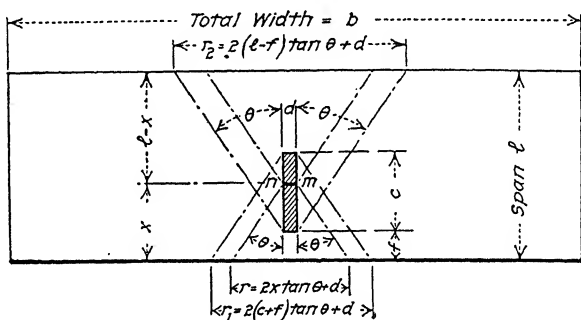


FIG. 244.

sideration of the matter leads to the conclusion that it is. If the farther support were moved in so that the element of load,  $mn$ , became central, the effective angles to the two supports would be equal. There would then be applied to the shifted support, along a length that may be called the effective reaction-width of the reduced span, a uniformly-distributed reaction which, when the first support was replaced in its original position, would become a concentrated load on the original span. The virtual load would be delivered to the support nearest to it, but farthest from the original eccentric element of load  $mn$  within the same effective angle as would apply to the nearer support in any case. It thus appears that the effective angles from any element of loading to the two supports are equal.

"When the selected element of loading is not at the center of the span and the reactions at the two supports are thus not distributed over the same effective widths, the question arises as to what should be the effective width of the slab for the calculation of resisting moment. It is probable that the average of the two reaction-widths would be the

correct width to assume for this purpose, and in the absence of direct experimental evidence on the matter, this assumption is recommended.

"Considering as a whole the concentrated load shown in Fig. 244 it follows that the part of it delivered to either support may be regarded as wholly transferred to that support within lines drawn through the remotest corners of the loaded area and making angles with the direction of the span of the slab equal to  $\theta$ , one-half of the effective angle. If  $f$  be the distance of that edge of the loaded area nearest a support, from the support, the effective reaction width,  $r_1$ , for the nearer support would be

$$r_1 = 2(c + f) \tan \theta + d$$

and for the farther support it would be,

$$r_2 = 2(l - f) \tan \theta + d$$

As in the case of an element of loading, the effective width of the slab for the computation of moment of resistance may be taken as the average of the reaction widths  $r_1$  and  $r_2$ .

"Where the concentrated load is a moving one, the critical position will be at the center of the span. The effective reaction-widths are then equal to each other and the effective width of the slab for the computation of moment of resistance is equal to either.

"Since loads arising from wheels or rollers are often applied over considerably elongated areas, the orientation of the load on the span is an important consideration. For such loads, the distance  $d$  is always small—in theory only the width of a line—but the distance  $c$  may, for rollers, be as much as 48 in., and is commonly from 12 to 20 in.

"The two extreme arrangements of the load, indicated in Fig. 245, will be compared. In Fig. 245(a), the axis of the machine or vehicle is at right angles to the direction of the span of the slab, while in Fig. 245(b), it is parallel to this direction. For the usual system of floor construction in a bridge, with the slabs supported on longitudinal stringers, the axis of the machine for the case shown in Fig. 245(a) would be parallel to the axis of the bridge and for the case indicated in Fig. 245(b), transverse to it. The latter is a contingency that must be considered in wide bridges. When the load is placed as shown in Fig. 245(a), it follows from what has already been said that the effective width of the slab  $e_1$  is given by the expression

$$e_1 = (l + c) \tan \theta + d$$

and when the arrangement is that of Fig. 245(b), the effective width is

$$e_2 = (l + d) \tan \theta + c$$

Since  $c$  is ordinarily very much greater than  $d$ ,  $e_1$  is greater than  $e_2$ .

and the location and orientation of a wheel load most seriously stressing a slab is as shown in Fig. 245(a) and *not* as shown in Fig. 245(b).

"For bearing areas differing in shape from those shown in Figs. 244 and 245, equivalent rectangles may be substituted.

"When the length  $b$  of the slab is less than twice the span length  $l$ , it becomes necessary to make some reduction in the effective width. The writer would suggest that until further experimental evidence is available the values of  $\tan \theta$  in any calculation of effective widths be

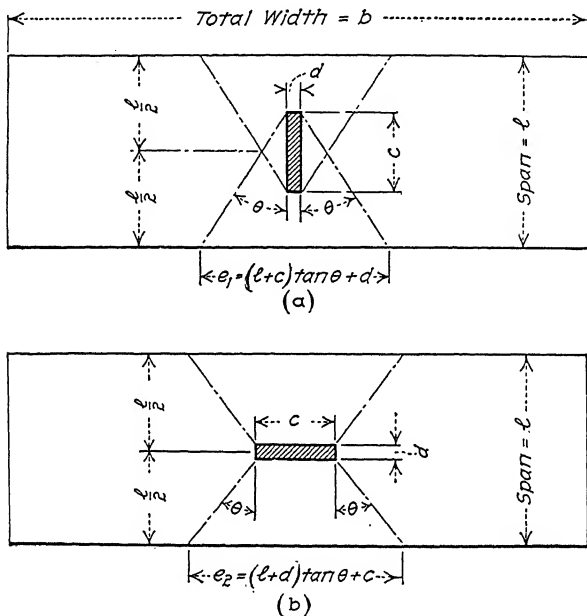


FIG. 245.

assumed substantially in accordance with those given by Mr. Slater's graph, or as follows:

$\frac{b}{l}$	$\tan \theta$
0.4	0.35
0.5	0.42
0.6	0.48
0.8	0.54
1.0	0.59
1.2	0.62
1.4	0.64
1.6	0.65
1.8	0.66
2.0 and over	0.67

"Although no experimental investigation of the relative distributing effects of various types of slab reinforcement has been made, it is probable that a form involving diagonal strands or rods is most efficient. Maximum stiffness along lines radiating from the load within the effective

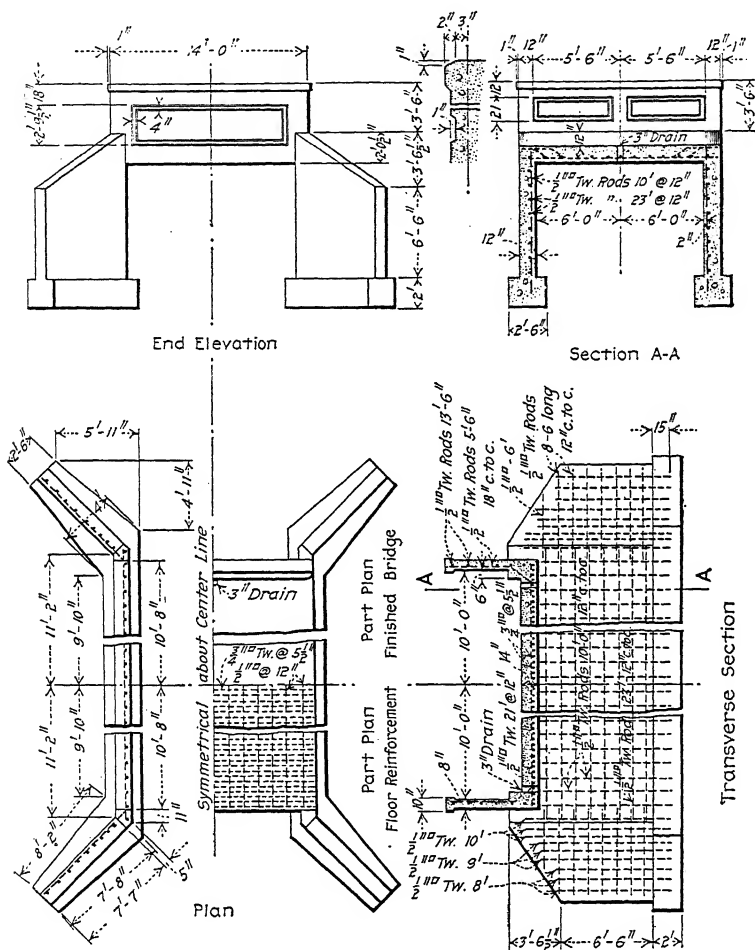
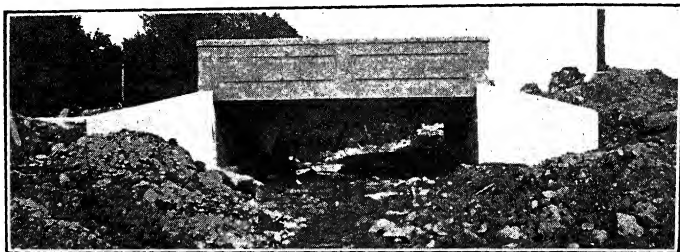


FIG. 246.—Standard design for slab bridges of 12 ft. span, Wisconsin Highway Commission.

angle and the provision of a large number of strands directly under the load would thus be secured. Upon these considerations the delivery of the load to the supports over a considerable effective width largely depends.



"The effect of a gravel cushion or other wearing surface in distributing concentrated loads over bridge floors has not been considered, as this is a matter not entering into the present discussion. Having found the area of the slab to which the load is applied by this surfacing, the problem is of precisely the same kind as arises when loads are applied directly to

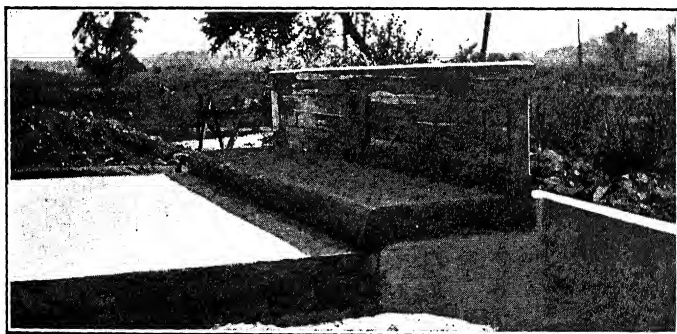


*Courtesy of Mr. M. W. Torkelson, Bridge Engineer, Wisconsin Highway Commission.*

FIG. 247.—Christiana bridge over Brewery Creek, Town of Cross Plains, Dane County, Wis.

the slab. The only difference is that the bearing area of the concentrated load is increased with the use of a wearing surface and consequently the effective width of the slab also becomes greater."

**66. Slab Bridges of Single Span.**—The floor of a slab bridge may be designed as any simply-supported slab except that shear-



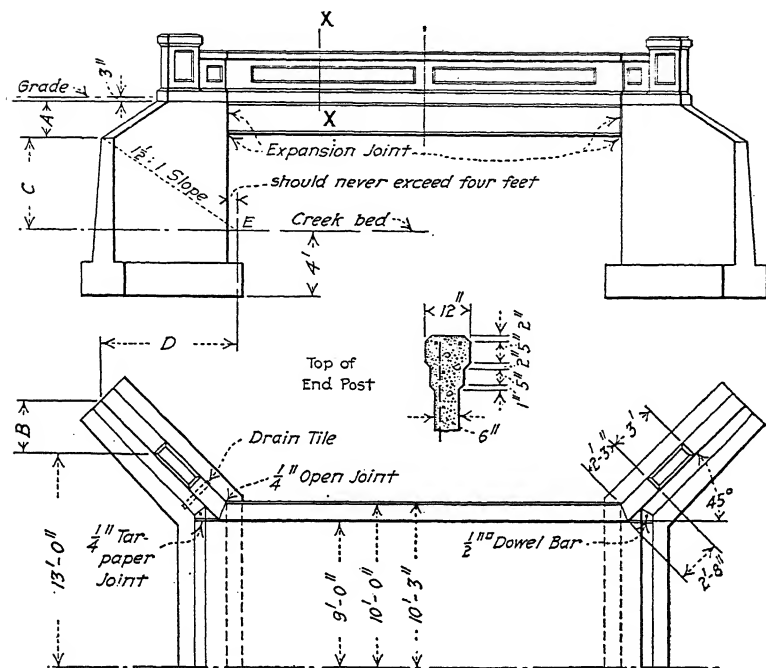
*Courtesy of Mr. M. W. Torkelson, Bridge Engineer, Wisconsin Highway Commission.*

FIG. 248.—Construction view of Christiana bridge, Town of Cross Plains, Dane County, Wis.

ing stresses may require very careful attention where the live load is relatively large, as in railroad structures. The whole reinforcing system may be made absolutely rigid by wiring the main reinforcing rods to the transverse reinforcement, employing extra transverse spacing rods at the ends of the bent-up



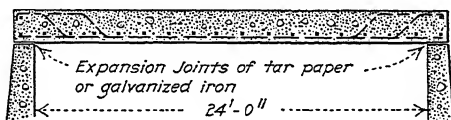




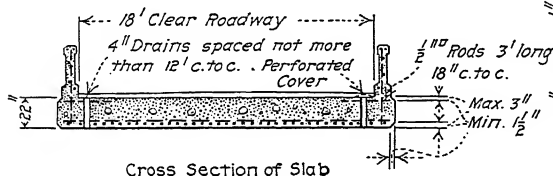
Half Plan View

Note: So proportion the wing length that  $A:B::C:D$  as  $1:1\frac{1}{2}$ . The point E where the  $1\frac{1}{2}:1$  slope from end of wing intersects the elevation of stream bed may be varied to suit local conditions.

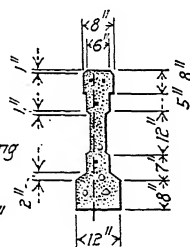
In streams whose channels are nearly the span width, or where there is a possibility of cutting and channel widening, the point E should be taken at abutment face.



Longitudinal Section



Cross Section of Slab



Section X-X

FIG. 251.—Typical slab superstructure, Iowa Highway Commission.



part of the abutment body is to shift the center of gravity of the entire mass farther from the stream face and thus reduce the eccentricity of pressure on the foundation. The horizontal reinforcing rods shown near the stream face of the abutment, and which are carried about 5 ft. into the wings, were employed

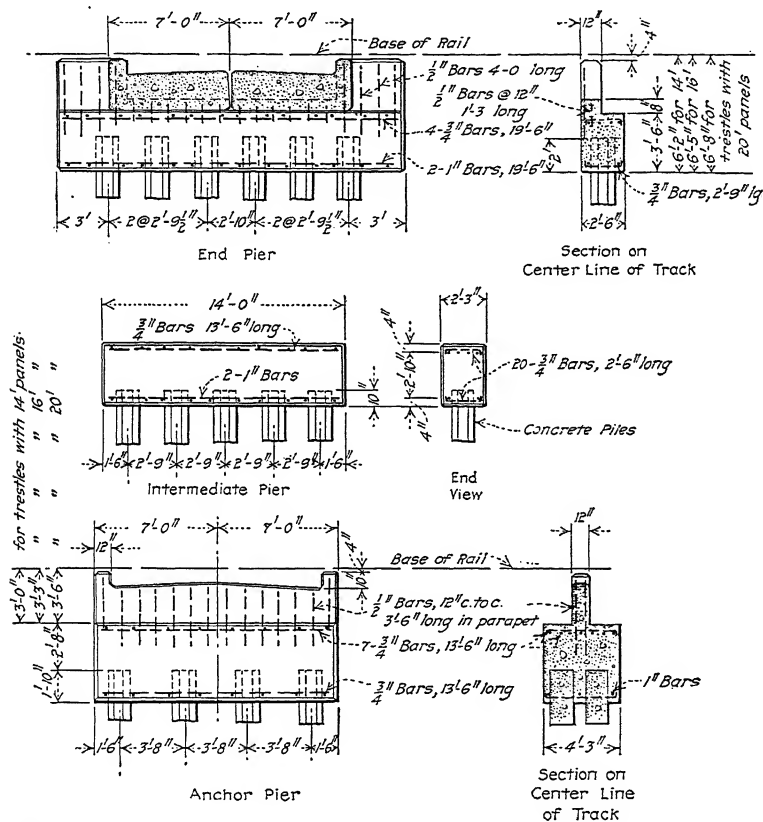


FIG. 253.—Details of substructure, standard concrete pile trestle, Illinois Central R. R.

to counteract a tendency to the formation of vertical cracks on the outside at the corner of wing and abutment. The vertical rods in the front face serve as a framework upon which to build the horizontal rods and they also prevent any tendency toward the formation of horizontal cracks in the stream face due to the clogging of an expansion joint.

### 67. Slab Bridges of Multiple Spans.—Slab bridges of

spans will be treated under the four following headings:

### Concrete pile trestles.

### Pier trestles.

### Trestles with framed bents.

### Cantilever flat-slab construction.

*Concrete Pile Trestles.*—Figs. 253 to 256 inclusive give the essential details of design of the pile trestles built by the Illinois

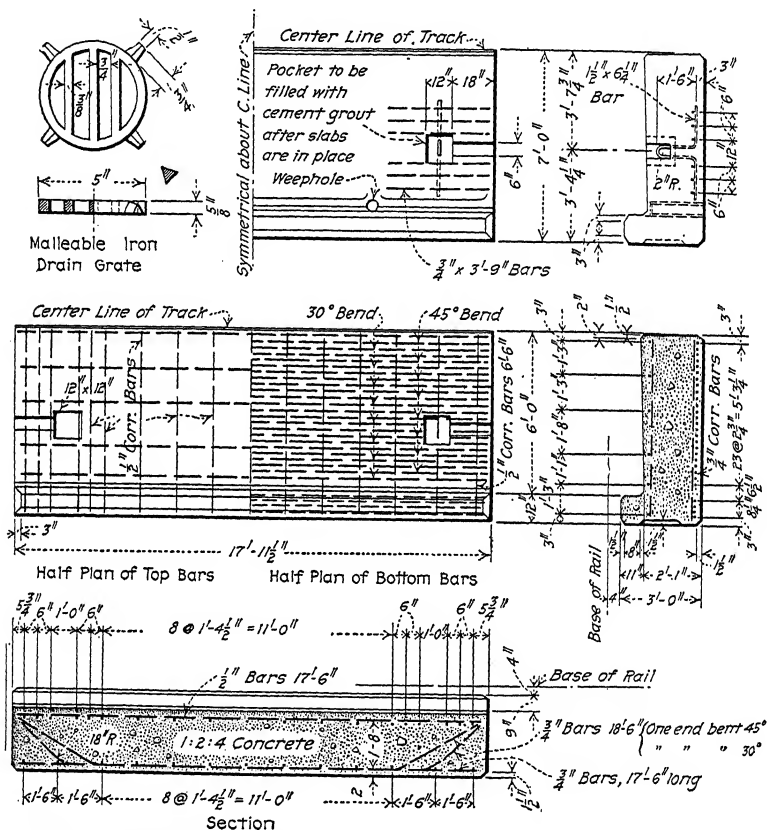


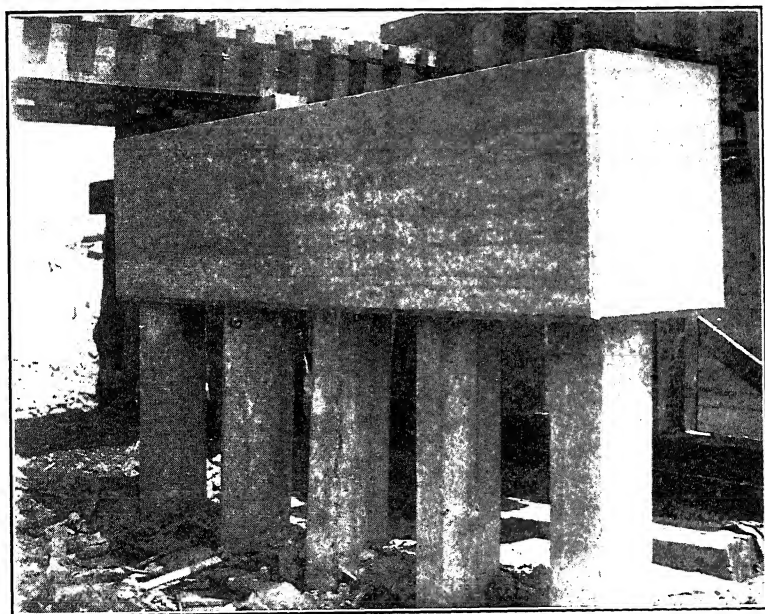
FIG. 254.—Standard slab for clear spans of 16 ft. Illinois Central R. R.

Central Railroad. They can be considered typical of concrete pile trestles in general. These trestles replace similar wooden structures over swamps and shallow streams which may not be filled and where bridges on more permanent supports would be extremely expensive because of their great length. The con-

struction consists of pile bents spaced generally from 16 to 20 ft. c. to c., and with a height above ground not greater than the span. The piles are capped with reinforced-concrete girders which support the floor slabs.



*Courtesy of Mr. Maro Johnson, Engineer of Bridges and Buildings, I. C. R. R.*  
FIG. 255.—Construction view of concrete pile trestle on Illinois Central R. R. near Obion, Tenn. Concrete bents ready for slabs.



*Courtesy of Mr. Maro Johnson, Engineer of Bridges and Buildings, I. C. R. R.*  
FIG. 256.—Typical bent of concrete pile trestle on Illinois Central R. R. near Obion, Tenn.

The piles and deck slabs are usually cast in a convenient yard, allowed to season from 60 to 90 days, and are then hauled to the bridge site. The lifting stirrups shown permit of the slabs being



set in place by a wrecking crane. The ballast and track are laid directly on the slabs after the longitudinal and transverse joints (except at anchor bents) are filled with cement mortar and

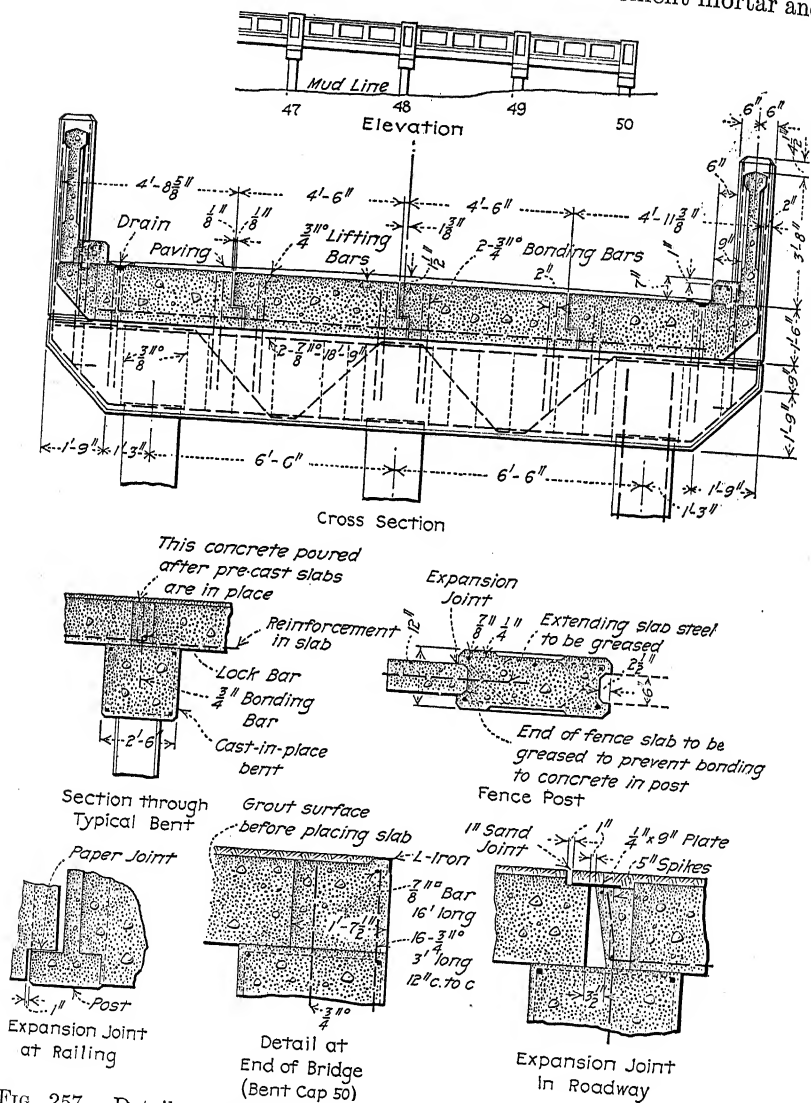
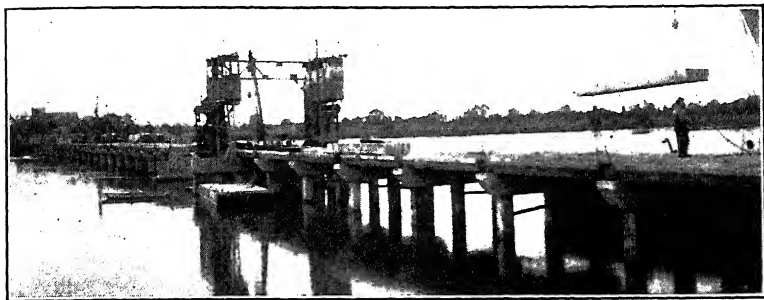


FIG. 257.—Details of pile trestle across the Miles River near Easton, Md. after the floor surface is thoroughly waterproofed. The slabs are set on a bed of grout on the pile caps. An anchor bent is

used at suitable intervals to take up longitudinal stresses due to tractive force and, by means of an expansion joint, to prevent any great accumulation of movement of the deck due to temperature changes.



Courtesy of Raymond Concrete Pile Co.

FIG. 258.—Construction view of pile trestle across the Miles River near Easton, Md.

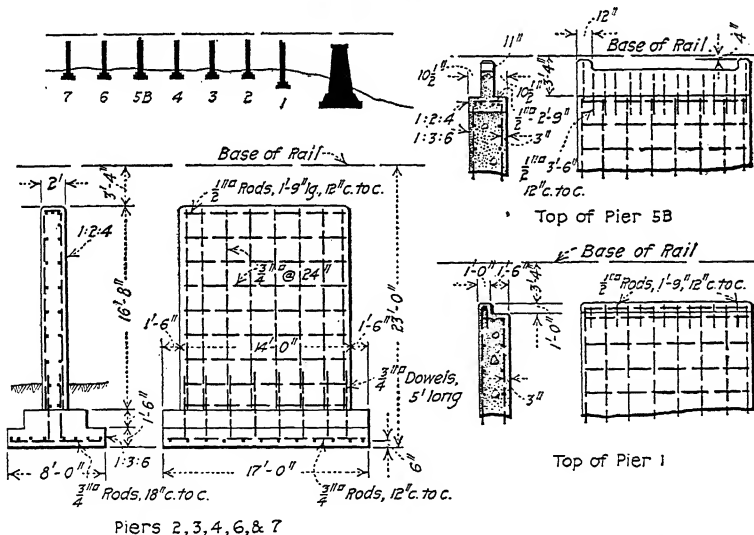
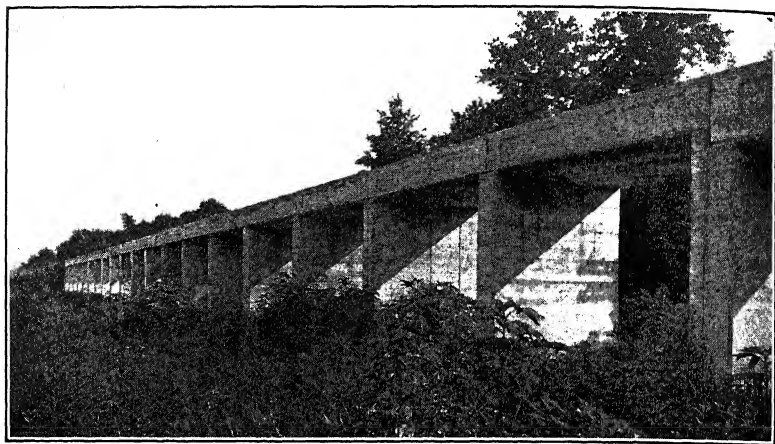


FIG. 259.—Pier details, Illinois Central R. R. trestle over Kaskaskia River near New Athens, Ill.

A concrete pile trestle for carrying a highway is shown in Figs. 257 and 258.<sup>1</sup> It was found economical to cast the piles, deck slabs, and railing slabs at Baltimore, 60 miles away, and transport them to the site on scows. Expansion joints were

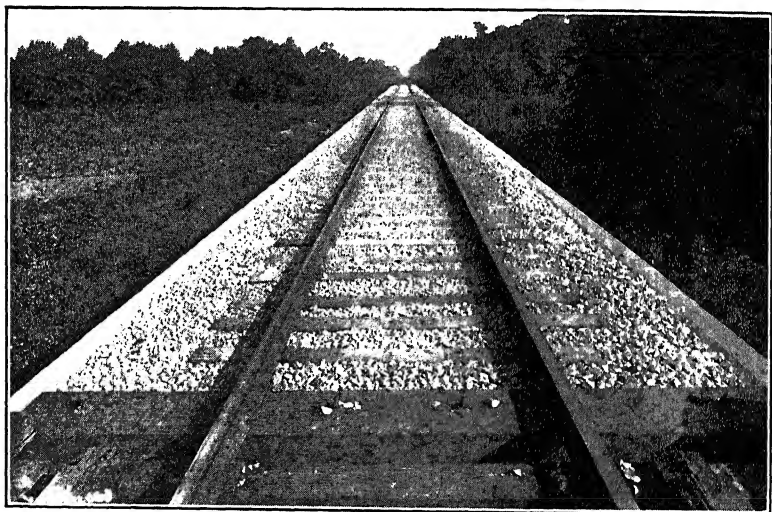
<sup>1</sup> See also *Engineering News*, issue of Feb. 5, 1914.

located in the roadway slabs, curb, and railing slabs at every fifth bent.



*Courtesy of Mr. Maro Johnson, Engineer of Bridges and Buildings, I. C. R. R.*

FIG. 260.—Solid benchwall type of concrete trestle on Illinois Central R. R. near New Athens, Ill.



*Courtesy of Mr. Maro Johnson, Engineer of Bridges and Buildings, I. C. R. R.*

FIG. 261.—Roadbed of trestle shown in Fig. 260.

*Pier Trestles.*—Thin concrete piers are preferable to pile bents when the height of bridge above the ground line is greater than

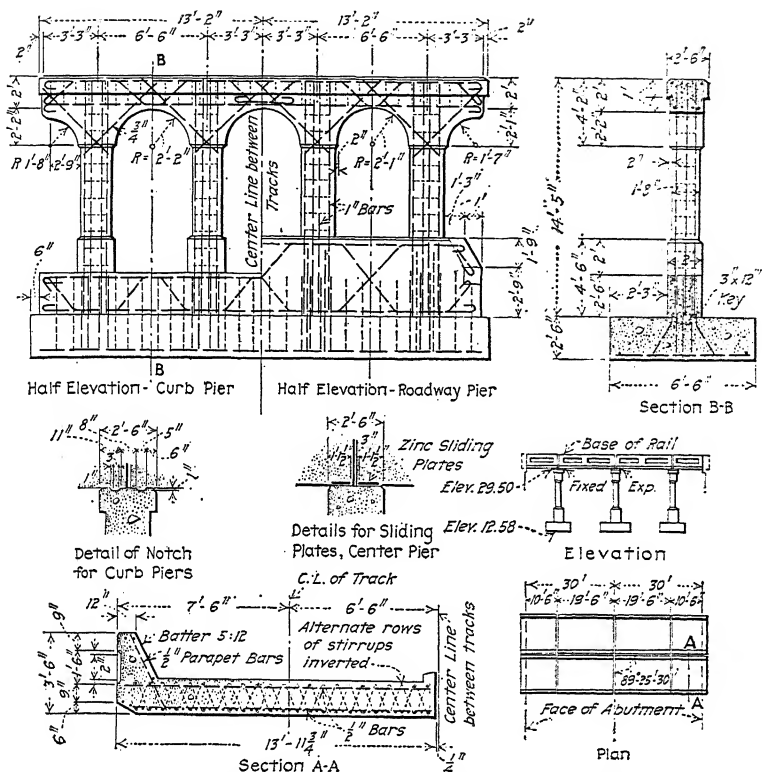
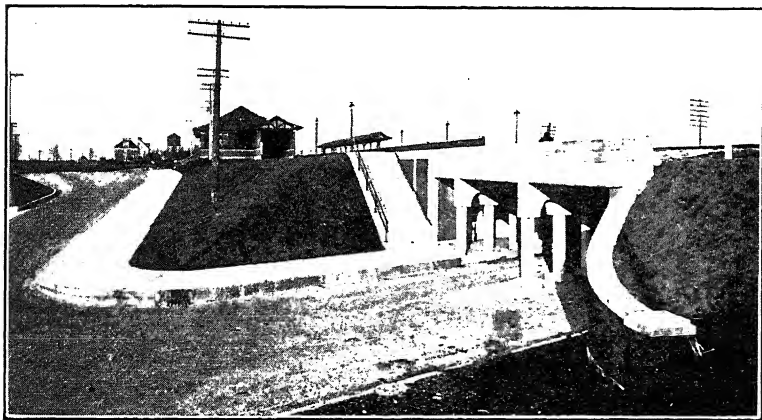
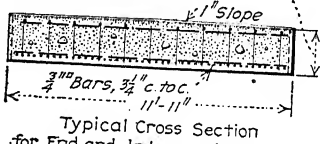
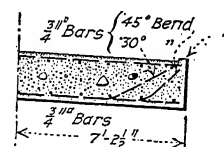
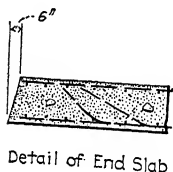
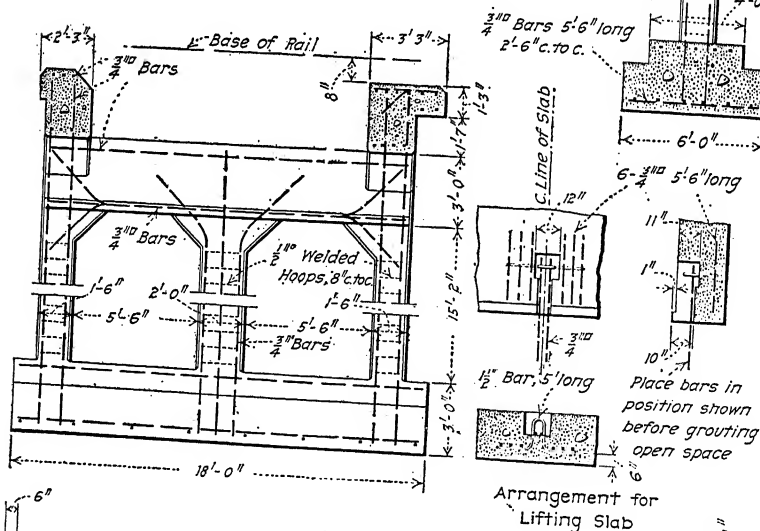
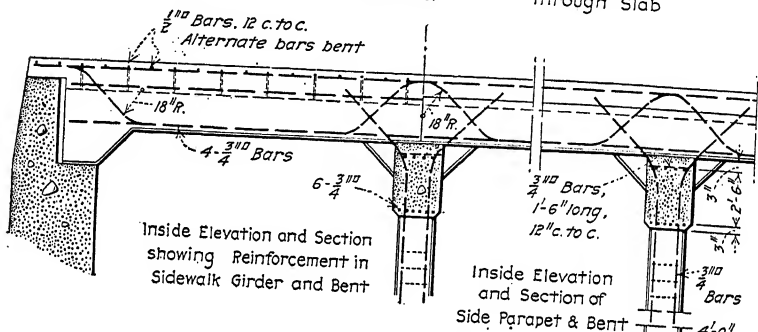
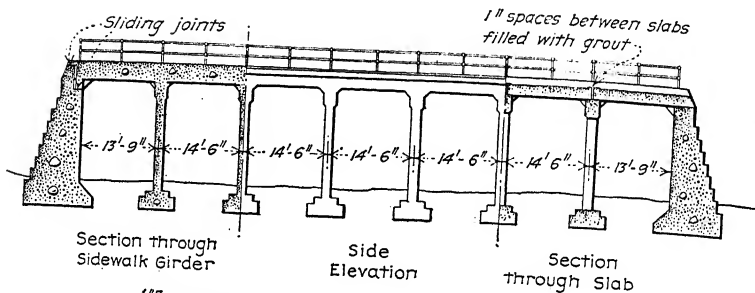


FIG. 262.—Details of Mozart Street subway, Bloomingdale Road track elevation, Chicago, Milwaukee & St. Paul Railway.



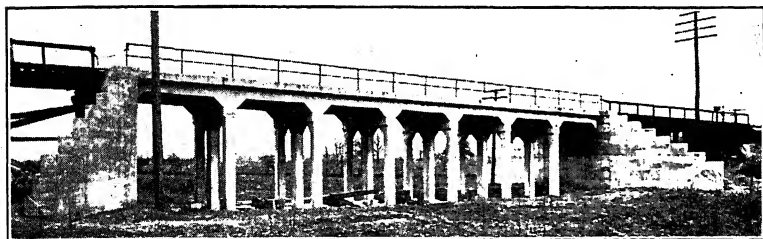
*Courtesy of Mr. Maro Johnson, Engineer of Bridges and Buildings, I. C. R. R.*



about 16 ft. Figs. 259, 260, and 261 show a typical trestle of the solid bench-wall type built by the Illinois Central Railroad.

*Trestles with Framed Bents.*—Slab bridges with framed bents forming subways are used on at least fifteen railroads in this country. A design which may be considered typical is shown in Fig. 262. The deck slabs may either be cast in place or cast at some central yard and placed in a similar manner to the slabs for pile or pier trestles. In Fig. 262 the design is shown for slabs to be cast in place. A general view of a typical Illinois Central subway is shown in Fig. 263.

A framed-bent trestle with continuous side girders to resist stresses due to traction is shown in Figs. 264 and 265. The girder on one side acts simply as a tie and parapet, while the



*Courtesy of Mr. Maro Johnson, Engineer of Bridges and Buildings, I. C. R. R.*

FIG. 265.—Trestle approach to Cumberland River bridge, Illinois Central R. R. Side girders continuous.

other with a cantilever projection at the side acts also as a sidewalk. The slabs were cast in a yard at some distance from the bridge site, loaded on flat cars, taken to the job, and swung into place with derricks. Expansion is allowed for at both ends by providing a sliding joint between the bridge superstructure and the abutments. The shallow 4-in. curbs at the ends of the slabs were provided to prevent seepage from getting into the 1-in. grout joint between slabs. The pier footings are reinforced longitudinally in top and bottom, and were figured as continuous T-beams uniformly loaded by the pressure on the soil. The cross girders at the top of the columns support the deck slabs previously referred to, and are made continuous.

*Cantilever Flat-slab Construction.*—Fig. 266 is a flat-slab structure of the Turner Mushroom type. The methods which may



be used in the design of the roadway slab are treated in Volume II. The hollow abutments should be noted.

A cantilever flat-slab bridge in which the abutments are of the ordinary reinforced-concrete type is shown in Fig. 267. The



*Courtesy of Mr. A. M. Wolf, Prin. Asst. Eng'r., Condrion Co., Chicago.*

FIG. 267.—Lafayette St. bridge, St. Paul, Minn.

abutment walls are considered as held at the top by the superstructure to which they are anchored by bending the vertical rods into the slab.



## SIMPLE GIRDER BRIDGES

Longitudinal Section through Girder

Elevation and Section of Post over Wing

Transverse Section through Girder

Elevation of Spindle Rail

### Table of Dimensions and Girder Reinforcement

Span	H	d	e	f	Stirrup Spaces			a	b	c	Girder Bars	
					12"	18"	24"				Top Row	Bottom Row
24'	2' 2"	2' 2 <sup>10</sup> "	3"	2' 2 <sup>11</sup> "	10	6	2	2' 3"	2' 3"	2' 0"	3 - 1 <sup>10</sup> "	3' - 1 <sup>10</sup> "
26'	2' 4"	2' 4 <sup>11</sup> "	3"	2' 4 <sup>12</sup> "	12	6	2	2' 6"	2' 1 <sup>11</sup> "	2' 5"	3 - 1 <sup>10</sup> "	3' - 1 <sup>10</sup> "
28'	2' 6"	2' 6 <sup>11</sup> "	3"	2' 6 <sup>12</sup> "	12	6	3	2' 5"	2' 2"	2' 11"	3 - 1 <sup>10</sup> "	2' - 1 <sup>10</sup> "
30'	2' 9"	3"	3 <sup>10</sup> "	2' 9"	10	6	5	2' 8"	2' 6"	2' 10"	3 - 1 <sup>10</sup> "	2' - 1 <sup>10</sup> "
32'	2' 10"	3"	3 <sup>10</sup> "	3"	10	6	6	2' 7 <sup>11</sup> "	2' 6 <sup>11</sup> "	3' 1"	3 - 1 <sup>10</sup> "	3 - 1 <sup>10</sup> "
34'	3' 1"	3"	4"	3"	10	10	4	2' 11"	2' 10"	3' 3"	2 - 1 <sup>10</sup> "	3 - 1 <sup>10</sup> "
36'	3' 3"	3"	4"	3"	10	10	5	3' 0"	2' 11"	3' 10"	3 - 1 <sup>10</sup> "	3 - 1 <sup>10</sup> "
38'	3' 5"	3"	4"	3"	10	10	6	3' 0"	2' 10"	3' 4"	2 - 1 <sup>10</sup> "	3 - 1 <sup>10</sup> "
40'	3' 8"	3 <sup>10</sup> "	4"	3 <sup>10</sup> "	12	6	9	3' 6"	3' 2"	3' 10"	3 - 1 <sup>10</sup> "	3 - 1 <sup>10</sup> "

FIG. 268.—Standard details of concrete deck girder bridges, Iowa Highway Commission.

ever sufficient head-room is available. The girders, of course, should be relatively thin and deep for the greatest economy, and

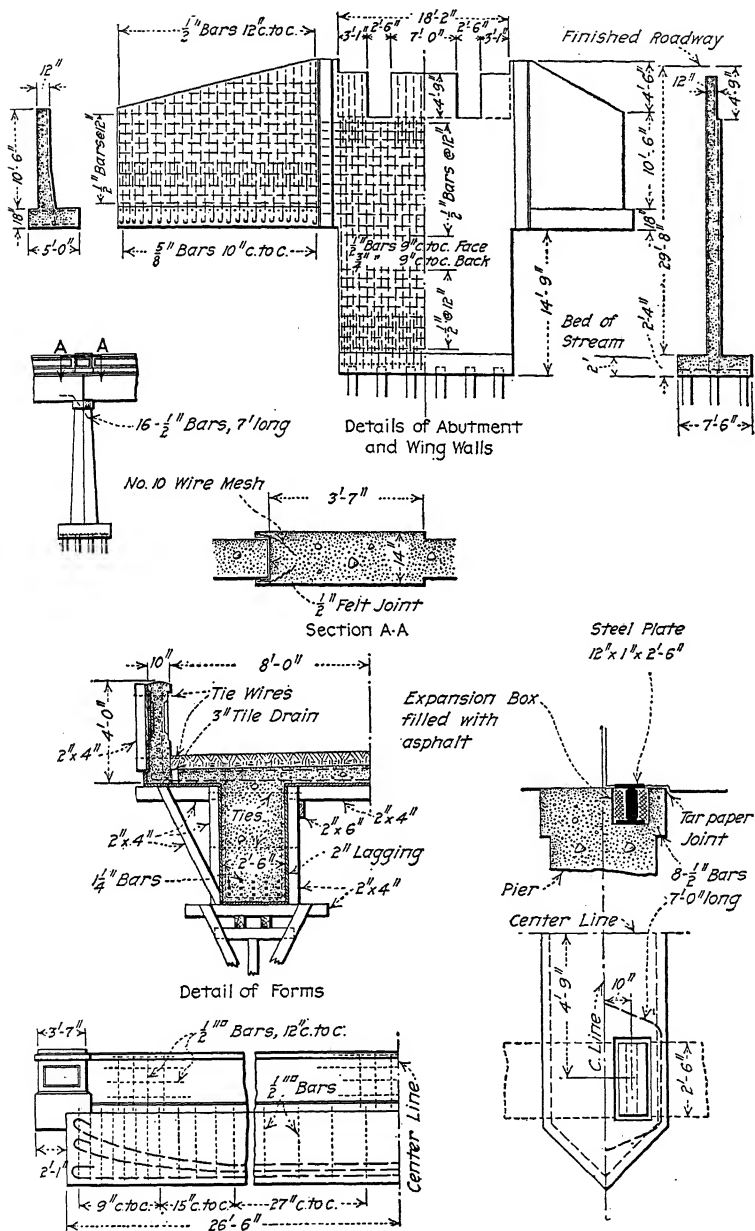
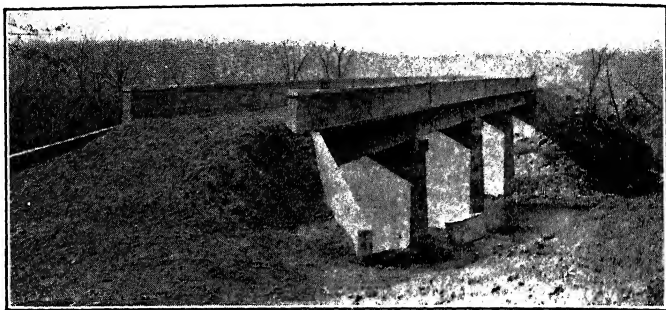


FIG. 269.—Details of Embarrass River bridge, Cumberland Co., Ill.

a curtain wall should be provided between the girders at each end of span to retain the earth fill, thereby avoiding complicated parapet walls on the abutments.

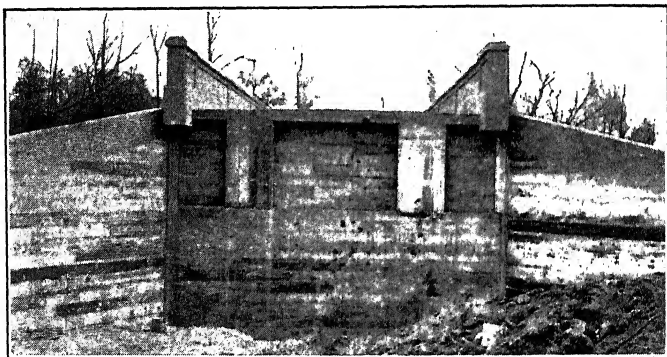
Standard details of deck-girder bridges designed by the engineers of the Iowa Highway Commission are shown in Fig.



*Courtesy of Engineering and Contracting.*

FIG. 270.—Embarrass River bridge, Cumberland Co., Ill.

268. The floor slab was analyzed both as fixed and as continuous, and was designed to resist maximum stresses caused by either method of analysis. The method of fastening the girder steel to anchor rods should be noted. Expansion joints are provided



*Courtesy of Engineering and Contracting.*

FIG. 271.—Rear view of abutment and wing walls, Embarrass River bridge, Cumberland Co., Ill.

under the girder stems by means of sliding steel plates anchored into the body of both superstructure and substructure.

Figs. 269, 270, and 271 illustrate the type of deck-girder bridge adopted as standard by the Illinois Highway Commission. The

following description of the methods employed in providing for expansion in girder bridges is given in the fourth report of the Commission:

"Two methods of providing for expansion in girder bridges have been used and both have proved satisfactory. In one method, the wing walls of one abutment are entirely separated from the abutment wall proper, the latter being free to move at the top with the expansion or contraction of the superstructure. The wing walls are designed to be self-supporting. As girder spans designed by the commission have so far been limited to 60 ft., the amount of movement either way from the normal is

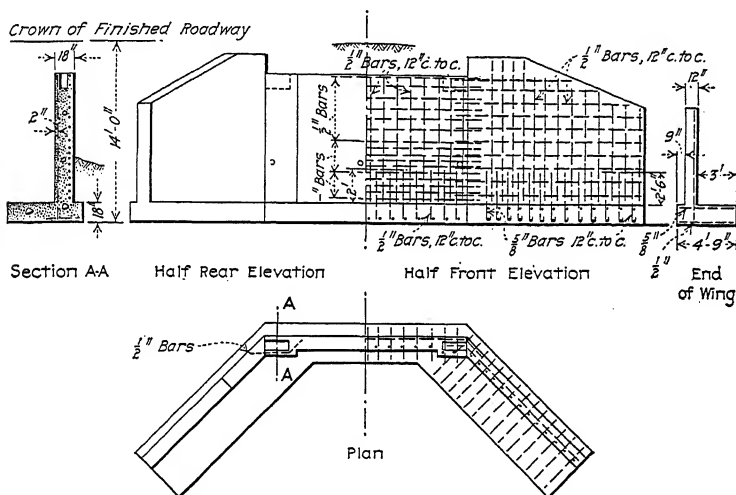


FIG. 272.—Type of abutment used for girder bridges by the Illinois Highway Commission. Wings of cantilever type. Main wall supported by wings as counterforts.

small and is taken up by deflection of the main wall or a slight rocking of the wall on the footing. Earth pressure against the wall is of little importance in this connection as it but tends to reduce the tension in the girder steel during expansion and to cause the abutment wall to follow the superstructure during contraction. It does not increase the stress in the compression area of the girder as the load is applied at the bottom of the girder, tending by this eccentricity of application to reverse the dead- and live-load stresses in the girder.

"This method has been found to be entirely successful, but is somewhat objectionable as a slight movement of the wings due to earth pressure and unequal settlement sometimes causes the wing walls to move forward slightly at the top, making a somewhat unsightly offset between the wing and abutment walls. This has never been more than

**Section A-A**

Continue wing to adapt itself to warped surface

This wing wall same as 9 ft. wing on other side

12" x 32"

2-3/8" Temp Bars in each bay

12" x 32"

12" x 32"

12" x 32"

A

1/2" Bars, 8" c.t.c.

Alternate bars bent

12" x 32"

20' - 0"

B

12" x 32"

Railing and caps for end posts poured in a separate operation

17' - 3 1/4"

Bush hammered

Spandrel ring and railing rubbed with coarse carborundum with water

Section B-B

Section C-C

2 or 3 in. for the highest walls, but as it is not understood by the ordinary observer, an impression of weakness is sometimes caused.

"The present method of providing for expansion is to design the abutments and wings in the ordinary way, separating the superstructure completely from one of the abutments by a thick paper joint and supporting each girder at the free end on a single cast-iron rocker of large diameter. The reaction is transmitted to the girder and abutment from the rocker through planed structural-steel plates stiffened with I-beams when necessary. The rocker surfaces in contact with the bearing plates are turned to insure perfect bearing on the plates. The diameter of the rocker is made proportional to the load imposed per linear inch, in the same manner as is commonly used in proportioning roller nests for



*Courtesy of Brenneke & Fay, Consulting Engineers, St. Louis, Mo.*

FIG. 274.—North Samuels Avenue viaduct, Fort Worth, Texas.

steel bridges. The upper and lower plates are bedded in the concrete of the superstructure and abutment. The rocker is located in a pocket built in the abutment. This pocket is filled with a soft asphalt to prevent the entrance of water or dirt and to protect the metal from corrosion.

"The rocker method of providing for expansion has proved very satisfactory and is but little more expensive than the other method, especially when it is considered that the wings may be tied to the main wall when rockers are used and advantage taken of the mutual support thus obtained."

Fig. 272 shows a type of abutment adopted by the Illinois Highway Commission in cases where the girders are supported on cast-iron rockers and the wings are nearly parallel to the roadway or make an angle of more than  $45^\circ$  with the face of the abutment. The wing walls are considered to act as counter-

forts and the reinforcing steel in the main wall is horizontal and placed near the stream face of the wall.

Fig. 273 gives the details of a girder bridge, the main portion of the abutments and the wings of which were designed and

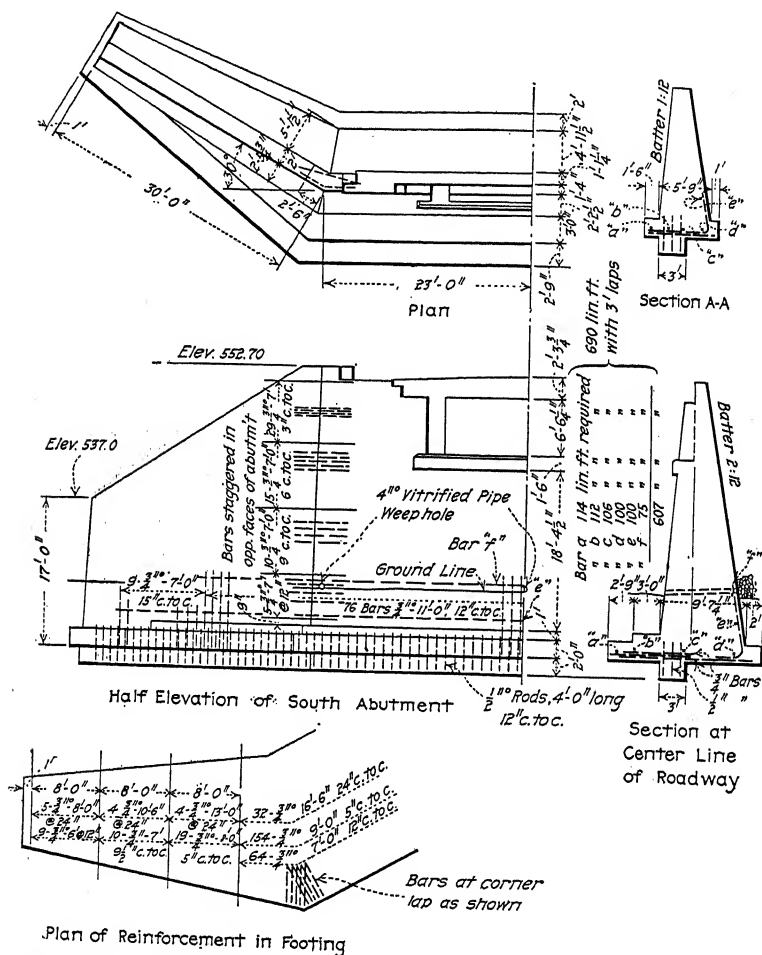


FIG. 275.—Details of south abutment, North Samuels Avenue viaduct, Fort Worth, Texas.

figured in the same manner as the slab bridges of Figs. 246, 249, and 250.

In the structure shown in Figs. 274 to 278 inclusive, cross girders and stringers were provided in addition to the longitudinal

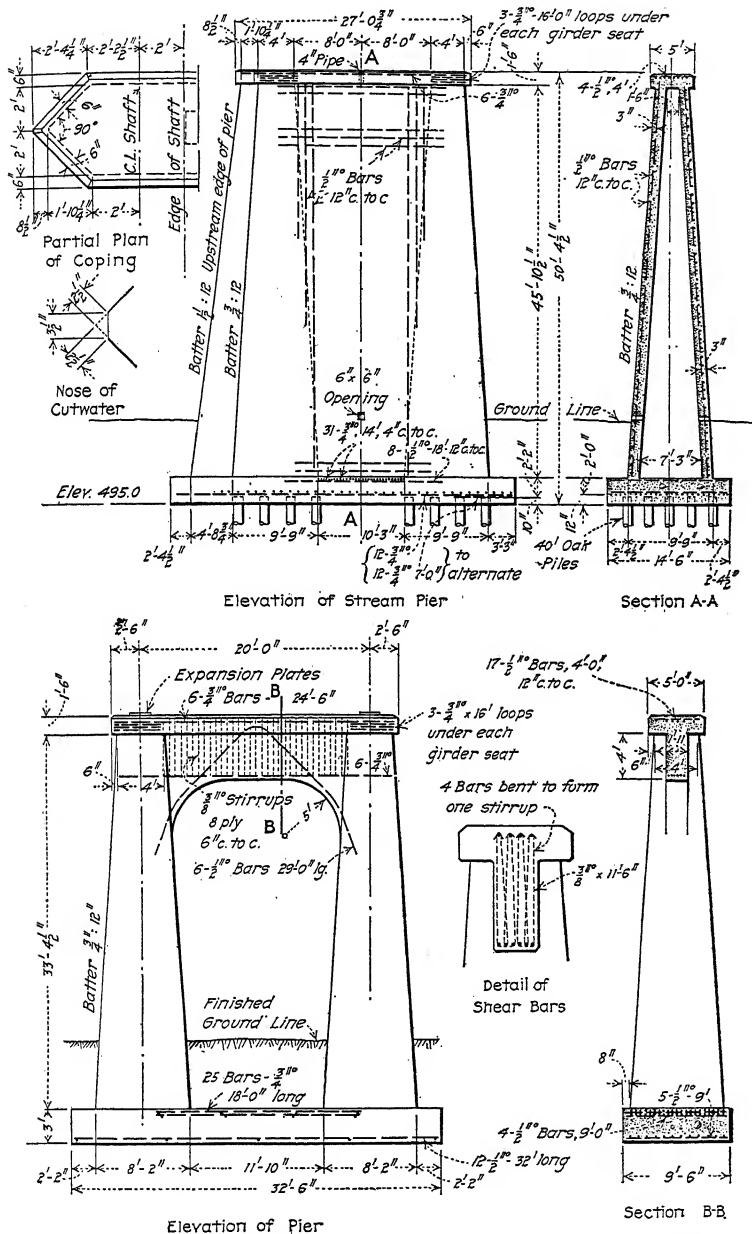


FIG. 276.—Details of typical piers, North Samuels Avenue viaduct,  
Fort Worth, Texas.



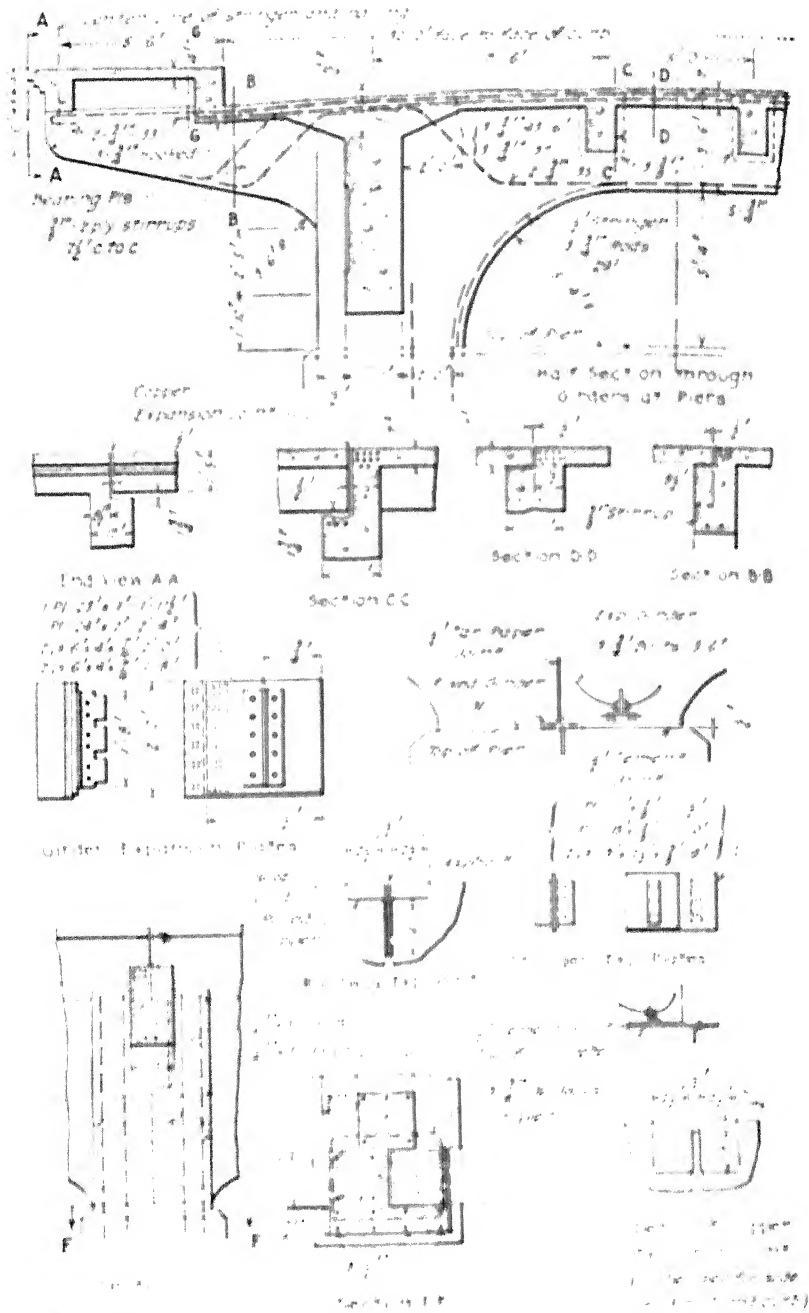


FIG. 227. Details of Bridge System, North Side. View as indicated.

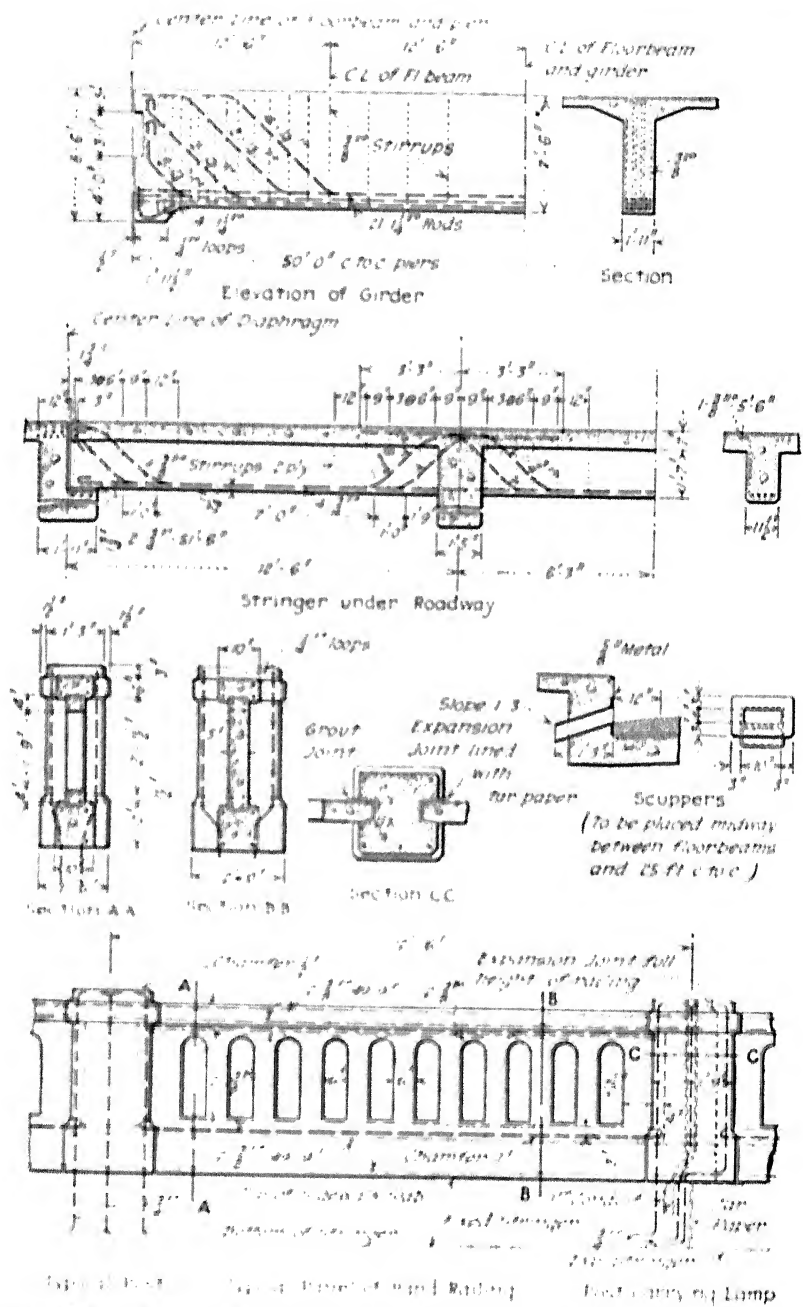


FIG. 278. Details of floor system and riling, North Samuels Avenue viaduct.

to the pier and the other end is allowed to expand and contract in a joint packed all around with  $\frac{1}{2}$ -in. of tar paper and bearing on a pair of milled steel plates. Expansion joints were also made in the roadway slab and railing. Cast iron scuppers were placed in each curb on 25-ft. centers. For maximum stresses in the cross girders, the sidewalks were assumed to be unloaded.

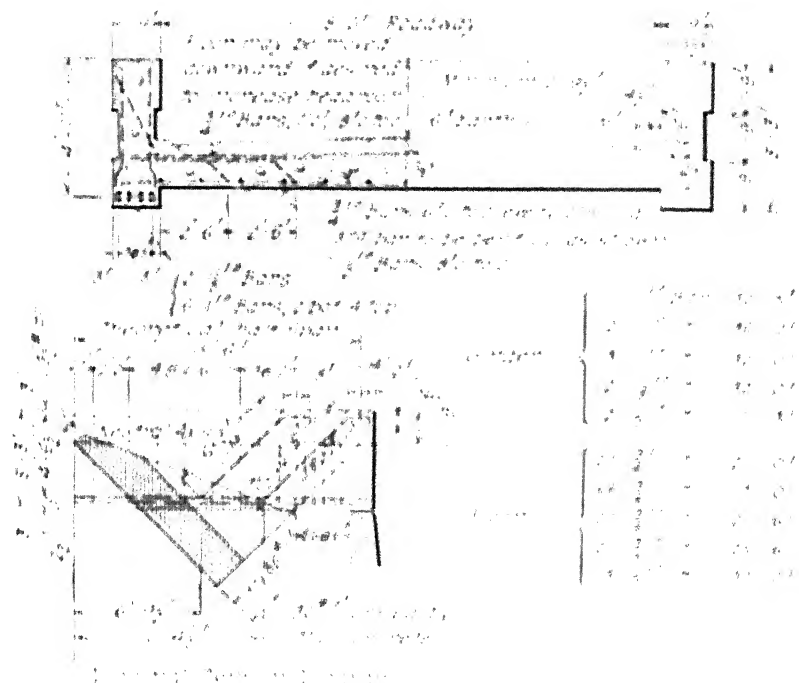


FIG. 279.—Standard sections for through girder bridges, 10 to 20 ft. span.  
Lowell Highway, California.

Reinforced-concrete deck girder bridges for railroad traffic are rather unusual, but a few such structures have been built. The superstructure in such bridges is usually supported by plain concrete piers and abutments.

**69. Through Girders.** From the standpoint of economy, the through girder bridge should not be built except where an sufficient head room or other local condition prevent the use of the deck girder.

The standard type of through girder bridge, adopted for the

Iowa Highway Commission for locations where the deck type is impracticable, is shown in Fig. 279. The girders themselves were designed as simple beams and the floor as a slab partially fixed, the point of contraflexure being arbitrarily assumed at about



Courtesy of Mr. M. W. Funkelien, Bridge Engineer, Wisconsin Highway Commission.  
FIG. 280—Funkelien bridge, Town of Christiansa, Dane Co., Wis.

1 ft. from the edge of the girder. This is approximately in accordance with tests made by the Illinois Highway Commission in 1907.

In the tests referred to, stress measurements were made on a through-girder span with an 18-ft. roadway loaded with crushed

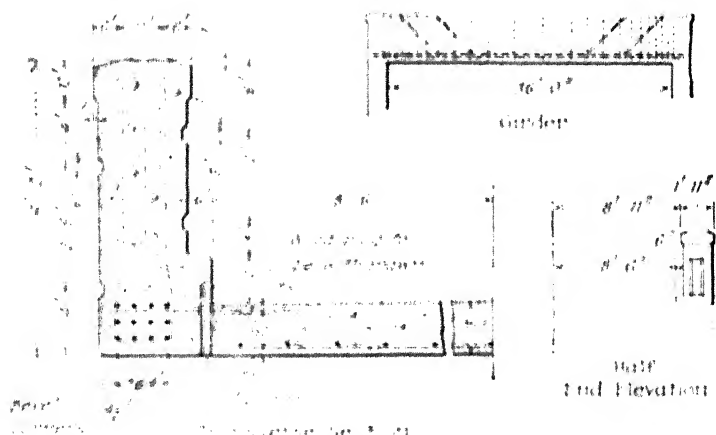


FIG. 281—Details of superstructure of Funkelien bridge, Town of Christiansa, Dane Co., Wis.

stone and pig iron. The full-applied load was 418 tons, which gave a distributed load per square foot of floor of 1450 lb. Deformation measurements were made in the reinforcing steel of the sus-



pended floor which indicated stress equivalent to that theoretically resulting from a simple span of 15.5 ft. In other words, since the roadway was 18 ft. between girders, the point of contraflexure was apparently about 15 in. from each girder face.

Figs. 280, 281, 282, and 283 illustrate other designs of through-girder superstructures.

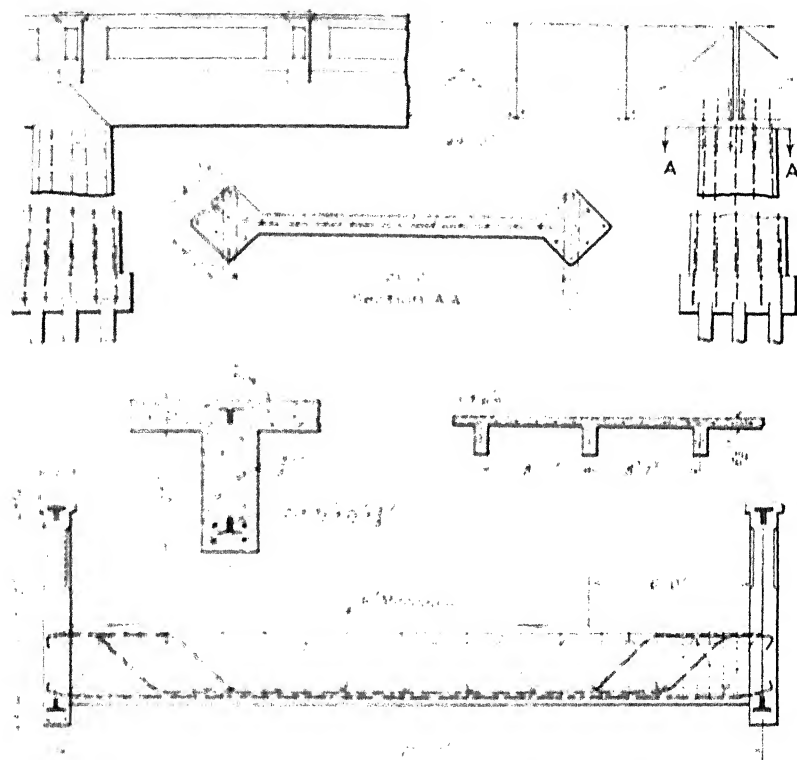


Fig. 280. Detail of bridge over Muddy Creek, Hamilton County, Ohio.

Figs. 284 and 285 show a rather unusual type of through bridge on account of the fact that the girder reinforcement is in the form of a truss of sufficient strength to carry the dead and construction loads. The piers are simply columns braced between by either a vertical slab or by struts. As no falsework is necessary, this type of construction is especially adapted for highway bridges over railroad and electric lines, or at locations where the soil is very soft.

## CHAPTER XVI

### CONTINUOUS GIRDER BRIDGES

**70. Durability of Monolithic Construction.** The designs of most of the continuous girder bridges built monolithic with supports are conservative and safe, but still there are some bridges of this type, especially those with exceedingly high piers or bents, which are classed by many engineers as dangerously extreme considering our present knowledge of reinforced concrete. The fact that light sections in concrete construction have quite often developed cracks to a more or less extent has made these engineers hold to the conservative idea that the difficulty in providing intelligently for movement due to temperature change in the moisture content of the concrete, etc., is so great as to make light construction something to be avoided wherever possible. It will suffice to say here that bridges of the monolithic type when carefully designed and constructed are giving entire satisfaction, and only time will prove whether or not such light structures are durable.

**71. Details of Design.** Since the superstructure and the piers are usually made monolithic, the latter may be made of comparatively small cross-section if properly reinforced for bending. The pier may become in reality nothing more than two or more columns connected by a suitable portal, and the stress due to bending in the columns, caused by longitudinal continuity of the floor loading, may be computed in the same manner as for columns in buildings. (See Chapter XIV of Volume II.) In order to prevent an accumulation of movement due to contraction and expansion, expansion joints should be provided at least every 100 ft. in length of the structure. If this is not done, severe stresses are likely to occur in the end columns. For high trestles, the columns should be braced longitudinally as well as laterally in the same manner as for high trestles of structural steel.

In most railroad trestles or viaducts the steel at the bottom of the longitudinal girder at the center of span is proportioned for the maximum bending moment produced by the given loading

for a simply-supported beam, and six-tenths of the reinforcement thus found necessary is placed in the top of the girders over supports to provide for the continuous action developed. In view of what has been said in Art. 69 of Volume II this method requires 25 per cent. more steel than if the girders were designed throughout for  $\frac{1}{2}w\ell^2$ . The above practice, however, is quite prevalent among designers of railroad structures in cases where safety is paramount, since if the piers should settle, or cracks should develop over the piers for other reasons, there would be enough reinforcement at the center of span so that the girders would carry the load as simply-supported beams.

In long bridges an expansion joint is usually provided between the superstructure and the abutments for the reason that, if an abutment with a heavy pressure of earth against it is rigidly connected with a number of continuous spans, the expansion and contraction tend to act in one direction only—that is, away from the abutment—the earth pressure back of the abutment not allowing movement in the opposite direction. Such a condition would lead to difficulties at the center of the bridge, or over the expansion piers next to the abutments, and the abutments and piers would also be severely over-stressed due to the continuous movement in one direction. Each time an abutment would move slightly due to contraction, the earth against it by reason of the heavy moving loads would fill in the small space left by the contractive movement, and when expansion again took place, the abutment would be restrained by the earth so that enormous stresses might be developed.

**72. Examples of Typical Bridges of the Continuous Girder Type.** A rather simple highway trestle, applicable to comparatively low crossings, is shown in Fig. 286. The longitudinal beams are continuous over three spans, an expansion joint occurring over every third pier. Intermediate piers are made monolithic with the floor by means of rods from the columns and struts from the cross beams. Because of the indeterminate degree of fixity, the lightness of the structure, and unknown construction factors, all members affected were designed both as fixed beams and as beams freely supported. The slabs were designed as continuous, with equal positive and negative steel throughout. The center longitudinal beam was designed as a T beam with a 36 in. flange. The pier web, or wall between



A low trestle or viaduct type of construction is shown in Figs. 287 and 288. The slab-beam-and-girder spans were selected since arches, it was thought, would not appear to advantage

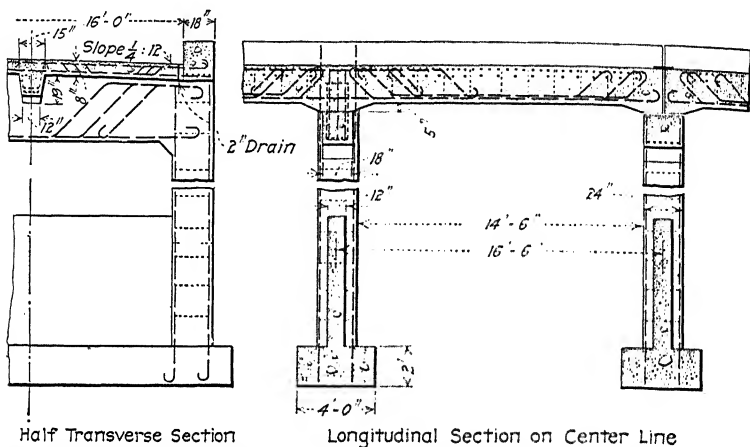
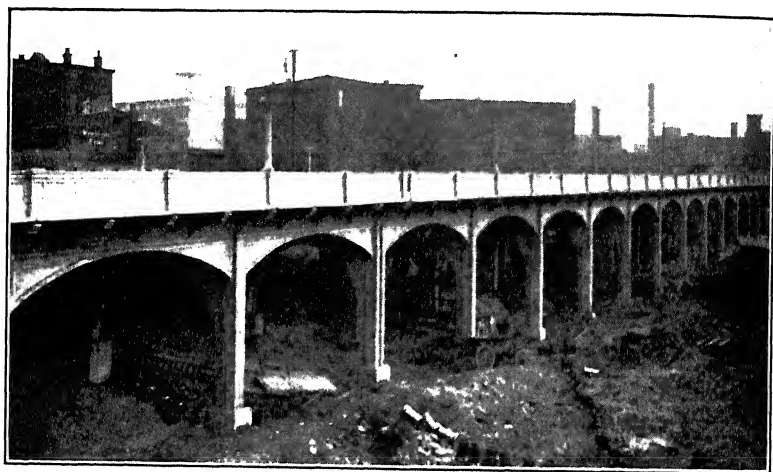


FIG. 286.—Details of standard trestle spans, Engineering Department, State of Arizona.



Courtesy of Mr. Frank L. Raschig, Division Engineer, Division of Structures, Cincinnati, O.  
FIG. 287.—Gilbert Avenue viaduct, Cincinnati, Ohio. Note expansion joint near center of illustration.

for such low construction. The cost of the girder type was also found to be much less than for a series of arches, due principally to decrease in the dead weight of the structure and

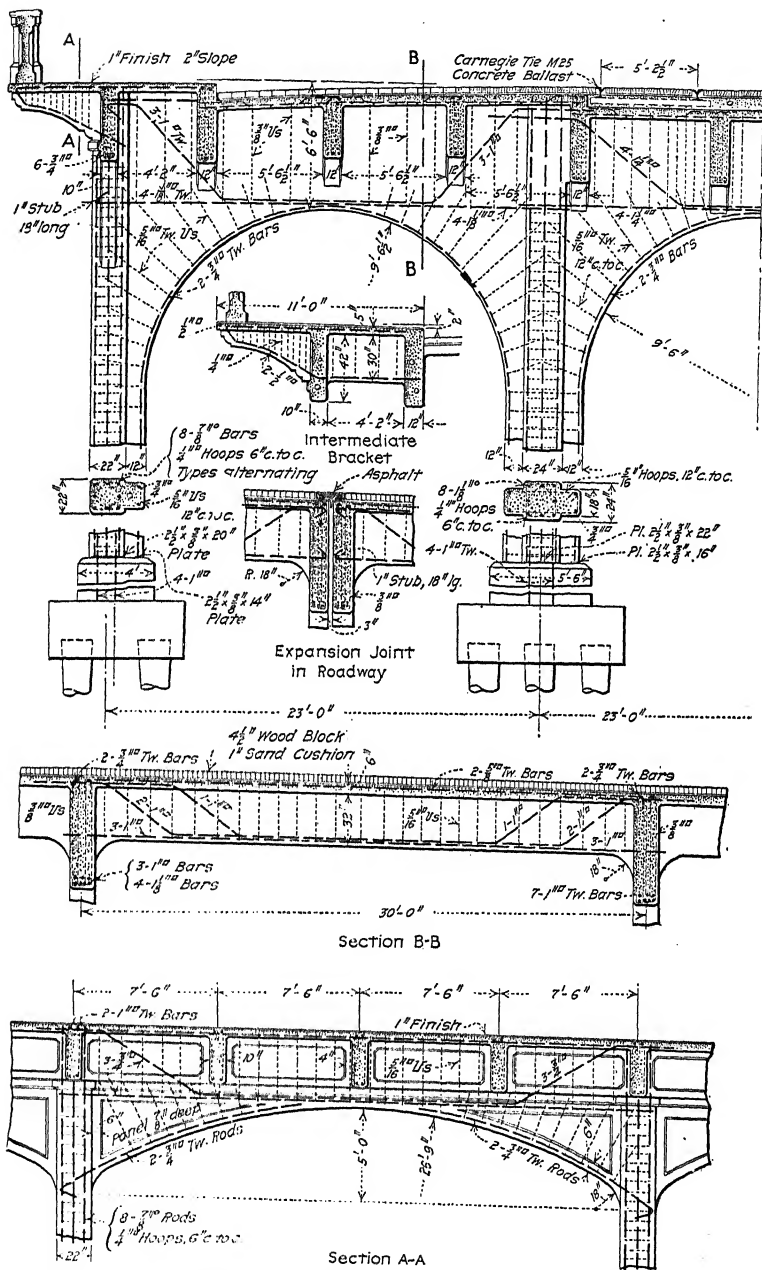


FIG. 288. Details of Gilbert Avenue viaduct, Cincinnati, Ohio.